VIBRATION RESPONSE ANALYSIS IN ORTHOPAEDICS AND ITS APPLICATION AT THE LUMBAR SPINE

by

Kevin Shek Chuen KWONG

(PDPT, MSc)

This thesis is submitted in partial fulfilment
of the requirements for the Degree of
Doctor of Philosophy in Bioengineering
in the Bioengineering Unit.

University of Strathclyde,
Glasgow, Scotland, U.K.

September, 1995.

DECLARATION

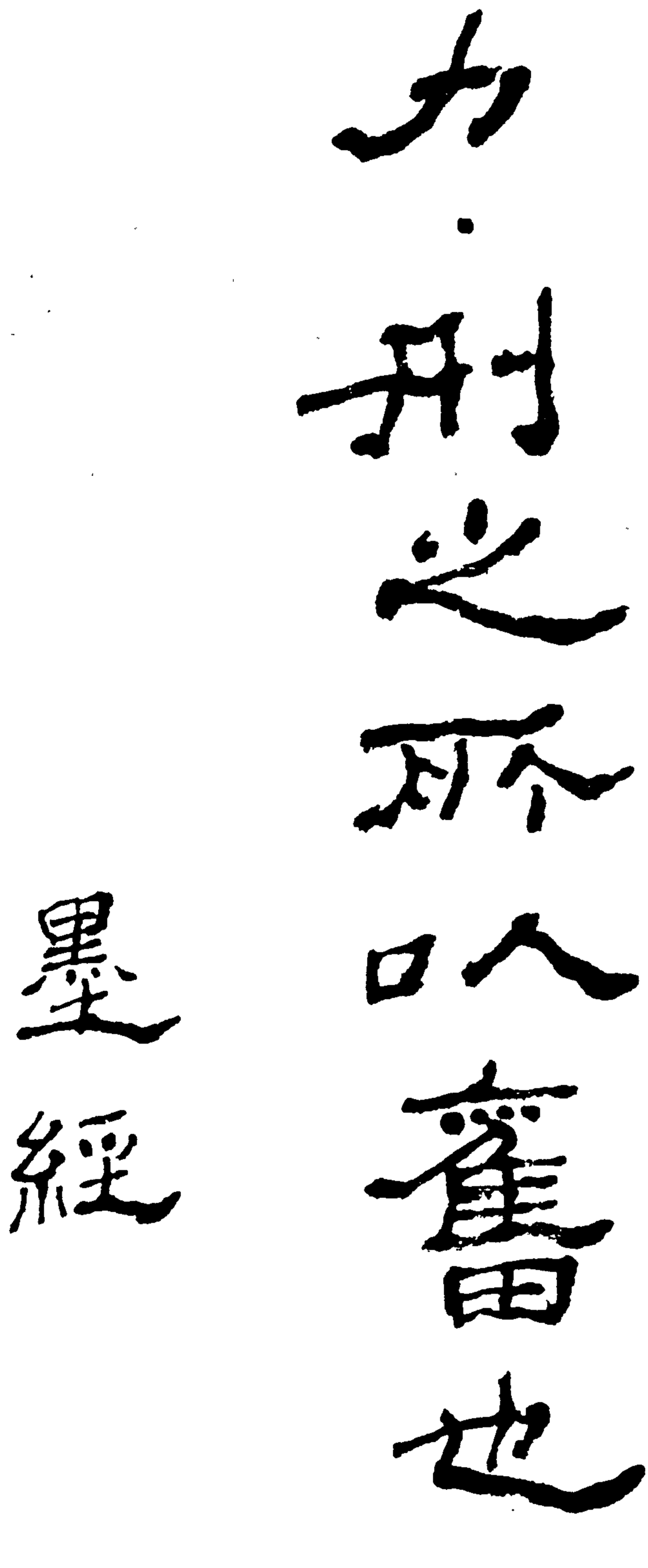
力
非
之
所
以
奮
也
墨
經

"Force is what sets a body in motion" - a law quoted from *Mo-jing* which is believed to be a publication of Mo-zi (circa 400 B.C.) and his fellow philosophers.

ACKNOWLEDGEMENTS

This research was supported by The Hong Kong Polytechnic University.

The author wishes to express his heart-felt appreciation to the guidance and encouragement offered to him by Professor John P. Paul and Professor John H. Evans. The author felt privileged to research under their tutelage.

Dr Jack C.Y. Cheng and Dr K.M. Poon kindly provided clinical material and professional advice. Mr Raymond Y.W. Lee designed the mounting cups for the test specimen. Colleagues of the Jockey Club Rehabilitation Engineering Centre offered technical support. Mr Dave Smith arranged specimens for tests. A group of young men and women volunteered to be the test subjects. To all of these people the author would like to express his very sincere vote of thanks.

ABSTRACT

Vibration response analysis has been carried out on human lumbar spines in-vitro and in-vivo. Random vibration in the frequency range between 20 Hz and 2 kHz was applied to the L5 spinous process in the antero-posterior direction while motion response was measured at the other spinous processes of the lumbar spine. Transfer mobility which defines the lumbar spine's motion response to vibratory force was evaluated by using the fast Fourier transform and spectral averaging technique. There was high damping during the in-vitro tests and the lumbar spine was found to behave as a segmented beam hinged at the thoracic and sacral ends. Fundamental mode shape was observed at frequencies lower than 150 Hz and this pattern was also observed with simulated fusion of the facet joints and interbody fusion. Mobility summated for the whole range of frequency could be modelled by an exponential expression. Useful parameters have been identified and they were found to relate to the lumbar spine's vibratory characteristics resulting from structural modifications. Vibration testing performed on normal subjects revealed that a relaxed lumbar spine was highly damped and non-resonant. First flexural vibration mode was observed only under the action of the back extensors. Averaged figures have been established for the coefficients of an exponential expression which fits closely to the summated mobility curve. The mobility and its attenuation coefficients in different frequency bands have been evaluated from twelve normal subjects. Localized attenuation of vibration response and the reduction in mobility were observed on a patient with osteoporotic lumbar spine. Mobility in the low frequencies was reduced while the medium and high band mobility were enhanced in patients with postero-lateral fusion and instrumentation for fixation of the lumbar spine. The attenuation pattern of these patients was consistent, and corresponded to the existence of structural enhancement.

CONTENTS

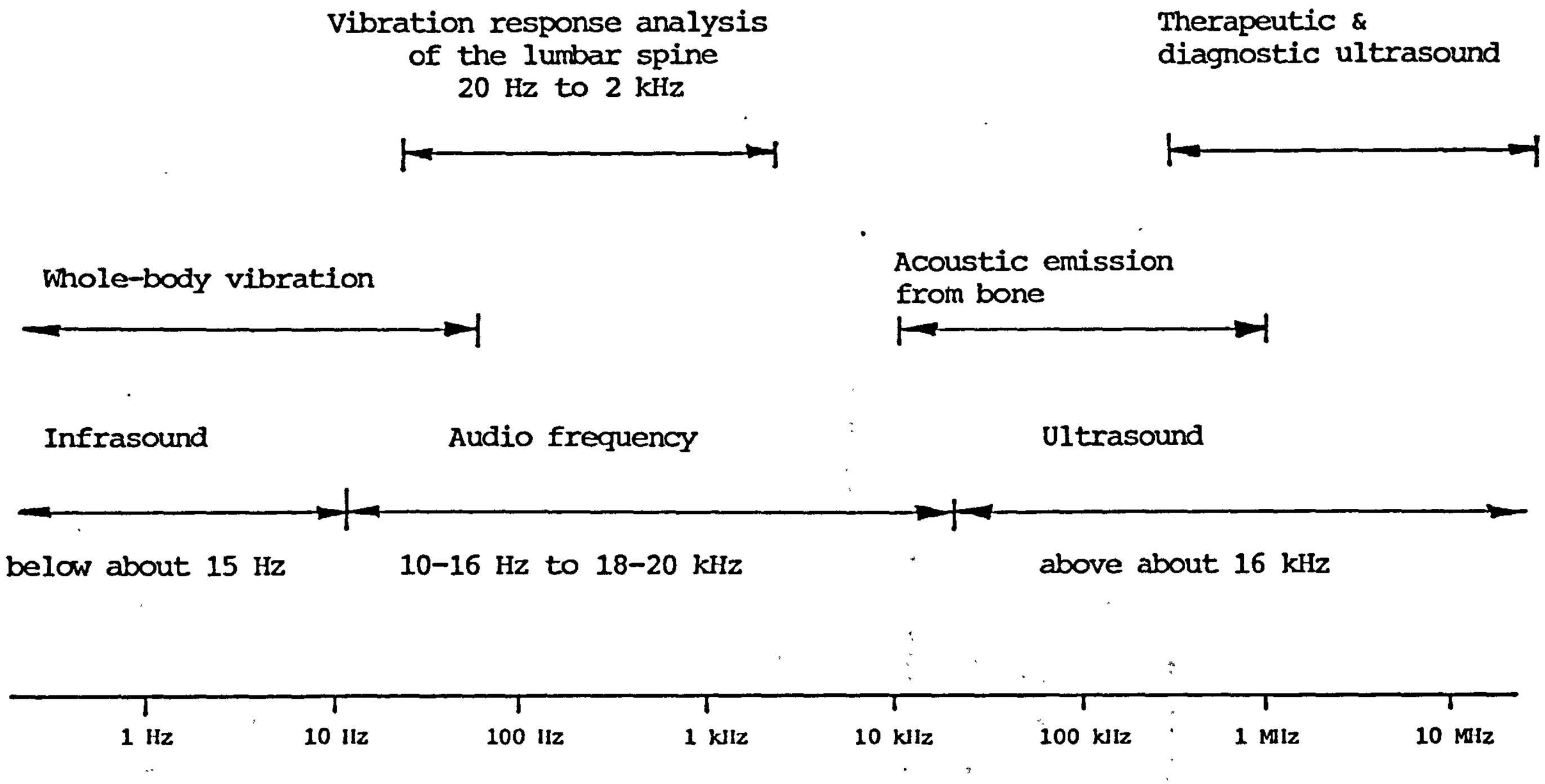

Fig 1.1 Acoustical frequency range.

CHAPTER 1

GENERAL INTRODUCTION

Traditionally, *acoustics* pertains to "the science of sound, including its production, transmission, and effects", and "an audio frequency is any frequency corresponding to a normally audible sound wave" (Beranek, 1972). Recent advancements in the field have extended the scope to infrasound and also to ultrasound far beyond the hearing range (fig 1.1). "*Acoustic* is used in relation to terms which denote things having the properties, dimensions or physical characteristics associated with sound waves, whilst *acoustical* is used when the concept does not relate to something explicitly having such dimensions" (Stephens, 1975). *Acoustical* also refers to the field which is not directly related to hearing but covers *vibration* which is a possible source of sound. In this thesis, the term *acoustical* adopts a more generic meaning nesting *vibration* which is defined as "oscillatory motion of a body upon which a force is acting" (Stephens, 1975). Here *vibration* refers to bone-borne transmission and propagation of acoustical energy, and the detection of associated motion at appropriate locations in the musculoskeletal system.

For centuries, auscultation and percussion have been well developed in the medical profession for clinical examination and diagnosis of cardiac and respiratory diseases. These two basic clinical skills utilize the principles of sound production and its transmission properties in the human tissues for the understanding of disease states in man. The orthopaedics specialty, which is primarily concerned with the pathological, anatomical and mechanical disorders of the musculoskeletal and locomotion systems, has relied heavily on the use of radiological imaging techniques. With the advancements of diagnostic ultrasound for imaging, this technique has been applied in the diagnosis of bone and joint disorders. Auscultation of bone and joints has been reported. However,

acoustic techniques have not been developed to the stage where they may be used routinely as standard diagnostic tools. The subjective appreciation of sound and the detection of vibration such as crepitus from joints do not yet constitute an essential part of routine clinical examinations. The ability to appreciate these physical signs and their interpretation in association with other clinical signs are highly experience dependent. This has limited the application of acoustic and vibration techniques in the practice of orthopaedics.

Vibration response analysis which examines the motion response of mechanical structures to vibratory force is a well established technique widely used in industry and engineering for monitoring machine health. Its applications in biomedical engineering for studying the effects of vibration and high *g* impacts on the human body are numerous and have been reported extensively elsewhere. Intrinsically generated vibrations developed during walking and other functional activities of the lower limbs have been studied. The assessment of the state of bone fracture healing, the detection of prosthetic loosening and the evaluation of the physical quality, such as stiffness, of long bones by vibration techniques are also drawing current attention. The transmissibility of shock waves through body structures like the spinal column has also been reported. However, former investigations have largely focused on the gross dynamic characteristics of the spine, lacking the intention of examining the mechanical characteristics of localised or finer structures. The study of local motion response of the spinal column to vibratory force has received much less attention and the use of vibration techniques for the examination of local vibratory characteristics of the lumbar spine has not been attempted.

No one would argue the diagnostic value of radiological imaging techniques and related processes. However, conventional imaging techniques adopt a positional standard of analysis derived in the main from subjective

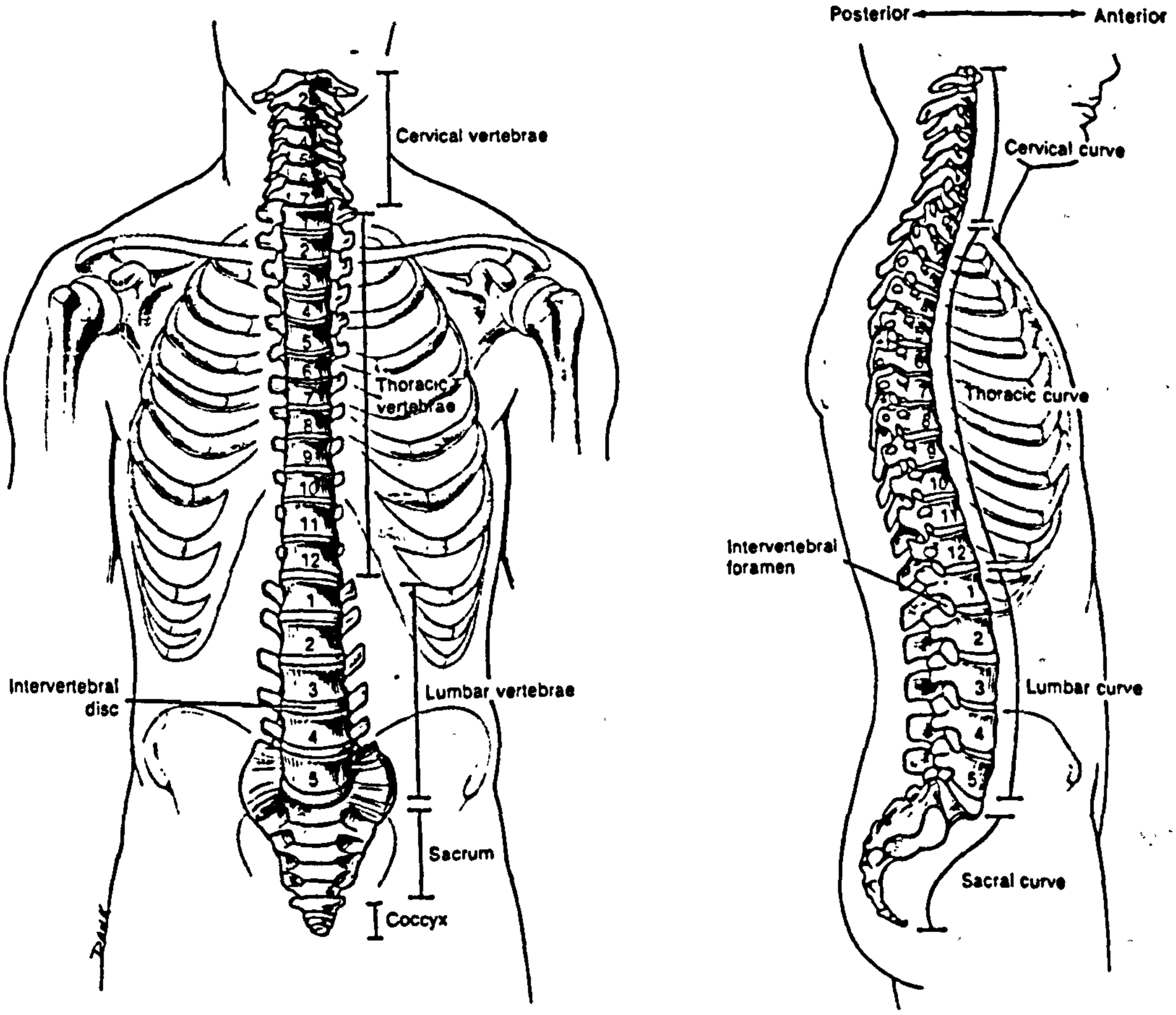

Fig 1.2 The lumbar spine consists of five segments forming the axial skeleton of the low back (from Tortora & Anagnostakos, 1987).

visual interpretation of data. Vibration techniques have the potential to utilize a mechanical standard of analysis derived from more objective data directly related to the dynamic response of the observed structure. The major advantage of vibration technique is its potential capability of revealing the dynamic mechanical behaviour of the bone and joint structures by objective measurements, which are not normally obtainable from routine clinical imaging procedures. The mechanical properties of bone and joint structures such as strength, integrity and stability could only be inferred from radiological images with reference to prerequisite clinical experience. However, vibration response analysis may give an indication of the mechanical weakness or strength of the bone and joint structures instead of merely the spatial relationship of their sub-structures as for the case of imaging techniques.

The spine (fig 1.2) is a structural assembly of bony masses and soft tissues of various geometry and mechanical properties. It has a primary function of supporting the load originating from the weight of the body and its motions. The spine both functionally and structurally demonstrates a good analogy of mechanical principles within the human body. It is hypothesized that the spine being a mechanical structure per se, should respond to vibratory force in an unique manner characteristic of its mechanical properties. Vibration response analysis is a technique widely used for testing the integrity of mechanical and building structures. It is here suggested that it should be equally applicable for the detection of structural weakness or strength of the lumbar spine by examining its dynamic response to vibratory force.

For long bones and the peripheral joints, use can be made of attempted manipulation and palpation in association with other clinical investigations for testing the changes in their stiffness as in the case of clinical examination of bone fracture. The lumbar spine, however, being deeply embedded in the surrounding soft tissues in the lower trunk

is practically inaccessible to manual contact except at the most prominent spinous processes, or through an invasive approach. The attempted test of the integrity or mechanical derangement of the lumbar spine by manual manoeuvre is difficult if not impossible. In-vivo mechanical tests using Instron-type of machines for the mechanical behaviour of the lumbar spine is not feasible for obvious reasons, not even to mention safety. It is highly desirable to develop a non-invasive, non-challenging and yet more discriminating technique which is capable of showing the structural integrity and dynamic mechanical behaviour of the lumbar spine. This research also aims to investigate and explore the technical feasibility of vibration techniques and the associated analyses of the lumbar spine to examine its dynamic mechanical characteristics. Results from this study, if proved positive, may possibly lead to the development of a clinically viable vibration technique for the examination of changes in the dynamic mechanical characteristics of the lumbar spine as a result of surgical and pathological fusions. The outcomes of this research may also help to identify some other potential areas of application of the technique in orthopaedics.

Previous vibration studies on the spine focused on the use of vibrations in the infrasonic or the lower audio frequency range. Those are basically tests for the mechanical behaviour attributable to the gross geometry i.e. the curvature and the anatomical form of the spinal column. Diagnostic ultrasound, on the other extreme, utilizes frequencies in the order of mega-Hertz. There seems to be a gap between these two extreme ranges of frequency in the acoustical spectrum. This is the domain in which this research attempts to explore. The frequencies of interest of this study are confined to audio range.

This study examines the transmission of bone-borne vibration in the lumbar spine and its motion response to external vibratory force. A vibration technique has been developed to detect the changes in vibration response of

the lumbar spine specimens with simulated fusions. The changes in the in-vivo vibration response of surgically fused lumbar spines of patients are also investigated with reference to a group of normal subjects. This study also investigates the potential capability of this vibration technique as a diagnostic tool for problems related to structural modifications of the lumbar spine.

For the purpose of this investigation, the bone substance and associated soft tissues of the lumbar spine are considered homogeneous. The spinal segments, and the associated intervertebral discs and the zygapophyseal joints are the primary structures for the transmission of vibratory stress while the paraspinal musculature is considered as insulation material to vibration. The microstructure of bone substance and soft tissue are not subject matters for discussion in this thesis. The lumbar spine is considered as a passive linear system exhibiting no viscoelastic behaviour under minimal stress condition experienced in the vibration tests. This assumption of system linearity is subject to tests which are reported and discussed in the appropriate chapters.

This thesis reviews the theory and literature on acoustical techniques and associated analyses applied for research and clinical practice in orthopaedics. The review forms the basis for the development of a safe and reliable technique for the examination of vibration response of the lumbar spine. Special considerations of the experimental approach and technical feasibility are discussed. The main experimental studies involved vibration testing carried out on human lumbar spine specimens and on similar ones with simulated facet joints fusion and interbody fusion. Vibration testing with a similar but modified experimental technique was also carried out on normal subjects and patients. Results are presented of the vibration response of healthy individuals and patients with confirmed orthopaedic problems such as postero-lateral fusion and osteoporosis of the lumbar spine.

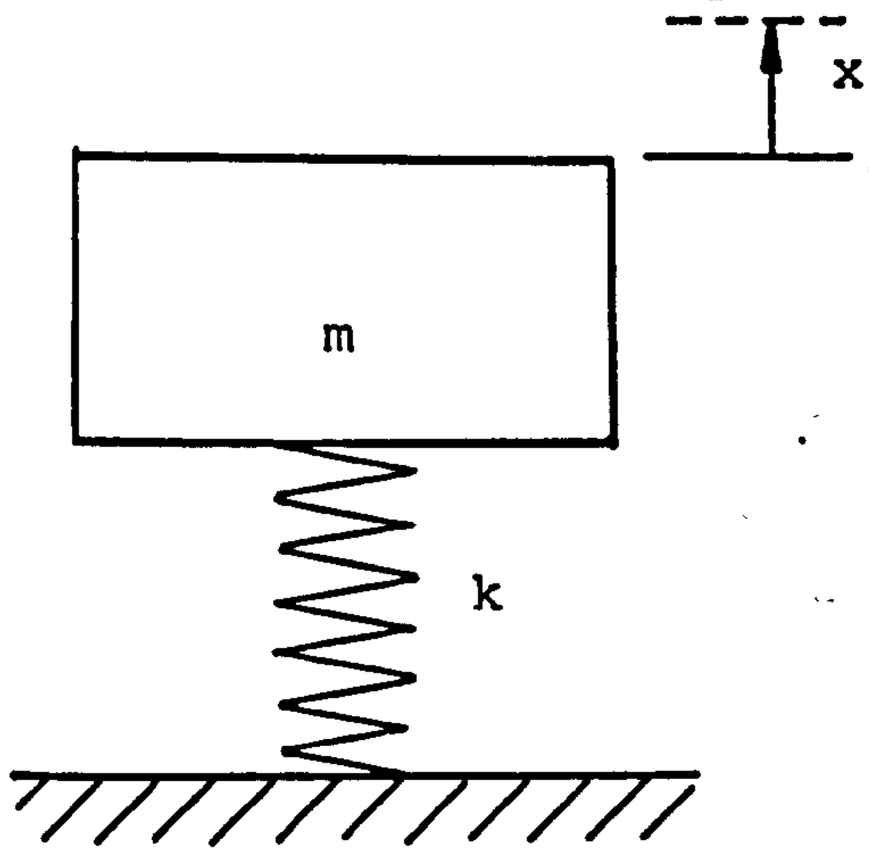

Fig 2.1 A simple mass-spring system.

CHAPTER 2

REVIEW OF THEORY AND LITERATURE

2.1 INTRODUCTION

The subject matter presented in this review covers the theoretical basis of mechanical vibration, vibration signals and their analyses in the time and frequency domains. The theory and mathematical concepts summarized in this chapter are deemed essential for the development of frequency response analysis of vibration systems - an approach which is also described as vibration response analysis in this thesis. Based on published work, the acoustical properties of biological tissues and structures in the musculoskeletal system are discussed and summarized. Acoustic and vibration techniques applied in the field of biomedical engineering, particularly those of potential clinical applications are outlined. This review also highlights the technical difficulties, uncertainties, and limitations in the development of an appropriate experimental approach to the vibration response analysis of the lumbar spine.

2.2 BASIC VIBRATION THEORY

2.2.1 Mechanical Vibration

Mechanical vibration is an observable and measurable response of a physical system to an excitatory force, intrinsic or extrinsic. This response of the system can be expressed as motion in terms of displacement, velocity or acceleration. The mechanical characteristics of a vibration system which exhibits an oscillatory motion initiated by an excitation can be illustrated by a simple mechanical model which comprises a mass and a spring (fig 2.1). Mathematically, the oscillatory motion of this system can be expressed as a sinusoidal function of time:

$$x(t) = A \sin(2\pi f_n t + \theta) \qquad (2.1)$$

where

x is the instantaneous displacement (in m) of the mass about an equilibrium reference position;

A is the amplitude (peak) of the motion in m;

f_n is the natural frequency (in Hz) at which the system would oscillate indefinitely under undamped condition;

θ is the phase angle in rad; and

t is the time in s.

The natural frequency f_n is dependent on the physical characteristics of the system, and is given by:

$$f_n = \frac{1}{2\pi}\sqrt{\frac{k}{m}} \qquad (2.2)$$

where

k is the elastic constant of the spring in N/m; and

m is the mass in kg.

2.2.2 Damping

In this real world, every practical vibration system incorporates damping elements of various nature which thus modify the behaviour of the previously described system by causing a decrease of the amplitude with time and a change in its natural frequency, both of which depend on the amount of damping. In this thesis, only viscous damping is considered, i.e. damping force = c.V, where c is the damping coefficient and V the velocity. The resulting oscillatory motion depends largely on whether c is equal to, greater than, or less than the critical damping coefficient c_c. Critical damping corresponds to a limiting condition between an oscillatory and a non-oscillatory transient state of free vibration (BS 3015, 1991). The damping ratio $\zeta = c/c_c$ which is defined as the fraction of critical damping conveniently expresses the amount of damping in a system. With damping less than critical, i.e.

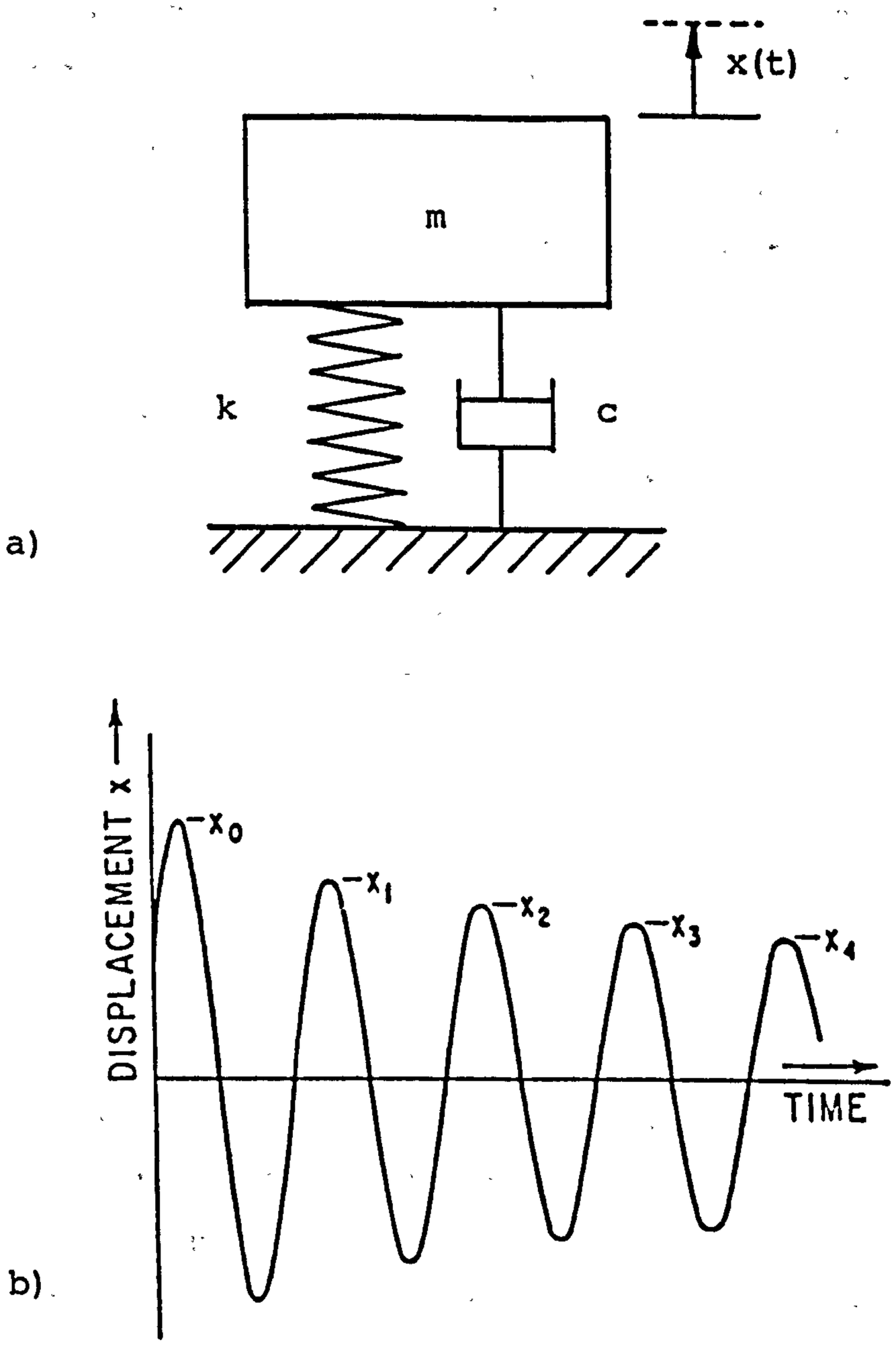

Fig 2.2 a) A mass-spring-damper system and b) the amplitudes of displacement maxima under damped free vibration (from Blake, 1988).

$\zeta < 1$, equation 2.1 is then modified as the following expression for free vibration of the damped system:

$$x(t) = Ae^{-\zeta(2\pi f_n)t}\sin(2\pi f_d t + \theta) \qquad (2.3)$$

where

e is the base of natural logarithm (2.71828); and

f_d is the damped natural frequency in Hz.

The ratio of any two displacement maxima separated by n cycles of oscillation will then be given by:

$$\frac{x_n}{x_0} = e^{-2\pi n\zeta/(1-\zeta^2)^{1/2}} \qquad (2.4)$$

Figure 2.2 shows the amplitudes of displacement maxima which bear a logarithmic relation with the successive ones. The logarithmic decrement δ is the natural logarithm of the ratio of the amplitudes of two successive displacement peaks of the damped free vibration of the system:

$$\delta = \ln\frac{x_n}{x_{n+1}} \qquad (2.5)$$

or

$$\frac{x_{n+1}}{x_n} = e^{-\delta} \qquad (2.6)$$

Hence, when referring to equation 2.4, with n = 1,

$$\delta = \frac{2\pi\zeta}{(1-\zeta^2)^{1/2}} \qquad (2.7)$$

Equation 2.7 indicates that the damping ratio could be estimated from an experimentally determined logarithmic decrement of the displacement maxima.

For a highly damped system, i.e. when $c = c_c$ ($\zeta = 1$), or $c > c_c$ ($\zeta > 1$), there is no oscillation, unless excited by a continuously applied excitatory force. This situation is described as a forced vibration.

2.2.3 Forced Vibration

If an external sinusoidal excitatory force is applied

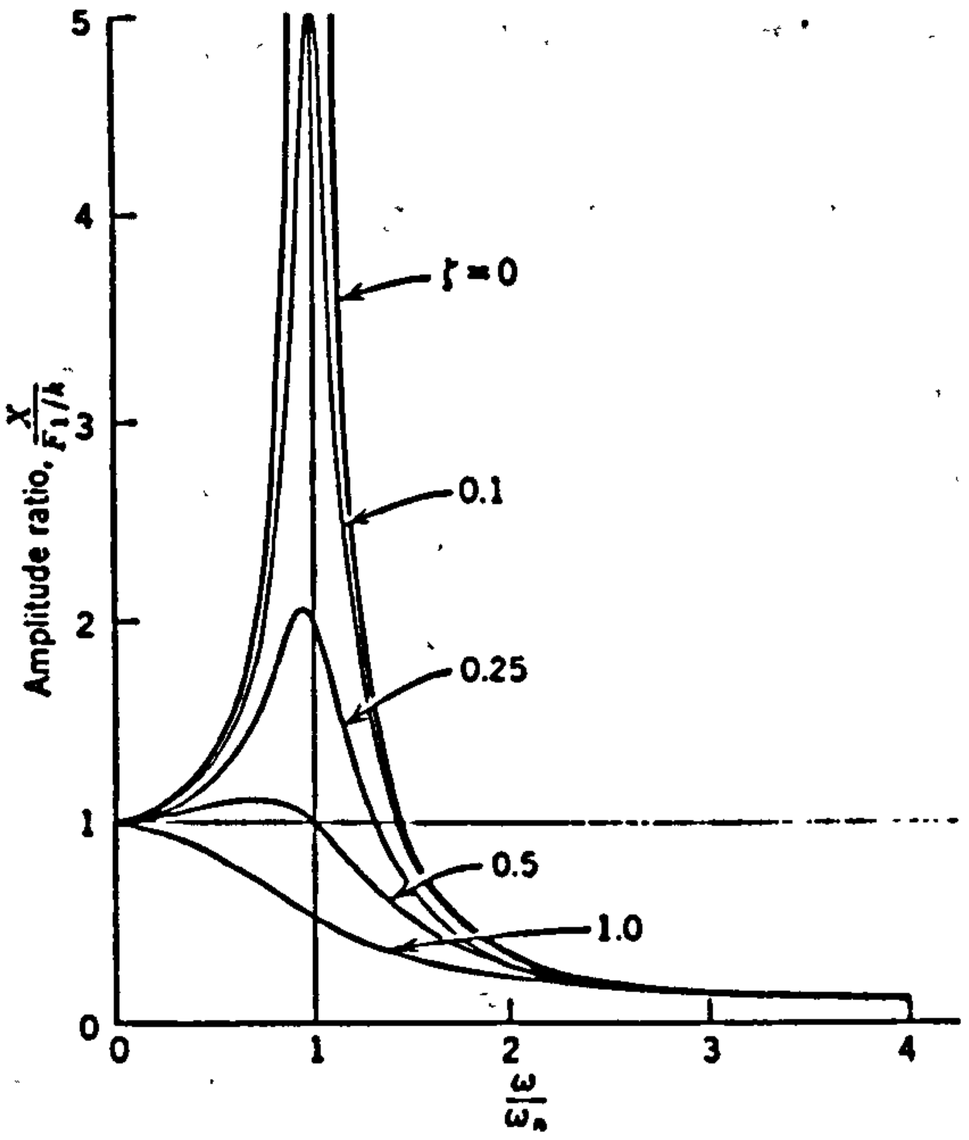

Fig 2.3 Motion response of a mechanical system under forced vibration. ω/ω_n is the ratio of forcing frequency to resonant frequency of the system (from Steidel Jr, 1989).

to a mechanical system, motion will follow the force which means the system vibrates with the same frequency as the external excitatory force, but with an amplitude which varies according to the ratio of the forcing frequency to the natural frequency of the system. Figure 2.3 depicts the motion response of such system to a range of excitation frequencies with various amount of damping in the system. At very low frequencies the displacement amplitude resembles the spring displacement that would occur as if the force is applied statically. The displacement amplitude rises to a peak at the resonant frequency of the system and approaches zero as the forcing frequency becomes very high. The above three frequency conditions may sometimes be described respectively as spring-controlled, damper-controlled, or mass-controlled as under these conditions the physical properties of the corresponding components dominate.

2.2.4 Degree-of-Freedom

The system described so far is considered as an ideal single degree-of-freedom (SDOF) system which exhibits motion in one direction only and the system comprises only one mass, one spring and one damper. Mathematically, its vibratory behaviour under a sinusoidal excitatory force of $F = F_0\sin(2\pi ft)$ is sufficiently described by one differential equation:

$$m\ddot{x} + c\dot{x} + kx = F_0\sin(2\pi ft) \qquad (2.8)$$

where

- m is the mass in kg;
- c is the damping coefficient in Ns/m;
- k is the elastic constant of the spring in N/m;
- F_o is the amplitude of the excitatory force in N;
- f is the forcing frequency in Hz; and
- t is the time in s.

Most systems especially biomechanical ones are complex and should be considered as multi-degree-of-freedom (MDOF)

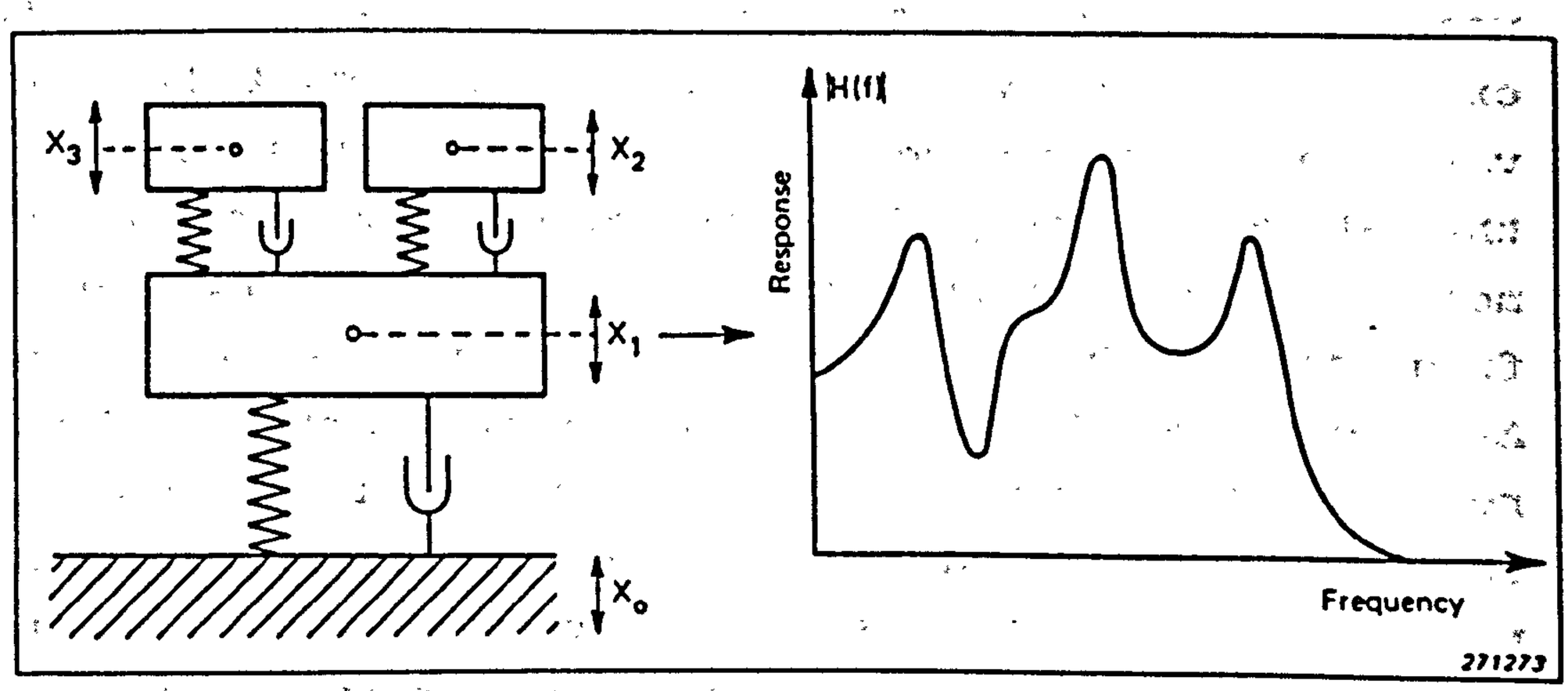

Fig 2.4 Multi-degree-of-freedom system and its frequency response function (from Broch, 1984).

systems which consist of interacting masses, springs, and dampers (Fig 2.4). All MDOF systems exhibit "combined" behaviour of a number of SDOF systems in accordance with the principle of superposition. Mathematically, it is more complex regarding the presentation and solution through an analytical approach.

2.3 ANALYSIS OF VIBRATION SIGNALS

2.3.1 Vibration Signals

The vibration signal, which is the time-record of the motion or force associated with a mechanical vibration, may take various forms. The simplest form consists of a sinusoidal wave of single frequency. A swept sine wave refers to one the frequency of which sweeps linearly or logarithmically within a preset range. However the motions of most mechanical systems usually comprise components occurring at different frequencies and phases which "combine" simultaneously forming complex waveforms. Non-sinusoidal signals, such as a square wave, can be separated into a number of harmonically related components each of which are sinusoidal in nature and are multiples of the fundamental frequency to which they are referred. In accordance with the principle of superposition, complex vibration signals can be decomposed into a number of sinusoidal components of various amplitudes and frequencies. A random vibration signal is one which is random in amplitude and phase. It does not have periodical or harmonically related components, and neither does it concentrate on a particular frequency. Its spectral components distribute uniformly across the frequency range of interest. This is sometimes described as "white noise" in some applications. While its instantaneous value cannot be predicted, a random vibration can only be described by its statistical properties i.e. the probability density distribution of its amplitude with time - a Gaussian distribution. A mechanical shock or impulse is a short duration burst of vibratory energy which takes place in a

finite length of time. Its frequency spectrum comprises spectral components distributed within a frequency band, the width of which is related inversely to the duration of the impulse.

2.3.2 Statistical Analysis

The mean absolute value of a time-signal x(t) is one of the statistical descriptors, and is given by:

$$\textit{Mean Absolute Value, } \overline{x} = \frac{1}{T}\int_0^T |x(t)|\,dt \qquad (2.9)$$

where T is the time duration in which the signal was recorded. The corresponding discrete form of the mean absolute value for a time series x(i) sampled at f_s samples per second with N (= $T.f_s$) sampled values within the series, is given by:

$$\textit{Mean Absolute Value, } \overline{x} = \frac{1}{N}\sum_{i=1}^{N} |x(i)| \qquad (2.10)$$

For complex signals e.g. random vibration, the root-mean-square (RMS) value is a useful descriptor which is a measure of the energy content of the signals. It may also be used to quantify the severity of exposure to vibration (Griffin, 1990). The mathematical expression of the RMS value of a time-signal x(t) is:

$$RMS = \sqrt{\frac{1}{T}\int_0^T x^2(t)\,dt} \qquad (2.11)$$

and accordingly its digital form is:

$$RMS = \left[\frac{1}{N}\sum_{i=1}^{N} x^2(i)\right]^{1/2} \qquad (2.12)$$

2.3.3 Time Domain Analysis

The time-history of a sinusoidal signal is straight

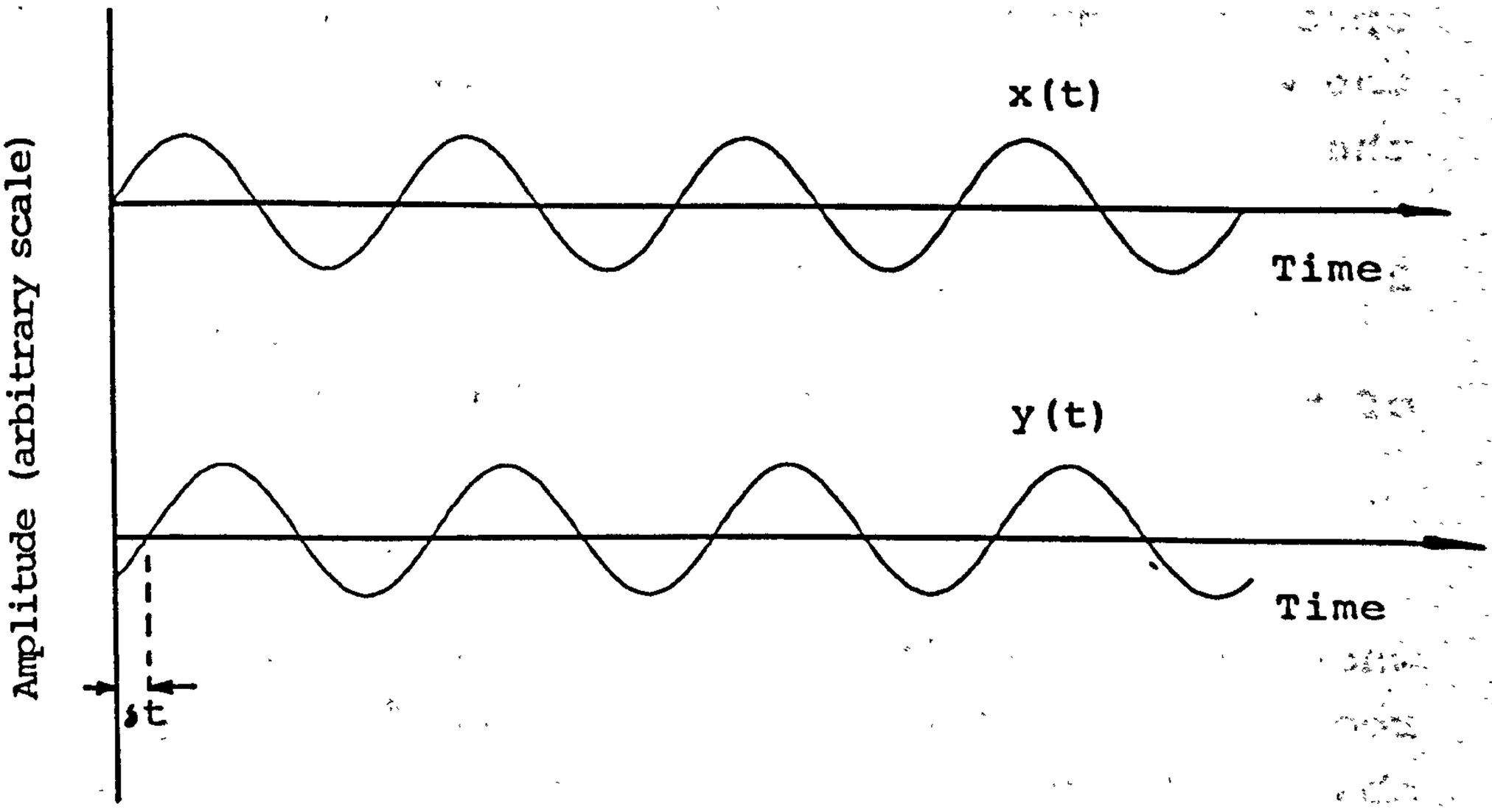

Fig 2.5 Time-delay between two sinusoidal waves of the same frequency.

forward. The three essential parameters: amplitude, frequency, and phase are sufficient in the description of the vibration signal. Amplitude ratio (A_y/A_x) can be used to describe the relative intensity of two stationary sinusoidal signals x(t) and y(t) of the same frequency; while the time-delay δt reveals their temporal relation in occurrence (fig 2.5).

Autocorrelation is a function which indicates to what extent a time-signal x(t) is similar with a displaced version of itself as a function of the displacement τ in time. It is useful for determining the periodicity in a signal, and hence the possible identification of a secondary signal existing as echo, or travelling through an alternative transmission path in a system. Similarly, cross-correlation gives a measure of the degree of similarity between x(t) and a displaced version of another time-signal y(t) as a function of the time displacement. It is useful in determining the time-delay in occurrence between two independent but simultaneous records of signals. The autocorrelation function $R_{xx}(\tau)$ of a signal x(t) and the cross-correlation function $R_{xy}(\tau)$ between two signals x(t) and y(t) are given by:

$$R_{xx}(\tau) = \lim_{T\to\infty} \frac{1}{T}\int_T x(t)\ x(t+\tau)\ dt \qquad (2.13)$$

$$R_{xy}(\tau) = \lim_{T\to\infty} \frac{1}{T}\int_T x(t)\ y(t+\tau)\ dt \qquad (2.14)$$

2.3.4 Frequency Domain Analysis

Time and frequency domains are two different, but closely related means of expressing the characteristics of a signal. Both the time-history of a signal and its frequency equivalent are capturing the same information about the signal. The former expresses the signal with respect to a time-scale while the latter describes its spectral components within a range of frequency. Through the effective use of frequency analysis, a complex waveform

can be expressed as a frequency spectrum which shows the relative amplitudes of its components on an appropriate scale. A well established practical approach of frequency analysis is based on the concept of the Fourier transform which converts a signal from the time domain into its equivalent form in the frequency domain (Bergland, 1969). The Fourier transform of a time-signal x(t) defines the complex spectrum X(f), and is given by:

$$X(f) = \int_{-\infty}^{\infty} x(t)\, e^{-j2\pi ft} dt \qquad (2.15)$$

$$x(t) = \int_{-\infty}^{\infty} X(f)\, e^{j2\pi ft} df \qquad (2.16)$$

Equation 2.16 is the expression for inverse Fourier transform. With the advancement of digital systems, the processes of data acquisition and analysis could well be implemented digitally. Equations 2.15 and 2.16 can then be replaced by their corresponding digital forms, and subsequently the transform is described as discrete Fourier transform (DFT) (Bergland, 1969). Equations 2.17 and 2.18 represent respectively the mathematically linked procedures of forward and inverse discrete Fourier transforms:

$$X_n = \frac{1}{N} \sum_{i=0}^{N-1} x_i e^{-j2\pi in/N} \qquad (2.17)$$

$$x_i = \sum_{n=0}^{N-1} X_n e^{j2\pi in/N} \qquad (2.18)$$

where

X_n is the Fourier components of the signal;

x_i is the time-signal sampled at discrete points of time;

i, n are integers; and

N is the number of samples in the time-record.

The fast Fourier transform (FFT) (Cooley & Tukey, 1965) is a much faster computational algorithm of the discrete

Fourier transform. FFT-based digital systems are readily available for the analysis of vibration signals. However the inherent drawbacks of using the DFT technique still exist and these have been documented (Bergland, 1969).

The autospectrum of x(t) is defined by:

$$S_{xx}(f) = X^*(f) \cdot X(f) \qquad (2.19)$$

where $X^*(f)$ is the complex conjugate of X(f). The autospectrum expresses the distribution of energy or power in the signal as a function of frequency. Thus it is synonymously described as power spectral density. The cross-spectrum S_{xy} between two signals x(t) and y(t) is defined by:

$$S_{xy}(f) = X^*(f) \cdot Y(f) \qquad (2.20)$$

The major practical use of cross-spectrum is seen by its role as the key function for the computation of frequency response function (FRF) in the analysis of vibration systems (equation 2.29).

In practice, autospectrum and cross-spectrum are estimated for each time-record block (i) of definite size, and averaging is performed over a finite number of blocks. The autospectrum of x(t) and the cross-spectrum between x(t) and y(t) are estimated by:

$$S_{xx}(f) = \lim_{k\to\infty} \frac{1}{k} \sum_{i=1}^{k} \hat{X}_i^*(f)\ \hat{X}_i(f) \qquad (2.21)$$

$$S_{xy}(f) = \lim_{k\to\infty} \frac{1}{k} \sum_{i=1}^{k} \hat{X}_i^*(f)\ \hat{Y}_i(f) \qquad (2.22)$$

where

$\hat{X}_i(f)$, $\hat{Y}_i(f)$ are the estimated spectra of each time-record block (i) of x(t) and y(t) respectively, using equation 2.17; and

k is the number of time-record blocks for averaging.

In this thesis, autospectra and cross-spectra are expressed with the corresponding one-sided spectra defined by:

$$\begin{aligned} G_{xx}(f) &= 2S_{xx}(f) && f > 0 \\ &= S_{xx}(f) && f = 0 \\ &= 0 && f < 0 \end{aligned} \qquad (2.23)$$

and

$$\begin{aligned} G_{xy}(f) &= 2S_{xy}(f) && f > 0 \\ &= S_{xy}(f) && f = 0 \\ &= 0 && f < 0 \end{aligned} \qquad (2.24)$$

Alternatively, use can be made of analogue or digital filters in association with other instruments to perform frequency analysis of a signal. However, this study is primarily based on the application of FFT-based frequency analysis technique, hence the use of digital filters (Randall, 1987) will not be elaborated in this thesis.

2.3.5 Cepstrum Analysis

Echo or delayed transmission of a vibration signal in an alternative or longer path may constitute a secondary signal which superimposes with the original one as a time-delayed version. This may not be easily noticed. Use can be made of the periodicity of a cepstrum analysis for the detection of the secondary signal. Cepstrum, a corruption of the term *spectrum*, is defined as the Fourier transform of the logarithm of the power spectrum of a signal (Beauchamp, 1987). The following equation expresses the computation of cepstrum K_i of a signal in digital form:

$$K_i = \frac{1}{N}\sum_{n=0}^{N-1} (\log_e |X_n|^2)\, e^{2\pi i n/N} \qquad (2.25)$$

where

X_n is the Fourier components of the signal;

i, n are integers; and

N is the number of points of the Fourier transform.

The parameters such as amplitude and time-delay of the echo exist as cosinusoidal terms in the power spectrum

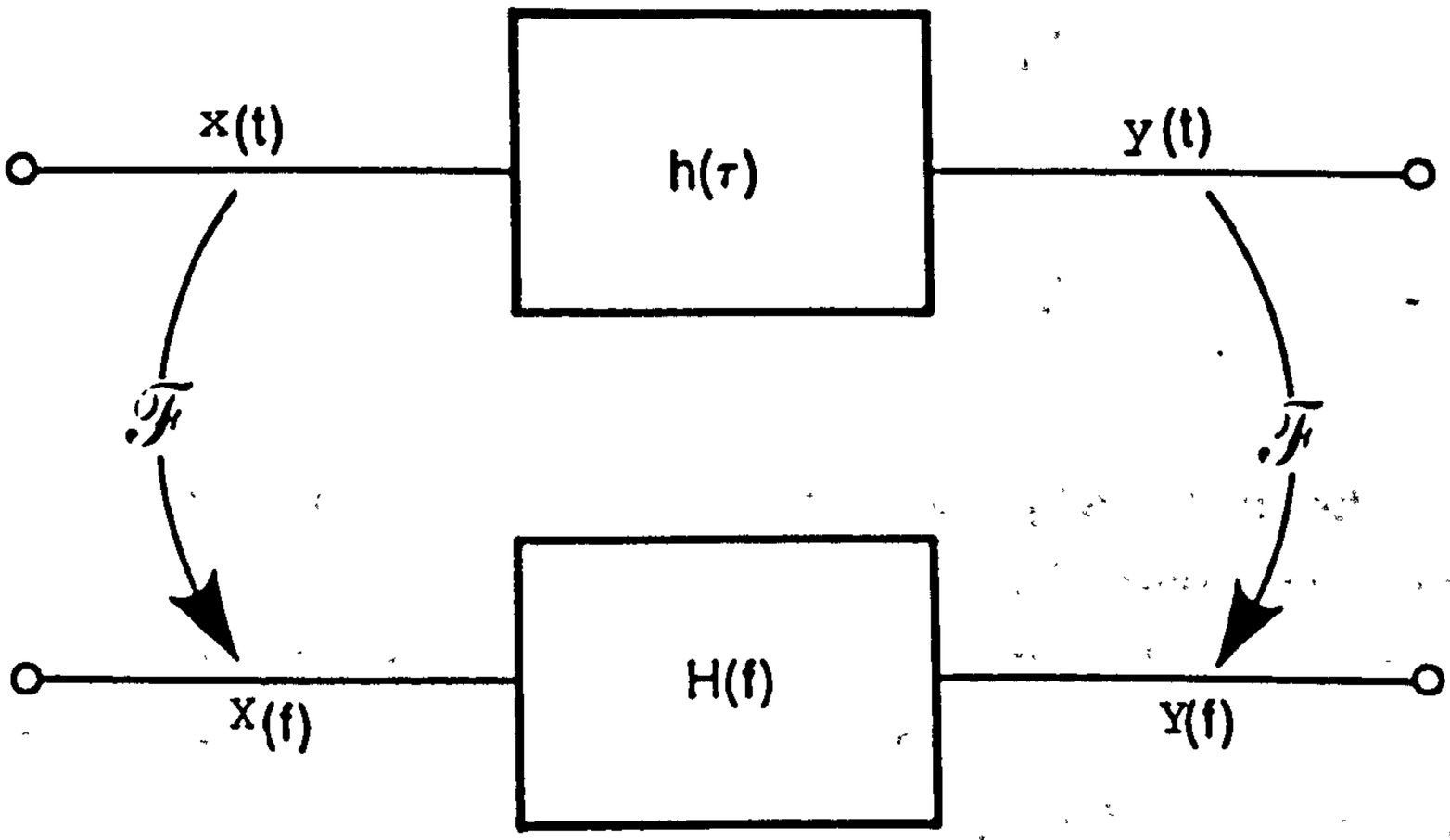

Fig 2.6 System with input signal x(t) and output signal y(t). The Fourier transform of x(t) and y(t) are X(f) and Y(f) respectively (modified from Herlufsen, 1984)

($|X(f)|^2$), and are not readily detectable. The logarithmic function converts the multiplication into addition. Hence the logarithmic power spectrum of the original signal will then be overlaid with a cosinusoidal ripple which indicates the periodicity (Summers, 1981). The time-delay of the echo can be detected by subsequent (inverse) Fourier transform back to the time domain. Section 3.9.2 outlines the validation of cepstrum analysis implemented on a digital system.

2.4 VIBRATION RESPONSE ANALYSIS OF SYSTEMS

2.4.1 Impulse Response Function

The main objective of system analysis is to establish an input-output relationship of a vibration system. The function h(t) is the impulse response function which describes the mechanical characteristics of the system as the theoretical response to an infinitely short duration unit impulse. The output signal y(t) could be considered as the result of a convolution of the input signal x(t) with the impulse response function of the system. This forms the basis of system analysis whereas the output can also be explained as a modulated form by the system characteristics of the input excitation. The mathematical relation between the input and output signals can be expressed by (Balmer, 1991):

$$y(t) = h(t) * x(t) = \int_{-\infty}^{\infty} h(\tau)\, x(t-\tau)\, d\tau \qquad (2.26)$$

where "*" denotes convolution and τ is a dummy time variable.

2.4.2 Frequency Response Function

An alternative system descriptor is the frequency response function H(f) in the frequency domain. H(f) and h(t) are related via the Fourier transform. The Fourier transforms of x(t) and y(t) are X(f) and Y(f) respectively (fig 2.6). In the frequency domain, the relation between

input and output signals is expressed by:

$$Y(f) = H(f) \cdot X(f) \qquad (2.27)$$

where "." denotes multiplication. The advantage of system analysis in the frequency domain is therefore significant. Equation 2.27 is expressing the equivalent form of a convolution in the time domain as a multiplication in the frequency domain. Hence, the computation involved is very much simplified and the frequency response function, which represents the system's steady state response to a harmonic forcing function with frequency f (Van der Perre, 1984), is readily defined by:

$$H(f) = \frac{Y(f)}{X(f)} \qquad (2.28)$$

Equation 2.28 is in fact a simplified form of the frequency response function which is normally computed in its complex form, i.e. in magnitude and phase expressions, or alternatively as real and imaginary parts. However, the magnitude is more important in practice, and is drawing major attention in discussions. The formal computation of a frequency response function $H_{xy}(f)$ in the complex form is:

$$H_{xy}(f) = \frac{G_{xy}(f)}{G_{xx}(f)} \qquad (2.29)$$

where $G_{xx}(f)$ and $G_{xy}(f)$ are respectively the autospectrum of x(t) and the cross-spectrum between x(t) and y(t), obtained by equations 2.23 and 2.24.

Frequency response function finds its extended uses in the analysis of vibration systems. Equation 2.28 can be extended to define a list of derived frequency response functions according to the type of measurements, as well as the spatial relationship of the locations at which the input and output signals of the system are measured. These

form the mathematical basis to characterize the system's motion response under forced vibration. It is referred to as vibration response analysis in this thesis.

Mobility measurement refers to the measurement of motion (as acceleration, velocity or displacement) of a system in response to a known excitatory force. Driving point mobility, or direct mobility is a generic term expressing the system's ability to absorb a vibration, and it also relates the excitatory force to the induced motion at the driving point. Apparent mass and mechanical impedance are inverse functions of direct mobility. They express the system's ability to resist a vibratory excitation at the driving point and they are also related to transmissibility. Figure 2.7 depicts a simple SDOF system for which transmissibility T is defined as:

$$T(f) = \frac{A_y(f)}{A_x(f)} \qquad (2.30)$$

Apparent mass AM is given by:

$$AM(f) = \frac{F_x(f)}{A_x(f)} = \frac{m.A_y(f)}{A_x(f)} = m.T(f) \qquad (2.31)$$

Mechanical impedance Z is given by:

$$Z(f) = \frac{F_x(f)}{V_x(f)} = \frac{m.A_y(f)}{A_x(f)/(j.2\pi f)} = j.2\pi f.m.T(f) \qquad (2.32)$$

where

m	is the mass;
x	denotes the driving point;
y	denotes the measuring point;
$F_x(f)$	is the force spectrum;
$A_x(f)$	is the acceleration spectrum;
$V_x(f)$	is the velocity spectrum; and
j	$= \sqrt{(-1)}$.

It can be seen from equations 2.31 and 2.32 that both apparent mass and mechanical impedance measured at the

driving point are suitable parameters indicating the transmissibility of vibratory energy at the driving point where the system is in contact with the vibratory stimulus. These two parameters provide the same information in the frequency domain except that the mechanical impedance would yield a frequency-weighted spectrum. Their value of use depend on their appropriateness in a particular measurement.

Transfer mobility describes the structure's ability to transmit or isolate a vibration. The transfer functions relevant to this study are transfer accelerance and transfer mobility defined by:

$$Transfer\ Accelerance = \frac{A_y(f)}{F_x(f)} \qquad (2.33)$$

$$Transfer\ Mobility = \frac{V_y(f)}{F_x(f)} = \frac{A_y(f)/(j.2\pi f)}{F_x(f)} \qquad (2.34)$$

It can be seen that both transfer accelerance and transfer mobility are related to each other by a frequency dependent factor $2\pi f$, and they reveal the same information. In practice, the choice of use depends on their appropriateness in each particular presentation.

Relative transmissibility is defined as the ratio of acceleration spectra measured at two different measuring points of the system (fig 2.8), and is defined by:

$$Relative\ Transmissibility = \frac{A_z(f)}{A_y(f)} \qquad (2.35)$$

where z denotes a second measuring point.

2.4.3 Modal Analysis

Modal analysis is a structural testing technique which examines the dynamic behaviour of a vibration system or

where $G_{xx}(f)$, $G_{yy}(f)$ and $G_{xy}(f)$ are the autospectra and cross-spectrum defined previously. At each particular frequency f, the coherence function assesses the degree of linear relationship between the two signals x(t) and y(t), and hence determines the amount of coherent components in the frequency response function. The coherence function ranges from 0 to 1, and a coherency close to unity indicates high causal relationship of two signals. If x(t) and y(t) are respectively the input and output signals of the system, a high coherency strongly suggests that y(t) is a genuine response to the excitation x(t) of the system. Otherwise, a low coherency indicates system non-linearity, the presence of noise or incoherent elements i.e. error in the measurements.

2.4.5 Noise and Error Estimation

The amount of noise and error due to incoherency in signals can be estimated by signal-to-noise ratio S/N which is defined as the variance of a signal to that of noise. For a particular frequency f, S/N can be obtained from the coherence function (Herlufsen, 1984):

$$S/N = \frac{\sigma_s^2}{\sigma_n^2} = \frac{\gamma^2(f)}{1 - \gamma^2(f)} \qquad (2.37)$$

Hence a high coherence function close to unity indicates that the system is relatively free from noise.

As mentioned in section 2.3.4, the autospectrum ($G_{xx}(f)$) and the cross-spectrum ($G_{xy}(f)$) required for the computation of frequency response function are obtained by the spectral averaging performed over a finite number of data blocks of a long time-signal. When the frequency response function is estimated by equation 2.29, and assume that the signals are random with Gaussian distribution of amplitude and phase, the error associated with the number of averages N and the coherence function can be determined. For a particular frequency f, the normalized random error of the magnitude of the estimated frequency response

$$\{\psi\}_1 = \begin{Bmatrix} 0 & 0 \\ 60 & 0 \\ 85 & 0 \\ 60 & 0 \\ 0 & 0 \end{Bmatrix}$$

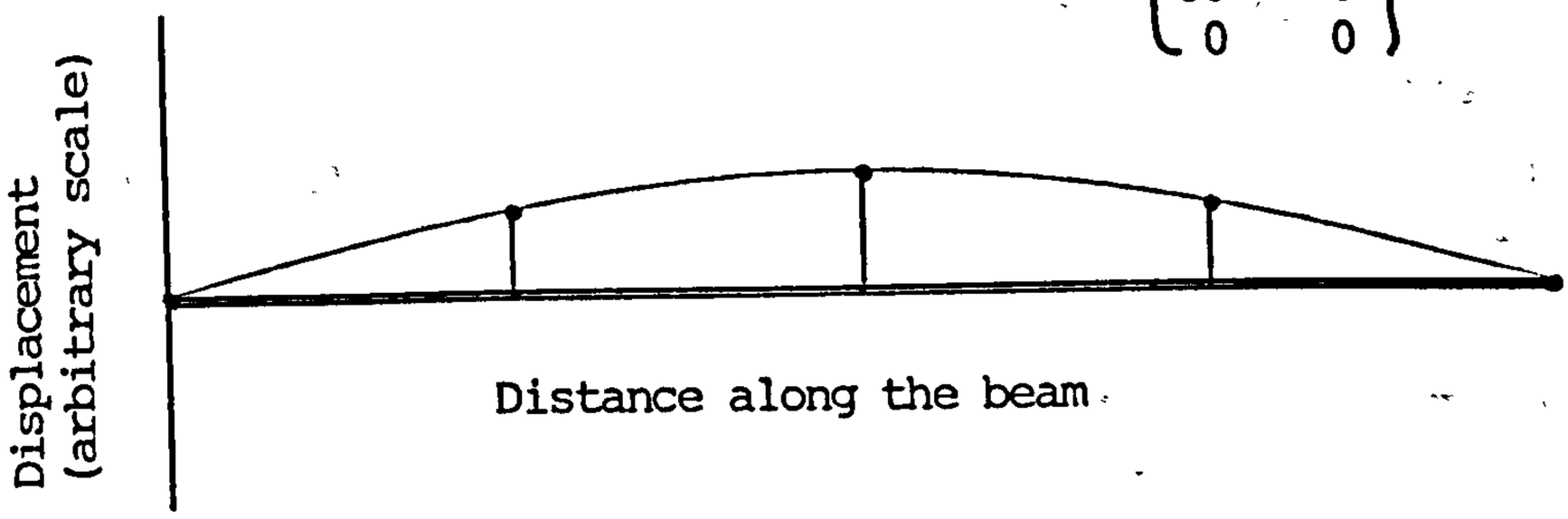

Fig 2.9 Mode shape of a vibrating beam for n=1.

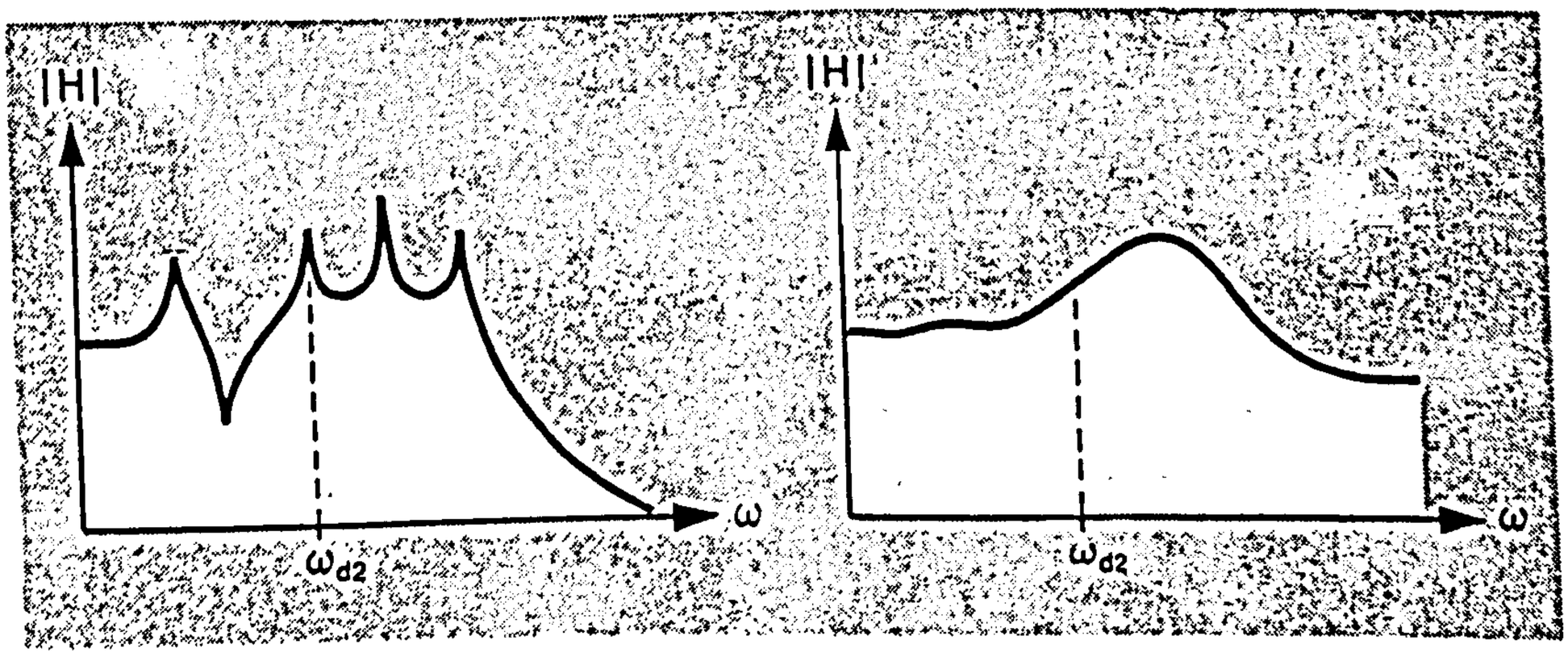

a) Lightly damped system.

b) Heavily damped system.

Fig 2.10 Frequency response function of a) a lightly damped system and b) a heavily damped system (from Døssing, 1988b).

structure in response to a known excitation by the expression of its modal parameters: modal frequency, modal damping and mode shapes, provided both temporal and spatial resolution are adequate. Figure 2.9 depicts a practical approach for the determination of the mode shape of a vibrating beam. The mode shape vector $\{\Psi\}_n$ which is an array of sampled mode shape, presents the magnitude and phase information obtained through mobility measurement performed at pre-determined points, such that the mobility at these points adequately represents the motion of the beam. The letter n denotes the mode number, where in this illustration, n = 1 represents the fundamental mode of the vibration structure.

A lightly damped structure behaves as a SDOF system around the resonant frequencies. Hence the modal frequencies are separated and shown clearly on the frequency response function H(f). In practice, the damping ratio could also be determined from the half-power point around a resonant frequency. For a structure of heavy damping, the frequency response function does not show clearly distinct modes, and the analytical determination of the modal parameters could be difficult (fig 2.10).

2.4.4 Coherence and System Linearity

The frequency response functions established in previous sections assume system linearity, and mathematically, they are the best linear fit in the least square sense of the system behaviour should any non-linearity exist. However, an objective monitoring of the linearity of the mechanical system is deemed mandatory. The coherence function $\gamma^2(f)$, defined below, corresponds to the correlation coefficient which is a statistical measure of the degree of linear dependency between two variables.

$$\gamma^2(f) = \frac{|G_{xy}(f)|^2}{G_{xx}(f) \cdot G_{yy}(f)} \qquad (2.36)$$

where $G_{xx}(f)$, $G_{yy}(f)$ and $G_{xy}(f)$ are the autospectra and cross-spectrum defined previously. At each particular frequency f, the coherence function assesses the degree of linear relationship between the two signals x(t) and y(t), and hence determines the amount of coherent components in the frequency response function. The coherence function ranges from 0 to 1, and a coherency close to unity indicates high causal relationship of two signals. If x(t) and y(t) are respectively the input and output signals of the system, a high coherency strongly suggests that y(t) is a genuine response to the excitation x(t) of the system. Otherwise, a low coherency indicates system non-linearity, the presence of noise or incoherent elements i.e. error in the measurements.

2.4.5 Noise and Error Estimation

The amount of noise and error due to incoherency in signals can be estimated by signal-to-noise ratio S/N which is defined as the variance of a signal to that of noise. For a particular frequency f, S/N can be obtained from the coherence function (Herlufsen, 1984):

$$S/N = \frac{\sigma_s^2}{\sigma_n^2} = \frac{\gamma^2(f)}{1 - \gamma^2(f)} \qquad (2.37)$$

Hence a high coherence function close to unity indicates that the system is relatively free from noise.

As mentioned in section 2.3.4, the autospectrum ($G_{xx}(f)$) and the cross-spectrum ($G_{xy}(f)$) required for the computation of frequency response function are obtained by the spectral averaging performed over a finite number of data blocks of a long time-signal. When the frequency response function is estimated by equation 2.29, and assume that the signals are random with Gaussian distribution of amplitude and phase, the error associated with the number of averages N and the coherence function can be determined. For a particular frequency f, the normalized random error of the magnitude of the estimated frequency response

function is given by (Herlufsen, 1984):

$$\textit{Random Error},\ e_r = \sqrt{\frac{1 - \gamma^2(f)}{\gamma^2(f)\,.2N}} \qquad (2.38)$$

It is clearly indicated by equation 2.38 that the higher the coherency is the less random error will there be in an estimate of the frequency response function, hence a higher statistical certainty in the measurement. More averaging is required to obtain statistical accuracy in a harsh measurement where noise or incoherency of signals are contributing problems.

2.5 ACOUSTICAL PROPERTIES OF BIOLOGICAL TISSUES AND SYSTEMS

Biological materials are complicated, complex and composite at both microscopic and macroscopic level. They possess unique mechanical characteristics which make them behave dissimilarly to non-biological ones. Non-homogeneity, anisotropy, viscoelasticity and time-rate dependency are well known characteristics, among others (Kenedi, 1980). Individual variability, site-specificity, gender-related and age-related characteristics make them mechanically unique and different even from sample to sample.

Vibration studies on the human body are inevitably faced with a series of questions at the outset. When the body surface is subject to a mechanical vibration, or in contact with a vibrating object, the local response of its surface determines quantitatively and qualitatively the mechanical energy being transmitted to the body. What follows is the question of how the vibratory energy is being dispersed or distributed to other parts of the body. This may involve the conversion into thermal effects in the tissue or waves of vibratory stresses propagating to other parts of the body. However, the thermal effects of vibratory energy are outside the scope of this study though

they are of therapeutic significance in physical therapy. The form of wave propagation, i.e. whether as shear (transverse) waves, compressive (longitudinal) stress, flexural waves or total attenuation depends on the physical properties, such as stiffness, elasticity and viscosity of the intervening tissues or structures along the transmission path.

How does the musculoskeletal system of a human body respond to mechanical vibration? The attempt to answer this question requires some knowledge of the acoustical properties of the tissues and structures involved. In this context, the response refers to the vibration levels in terms of motion measured at various locations in the system. Local response at specific points of a system could be expressed as motions relative to a reference point; or further summarized as an overall response in terms of a gross change in shape, or mode shapes of the system. By this token, the response, local or general of the system to externally applied vibratory energy could be interpreted as an indication of the physical characteristics of the structures through which these vibratory stresses propagate.

Recent advancement of diagnostic ultrasound and associated research in the field lead to some understanding of the transmission properties of ultrasound through soft and hard tissues. However, the scope of this discussion is confined only to acoustical properties of the musculoskeletal system in the audio frequency range. The local response of the spine will be examined, with particular attention to the lumbar region. Physiological responses of the human body to vibration is deemed beyond the scope of this study, and hence will not be discussed.

2.5.1 Skin

Non-invasive vibration techniques for in-vivo study or clinical application invariably require the measurement of vibration signals by attaching transducers over the skin at

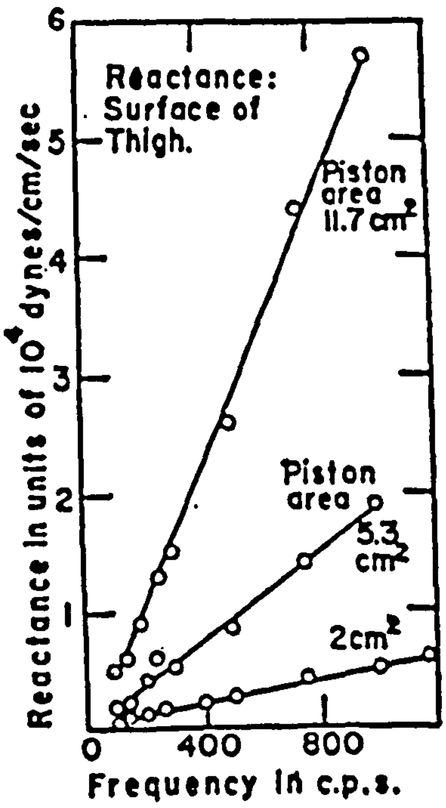

a)

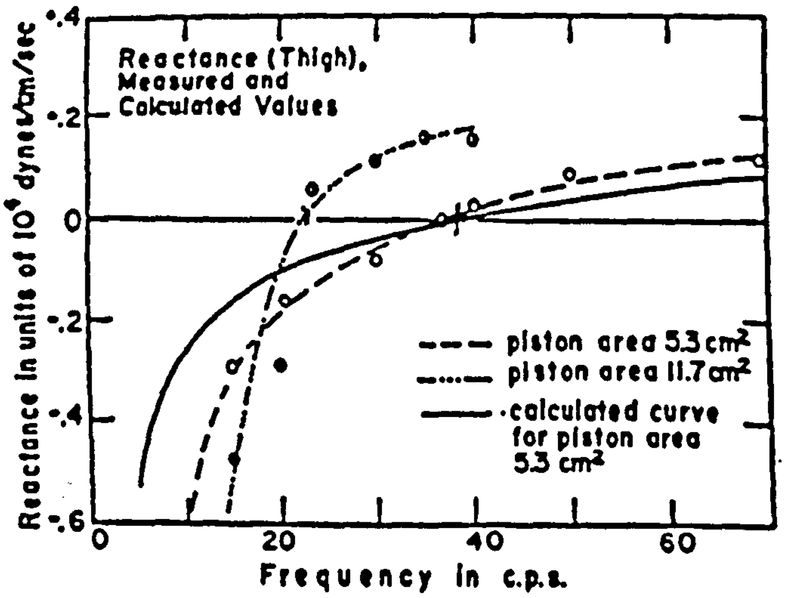

b)

Fig 2.11 Reactance of body surface over the thigh showing a) the mass effect in high frequency and b) predominant effect of elastic element in low frequency range (from Franke, 1951).

bony prominences, where the soft tissue layer is thinnest. The skin is therefore a very critical tissue structure which imposes great difficulty to vibration measurements on live subjects. However, full understanding of the vibratory transmission properties of skin is still lacking. Some early studies on the physical properties of skin and its underlying tissues were reported by Franke (1951), and supplemented by von Gierke and associates (1952). Their experimental studies attempted to characterize the mechanical behaviour of the skin by the measurement of mechanical impedance which is defined as the complex ratio of the vibratory force applied to a defined area of the body surface to the induced velocity of the area. The expression for mechanical impedance Z is given by:

$$Z = \frac{F}{V} \tag{2.39}$$

where both the force F and velocity V are complex vectors. The mechanical impedance can also be expressed in real and imaginary parts as:

$$Z = R + jX \tag{2.40}$$

where

R denotes the resistance;

X denotes the reactance; and

j $= \sqrt{(-1)}$.

The resistance is a measure of the viscous damping property of the skin. The reactance can also be expressed as (Hixson, 1988):

$$X = \omega m - \frac{c}{\omega} \tag{2.41}$$

where

ω is the frequency of vibration in rad/s;

m is the effective mass in kg; and

c is the elastic constant in N/m.

The reactance is a measure of the inertial and elastic

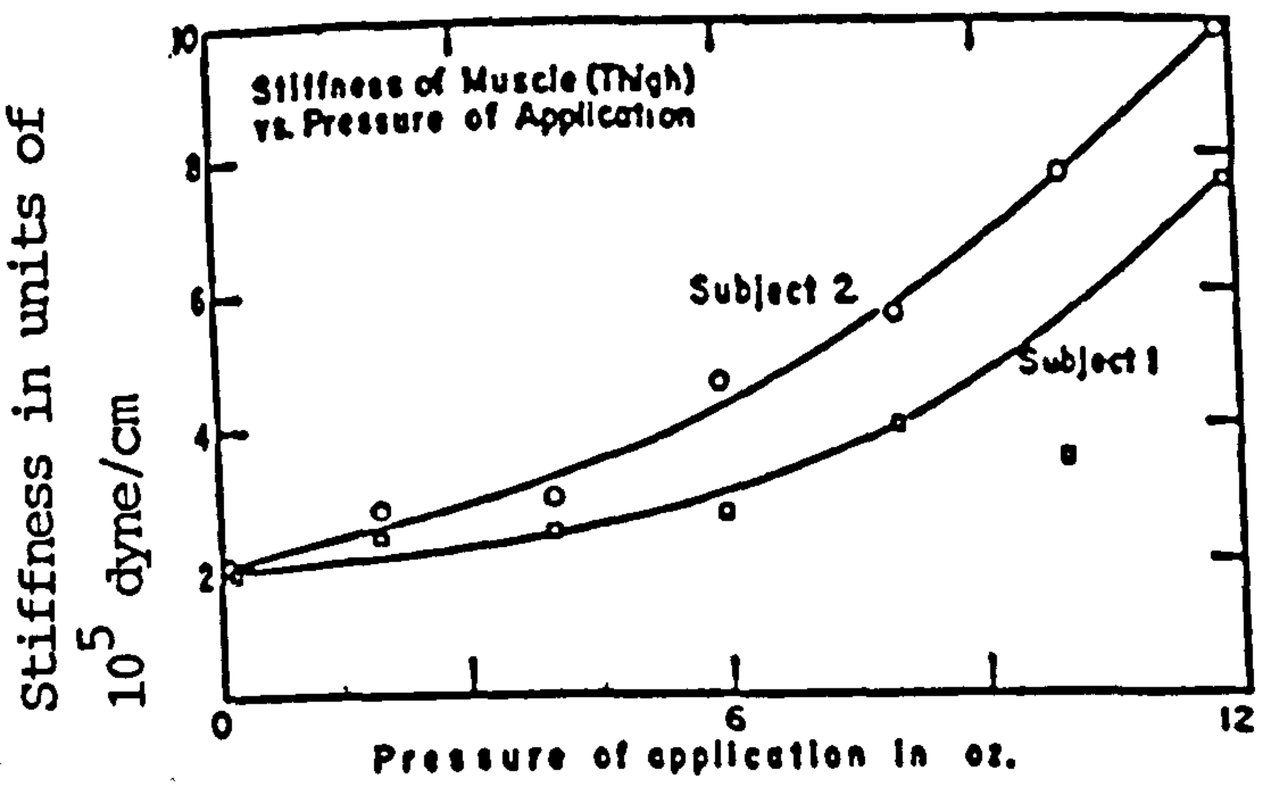

Fig 2.12 The effect of contact pressure on mechanical impedance of the skin (from Franke, 1951).

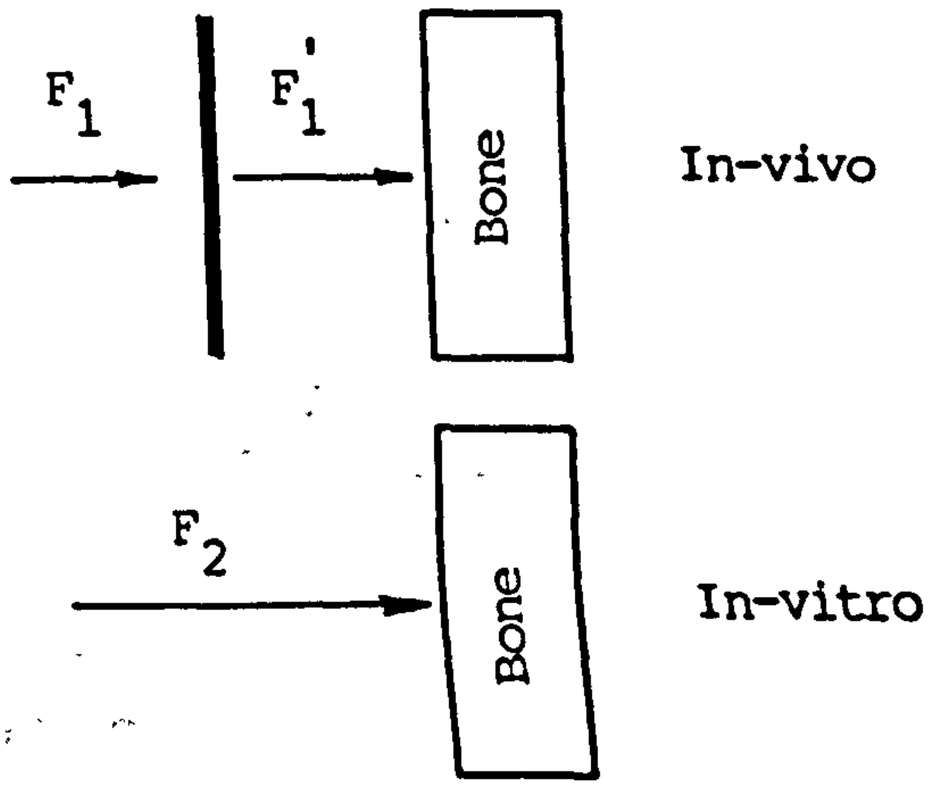

Fig 2.13 Schematic diagram showing forces at different interfaces (redrawn from Cornelissen et al, 1986).

properties of the skin. At resonant frequency, the reactance will be equal to zero.

Franke (1951) measured the mechanical impedance in the frequency range from 10 Hz to 1500 Hz for a small area of the body surface over the thigh by an instrumented vibrating piston in "zero" contact pressure with the skin. The complex mechanical behaviour of the skin and its underlying tissues, as indicated by the mechanical impedance, was found to comprise the effects of mass, stiffness and viscosity elements. A simple mass-spring-damper mechanical model was established. Resonance was observed below 50 Hz, above which the reactance increased with the frequency, showing the predominant mass effect in this frequency range (fig 2.11a). The reactance (in negative values) was also observed to vary inversely with the frequency below the resonance (fig 2.11b), revealing the predominant effect of the elastic element. The resistance remained fairly constant. The stiffness constant c was also reported in the original article: $c = 1.8 \times 10^5$ dyne/cm (or 1.8×10^2 Nm^{-1}). Franke (1951) and von Gierke et al (1952) also observed the surface waves propagating along the surface of vibrating skin, by a stroboscopic method. The waves propagated with a constant velocity of about 1.6 ms^{-1}, and the surface displacement decreased with increasing distance from the vibratory source.

In the context of this discussion, the skin can be simplified as a homogeneous layer of elastic and viscous elements with distributed mass, which exhibits resistive and reactive characteristics in response to local vibratory stress. This model is an adequate simplification of the body surface. Low stiffness of the skin, according to the derived value for the mechanical model suggests that the skin could be stiffened by compressive force to enhance transmissibility of vibration. In practical terms, compression can be accomplished by an appropriate preload method. Franke (1951) repeated the measurements of mechanical impedance with various contact pressure, and

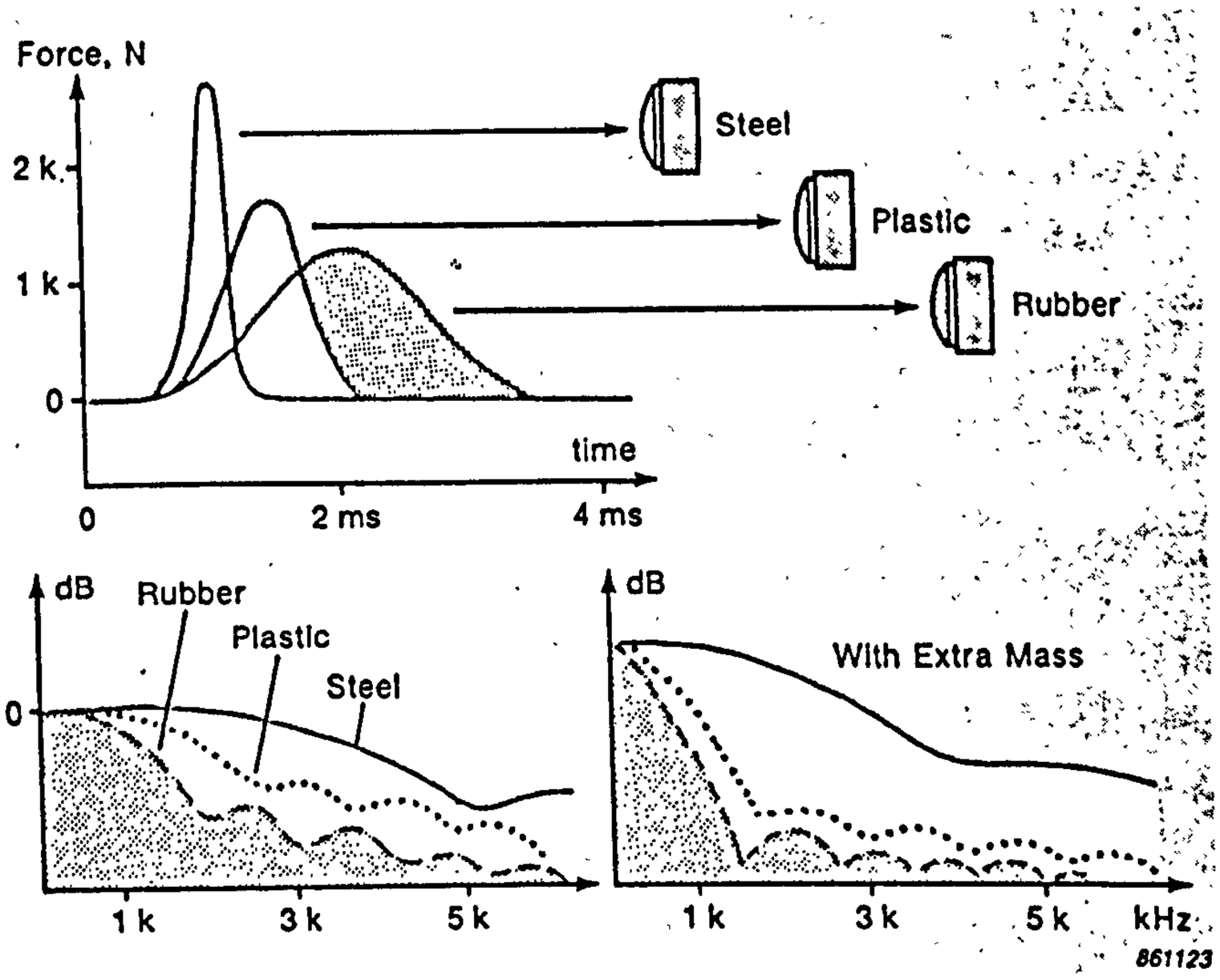

Fig 2.14 The frequency response of different hammer tips (from Døssing, 1988a).

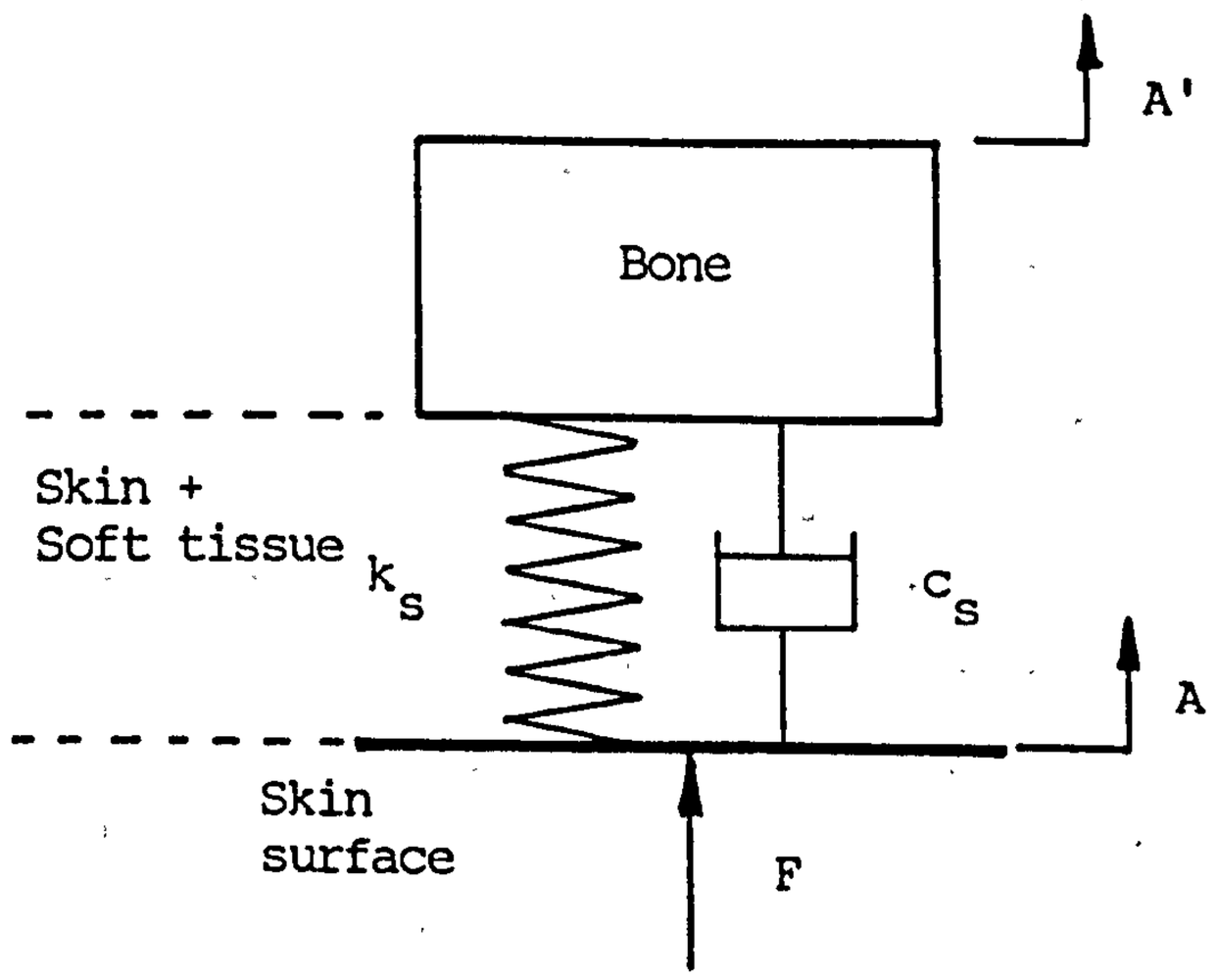

Fig 2.15 Mechanical model of skin at the driving point. k_s and c_s are the stiffness and damping factor of the skin.

found that the stiffness increased non-linearly with the contact pressure. Figure 2.12 shows the change of mechanical impedance of the skin with various contact pressure.

The mechanical property of skin affects vibration measurements in two ways. It influences the force transmissibility at the driving point i.e. the point at which the body is driven or excited, and more importantly the genuine measurement of vibration of the bone through overlying skin. Cornelissen et al (1986) explained that the skin does not significantly change the excitatory force signal. The force F_1 measured over the skin is not different from that force F_1' exerted at the bone through the skin, i.e. $F_1 = F_1'$ (fig 2.13). The force applied directly on the bone F_2 will be different from the force F_1' applied through the skin. The skin provides a "soft" interface which attenuates the high frequency components of the forcing signal and hence changes the effective band-width of the forcing signal. It however does not introduce significant discrepancy between the measured force and that actually applied on the bone. Cornelissen et al (1986) also drew an analogy between the skin and the tip of an impact hammer. The stiffness of the tip governs the effective frequency content of the impact force. A soft tip effects a longer impact duration and hence limits the force spectrum to low frequency range; while a hard tip provides a sharp contact of short duration, and extends the force spectrum to high frequency range (fig 2.14). Saha and Lakes (1977a) examined the response of femoral and tibial bones by applying a standardized impact force over the skin, and over the simulated soft tissue layers (rubber sheets) of various thicknesses covering an excised bone. Significant dependence of the impact force profile on the thickness, hence the stiffness of the interposing soft tissue layer was observed. As a consequence, the input excitation in high frequency range was limited.

The mechanical model suggested by Sandover (1982)

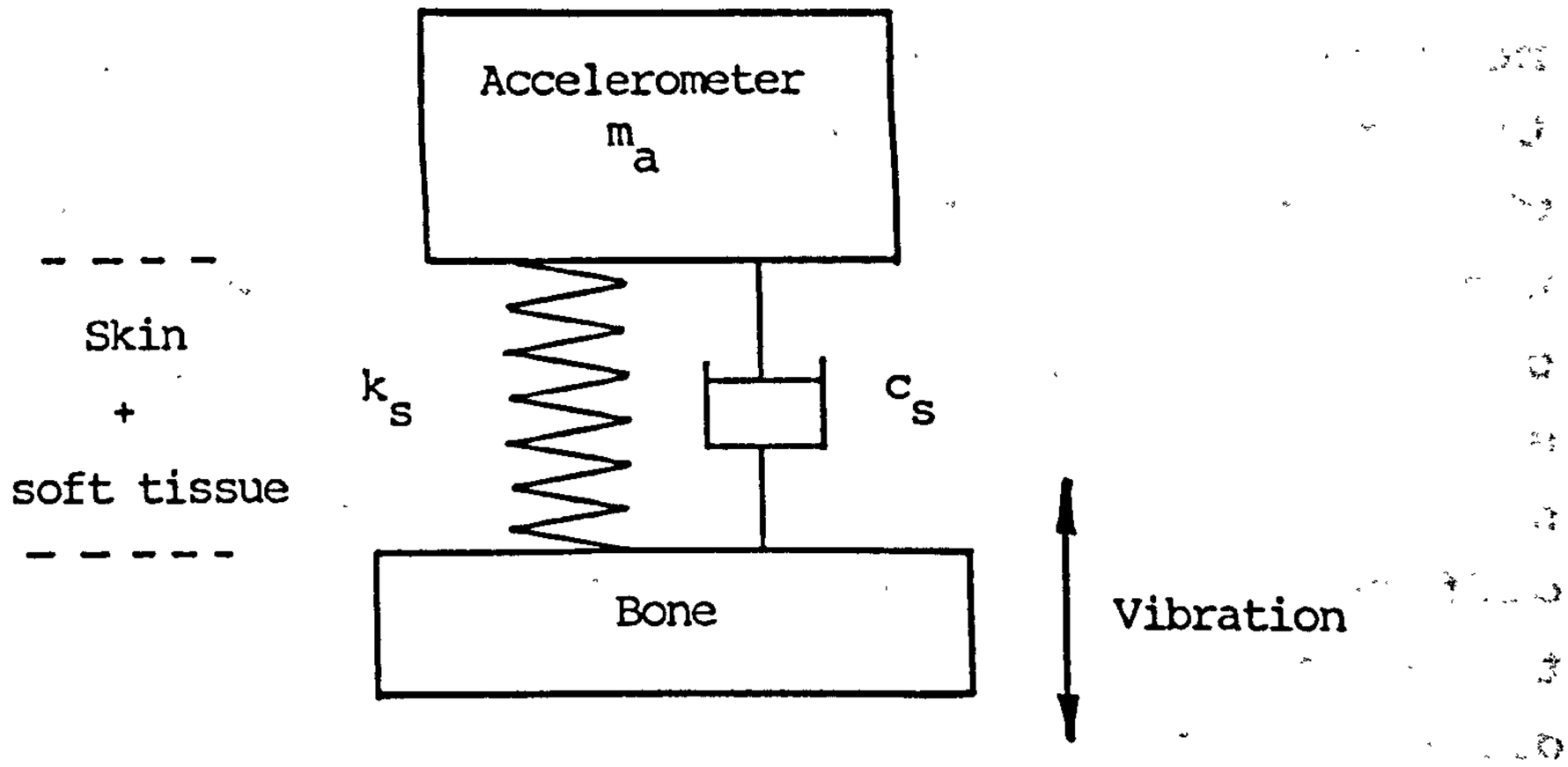

Fig 2.16 Mechanical model of skin at the measuring point. k_s and c_s are the stiffness and damping factor of the skin.

could also be used to explain the transmissibility of vibration at the driving point. Figure 2.15 depicts a simple mechanical model which includes the musculoskeletal system and its overlying skin. Transmissibility T is defined as:

$$T(f) = \frac{A'(f)}{A(f)} \qquad (2.42)$$

where

A'(f) is the acceleration spectrum set up or transmitted in the system; and

A(f) is the acceleration spectrum at the driving point.

It can be shown that apparent mass AM as defined below will yield the same spectrum as transmissibility:

$$AM(f) = \frac{F(f)}{A(f)} = \frac{m.A'(f)}{A(f)} = m.T(f) \qquad (2.43)$$

where

F(f) is the force spectrum at the driving point; and

m is the effective mass of the system.

Comparing equations 2.42 and 2.43, it shows that the force spectrum F(f) gives the same spectrum as the transmitted acceleration of the system. Hence the force measured at the driving point over the skin is considered a genuine measure of the vibratory excitation applied to the musculoskeletal system. If the simple model holds well for all situations of external excitation by driving through the skin, it is suggested here to stiffen the skin by suitable compression to enhance the transmissibility of high frequency vibration.

As mentioned previously, the skin also influences the measurement of vibration through the skin overlying the bone. If the skin comprises viscoelastic elements as described previously, attenuation of the high frequency components would render measurements inaccurate. This problem is more difficult to tackle, and has been

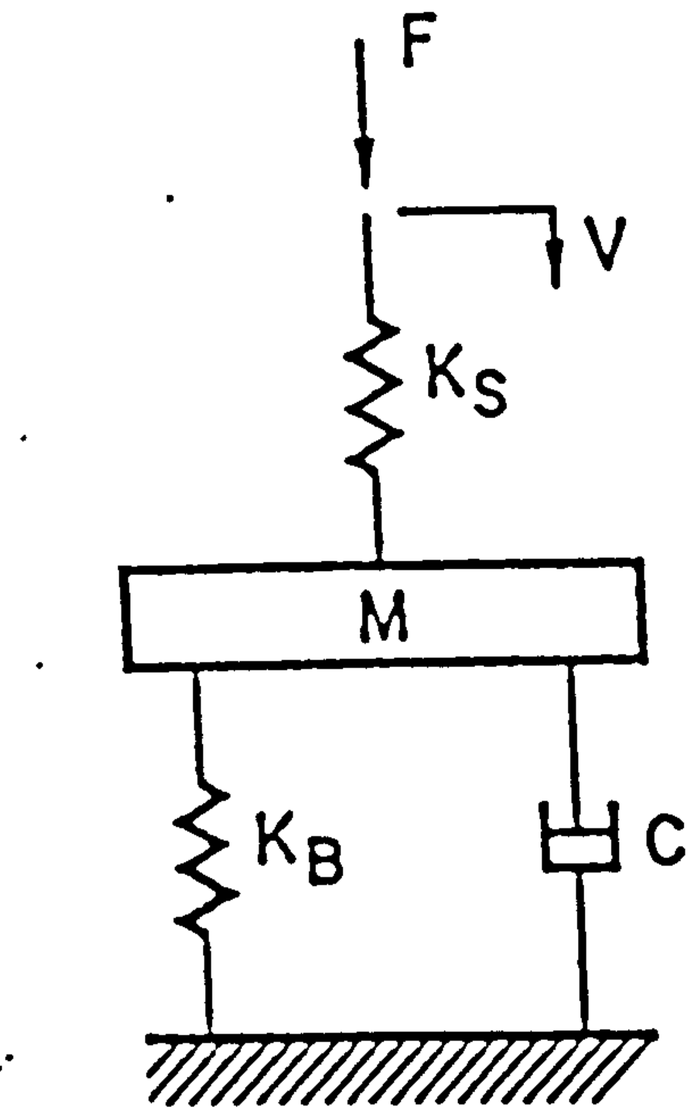

Fig 2.17 Mechanical model which approximates ulnar response. K_s is the stiffness of skin (from Thompson, 1973).

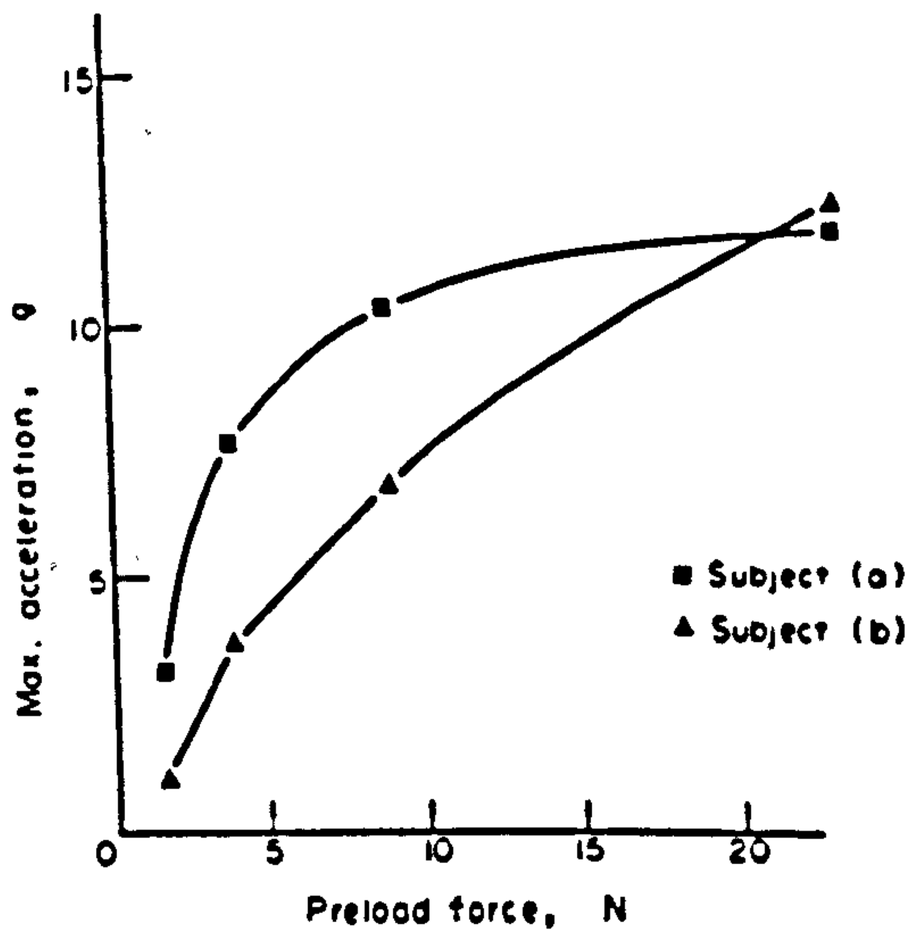

Fig 2.18 Maximum acceleration of skin over human tibia as a function of preload force (from Saha & Lakes, 1977a).

investigated by a number of research teams. Depending on the applications, vibrations are measured either longitudinally or transversely over the body surface i.e. parallel or perpendicular to the skin surface by the use of accelerometers. The physical set-up can be illustrated by the mechanical model in figure 2.16. Vibration of the bone which forms the foundation of the model excites the accelerometer-skin complex. The response is then detected by the accelerometer. Obviously the motion transmissibility depends on the mechanical behaviour of the system. At very low frequency below resonance, the mass m_a (accelerometer) vibrates coherently with the foundation (bone) and in this situation the measured vibration is a true reflection of the motion of the bone. At resonance, the system vibrates with an exaggerated amplitude depending on the damping c_s of the skin and its underlying tissue. Vibration at high frequency will then be attenuated due to the low response of the system. So ideally, the working frequency range of such system should be brought to well below the resonance. As indicated by the experimental results by Franke (1951) and von Gierke et al (1952), the skin possesses low stiffness, and hence resonates at a low frequency. This would limit the working frequency range. Technically, this could be "solved" or rather improved by the use of a light accelerometer to reduce the mass m_a; and to stiffen the skin, i.e. to increase k_s by a compressive preload force which could be achieved either by an additional mass; or by the use of a spring system. However, the additional mass will compromise the frequency range by lowering the resonant frequency and hence is not an acceptable method. Spring preload apparently becomes the only choice.

Thompson (1973) measured the mechanical impedance of the ulna fixed at the wrist and elbow. A static preload force between 2 N and 6 N was applied to a vibrating probe which excited the forearm at its mid-span. The mechanical behaviour of the forearm as indicated by the mechanical impedance stabilized with a 4 N preload force. Thompson

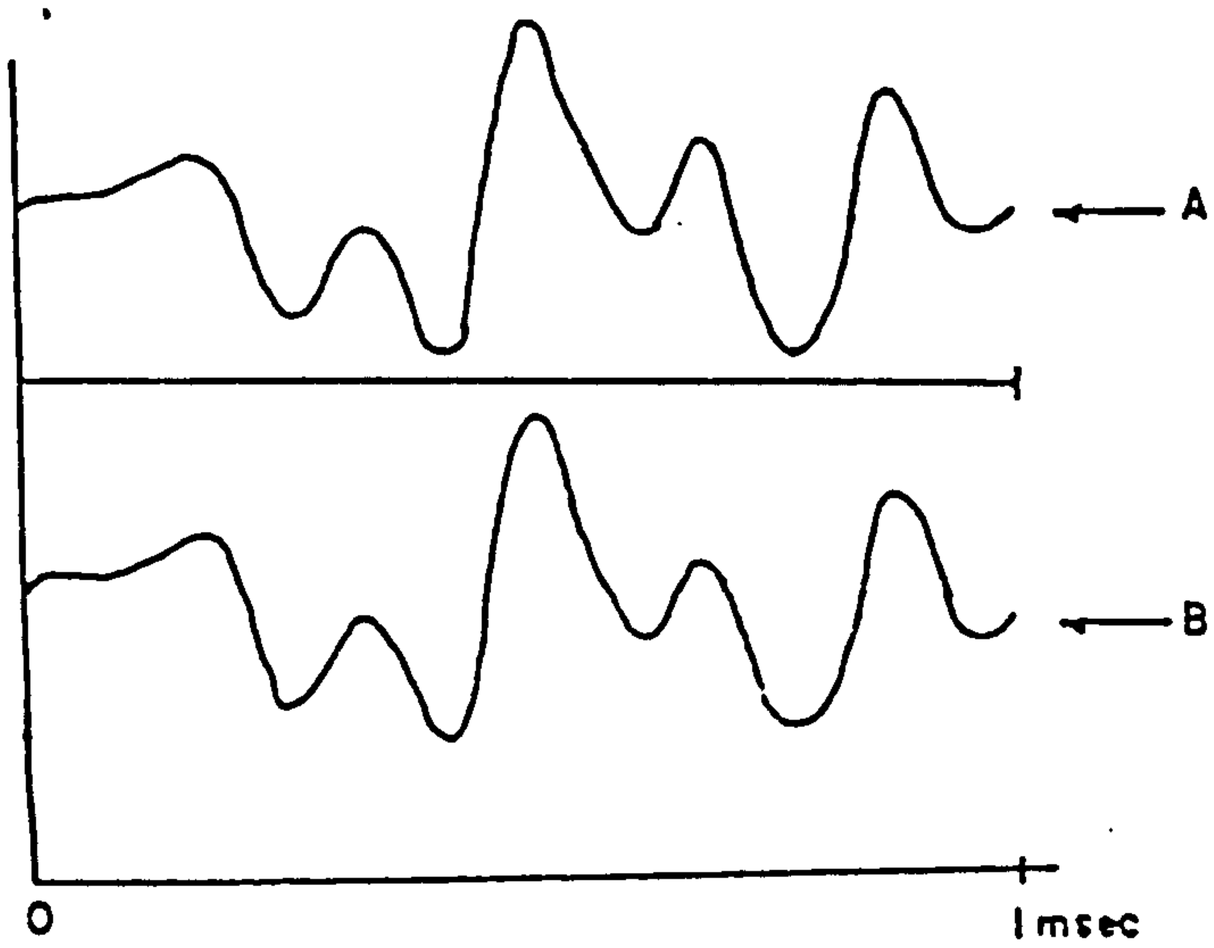

Fig 2.19 Accelerometer test: A) hand-held needle-mounted accelerometer and B) adjacent rigidly mounted accelerometer (from Ziegert & Lewis, 1978).

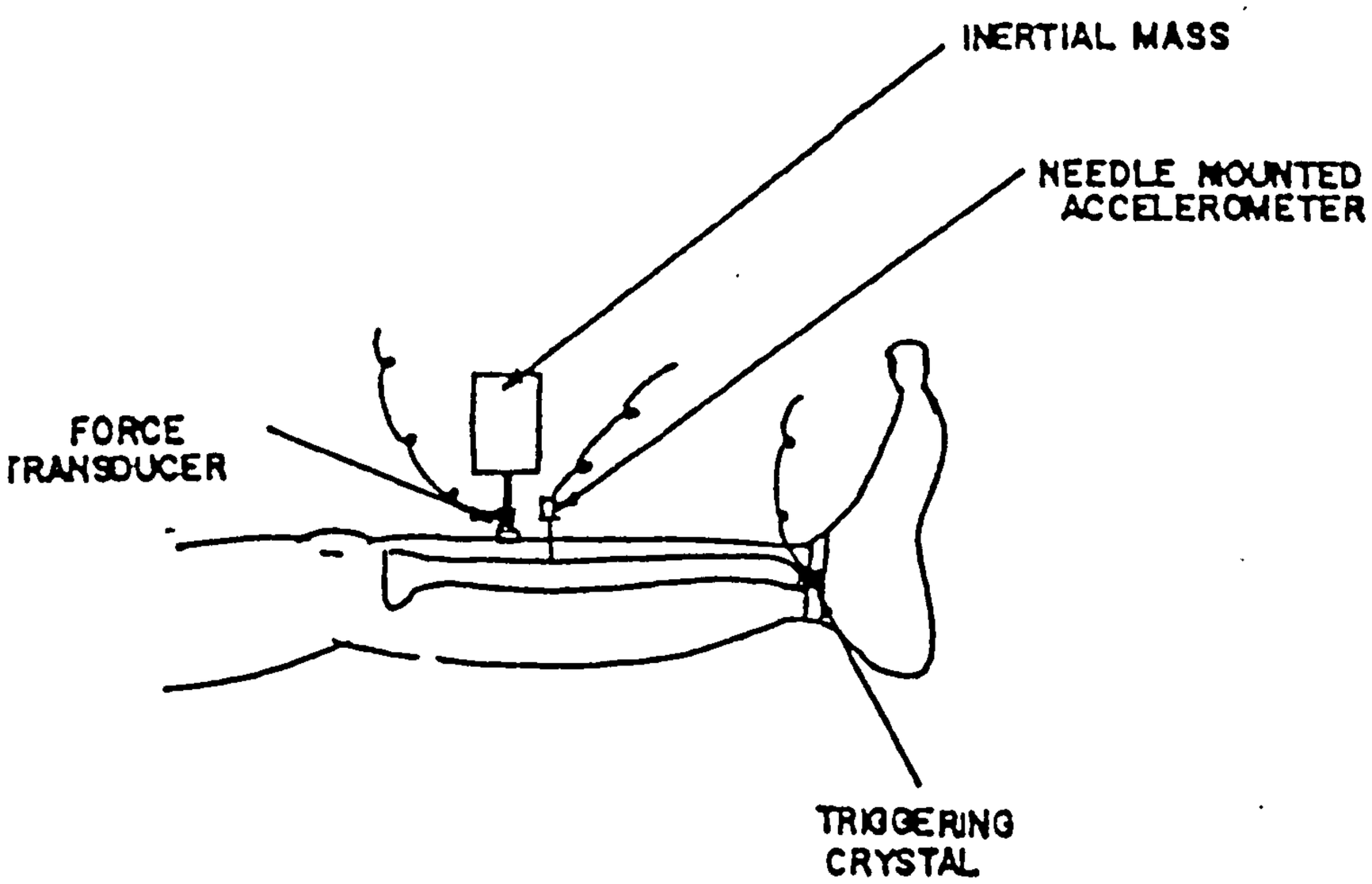

Fig 2.20 Ineffective use of an inertial mass as motion detector (from Ziegert & Lewis, 1978).

modelled the skin as a discrete springy element (fig 2.17), and explained that the static coupling force of 4 N or above "was sufficient to raise the stiffness of the skin layer above the effective bending stiffness of the ulna". The stiffness constants of the skin layer was found to be 2.8×10^5 Nm^{-1}. This figure obtained under a compressed condition was of course much higher than the value determined by Franke (1951). It also agreed with the Franke's finding that the skin became stiffened under mechanical pressure. Orne and Mandke (1975) revised Thompson's model for the skin as a spring-spring damper system.

Saha and Lakes (1977a) also observed that the effect of preload force level on the response acceleration was significant and inter-subject variability was noticed. The test results did not indicate, within pain tolerance, any asymptotic value of preload force beyond which the response became consistent and invariant (fig 2.18). The use of two preload methods by mass and by spring had been investigated. It was found that the application of an accelerometer preloaded by a spring rendered some parameters (e.g. time-delay between response peaks, and the ratio of peaks) of the response signals less sensitive to changes in preload force level and thickness of interposing soft tissues.

Ziegert and Lewis (1978), in an impact test on the tibia, demonstrated the possibility of obtaining high frequency components of the response displacement signal by the use of a hand-held needle-mounted accelerometer with the needle inserted through anaesthetized skin to achieve a firm contact with the bone. The hand-held accelerometer was also found to produce the same signal as that measured by a comparable light accelerometer cemented over excised bone (fig 2.19). The use of a mass of 2.3 kg mounted with an accelerometer as a motion detector held over the skin was not successful as the mass was found to be literally motionless (fig 2.20). Ziegert and Lewis (1979) also

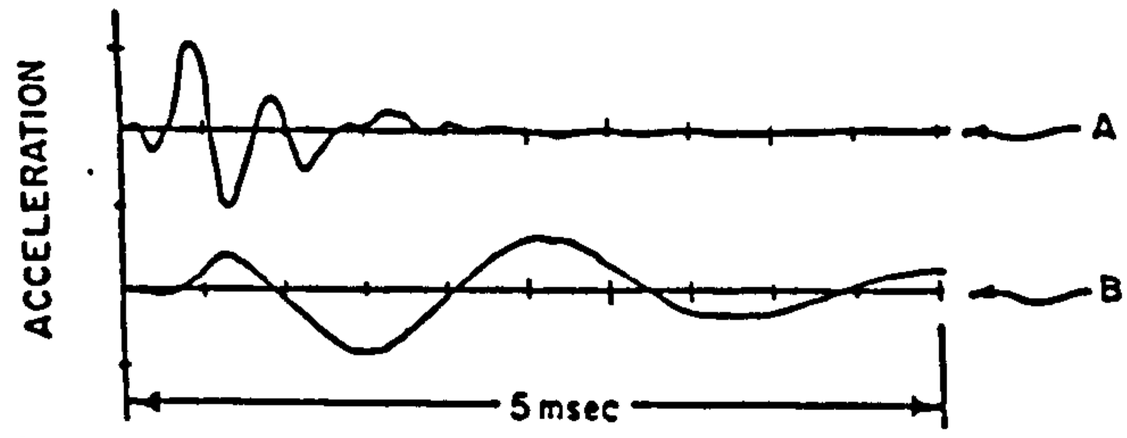

Fig 2.21a Comparison of actual bone acceleration to skin acceleration using a 34-g accelerometer. (A) needle-mounted accelerometer on bone; (B) 34-g accelerometer mounted on skin.

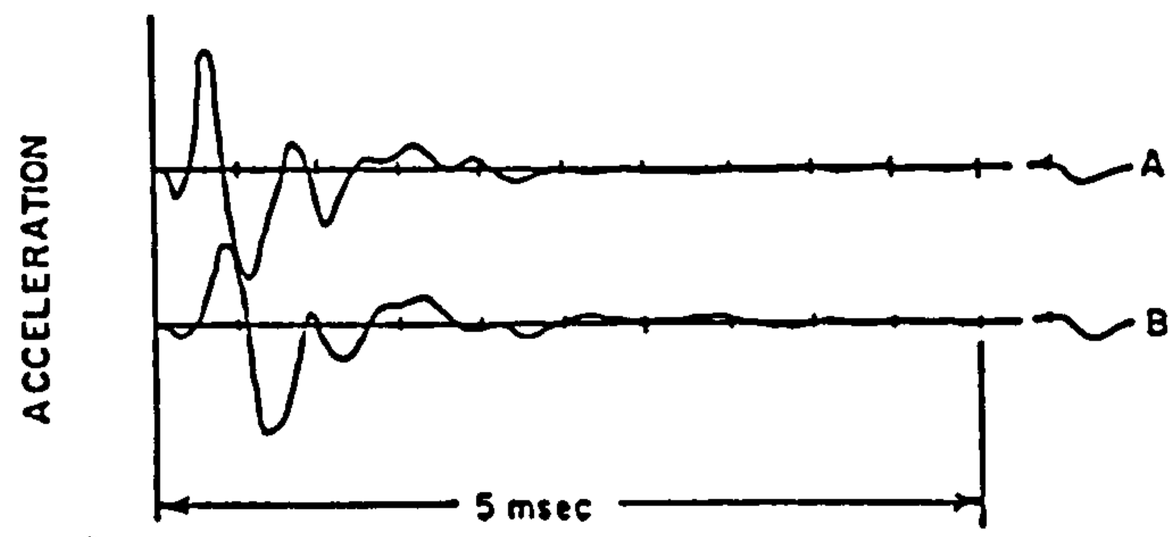

Fig 2.21b Comparison of actual bone acceleration to skin acceleration using a 1.5-g accelerometer. (A) needle-mounted accelerometer on bone; (B) 1.5-g accelerometer mounted on skin.

(from Ziegert & Lewis, 1979)

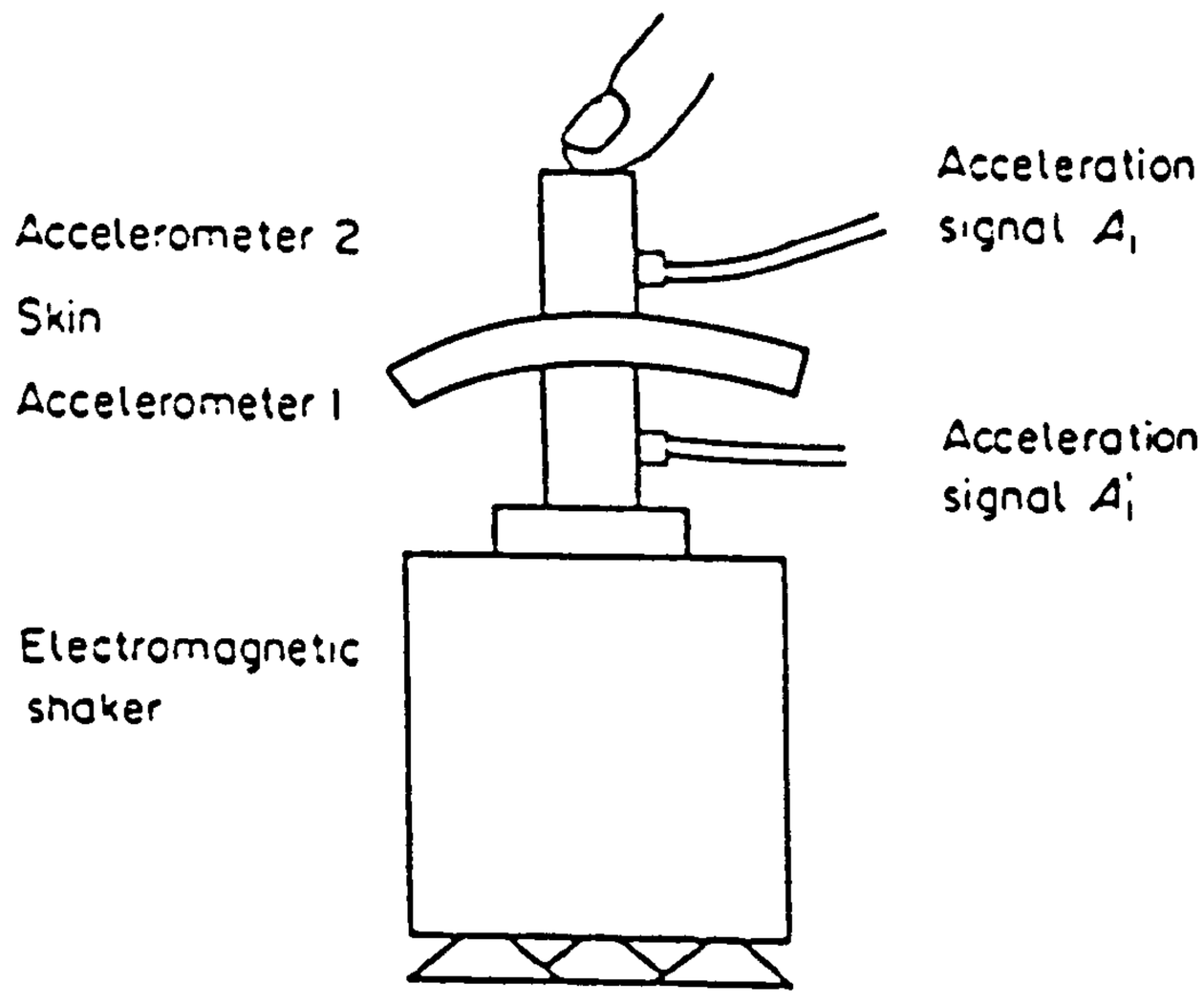

Fig 2.22 Experimental set-up to determine transmissibility of skin (from Cornelissen et al, 1986).

measured bone vibration by accelerometers attached over the skin by an elastic strip, and by a needle-mounted accelerometer described above. A light (1.5 g) skin-mounted accelerometer gave a measurement with close resemblance to the needle-mounted one; while the heavy (34 g) one showed gross discrepancy (fig 2.21). The results suggest that a test condition of suitable compressive preload to a light skin-mounted accelerometer is adequate in detecting bone vibration.

The effect of soft tissue on the output from skin-mounted accelerometers was also studied by Nokes and associates (1984a). An allowable range of preload force had been obtained for skin-mounted accelerometer used over skin of various thicknesses. The overall suggested range was 3.8 to 5.2 N, while the optimal preload was reported as 4.2 N. The group recommended the use of appropriate preload for skin-mounted accelerometer to overcome the damping effects of the skin and its underlying tissues; but warned that excessive preload would distort the recorded signal by contributing high frequency components unrelated to the bone vibration.

Cornelissen and associates (1986) described a set-up to determine the transmissibility of skin directly by comparing the accelerations measured on both the inner and outer surfaces of a piece of human skin (fig 2.22). The finger which applied a force of 18 N over the skin effected a spring preload system which compressed and stiffened the skin. It was found that the transmissibility of the skin was equal to unity up to 1600 Hz, and there was no phase shift. This preload force or pressure level is significantly much higher than that suggested by Thompson (1973), if assuming the contact areas were comparable. Nokes and Thorne (1988) commented that the 6 N preload used by Thompson (1973) was "close to the threshold of discomfort". The preload force of 18 N Cornelissen et al (1986) used on the specimen of human skin would then have greater difficulty in its in-vivo applications, unless

incorporated with local anaesthesia of the skin.

Currently attention has also been drawn to the measurement of bone vibration along the main axis of long bone and the spinal column during normal locomotion or sports activities of human subjects. The advocated non-invasive technique brings forth the use of skin-mounted accelerometers to measure longitudinal vibration over the surface of skin. Attachment through elastic straps applied around the limbs or adhesive tape over the spinous process of the vertebral column has been the preferred method (Wosk & Voloshin, 1981; Helliwell et al, 1989). Unfortunately, the skin in association with its underlying soft tissue is mechanically much less stiff longitudinally than is transversely. Whether the compressive force offered by the circumferentially applied elastic straps or whatever attachment is adequate to stiffen the skin to an acceptable extent is the major question. Subsequently, the inherent error resulting from the relative movement between the skin and the underlying bone raises a big question about the fidelity of the measurement made by a skin-mounted accelerometer over loose skin. Attempts have been made to tackle the problem by obtaining prerequisite knowledge of the skin's mechanical properties from an independent method, followed by appropriate correction or transformation. Hinz et al (1988) applied an impulse response technique to obtain the transfer function of the skin layer between the accelerometer and the bone. Subsequent use of the inverse transfer function estimated vibration of the bone, as illustrated below:

$$A_b(f) = H^{-1}(f) \cdot A_s(f) \qquad (2.44)$$

where

$A_b(f)$, $A_s(f)$ are the acceleration spectra on bone and skin respectively; and

$H^{-1}(f)$ is the inverse transfer function of skin.

Kim and associates (1993) developed a single degree-of-freedom model for the interposed skin between the bone and accelerometer. Both stiffness and damping parameters were obtained through a "parameter estimation approach" from measurements made by skin-mounted and bone-mounted accelerometers. The transfer function was used as a correction factor for subsequent measurements of skin vibration to obtain information of bone vibration. It was also shown that the approach was only valid up to about 50 Hz, and the estimated parameters were site-specific, lacking general applicability. Measurement of longitudinal bone vibration by a skin-mounted accelerometer presents a primary limitation which comes from the lack of rigidity of the skin and its underlying soft tissues at the mounting site of the accelerometer. This effects a low resonant frequency, and subsequently a limited frequency band-width for the measurement system.

To summarize, skin possesses complex inertial, elastic and viscous properties. For the detection of mechanical vibration through the skin over a bony prominence, skin-mounted accelerometry with the application of compressive preload force to stiffen the skin and its underlying soft tissue remains a simple and effective method, though a consensus over the optimal preload force level does not exist within pain tolerance. The employment of a light accelerometer gains general acceptance as to raise the resonant frequency and hence to extend the allowable working frequency range for vibration measurement. However, skin-mounted accelerometry for the measurement of bone vibrations in the axial direction of long bone and spinal column still suffers great limitations, due to its limited band-width.

2.5.2 Bone

As the primary load-bearing structure of the musculoskeletal system, bone plays a key role in the transmission of mechanical loads and stresses resulting

from the weight of the human body and its movements, both in static and dynamic situations. The mechanical property of bone, normal or pathological, inevitably has been and still is a major subject of research interest in biomechanics and related fields. Bone has been studied extensively in-vivo and in-vitro under loaded or unloaded conditions. Vibration analysis of human bone is a specific area of study on the dynamic response of this structure to vibratory excitation.

Among the long bones, the ulna and tibia are the most extensively investigated because of their relatively simple geometry, ease of access and convenience of positioning in well defined support conditions. Furthermore, these two bones have ample subcutaneous surface and bony prominences which are not crucial anatomical parts for invasive procedures in vibration tests. The vibratory properties of femoral bone have also been studied, but mostly confined to embalmed or excised specimens.

Vibration measurements including the velocity of wave and stress propagation along the bone, the determination of mechanical impedance and resonant frequency, and more recently the modal parameters have been reported. Vibration techniques for clinical applications in the monitoring of fracture healing, and the assessment of bone pathology e.g. osteoporosis are discussed in section 2.6. Various vibration tests have been developed which apply impulse response, sinusoidal vibration, swept sine vibration, or random vibration techniques.

This section attempts to summarize the general acoustical properties of long bones by referring to published studies on the ulnar, tibial and femoral bones. Measurements of mechanical impedance, resonant frequency, wave propagation velocity and modal parameters which are deemed particularly relevant to this study will be discussed.

Velocity of Wave Propagation. Wong and associates (1976) studied the propagation of flexural waves along

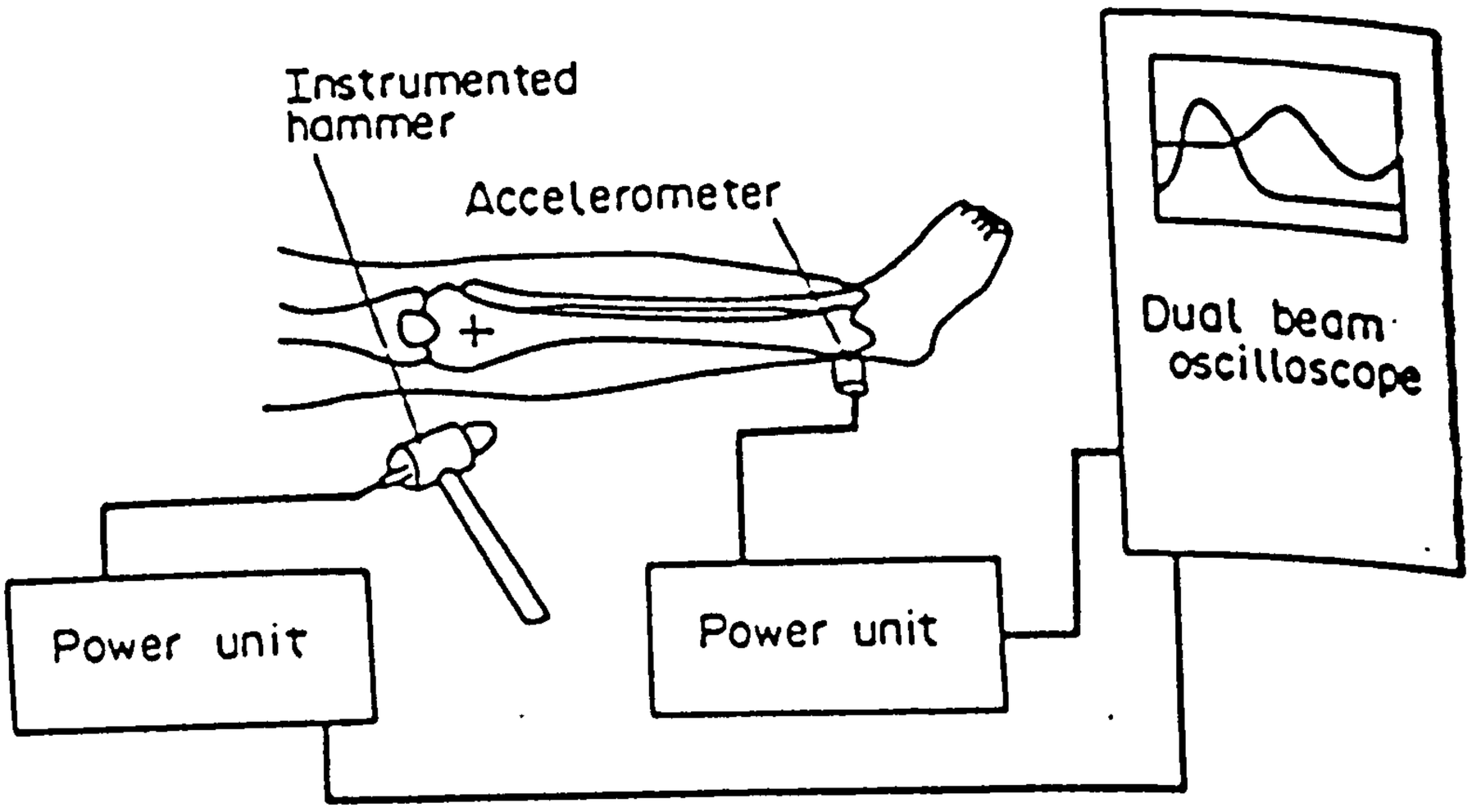

Fig 2.23 Experimental set-up to determine the velocity of flexural wave propagation in bone (Wong et al, 1983).

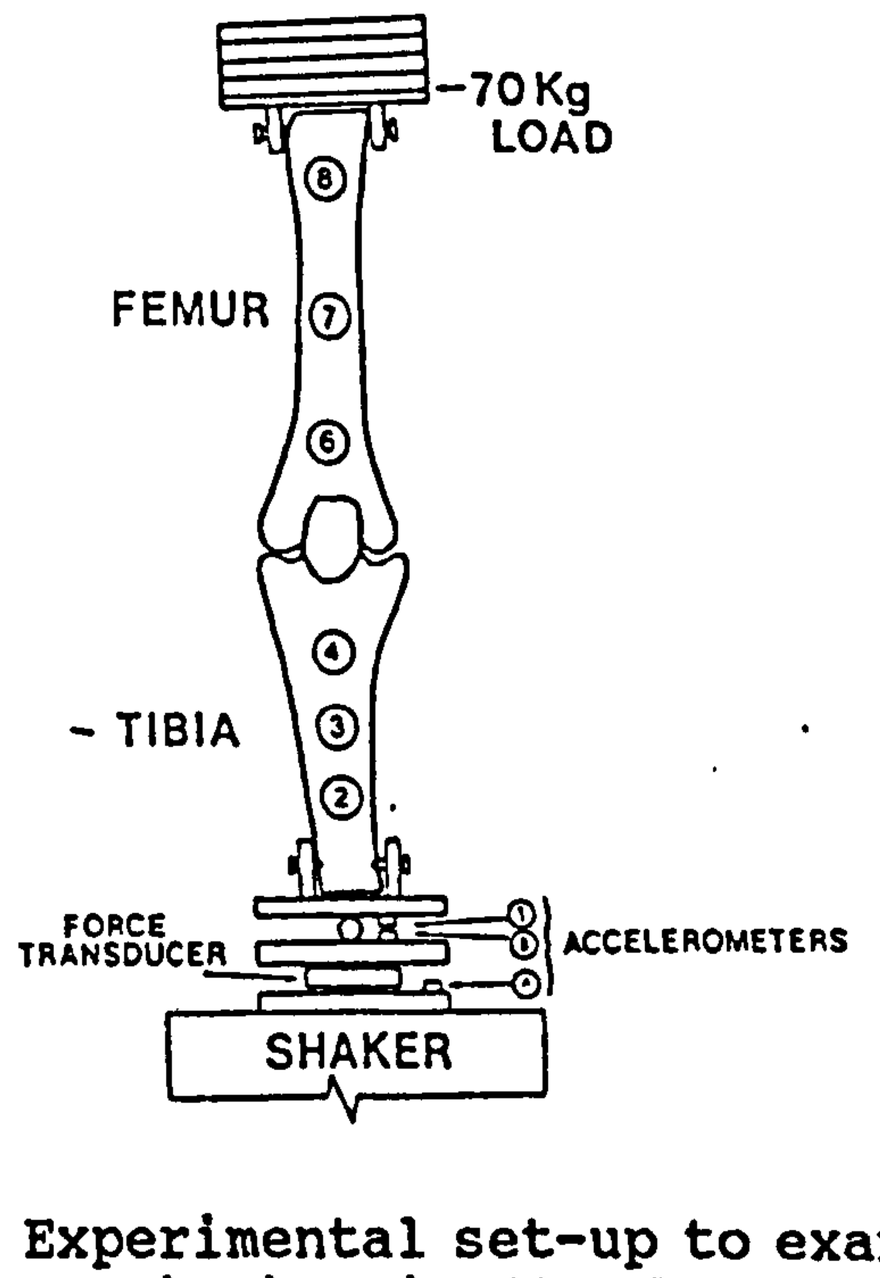

Fig 2.24 Experimental set-up to examine impulsive force transmission in the lower extremity of a cadaver (from Chu et al, 1986). Circled numbers indicate accelerometer locations.

embalmed tibial bone by applying a transverse mechanical impact at the mid-span of the bone supported in a free-free condition, and with the responses being detected at prescribed positions along the bone. The reported velocity of wave propagation was in the order of 1500 ms^{-1}. Associated longitudinal waves was also observed, with a velocity of 3500 ms^{-1}. Significant damping was noticed when the waves travelled along the bone and rendered great difficulty in the identification of the response impulses.

Wong et al (1983) conducted a transverse impact test on the tibiae of volunteers and embalmed tibial bones (fig 2.23). Results showed that the velocity of wave propagation for the male subjects (351 ± 118 ms^{-1}) was higher than that for the female ones (266 ± 69 ms^{-1}). These values are close to that (328 to 351 ms^{-1}) reported by Buturla and Pope (1973), and quoted by Saha and Lakes (1977a). Wong et al (1983) also noted the negative correlation between the wave velocity and age in both sexes. The average wave velocity determined for the embalmed specimens was 1137 ms^{-1}, ranged between 753 and 1142 ms^{-1}. The test results also indicated that wave velocity correlated with bone mass per unit length; and negative correlation was found with bone density measured by standardized osteoporosis index. There was also an indication that the measured wave velocity was related to the subjects' level of sports activities and disease states e.g. diabetes mellitus and arthritis.

Chu and associates (1986) investigated the transmission of impulsive waves through the lower extremity by experimenting on cadaveric specimen (fig 2.24). The impulse waves were observed to propagate at an average speed of 3100 ± 50 ms^{-1}. This is in close agreement with the value 3228 ± 110 ms^{-1} measured by Pelker and Saha (1983), and 3500 ms^{-1} by Wong et al (1976). Pelker and Saha (1983) also reported that the wave velocity was not significantly different whether in fresh or embalmed, wet or dry specimens.

Wosk and Voloshin (1981) measured the longitudinal

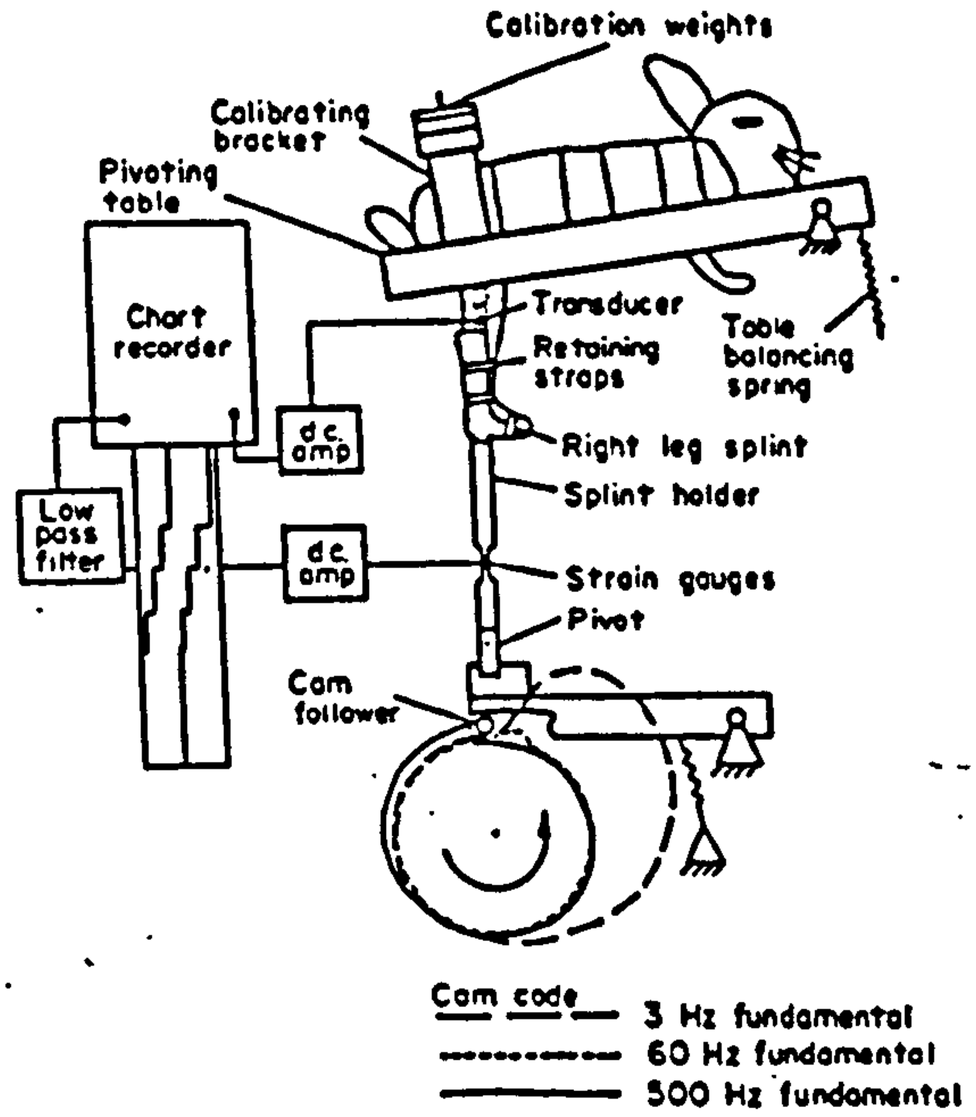

Fig 2.25 Dynamic test by impulsive force on the leg of rabbit (from Paul et al, 1978).

vibrations at various locations along the lower limbs on a group of healthy subjects during normal barefooted walking. Longitudinal waves were noted to be transmitted through the locomotion system and attenuated by shock absorbers i.e. the bone and soft tissues as suggested. Asymmetrical patterns of transmitted waves were observed in a group of normal subjects who satisfied the initial selection criteria as "healthy" persons. It was hypothesized that these subjects had changed their walking patterns due to underlying insufficient shock absorbing capacity of their locomotion system, resulting in asymmetry in the transmitted waveforms along the lower limbs.

Waves propagating along the bone inevitably suffer attenuation due to damping of bone and associated soft tissues. Pelker and Saha (1983) reported the mean attenuation coefficient of 0.023 cm^{-1} (0.2 dB/cm) for stress waves along fresh human long bones. This figure is much smaller than the values of 12 dB/cm and 30 dB/cm at 2.0 and 8.0 MHz respectively for the ultrasonic transmission in bone (Garcia, 1980). The group also discovered both linear and parabolic relationships between the bone's cross-sectional area A and the attenuation coefficient α, expressed respectively by the following equations:

$$\textit{Linear}: \quad A = 0.746 + 94.3\alpha \tag{2.45}$$

$$\textit{Parabolic}: \quad A = 1.57 + 135\alpha - 908\alpha^2 \tag{2.46}$$

This implies that one could extrapolate the cross-sectional area of a bone from the measurement of attenuation of a travelling wave. A parabolic relationship between the porosity of the bone and the attenuation coefficient was also observed. Dispersion was also observed as broadening of the wave pulse along the bone.

Paul et al (1978), performed a dynamic test by applying impulsive force of various frequencies on the legs of rabbits with a force transducer implanted in their upper tibial shafts (fig 2.25). The bone was found to attenuate

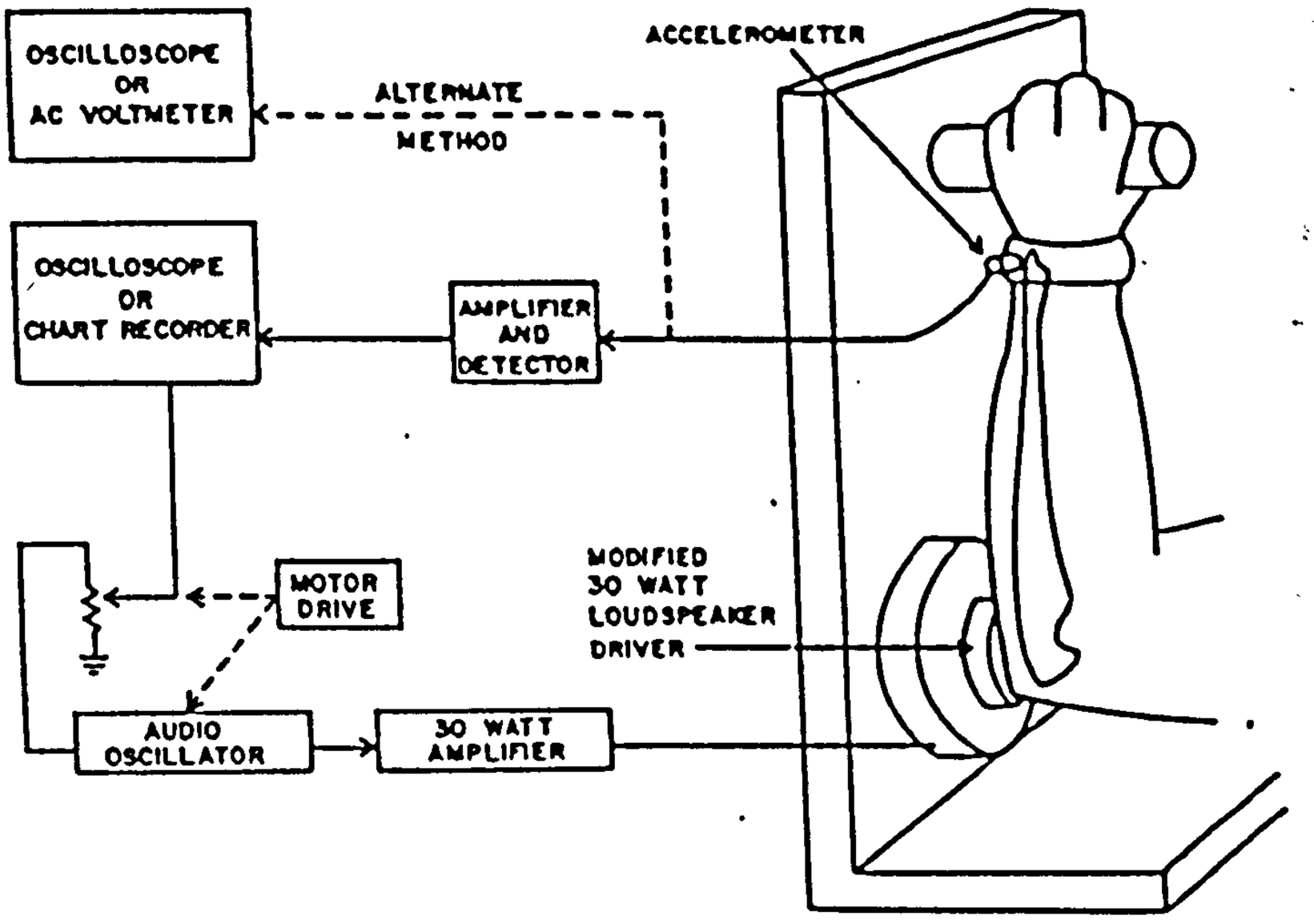

Fig 2.26 Apparatus used to measure ulnar resonant frequency (from Jurist & Dymond, 1970).

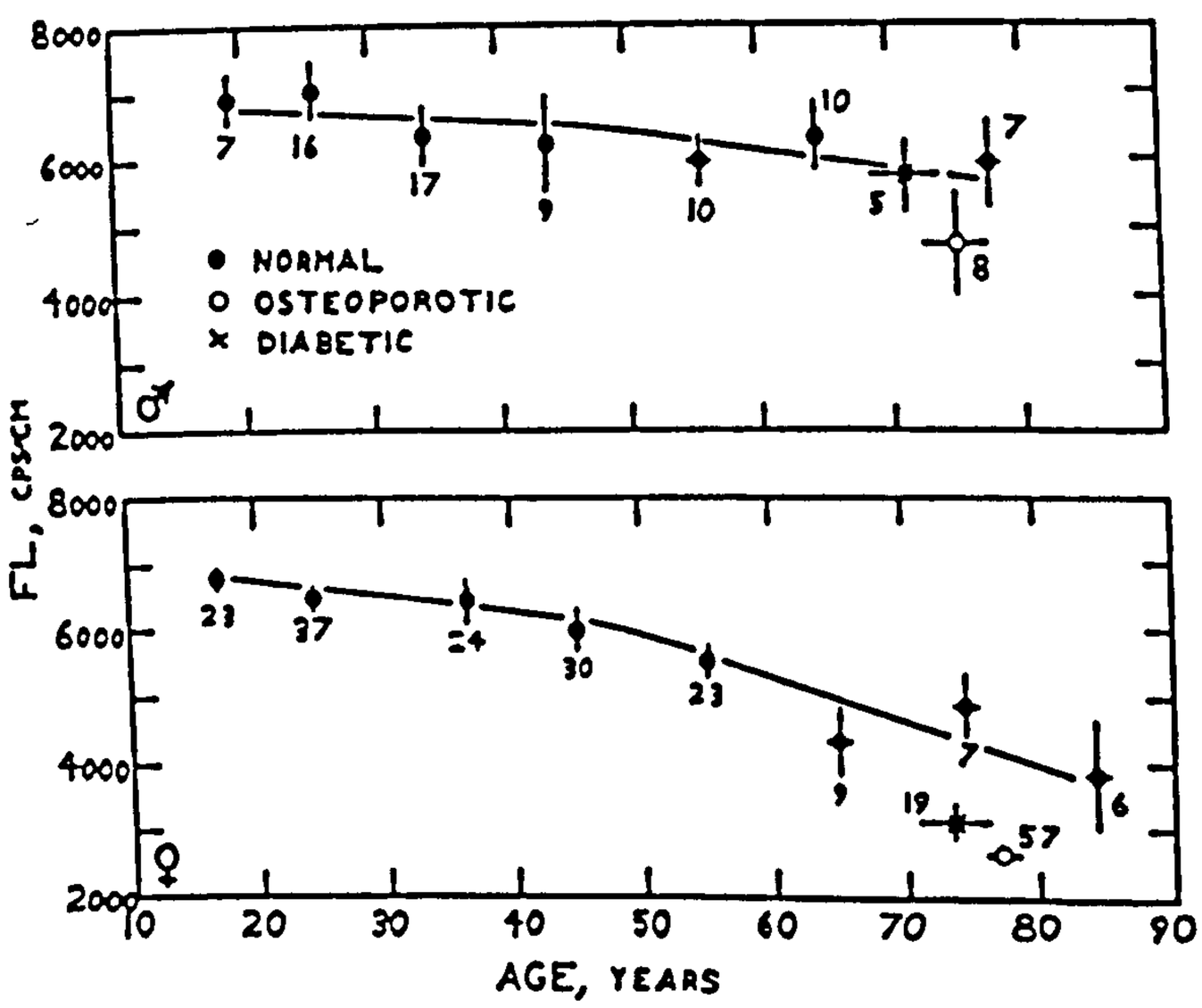

Fig 2.27 The use of FL value as an indication of osteoporosis (from Selle & Jurist, 1966a). F is the resonant frequency and L is the length of the ulnar bone.

dynamic force of higher frequency, and that attenuation increased with increasing frequency (18% at 60 Hz and 98% at 360 Hz).

Resonant Frequency. The principle of `resonant frequency measurement was to establish a reliable relationship between the vibration response characteristics and the physical characteristics of bone, such that this relationship could be utilized in clinical applications.

Jurist and Selle (1965), Selle and Jurist (1966a), and Jurist and Dymond (1970) were the first groups who determined the resonant frequency of the ulna (fig 2.26) and used the product of resonant frequency F and length L of the bone as an indication of osteoporosis (fig 2.27). The investigation was based on the concept that while the ulnar bone is treated as a vibrating bar, this product FL = KC, where C is the speed of sound propagation through the bone and K is a proportionality constant which depends on the shape, cross-sectional area of the ulna, support conditions, and mode of vibration. Hence FL may be taken as an indicator of the bone's relative stiffness which is a function of its mineral density (fig 2.28). However, the technique suffered inconsistency from positioning of the accelerometer against the wrist which accounted for 50% of the variance in the measurement of resonant frequency. Wrist position was less critical and the oedema of the forearm did not significantly affect the measurement.

Referring to Jurist's (1970a) publication, Doherty and his associate (1974) explained, in elaborated text, the invalidity of resonant frequency as an indicator of the physical properties of the ulna. It was pointed out that the natural frequency of a vibrating system depends on $\sqrt{(k/m)}$, where k and m are the generalized stiffness and generalized mass respectively. Both k and m are dependent on the bone density, and would decrease in osteoporotic bones. Hence the resonant frequency alone is not sufficient in the detection of osteoporosis or any loss of bone content. Vibration tests by applying steady state sine wave

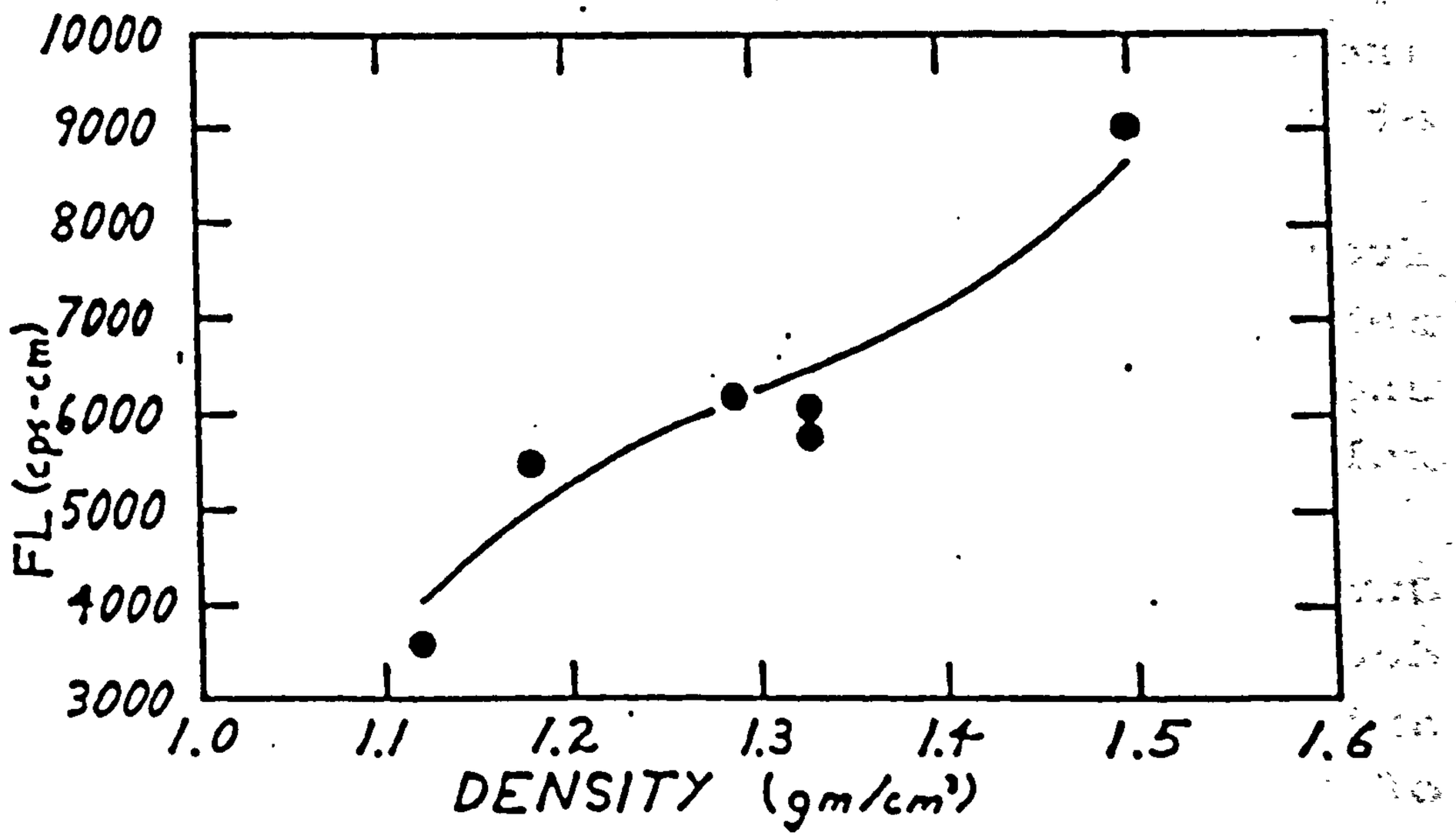

Fig 2.28 FL value versus density of bone (from Selle & Jurist, 1966b). F is the resonant frequency and L is the length of the ulnar bone.

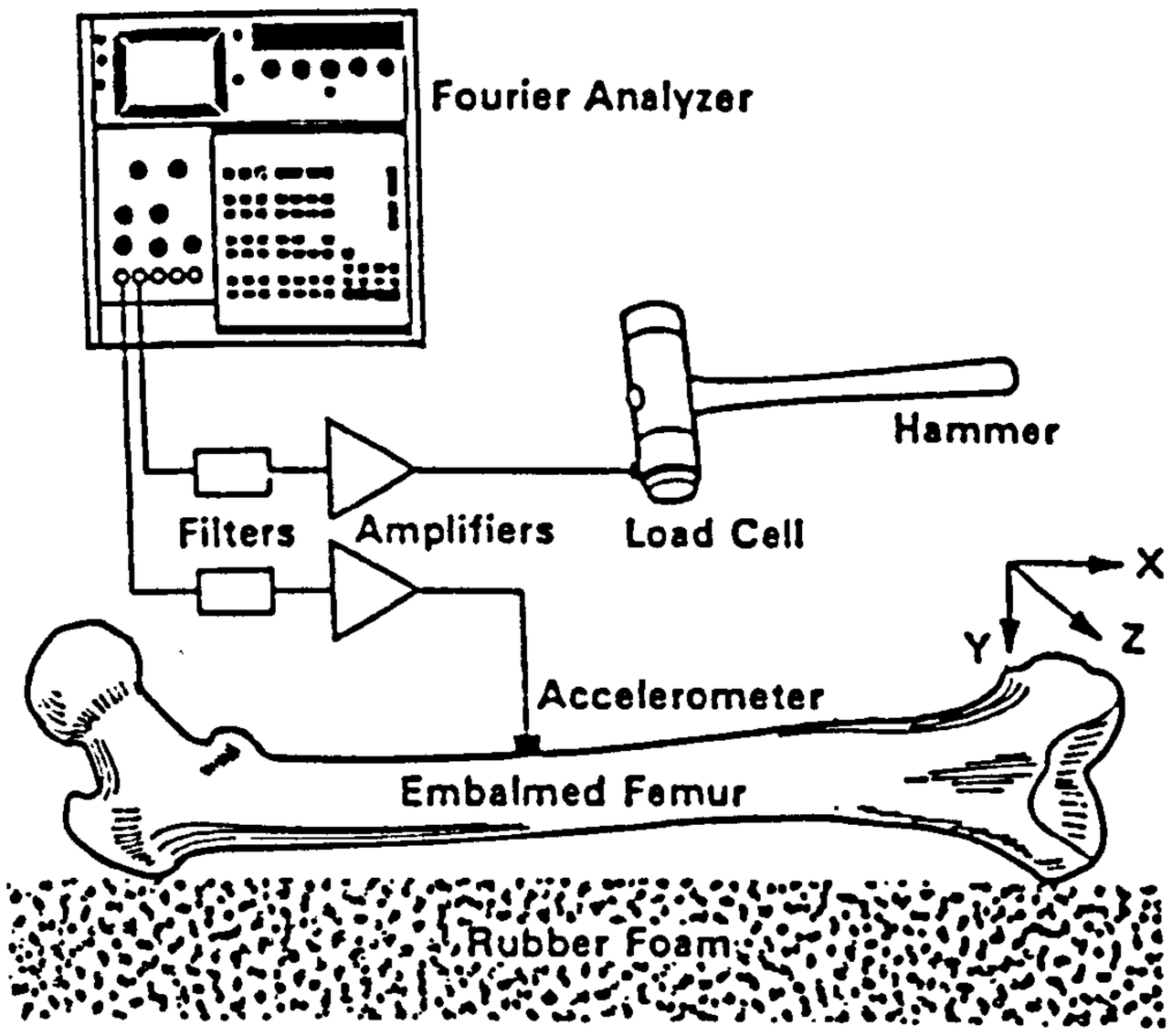

Fig 2.29 Experimental set-up to examine the vibratory characteristics of embalmed human femur (from Khalil et al, 1980).

over a frequency range was performed on human tibiae, and the results demonstrated that resonant frequency was less sensitive to the change in physical state of the bone than either generalized stiffness such as flexural rigidity and generalized dynamic mass. It was also suggested that the non-rigid in-vivo support of the bone, and the non-linear filtering effect of the soft tissues would render clinical application difficult.

Hight et al (1980) looked into the effects of geometry and boundary conditions on the dynamic response of the tibia using a beam-type finite element computer model to predict the natural frequency response of the bone. It was found that the boundary conditions caused the major influence on the predicted lateral natural frequency - for example the first natural frequency decreased by a factor of 5 from a fixed-fixed to a fixed-free case. The geometrical variables, for example twist and curvature, changed the predicted frequencies by less than 10%, and the changes were significant.

Khalil et al (1980) examined the vibratory characteristics of embalmed human femur under impact force in free-free boundary conditions (fig 2.29). A mathematical model was also developed to predict the femur's resonant frequencies and mode shapes with the inputs of geometrical parameters and material characteristics of the bone. A total of 20 resonant frequencies had been identified and it was shown that the experimental data matched those determined by the mathematical model. The resonant frequencies were also found to correspond to flexure, torsion and longitudinal extension.

Contrary to the findings of Khalil et al (1980), Thomas and associates (1991) only observed a simple mass-like mode when a human femoral bone was subject to random mechanical vibration in free-hinged conditions (fig 2.30). When the ends of the bone were clamped with a loading between 0 and 500 N, single resonant frequency was observed between 138 and 177 Hz, with the higher resonant frequency

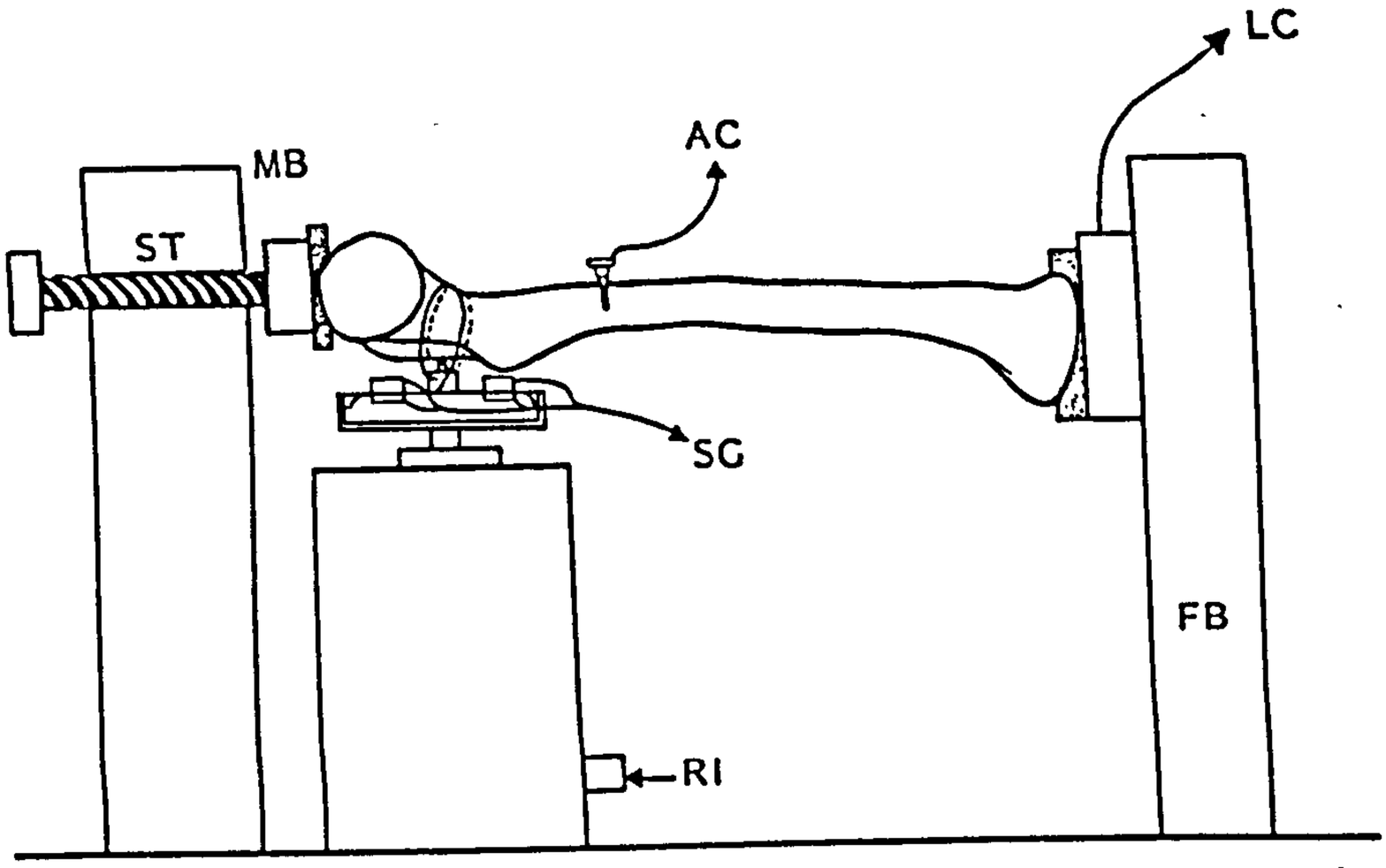

Fig 2.30 Vibration test on isolated femur (from Thomas et al, 1991).

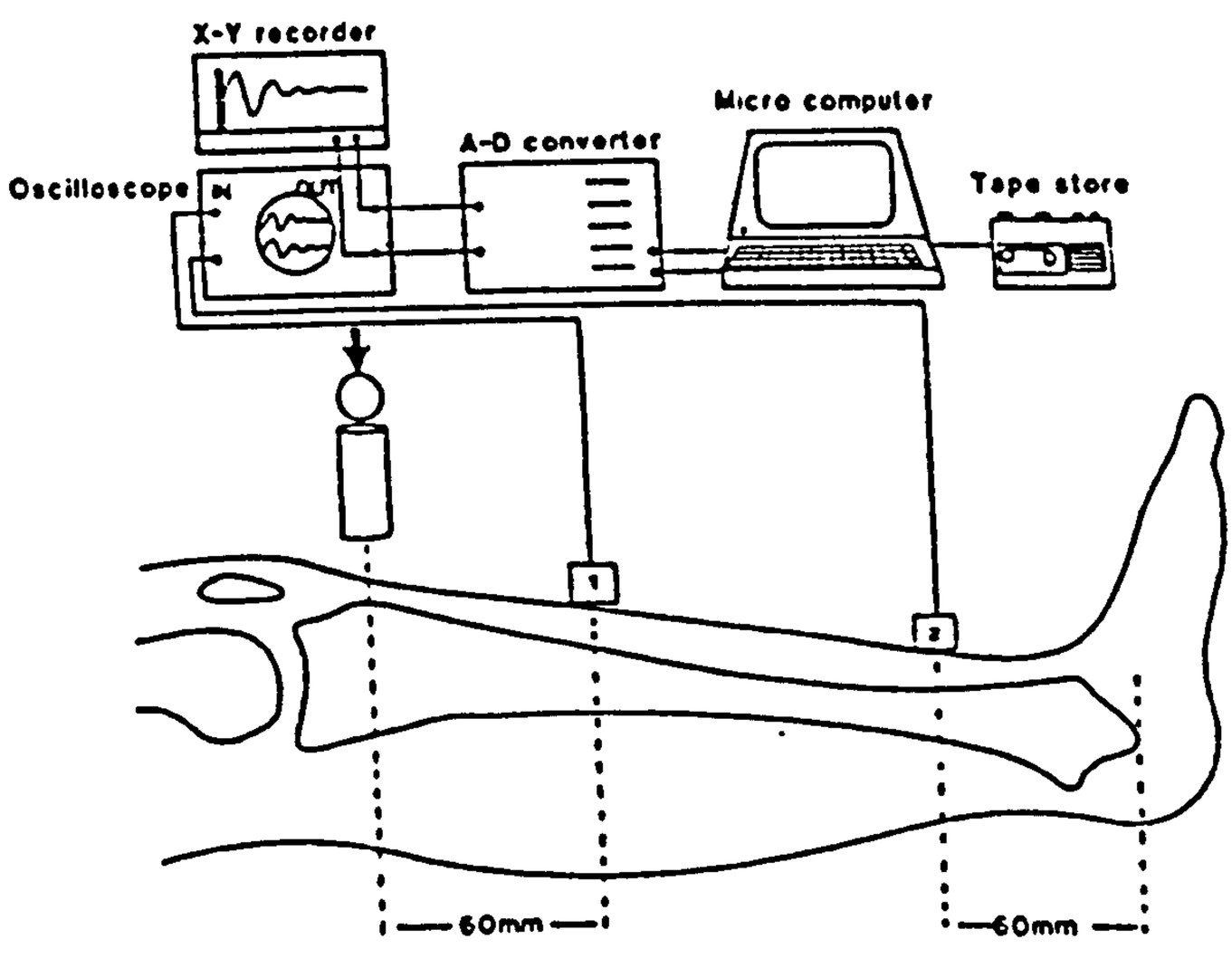

Fig 2.31 Apparatus used to derive the tibial natural frequency by impact method followed by fast Fourier transform (from Nokes et al, 1984b).

happening at the higher clamping load. The results presented were in agreement with the conclusion made on boundary conditions by Hight et al (1980).

Impulse response technique followed by the fast Fourier transform, and direct frequency domain analysis using steady sinusoidal vibration have been employed in the in-vivo determination of natural frequency of the tibia (fig 2.31 & 2.32). Nokes et al (1984b) demonstrated the use of these two techniques, and reported the first mode of vibration of living tibiae ranged from 250 to 530 Hz. It was also observed that direct measurement by frequency domain analysis yielded more consistent results.

Evans (1985a) performed vibration tests on isolated human ulnas in an attempt to determine the effect of geometrical factors on the dynamic response of the bone. Vibration signals were monitored at eight equiangular positions around the circumference which was marked at 11 equidistant locations along the bone, while white noise was used as the excitation. The directions and shapes of various vibration modes were identified. Results drawn from two different specimens showed individual variability due to the influence of complex geometry. It was also suggested that vibration methods for the assessment of relative changes in the bone properties e.g. in the assessment of fracture healing for a particular individual would give reliable results. In cases, for example the diagnosis of osteoporosis where the absolute measurement is required to compare with a statistical norm, individual variability would cause difficulty in the interpretation of experimental data.

Saha et al (1992) carried out impact testing technique on embalmed human ulnas in an attempt to relate the resonant frequency to the bones' load carrying capacity. A resonant frequency parameter Y (= FL^2) was defined, where F is the resonant frequency and L is the length of the bone. It was shown that this frequency parameter demonstrated a positive correlation with the bending

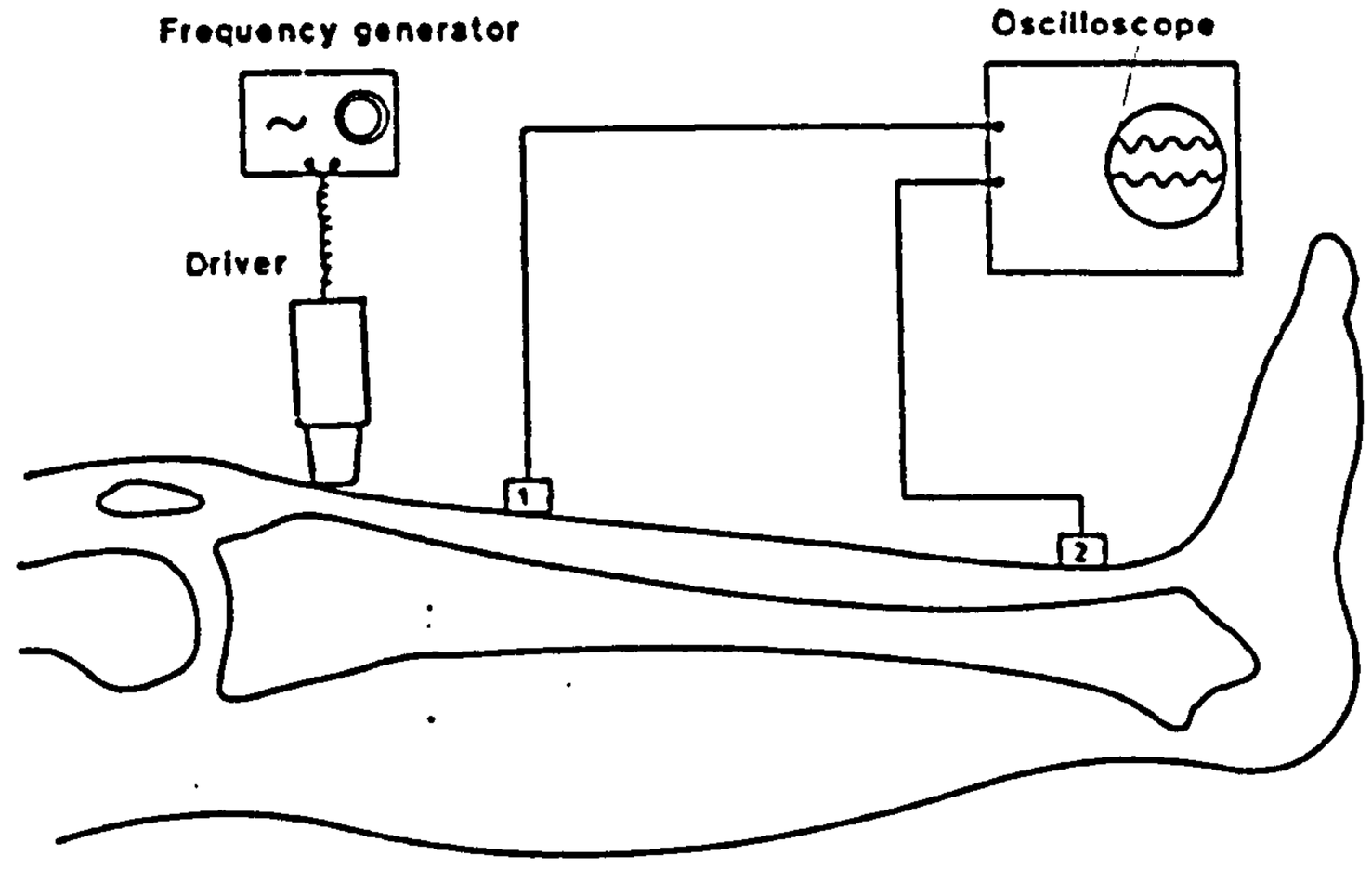

Fig 2.32 Apparatus used for direct determination of tibial natural frequency by sinusoidal vibration (from Nokes et al, 1984b).

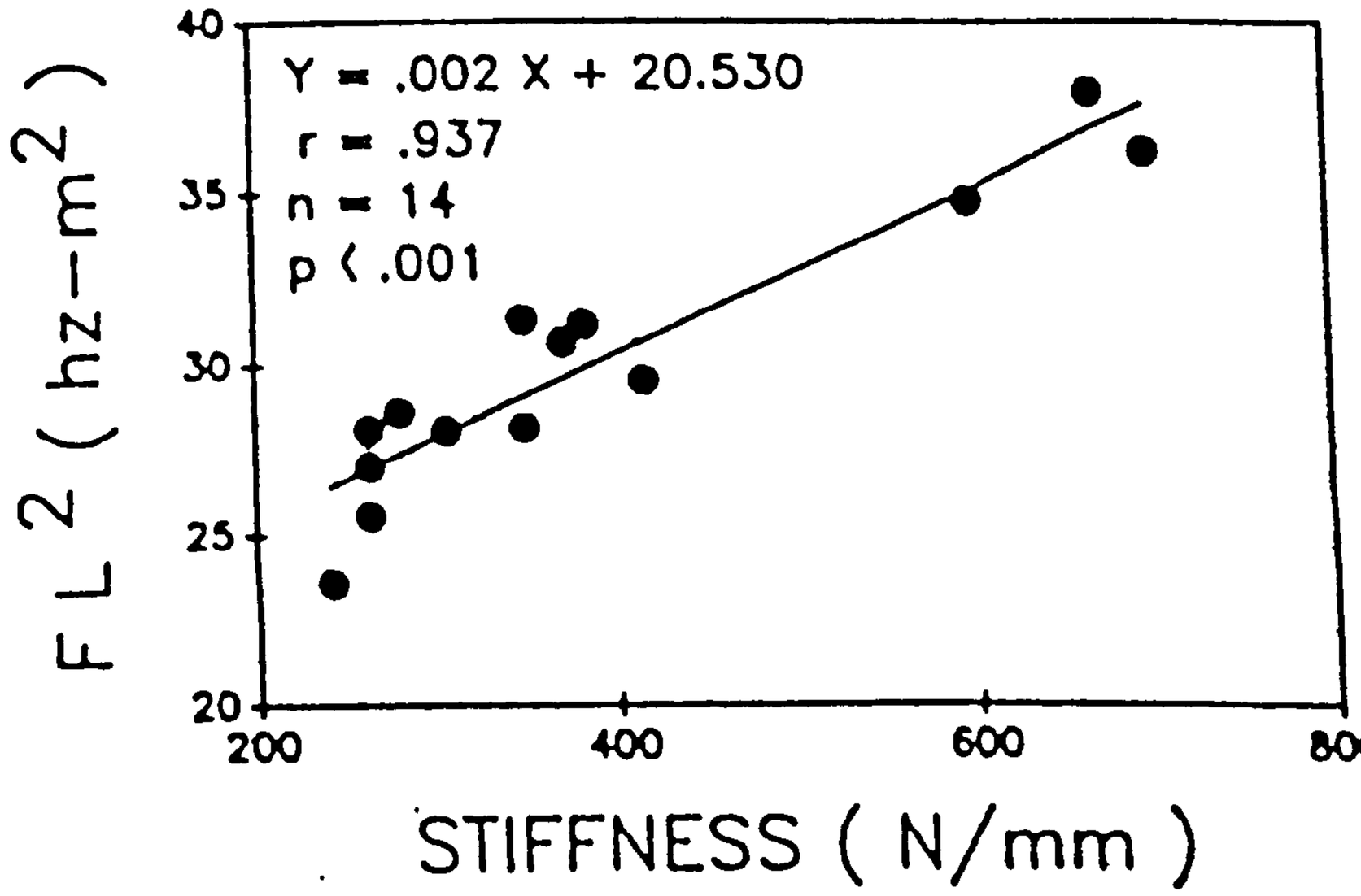

Fig 2.33 FL^2 value versus stiffness of embalmed human ulnar bone (from Saha et al, 1992).

stiffness (fig 2.33), and the load carrying capacity i.e. the load to failure in bending (fig 2.34) of the bone. The load to failure was also found to have significant positive correlation with the mineral content. It was also suggested that the resonant frequency parameter Y defined above could be used to predict the mechanical characteristics and the relative mineral content of human long bones. Lowet et al (1993) demonstrated linear correlation between resonant frequencies and torsional stiffness of the femoral bones of sheep and dogs, measured experimentally and estimated mathematically. The results again suggested the relevance of resonant frequency as a measure for the mechanical characteristics of long bones.

Mechanical Impedance. Mechanical impedance defined in equation 2.32 allows the determination of stiffness, mass and damping parameters of a vibration system separately. Campbell and Jurist (1971) measured the mechanical impedance of intact excised femur, and then repeated the test after the removal of a small bone wedge from the neck, after removal of the head and after re-attachment of the head (fig 2.35). Marked differences in the reactance were discovered with these changes. It was suggested that mechanical impedance measurement of the femoral bone could be used to determine the degree of union of healing fracture of this bone.

Thompson (1973) measured the mechanical impedance of the ulna in-vivo. The experimental data matched closely the proposed mechanical model. The analytical expression of the model enabled the determination of bending stiffness of the bone, which was shown to be an index of the bone's ability to resist bending.

Measurement of driving point mechanical impedance was utilized by Steele et al (1988) for in-vivo comparison of stiffness and bone mineral content in human forearm bones. A dynamic analyzer system enabled the physical parameters of a model to be determined after the measurement of vibratory force and motion at the driving point. It was

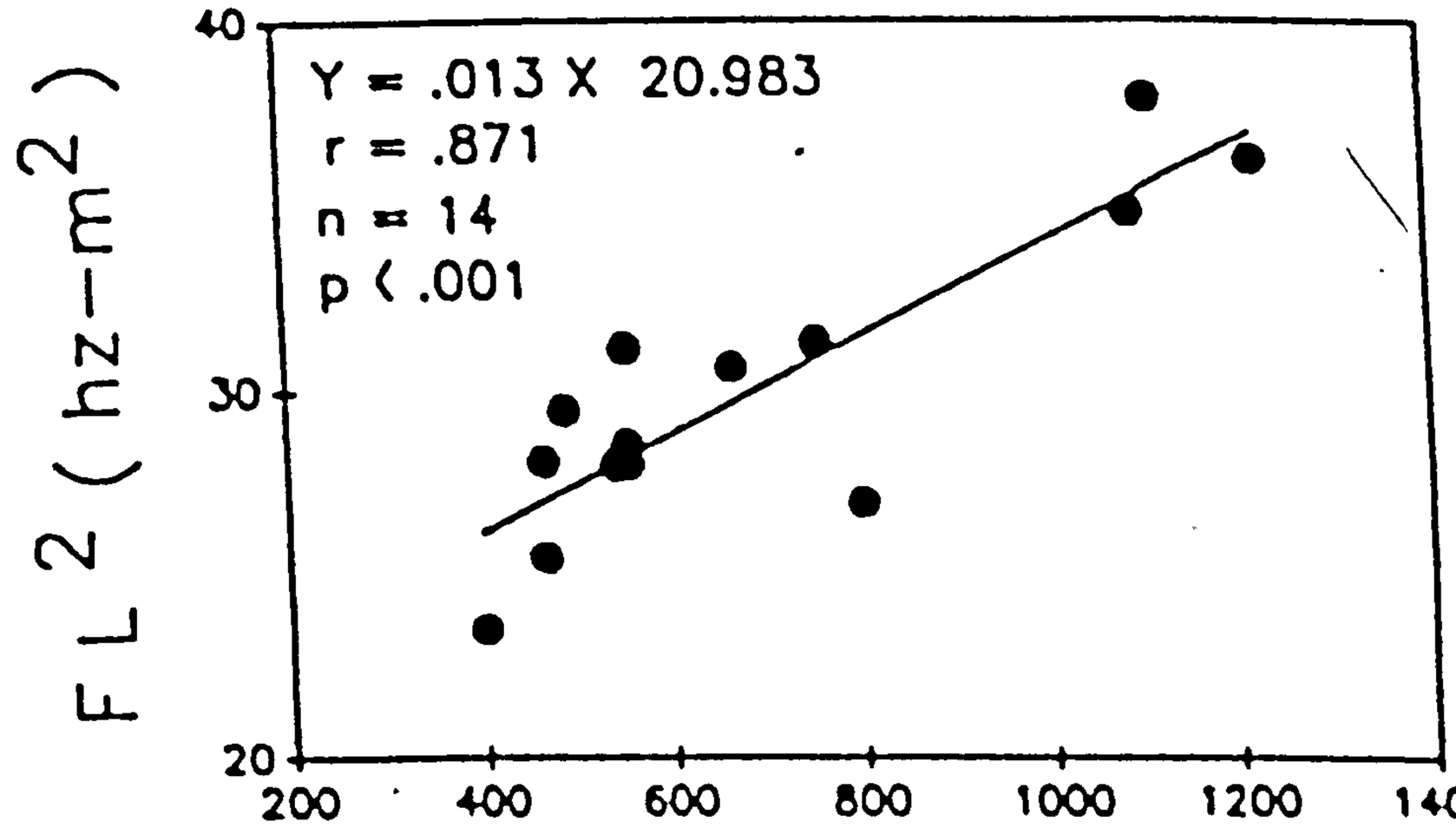

Fig 2.34 FL^2 value versus the load to failure of embalmed human ulnar bone (from Saha et al, 1992).

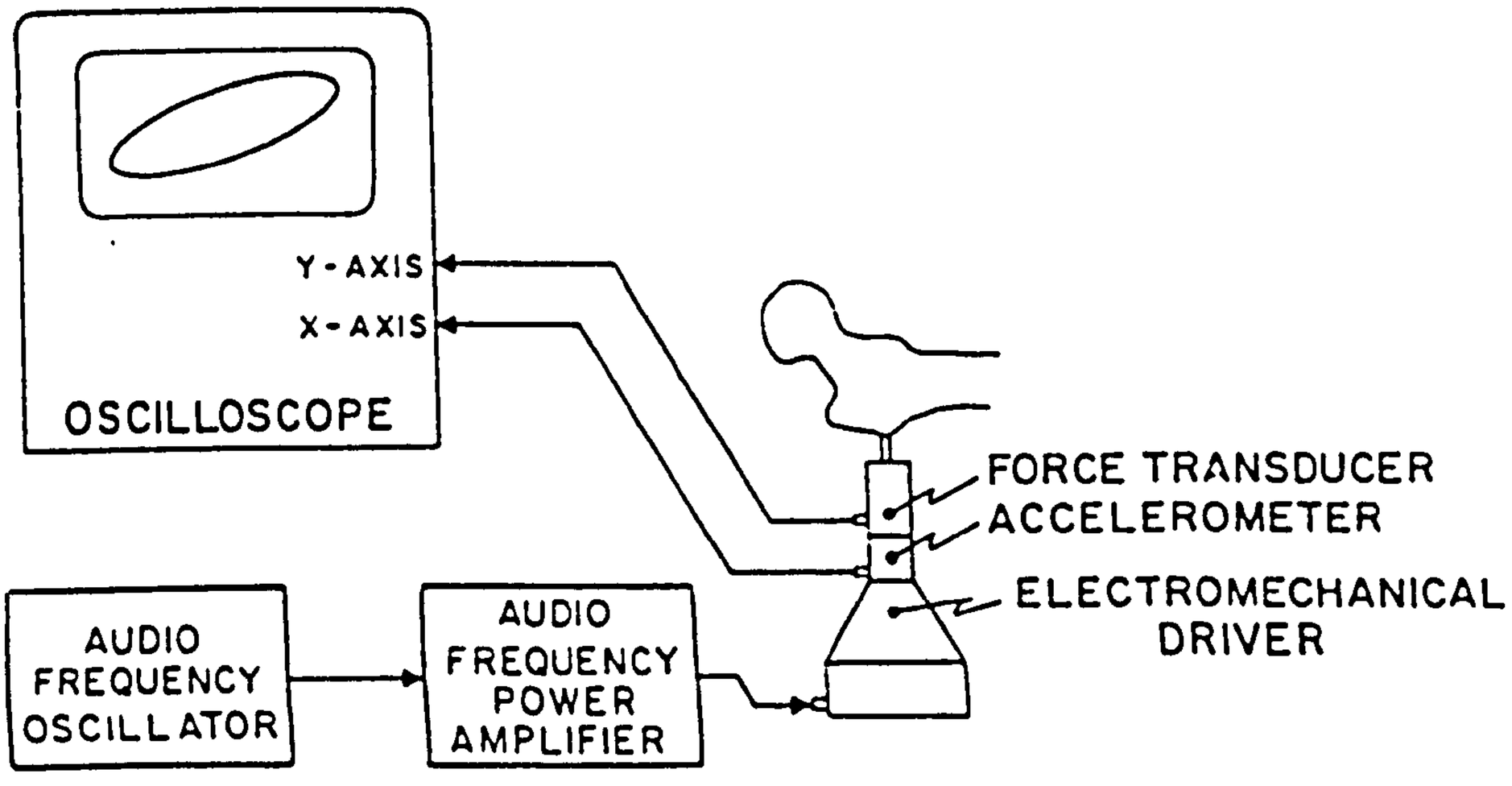

Fig 2.35 Apparatus for determination of mechanical impedance of excised femur (from Campbell & Jurist, 1971).

found that the correlation between elastic bending stiffness and bone mineral content was high. It was commented that mechanical impedance measurement could be employed to understand the factors related to bone's health and disease states.

Van der Perre (1984) commented that the impedance response was more sensitive to changes in cross-sectional dimensions than Young's modulus or density. It was also pointed out that mechanical impedance was also influenced by factors like: skin compliance, point of application of excitatory force, and muscle parameters. These remarks in fact reiterated the high influence of individual variability, and the fact that external factors impose great inconsistency in the measurement of mechanical impedance.

Modal Analysis. This is a technique applied only recently in biomechanical engineering. The major interest of using the technique is to understand the vibratory behaviour of long bone under excitation, by determining the modal parameters: modal frequency, modal damping and mode shape (section 2.4.3). Modal analysis technique can be implemented by two different approaches: Bone Resonance Analysis (BRA) and Impulse Frequency Response (IFR) (Christensen et al, 1986). BRA employs a sweeping sinusoidal excitation to the bone and the motion response is being monitored by an accelerometer or suitable transducer (fig 2.36). Resonances are determined by the maximum motion response of the bone. IFR applies a known impact force onto the bone, and the motion response is measured simultaneously (fig 2.37). The frequency response function is then computed using the fast Fourier transform, giving the ratio of the motion response to the applied force as a function of frequency. Measurement by both approaches could be repeated at various points on the bone, such that the motion response detected at these points adequately represents the motion of the bone.

Christensen et al (1986) also performed a comparative

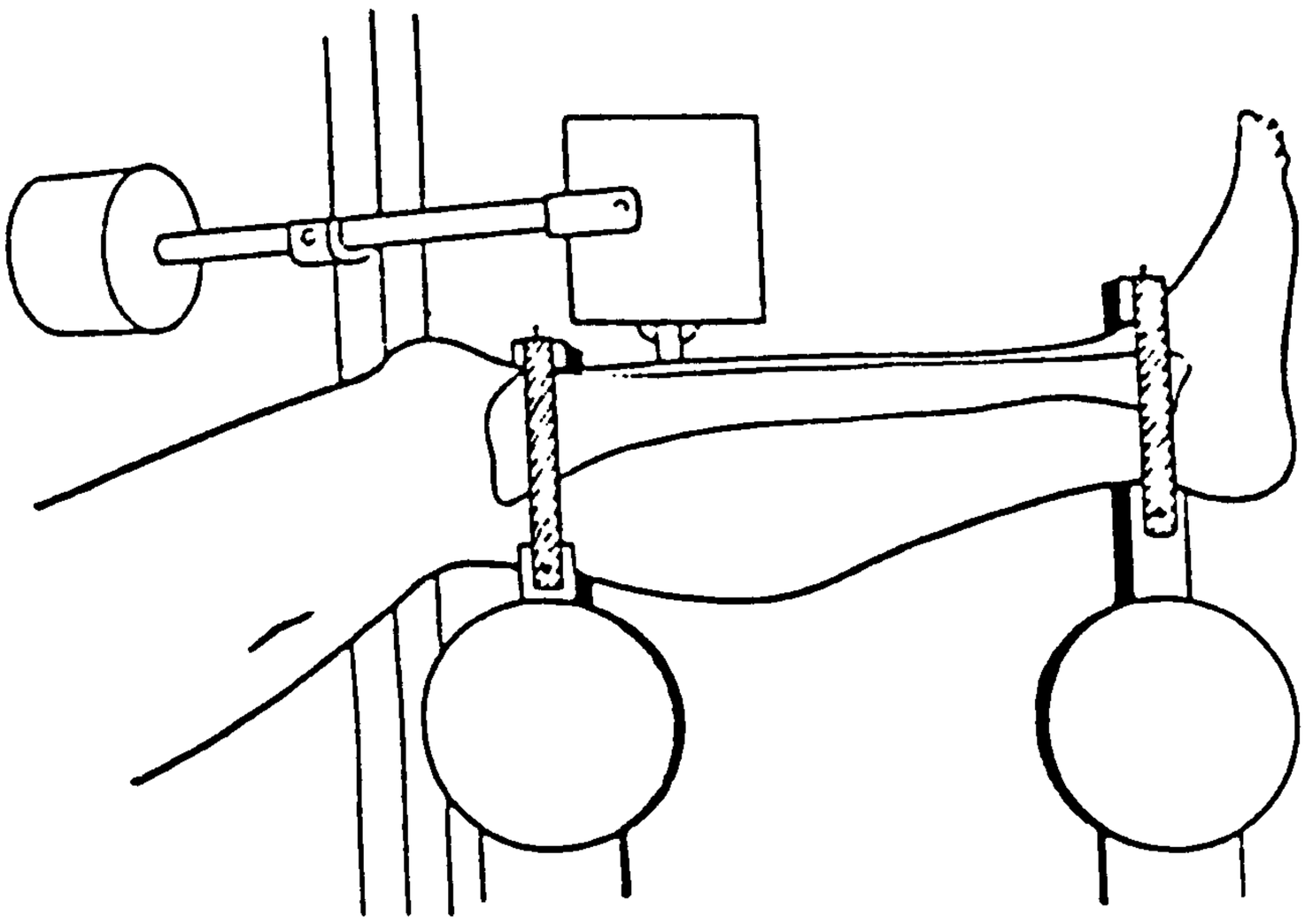

Fig 2.36 Bone resonance analysis method (from Christensen et al, 1986).

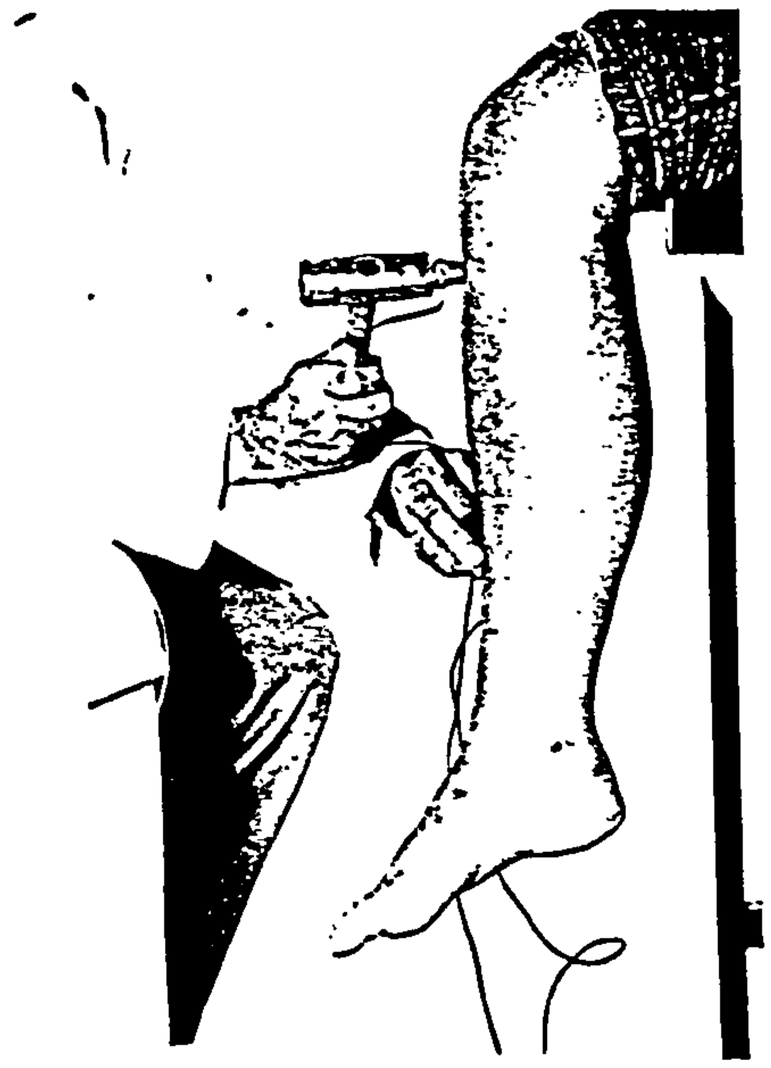

Fig 2.37 Impulse frequency response method (from Christensen et al, 1986).

study of the compatibility of the two techniques - BRA and IFR, on excised tibia and amputated lower leg, under various support conditions. It was found that the support conditions had great influence on the mode shape and frequency of the single bending mode. There was no significant difference in the natural frequencies determined by the two techniques. However the higher modes were found to vibrate in different planes. It was explained that for a beam of complex geometry, such as the tibia, twisting of the beam would influence the results. Furthermore, the rigidity of the support conditions was also a critical factor which varied the results. The group also commented that modal analysis was time consuming and technique demanding. Though not quite ready for routine clinical application, the technique could be used to monitor the sensitivity of the different modes to changes in the stiffness of the tibia.

Cornelissen et al (1986) reported the performance of modal analysis on amputated lower legs, incorporating staged resection of the soft tissues and the fibula. Removal of the soft tissues was found to raise the damped resonant frequency and decrease the damping ratios, but did not change the mode shapes. The fibula was found to have a stiffening effect on the tibia. The resonant frequency decreased when the fibula was cut away. The group also commented that the influence of soft tissue, joints and the fibula created difficulty in the exact interpretation of the vibration measurements of the tibia.

An in-vivo modal analysis has been reported by Lowet et al (1992) on the tibiae of healthy persons. Three vibration modes were identified. They were: rigid-body in the antero-posterior direction; a single bending mode and a double bending mode, both in the medio-lateral direction. The mean values and standard deviations were established for the group of healthy subjects tested.

To summarize, bone is a complex structure, and is the major medium for wave propagation in the body. Longitudinal

waves and flexural waves have been demonstrated with attenuation, the degree of which is frequency dependent and the wave propagation has been shown to be related to the physical properties of the bone. The complex geometry of the bone contributes to the complex modes and frequencies in vibration. Besides the bone's intrinsic mechanical properties and individual variability, the end conditions and the effect of musculature are factors which present a high influence on the vibratory behaviour of bone.

2.5.3 Peripheral Joints

Traditionally, articular cartilage has been considered as the major shock absorption or force attenuation component of a synovial joint because of its demonstrated compliance relative to subchondral bone. In-vitro dynamic compressive tests were carried out separately on bovine specimens of these two intra-articular structures in the metacarpohalangeal and metatarsophalangeal joints (Radin et al, 1970). Results showed that subchondral bone was 10 to 15 times less compliant than articular cartilage, and the synovial fluid was shown to have no significant force attenuating effect. From the experimental data obtained in the tests, the group also proposed that the subchondral bone was of equal capability to that of articular cartilage in the attenuation of dynamic force due to the bone's greater thickness and hence the total amount of allowable deformation. The cartilage was contributing additional function in distributing the load and allowing relatively larger load-bearing area. If both subchondral bone and articular cartilage are considered as homogeneous isotropic continuum, the longitudinal stress wave velocity can be given by: $V = \sqrt{(E/\rho)}$, where E denotes the Young's modulus and ρ is the mass density (Anderson et al, 1991). The longitudinal wave velocity V for subchondral bone is approximately 1600 ms^{-1}, and for articular cartilage, roughly 200 ms^{-1}. These figures are smaller than those estimated for cortical bone by Wong et al (1976), Pelker

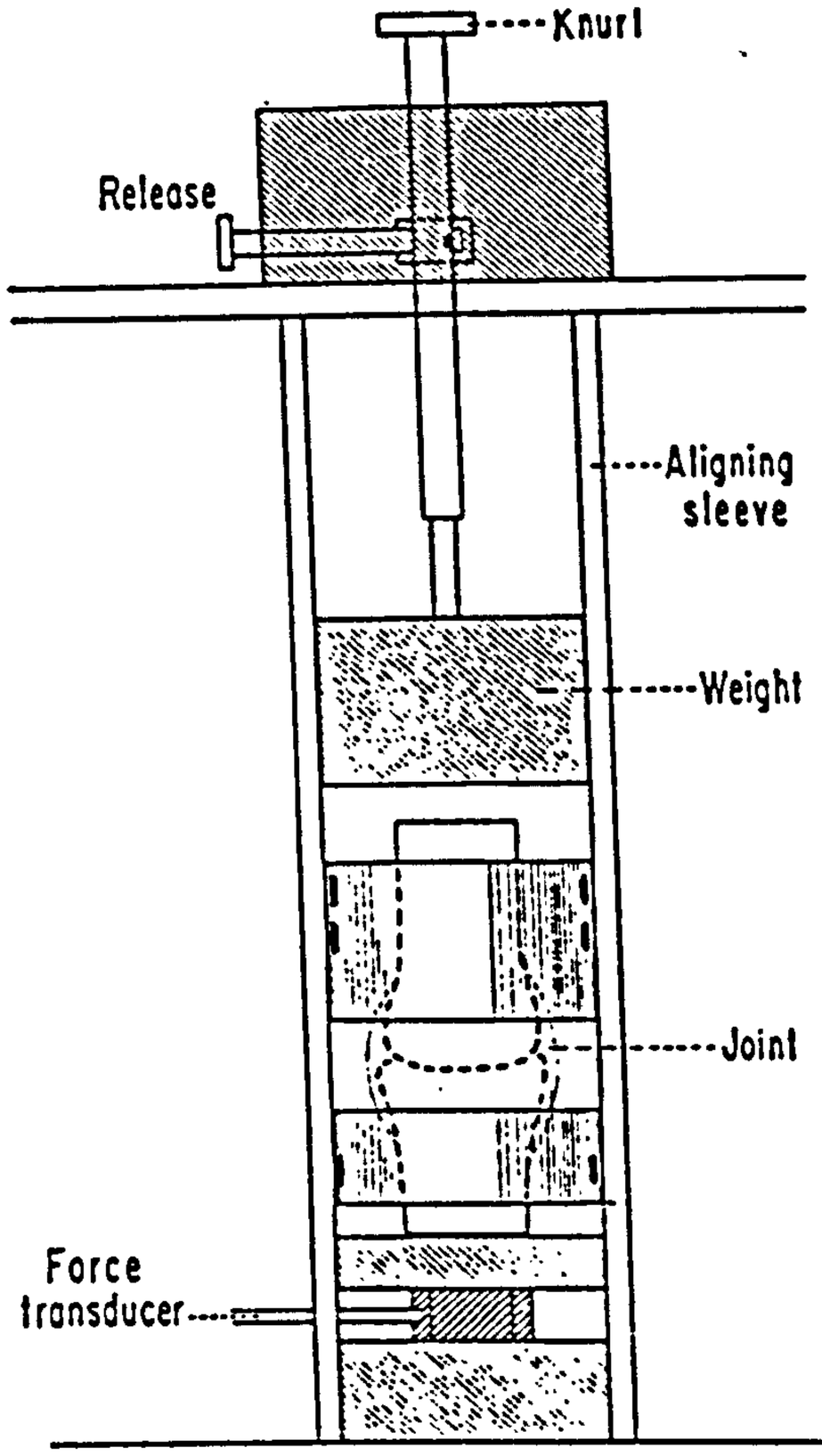

Fig 2.38 Apparatus for impact testing on bovine interphalangeal joint (from Radin & Paul, 1970).

and Saha (1983), and Chu et al (1986). These intra-articular structures are contributing some degree of attenuation and delay in the longitudinal wave propagation due to their relative compliance with respect to cortical bone. A dynamic contact finite element analysis performed by Anderson et al (1991) revealed that when compressive stress waves propagate through the epiphyseal bone towards the articular cartilage, their magnitude was substantially attenuated by the relatively compliant metaphyses. The stress waves were broadened and distorted. However, transient stress of high amplitude was observed at the articular surface. This observation is in agreement with the experimental data reported by Radin et al (1970), but contradicts the traditional incorrect assumption that the articular cartilage is to act as a shock absorber.

Radin and Paul (1970) who performed in-vitro impact testing on fresh bovine interphalangeal joints found that the subchondral bone was the major shock absorption element of the joint rather than the articular cartilage (fig 2.38). This findings has gained support from a direct measurement of the transmissibility of impulsive stress across the embalmed human knee joint carried out by Chu et al (1986). The knee joints were found to attenuate about 59% of the impulsive wave when intact, and 54% with mechanically abraded articular cartilage. This small difference in the attenuation capability suggests that the articular cartilage does not play an important role in the attenuation of impulsive force at the joint.

A comparative study on the force attenuating capacity of painful and meniscectomized knees with normal ones has been performed by Voloshin and Wosk (1983). Acceleration signals registered at the tibial tuberosity and the femoral condyle, as a result of the impulsive force at heel-strikes during normal walking, were compared. The healthy knees were found to show 20% greater shock absorbing capacity than the painful and meniscectomized ones.

To summarize, peripheral joints are complex structures

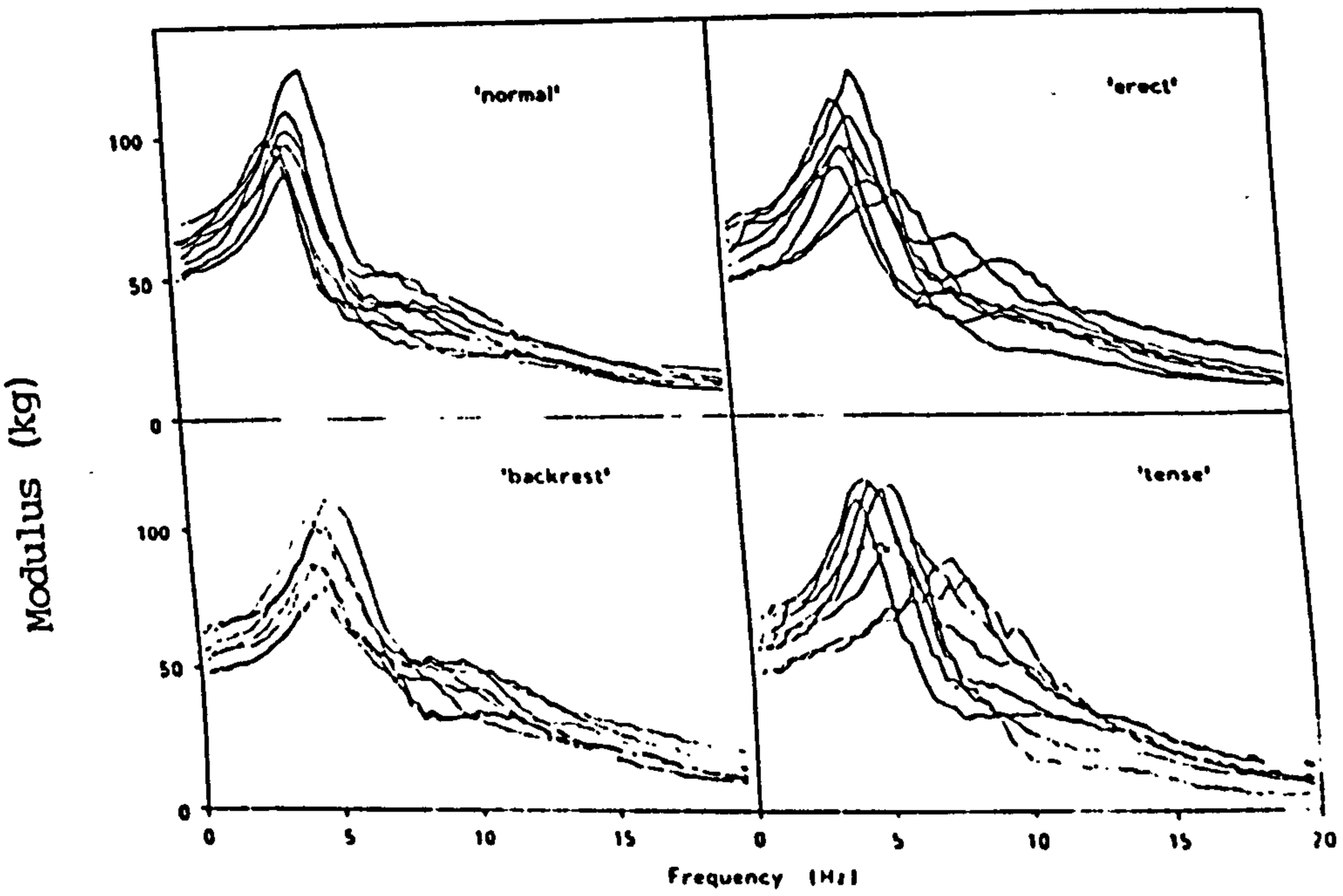

Fig 2.39 Apparent masses of eight people for four different conditions (from Fairley & Griffin, 1989).

comprising materials of various acoustical properties. Stress waves will be distorted and distributed when propagating across various components of the joint. Substantial attenuation is expected due to the compliance of subchondral bone.

2.5.4 The Spine

Whole-body vibration study becomes a major area in the biomechanical study of the spine in the light of growing concern over industrial health and safety, and due to the advancing development in aeronautical and motor industries. Studies of this kind entail a lot of vibration tests in the field or in a simulated environment in the laboratory. Attention lies in the measurement of the dynamic response of the human body under vibratory situations. Two major experimental approaches have been used (Griffin, 1990). The first method typically examines the vibration transmitted to the body by the measurement of mechanical impedance at the driving point at the buttock-seat interface. The mechanical impedance, or apparent mass (section 2.4.2) give some indication of the body's dynamic characteristics by quantifying the force required to produce a unit measure of motion (velocity or acceleration) as a function of frequency. The measurement of mechanical impedance, as a complex function, also helps to characterize the body's mechanical behaviour as mass-like or spring-like across the frequency range of interest. Subsequently, the mechanical parameters e.g. mass, spring constant, and damping ratio could be determined by suitable modelling and curve-fitting techniques. Representative works have been reported by Sandover (1982), and Fairley and Griffin (1989) (fig 2.39). The second method examines the transmission of vibration through the body by comparing the vibration level at a point e.g. the head on the body with that at the driving point - usually the seat in sitting or the heel in standing or walking postures. Paddan and Griffin (1992) determined the head's movement in all axes at various locations at the

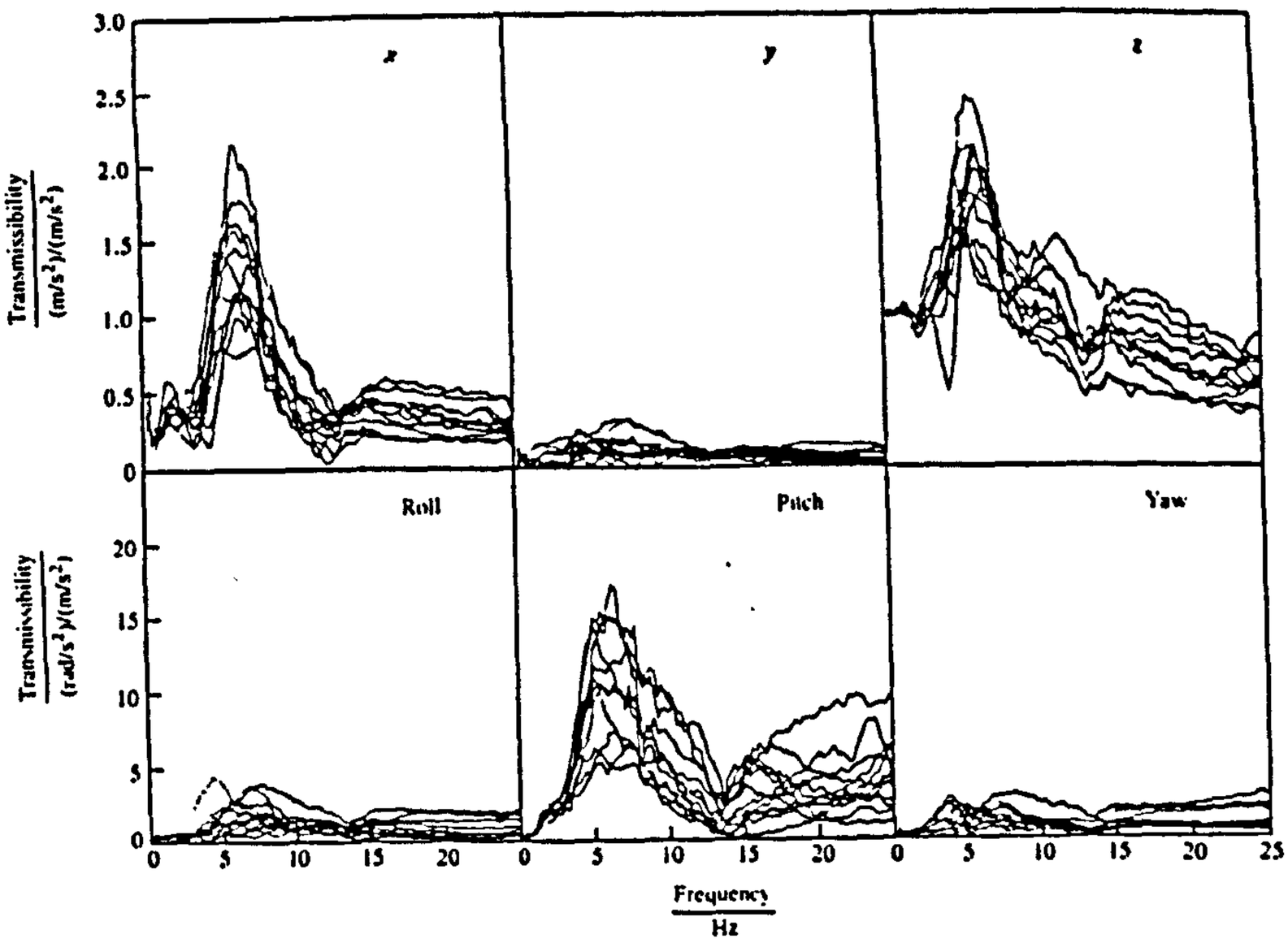

Fig 2.40 Transmissibility for 12 subjects in a 'back-on' posture during vertical seat motion (from Paddan & Griffin, 1992).

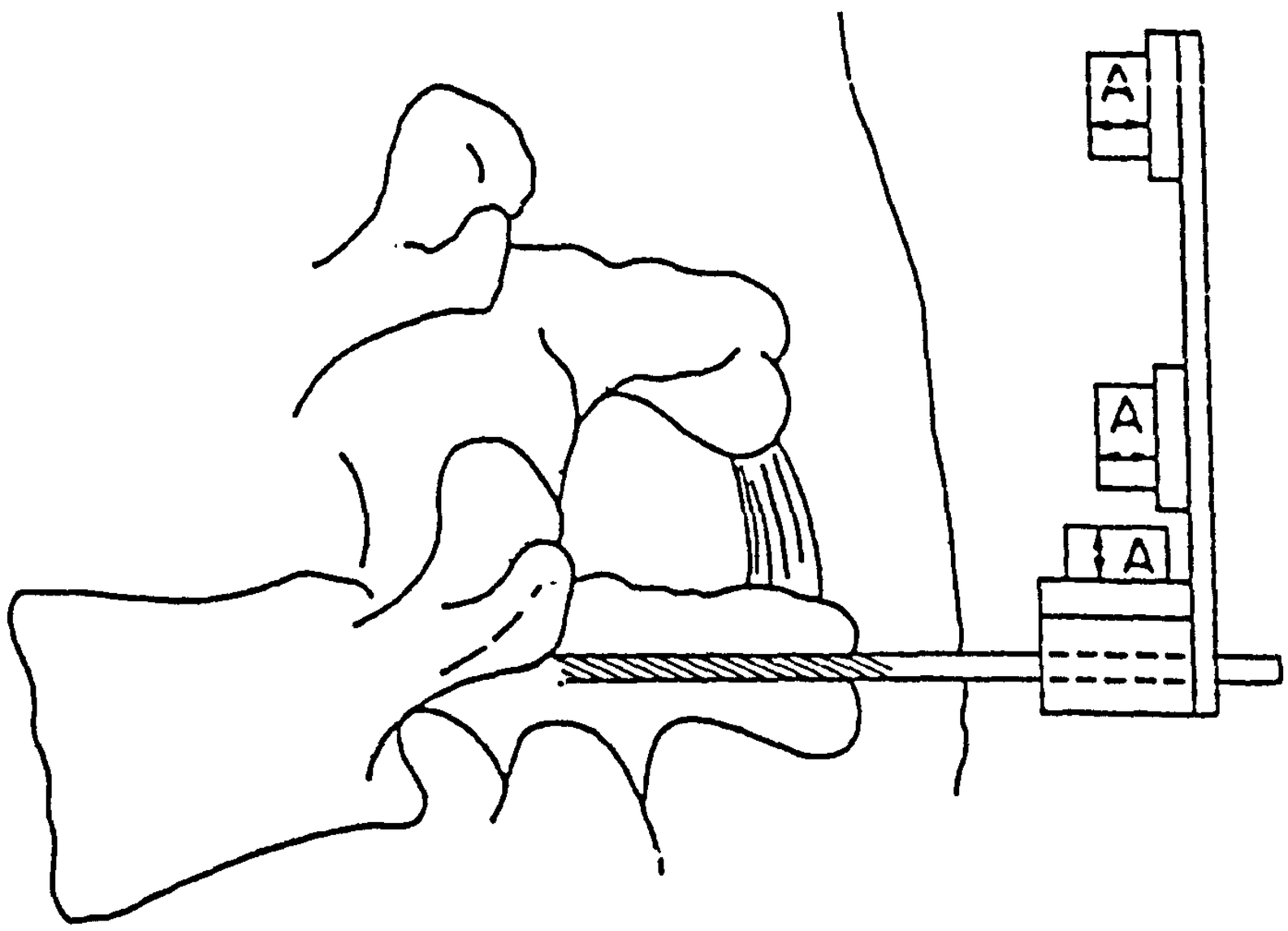

Fig 2.41 Vibration measurement by accelerometers on pins screwed into the spinous process (from Pope et al, 1986).

head with the subjects exposed to vertical seat vibration (fig 2.40). Transmissibility is given by the magnitude of the transfer function. Measurement of seat-to-head transmissibility is usually confined to the direction of the long axis of the trunk i.e. the z-axis, in accordance with BS 6841 (1987). Paddan and Griffin (1988b) have also studied the seat-to-head transmissibility in horizontal seat vibration. Work recently reported by Paddan (1991) has extended the investigations to the body's dynamic response in horizontal motions, i.e. in x- and y-axes, in sitting and standing subjects. The study also included vibration tests incorporating different trunk postures and limb positions.

Griffin (1990) has commented that "there have been few attempts to relate vertical seat-to-head transmissibility data to measure of discomfort, activity disturbance or health effects". Furthermore, most published work has been limited to the dynamic response of the entire body, and in frequency range up to about 50 Hz. Of interest relevant to this study reports on the local response of the spinal column, particularly the lumbar spine are scanty. This is mainly related to the technical difficulty of attaching appropriate transducers at the lumbar spine by non-invasive techniques. As discussed in section 2.5.1, skin-mounted accelerometry demonstrates a limited working frequency range, and has its other disadvantages. Discrepancies in the measurements made by skin-mounted and bone-mounted devices have been assessed. Pope et al (1986) employed an opto-electronic system to compare the vibratory movements of markers fixed rigidly to the L3 spinous process through a pin, with that measured by skin-mounted markers attached at the same level (fig 2.41). Discrepancies in these measurements were substantial, and were found to be greater when the skin-mounted markers were located farther away from the mid-line. In spite of the drawbacks in its use, skin-mounted accelerometry remains the most acceptable non-invasive technique. The problem of the skin's lack of

stiffness and the possible solution for improvement have been discussed in section 2.5.1. Hinz et al (1988) determined the inverse transfer function for the skin between the accelerometer and bone. The inverse transfer function was used subsequently in the estimation of bone vibration from that measured on the skin. Smeathers (1989b) used similar correction factors for the measurements made by skin-mounted accelerometers at the T2 and S2 spinal levels. Transmissibility between the two sites during walking was subsequently estimated.

Panjabi et al (1986) measured the vibrations in the lumbar vertebrae in-vivo by employing accelerometers attached on Kirschner wires inserted into the spinous process. Measurements were made at L1 and L3 spinous processes and at the sacrum, while the human subject was exposed to vertical vibration in a seated position. Resonance was observed in the vertical vibration at about 4.4 Hz, and the L1 and L3 vertebrae were found to vibrate synchronously, showing no sign of differential vibration or resonance between these two levels in the lumbar spine, in the frequency range up to 15 Hz. A similar resonance pattern was observed for the sacrum, though at a slightly higher frequency (4.7 Hz). The observed resonance was probably set up in the intervening tissue structures between the seat and the sacrum. The group commented that the result implied the local stiffness of the lumbar spine within the frequency range up to 15 Hz.

Ray and associates (1992) reported the use of a 3-axis accelerometers inserted into the L3 spinous process in the measurement of transmitted vibration, in response to impact force applied at the heel in standing and generated during walking. Resonances were observed at 4, 12 and 23 Hz, during the two activities. Frequencies above 25 Hz were effectively attenuated at the. level of L3. Ray and associates suggested that the result indicated the shock absorption effect of the intervertebral discs and the general compliance of the spine. This result was basically

in agreement with that observed by Panjabi et al (1986), but the groups have drawn contradicting conclusions. Apparently, information obtained by Ray et al (1992) was not adequate to differentiate the transmission properties of the structures from the foot to the sacrum, and that from the sacrum to the L3 vertebra.

Direct in-vivo measurement of the relative movements between two adjacent segments of the lumbar spine has been attempted. Pope et al (1991) reported the use of an Intervertebral Motion Device (IMD) which is a transducer system linked with pins that are rigidly attached to adjacent spinous processes in the lumbar spine. The system gives information of the relative displacement between the corresponding vertebral segments. Coupled translational motion accompanied by rotation was observed in the adjacent motion segments of a seated human subject exposed to vertical vibration of 5 Hz. This was a strong indication of the compliance of the lumbar spine at this frequency, contrary to the conclusion made by Panjabi et al (1986).

As a summary, the spine is both anatomically and biomechanically complex. The combination of its lateral flexibility and axial incompressibility render some uncertainty to the analysis of the transmission of vibratory and impulsive stresses through the system. Local response, particularly that of the lumbar spine have not been intensively studied. The limited capability of non-invasive techniques has restricted the accuracy and also the effective frequency range of vibration tests on the spine. Invasive techniques, though subject to ethical constraints, have been proved effective in the direct detection of vibratory movement of individual vertebrae. However, vibration tests on human subjects, in-vitro or in-vivo, are inevitably faced with the problem of inter-subject variability. This could introduce limitations in situations where a single measurement has to be compared with a statistical norm which itself is lacking confidence. Intra-subject variability can be controlled by

standardizing the test protocols.

2.5.5 Muscles and Ligaments

Skeletal muscles cover the outer surface of the bones and are attached to them through periosteum, aponeurosis, or tendons. Except at the joints, bony prominences and over subcutaneous bony surfaces, skeletal muscles form a thick cushioning or padding layer "insulating" the bone acoustically from the outside. Since the skeleton forms the major structure and medium through which the impulsive stresses transmit, it is logical to suggest that bones play a major role in the transmission of vibration and acoustic waves in the musculoskeletal system. Because of their relative compliance, muscles are not expected to contribute to an extent comparable to that played by the bone and joint structures. However, since muscles have definite mass and high fluid content, their effects on the vibration response of the bones are expected to be significant. It is interesting to know how these physical properties of the muscles would affect the resonance and damping of a vibrating bone.

Orne and Mandke (1975) noticed the existence of what they referred to as "sub-resonance" associated with the measurement of mechanical impedance on the ulna by Thompson (1973), and suggested a revised version of the mechanical model which included the muscle as an entity of a distributed mass-spring-damper system attached to the bone. This revised model was found to fit more closely to the experimental data obtained previously. Lim (1989) observed additional resonance at a frequency lower than the first mode resonance when mechanical impedance was measured on fractured tibiae with swollen surrounding soft tissues. This vibratory behaviour of the fractured bone was similar in nature to what Orne and Mandke (1975) suggested of the "sub-resonance" associated with the mechanical characteristics of the attached musculature, but in a more pronounced manner probably due to the acuteness of

swelling. Jurist and Dymond (1970) applied an inflatable cuff to occlude venous return of the forearm to introduce an oedematous state of the soft tissues when testing the resonant frequency of a vibrating ulna. However, there was no significant change in the resonant frequency detected.

Hansson et al (1992) examined the transmission of vertical impulsive stress through the lower limbs and the spine in a standing posture. The effect of musculature on the amplification and the resonant frequency was observed. The stiffening of the skeletal system by muscle action and modified posture shifted the resonant frequency from 2-3 Hz to 4 Hz, and increased the peak value at resonance. Collier and Donarski (1987b) measured in patients the resonant frequency of fracture of the tibia. The effect of muscle tension on the resonant frequency was noticeable, especially on nervous patients who were being tested for the first time. The resonant frequency was increased, while the damping was increased. It was explained (Collier & Donarski, 1987b) that the muscle's contraction, particularly the quadriceps, affects the coupling of the tibial bone with the rest of the body. In this situation, the end conditions are expected to have been altered.

An in-vivo study of the force transmission through the tibiae of rabbits under impulsive loading has been reported by Paul et al (1978). The transmitted force patterns recorded with the animal anaesthetized, fully awake, or deceased, have been Fourier transformed and compared. The muscle tone did not appear to have any significant effect on the force transmission, though it was commented that the muscle's active contraction would have effect only in the lower frequency range below 10 Hz.

The effect of attached musculature on the vibratory behaviour of a long bone has also been reported by Cornelissen et al (1986) in the determination of mode shapes of a vibrating tibia. It was found that the removal of the attached musculature increased the resonant frequency and decreased the damping ratio, but without

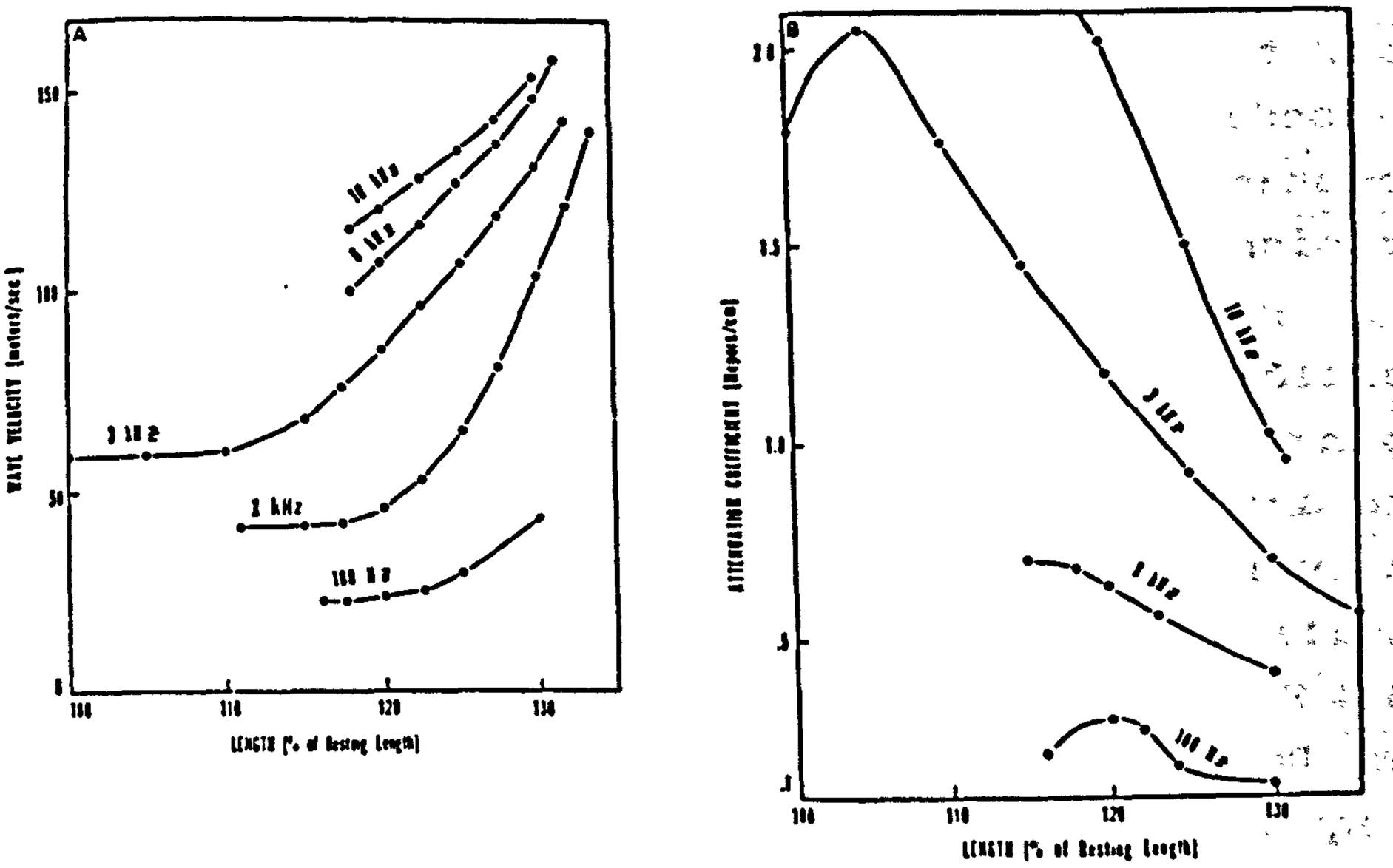

Fig 2.42 a) Wave velocity versus muscle length for various wave frequencies. b) Wave attenuation coefficient versus muscle length for various wave frequencies. (from Truong, 1974).

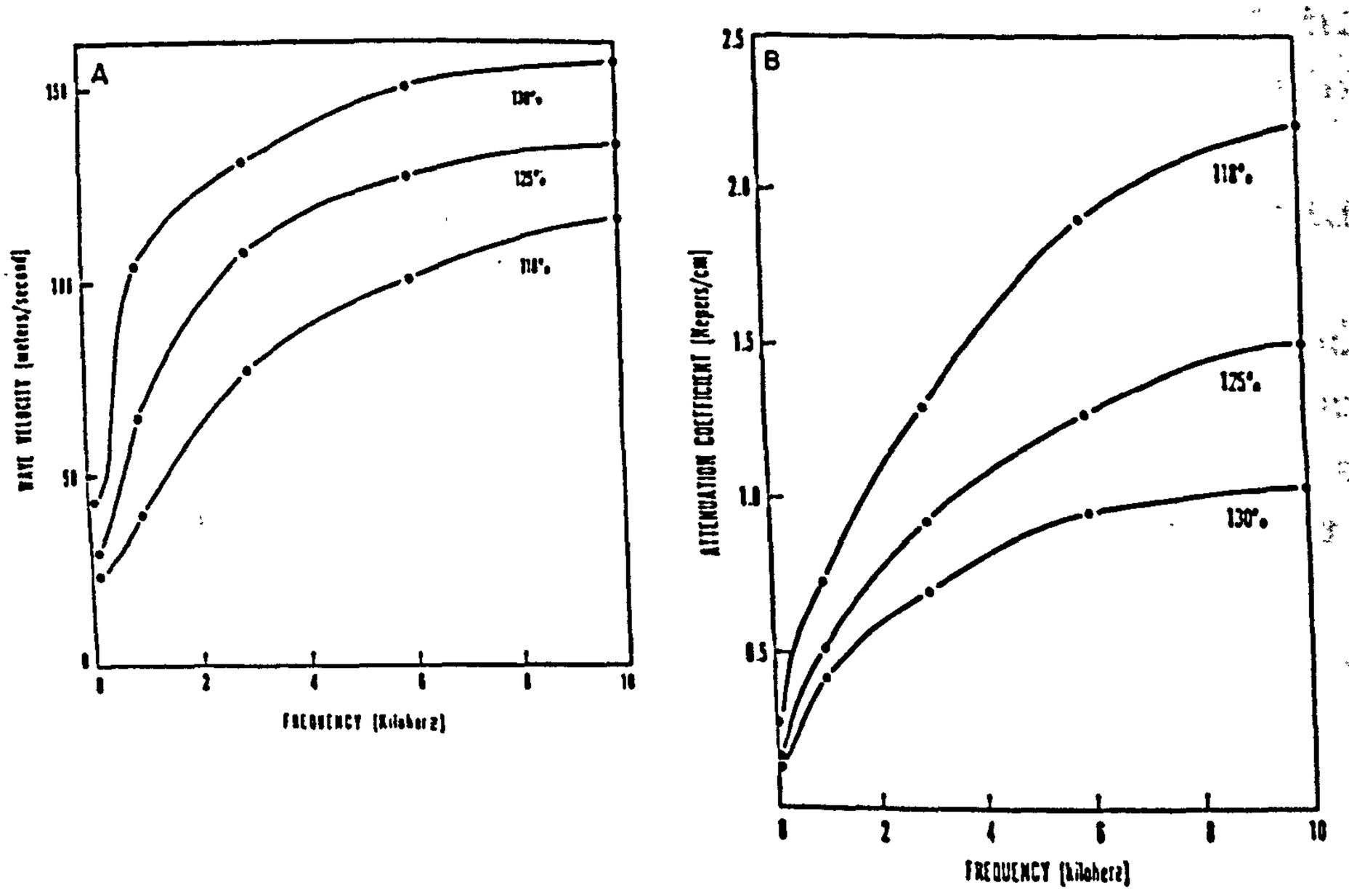

Fig 2.43 a) Wave velocity versus frequency for muscle lengths of 118, 125, and 130%. b) Attenuation coefficient versus frequency for muscle lengths of 118, 125 and 130%. (from Truong, 1974).

causing any change to the mode shapes. It was also suggested that the viscous fluid of muscles and their mass caused these shifts in the resonant frequency and the changes in the damping ratio.

Truong (1974) has reported on the direct measurement of propagation constants of compressive waves of various frequencies in an isolated sartorius muscle of frog. Both the wave velocity and attenuation coefficient along the muscle were detected with various excitation frequencies and in two different states of the muscle:- relaxed but stretched, and in isometric tetanic contraction caused by electrical stimulation. Stretching was found to increase the wave velocity at all test frequencies from 100 Hz to 10 kHz with an exponential rise to greater extension range. The attenuation coefficient showed an initial rise, followed by a decline when the muscles were being stretched (fig 2.42). For a given length of muscle, the wave velocity and attenuation coefficient increased with higher frequency waves, showing a tendency to level off (fig 2.43). The wave velocity has been shown to have direct relationship with the tension set up in the muscle, and the pattern demonstrated similarity to the tension-length diagram shown on standard text of physiology (Emslie-Smith et al, 1988) (fig 2.44a & b). When referring to the muscle tension, the wave velocity in a contracting muscle is higher and showing a greater slope towards the higher tension than that in a resting one, and its relationship with the muscle tension is fairly linear (fig 2.44c). Active contraction of the muscle was found to decrease the attenuation coefficient, and the amount appeared to be directly related to the developed muscle tension. Typical values, as interpreted from the published graphs, for the velocity and attenuation coefficient (Kolsky, 1963) of a 3 kHz wave were 60 ms^{-1} and 1.7 neper/cm (14.7 dB/cm) respectively in relaxed muscle and that for contracting muscle were 130 ms^{-1} and 0.7 neper/cm (6.1 dB/cm). In comparison with the velocity and attenuation coefficient Pelker and Saha (1983) determined

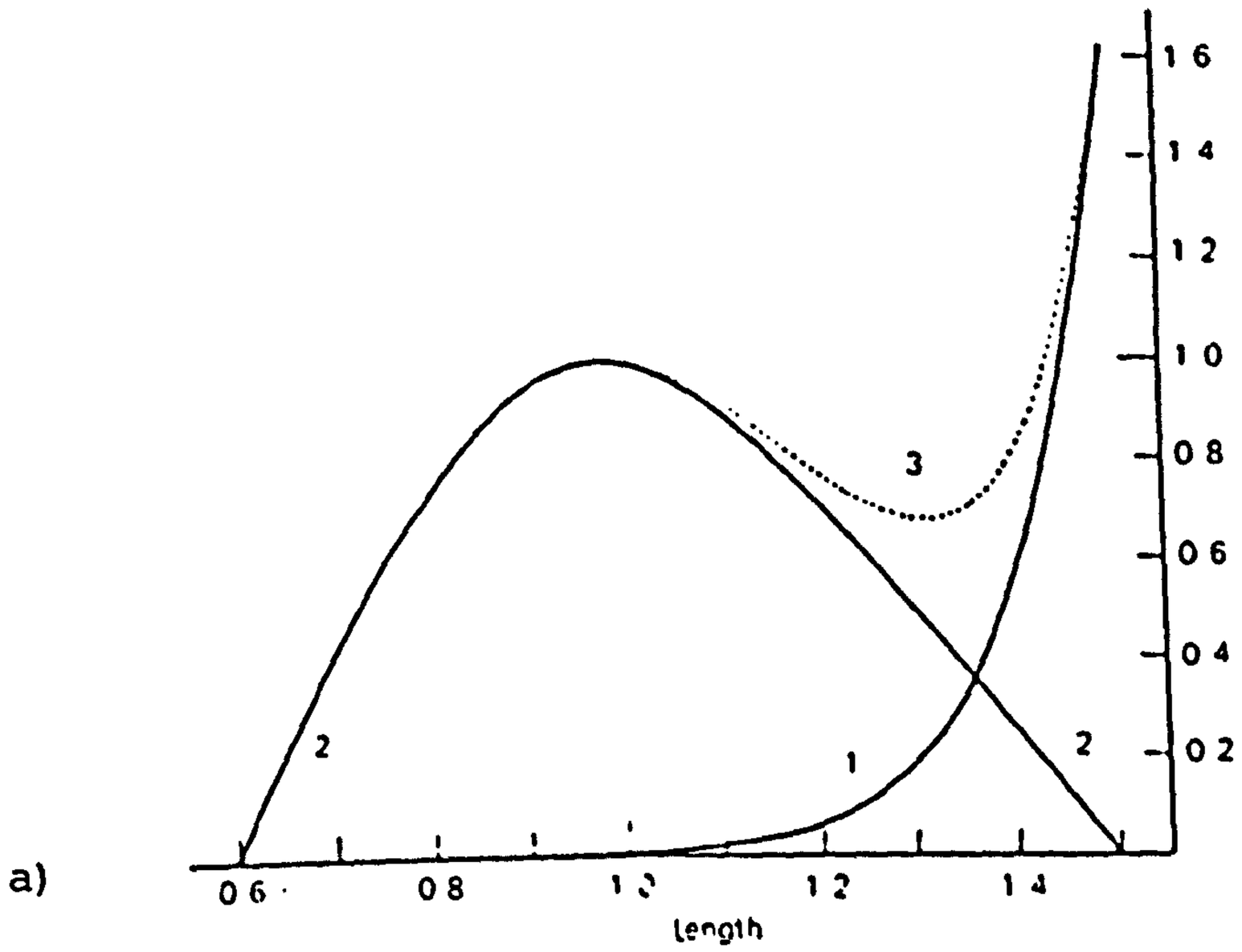

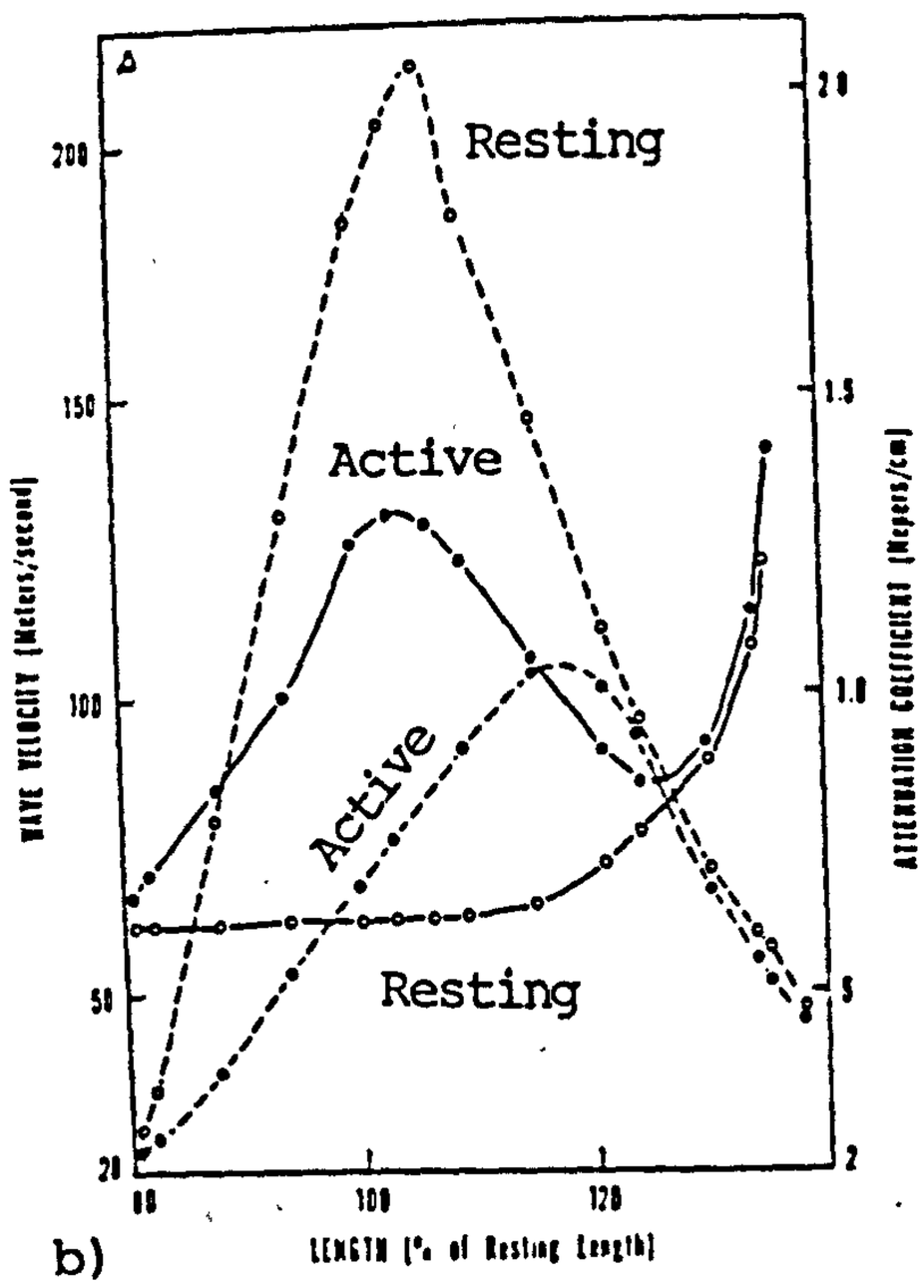

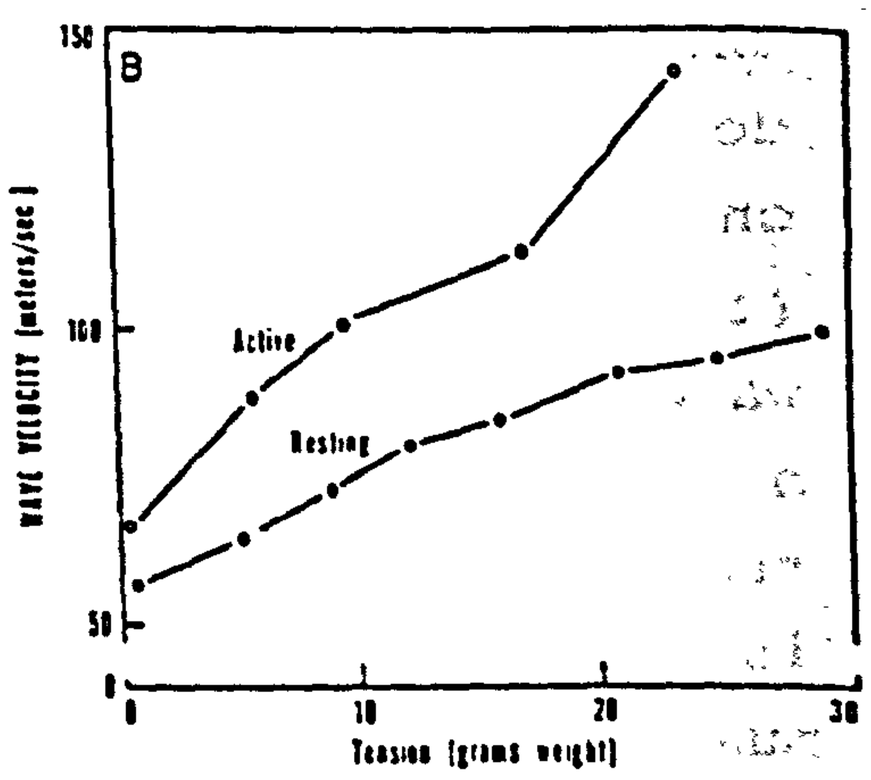

Fig 2.44 a) Diagram of tension-length relations of sartorius muscle of frog. 1) At rest passively stretched; 2) extra force developed during maximal tetanus; 3) total force in maximal tetanus. (from Emslie-Smith, 1988). b) Wave velocity (———) and attenuation coefficient (·····) versus muscle length. c) Wave velocity versus muscle tension (from Truong, 1974).

for fresh bone, these values reveal that longitudinal wave velocity in muscles is about 1/50 of that in bones, and muscles have a wave attenuation effect almost 70 times higher than bones. Schoenberg et al (1974) performed an independent test using a different measurement technique on the same muscle - frog's sartorius. A figure of 170 ms^{-1} for longitudinal impulse wave velocity along the contracting muscle was determined, in close agreement with that reported by Truong (1974). The wave velocity in resting muscle was found to be about 1/3 of that in the activated condition.

Oestreicher (1951) applied the values of the physical parameters such as shear elasticity, shear viscosity, and compressibility of muscles in an theoretical analysis of the wave propagation behaviour in a medium of elastic, viscous, and relaxational properties. The assumption of isotropy and homogeneity was found valid for muscular tissues up to 200 kHz.

As an associated structure for wave propagation in the musculoskeletal system, muscle possesses mass and viscous properties which have been found to modify the bone's response to vibration. However, the fundamental mechanical behaviour of the bone has not been changed. Active muscle contraction has demonstrated some effects on the vibratory response of the bone, but a resting muscle apparently does not cause any significant change. Longitudinal waves have been observed to propagate in skeletal muscles. However, if both bone and muscle are set as parallel structures through which stress waves are allowed to propagate, it is expected that the musculature will play a less important role due to the much lower wave velocity and higher attenuation in muscles. Furthermore, due to the mismatch in the acoustical properties of the two media as a result of different stiffness, waves travelling across the interface from bone to the muscle will be greatly dispersed and the intensity of that dispersed wave being re-admitted to the bony structure will be very much reduced. Due to its inherent

compliance, and also its viscous properties, acoustical energy will be dissipated, hence the muscle will only serve as an acoustical insulator for the bone through which stress waves propagate. The skeletal muscle, especially in its resting state does not play any active role in the transmission and propagation of stress waves.

Ligaments, periarticular or intra-articular, have the primary function of maintaining the anatomical alignment of the bone segments which constitute the articulating components at the joint. Ligaments also show viscoelastic characteristics which implies a greater resistance to elongation at higher strain. The result of this helps to confine the movements of the joints to within a physiological limit. There is no active element in a ligament, which then does its job by its inherent stiffness, i.e. resistance to elongate. This resistance, together with the negative pressure established in the (synovial) joints cavity, help to maintain a good contact between the articulating surfaces.

Pintar et al (1992) determined the biomechanical properties of the major ligaments of the lumbar spine. The force-deformation curves showed linear portions, which was described as the "physiological range" by White and Panjabi (1990). Unfortunately specific acoustical properties of ligaments have not been available to the author. However by this token, if a vibratory excitation is applied to the bone with the joints in a near-to-neutral position, and with a limited amplitude to avoid substantial deviation from a normal or neutral alignment of the articulating components, the ligaments involved would then be expected to behave linearly under this situation of minimal strain. Hence the ligaments are not expected to induce any non-linear behaviour to the vibrating bone structure in these circumstances.

2.6 CLINICAL APPLICATIONS OF VIBRATION TECHNIQUES

The general acoustical properties of major tissues and

structures of the musculoskeletal system have been summarized. The following sections attempt to outline some of the clinical applications of vibration techniques which are designed to address specific clinical problems related to the transmission of vibration in bone, peripheral joints, and the spine. For comprehensiveness, it is deemed necessary to include auscultation of the joints, which is basically an acoustic technique for the detection of vibrations i.e. crepitus inside the joints, though acoustic technique and the transmission of air-borne vibration are not the major subject matter of this study.

2.6.1 Diagnosis of Osteoporosis

Osteoporosis is defined as a loss or decrease in the mineral content in bone (Hoerr & Osol, 1956). Degeneration due to ageing, hormonal disturbance, bone pathology (e.g. neoplasm), and prolonged disuse are the possible causes, leading to systematic or local demineralization and porosity of the skeleton. Vibration technique for the diagnosis of osteoporosis is based on the principle that for a given geometrical shape and construct, the vibratory behaviour of a bone e.g. resonant frequency is dependent on its stiffness, and hence the Young's modulus which is again related to the mineral content of the bone.

Jurist and Selle (1965) reported the use of an acoustical technique for the detection of osteoporosis, and claimed that the method was 3 to 5 times more sensitive than the radiographic method. The 50 osteoporotic patients being tested showed a mean FL product of approximately 50% of that for the normal subjects, where F and L are the resonant frequency and the length of the ulna respectively. The study had been extended to a bigger sample of patients and normal subjects, mainly women. It was concluded that the vibration technique was useful for the early detection and aetiological study of osteoporosis, and it would probably help to evaluate therapeutic intervention of the condition (Selle & Jurist, 1966a). However, it appeared

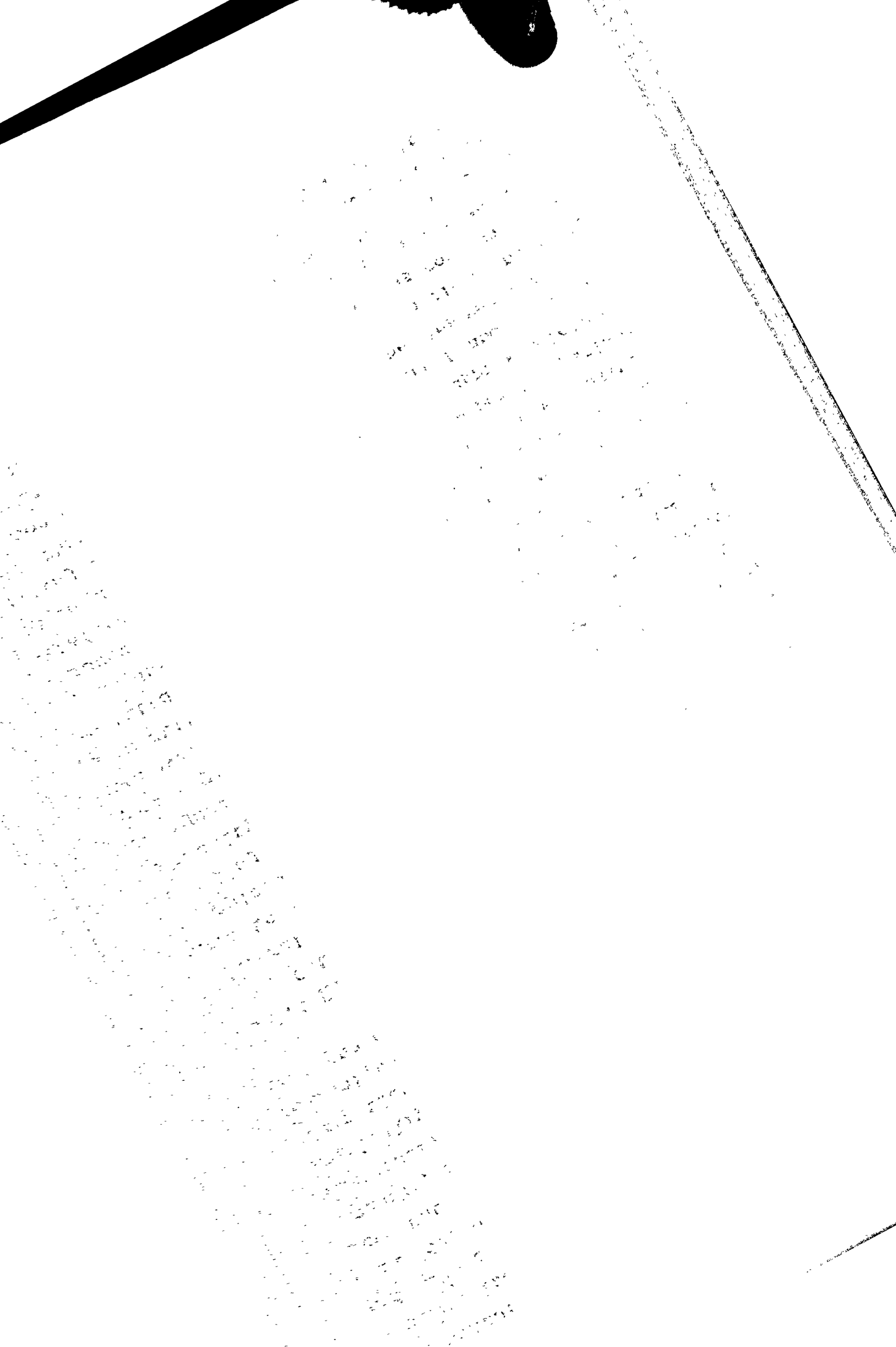

that there was significant overlap of the FL values between the normal and osteoporotic bones. The discriminant value of FL could only be drawn arbitrarily to eliminate the number of false positive and false negative cases. Though it had been commented that radiographic technique was not able to detect osteoporosis until at least 30% of deossification (Selle & Jurist, 1966b), the vibration technique did not explain for itself its sensitivity over radiographic technique for this low degree of osteoporosis. Doherty et al (1974) also commented on the insensitivity of using the resonant frequency alone for the detection of changes in bone's mineral content.

The velocity of the flexural wave generated in the tibia by a mechanical impact has been found to correlate negatively with the degree of osteoporosis, and positively with the mass per unit length of the bone (Wong et al, 1983). Pelker and Saha (1983) discovered that the cross-sectional area of the bone was positively correlated with the attenuation coefficient, which suggested that the attenuation coefficients could be used as an indication of thinning of cortical bone in a disease state. Porosity of the bone, as measured by radiographic technique was shown to have a parabolic relationship with the wave attenuation coefficient and the feasibility of estimating the porosity of bone from its attenuation coefficient was suggested. However, routine clinical applications of these vibration techniques for the diagnosis of osteoporosis have not been reported. There has not been any significant breakthrough in previous decades. The inherent difficulty of determining a confident discriminant value of the parameters such as resonant frequency and attenuation coefficient for diagnostic purpose has not been overcome. This limits the development of this application in the clinical setting.

2.6.2 Monitoring of Bone Fracture Healing

Fracture is a break or interruption of the continuity of a bone (MacNalty, 1965). Though good alignment and

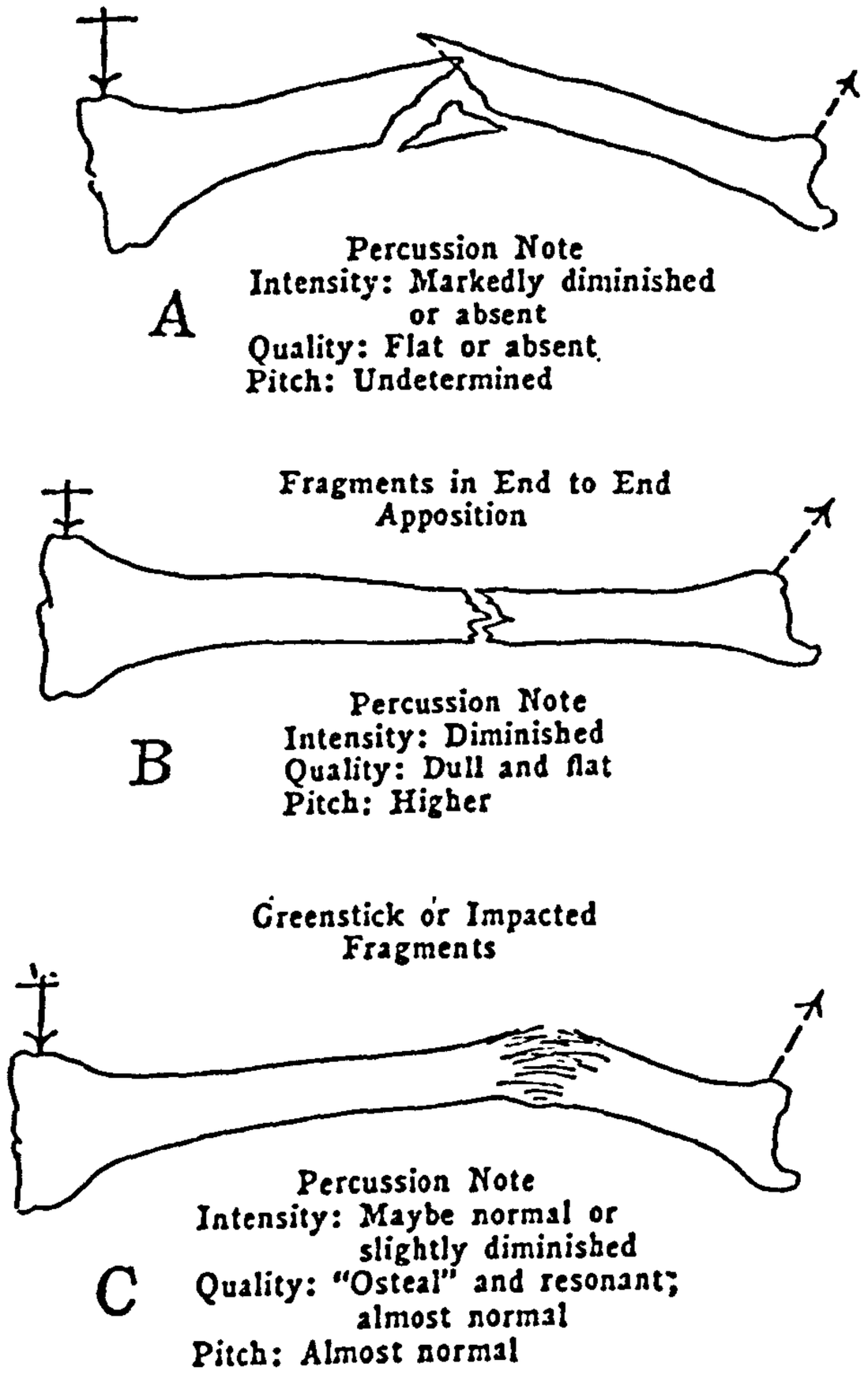

Fig 2.45 Effect of the position of fragments on the percussion note (from McGaw, 1942).

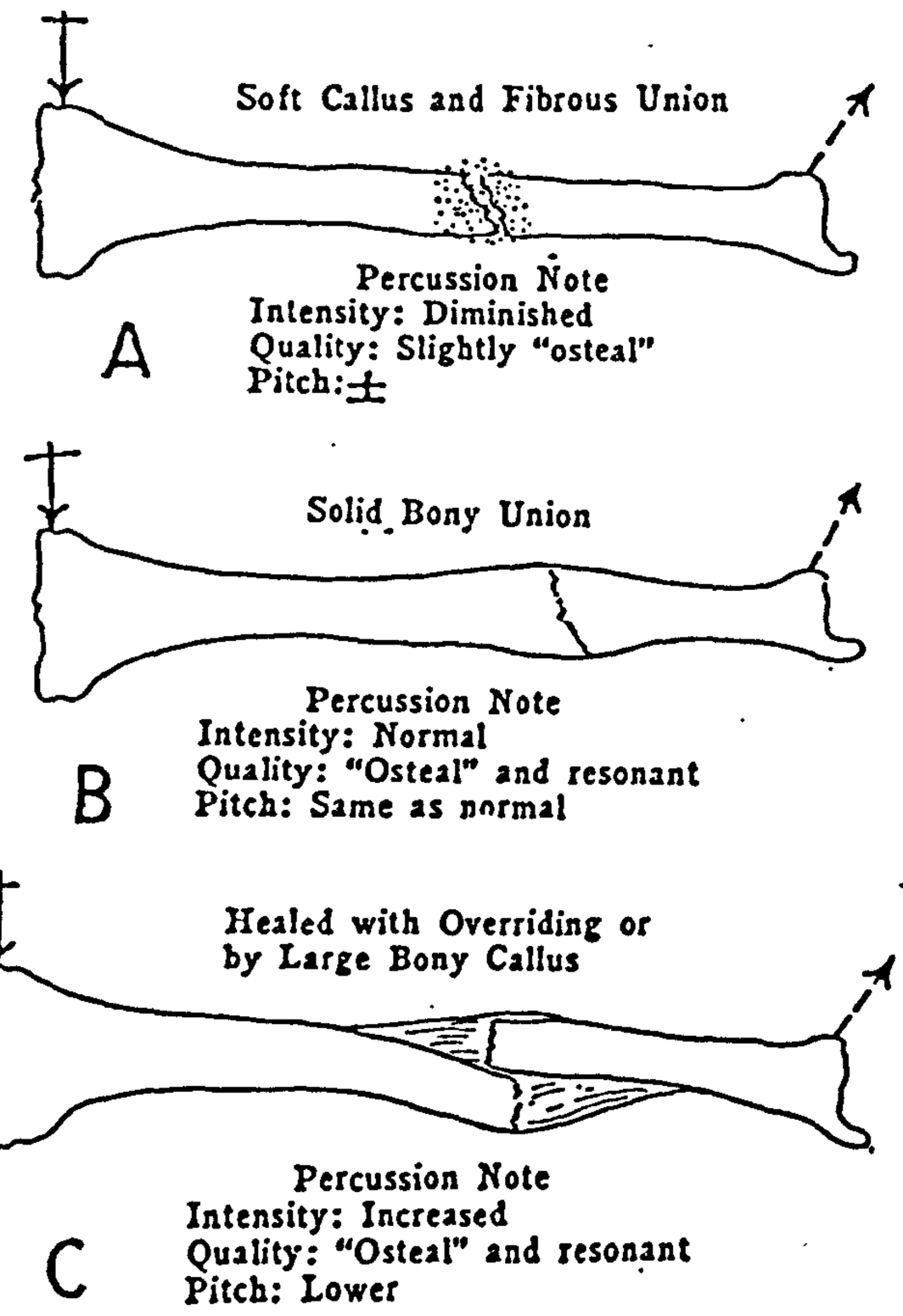

Fig 2.46 Effect of healing on the percussion note (from McGaw, 1942).

secure contact of the fracture segments might have been achieved by suitable medical management, and maintained by muscle tension and external support, the resulting deviation from a normal anatomical and physical characteristics of the bone is definite. A fractured bone demonstrates fragmented bony mass, altered end conditions due to the coupling effect at the fracture site and the swollen surrounding soft tissues. There may also be a gross decrease in mineral content due to disuse. In the course of healing, the fracture site will be gradually bridged by woven bone or fluffy callus to establish union; and further ossification by the formation of solid lamella bone towards consolidation (Apley & Solomon, 1993), the bone then approximates a normal one. These gradual alteration in the mechanical conditions will be manifested as changes in the bone's vibratory characteristics. Acoustical technique would then be in a good position to detect these changes during the course of bone healing. Resonant frequency, wave velocity and attenuation factor are the major parameters which have been claimed to have some clinical value in the diagnosis and monitoring of bone fracture. There has not been any intention to replace the use of radiographic examination which has been well developed as a clinical routine ever since the invention of roentgen rays. It is rather to consider the acoustical technique as an objective method supplementary to conventional procedure. Vibration techniques fall within two major categories regarding the methods of excitation:- impact and vibration testing. Measurement of the mechanical impedance and vibration mode shapes of fractured bones have also been reported.

Impact Testing. Early use of vibration technique in the diagnosis of fracture in long bones dated back to the 30's or probably earlier. Lippmann (1932) outlined the physical principles adopted in the clinical use of auscultatory percussion for the examination of bone fractures and McGaw (1942) reiterated the usefulness of percussion-auscultation technique. This technique had been

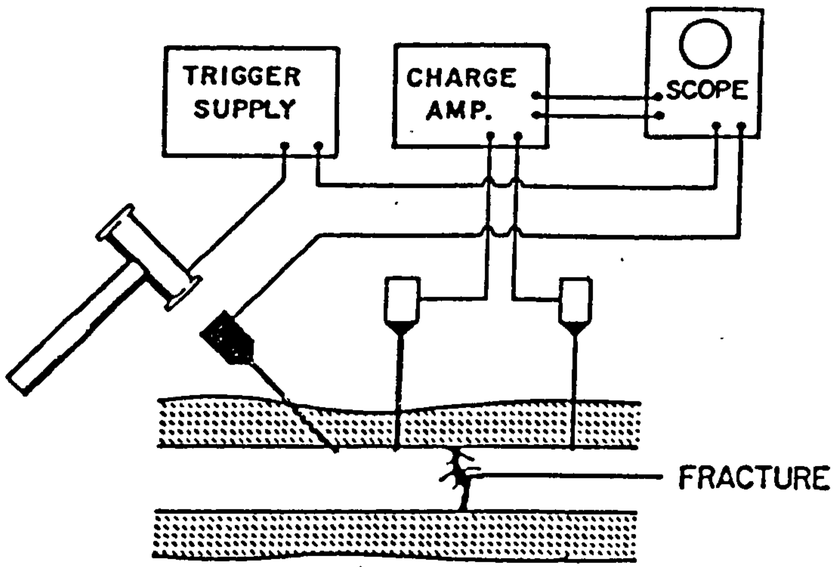

Fig 2.47 Technique as utilized with an impulse source imparted at the excitation needle (from Sonstegard & Matthews, 1976).

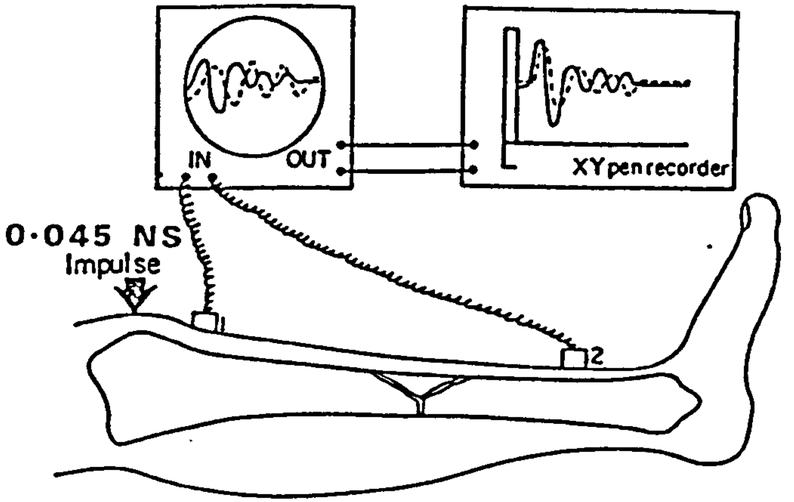

Fig 2.48 Apparatus for the measurement of vibration response (from Nokes et al, 1985).

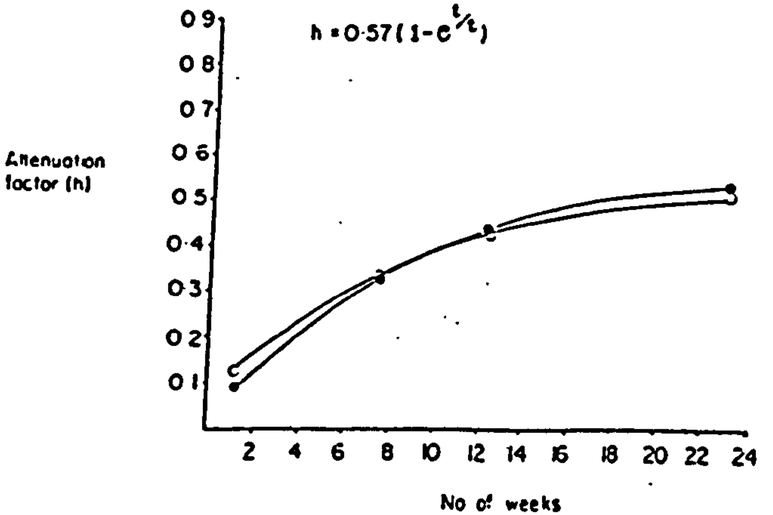

Fig 2.49 Attenuation factor versus time after fracture (from Nokes et al, 1985).

employed in helping diagnosis, to check reduction, and to monitor bone healing during subsequent follow-ups. It was explained that if an intact long bone is being percussed or struck by an impact force at its bony prominence, vibration will be set up and the sound picked up at the other end through auscultation, or by the use of suitable device has a moderate resonance of high pitch, and with an "osteal" quality characteristic of the bone's physical quality, e.g. elasticity. An intact bone was found to give a sharply distinct and resonant tone which was transmitted mainly through the bone and the joint. In a fractured bone, each fragment has different size, shape, and mass to the intact bone. The response of the fragments to percussion will demonstrate unique vibratory characteristics, and hence alter the quality and pitch of the sound detected through auscultation. It was found to demonstrate a soft, dull and non-resonant tone. However, the intensity of transmitted sound is directly related to the bone's ability to conduct vibration, and it would need only a slight bony contact at the fracture site to effect a good conduction. Therefore a fractured bone may not necessarily demonstrate marked reduction in the conduction amplitude, unless the fragments are sufficiently separated. Both the quantity and quality of the auscultation note were found to change, and get closer to a normal tone during the course of bone healing, and they varied with the type of fracture, the position of fracture and the degree of healing (fig 2.45 & 2.46).

Systematic impact testing was carried out by Sonstegard and Matthews (1976). Hypodermic needles were employed to allow direct application of an impact force onto the bone, and simultaneously pick up the response at two points over opposite sides of the fracture site in a long bone (fig 2.47). Amplitude ratio, slope ratio, and propagation velocity were determined from the output signals. Clinical experience on 11 patients had shown that the technique was suitable and capable of identifying the non-union cases. Nokes et al (1985) employed a similar

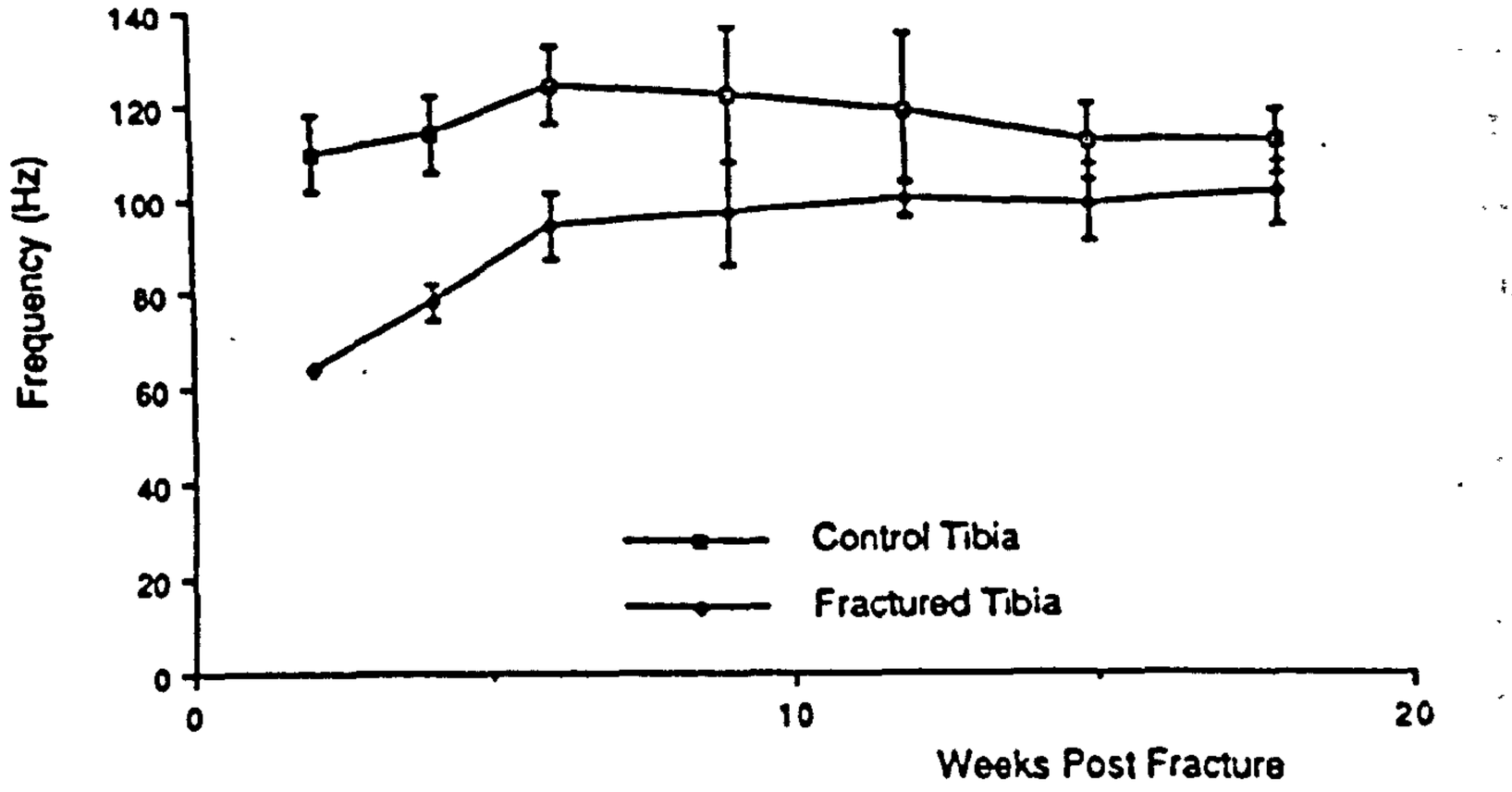

Fig 2.50 Frequency of rigid-body vibration with time after fracture (from Cunningham et al, 1990).

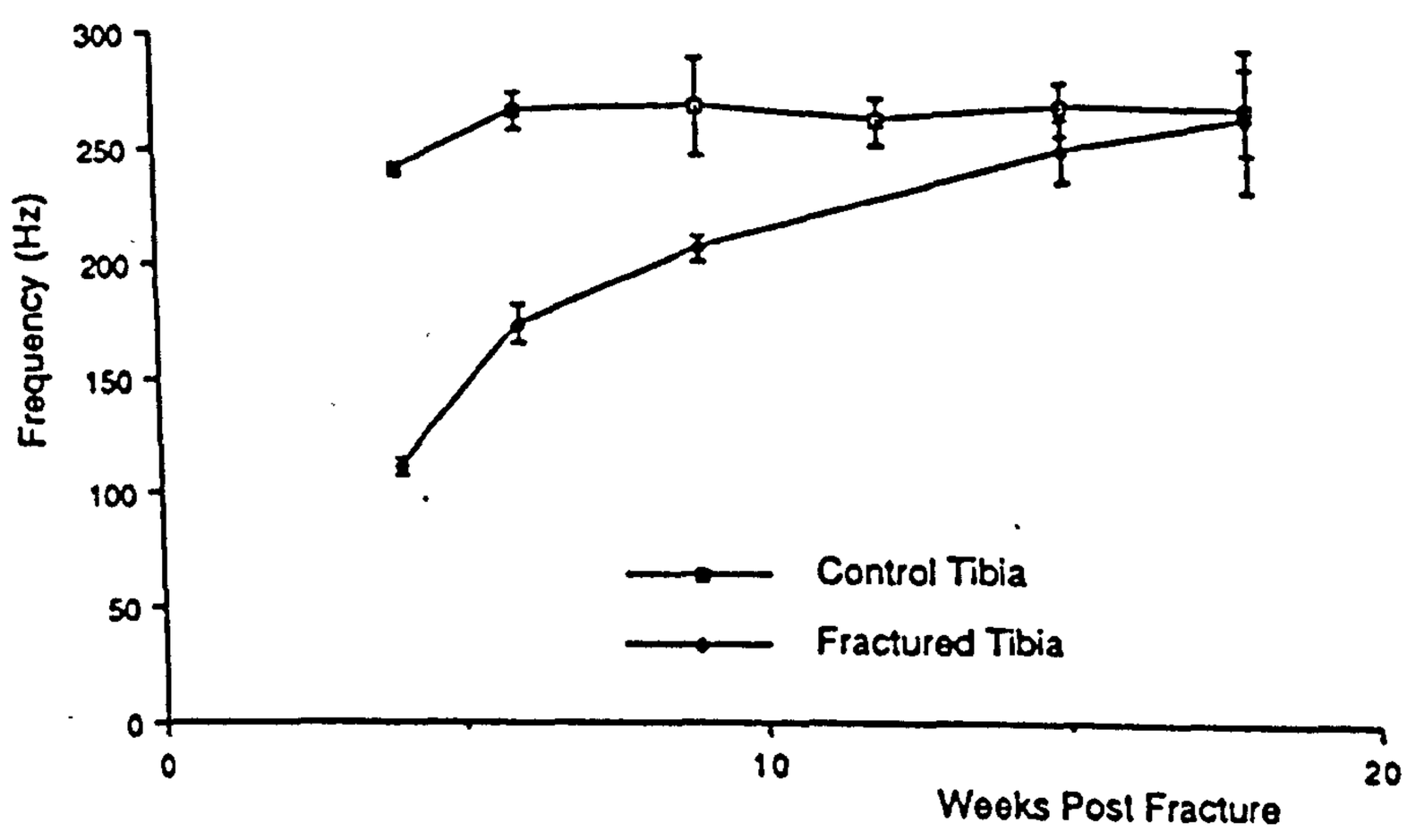

Fig 2.51 Frequency of the first single bending vibration mode with time after fracture (from Cunningham et al, 1990).

technique with non-invasive detection of the response signals over two points on opposite sides of a bone fracture (fig 2.48). Attenuation factor h, defined as the amplitude ratio of the distal to the proximal signal was found to correlate well with the clinical and radiological findings of bone union, and it levelled at a mean value of 0.57. It was a useful index of the healing state of the fracture (fig 2.49). The use of a wave analyzer has been reported by Sekiguchi and Hirayama (1979) in a frequency analysis of the percussion note produced on fractured tibial bone. The patterns of the frequency spectra were examined, and they showed marked attenuation in the high frequencies when compared with the intact bone. As the fracture healed, the frequency spectra improved and approached the normal ones. The technique was also found useful in identifying cases of delayed union which did not show any improvement after a sufficient length of time. Doemland et al (1986) developed a microprocessor-based analysis system to obtain the power spectrum, via the Fourier transform, of the impulse response of a fractured bone. The resonant frequency determined from the frequency spectrum was found to have clinical value as an indication of the stiffness of the bone fracture, and hence the state of healing.

Cunningham et al (1990) described the use of an impact testing technique to determine the rigid-body and the first bending vibration mode of the fractured tibia. The modal frequencies of the fractured bone was always lower than the intact one, and the discrepancy decreased with healing. The rigid-body and 1st single bending mode were found to approach normal at about 18 weeks post-fracture (fig 2.50 & 2.51). In a case of delayed union, the frequency was found to converge after bone grafting, reflecting a gain in the mechanical integrity of the bone fracture. The group also described the use of three different techniques for biomechanical measurement of fracture healing. They were fracture stiffness measurements i.e. deflection under a

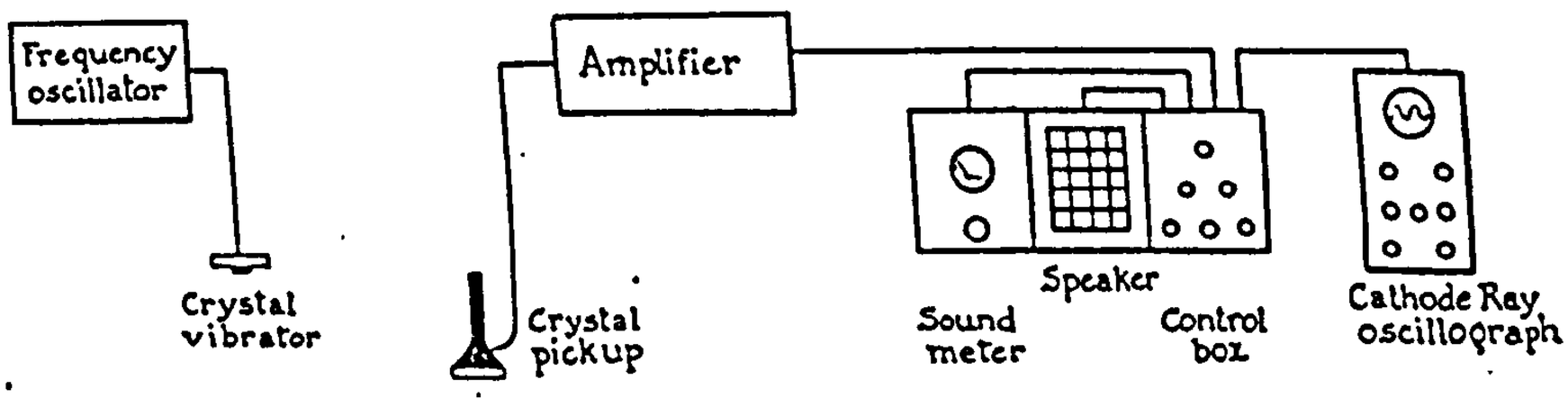

Fig 2.52 Vibration technique to measure the intensity of transmitted vibration through bone fracture (from McGaw, 1942).

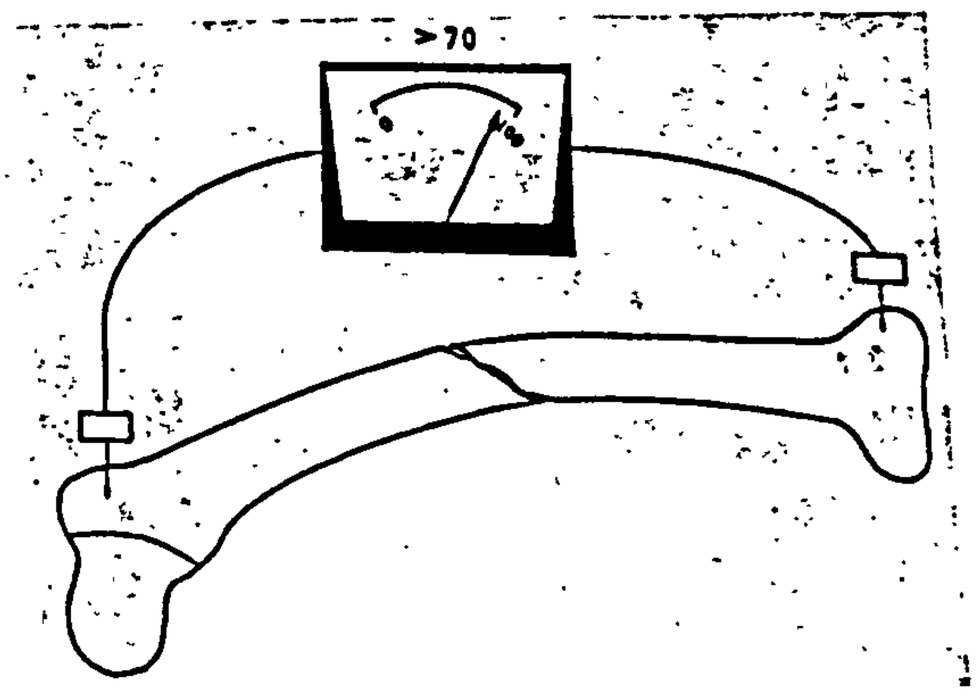

Fig 2.53 Conduction across fractures in which the bone ends are in contact (from Dencker & Moberg, 1968).

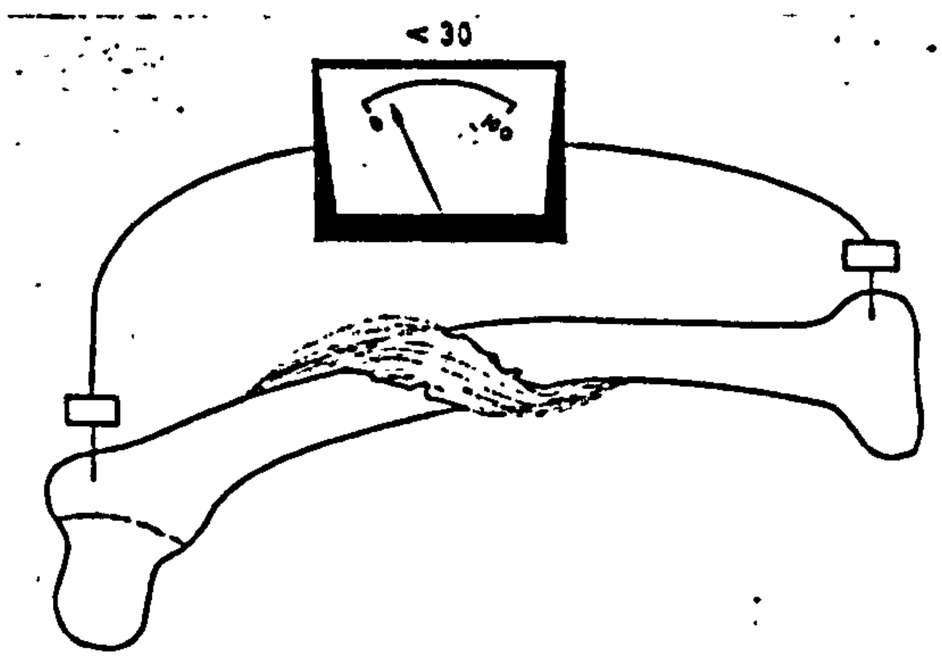

Fig 2.54 Conduction across fractures with soft tissue interposition (from Dencker & Moberg, 1968).

known applied load, vibration measurement using impact testing, and the measurement of transmission velocity of ultrasound. A comparison based on the merit of applicability and practicality of the three techniques has been made. However, there was no direct comparison of the findings obtained by the three different techniques concurrently on the same group of subjects.

Vibration Testing. McGaw (1942) also measured the intensity of the transmitted sound by using an electronic system which comprised a crystal vibrator as the source of excitation, a crystal pick-up incorporating an amplifier system, and an oscilloscope for the display of acoustical signals (fig 2.52). The radiographic image, auscultation-percussion note, and the intensity "meter" reading were found to have good correlation with each other in the indication of the healing state of the fractured bone. Dencker and Moberg (1968) reported the use of a vibration instrument comprising a transducer which generated vibratory excitation of 1 kHz to the bone, either invasively through a pin or non-invasively through skin. A receiver transducer picked up the vibration level across the fracture site. A weaker conduction amplitude was noticed in a case with interposition of soft tissues, which was confirmed at subsequent operation. Those cases which presented high conduction amplitudes united uneventfully (fig 2.53 & 2.54). Jernberger (1967) applied a vibratory excitation invasively through a nail inserted at mid-shaft of the tibia. Vibration levels at two points, proximal and distal to the vibration source were picked up by microphones attached to the bone with nails. The transmission was found to be markedly reduced when measured at a point distal to an unstable fracture in the bone. However, Jernberger (1967), and Dencker and Moberg (1968) reported the insufficiency of the measurement of conduction amplitudes because only a trivial bone contact of the fracture fragments was needed to effect good transmission. Hence this technique could only differentiate a fracture

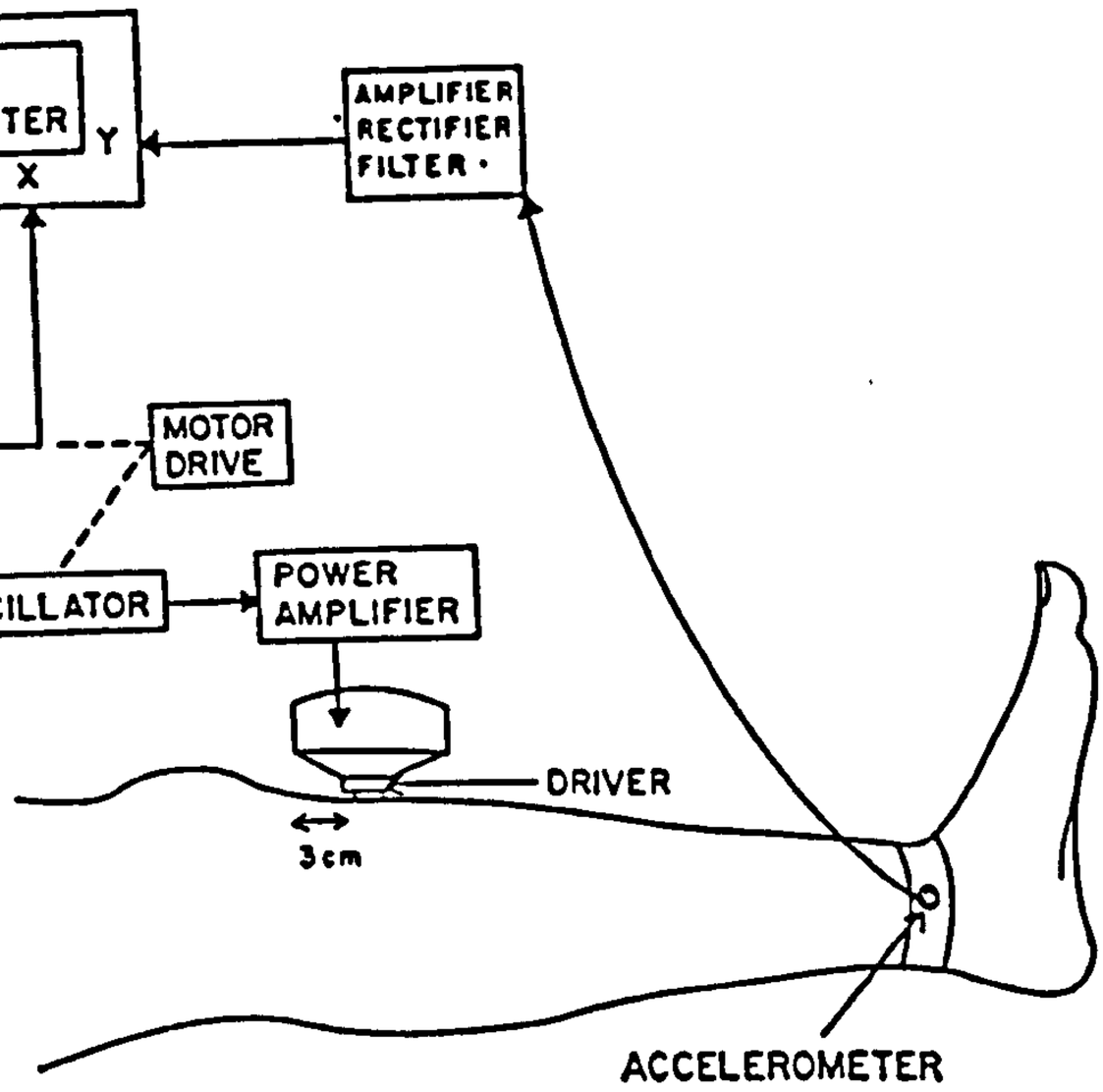

Fig 2.55 Apparatus for measurement of tibial resonant frequency (from Markey & Jurist, 1974).

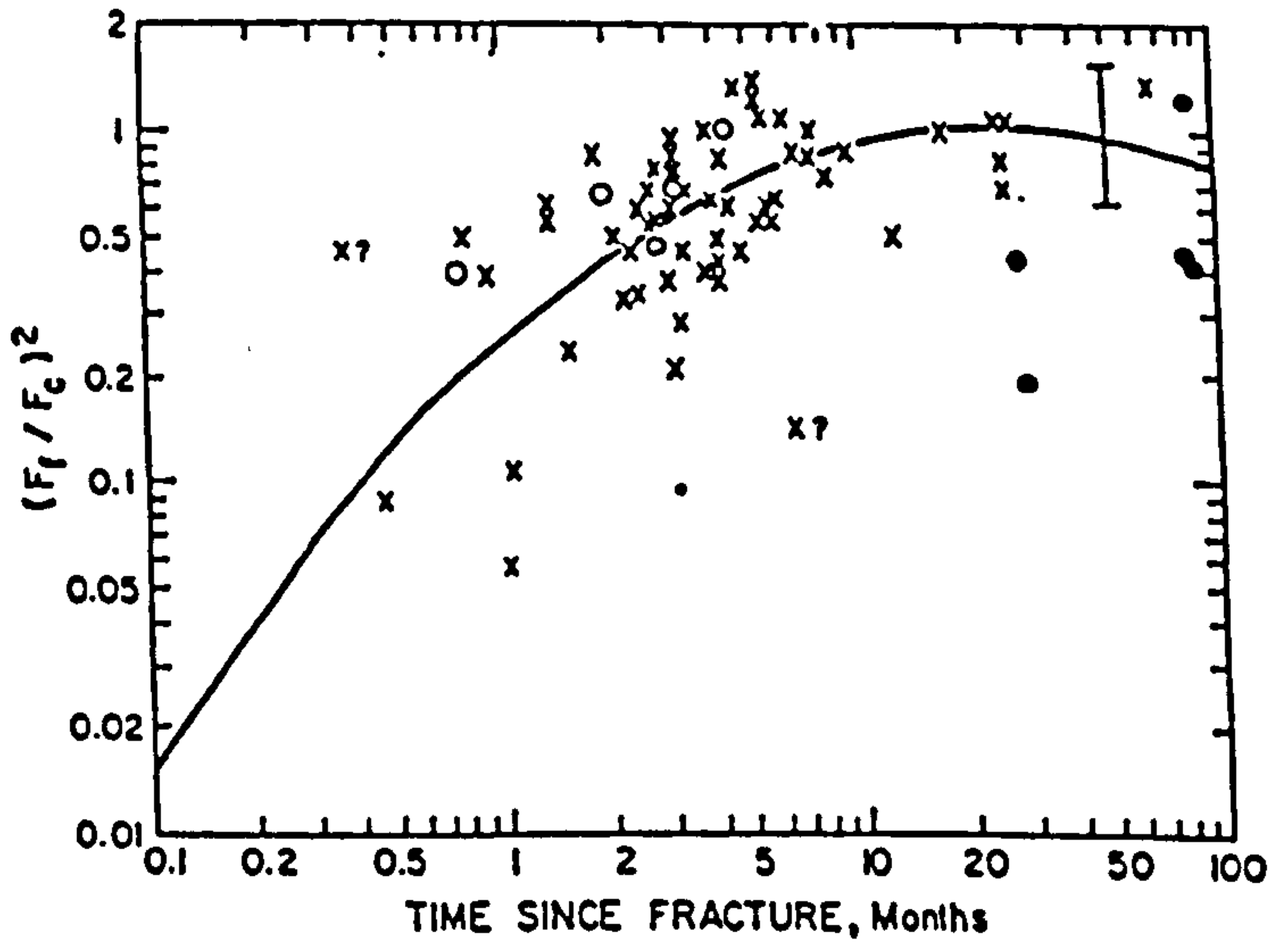

Fig 2.56 $(F_r/F_o)^2$ value versus time since fracture (from Markey & Jurist, 1974).

with sufficient separation of bone fragments, e.g. one with interposition of soft tissues, or under excessive distraction. The detection of cracks in bone using vibration technique is difficult in practice.

Resonant frequency has been used as an indication of bone fracture, and also as a parameter to monitor the stage of healing. The physical principles of this technique are again based on the altered mechanical properties such as mass, stiffness, and end conditions of the bone fragments against an intact bone. These changes in mechanical properties or environment will be manifested as alterations in acoustical properties. Resonant frequency of a fractured bone will shift from a normal one. As times goes on and the fracture healing progresses, so does the mechanical coupling between the bone fragments whose acoustical characteristics will approach that of an intact bone. Vibration techniques for the measurement of resonant frequency entailed the application of a mechanical vibration onto the fractured bone, and accelerometers or microphones were used to pick up response signals from the bone fragments (Markey & Jurist, 1974; Nokes et al, 1984c; Collier & Donarski, 1987b; Singh et al, 1989). The resonant frequency was determined at which the response signals showed the highest amplitudes. Markey & Jurist (1974) determined the square of the resonant frequency ratio $(F_f/F_c)^2$ where, F_f and F_c are respectively the resonant frequencies of the fractured and contralateral intact bone (fig 2.55). The ratio progressed with time since fracture, and was found to correlate with the estimated strength of the fracture and the score of union, based on roentgenographic findings and standardized criteria (fig 2.56). The ratio was suggested as a valid index of fracture healing. Collier & Donarski (1987b) noticed the dropping of resonant frequency of a fractured bone with respect to an intact one. The shift back towards normal resonant frequency in association with an increase in high frequency response suggested regaining in strength of a healing bone.

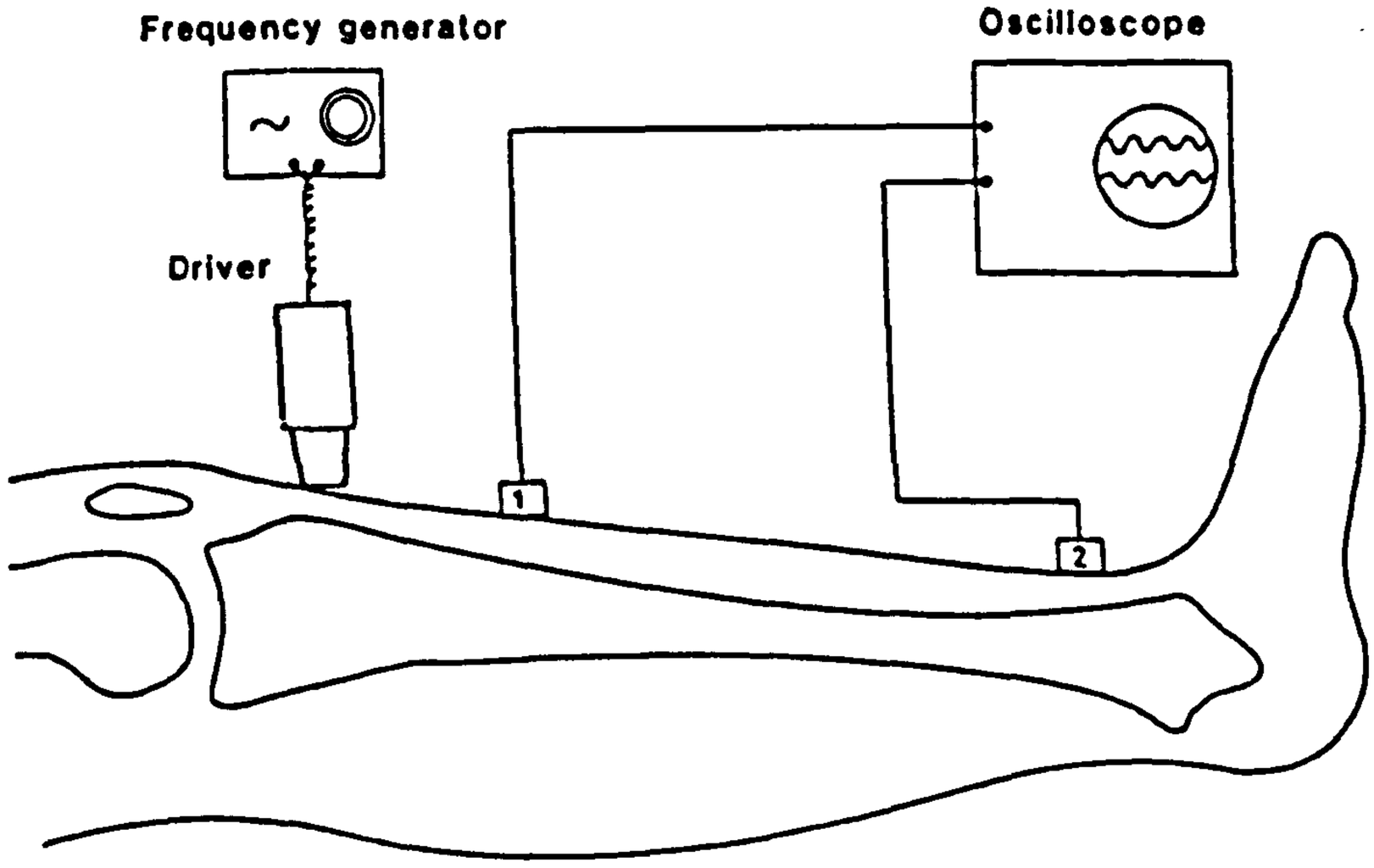

Fig 2.57 Apparatus for measurement of resonant frequencies of fracture fragments (from Nokes et al, 1984c).

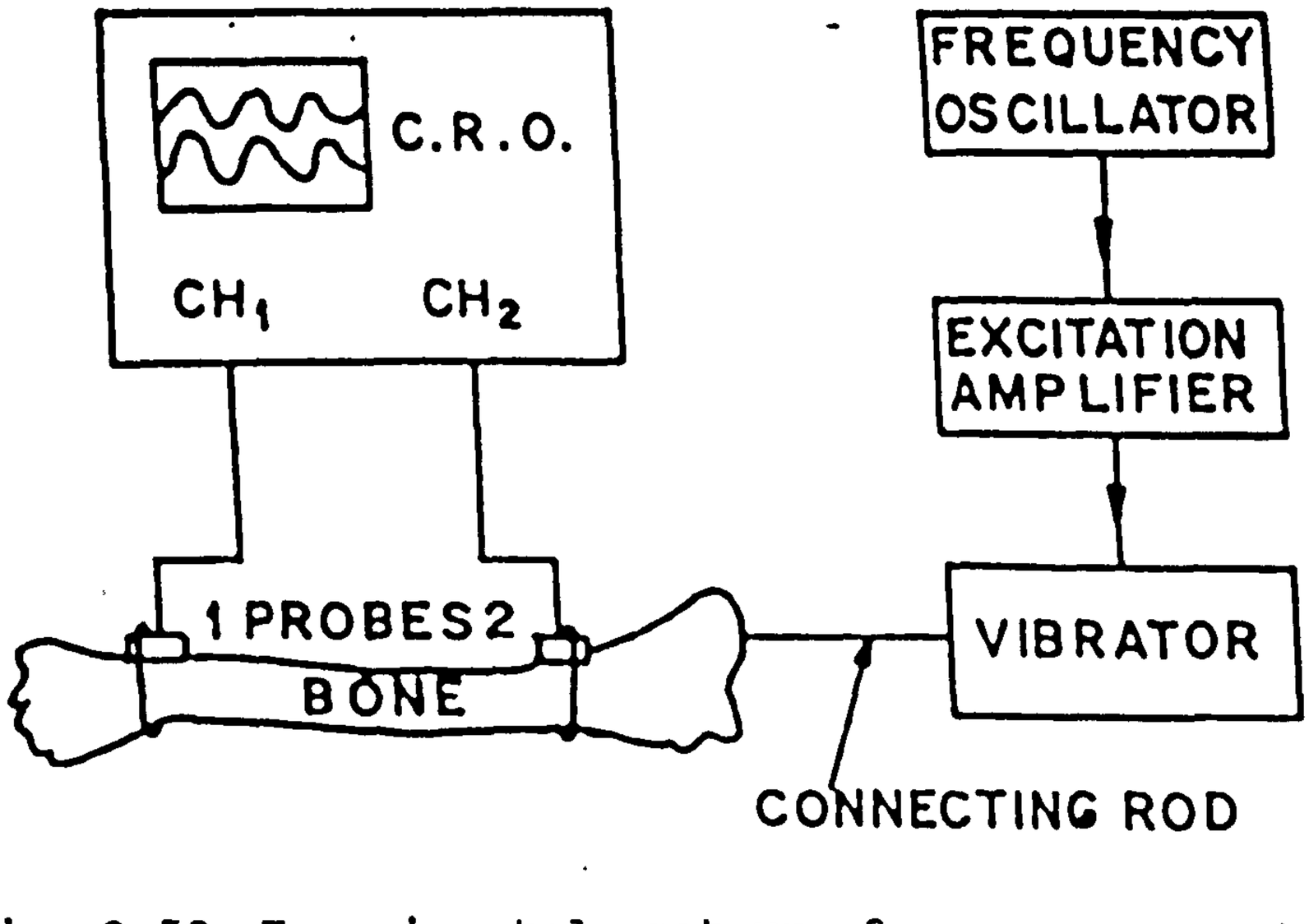

Fig 2.58 Experimental set-up for measurement of resonant frequencies of fracture fragments (from Singh et al, 1989).

Nokes et al (1984c) and Singh et al (1989) compared the resonant frequencies of the proximal and distal fracture fragments (fig 2.57 & 2.58). It was noticed that the discrepancy narrowed when the bone was healing. Nokes and associates (1984c) also established a mathematical model which describes the mean frequency difference Y in Hz as a function of time t in days after fracture: where $Y = 170(0.9053)^t$. This model was also found to fit closely with the experimental data as well as the clinical and radiological findings in the events of successful union of mid-shaft fracture of the tibia. The general applicability of this technique was still uncertain. However, Singh et al (1989) noticed the incapability of the resonant frequency technique to detect hairline fracture or impacted fracture in which the fracture fragments had already gained sufficient bony contact, and hence the acoustical behaviour showed no significant difference from an intact bone. This incapability corresponds to that same problem associated with the measurement of conduction amplitude discussed previously.

Resonant frequency of a fractured bone could also be determined by the simultaneous measurements of the velocity and the driving force at the point where the bone is excited. Matthews et al (1989) computed the ratio of amplitude of the response velocity to the forcing vibration as a function of frequency. An isolated fracture of the tibia showed a lower resonant frequency than the uninjured one. The difference was more pronounced, and the second resonance at higher frequency was absent with fracture of both the tibia and fibula. The resonant frequency was found to gradually increase to normal when the fracture healed.

Nikiforidis et al (1990) observed strong coupling between the lateral and axial vibration of a fractured tibia, which suggested non-uniformity in the stiffness of the bone at the fracture site during healing, by referring to an established analytical model. Subsequent radiological examination confirmed the findings.

2.6.3 Identification of Joint Problems

Arthritis developed in the course of degeneration and ageing, or as a result of joint pathologies (e.g. rheumatism) are inevitably accompanied by destruction of the joints to various extent (Apley & Solomon, 1993). The articular cartilage and the subchondral bone are particularly vulnerable. Associated involvements of the joint include: thinning of articular cartilage due to persistent wear and tear, roughening of the articular surfaces and damage to the subchondral bone. Without early intervention, mechanical disorders arise from these pathological changes, insidious destruction, or direct trauma to the fine structures of the joints, for examples in sports injuries, would lead to advanced mechanical derangement. Early detection of mechanical disorders or malfunctions could be accomplished by the detection and interpretation of a clinical observation described as vibration emission (Mollan, 1981). Human joints when set in motion emit vibrations which could be felt through manual contact or through auscultation by using a stethoscope over the joint. The observation of these subclinical signs has been claimed to have diagnostic value (Kernohan et al, 1986). The following paragraphs attempt to outline the development from an acoustic technique in the early days to a vibration technique which is more ready for clinical application.

Acoustic Techniques. Though simple in its construction, a stethoscope can be considered as an acoustic instrument, perhaps the very first device of this nature available to the medical profession. Early acoustical study of the mechanical disorders of the peripheral joints involved solely the use of the stethoscope for auscultation. The earliest recording of sounds emitted from human joints was reported by Blodgett (1902) who detected the sound generated within the knee joints through auscultation. Dots, vertical strokes and dashes were used to record the occurrence of three distinct

types of sounds which were described respectively as snapping, creaking sound; rough and coarse grating sound, and squeaking sound. The sounds were recorded with respect to the joint position. It was found that both the quantity and quality of the emitted sound were related to the pathology of the joint as well as the age - joint sound was increased in old people. Walters (1929) described the joint sounds obtained through auscultation as smooth, rough, grating. It was found that the degree of grating was related to clinical signs and symptoms and that there was a steady trend of increase in severity with age.

With the advancement of electronics, microphones in association with amplifying and filtering systems become available for recording joint sounds. A more systematic recording of joint sounds was made by Steindler (1937) who used a cardiophone (modified microphone) to pick up sounds emitted from the knee joint. The amplified signals were then suitably filtered and displayed on an oscillogram together with information of the joint position and a time-trace. The intensity and characteristics of the joint sounds were studied for a range of joint conditions. The technique was able to locate the origin of sound by repeated measurements on the four quadrants defined over the patella, and by referring to the position of the joint. Peylan (1953) used a type of "throat microphone" which picked up the joint sounds from contact with the skin, such that the system was relatively free from ambient noise. The system consisted of an amplifier with independent control of the amplification of high and low frequencies. Direct auscultation was made for a range of rheumatoid and related joint conditions. Various types of characteristic joint sounds were detected, and were found to have explainable anatomical and pathological backgrounds.

In the 60's and 70's, there was no significant advancement in the auscultation of joints except in the methods of storage and analysis of the sound signals. The microphone was still the only feasible sensor for joint

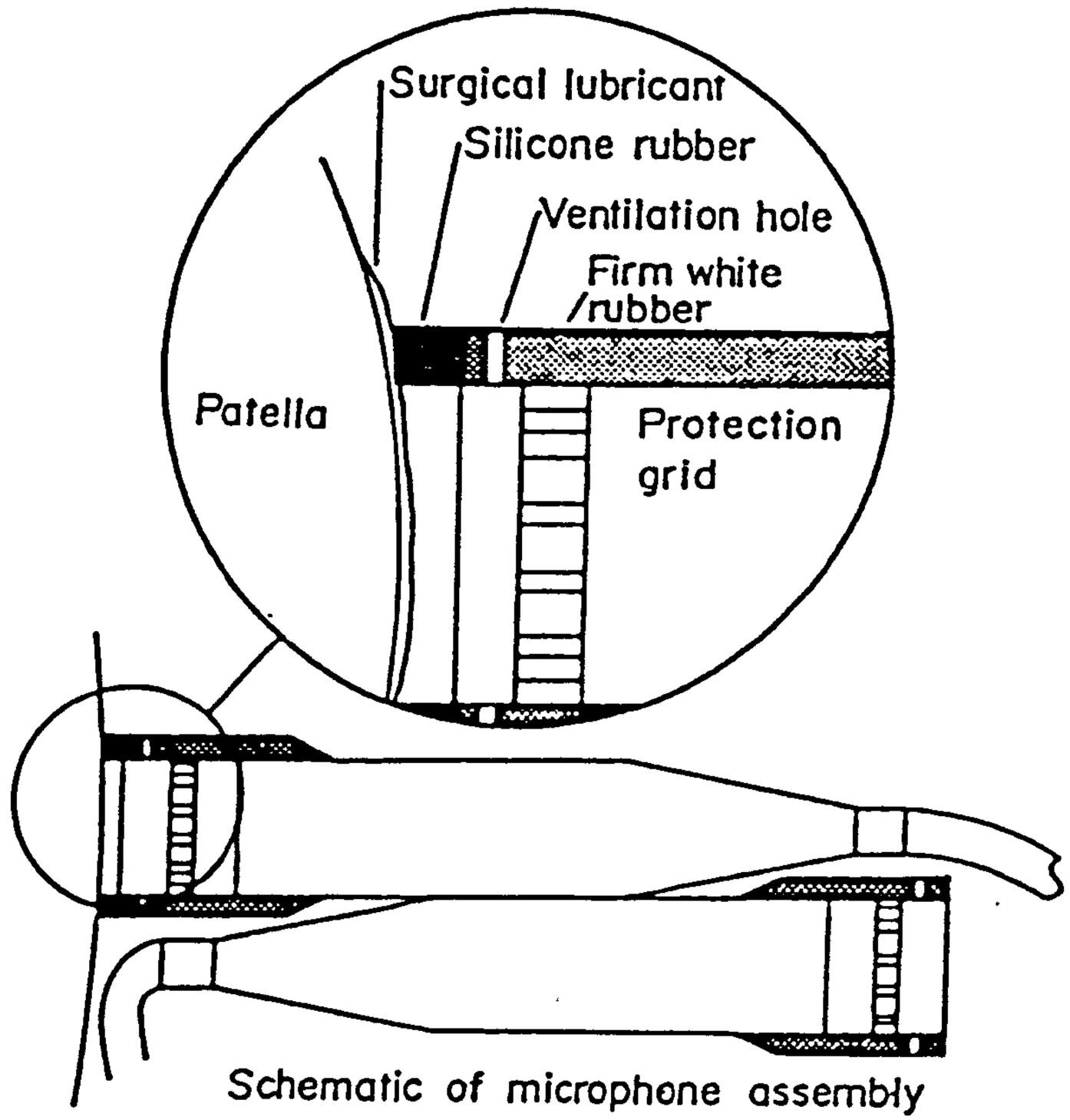

Fig 2.59 Double microphone assembly (from Chu et al, 1976a).

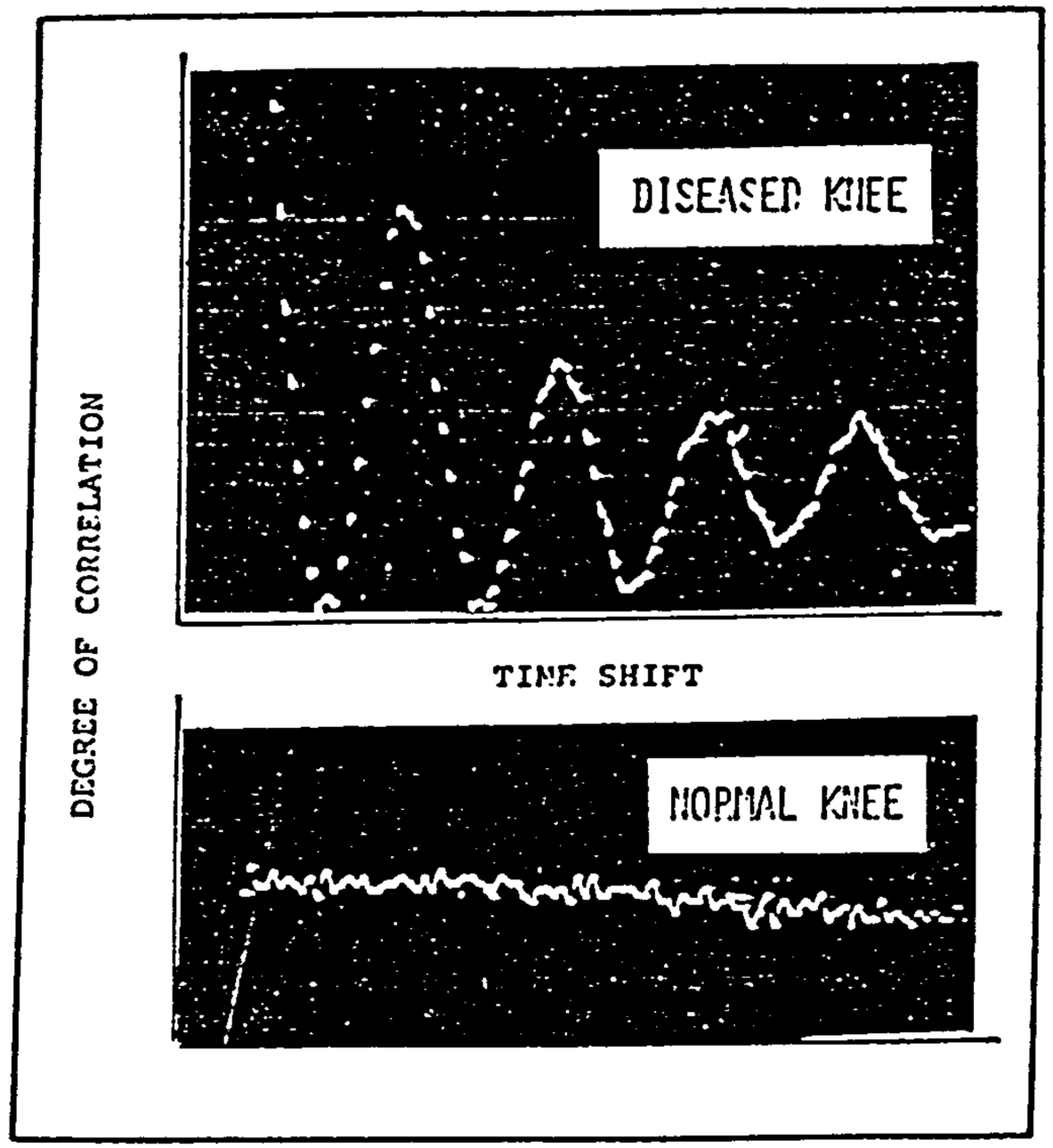

Fig 2.60 Typical normal and diseased knee autocorrelation function (from Chu et al, 1976b).

sounds. Fischer and Johnson (1960) used a microphone incorporated in a rubber bell attached over the patella by suction. Joint sounds picked up by the microphone were recorded on photographic paper, while the position of the knee joint was registered. The waveform was also integrated and summated continuously at regular one-second intervals to indicate the intensity, and was then analyzed by a frequency analyzer. The characteristics of joint sounds in terms of the regularity, intensity and frequency of sounds were compared for normal, rheumatoid, and degenerative knees. Degenerative knees showed distinct characteristics in its high frequency, high intensity bursts recorded at regular intervals. Rheumatoid patients showed an irregular pattern of low frequency, with occasional bursts of higher frequency. Chu et al (1976a) reported the design of a double microphone assembly for noise cancellation, so that the detected joint sounds were relatively free from ambient noise (fig 2.59). The characteristic acoustical signals for normal, rheumatoid and degenerative knees were recorded by photographic means, while at the same time fed into a frequency analyzer to obtain the power spectrum and autocorrelation function. It was found that the amplitude of the time-record of joint sounds appeared to correspond to the severity of damage of the cartilage, being highest in the degenerative cases. The peak magnitude and band-width of the power spectra were also found to correspond to the severity of the disease. The autocorrelation function of degenerative joint sounds indicated some periodicity, i.e. presence of deterministic signals, while that for a normal joint revealed a random and non-periodic joint sound (fig 2.60). The technique enabled the determination of an acoustical "signature" of the joints, which was found to be related to the type and severity of the disease conditions. A statistical analysis showed high reliability of the technique when compared with diagnosis made by medical personnel.

Mollan (1981) critically investigated the various

technical aspects associated with acoustic technique and evaluated its capability for the detection of vibration emission from peripheral joints. It was found that vibrations emitted from joints were in the extremely low range of audio frequency. In this range, acoustic technique suffered from inherent deficiency in limited dynamic sensitivity and limited frequency response of the apparatus, particularly that of the microphone. It was also difficult to exclude ambient noise in a clinical situation. Mollan et al (1982a & b) also commented that acoustic registration of joint sounds would be problematic if these limitations were not appreciated.

Vibration Arthrometry. Vibration arthrometry is a vibration technique developed with the intention of replacing acoustic techniques for the detection of vibration emission from joints (Kernohan et al, 1990). Accelerometers are used to detect vibration signals by direct contact with the skin over the joint. Commercially available accelerometers could have a frequency response extending well below 1 Hz (Broch, 1984), covering the subsonic range required for the detection of vibration emission, and with an adequate dynamic sensitivity for low vibration level especially at low frequencies. In this frequency range, microphones would suffer technical incapability due to mismatch in acoustic impedance.

Vibration arthrometry has been developed as a diagnostic aid in diseases of the knee joint, and the detail technical aspects have been outlined elsewhere (McCoy et al, 1987). Basically, two major types of knee vibration signals i.e. the transient and continuous ones have been identified, and they have been found to have diagnostic value (Kernohan & Mollan, 1991). The transient type of knee vibration signals can be detected by three accelerometers: one attached over the patella and the others over the medial and lateral femoral condyles (fig 2.61). Active and passive manoeuvres, including McMurray's test (Apley & Solomon, 1993) which involves the medial and

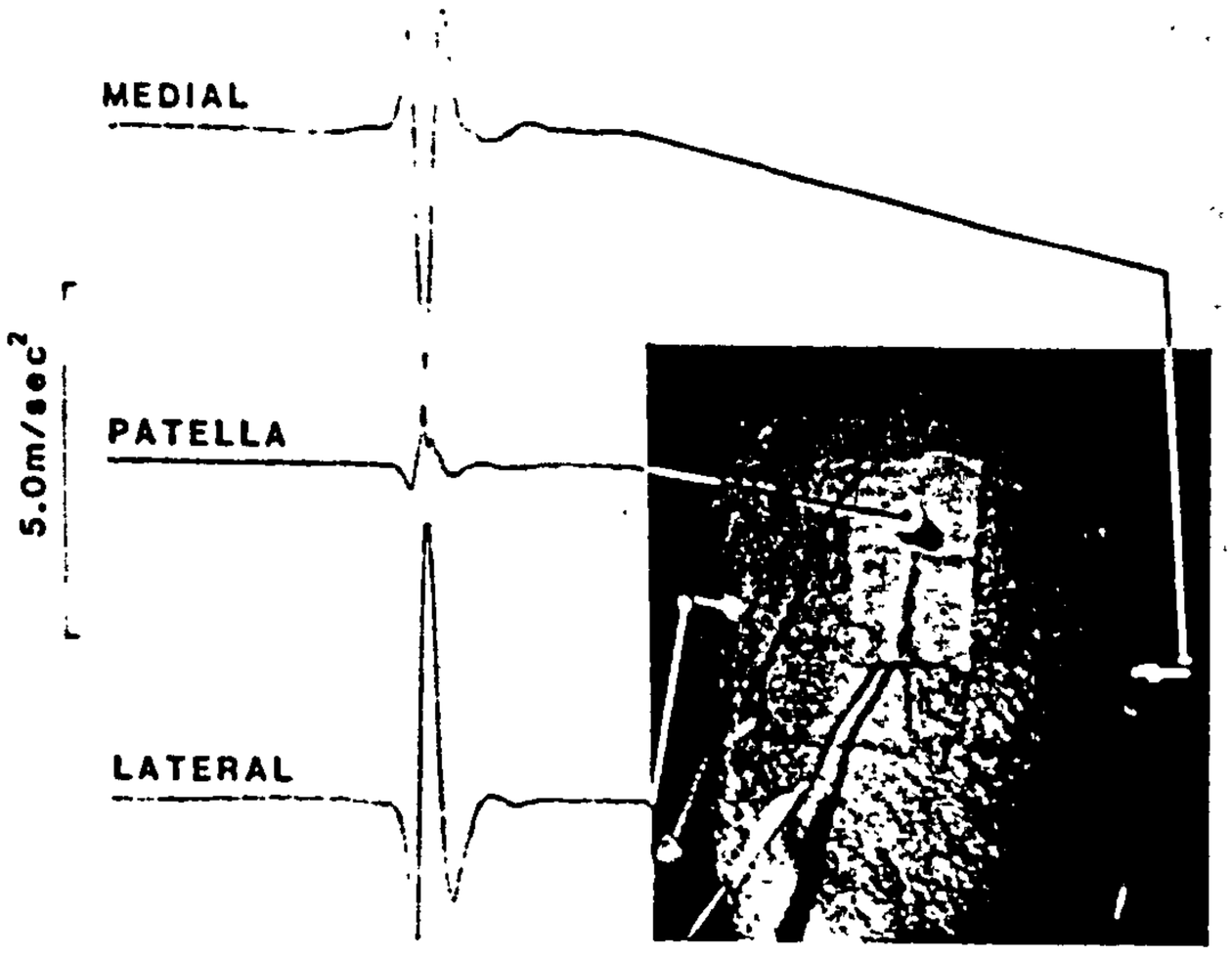

Fig 2.61 Cartilage damage in the menisci was manifested by transient vibrations recording during flexion and extension of the joint (from Kernohan & Mollan, 1991).

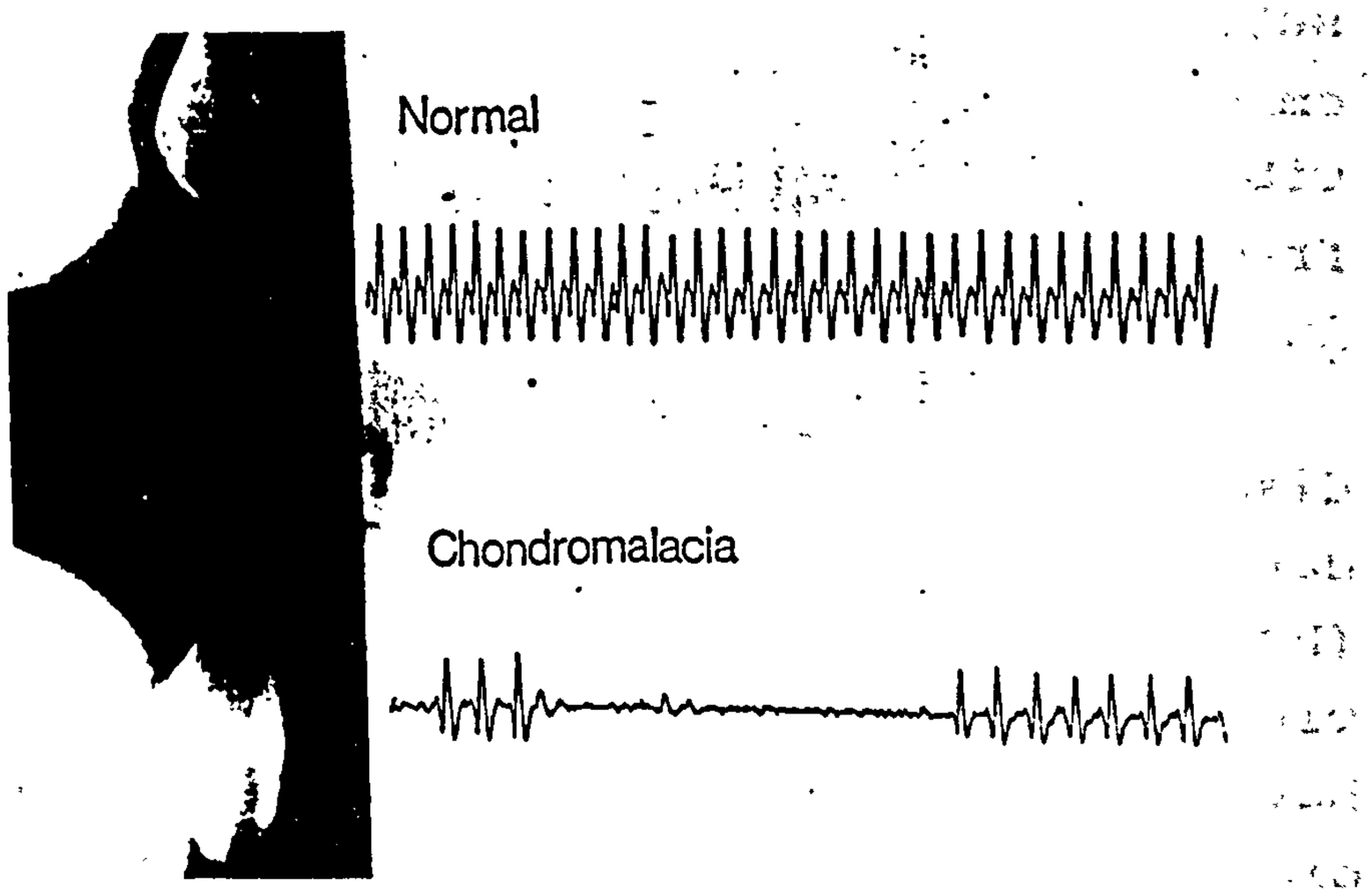

Fig 2.62 Detection of vibration from normal and diseased patello-femoral joint (from Kernohan & Mollan, 1991).

lateral rotation of the leg while the knee is slowly extended, were carried out to elicit the characteristic click indicative of meniscal destruction. The source of origin, or the site of lesion, could be located by examining the relative amplitudes of the signals detected by individual accelerometers. The technique was able to detect 86% of the cases with confirmed diagnosis by arthroscopy (Kernohan et al, 1986). The continuous type, described as crepitus can be explained by a "stick-slip" phenomenon taking place between the articular surfaces of femur and patella when the knee is gently moved at a low angular velocity (Hamilton, 1989). Fine and regular physiological crepitus could be detected continuously on normal knee joints, and was observed to increase substantially after isometric load. The pattern of these continuous knee vibration signals were able to reveal the surface quality of the articular cartilage (fig 2.62). Disrupted and irregular beats were observed in patellofemoral pathology associated with diseased cartilage for example in chondromalacia patellae. Beverland et al (1986) claimed that the technique could be used to quantify joint cartilage degeneration before changes appeared on radiographic images.

Clinical application of vibration emission has been extended to the early screening of congenital dislocation of the hip (CDH). The classical sign of Ortolani's test (Apley & Solomon, 1993) felt as soft "clunk" could be detected when a displaced hip of the neonate reduces upon a gentle abduction force at the affected hip. A sharp "click" may be felt over a healthy hip joint upon the same manual manoeuvre, and an inexperienced examiner might be confused. The vibration arthrometry in this application was based on the acquisition and frequency analysis of the joint's vibration sound emitted during the Ortolani's test or Barlow's test (Barlow, 1962). Vibration signals were detected by piezoelectric accelerometers attached over the greater trochanters and other points around the neonate's

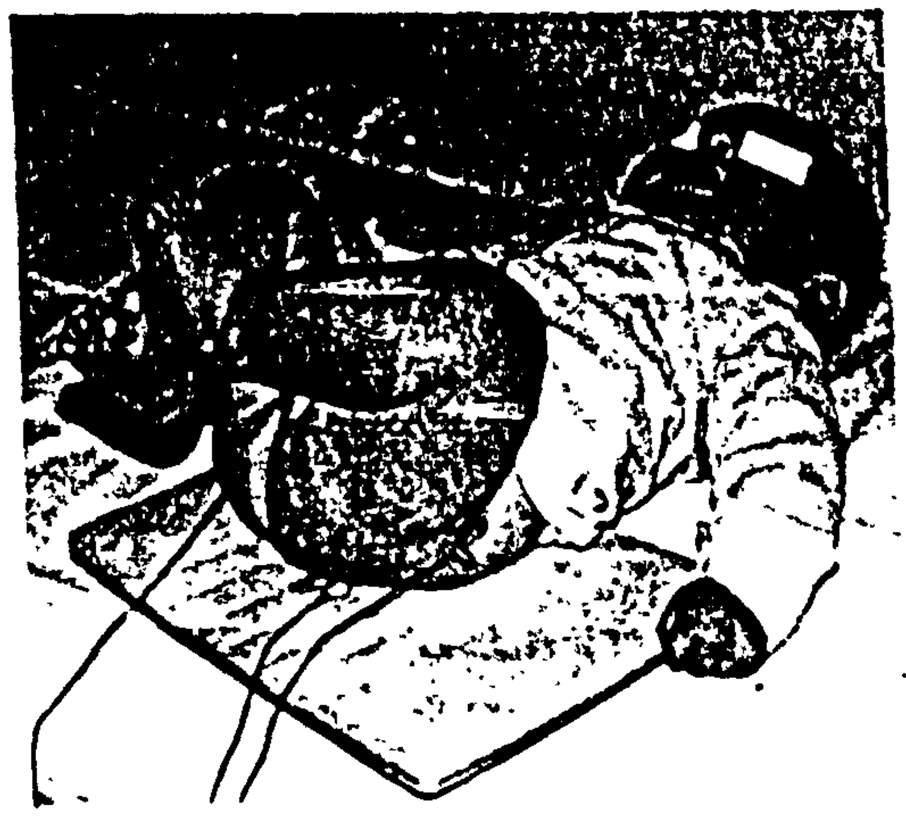

Fig 2.63 Neonate with three accelerometers in position for vibration arthrometry (from Kernohan et al, 1991).

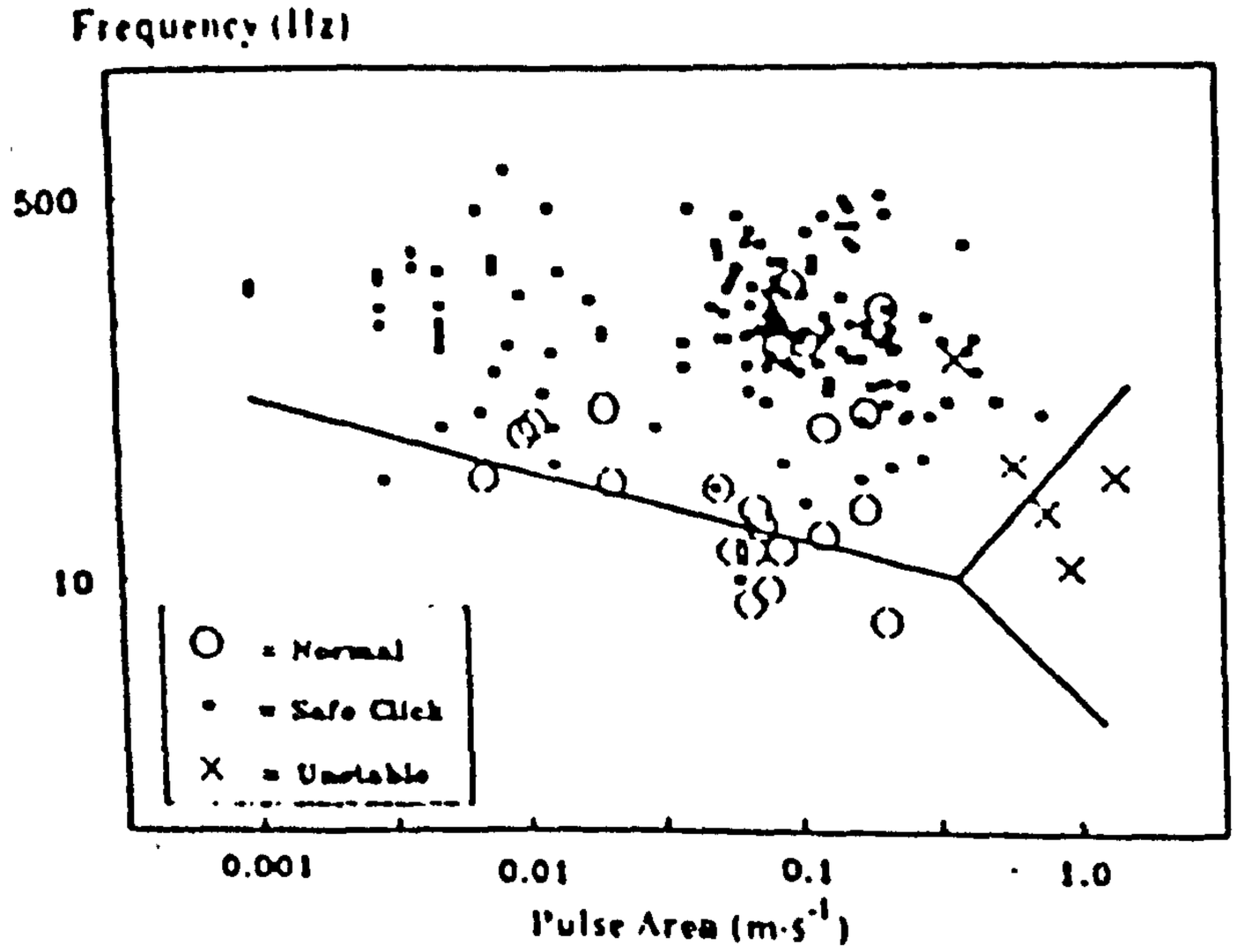

Fig 2.64 A scattergraph of pulse area and frequency content indicates how discrimination lines can be used to aid diagnosis of hip dislocation (from Kernohan et al, 1991).

pelvis (fig 2.63), and then analyzed to obtain the frequency spectra. It was found that the "clunk" produced a low frequency vibration which was significantly different from the high frequency signal of the normal "click" (Cowie et al, 1983). The frequency spectra, in association with other parameters e.g. pulse area and peak frequency were found to have diagnostic power in detecting instability of the neonate's hip (Kernohan et al, 1991) (fig 2.64). The technique was found to have a positive predictive value of 86% and a negative predictive value of 99% with $p < 0.005$ (Kernohan & Mollan, 1991).

It is worth to mention an independent study on the same clinical problem by examining the volume of sound transmitted across the hip joints of the neonates (Stone et al, 1987). A discrete tone generated by a tuning fork was applied over each patella while a stethoscope was placed over the pubic symphysis to listen to the transmitted sound. A reduction in sound transmission suggested a dislocation of the affected hip joint. This technique is still suffering from subjectivity in the evaluation of sound volume, and is lacking detail analysis. It could only be considered as an test adjunct to other clinical examinations. However, this is one of the few examples which utilize acoustic transmission across the joints as a diagnostic tool.

2.6.4 Evaluation of the Integrity of Hip Joint Prosthesis

Aseptic loosening is a common cause of failure for internal prosthesis of the hip. Early detection is difficult, and the loosening might already be too advanced when clinical symptoms and radiological evidence show up. Rosenstein et al (1989) has developed a vibration technique to differentiate a loose femoral component of the hip prosthesis from an intact one. Vibratory excitation of known frequency was applied by a mechanical vibrator at the lateral femoral condyle, while a hand-held accelerometer was placed over the greater trochanter to pick up the

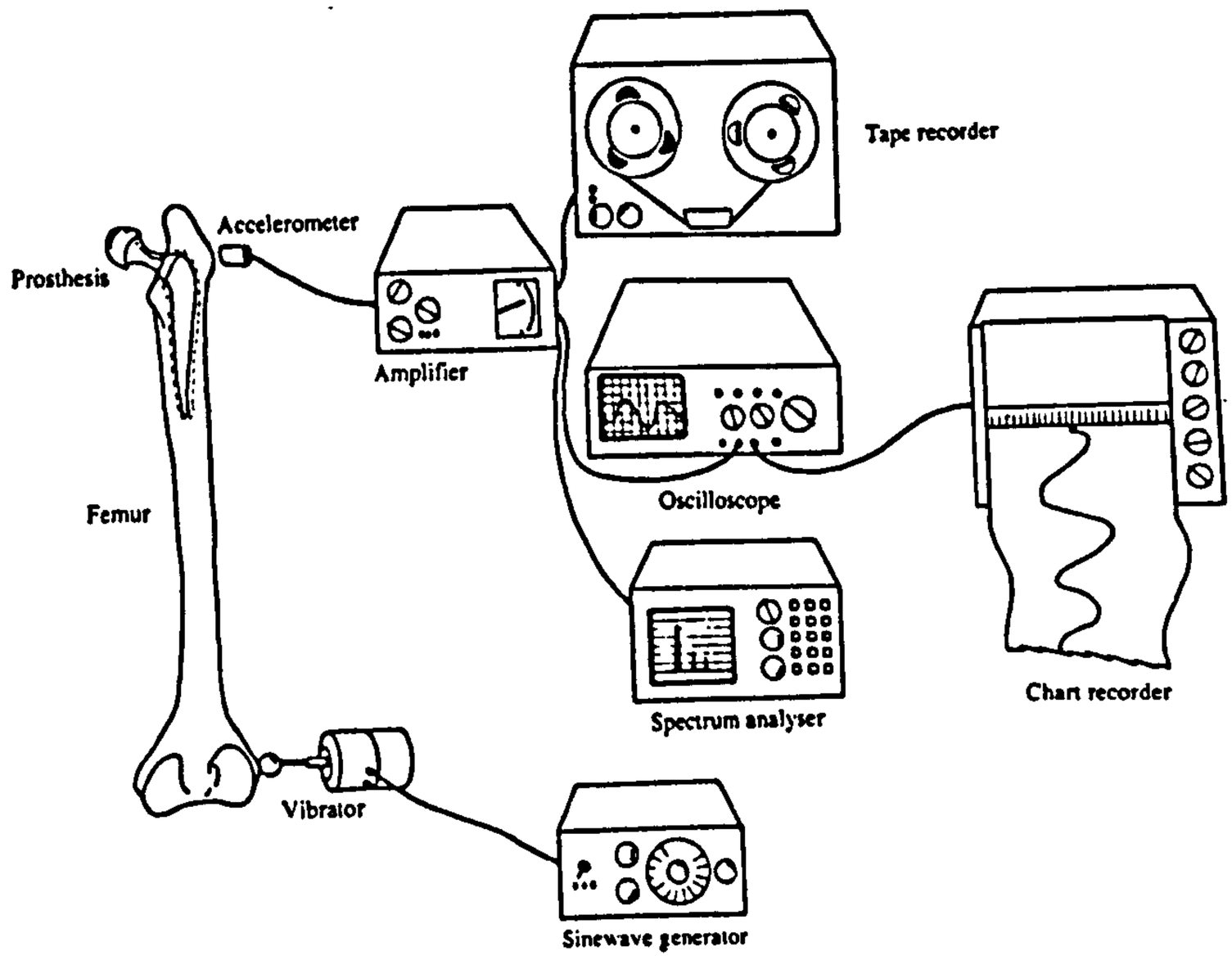

Fig 2.65 Equipment for vibration testing on hip prosthesis (from Rosenstein et al, 1989).

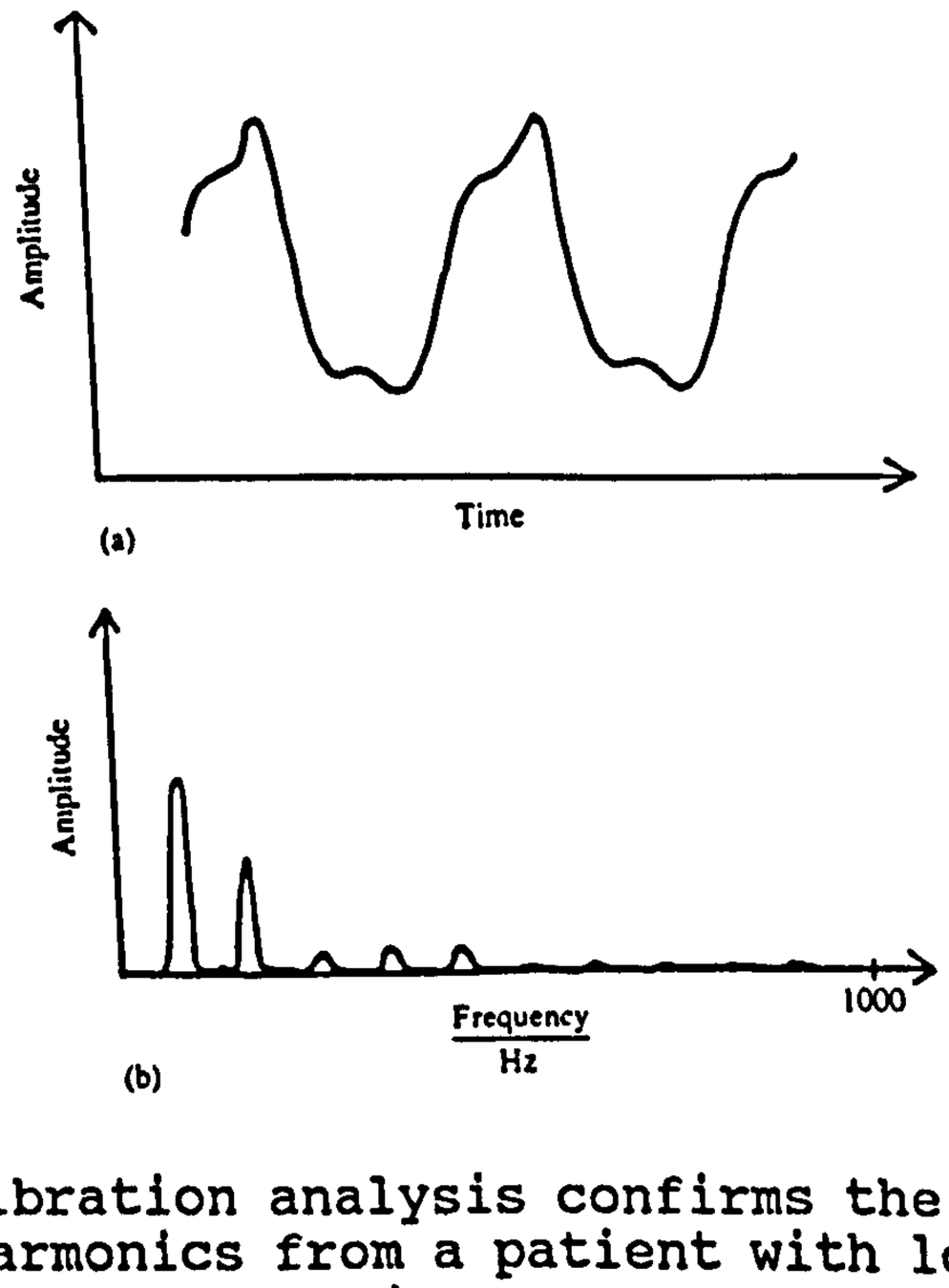

Fig 2.66 Vibration analysis confirms the presence of multiple harmonics from a patient with loose femoral implant (from Rosenstein et al, 1989).

response signals for analysis (fig 2.65). A pure sinusoidal wave was obtained if the prosthesis was secure. A non-sinusoidal wave with multiple harmonics was found on those patients with loose femoral implants (fig 2.66). In all these cases, subsequent operation on the hip confirmed the findings of the vibration technique. The technique was based on the mechanical principle that for a secure prosthesis, the bone and prosthesis vibrate as a single unit. When loosening happens the components respond separately and the mechanical behaviour of the whole system depends on the degree of coupling between the bone and the prosthesis.

Experimental and analytical work by Poss et al (1984) demonstrated the possibility of assessing the integrity of the bonding between hip prosthesis and bone cement (fig 2.67). Vibration tests performed on the prosthesis-cement complex demonstrated two resonant frequencies which were found to separate apart gradually during the course of cement curing. The second harmonic stabilized in approximately 12 minutes after the cement had been cooled to room temperature (fig 2.68). This suggested that the temperature of the curing cement is not a reliable indicator of the state of polymerization of the bone cement. It was also suggested that the vibration technique could be used during the operation to evaluate the firmness of cement fixation as well as a post-operative measurement to form a baseline against which future reference can be made.

2.6.5 Aetiological Study of Back Problems

The transmission of shock and vibration in the spine has been the major concern in industrial health and safety as well as in vehicular transportation. Pope and Hansson (1992) summarized a series of epidemiological factors of low back pain (LBP). It is apparent that exposure to whole-body vibration in some occupations e.g. truck or tractor driving showed some relationship with LBP, and the

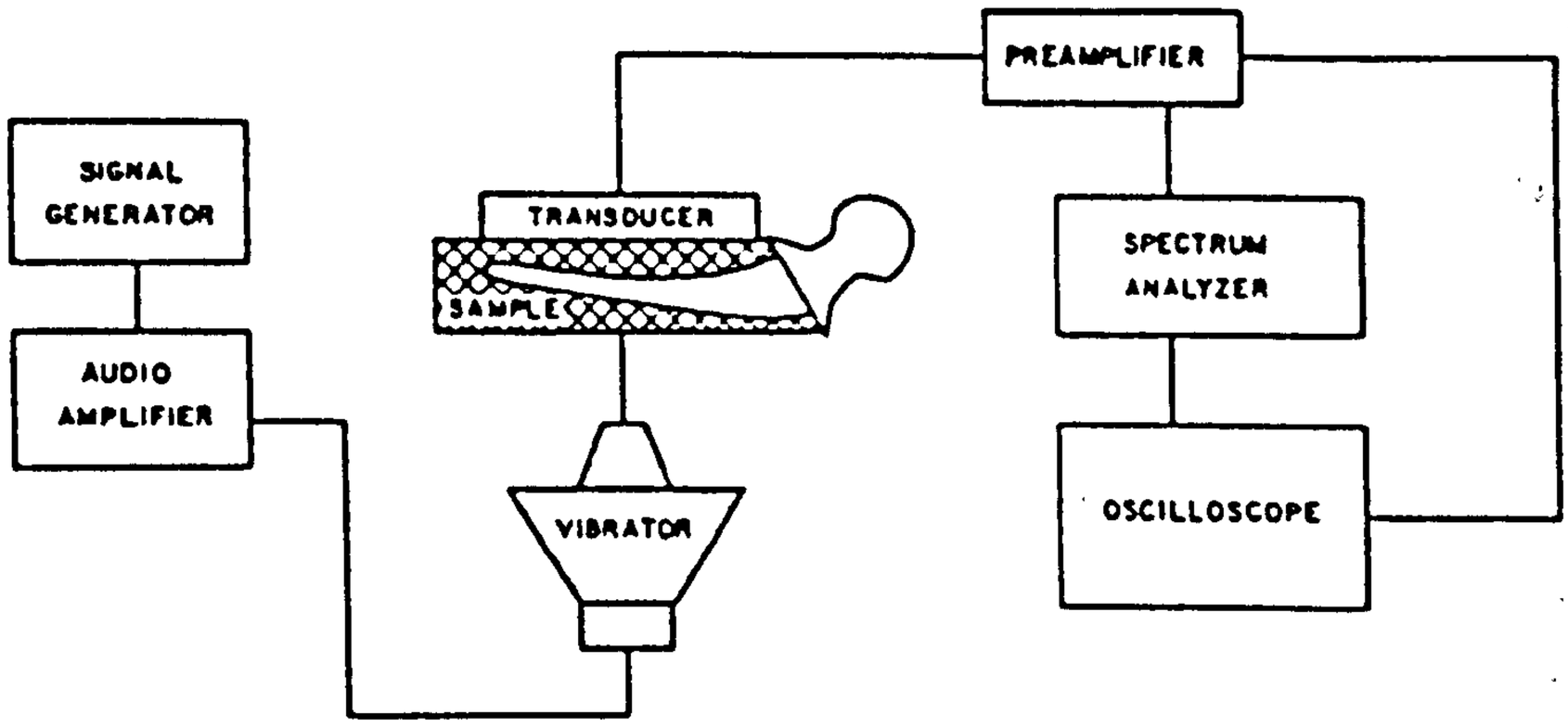

Fig 2.67 Instrumentation used for assessment of integrity of prosthesis-cement complex (from Poss et al, 1984).

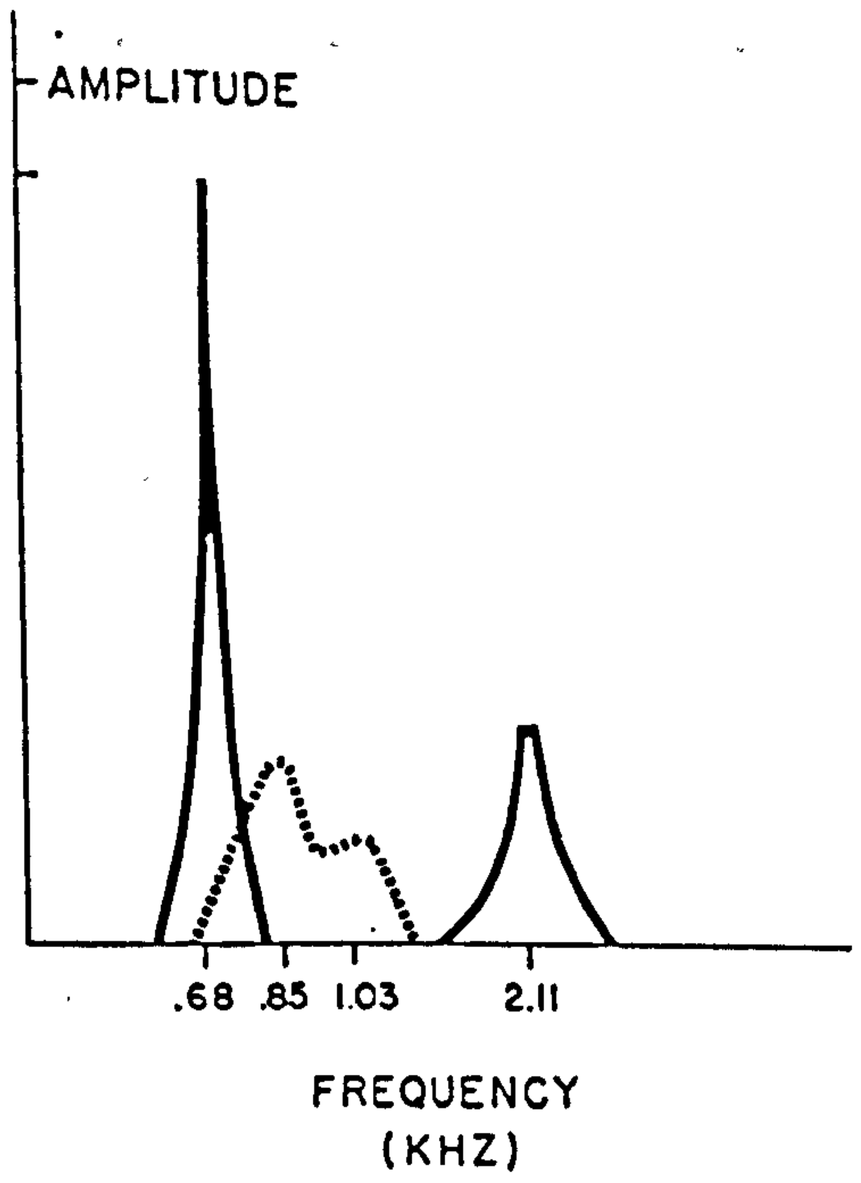

Fig 2.68 Sonic monitoring of cement polymerization (from Poss et al, 1984). Dotted line shows the sonic response at 13 minutes after cement mixing and solid line at 34 minutes.

incidence of complaints increase as the amount of exposure to vibration increases. Impact study on a seated human subjects revealed that the resonance occurred between 4 and 6 Hz was due to vertical vibration of the trunk relative to the pelvis. A bending vibration of the upper trunk with respect to the lumbar spine was observed between 10 and 14 Hz. These would lead to muscle fatigue. Studies on animals revealed that chronic exposure to vibration also lead to histological changes in the nerve roots, cartilage, muscles and bones. All these are predisposing factors of low back pain.

Voloshin and Wosk (1982) evaluated the shock absorbing capacity of the spine by comparing the vibration levels at the forehead with that at the femoral condyle during barefooted walking. It was found that the group of patients with chronic low back pain presented lower shock absorbing capacity than the healthy subjects and those with knee problems. The results also show that the LBP patients modified their patterns of walking to reduce the incoming shock waves, as revealed by the reduced absolute vibration levels measured at the femoral condyle. However, the study did not explained whether the reduction in shock absorbing capacity in the spine is a cause or is in fact a result of low back pain.

Helliwell et al (1989) studied the vibration generated during heel-strike in normal subjects and patients with ankylosing spondylitis of the spine. Transmissibility between the fourth lumbar and the second thoracic vertebrae were investigated using skin-mounted accelerometers and the correction technique discussed in section 2.5.1. In normal subjects, significant attenuation was observed for frequencies between 15 and 40 Hz, while this attenuation was not observed in subjects with ankylosing spine (fig 2.69 & 2.70). This finding suggests the shock absorbing effects due to the flexibility of a normal spine. An ankylosed spine behaves as a stiff strut and therefore lacking this ability. It has also been suggested that the

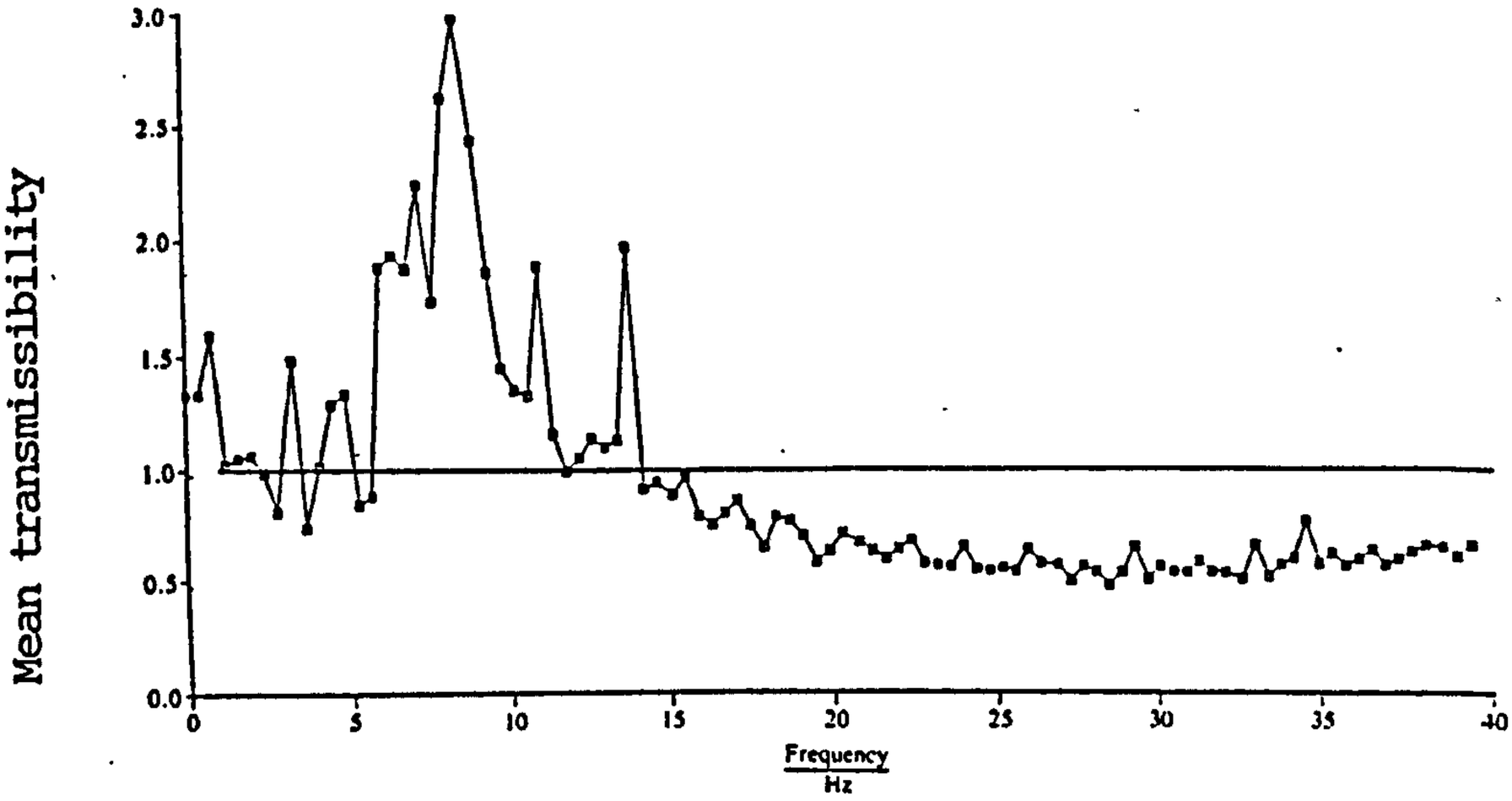

Fig 2.69 Mean transmissibility of the dominant frequency components in the healthy control group (from Helliwell et al, 1989).

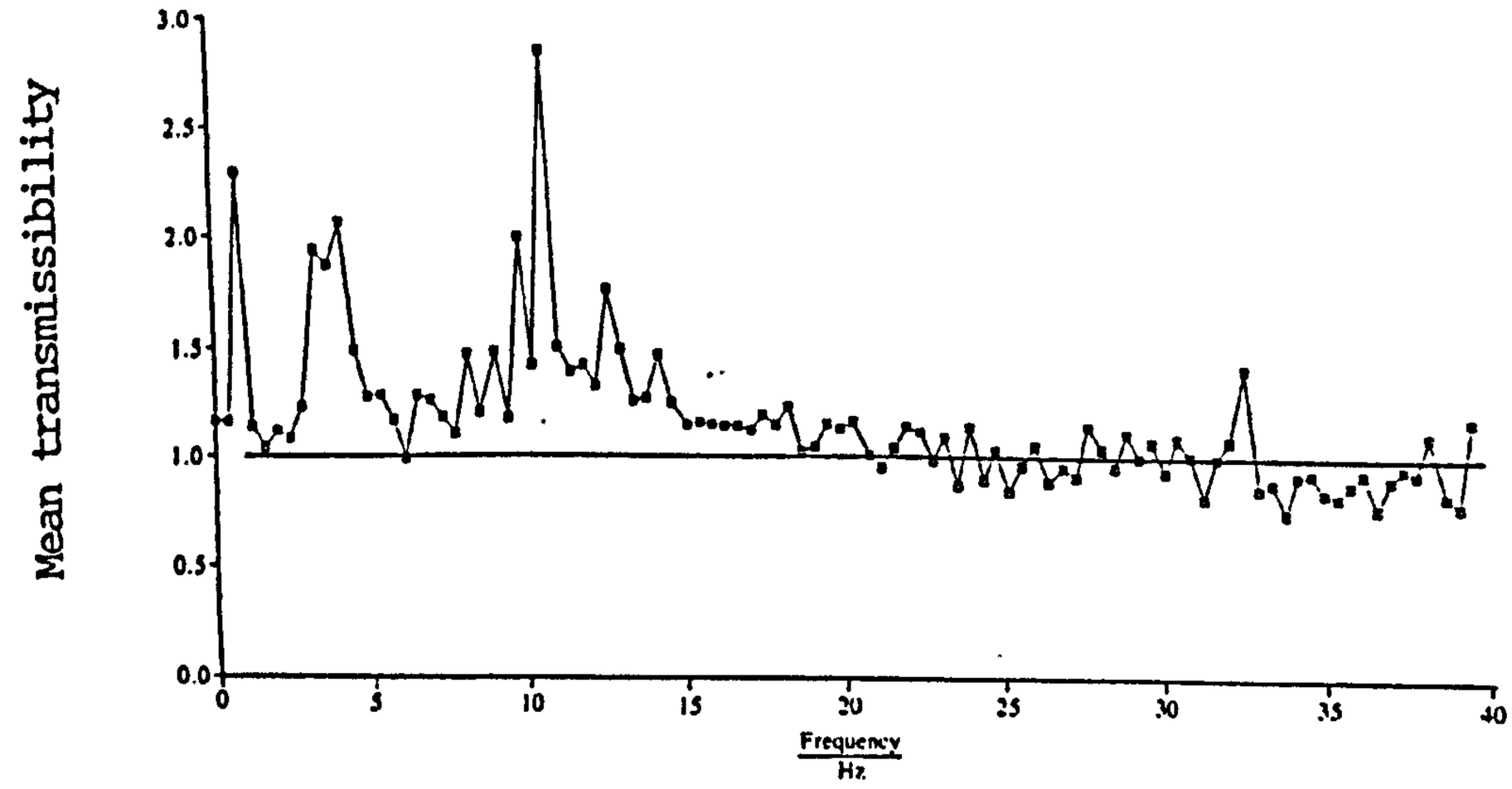

Fig 2.70 Mean transmissibility of the dominant frequency components in the ankylosing spondylitis group (from Helliwell et al, 1989).

transmissibility measurement can be used for other study of the patho-physiological states of the spine.

2.7 SUMMARY

Basic vibration theories have been summarized with special reference to the analysis of vibration signals and systems. The general acoustical properties of the major tissues and structures of the musculoskeletal system have been outlined. The skin has an unique mechanical characteristic which affects the detection of vibration in the underlying bone, and this problem can be improved by suitable use of a light accelerometer in association with compressive preload force regarding the placement of vibration sensors. The bone is the major structure or medium through which vibration waves propagate, and bone possesses vibratory characteristics sensitive to changes of its own mechanical characteristics such as integrity, stiffness and support conditions. Muscles are not playing an active part in the transmission of sound and vibration, though they demonstrate some modifying effects e.g. damping on the vibratory characteristics of the bone onto which they are attached. The spine remains as a complex structure showing axial incompressibility, resulting in attenuation capacity in axial transmission of the vibratory stress. However, the spine's response to lateral vibration has been receiving less attention. Local response of the spine, particularly in the lumbar region warrants further investigation.

Acoustic and vibration techniques have been developed to facilitate the diagnosis of clinical problems of the bones and joints. The techniques are based on well accepted physical principles derived from knowledge on mechanical systems. The useful parameters are: wave transmission velocity, attenuation factors, resonant frequency, mechanical impedance, modal frequency and mode shapes, and frequency spectrum. Like many other biological and medical measurements, vibration techniques suffer a major

limitation due to inter-subject variability. Relative measurements which compare parameters estimated at different points in time, or determined over contralateral limbs could be useful as a monitoring index of the progress or deterioration of a disease state. However, absolute measurement is lacking confidence as it is still difficult to establish a statistical norm or a discriminant value against which a definite clinical decision or diagnosis could be made.

CHAPTER 3

METHODOLOGY AND INSTRUMENTATION

3.1 INTRODUCTION

One of the primary aims of this study is an attempt to answer a fundamental question of how the lumbar spine responds when it is exposed to external vibratory stimulus. It also looks into the general and specific dynamic behaviour of the lumbar spine in a vibratory situation. This requires firstly the knowledge of the effectiveness of vibratory energy transmission into the body at the driving point where it is in contact with the excitation. It is then required to examine how this vibratory energy is absorbed or propagated in the body tissue, and the path in which this propagation takes place. Furthermore, this study is directed towards the motion response of the lumbar spine and the form of waves when vibration propagates along the spine. These requirements entail the development of a vibration technique for in-vitro studies, and one which could be applied safely on human subjects in accordance with some established regulations or recognized standards. These techniques could be developed on the basis of established dynamic analysis techniques widely used in engineering and industry. However, some relevant physical parameters will need to be identified. Their physical interpretations and their applicability as a diagnostic tool require careful investigation.

In this chapter, the general experimental approach is discussed. Technical issues regarding the methods of excitation and the measurements made by a microprocessor-based digital system are outlined. Suitable signal processing and analysis techniques are developed on the theoretical basis summarized in chapter 2. The design of test conditions is discussed to find a realistic model of the lumbar spine under vibration tests. The general and specific dynamic characteristics of the lumbar spine are the major aspects for examination. This chapter also

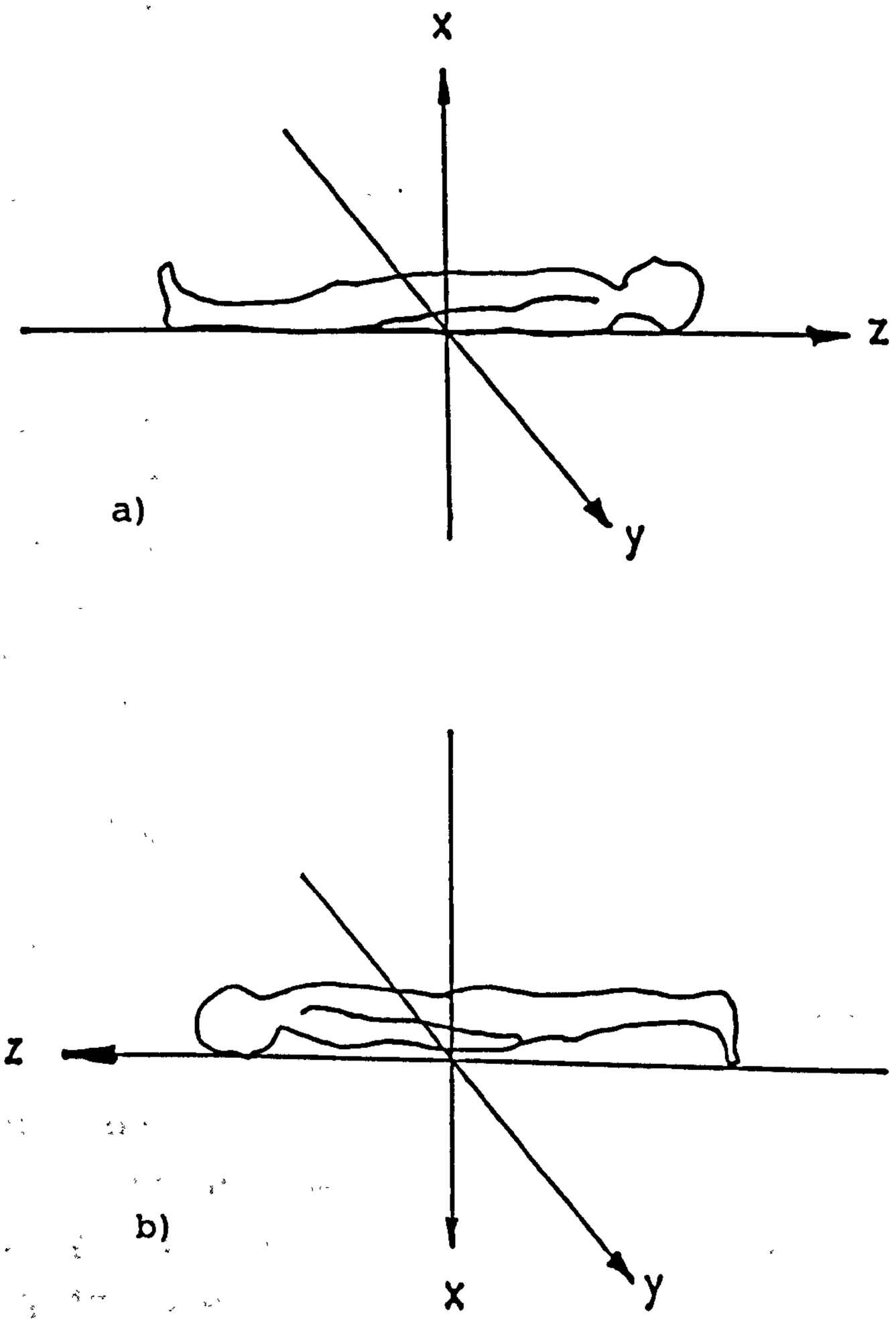

Fig 3.1 Basicentric axes for a) a supine person, and b) a prone person.

highlights the major specifications of the equipment used for this study. Hardware calibration and the validation of software are reported.

The following discussion is based on the anticipated arrangement that experiments will start on specimens of the human lumbar spine, followed by in-vivo tests on normal subjects and patients at a later stage. General technical aspects are taken into consideration of their feasibility in situations when tests are to be conducted on normal subjects and patients. Detailed experimental design and specific test protocols are reported in appropriate sections.

It is necessary to define the coordinate system which will be adopted in the following discussion and in the experimental study. The basicentric axes system as recommended by British Standard Institution (BS 6841, 1987) will be followed. Assume a human body in supine position, the x-axis is defined as that pointing in the postero-anterior direction with the forward direction as positive (fig 3.1a). The positive y-axis is that which points to the left on a transverse plane. The axis which runs along the longitudinal axis of the trunk in the caudo-cranial direction is defined as the z-axis. These three mutually perpendicular axes form a right-handed orthogonal coordinate system. The corresponding coordinate system for a human body in prone is illustrated in figure 3.1b.

3.2 EXPERIMENTAL APPROACH

To study the dynamic or vibratory behaviour of a system or structure, two basic approaches can be adopted (Ewins, 1991). The first approach is where the vibration response of a system is examined during its "operational condition", while the second one involves a system or its components being excited with a known external vibratory stimulus or excitatory force. The following sections discuss the technical aspects in the consideration of these two experimental approaches.

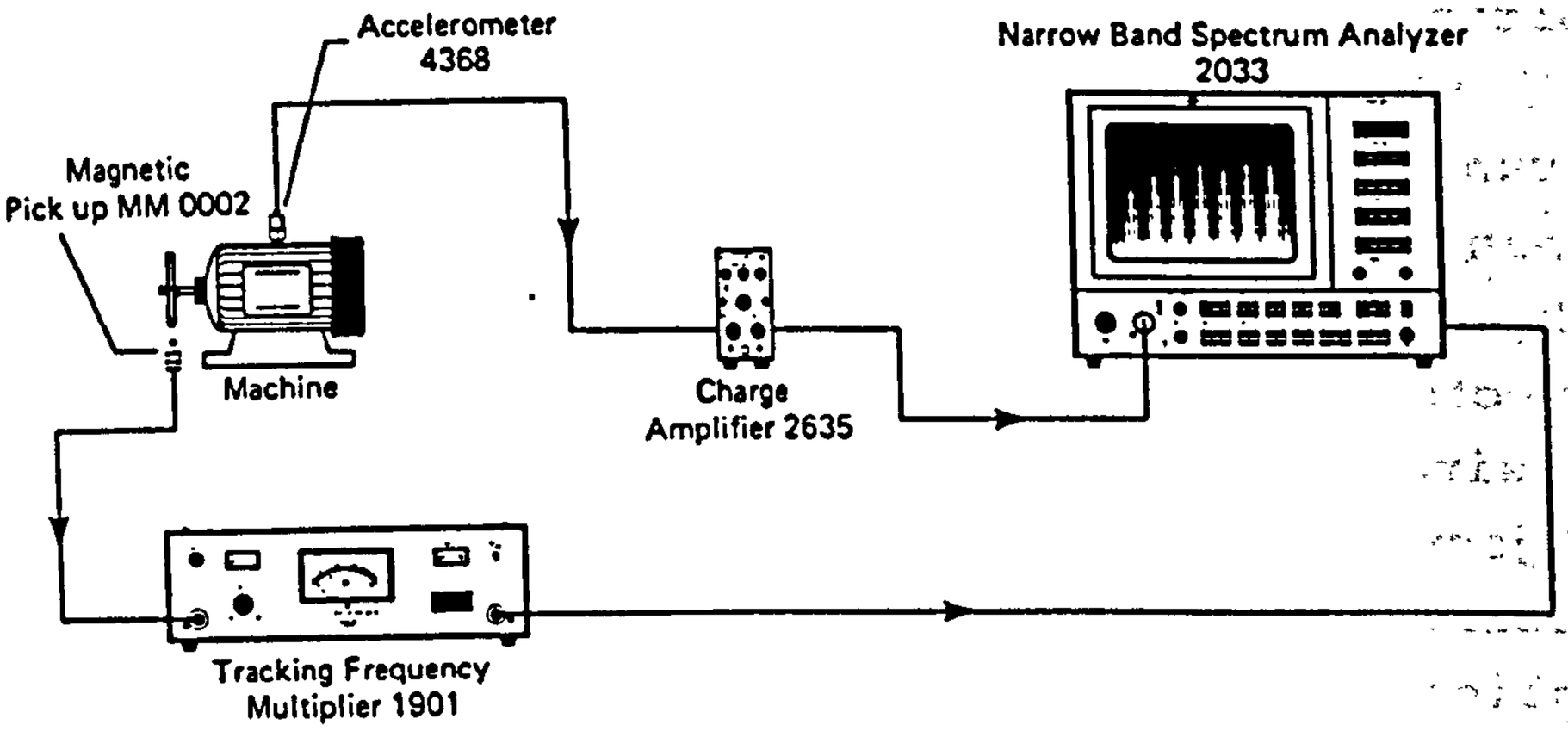

Fig 3.2 Monitoring of machine health (from Broch, 1984).

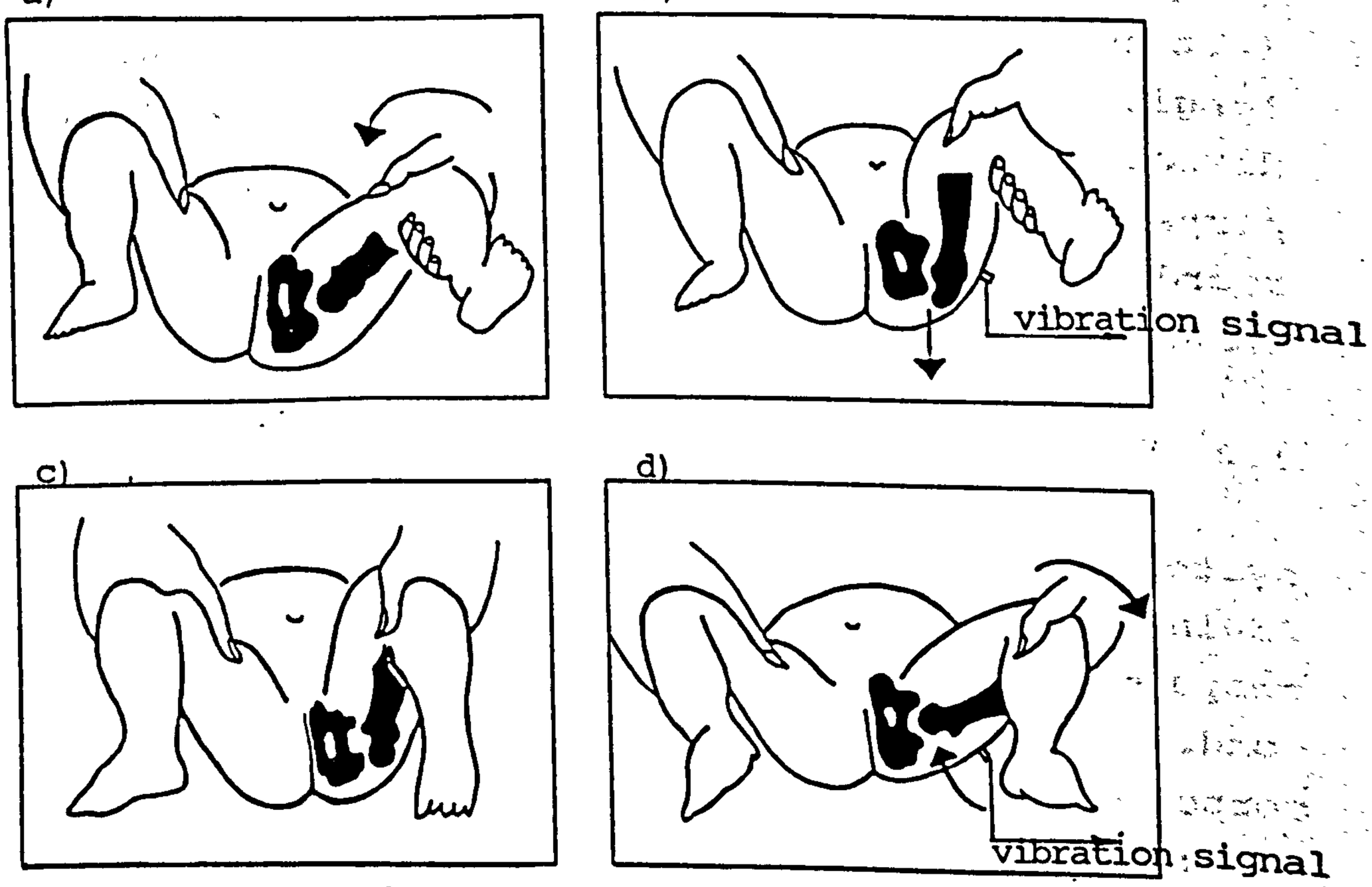

Fig 3.3 a & b) Barlow's test. Detection of vibration during dislocation; c & d) Ortolani's test. Detection of vibration during reduction. (modified from Mubarak et al, 1987).

3.2.1 Signal Analysis

The first approach involves the system being tested under a standardized operational condition in which intrinsically generated or self-induced vibration is measured and monitored at salient locations of the system. The vibration signal is then processed and analyzed in the time and frequency domain to extract useful information on the mechanical strength or weakness of the structure. A knowledge of the mechanics of the system allows the identification of the sources of erroneous noise and vibration by relating the frequency components with specific mechanical components of the system. This approach is described as signal analysis (Døssing, 1988a), and is suitable for examining the performance of systems with a well defined operational mode such as electric motors or diesel engines. The signal analysis approach is often used in routine monitoring of machine health (fig 3.2). The work on the screening of congenital dislocation of the hip by a group in Belfast (Kernohan et al, 1991) is based on a similar approach. The screening procedure involves the manual manipulation of the neonate's hip in accordance with standard clinical manoeuvres - the Ortolani's test and the Barlow's test (section 2.6.3). The vibration signals generated from within the hip joint during its reduction or dislocation respectively are frequency analyzed to reduce relevant parameters to help diagnosis. This vibration emission or vibration arthrometry technique proved useful on the assumption that these two clinical tests (Ortolani's and Barlow's) and hence the vibration signals generated at the hip are reproducible and the signal intensity emitted at the body surface is high enough to be picked up by skin-mounted sensors (fig 3.3). Unfortunately, there is no such standardized "operational condition" of the lumbar spine. Even under well controlled physiological movements such as flexion and extension, the lumbar spine is not envisaged to generate intrinsically vibration signals with a considerable signal-to-noise ratio, and of an intensity

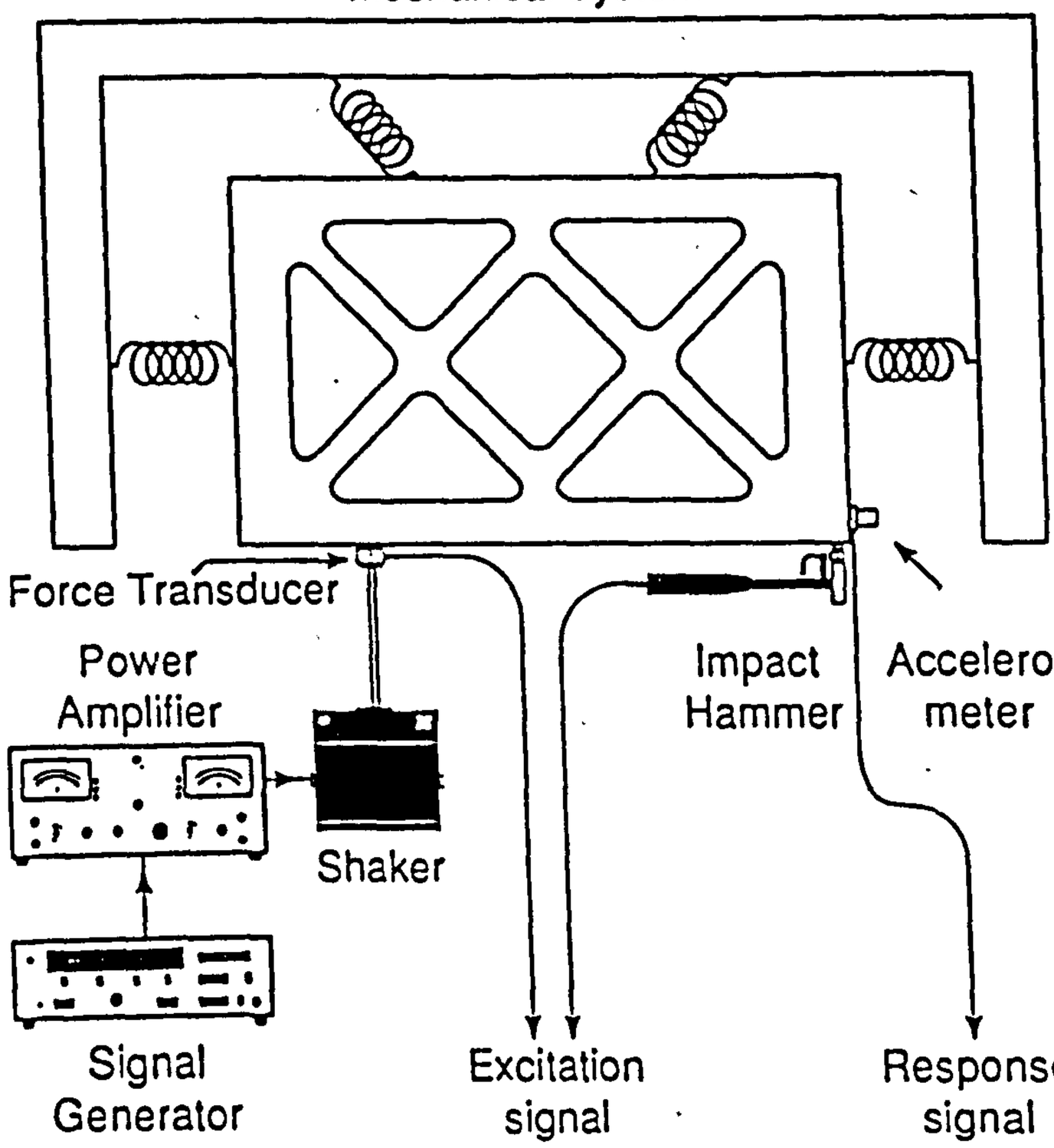

Fig 3.4 Vibration response analysis of a mechanical system (from Brüel & Kjær).

high enough to be detected. Measurement of vibrations over a moving lumbar spine would be technically difficult especially with the attachment of vibration sensors by non-invasive techniques. Thus the signal analysis approach was deemed unsuitable and an alternative approach, system analysis (Døssing, 1988a) was adopted.

3.2.2 System Analysis

The second approach involves a test system vibrating under an externally applied or transmitted excitatory force of controllable and measurable parameters. This excitation is considered as the input to the system. The response of the system is measured as vibration levels at specific locations (fig 3.4). This output response of the system is compared with the input excitation to obtain information on the inherent system characteristics. Assuming that the system has linear mechanical characteristics, a linear analytical technique e.g. frequency response function can be applied to reveal the dynamic behaviour of the system under vibratory excitation (section 2.4.2). The major advantage of the system analysis approach is that the dynamic characteristics of a system remain independent of the form of excitation. This allows flexibility in the choice of input stimulus to the test system. However, the input excitation is required to contain sufficient energy in all frequency components within the frequency range of interest.

This study adopts a system analysis approach in the examination of the vibration response of the human lumbar spine. This approach requires the lumbar spine to be excited by a forcing vibration of measurable and controllable level within a defined frequency range. The vibration response of the lumbar spine can then be measured at salient points to examine its dynamic characteristics. An adequately strong and yet safely controlled vibratory force is introduced into the lumbar spine to induce a motion response. The lumbar spine under test is considered

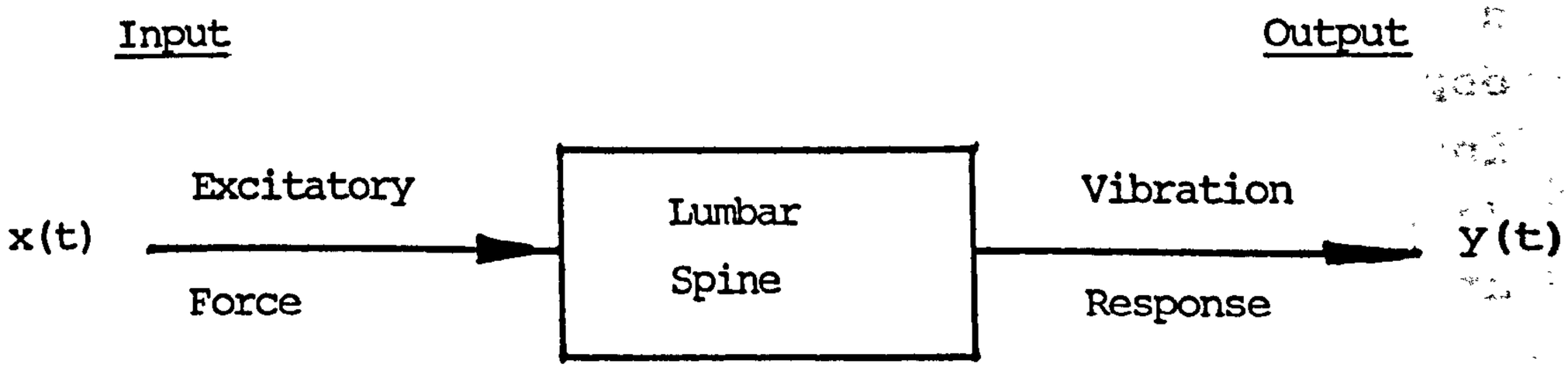

System Linearity:

In time domain

If $x_1(t) \longrightarrow y_1(t)$

$x_2(t) \longrightarrow y_2(t)$

then $x_1(t) + x_2(t) \longrightarrow y_1(t) + y_2(t)$

and $k.x_1(t) \longrightarrow k.y_1(t)$

$k.x_2(t) \longrightarrow k.y_2(t)$

where k is a constant.

In frequency domain

Frequency response function $H(f) = \frac{Y(f)}{X(f)}$ remains constant.

Fig 3.5 A black box model of passive linear mechanical system.

as a passive linear mechanical transmission system. These properties require that the system by itself does not induce any change in mechanical characteristics due to inherent factors for example physiological and psychological activities. It is assumed that the system does not generate any vibratory energy without external stimulus, and none of its components will intrinsically generate any source of vibration due to anatomical changes or physiological activities inside the body. By this token, the resonance set up in the thoracic, abdominal and pelvic cavities is considered insignificant for the purpose of this study. The system is also considered time-invariant, and will behave linearly under a specified frequency range of vibratory excitation in accordance with the principle of linearity illustrated by figure 3.5. The system is able to transmit vibratory energy to other locations of the system such that a motion response can be detected at appropriate points. These assumed system characteristics are subject to validation in the experimental studies.

Figure 3.5 also shows a black box model which illustrates the test of system characteristics, and explains the basic approach of system analysis. The frequency analysis to be used is primarily based on the fast Fourier transform algorithm. The frequency response functions as defined in section 2.4.2 are widely used in this study to reveal the vibration response of the lumbar spine.

3.3 EXCITATION

Excitation refers to the mechanical stimulus applied to a specimen or system during a vibration test. The point at which the lumbar spine is driven by a vibratory force is described as the driving point. This section attempts to discuss the technical issues regarding the application of a suitable form of vibratory excitation to induce a motion response of the lumbar spine. The magnitude of excitation should be to the extent that the induced response can

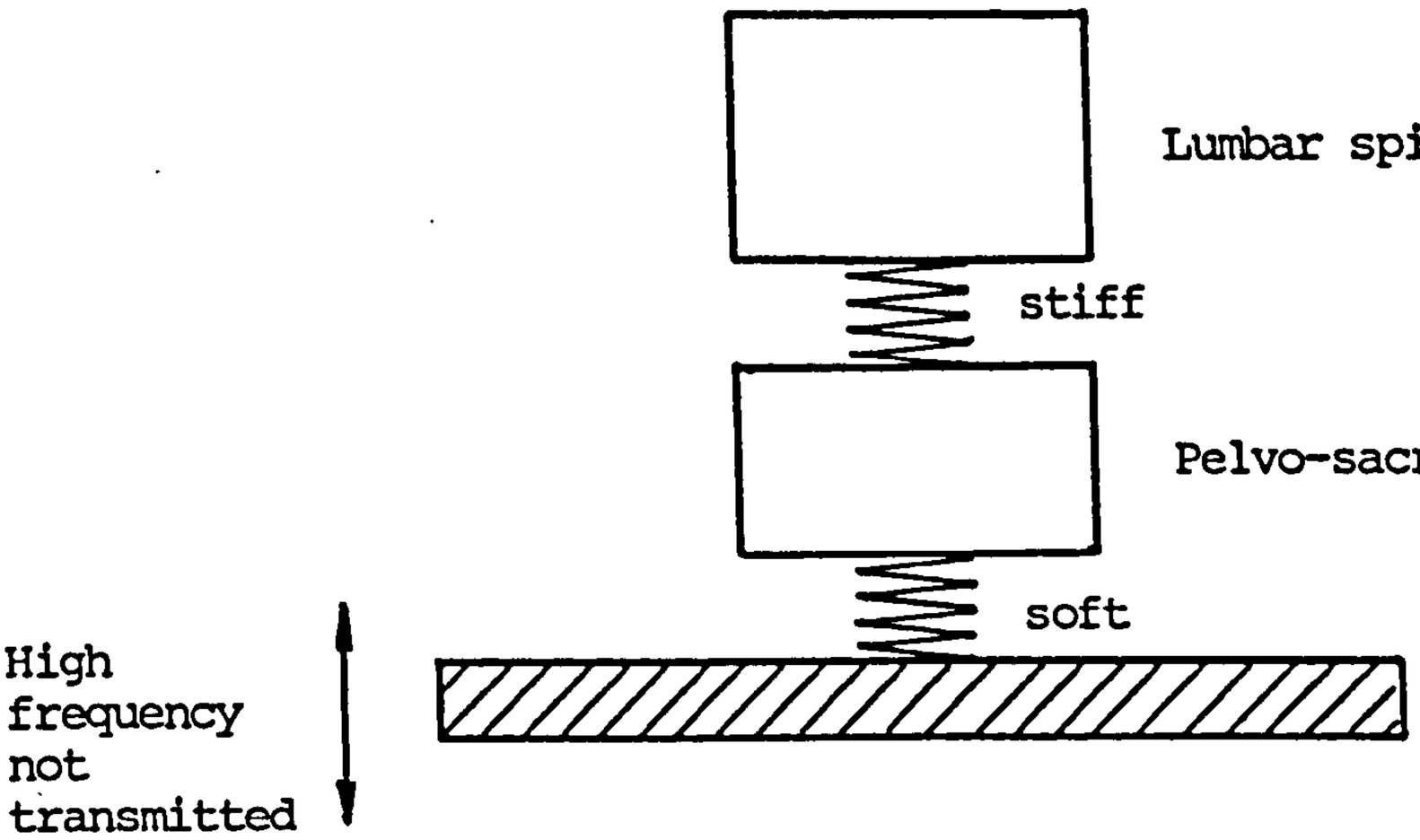

Fig 3.6 A mechanical model to illustrate ineffective transmission of high frequency vibration from the seat to the lumbar spine, and the difficulty of getting different vibrations between the lumbar spine and the pelvo-sacrum in the axial direction.

provide enough information on the mechanical stiffness or weakness, and be sensitive to changes in the mechanical integrity of the structure of the lumbar spine. However, the excitatory stimulus should not induce any adverse effect on the structure of the lumbar spine and associated tissues. This requirement is extremely important in situations of in-vivo tests.

3.3.1 Direction of Excitation

Workers in the field of whole-body vibration have been exploring extensively the response in the z-axis of the body, i.e. along the direction of the trunk. Recently, interest has been extended to study of the vibration response in the x-axis, i.e. fore-aft direction of the body (Paddan, 1991). Assuming a seated person under tests, excitatory force and acceleration can be easily measured and monitored at the buttock-seat interface. However, this is only an indirect and ineffective application of excitatory force to the lumbar through the complex structure of the pelvis and the thigh. There is practically no easy access point to the lumbar spine, except at the spinous processes. The transmission of vibratory energy from the seat to the lumbar spine is very much limited by the tissue characteristics at the buttock. The in-vivo measurement of spinal column vibration reported by Panjabi and his associates (1986) gave a clear message that the transmission of high frequency vibration from buttock to the spine was not effective. The lumbar spine was found to have a local transmissibility equal to unity in the longitudinal axis. Figure 3.6 depicts a possible model inspired by the findings of that group, and the composite system explains why their approach did not reveal any "difference" between the vibration signals taken at the lumbar spine and that at the sacrum. The model also helps to explain the ineffective transmission, particularly of the high frequency vibration axially through the soft tissue between the buttock and the seat. The mechanical

characteristics of axial incompressibility and lateral flexibility of the lumbar spine as described by Evans (1985b) also helps to explain why vibratory excitation in the longitudinal axis may not yield fruitful results. Hence vibration in the axial direction may not be suitable or effective for tests of the local response of the lumbar spine. Sandover (1982) also suggested the dependence of vibration measurement on posture and position, and also on the geometrical configuration e.g. curvature of the trunk. The direction of excitation should also be considered in conjunction with the choice of frequency band-width for the tests. Vibration tests on the spine in the z-axis are very much limited to low frequencies, as the soft tissue at the buttock region and the intervertebral discs are expected to attenuate high frequency vibration as it propagates up from the seat. Invasive techniques to achieve a direct application of excitatory force to the lumbar spine are not considered for the purpose of this study due to ethical constraints.

Excitation in the x-direction has several advantages. The lumbar spine can be excited at specific locations in the antero-posterior direction by placing suitable instrumented probes or sensing devices attached over the skin at the appropriate spinous processes. The skin can be stiffened to enhance the transmission of vibration under suitable compressive preload (section 2.5.1). Both the excitatory force and the motion response can be measured at the spinous processes of the lumbar spine. This method provides adequate spatial resolution for the examination of the local vibration response of the lumbar spine. The lumbar spine is relatively mobile in the sagittal plane to perform trunk flexion and extension. The allowable movement in the x-axis is bigger compared to that in the z-axis as the relative incompressibility of the intervertebral joints limits axial movement (Smeathers, 1984). Hence the vibration response of the spine is expected to be sufficiently strong in the x-axis for investigation.

Assuming a prone person positioned in a relaxed manner for tests, the posture and position of the subject can be standardized to avoid postural variation which might affect the response, and the influence of muscle tension will be minimized. It was decided that both the excitatory force and the vibration response be measured in the x-axis.

3.3.2 Methods of Excitation

There are several well established and routinely used excitation methods for vibration tests on mechanical and civil structures. The technicality and feasibility of using these various methods of excitation are to be considered. However, the pattern of vibratory force for this study cannot be drawn from any specific work environment or simulated exposure to vibration in relation to a particular occupation. The following discussion emphasizes the suitability and safety of their use for tests on the human lumbar spine. Technically, it is required that the excitation carries sufficient vibratory energy distributed over the entire frequency range of interest. Though of secondary importance, the availability of instrumentation, the time for taking measurements and analysis, and the cost of subsequent storage of data are also points for consideration.

Impact Testing. Impulsive force can be conveniently generated by a hand-held hammer striking at the spinous process. It has to be applied at sufficient intervals to allow the lumbar spine to settle before the next impact comes. The lumbar spine's mechanical characteristics can be revealed by its response to the impact force. However, the total energy generated by an impact force is small and may not be adequate to induce sufficiently strong response for analysis. Furthermore, the impulsive signal has a high crest factor which is defined as the ratio of the peak value to the standard deviation. Technically it is difficult to control the magnitude of the impulsive force and it also runs the risk of driving the lumbar spine

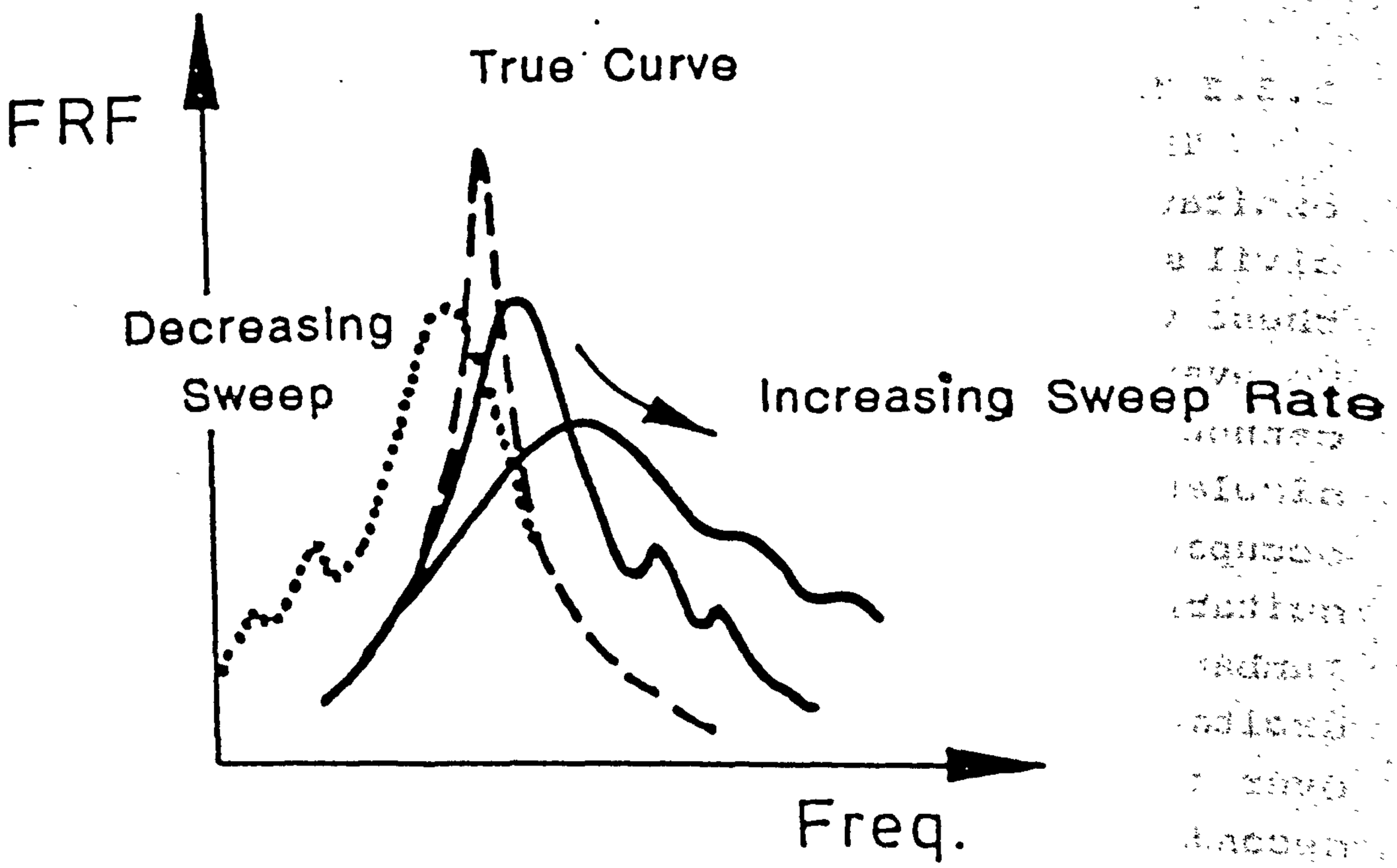

Fig 3.7 Distorting effect of sweep rate (from Ewins, 1991).

beyond its linearity limit, though an instrumented hammer could be used to measure the impact force. Impulsive force in the form of an impact through non-invasive means would be difficult to apply on human subjects if consistency, repeatability and safety are major concerns. Moreover, an impact force over the spinous process would induce discomfort and may not be acceptable to most people.

Swept Sine Testing. Slowly swept sine wave delivers vibratory excitation to the lumbar spine within a range of frequency. In practice, it is required that the sweep rate be sufficiently slow to achieve a steady-state response condition before a measurement is made. However, the sweep rate suffers some limitations in that both too slow or too fast sweeping can produce a distorted frequency response function plot (fig 3.7), and hence errors in the determination of the resonant frequency of the system (Ewins, 1991). The major concern of using swept sine wave stimulation would be that the tests will take a longer time than would be tolerated by the test subjects. Furthermore, there is a risk of setting up standing waves when the sweeping frequency reaches the resonant frequency of the lumbar spine. This will impose potential danger especially to patients who have undergone surgical fusions, and the bone substance or joint components are not strong enough to withstand high vibratory stresses induced by resonance.

Discrete Frequency Vibration Testing. Discrete frequency vibration testing examines the response of the lumbar spine induced by sinusoidal excitatory force of single frequency. The input-output relationship of a system can be established by the amplitude ratio of the vibration response to that of the excitatory force at each frequency. The biggest advantage of using discrete frequency sinusoidal vibration is that the input force of each specific excitation frequency can be controlled, and sufficient vibratory energy can be transmitted into the lumbar spine. By closely monitoring the input and output signals, the lumbar spine may be prevented from being

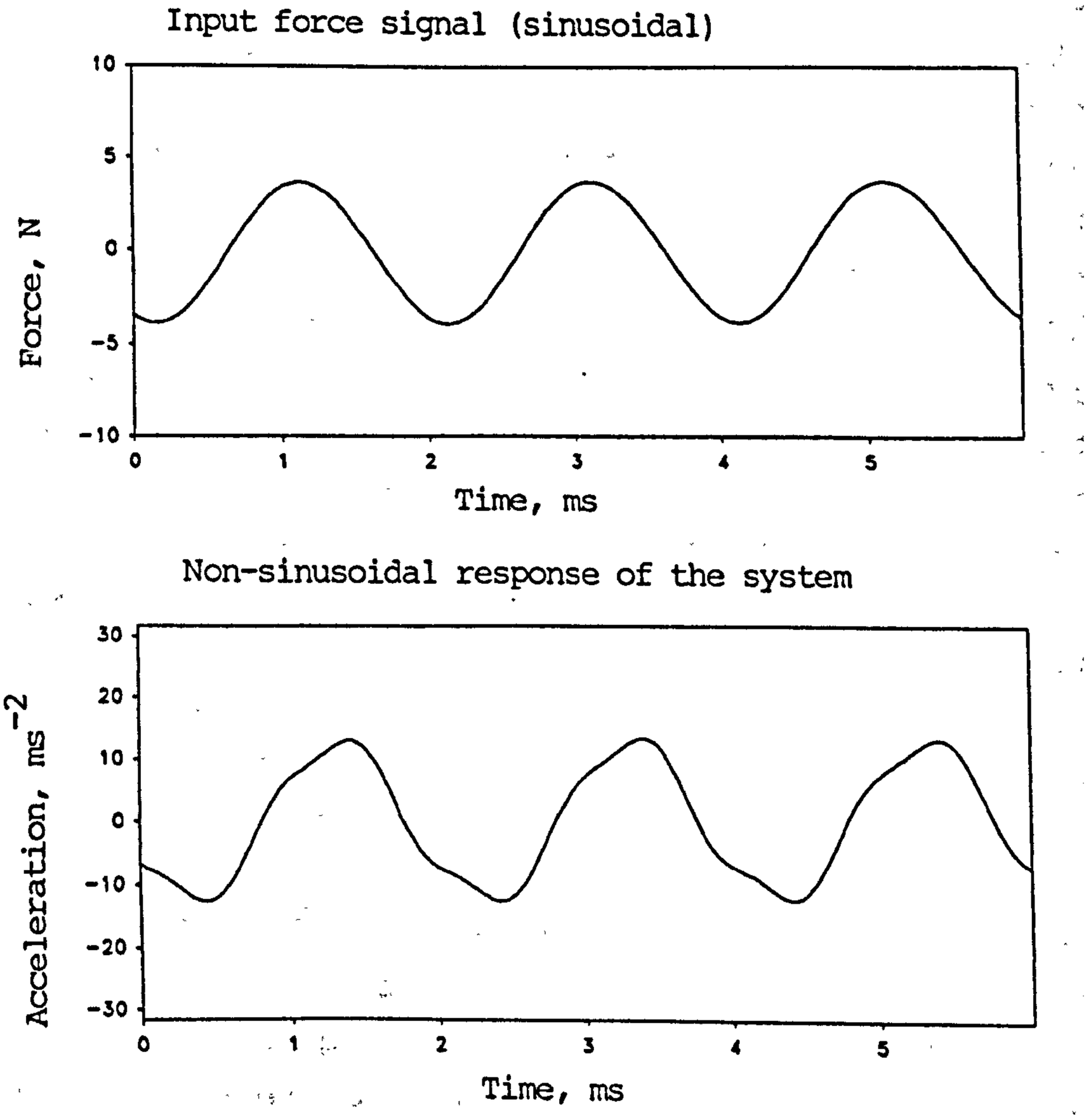

Fig 3.8 System non-linearity.

driven beyond its linearity limit. Figure 3.8 illustrates the non-sinusoidal response of a system which was being driven beyond its linearity limit. When a time-record of the input and output signals is available, the temporal relationship between these two signals can be identified. Vibration tests can be carried out using sine waves of discrete frequencies, for example 100, 200, 500, 1000, and 2000 Hz. The chance of forming standing waves in the lumbar spine is low, and it can be prevented if the excitation is delivered in the form of repeated tone bursts of short duration. This would not be a concern if the lumbar spine be proved as a structure of high damping. The probability of having these chosen frequencies coincide with the resonant frequency is low. The major disadvantage of using discrete frequencies is that the subsequent data analysis will be limited to the system's response at the chosen frequencies. The comprehensive mechanical characteristics of the lumbar spine, particularly that at resonance will not be revealed. Hence the subsequent data analysis may be considered incomplete. From a practical point of view, discrete frequency vibration testing has its limitations because tests have to be repeated at various frequencies, and is therefore time consuming. However, it is still worthwhile to perform discrete frequency vibration testing to allow cross-referencing the results with other techniques such as the random vibration testing. This also provides the opportunity to look into the feasibility of developing a simple and portable instrument which could only implement discrete frequency vibration testing technique for clinical application.

Random Vibration Testing. Random vibration refers to one which is random in frequency, magnitude and phase. White noise with a flat spectrum covering a wide band of frequency is readily available from standard generators. Taped white noise played back from a tape-recorder also serves as a handy source of random vibration. Theoretically, a flat forcing spectrum is preferred because

it guarantees a uniform distribution of vibratory energy across the frequency range of interest. In practice, it still depends on the compliance of the lumbar spine at the point where the excitatory force is applied. More importantly, it relies on the end support conditions and the overall dynamic characteristics of the lumbar spine. As a consequence, a flat input forcing spectrum may not be achieved. However, it is not a great technical problem as long as the input force is measurable, and controlled within an appropriate magnitude range. Frequency response functions can be used to obtain information on the system's dynamic characteristics by plotting the ratio of the motion response to excitation as a function of frequency. It is assumed that the linearity of the system and its mechanical characteristics remain the same, and are independent of the excitation level at any particular frequency. Random vibration has the advantage of testing the system through a wide range of frequency components simultaneously - a feature which is sometimes described as parallel analysis. This possibly shortens the test time, and allows a longer record to be taken of the vibration signals. This also facilitates the spectral averaging process of a longer signal record to achieve a better statistical confidence (section 2.3.4).

Random vibration and discrete frequency vibration are the major techniques to be used for this study. Other methods of excitation will be used when deemed necessary.

3.3.3 Frequency Range

The test frequency is governed by several factors. It depends on the effectiveness of transmission of vibratory stimulus to the lumbar spine. Direct mechanical coupling between the vibration exciter and the bone could be achieved effectively by suitable use of pins or screws in-vitro. However, for in-vivo study using a non-invasive technique, the compliance of skin at the driving point would limit the frequency range. Suitable compressive

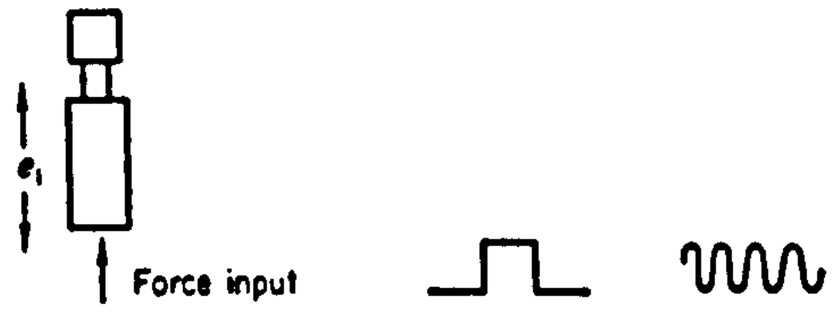

Low frequencies λ shear $\gg e_1$	Middle frequencies λ shear $\leq e_1$	High frequencies λ compr $\leq e_1$
Lumped parameter model for longitudinal, torsional and bending ..... vibrations	Shear waves, Surface waves	Compression waves, Shear waves
Stress concentrated in 'spring' which is determined by inhomogeneities and geometry	Stress pattern determined by shear resonances	Stress pattern determined by compression resonances

Compression
Rarefaction
Compression
Rarefaction
Compression

Fig 3.9 Different modes of propagation of mechanical energy in body tissue (from von Gierke, 1964).

preload may be used to stiffen the intervening skin to achieve an effective transmission interface. As discussed in section 2.5.1, this is extremely important at the measuring point where a flat frequency response of the interface i.e. the skin between the bone and the vibration sensor is required. The frequency range is also limited by the overall stiffness or compliance of the lumbar spine under test. At higher frequency particularly near resonance, the test system will be compliant and less able to withstand or to resist vibratory force, hence the effective excitation will be small (Ewins, 1991).

The form of vibration waves is also determined by the relative geometrical dimension of the transmission medium or structure with respect to the wavelength of the vibration (von Gierke, 1964). A structure being excited by low frequency vibration will behave as a lumped mass incorporating spring and damping elements (fig 3.9). However, if the wavelength of vibration is of the same dimension as the physical length of the structure, vibratory energy will be propagated as shear waves along the structure. The response when monitored at various locations of the system will present temporal and spatial parameters which are sufficient to reveal the specific mechanical characteristics.

The choice of excitation frequency also depends on the system's general vibratory behaviour with respect to its physical dimensions and resonant frequency (von Gierke, 1959). A system, when excited by very low frequency vibration will behave as a lumped mass and the system's dynamic characteristics will not be revealed. The same system under vibratory excitation in a frequency range close to its resonant frequency will exhibit different responses at various locations. These help to reveal the dynamic characteristics of the structure of the system. At very high frequency, the vibratory energy will be propagated as compression waves. The system will behave as a medium for the propagation of vibratory energy. Both the

shape, the physical size and material properties will have effects on the waves' transmission. Analysis of waves in this frequency range is complex, and it falls into the category of ultrasonic imaging which reveals only spatial information. It may not reveal the structure's dynamic mechanical characteristics, and is therefore considered beyond the scope of this study.

This study will be confined to the use of audio frequencies for the experimental study. Assuming the vibratory energy will be mainly transmitted through the bone and intervertebral joints, it is expected that these structures will exhibit significant damping and attenuation to high frequency energy. This is another limiting factor that prevents the successful use of high frequency vibration.

The initial plan of this study is to examine the response of the lumbar spine in the audio frequency range up to 2 kHz. This range of frequency has not been investigated of the dynamic response of the human lumbar spine as explained in chapter 1. This choice of frequency range will be subject to adjustment during the actual tests, and will be modified, if necessary, according to the actual response of the test specimens and subjects.

3.3.4 Magnitude and Duration

Safety is the primary concern of vibration tests on human subjects. Every endeavour must be taken to prevent vibration that is too severe in terms of magnitude and duration. For the measurement of severity of vibration exposure, British Standard Institution (BS 7085, 1989) recommends the use vibration dose value VDV in $ms^{-1.75}$ which is defined as:

$$VDV = \left(\int_0^T a^4(t)\, dt \right)^{\frac{1}{4}} \qquad (3.1)$$

Table 3.1 Weighted acceleration equivalent to a vibration dose value of 15 $ms^{-1.75}$ for continuous mechanical vibration at constant magnitude (from BS 7085, 1989).

Duration of exposure	1 s	4 s	16 s	1 min	4 min	16 min	1 h	4 h	8 h
Weighted acceleration, RMS (in ms^{-2})	10.71	7.57	5.36	3.84	2.72	1.92	1.38	0.98	0.82

where

a(t) is the frequency-weighted acceleration in ms^{-2}; and

T is the total period of exposure in s.

For statistically stationary vibration, the estimated vibration dose value eVDV can be calculated by:

$$eVDV = [(1.4a)^4 \ t_0]^{\frac{1}{4}} \qquad (3.2)$$

where

a is the root-mean-square value of acceleration in ms^{-2}; and

t_o is the duration in s.

The same document recommends that the attendance of medical personnel is not required if a total daily exposure of any subject does not exceed 15 $ms^{-1.75}$. The vibration level equivalent to this vibration dose value is illustrated in table 3.1. This study follows the recommendation in the control of severity of vibration exposure of the test subjects. However, this British Standard Guide assumes a whole-body exposure, or transmission of vibration to the body as a whole. This vibration investigation involves the local application of excitation only to the lumbar spine, and the rest of the body is relatively stationary. So it will be very safe if the vibration dose value be controlled to within 15 $ms^{-1.75}$. Furthermore, the same document refers only to vibration transmitted to the human body in the frequency range between 0.5 and 80 Hz, whilst this study covers a wider frequency range up to 2 kHz. Hence strict reference to this guide may not be appropriate.

It would be an ideal situation if the lumbar spine maintained its linear mechanical behaviour within a wide dynamic range of the excitation. A smaller excitatory force would then be sufficient to induce coherent response of the lumbar spine without the risk of driving it beyond the linearity limit. The vibration technique would thus be safe. The dynamic range of linear response of the lumbar spine can be ascertained in the in-vitro study using an

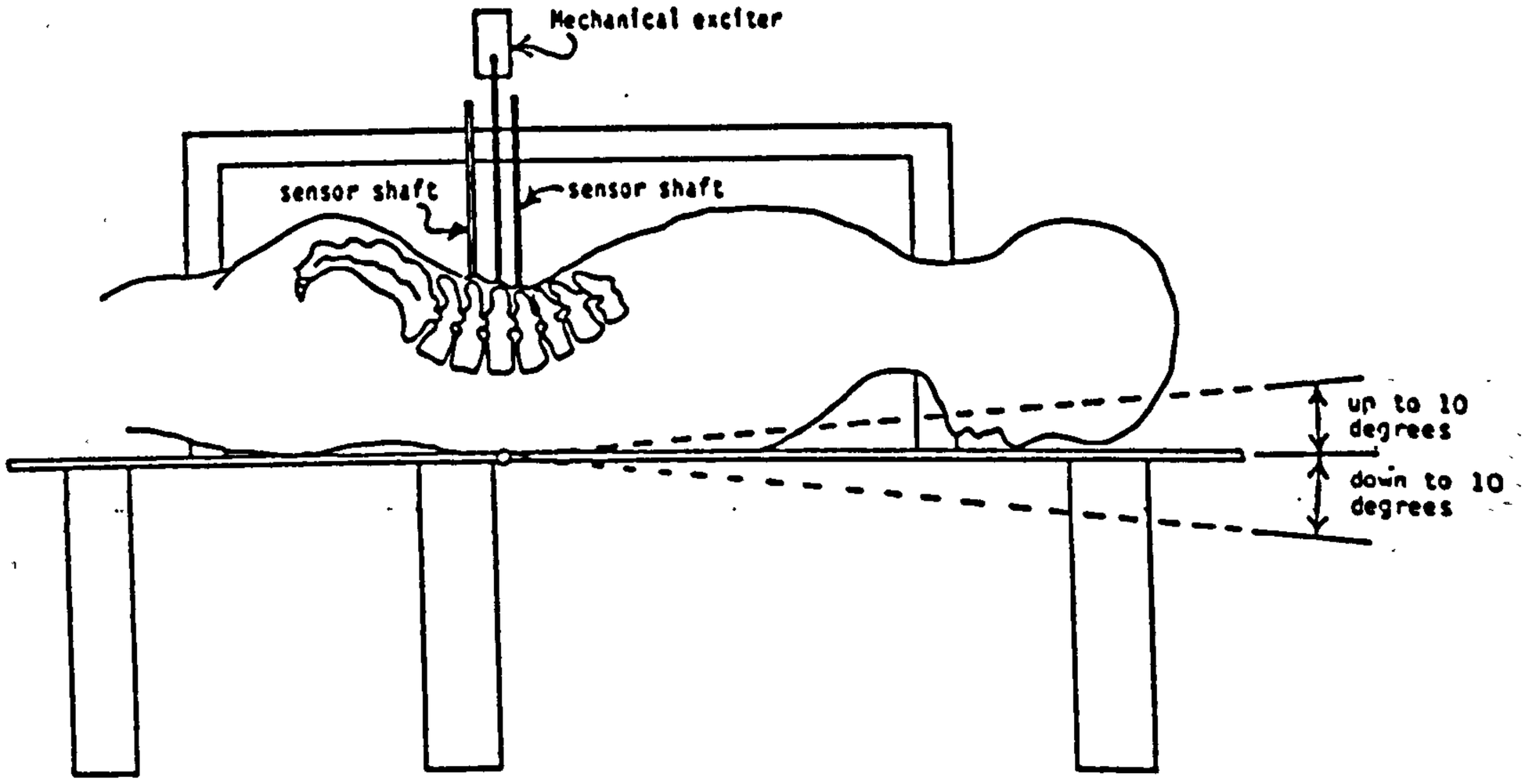

Fig 3.10 Vibration test on the lumbar spine in the antero-posterior direction (from Huston et al, 1991).

isolated lumbar spine. The test subject's feelings and physiological response could be used as indicators to check if the vibration dose value is beyond his tolerance to produce anxiety, restlessness or any discomfort. Every endeavour will be made to ensure the subject's acceptance of the excitation level by trying the vibratory stimulus at the extremities first so that he is familiarized with the feeling, or by comparing with vibratory types of home appliance such as a hand-held massager. The subject will be closely monitored on his feelings and physiological responses during the vibration tests.

There are no previous reports on the allowable maximum limit of magnitude for vibration tests on human subjects up to 2 kHz. Previous work on the vibration response of the human body in the antero-posterior direction only relates to the occupational or work environment. However, there has been no report of the optimal magnitude for the excitatory force suitable for vibration analysis of this nature. Huston and associates (1991) performed a vibration response analysis on the lumbar spine by applying vibratory force through an instrumented stiff rod over the spinous process in the x-axis (fig 3.10). However, the group did not report the magnitude of vibratory force and other parameters used.

When testing on live subjects, the duration of tests has to be limited to avoid any discomfort or shift of position. This also ensures that the lumbar spine is time-invariant and its characteristics remain unchanged during the test period. Attempts will be made to limit each trial to within 10 s, with sufficient rest intervals between each trial.

3.4 MEASUREMENT OF VIBRATION RESPONSE

The bone, being the hardest tissue in the lumbar spine, is expected to be the major structure or medium for the transmission and propagation of vibration. Attention will then be brought to the mechanical features of bone-borne vibration. Measurement of the vibration response can

be conveniently measured by a vibration sensor which is attached at appropriate locations on the lumbar spine. An accelerometer with direct mechanical coupling with the lumbar spine will be deemed suitable for such purpose. The detailed specifications of the accelerometer are outlined in section 3.8.2.

Acoustic techniques offer an alternative method for the examination of vibration within the bone. However, the skin surface has low acoustic emittance, and the acoustic energy emitted from a vibrating lumbar spine is expected to be weak. Measurement of vibration signals using a microphone or a similar kind of sensor is not effective, though not impossible. There is still a problem of mismatch in the acoustic impedance between a vibrating structure and an acoustic device coupled by air. Mollan and his associates (1982b) critically appraised the use of acoustic techniques for the detection of vibration emission in bone and joints. It was also a critical comment on the technique's ineffectiveness due to unsolved problems of ambient noise and noise coming from skin friction. Acoustic techniques will have further limitations in the measurement of low frequency vibration because of the insensitivity of microphone below 50 Hz (Mollan 1981). Mollan's pioneer work and subsequent research on the vibration technique in other applications by his group have indicated that the technique is a more effective means of picking up vibration signals emitted from the musculoskeletal system for the identification of joint problems (Kernohan et al, 1990).

Having mentioned the disadvantages of acoustic devices, it was thought worthwhile to investigate further the applicability of acoustic techniques using modified forms of acoustic sensors for in-vivo measurements. A microphone insert was installed in a housing modified from the head of a neonatal stethoscope. Acoustic signals could be picked up by placing the stethoscope head over the bony prominence. The associated amplifier provides adequate amplification to the signals for acquisition and further

processing. A hydrophone was immersed in a specially designed glass tube filled with water to enhance acoustic coupling with the body. It was also the intention of these modifications to solve the problem of noise from the test environment. Some preliminary tests have shown that with the special housings the microphone and the hydrophone are workable sensors (with limitations) for picking up acoustical signals from the musculoskeletal system. They were found to be free from ambient noise. The detailed specifications and designs are outlined in sections 7.4.1 and 7.4.2. Their technical applicability are examined and also reported in the same sections.

3.4.1 Location and Direction of Measurement

The lumbar spine will be excited in the antero-posterior direction. Hence the measurement of vibration signals and subsequent analysis of the motion response will also be in the same direction. The spinous processes are the only subcutaneous bony prominences of a lumbar spine which are accessible for the placement of an accelerometer. Vibration signals can be picked up at various spinous processes to reveal the vibration response of different segments of the lumbar spine. Referring to section 2.5.1 on the acoustical characteristics of skin, mechanical coupling can be achieved through the use of suitable pin or screws for in-vitro measurements. For non-invasive placement of accelerometers, compressive preload has to be applied to stiffen the skin. It aims to enhance the transmission of vibration signal, particularly for the higher frequencies.

It is technically difficult to measure vibration in the z-axis at the spinous process by non-invasive skin-mounted sensors due to the compliance of skin in this direction. There will be poor mechanical coupling, and this would limit measurement at high frequency. Furthermore, it occurs in a direction perpendicular to the excitatory force, and the response in this direction would not be significant.

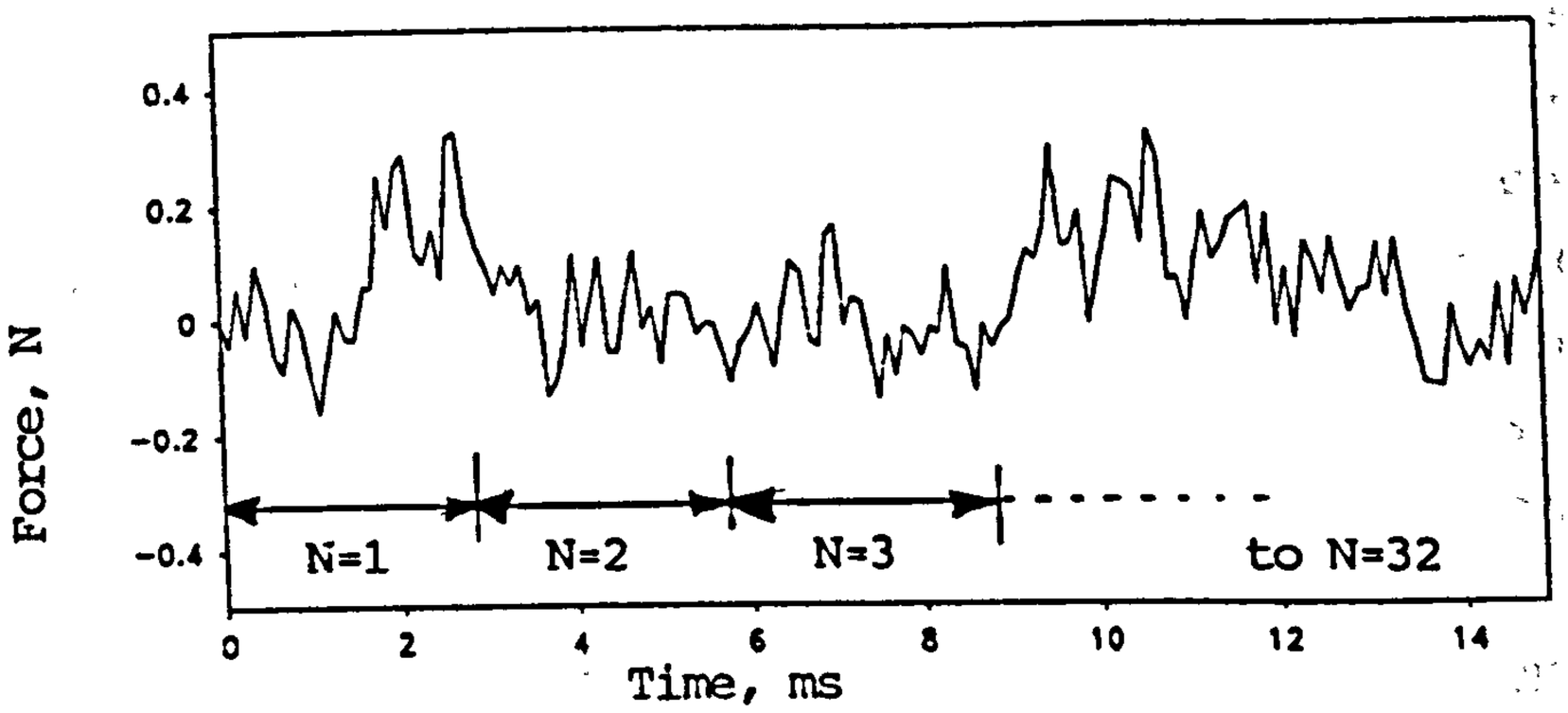

Fig 3.11 Time-records of vibration signals (force and acceleration) are divided into frames of 2048 samples each. The frequency response function is computed for each frame by using the fast Fourier transform, and is subsequently displayed as an averaged spectrum for the 32 frames of the records.

3.4.2 Types of Measurement

Mechanical vibration can be measured in terms of acceleration, velocity or displacement at an appropriate point which is described as the measuring point. Measurement of high frequency motion by acceleration is more suitable because of the small magnitude in displacement which may be below the sensitivity of displacement sensors. Measurement of low frequency vibration can be made by velocity or displacement since at low frequencies the acceleration is small. However, sensitive and reliable accelerometers are more conveniently available on the market. Vibration signals measured as acceleration can be integrated electronically by the conditioning circuits built into the charge amplifier to be described in section 3.8.2. Similarly integration can be achieved mathematically in the time domain, or by the use of a frequency-weighted conversion factor $2\pi f$ when expressing in the frequency domain (Griffin, 1990). In the experimental study all vibration response signals were measured as acceleration.

3.5 SUPPORT CONDITIONS

The mechanical response of a system is affected by the support conditions. The two ideal extreme support conditions for a lumbar spine under vibration tests could be free-free or fixed-fixed at both ends. However, in the real situation, the lumbar spine is attached caudally to the sacrum and pelvis, and cranially to the thoracic spine. Both ends can be considered relatively stationary due to their mass and inertia, assuming a prone position. Nevertheless, the ends of a lumbar spine are not perfectly fixed. It is envisaged that the real end support conditions for the lumbar spine are somewhere between a free-free and a fixed-fixed condition. For the purpose of simulating a realistic support condition for the lumbar spine in an in-vitro study, some form of anchorage could be used to provide relatively stationary supports at both ends, and

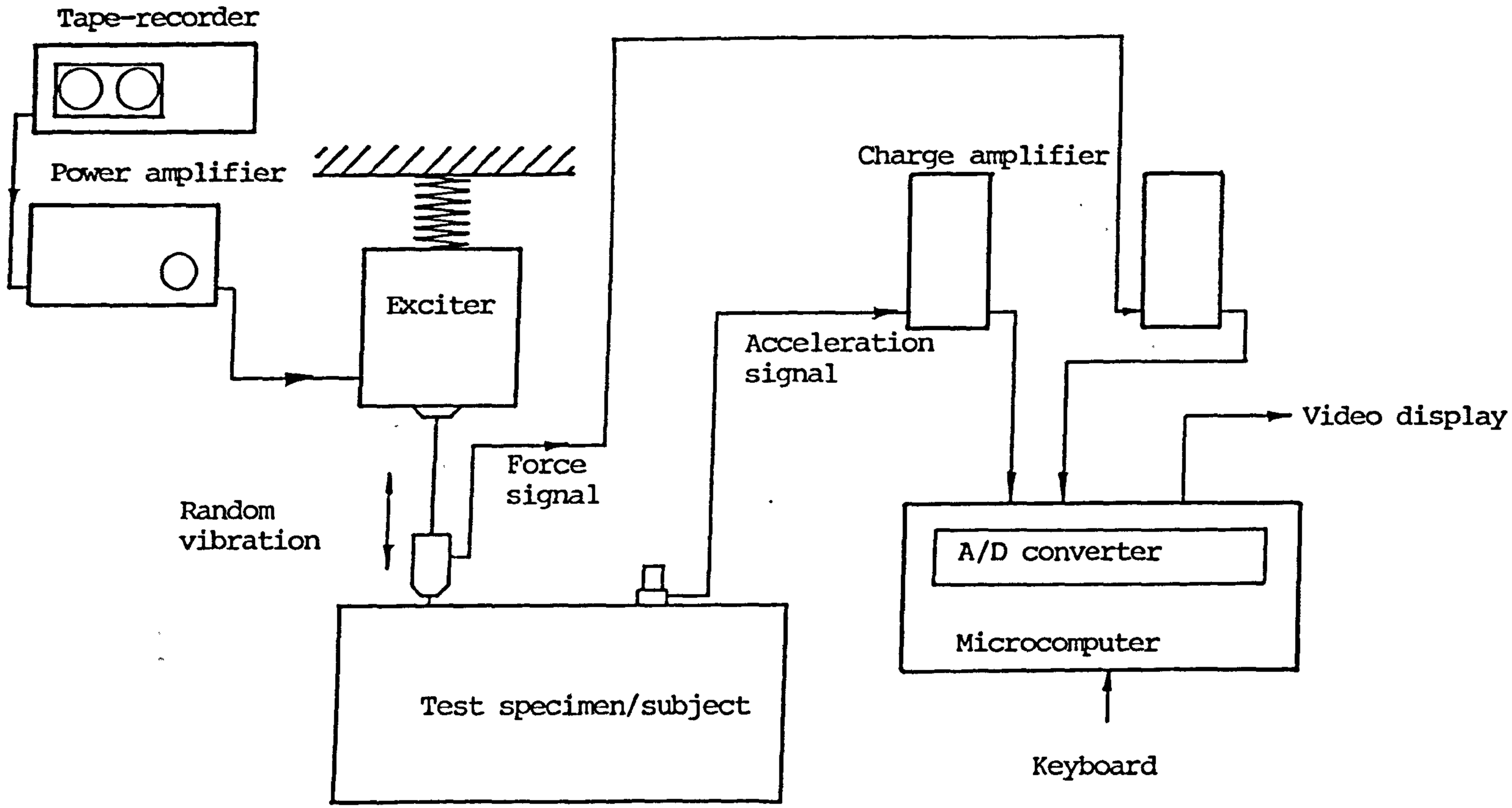

Fig 3.12 Schematic diagram showing the general experimental set-up. The tape-recorder is replaced by a signal generator during discrete frequency vibration testing.

suitable weights could be added to simulate the inertia of the pelvis and the thoracic cage. The detailed experimental designs for in-vitro and in-vivo studies are described in the appropriate sections.

3.6 DATA ACQUISITION AND ANALYSIS

The band-width of vibration response analysis covers the audio frequency up to 2 kHz. With the low-pass cut-off frequency set at 3 kHz during data acquisition, a sampling rate of 10 kHz is adequate to prevent aliasing (Bergland, 1969). A record size of 65536 samples requires about 6.5 s for acquisition. In the subsequent frequency analysis, if the FFT size is set at 2048 points per frame (fig 3.11), this achieves a frequency resolution of about 4.88 Hz. On statistical analysis, the degree-of-freedom N = 32, and hence a substantial reduction in the variance of error from noise or incoherent signal is possible. Assuming a coherence function of 0.95, the normalized random error estimated by equation 2.38 will be less than 3% which is acceptable for this study. It also implies high statistical confidence. Data acquisition and the subsequent computation of frequency response functions discussed in section 2.4.2 will be implemented on a digital system which is described in section 3.8. This data analysis protocol is deemed appropriate and has been established after some preliminary work and pilot study.

Cepstrum analysis as described in section 2.3.5 is also suggested for testing the existence of any echo or reflection at the ends of the lumbar spine particularly in an in-vitro situation, and to detect any alternative transmission path along the lumbar spine. However the capability of this analysis technique will need to be ascertained, and it is reported in section 3.9.2.

Time domain analysis is used to reveal the attenuation and time-delay of a vibration signal propagating along the lumbar spine. It is envisaged that some useful parameters could be drawn from the time domain analysis.

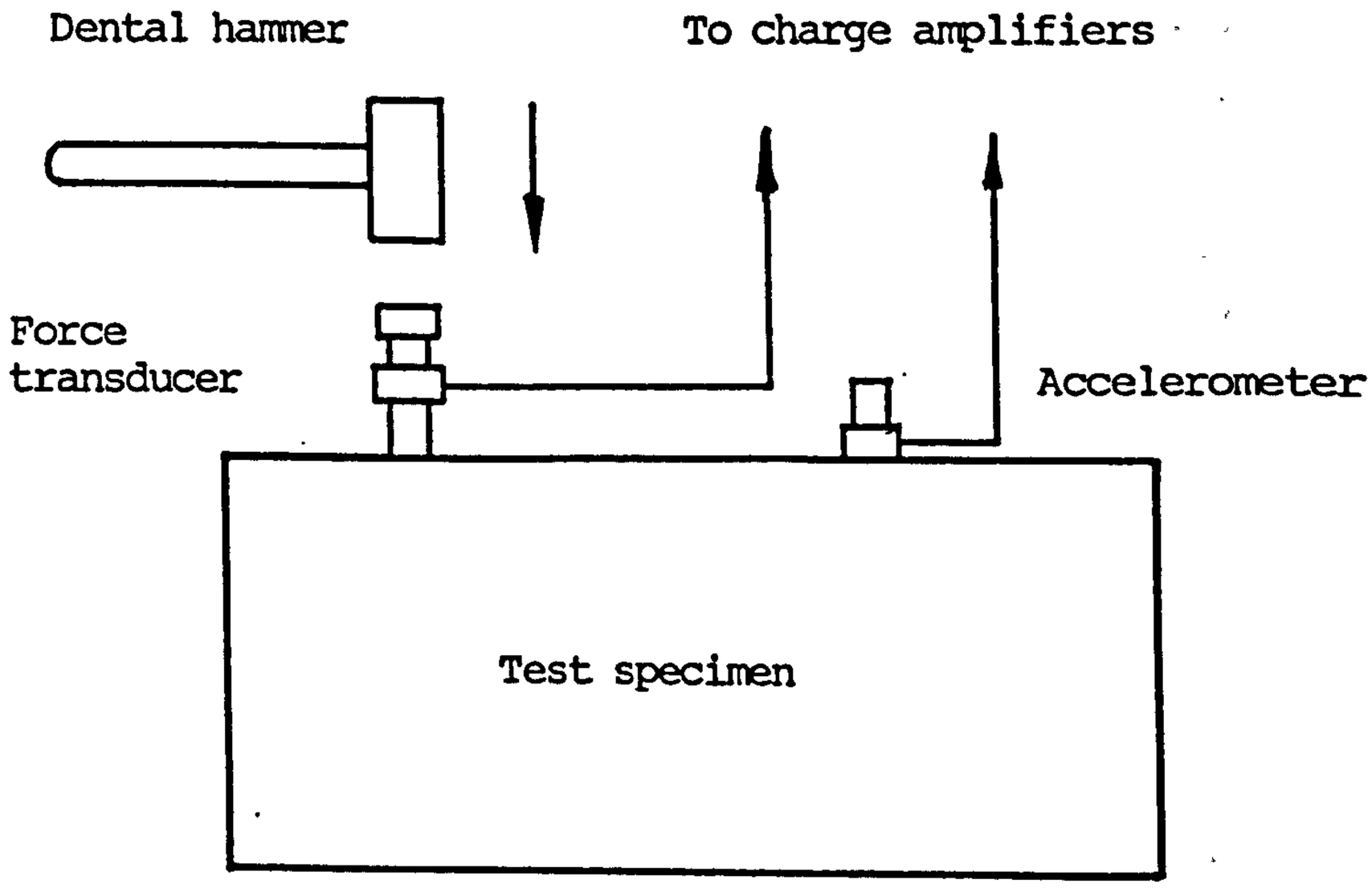

Fig 3.13 Schematic diagram of experimental set-up for impact testing.

3.7 SYSTEM CHARACTERISTICS

3.7.1 General System Characteristics

It is required to examine the general characteristics of a lumbar spine before going into specific analysis in detail. These general characteristics include:-

Linearity;

Repeatability;

Effect of misalignment;

Dynamic range;

Error estimation;

Effects of boundary condition; and

Assessment of ambient vibration.

3.7.2 Specific System Characteristics

Specific system characteristics include those parameters which are able to reflect the dynamic behaviour of a lumbar spine. It is required to understand the mechanical characteristics of the lumbar spine, and should be able to show any changes in the mechanical properties of the lumbar spine after some modifications of its structure.

The following system parameters and their derivatives will be used to characterize the lumbar spine's dynamic behaviour:-

-Apparent mass;

-Transmissibility; and

-Transfer mobility.

These parameters have been defined in section 2.4.2. However, other derived parameters will be defined and used in the vibration response analysis of the lumbar spine whenever necessary.

3.8 VIBRATION MEASUREMENT SYSTEM

This section outlines the major equipment of the system for the implementation of vibration response analysis technique on the lumbar spine. These include a system to generate vibratory force to the lumbar spine specimens or test subjects; a system to pick up vibration

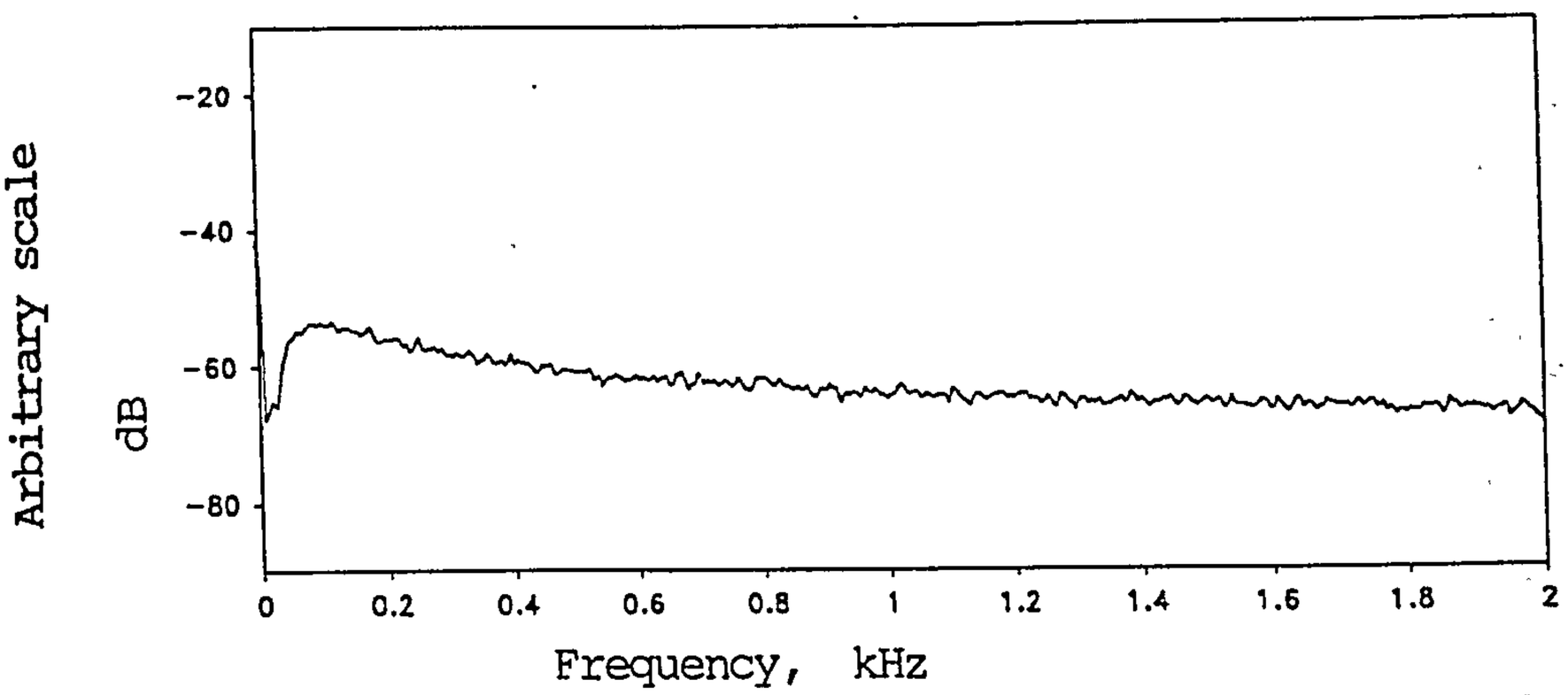

Fig 3.14 Spectrum of white noise from tape-recorder.

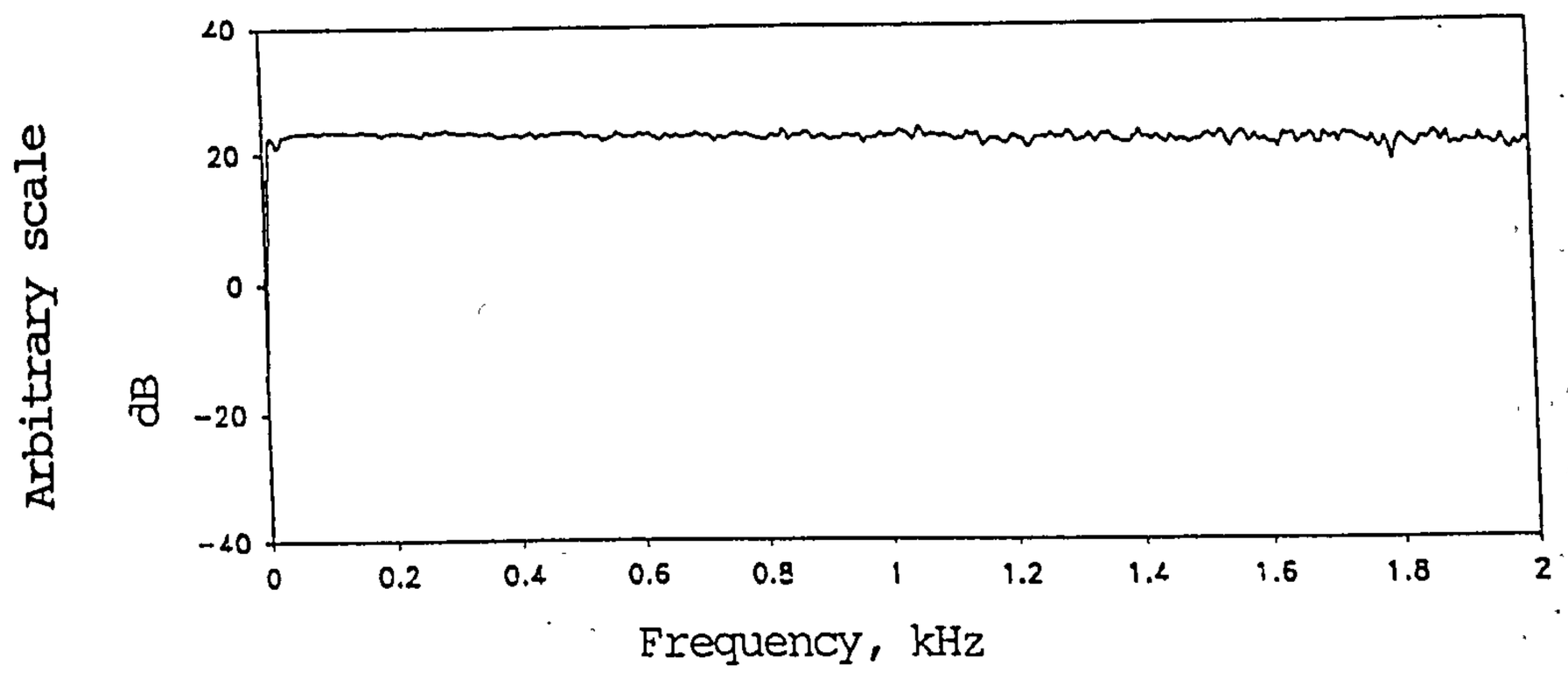

Fig 3.15 Frequency response function of the power amplifier.

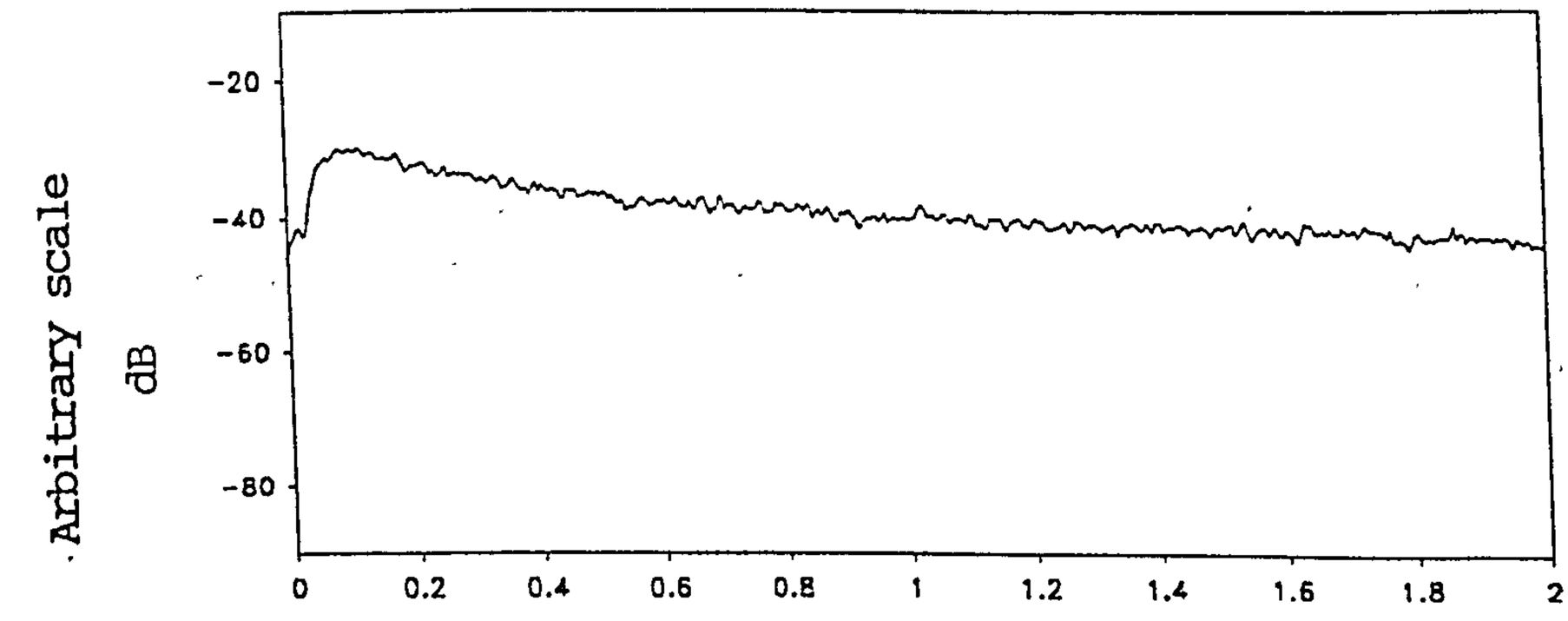

Fig 3.16 Spectrum of random vibration generated by the electrodynamic exciter.

signals; a digital system to acquire the signals, and subsequently to process and analyze the data to reveal the vibratory behaviour of the lumbar spine. Specific modifications are described in detail in the appropriate sections in which the experimental procedures are reported.

Specifications of these equipment are included in appendix IV. Figure 3.12 & 3.13 show the schematic diagrams of the major experimental set-ups.

3.8.1 Excitation System

This system includes a signal generator (BK Precision 3040) which generates sine waves of 100, 200, 500, 1000 or 2000 Hz. Repeated tone bursts can be generated by manually controlling a push-button in the circuit. A swept sine waves can be controlled manually by turning a dial-knob on the front panel. A tape-recorder (AKAI GXC-710D) plays back taped white noise signal. The frequency spectrum of the white noise is flat up to 2 kHz (fig 3.14). The noise signal is fed to a power amplifier (Brüel & Kjær Type 2706) to supply the electrodynamic exciter. The power amplifier's output impedance matches that of the exciter, so that the driving signal is not distorted and a flat frequency spectrum is maintained. Figure 3.15 shows that the amplifier has a uniform frequency response within the frequency range of interest. There is an attenuator to control the output by 10 dB steps. The amplifier is equipped with an overload protection circuit to limit the output in the events of overload or on the reception of erroneous signal. This is to ensure that the specimen or test subject are not driven by excessive force. An electrodynamic exciter (Brüel & Kjær Type 4810) was used to excite the specimen or test subject. The exciter is able to generate a peak vibratory force of 10 N in compression and tension in the frequency range up to 2.5 kHz in accordance with the power drawn from the amplifier. Figure 3.16 shows the frequency response of the exciter. This ensures that sufficient and uniform vibratory energy can be delivered

into the lumbar spine across the test frequency. A special drive-rod or instrumented probe was used to deliver vibratory force into the lumbar spine. An oscilloscope was included in the circuit to monitor the excitatory force. A stop-switch was used during an in-vivo testing to cut off the power to the exciter when the test subject administered an over-riding stop in the event of adverse situation.

Impact force was generated by a hand-held dental hammer which incorporated a hard plastic tip, and weighed about 2.4 N.

3.8.2 Transduction System

For impact tests, a piezoelectric force transducer (Brüel & Kjær Type 8203) was used to measure the transmitted force applied at the driving point. The force sensor has a force rating of 1000 N and sensitivity of 3.6 pC/N. Force can be measured in its longitudinal axis up to 10 kHz. For random vibration, discrete frequency vibration and swept sine tests, the excitatory force was measured by an impedance head (Brüel & Kjær Type 8001) which has a piezoelectric accelerometer and a force transducer in the same housing and mounting point. This allows simultaneous measurements of the force and acceleration at the driving point. The maximum force in tension and compression are 300 N and 2000 N respectively. The force and acceleration sensitivity are 370 pC/N and 3 pC/(ms^{-2}) respectively, and both sensors have a frequency range up to 10 kHz. Miniature piezoelectric accelerometers (Brüel & Kjær Type 4393) were available for the measurement of acceleration at the measuring point. All these piezoelectric transducers have insignificant acoustic and magnetic sensitivity so that they are immune from environmental factors like ambient noise and magnetic fields from nearby machinery. They are working in a stable room temperature and are therefore not affected by this factor.

The outputs of the piezoelectric transducers are led to a charge amplifier (Brüel & Kjær Type 2635). This

amplifier is equipped with a band-pass filter with low cut-off frequency at 0.2 or 2 Hz, and high cut-off frequency selectable stepwise from 100 Hz to 100 kHz. The maximum output voltage from the conditioning amplifier is ±8 V, with 10 dB steps from 0.1 mV to 1 V per mechanical unit which is either force in N or acceleration in ms^{-2}. A built-in electronic integrator converts the acceleration signal to velocity and then to displacement after a second integration.

3.8.3 Data Acquisition System

A digital system based on an Intel 80386DX microprocessor and 80387 mathematical coprocessor was available for data acquisition. Connection of vibration signals was via a screw terminal panel (Data Translation DT707) which accepts 8 channels of differential input. For analogue-to-digital conversion, the data acquisition board (Data Translation DT2821-G-8DI) accepts software programmable input settings to cope with a wide range of input voltage (±1.25 V, ±2.5 V, ±5.0 V and ±10.0 V). The maximum throughput of the board is 250 kHz, with direct memory access to the disk, i.e. the acquired data could be written directly to the hard-disk for storage. In the experimental study, the sampling rate was set to 10 kHz unless specified, and with a 12 bits resolution. Data acquisition is operated on GLOBAL LAB Data Acquisition Package (Data Translation SPO147). The analogue-to-digital (A/D) module of the system allows the user to define the parameters for the input channels such as the channel name, input range, units, sampling rate, sample size, storage area, filename and other essentials for data acquisition. Before each test, a trial run allows the user to check the setting of all the parameters by observing the display on the monitor, to see if the acquisition is running in the proper range. In the actual tests, the software allows repeated acquisitions in the same set-up and subsequent storage in binary format of data with different filenames.

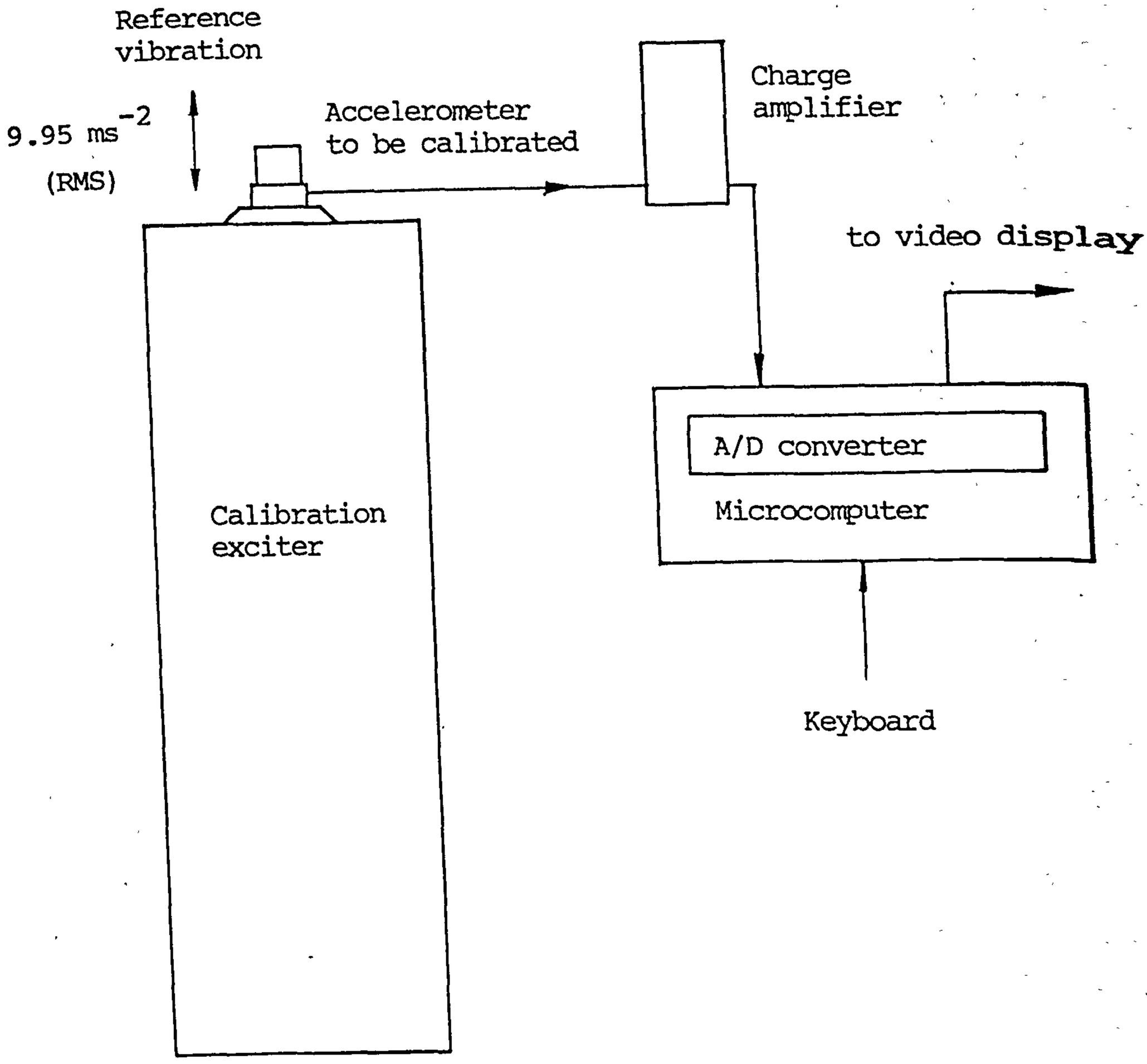

Fig 3.17a Calibration of accelerometer.

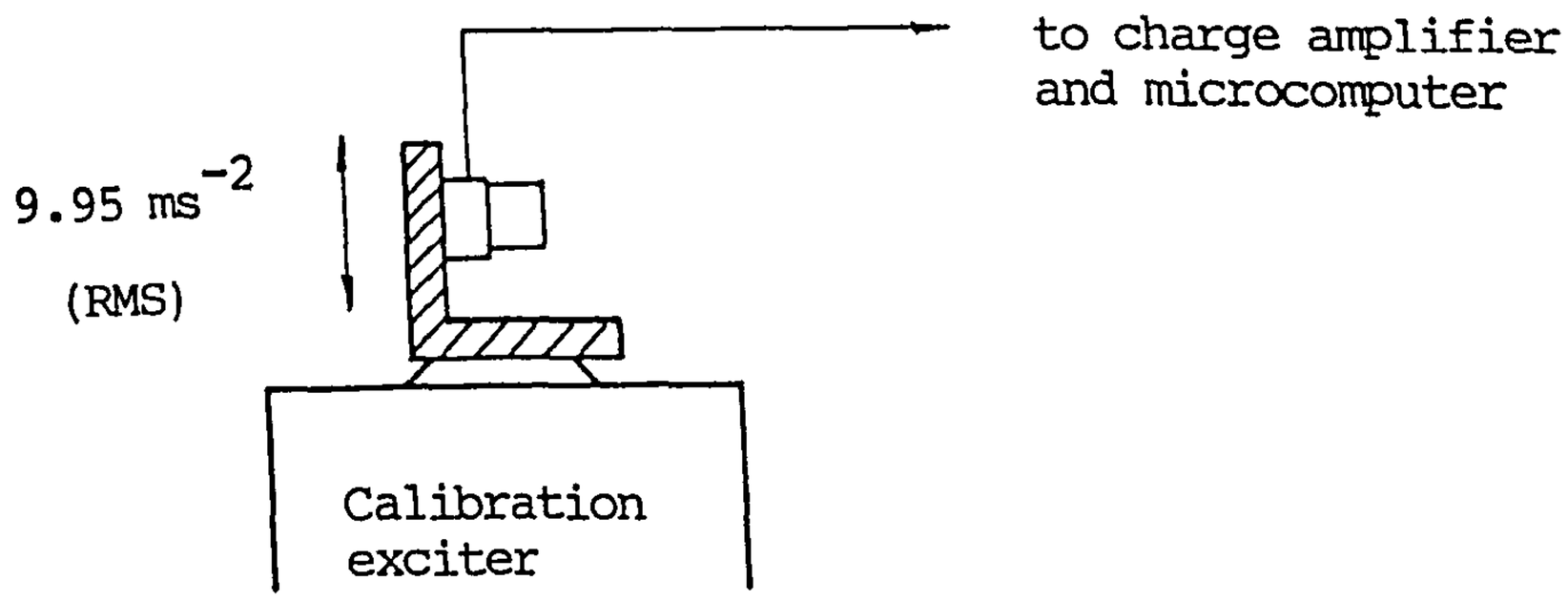

Fig 3.17b Checking cross-sensitivity of an accelerometer in a perpendicular axis.

The captured data can also be transferred in bulk to an external backup system (JUMBO 120 Mbytes, Colorando Memory Systems) for massive archive on magnetic tapes (3M DC2120 Mini Data Cartridge tape) of 120 Mbytes capacity each. The archived tape can be restored back to the hard-disk for subsequent analysis.

3.8.4 Data Analysis System

The STATPACK Signal Processing Module (Data Translation SP0177) of GLOBAL LAB software is used for signal analysis. Time domain analysis allows measurement of the signal parameter to be made by moving a cross-wire cursor on the screen. Autocorrelation of a signal itself and cross-correlation with another signal are possible. Spectral analysis of signals can be made by the fast Fourier transform (FFT) (Bergland, 1969) implemented by the software. Windows of definite FFT sizes (256, 512, 1024, 2048 or 4096) can be defined so that spectral averaging can be computed for a definite number of frames (N) depending on the record size. A record size of 65536 data points can be analyzed by a FFT size of 2048 to achieve a degree-of-freedom N = 32, which is adequate for most tests in this study.

Documentation by hardcopies of graphs can be generated by GRAPHPACK Printing Module (Data Translation SP0197) which creates graphs of various size and resolution, with suitable annotations.

3.9 CALIBRATION AND VALIDATION

The aims of calibration is to determine the sensitivity factor of the force and acceleration transducers, and to ascertain the validity of the frequency response function and cepstrum function implemented by the software.

3.9.1 Hardware Calibration

Figure 3.17a shows the schematic diagram of the set-up

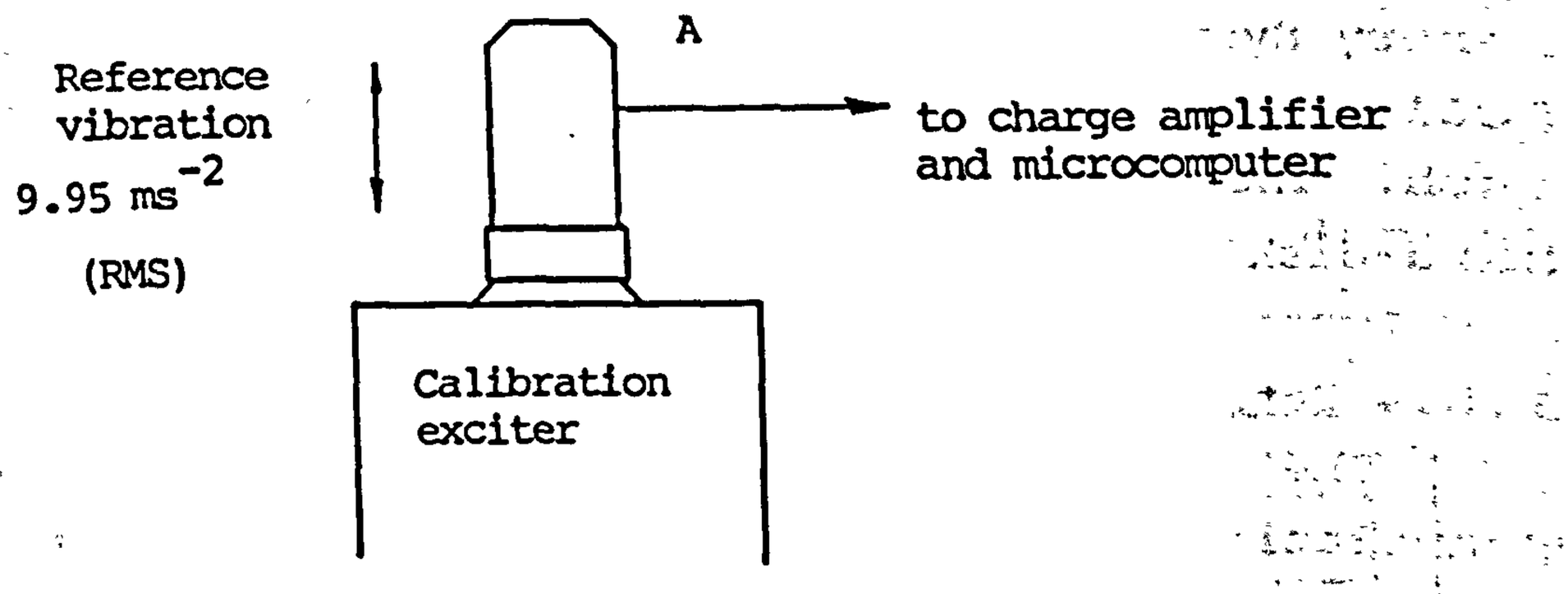

Fig 3.18a Calibration of accelerometer of the impedance head.

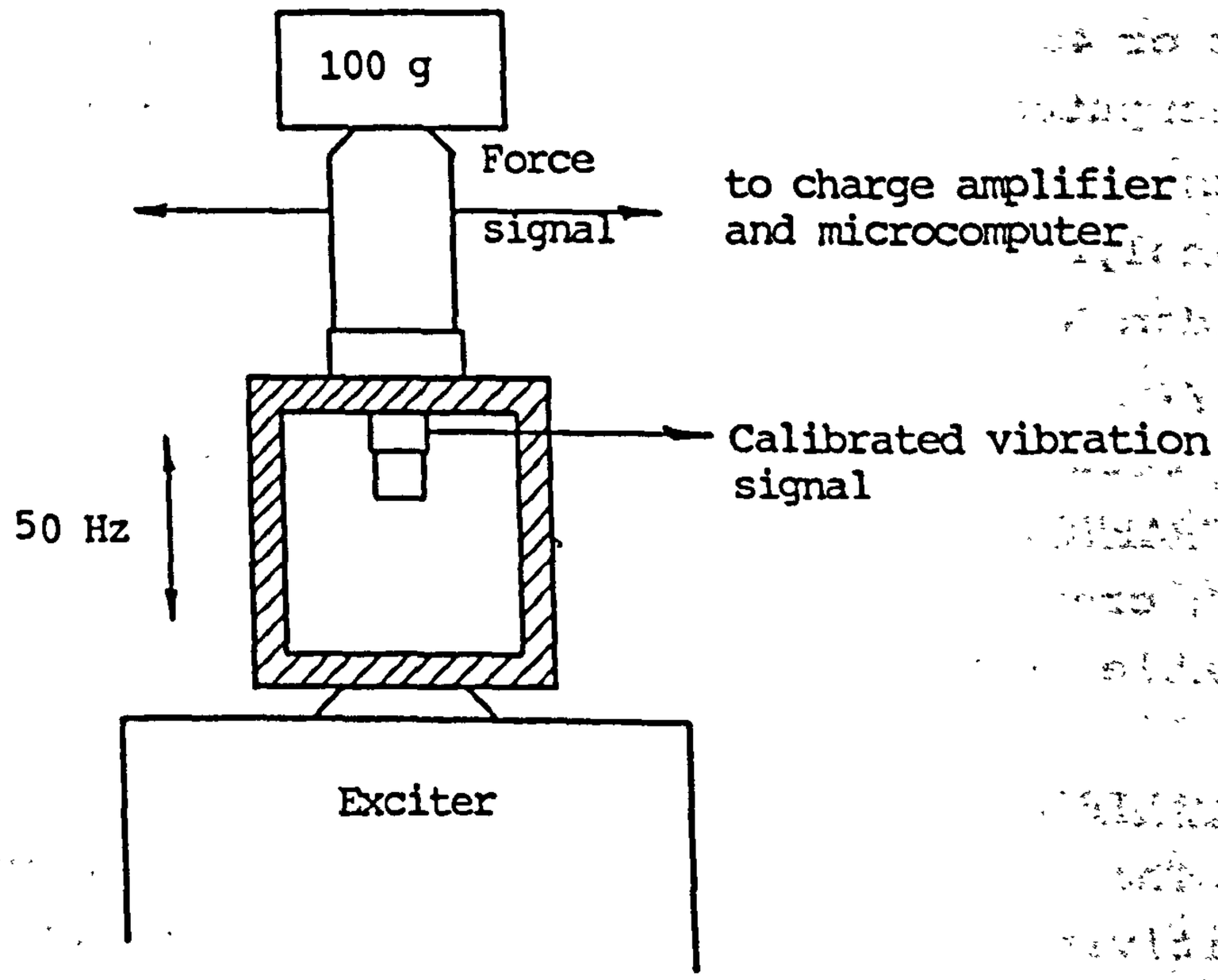

Fig 3.18b Calibration of force transducer of the impedance head.

of the hardware for calibration. A calibration exciter (Brüel & Kjær Type 4294), traceable to the National Institute of Standards and Technology, Maryland, U.S.A., generated a reference sinusoidal vibration level of 9.95 ms^{-2} (RMS) at 159.15 Hz. This vibration level was picked up by the accelerometer which was to be calibrated. The vibration signal was conditioned by the charge amplifier which was set according to the sensitivity S_o in $pC/(ms^{-2})$ indicated on the document supplied with the accelerometer. The amplified signal was then acquired by the data acquisition system described in section 3.8.3, and the RMS vibration level A in ms^{-2} was noted. The calibrated sensitivity S_c of the accelerometer was then determined by the equation:

$$\textit{Calibrated Sensitivity, } S_c = S_0 * \frac{A}{9.95} \qquad (3.3)$$

The same procedure was repeated for other accelerometers. It was found that there was less than 0.1% discrepancy between the documented and the calibrated figures.

The accelerometers were also mounted in a perpendicular position so that the cross-sensitivity was tested while vibration took place in other perpendicular axes (fig 3.17b). It was found that the cross-sensitivity was about 0.4%. Hence the accelerometer can be considered insensitive to vibration in other axes.

The acceleration transducer of the impedance head was calibrated with a similar set-up (fig 3.18a), and its force transducer was calibrated at 50 Hz in a set-up shown in figure 3.18b. The mass of load was chosen at 0.1 kg. The vibration level was set at 100 ms^{-2} (RMS), and was monitored by a calibrated accelerometer linked up with the same circuit as used in the calibration of the accelerometer. The calibrated sensitivity S_c in pC/N was determined by the equation:

$$\textit{Calibrated Sensitivity, } S_c = S_0 * \frac{F_1 - F_0}{m * A} \qquad (3.4)$$

Table 3.2 Multisinusoidal signals for software validation.

Input signal x(t):

Relative amplitude	Frequency, Hz	Phase, °
1	100	0
2	200	0
5	500	0
1	1000	0
2	2000	0

Output signal y(t):

Relative amplitude	Frequency, Hz	Phase, °
2	100	0
5	200	0
1	500	0
2	1000	0
5	2000	0

Table 3.3 Transfer function (Y(f)/X(f)) computed by the STATPACK module of GLOBAL LAB.

Frequency, Hz	Magnitude (ratio)	Phase, °
100	2	0
200	2.5	0
500	0.2	0
1000	2	0
2000	2.5	0

where

m is the mass in kg;

A is the RMS acceleration (in ms^{-2}) of the mass;

F_o is the RMS force in N measured without the mass;

F_1 is the RMS force in N measured with the mass; and

S_o is the sensitivity setting (in pC/N) for the force transducer during calibration.

It was found that the calibrated sensitivity of the force transducer was about 1.5% off the documented value supplied by the manufacturer.

3.9.2 Software Validation

Attempts have been made to ascertain the spectral analysis module of the signal processing software. Two multisinusoidal signals of various amplitudes but of the same phase differences as listed in table 3.2 were generated by the programme. One of the signals was used as input and the other as the output. Spectral analysis procedure was used to evaluate the magnitude and phase information obtained by the transfer function with respect to each particular frequency. The results listed in table 3.3 show the magnitude ratios of the output to input signals, and the phase at various frequencies. These results show that the computed amplitude ratio as indicated by the magnitude of the transfer function was accurate up to 100% and there was no inherent shift in phase due to computation error. The coherence function was found to be equal to unity. However, as was expected, the use of Hanning window function (Parks & Burrus, 1987) yields about 50% of the figures in the signals' power spectral density (by autospectrum) compared with figures processed without any window function. This shows that absolute measurement of the power function requires careful attention for its use. In this study, the ratio of the output to the input signals was of primary interest. Hence the spectral analysis procedure was confirmed to be up to the

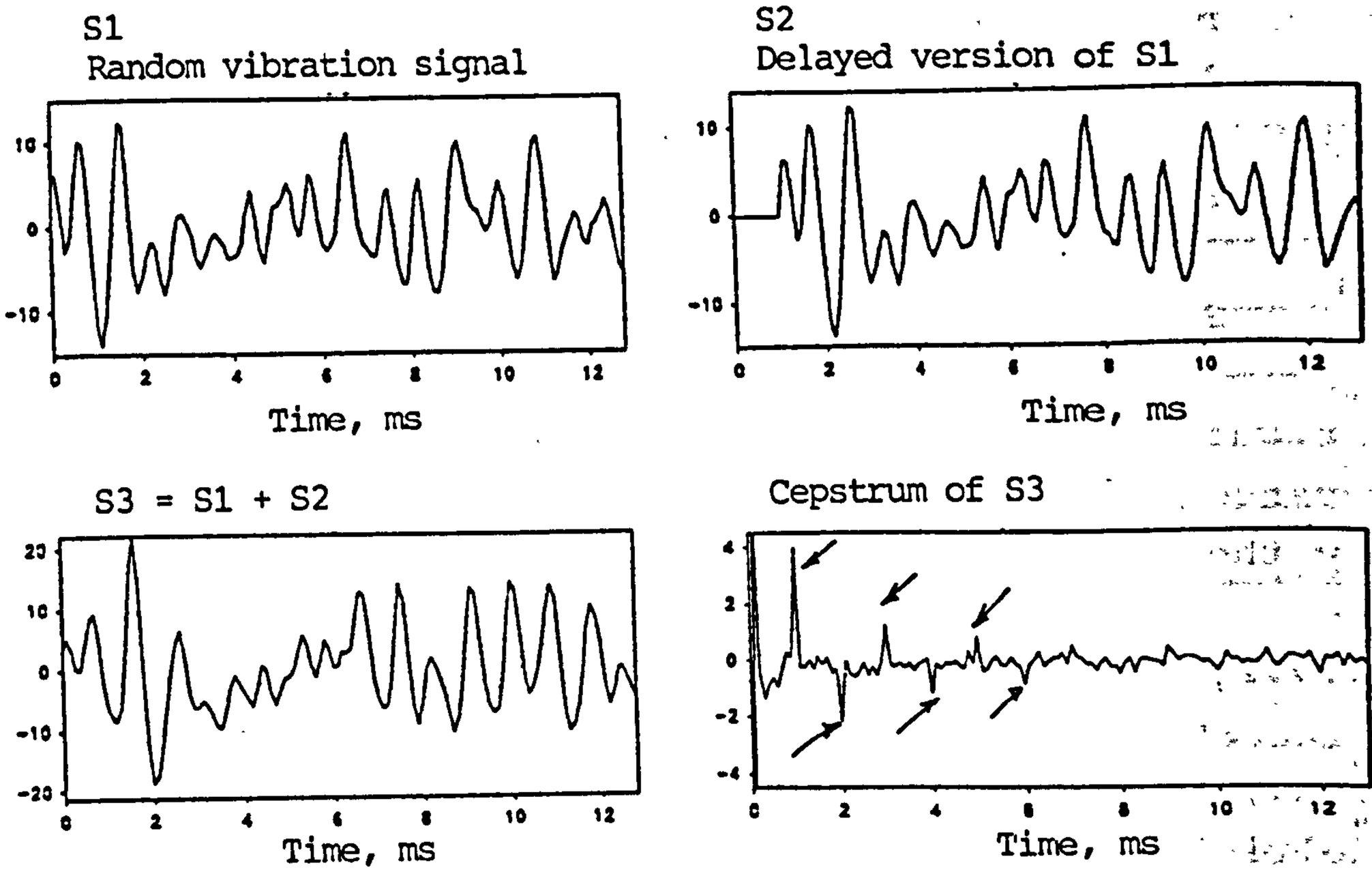

Fig 3.19 Cepstrum analysis of composite signals, showing periodicity when the amplitude of the delayed signal is greater than half of that of the original one. (Vertical axes in arbitrary scale).

requirement of this study.

Cepstrum analysis has been claimed useful for the detection of the time-delayed version of a signal in itself (section 2.3.5). It may be due to a secondary signal as a result of an echo, or delayed transmission in another, or a longer path. Attempts have been made to ascertain the capability and usefulness of the cepstrum function. A random signal was superimposed on a time-delayed version (by 1 ms) of itself. Cepstrum analysis was performed on the complex signal while using various amplitudes for the delayed component. It was found that the cepstrum was able to show the periodicity of T = 1 ms, which was found to correspond well with the time delayed (fig 3.19). However, the cepstrum analysis was found to be useful only when the delayed component has an amplitude of more than half of that of the original signal, otherwise the periodicity would be very vague. This results shows that cepstrum analysis would have limitations in its use when the echoed or delayed signal is weak.

3.9.3 System Error and Baseline Drift

The major source of electronic noise was coming from the charge amplifier. With maximum amplification sensitivity of 1 mechanical unit/V the typical output noise was about 3.5 mV (RMS). Quoting the worst case in which the signal level was about 0.5 V (RMS) after amplification, this represents a signal-to-noise level of more than 40 dB. However in the majority of cases, the amplifier sensitivity was set to 100 mechanical unit/V, at which the noise level was only about 0.7 mV (RMS). The measured electrical signal levels in most of the measurements ranged between 5 and 7.5 V, representing a signal-to-noise ratio of better than 80 dB, which suggested that the electronic noise level was negligible.

The analogue-to-digital conversion system quantized analogue signals to discrete levels with 12 bits resolution, resulting in quantization error which relates

to the input range and hence the size of each quantization step (Hamming, 1983). However, the software associated with the analogue-to-digital converter allows a programmable gain to cope with the input range as small as ±1.25 V. The variance of error E due to quantization is given by:

$$E = \frac{(2.5/4096)^2}{12} = 3.1 \; x \; 10^{-5} \; mV \qquad (3.5)$$

Assuming a difficult situation of acquiring a weak signal of 0.1 V (RMS), this corresponds to a signal-to-noise ratio of greater than 50 dB. Hence the noise level due to analogue-to-digital conversion was insignificant.

The acquisition system was found to have a baseline drift of about 1.8 ± 5 mV (mean ± SD) which did not justify specific adjustment of the offset of the vibration signals, except that the information in the extremely low frequencies would not be reliable.

3.10 OVERALL PLAN OF THE EXPERIMENTAL STUDIES

It is anticipated that some fundamental questions related to vibration analysis of the spine will be answered before proceeding on to in-vivo studies. Specimens of human lumbar spine will be tested under a simulated and well controlled condition to reveal its response to mechanical vibrations within a frequency range of 2 kHz. Particular attention is paid to test the capability of the vibration technique and the associated analysis in the detection of the changes in the mechanical characteristics of the lumbar spine as a result of its structural modifications. The vibration response of simulated fusion of the lumbar spine will be of particular interest, with the aim to test the sensitivity of the technique in the detection of changes in the structure of the lumbar spine. Normal subjects will be recruited to assess the specific vibration response of the lumbar spine in-vivo before the technique is applied on a selected group of patients. It is planned to develop a vibration technique and test protocol for the detection of

abnormality or structural changes of the lumbar spine due to surgical intervention or other pathologies.

3.11 SUMMARY

A system analysis approach will be adopted. The lumbar spine will be considered as a passive linear mechanical transmission system. Mechanical vibrations mainly in the forms of random vibration and tone bursts of discrete frequencies will used to excite the lumbar spine. Measurement of vibration response will be taken at appropriate spinous processes. The frequency response function which defines the ratio of motion response to excitatory force will be analyzed to reveal the dynamic characteristics of the lumbar spine in the audio frequency range up to 2 kHz. Suitable time parameters and amplitude parameters will be drawn from analysis in the time domain. Details of the experimental designs and findings are described in the appropriate chapters.

CHAPTER 4

PILOT STUDIES

4.1 INTRODUCTION

It is always easier to start tests on a simple model for all mechanical tests. Pilot studies have been carried out to investigate some fundamental technical aspects regarding the use of vibration technique for the examination of mechanical properties of disc-vertebrae complex. Segments of bovine coccygeal spine were used as a model for its simplicity in geometry and gross anatomy. Both random vibration and impact testing techniques have been applied for the tests, bearing the following objectives:-

i. to study the mechanical characteristics of the intervertebral disc and the vertebral body under low magnitude longitudinal stress from vibratory and impact force;

ii. to explore and decide an appropriate frequency range for vibration tests on human lumbar spine specimens;

iii. to study the applicability of the techniques mentioned in i) for the examination of changes in the mechanical properties of intervertebral disc;

iv. to test the linearity of the system under the test conditions; and

v. to test the feasibility of the measurement techniques and analysis protocols discussed in chapter 3.

For iii), changes in the mechanical properties of the intervertebral disc induced by freezing the specimen at about -15 °C and subsequent thawing to room temperature were examined. Random vibration tests were performed during the 28 hours of thawing. The changes in the frequency response of the intervertebral discs were monitored, to test if the vibration technique was sensitive enough to

detect the changes in their mechanical properties.

Linearity of behaviour, especially for biological systems, is a major concern as the system analysis technique (section 3.2.2) and its associated analysis e.g. frequency response functions (section 2.4.2) to be used in this study are based on the assumption that the system behaves linearly under the test conditions. Any non-linearity of the system would render the tests and analysis invalid. This is again one of the aspects which will be considered and investigated in this pilot study.

A porcine specimen which comprised the whole lumbar spine was mounted for vibration tests in a similar experimental set-up designed for tests on the human lumbar spines. The intention was to gain experience of the technique and to explore the use of several designs of attachment pins for the force and acceleration transducers which were to be used in in-vitro study on human specimens.

This chapter only reports the experimental set-ups for the pilot studies. Specifications of the equipment have been described in chapter 3 and appendix IV. The data acquisition protocol and the subsequent data analysis have been described in section 3.6.

4.2 IMPACT TESTS ON BOVINE COCCYX

A cylindrical block of stainless steel was suspended horizontally by thin steel wires forming a ballistic suspension. The bovine specimen which comprised two coccygeal vertebrae and the intervening disc was mounted on one end surface of the block with epoxy adhesive so that its longitudinal axis was colinear with the axis of the block (fig 4.1). The specimen was covered by gauze saturated with normal saline to prevent dehydration during thawing at room temperature, and in the intermissions between tests. Repeated impulsive excitations were applied by a hand-held dental hammer which struck the other end of the cylindrical block at intervals of about 1 s. The input excitation signal to the bovine specimen was measured by a

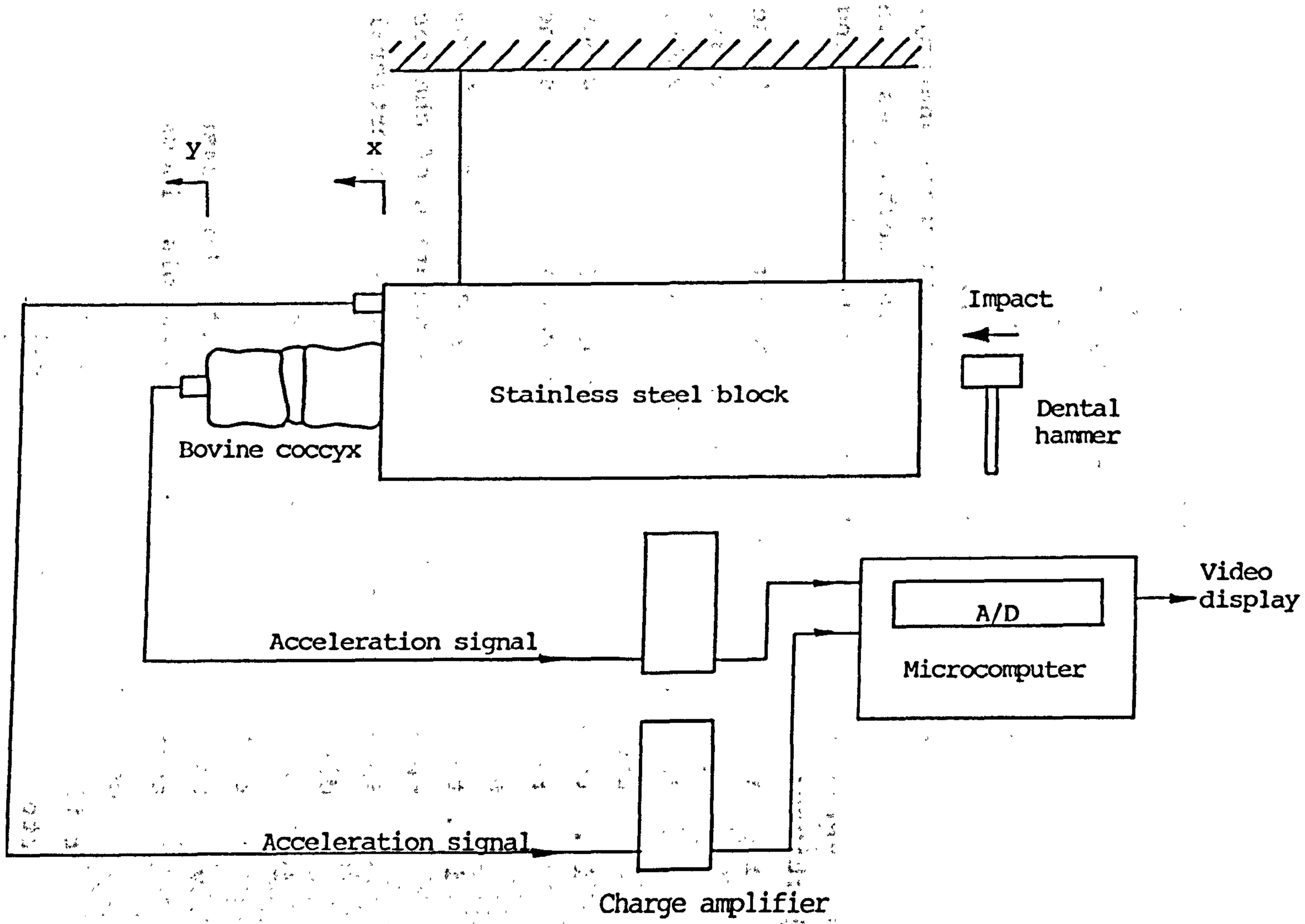

Fig 4.1 Schematic diagram of the experimental set-up for impact tests on a bovine coccyx specimen.

detect the changes in their mechanical properties.

Linearity of behaviour, especially for biological systems, is a major concern as the system analysis technique (section 3.2.2) and its associated analysis e.g. frequency response functions (section 2.4.2) to be used in this study are based on the assumption that the system behaves linearly under the test conditions. Any non-linearity of the system would render the tests and analysis invalid. This is again one of the aspects which will be considered and investigated in this pilot study.

A porcine specimen which comprised the whole lumbar spine was mounted for vibration tests in a similar experimental set-up designed for tests on the human lumbar spines. The intention was to gain experience of the technique and to explore the use of several designs of attachment pins for the force and acceleration transducers which were to be used in in-vitro study on human specimens.

This chapter only reports the experimental set-ups for the pilot studies. Specifications of the equipment have been described in chapter 3 and appendix IV. The data acquisition protocol and the subsequent data analysis have been described in section 3.6.

4.2 IMPACT TESTS ON BOVINE COCCYX

A cylindrical block of stainless steel was suspended horizontally by thin steel wires forming a ballistic suspension. The bovine specimen which comprised two coccygeal vertebrae and the intervening disc was mounted on one end surface of the block with epoxy adhesive so that its longitudinal axis was colinear with the axis of the block (fig 4.1). The specimen was covered by gauze saturated with normal saline to prevent dehydration during thawing at room temperature, and in the intermissions between tests. Repeated impulsive excitations were applied by a hand-held dental hammer which struck the other end of the cylindrical block at intervals of about 1 s. The input excitation signal to the bovine specimen was measured by a

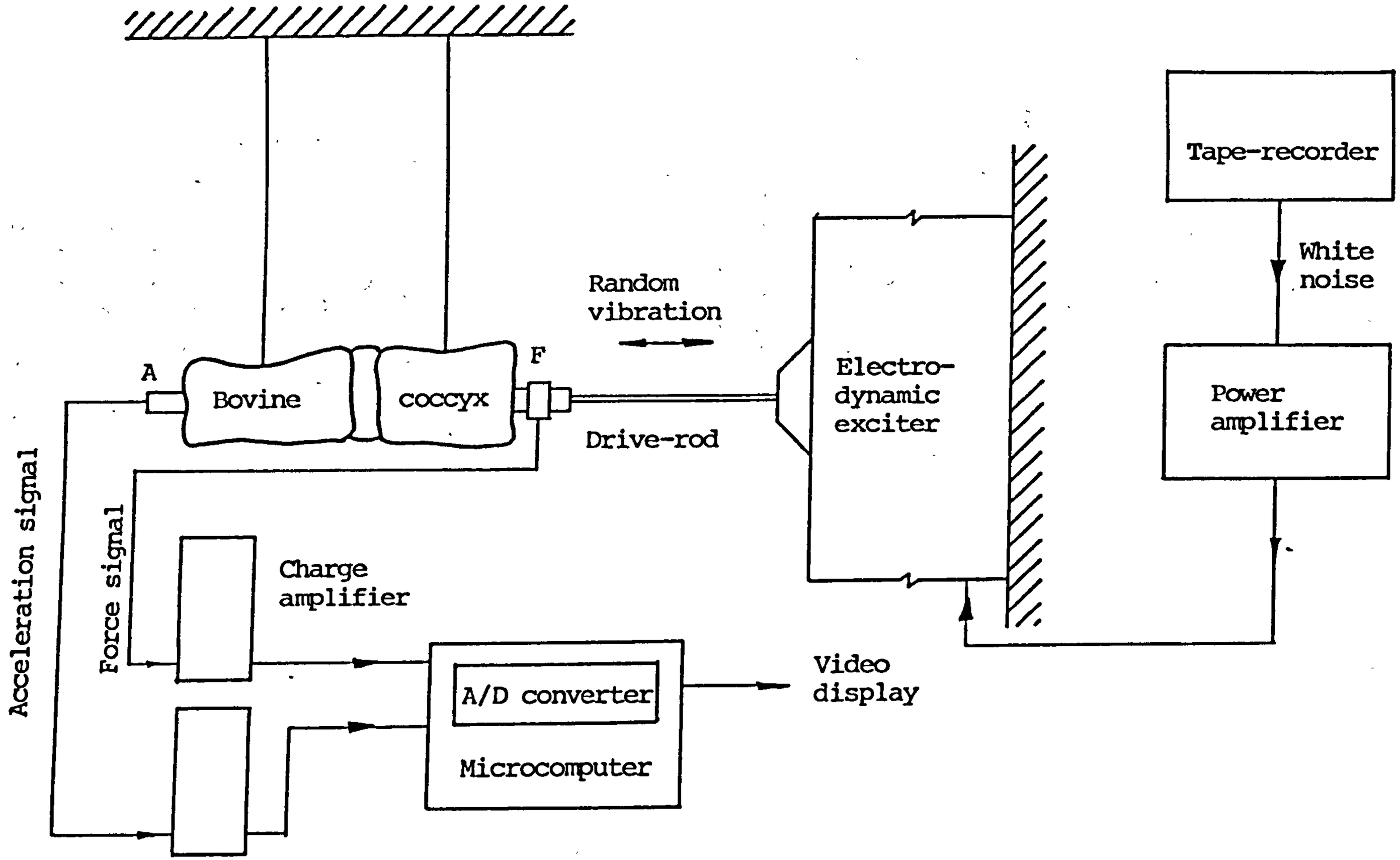

Fig 4.2 Schematic diagram of the experimental set-up for random vibration tests on a bovine coccyx specimen.

miniature piezoelectric accelerometer mounted by using a thin layer of beeswax on the end surface adjacent to the specimen. An identical accelerometer was fixed to the vertebra at the free end of the specimen on a stud through a tapped mounting screw (diameter 5 mm) which was then fixed in the bone substance. The input (x) and output (y) acceleration signals were picked up simultaneously by the accelerometers and then conditioned by two charge amplifiers with built-in analogue band-pass filters of low and high cut-off frequencies at 2 Hz and 3 kHz respectively. A microprocessor-based system, interfaced with an analogue-to-digital converter sampled the signals at a rate of 10 kHz with 12-bits resolution (section 3.8.3). The signals were then processed digitally and the frequency response function $H_{xy}(f)$ which defines the transmissibility of impulsive stress in the disc-vertebrae specimen was then calculated by applying the following computation algorithm and spectral averaging:

$$H_{xy}(f) = \frac{\hat{G}_{xy}(f)}{\hat{G}_{xx}(f)} \qquad (4.1)$$

where

$\hat{G}_{xy}(f)$ is the estimated cross-spectrum between x and y; and

$\hat{G}_{xx}(f)$ is the autospectrum of x.

4.3 RANDOM VIBRATION TESTS ON BOVINE COCCYX

The set-up for impact tests was modified so that a similar specimen was suspended directly by thin wires forming a ballistic suspension (fig 4.2). The specimen had been thawed to room temperature under similar conditions to that mentioned in section 4.2. A random vibratory force of frequency ranging from 20 Hz to 2 kHz was applied to the specimen by an electrodynamic exciter via a piezoelectric force transducer which was attached colinearly with the proximal vertebral body through a screw fixed in the bone

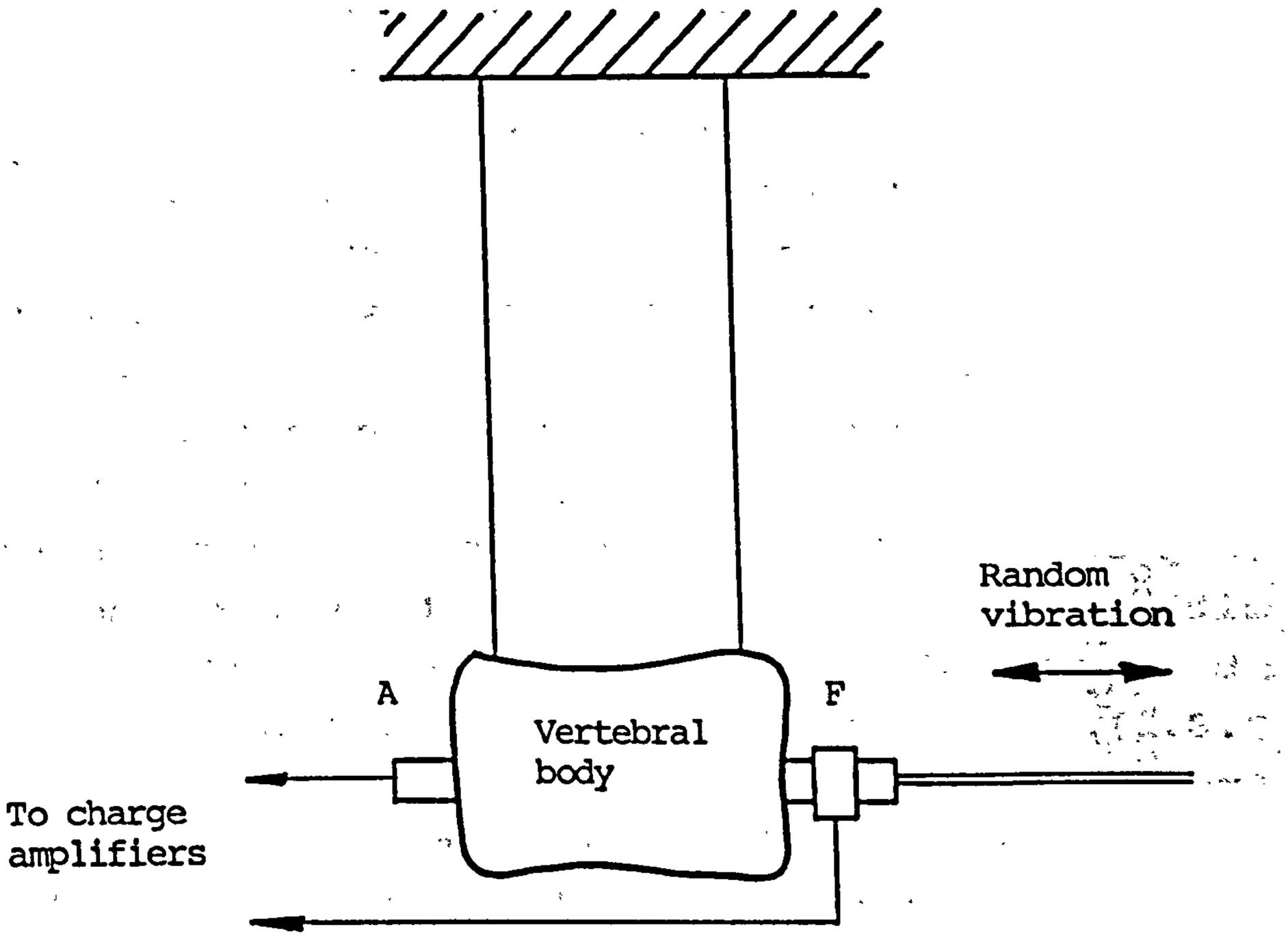

Fig 4.3 Schematic diagram of the experimental set-up for random vibration tests on a vertebral body of bovine coccyx. F and A are respectively the force and acceleration signals.

substance. The vibratory force (F) was measured both in compression and tension. The motion response (A) was detected by the miniature piezoelectric accelerometer fixed in the same manner as in the impact tests on the free surface of the distal vertebral body of the specimen. The input and output signals were conditioned by the charge amplifiers and were then acquired by the same digital system described above, at a sampling rate of 10 kHz. The frequency response function $H_{FA}(f)$ which expressed the motion response in terms of transfer accelerance, and the coherence function were obtained by the fast Fourier transform using the following computation algorithm:

$$H_{FA}(f) = \frac{\hat{G}_{FA}(f)}{\hat{G}_{FF}(f)} \qquad (4.2)$$

where

$\hat{G}_{FA}(f)$ is the estimated cross-spectrum between F and A; and

$\hat{G}_{FF}(f)$ is the autospectrum of F.

An identical random vibration test and data analysis procedure was also performed on a single vertebral body (fig 4.3). Frequency response function and coherence function were computed for the excitatory force (F) and the motion response (A) measured at opposite ends of the vertebral body. The closeness of the mechanical characteristics of the vertebral body to a rigid-body was tested. This procedure would differentiate the mechanical properties of the vertebral body from those of a disc-vertebrae complex; hence the transmissibility of the disc could be found.

4.4 RESULTS

It was found that, with practice, the hand-held impact hammer was able to generate a consistent impulsive excitation of short duration (0.5 ms) to the system. The low frequency components due to translational and torsional

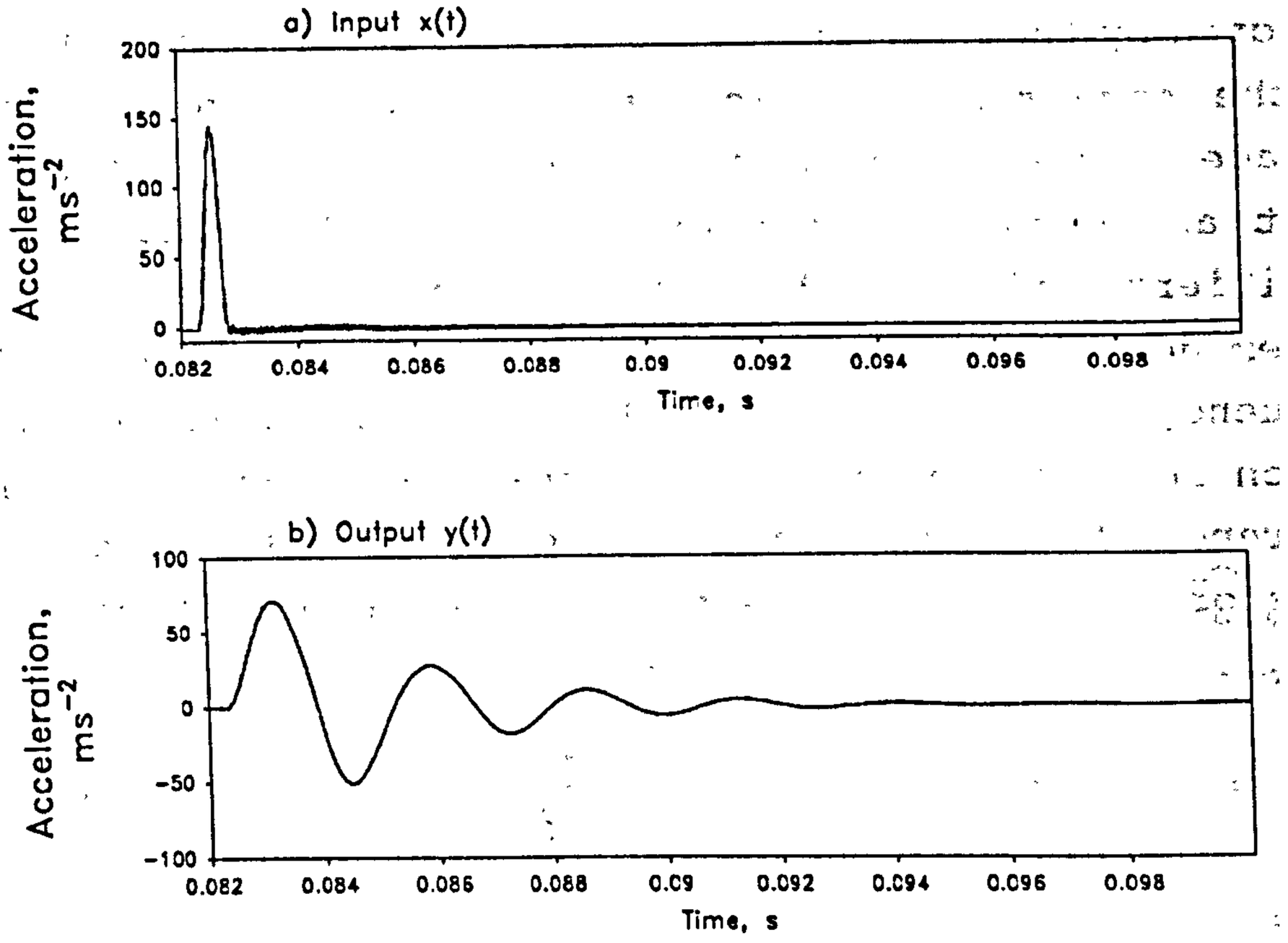

Fig 4.4 Vibration response of Specimen A under an impact test.

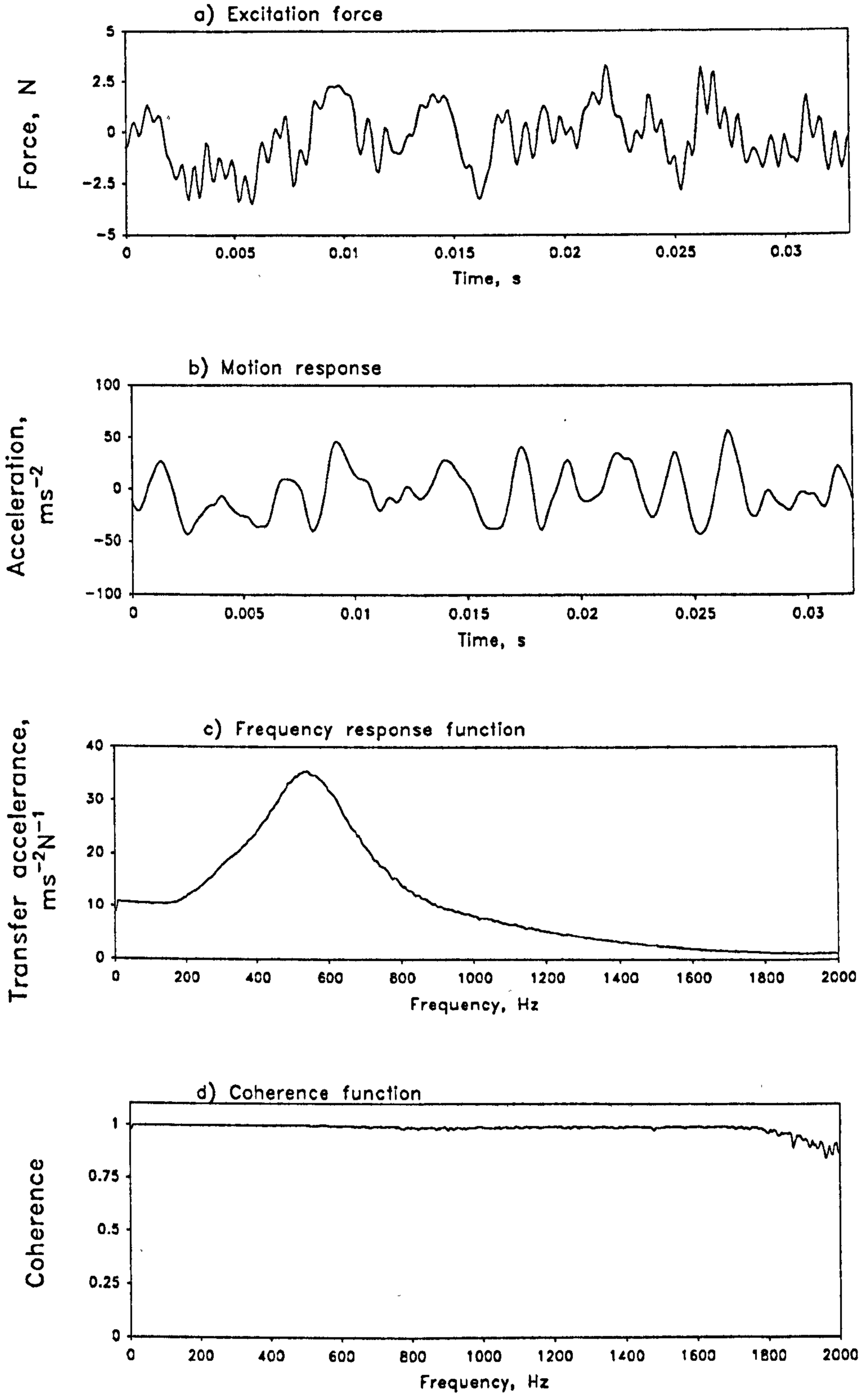

Fig 4.5 Vibration response of Specimen B under a random vibration test.

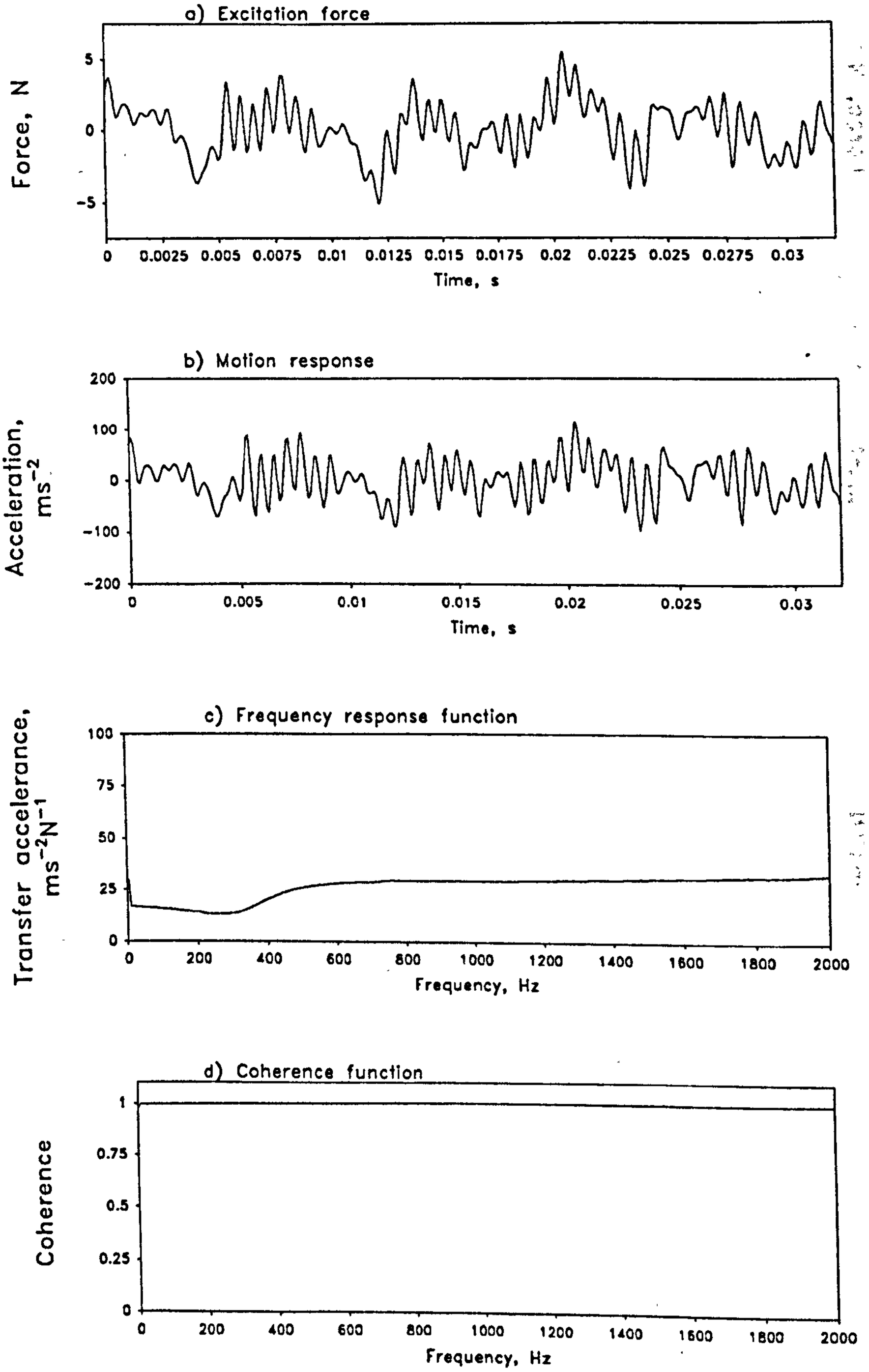

Fig 4.6 Vibration response of a vertebral body of bovine coccyx under random vibration test.

oscillations of the pendular system, and the high frequency components due to ringing of the metal block under impact were filtered off. The set-up was thus able to limit unwanted signals due to cross-sensitivity as a result of movement of the specimen in the horizontal and vertical directions perpendicular to the longitudinal axis of the specimen. Figure 4.4 shows the input and output signals as picked up by the accelerometers during an impact test. There was a short delay of 0.07 ms of the output signal after the impulsive input signal. The output signal also exhibited logarithmic decrement in its amplitudes, consistent with a damped vibration. The frequency response function of the disc-vertebrae complex (Specimen A) demonstrates a clearly defined peak at 354 Hz. These vibratory characteristics suggest that the bovine specimen behaved as a mechanical vibration system with single degree-of-freedom, and damping.

Figure 4.5 shows the input vibratory force and the output motion response signals during a random vibration test on another bovine specimen (Specimen B). It can be seen that the high frequency components are highly attenuated. The frequency response function shows a definite peak at 540 Hz for this particular test specimen, in a similar manner to that observed in the impact test. The frequency response function also shows some degree of damping when compared with figure 2.3.

It was found that the vertebral body exhibited a fairly flat frequency response during a random vibration test (fig 4.6). This finding suggests that the vertebral body can be considered relatively rigid compared to the intervening disc, and that it behaved as a solid mass when subject to random vibration within the specified frequency range. This finding also suggests that the attachment screws were strong enough to provide a rigid interface between the transducer and bone substance under the test condition.

The coherence function γ^2 between the input and output

Table 4.1 Typical values of damping ratio (from Steidal Jr, 1989).

Materials or structures	ζ
Automobile shock absorbers	0.1-0.5
Rubber	0.04
Rivet steel structures	0.03
Concrete	0.02
Wood	0.003
Cold rolled steel	0.0006
Cold rolled aluminium	0.0002
Phosphor bronze	0.00007

signals was determined by equation 2.36. For all impact and random vibration tests, the coherence function was very close to unity throughout the frequency range of interest, showing a high causality relationship between the input excitation and the output motion response (fig 4.4d, 4.5d & 4.6d). This high coherency also indicates that the test system behaved linearly under the test conditions and was free from noise.

4.5 MODELLING

A single degree-of-freedom lumped parameter model was set up to illustrate theoretically the mechanical behaviour of the disc-vertebrae complex. The system comprises a mass, a spring and a viscous damper similar to that shown in figure 2.2. From the experimental results under impact tests, it was noted that the bovine specimen behaved as a vibration system showing a logarithmic decrement in its amplitudes of response with the damping ratio $\zeta = 0.15$. This is a high value when compared with other biological and engineering materials as shown in table 4.1 (Steidal Jr, 1989). This finding also suggests the disc-vertebrae complex is a highly damped structure and that the human lumbar spine might have similar mechanical characteristics.

For the simple theoretical model depicted in figure 2.2, transmissibility of motion is defined as (Blake, 1988):

$$Transmissibility,\ T(\omega) = \sqrt{\frac{1 + (2\zeta\omega/\omega_n)^2}{(1 - \omega^2/\omega_n^2)^2 + (2\zeta\omega/\omega_n)^2}} \qquad (4.3)$$

where

ζ is the damping ratio;

ω_n is the natural angular frequency in rad/s; and

ω is the forcing angular frequency in rad/s.

An attempt has been made to curve-fit by non-linear regression procedure the theoretical transmissibility to

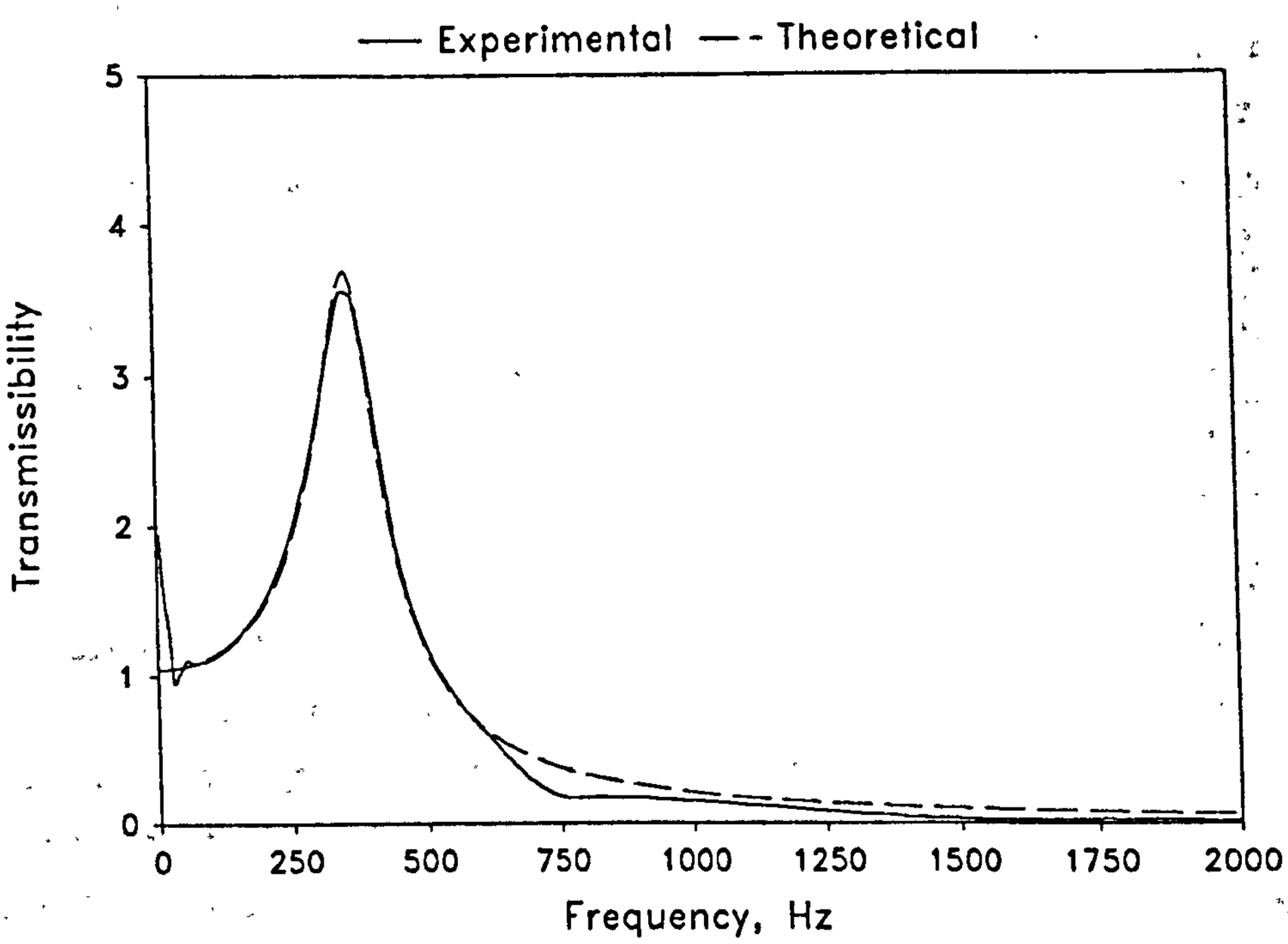

Fig 4.7 Curve-fitting for the transmissibility of a bovine disc-vertebrae complex (Specimen A) under impact test.

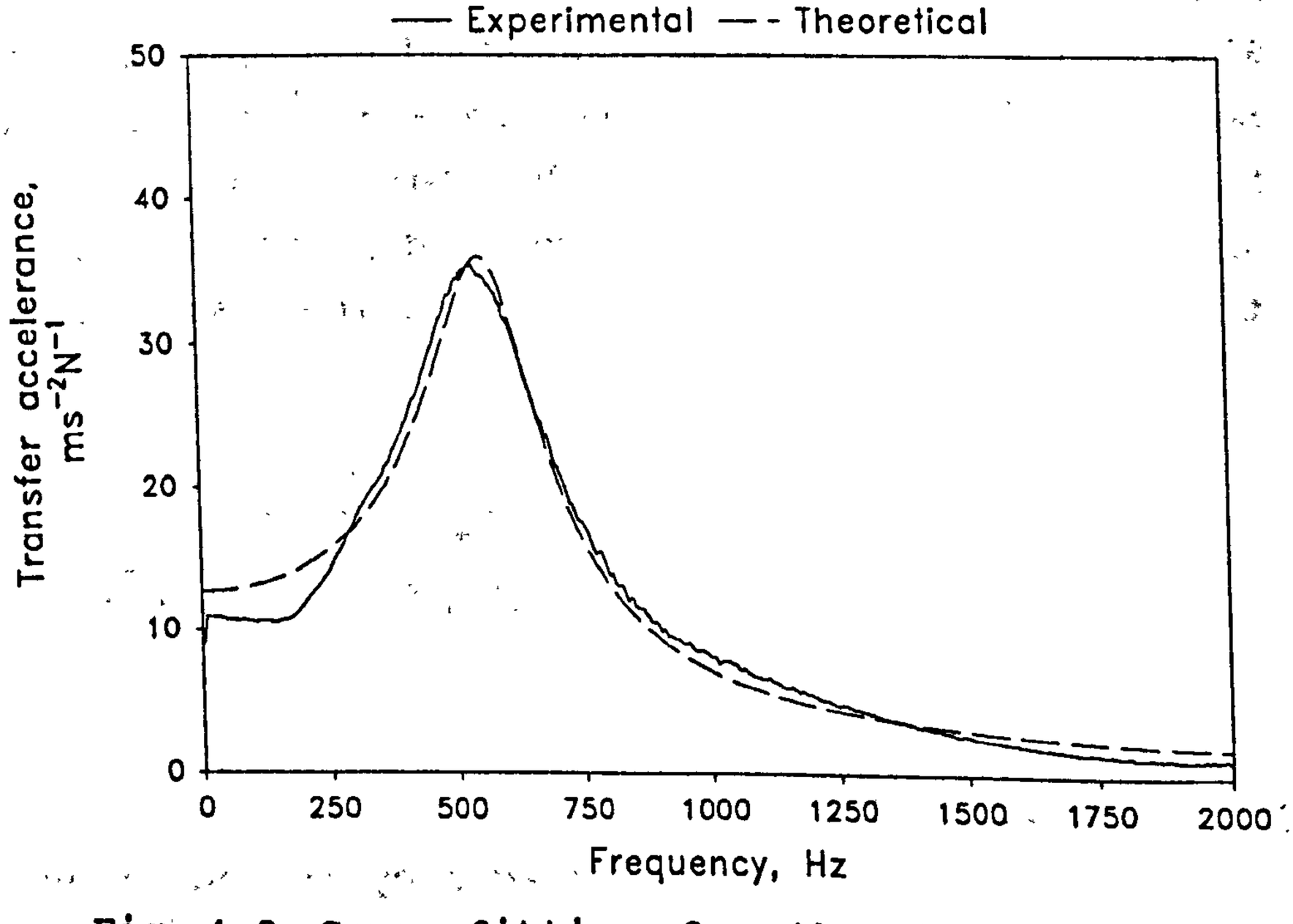

Fig 4.8 Curve-fitting for the frequency response function of a bovine disc-vertebrae complex (Specimen B) under random vibration test.

the experimentally determined frequency response function. Figure 4.7 shows that the transmissibility curve as shown in figure 4.4c fits closely to equation 4.3, with the coefficient of determination R^2 = 0.986. Similar curve-fitting procedure has been made to the frequency response function determined for another bovine specimen during random vibration test (fig 4.5c). Figure 4.8 shows that the experimental data also fit closely to the theoretical curve, with R^2 = 0.985. The damping ratio and damped natural frequency could then be determined experimentally (table 4.2). These results suggest that the disc-vertebrae complex of bovine coccyx behaved closely to a simple mass-spring-damper system with single degree-of-freedom when excited by under impact force and random vibration. The experimental approach, in association with the subsequent data analysis technique, can be considered adequate in revealing the bovine specimens' vibratory characteristics.

4.6 RANDOM VIBRATION TESTS DURING THAWING

Freezing at sub-zero temperature is a commonly used method of preserving specimens of the musculoskeletal tissue for biomechanical studies. It is generally accepted by investigators in the field that the procedure of deep freezing followed by thorough thawing does not affect the mechanical properties of biological tissue (Smeathers & Joanes, 1988). The process of thawing of a specimen from a deeply frozen state involves a transition state through which the mechanical characteristics of the specimen gradually change and approach to *normal*, or to a state closely resembling the natural condition. Thawing from a frozen state is also a handy means of inducing changes in the physical properties of the intervertebral disc without any mechanical or structural intervention.

Attempts have been made to investigate whether the system analysis approach and the frequency response function would be sensitive enough to indicate the changes in the mechanical behaviour of the disc-vertebrae complex

Table 4.2 Damping ratios and damped natural frequencies determined experimentally.

Specimens	Damping ratio ζ	Damped natural frequency f_d
Specimen A under impact test	0.150	367 Hz
Specimen B under random vibration test	0.192	574 Hz

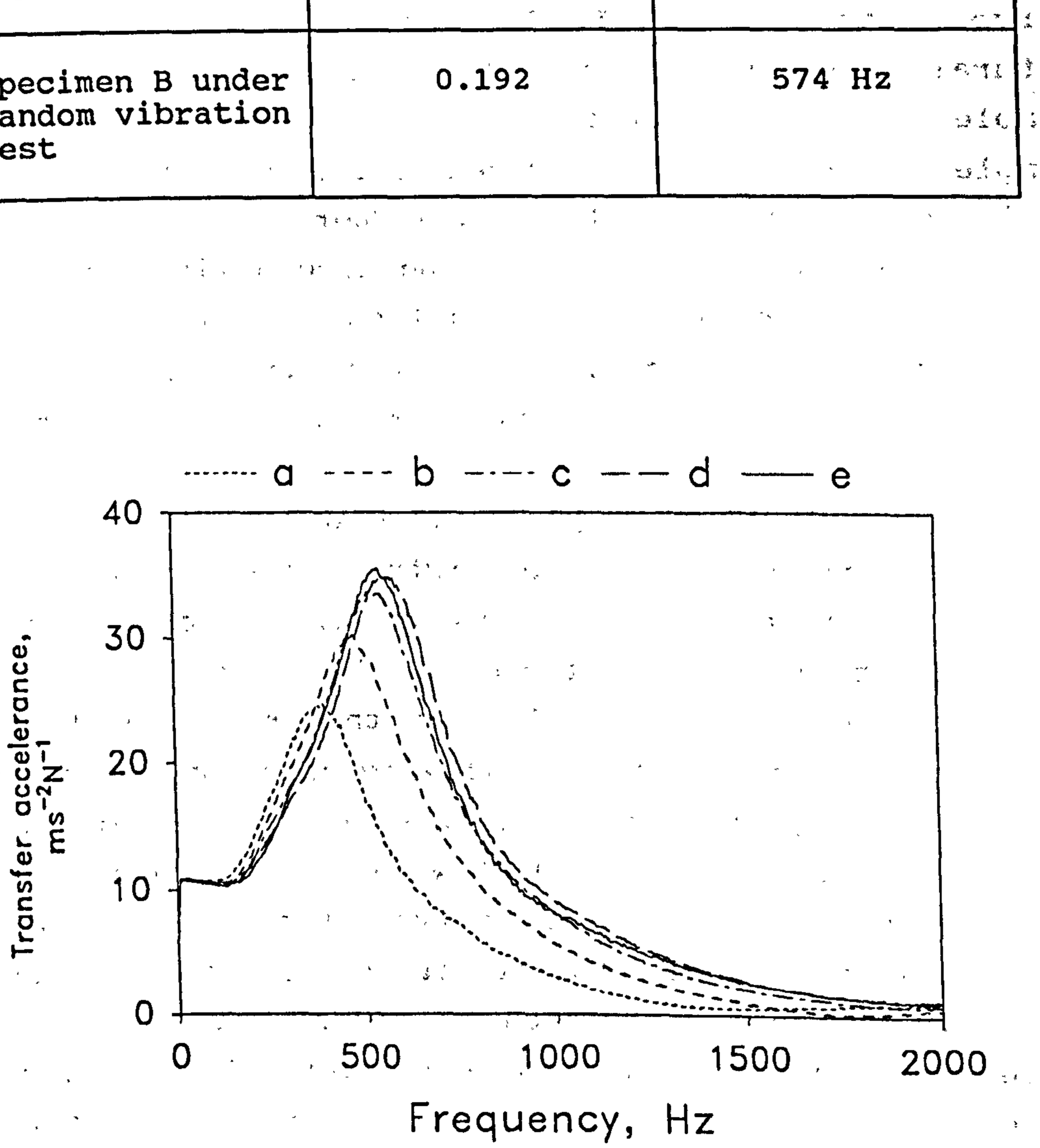

Fig 4.9 Frequency response functions of a bovine disc-vertebrae complex under random vibration during thawing. a) 1 h; b) 5 h; c) 9 h; d) 17 h; e) 28 h of thawing.

during thawing. Random vibration tests were then carried out to examine the changing mechanical characteristics of similar segments of bovine coccyx during the 28 hours of thawing from a frozen state at -15 °C. The data would provide an indication of the time taken to thaw the specimen and to achieve a stable mechanical response.

The same test procedure as outlined in section 4.3 was repeated for similar bovine specimens. In this pilot study, the specimen which comprised two bovine coccygeal vertebrae and the intervening disc had been wrapped in cellophane and stored at -15 °C for over one week. The specimen was wrapped in cotton gauze soaked with normal saline to prevent dehydration during thawing, except during the vibration tests. The vibration tests commenced soon after the specimen had been removed from the freezer and set up for testing. The tests were conducted at intervals for the following 28 hours in an ambient temperature between 20 and 23 °C. The same analysis technique was applied and the frequency response function was computed by equation 4.2.

As shown in figure 4.9, the frequency response function exhibits a gradual shift to the higher frequency, indicating a gradual increase in resonant frequency with thawing and also, a gradual decrease in the damping ratio. The biomechanical characteristics tend to stabilize in about 10 hours of thawing.

Based on the mechanical characteristics of the specimen obtained during thawing, it was noted that the measurement of the frequency response function was sensitive enough to detect the gradual changes in mechanical behaviour of the disc-vertebrae complex and that the vibration technique was a powerful tool suitable for the examination of the mechanical characteristics of the intervertebral joint and its associated structures.

As an ancillary finding regarding the extent of thawing, it is logical to suggest that for similar specimens of the spinal column under comparable conditions, at least 10 hours of thawing at an ambient temperature of

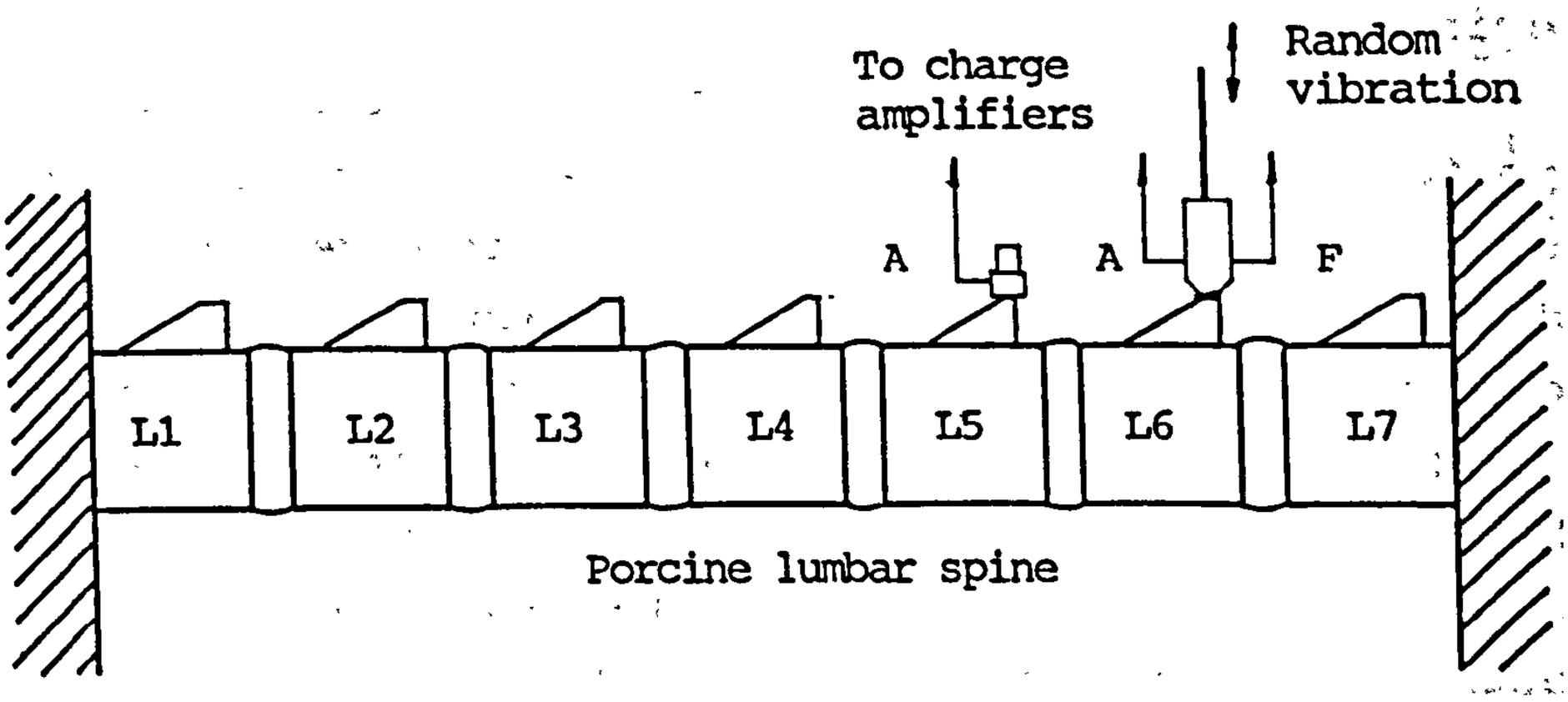

Fig 4.10 Schematic diagram of the experimental set-up for random vibration test on porcine lumbar spine in vitro.

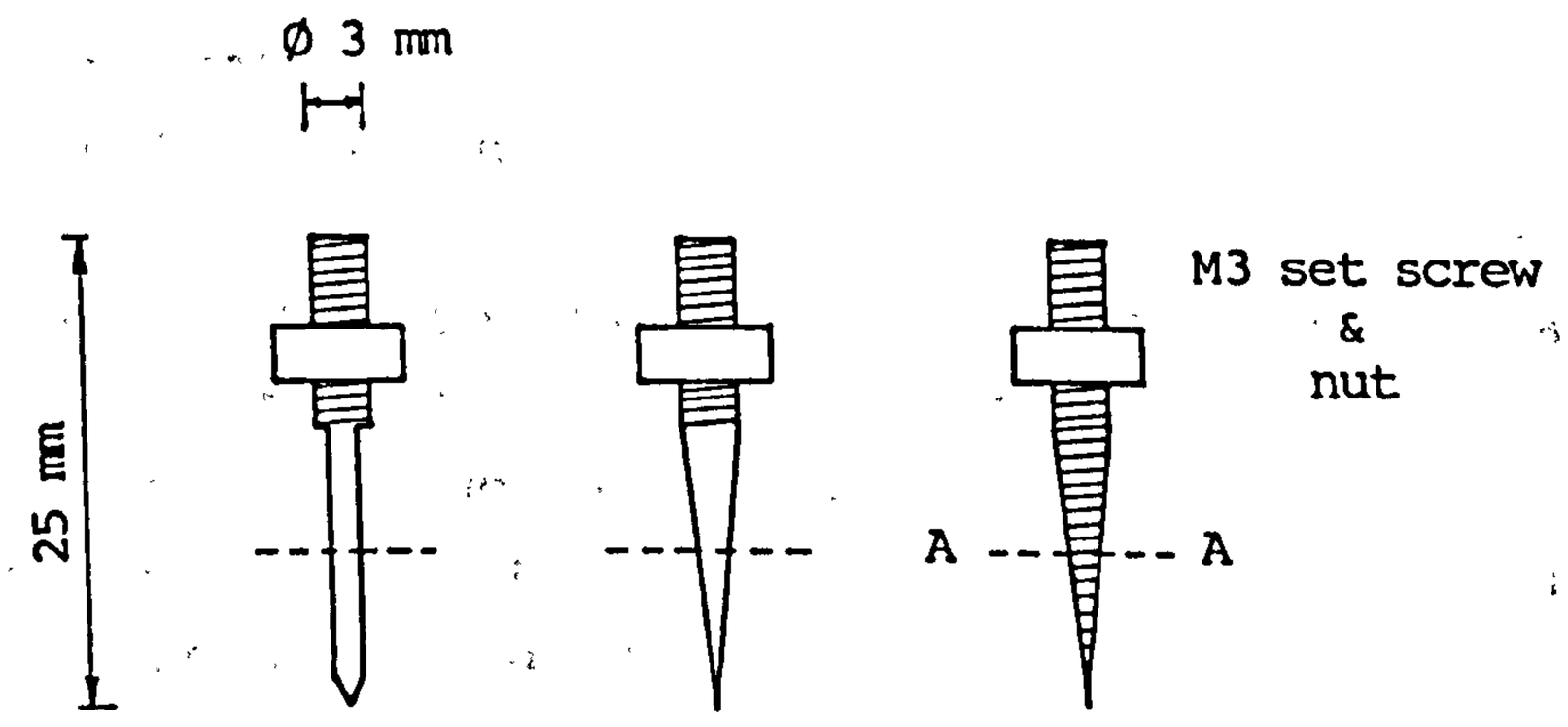

Fig 4.11 Designs of attachment pins for vibration transducers. a) A thin pin; b) a round pin with tapered shape; c) a flat pin with tapered end.

about 20 °C is required prior to mechanical test. For larger specimens such as the human lumbar spine, probably a longer period of thawing is needed to ensure that the disc's mechanical behaviour is stabilized. It is again a useful guideline which has been followed regarding the preparation of all test specimens for this study.

Although the temperature within the disc was not monitored during thawing, it can be assumed that the frequency response of the intervertebral disc is temperature dependent. Whether this characteristic is due to temperature dependence of the stiffness or of the viscosity of the disc, or of both, has yet to be investigated.

4.7 VIBRATION TESTS ON PORCINE LUMBAR SPINE

Random vibration testing was also carried out on a specimen of porcine lumbar spine which comprised the L1 to L7 vertebrae. To simulate the biomechanical conditions experienced in the body of the animal in a standing posture, the lumbar spinal column was mounted horizontally between two metallic brackets which were clamped securely on two bench vices. The specimen was further secured by epoxy-based filler and wood screws which were inserted through the bone substance of the vertebral bodies at both ends of the specimen. Random vibratory force of less than 5 N (peak) in the frequency range from 20 Hz to 2 kHz was applied in the antero-posterior direction to the L6 spinous process of the lumbar spine. Vibration response was measured as acceleration in the same direction at other spinous processes in turn. The force and acceleration transducers were attached at the appropriate spinous process through 2.5 cm pins modified from M3 set screws (fig 4.11a). Figure 4.10 shows the schematic diagram of the experimental set-up. Frequency response function defined by equation 4.2 was computed by using the fast Fourier transform and spectral averaging.

Results show that the porcine lumbar spine behaved in

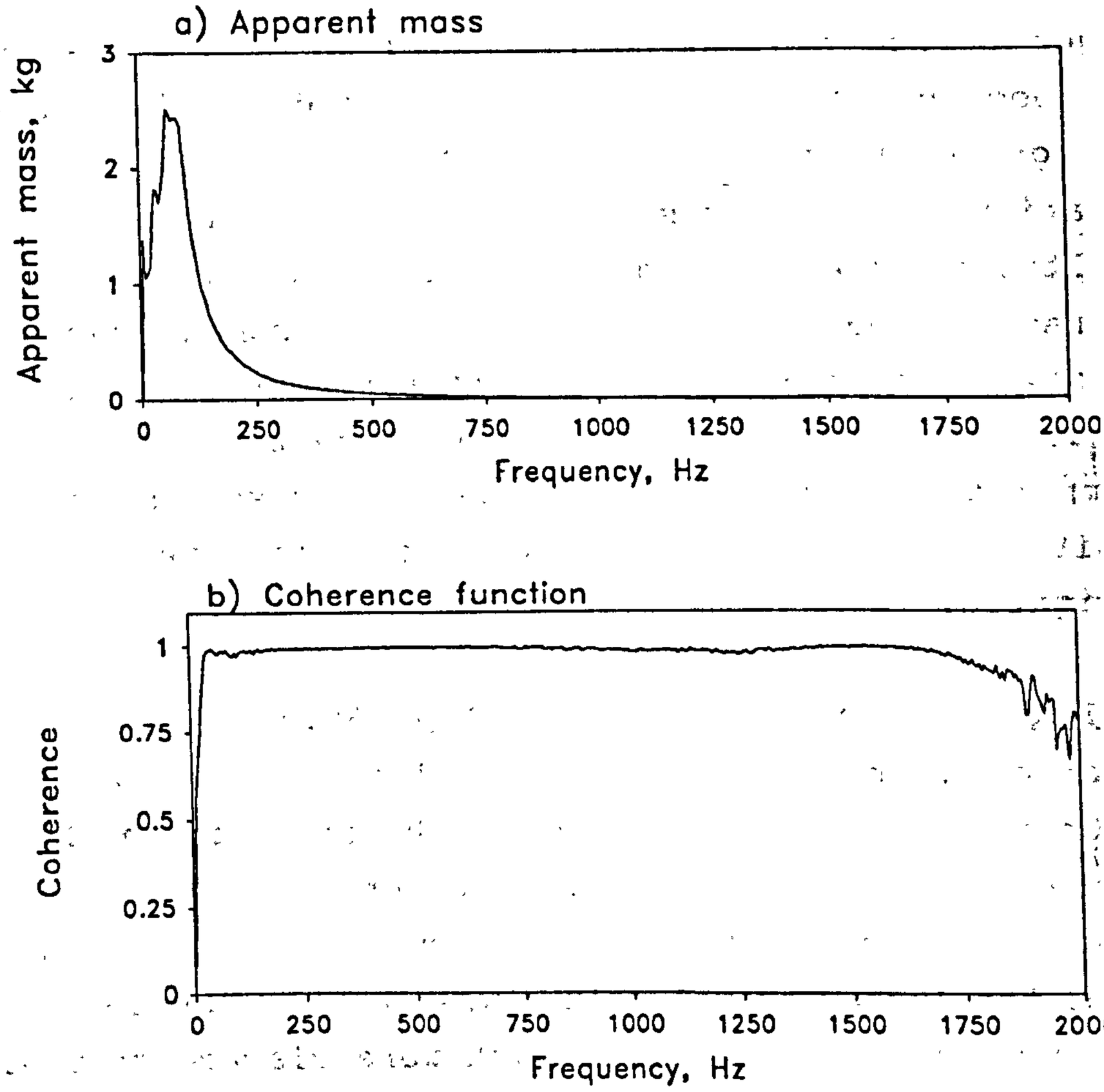

Fig 4.12 Apparent mass measurement at L6 spinous process of a porcine lumbar spine.

a different manner from a relatively simpler disc-vertebrae complex of the bovine coccygeal specimen when excited by random vibratory force in the antero-posterior direction. Figure 4.12 shows the apparent mass measurement which expresses the transmissibility at the L6 spinous process of the porcine lumbar spine. The transmissibility was low in the frequency above 1 kHz, which means that the vibratory force above this frequency was not effectively transmitted to the porcine specimen. This ineffective transmissibility may be due to the unsatisfactory design of the drive-pin as shown in figure 4.11a. The drive-pin did not provide a secure attachment of the transducers at the spinous processes. This led to some pin-loosening, hence poor transmission of vibration. The pin was then redesigned as shown in figures 4.11b & c. The flat pin with a tapered end was found to be most suitable when manually checked of its firmness of attachment at the spinous process. It was found to provide a firm anchorage by plug-fitting itself in the bone substance when inserted into the spinous process. This design of drive-pin was then used in the subsequent in-vitro tests on the human lumbar spine. However, vibration measurements on the porcine lumbar spine was found to have high coherence as shown in figure 4.12b. Experience from the pilot study also showed that the set-up of the lumbar spine specimen in a horizontal position was a suitable simulation of the end conditions in-vivo. The method of fixation of the specimen on the metallic brackets with epoxy-filler was effective. However some modifications would be required for the human lumbar spine for its bigger size. A deeper cup would be required for complete embedment of the vertebrae at the ends. This pilot test also suggested that a vibratory force of about 5 N (peak) would be adequate for a test of this nature. The accelerometer was found to be a suitable transducer for the measurement of vibration response of the lumbar spine.

4.8 SUMMARY

The results obtained from these pilot studies on bovine and porcine specimens are positive and the objectives have been achieved. The findings indicate that the instrumentation, measurement techniques and analysis procedures are suitable for use in further study. The measurement of frequency response function is applicable, and is sensitive enough for tests on the mechanical characteristics and their changes induced by structural modification of the spinal specimens. The setting of test specimen of porcine lumbar spine in a horizontal position is suitable for in-vitro test of the human lumbar spine though refinement and modification of the end supports are needed. Experience from these pilot studies also suggests that the frequency range up to 2 kHz is adequate for vibration response analysis of the lumbar spine. Vibration testing in a higher frequency range would not be appropriate as it is envisaged that no further information regarding the vibratory characteristics of the test specimens would be obtained.

CHAPTER 5

VIBRATION RESPONSE OF THE LUMBAR SPINE IN-VITRO

5.1 INTRODUCTION

The main aims of this in-vitro study were to examine the motion response and dynamic characteristics of intact lumbar spine under a well controlled vibratory condition. It would be essential to establish a knowledge basis for further investigation into one which presents with structural modifications or abnormalities e.g. fusions of the intervertebral joints. It was also envisaged that some useful parameters be identified to characterize the in-vitro mechanical characteristics of the intact lumbar spine before in-vivo studies could be extended to normal subjects and patients. This study also examined the effect of the end support conditions on the vibration response of the lumbar spine. At the present moment a knowledge of the precise end conditions for the lumbar spine in-vivo is not available.

Vibration tests on specimens of human lumbar spine were carried out in the Tissue Mechanics Laboratory of the Bioengineering Unit at the University of Strathclyde. The test environment was noted and it was found to be fairly stable in terms of temperature and relative humidity which may have effect on the mechanical properties of the soft tissues and structures of the test specimen. The vibration level of the test bench which supported the specimen and mounting device was checked to ensure that the testing system was adequately insulated from vibrations transmitted from the floor and nearby machinery.

The objectives of the in-vitro vibration tests were to reveal the following dynamic characteristics of the lumbar spine in free and fixed support conditions (section 5.2.1):

-rigid-body vibration mode;
-flexural vibration mode;
-mechanical impedance and apparent mass; and
-mobility response and other associated parameters.

This chapter describes the experimental design and outlines the general mechanical characteristics of isolated specimens of the lumbar spine under vibration tests. The gross motion response of the specimen in both free and fixed conditions are studied first. Apparent mass and its relation to transmissibility is examined to reveal the effectiveness of transmission of vibratory energy to the lumbar spine from an external excitatory force. Transfer mobility, summated mobility, total mobility, and band mobility which describe the generalized mechanical characteristics of the specimen are analyzed and reported. Attenuation of vibration at different lumbar segments is also reported. Specific and local response within a single vertebra of the specimen are outlined and discussed in the sections that follow. The results of vibration tests using tone bursts of discrete frequencies and their analysis in the time domain would give further insight into the transmission time of vibration waves and the associated time-delay along various segments of the lumbar spine. All results reported in this chapter refer to the findings of the tests performed on intact specimens supported in free or fixed end conditions. The testing equipment has been described in chapter 3. Specifications of the equipment are described in appendix IV. The mathematical and mechanical principles of the measurements are drawn from chapters 2 and 3.

5.2 EXPERIMENTAL DESIGN

Ten human lumbar spines including the 12th thoracic vertebra and the sacrum were harvested. The individual particulars of the specimens are listed in appendix I. Each specimen was cleared of attaching musculature leaving the ligaments, intervertebral discs and the zygapophyseal joints intact. Efforts had been taken to avoid destroying the joint capsules and ligaments by excessive removal of the paraspinal muscles. The specimen was checked to exclude fusions of the spinal joints or the intervertebral discs,

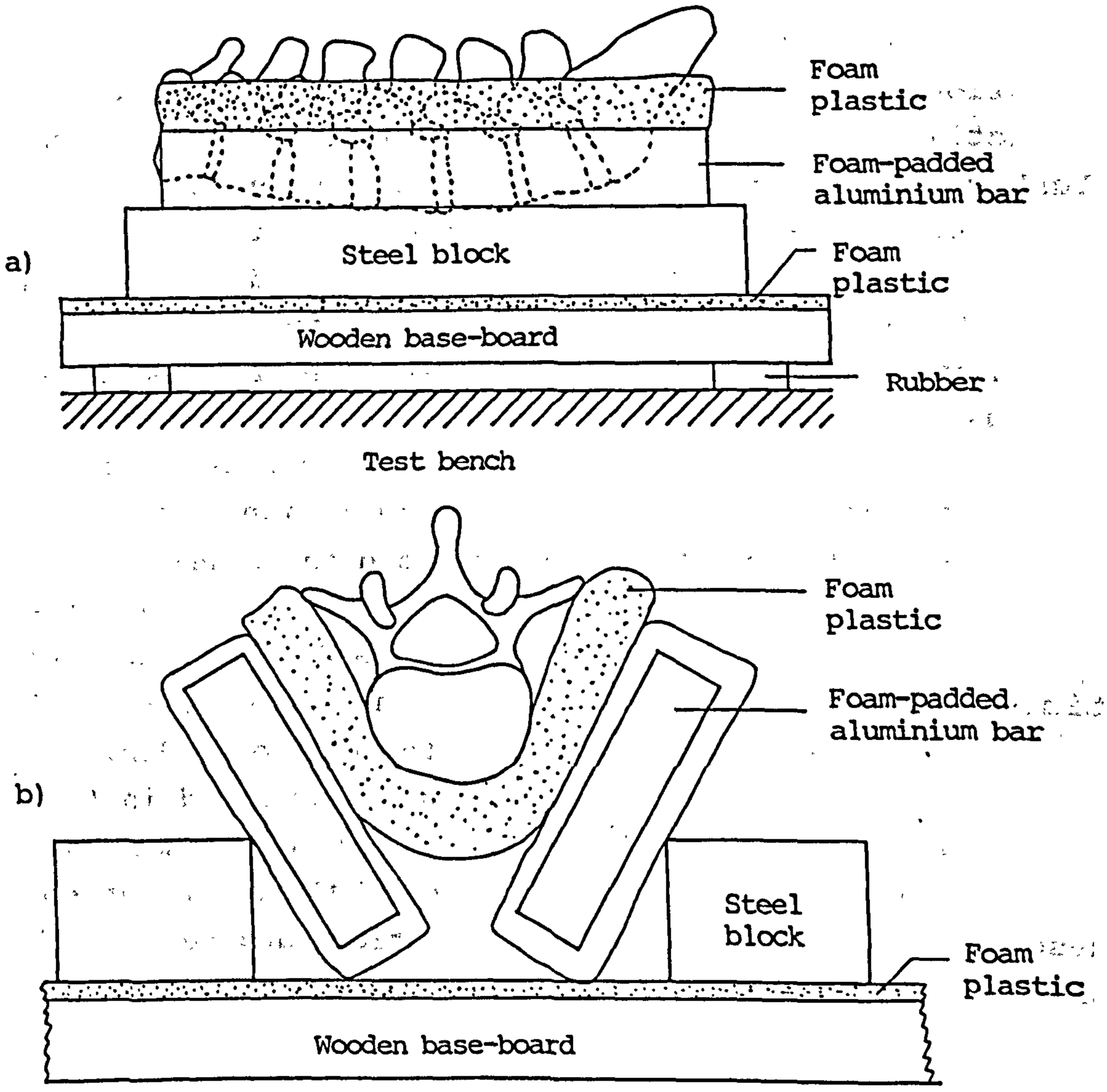

Fig 5.1 Free support condition of the lumbar spine. a) Lateral view; b) End-on view.

and to detect by manual manipulation any limitation in intersegmental flexion-extension movement. There were further opportunities to confirm non-existence of intervertebral fusions or destruction of bone by lateral roentgenograph of the specimen taken at a later stage. At the termination of all vibration tests, the specimen was then dissected for direct inspection of the facet joints and intervertebral discs to confirm non-existence of previous fusions. The grading of degeneration according to Rolander (1966) was also noted for each intervertebral disc (appendix I.2).

The prepared specimen was prevented from drying up by a thin layer of wet tissue paper, and was then wrapped in cellophane film to keep the moisture. Additional water was applied to moisten the specimen when necessary. The specimen was tested as far as possible on the day it was harvested. In situations when tests had to be carried out or to be continued on other days, the specimen was then frozen at -15 °C, and subsequently thawed in room temperature for about 18 to 24 hours before use.

5.2.1 Support Conditions

The specimen was mounted in a horizontal position and supported at its ends to simulate the conditions experienced in the body in a prone lying position. It was intended to create two ideal support conditions i.e. free-free and fixed-fixed at both ends. It was envisaged that the real support condition for the lumbar spine in-vivo would be somewhere in between. However, as discussed in section 3.5, perfectly free or fixed end conditions are difficult to achieve, if not impossible. To create a free support, the specimen was placed horizontally between two aluminium bars which were padded with thick layers of soft foam plastic (fig 5.1). The bars were placed in a V-shaped configuration to stabilize the specimen, and to prevent it from rotational movement about its long axis (z-axis). It is described as free lumbar spine in this thesis. In order

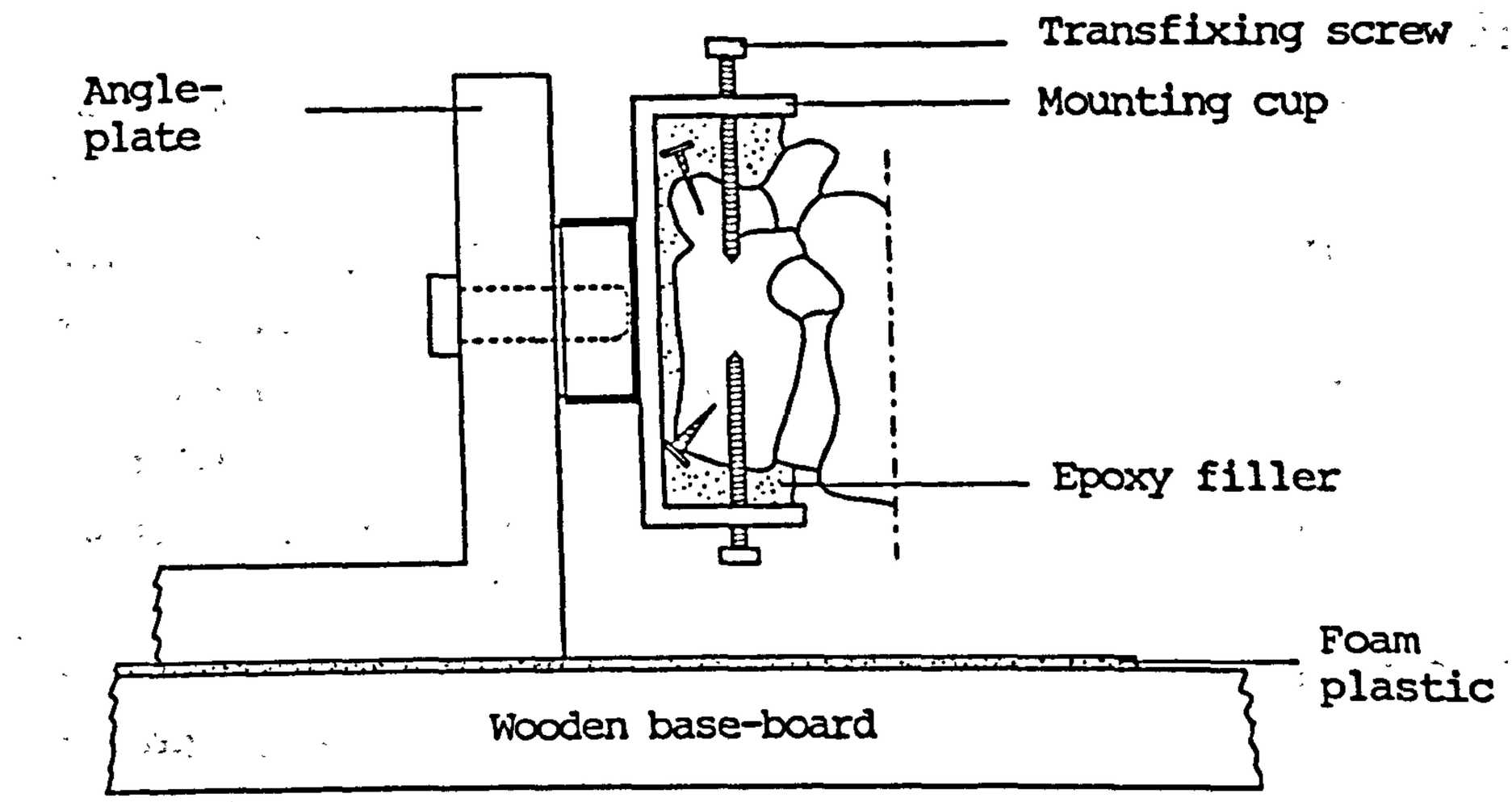

a)

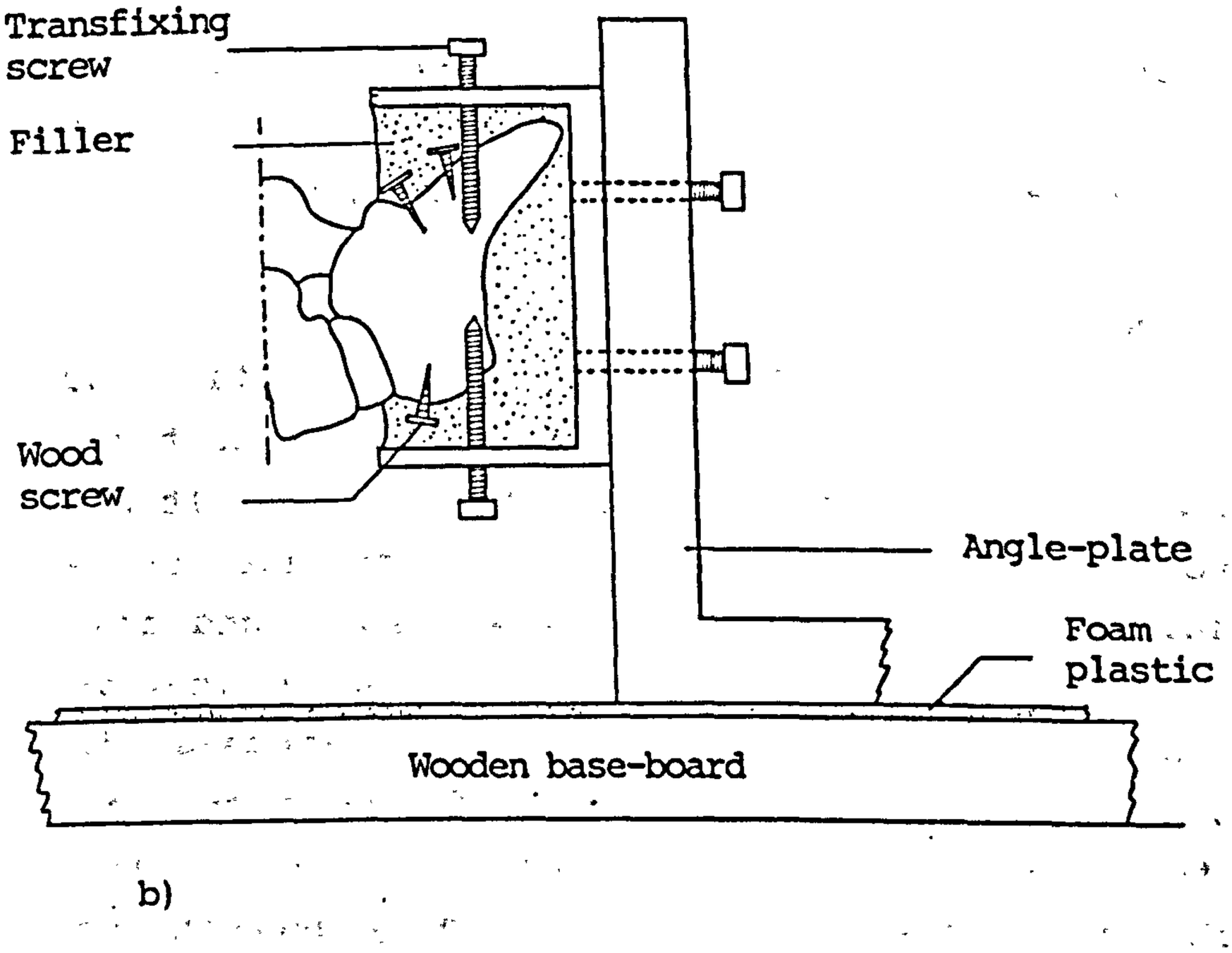

b)

Fig 5.2 Fixed support condition a) at the T12 thoracic vertebra, and b) at the sacrum.

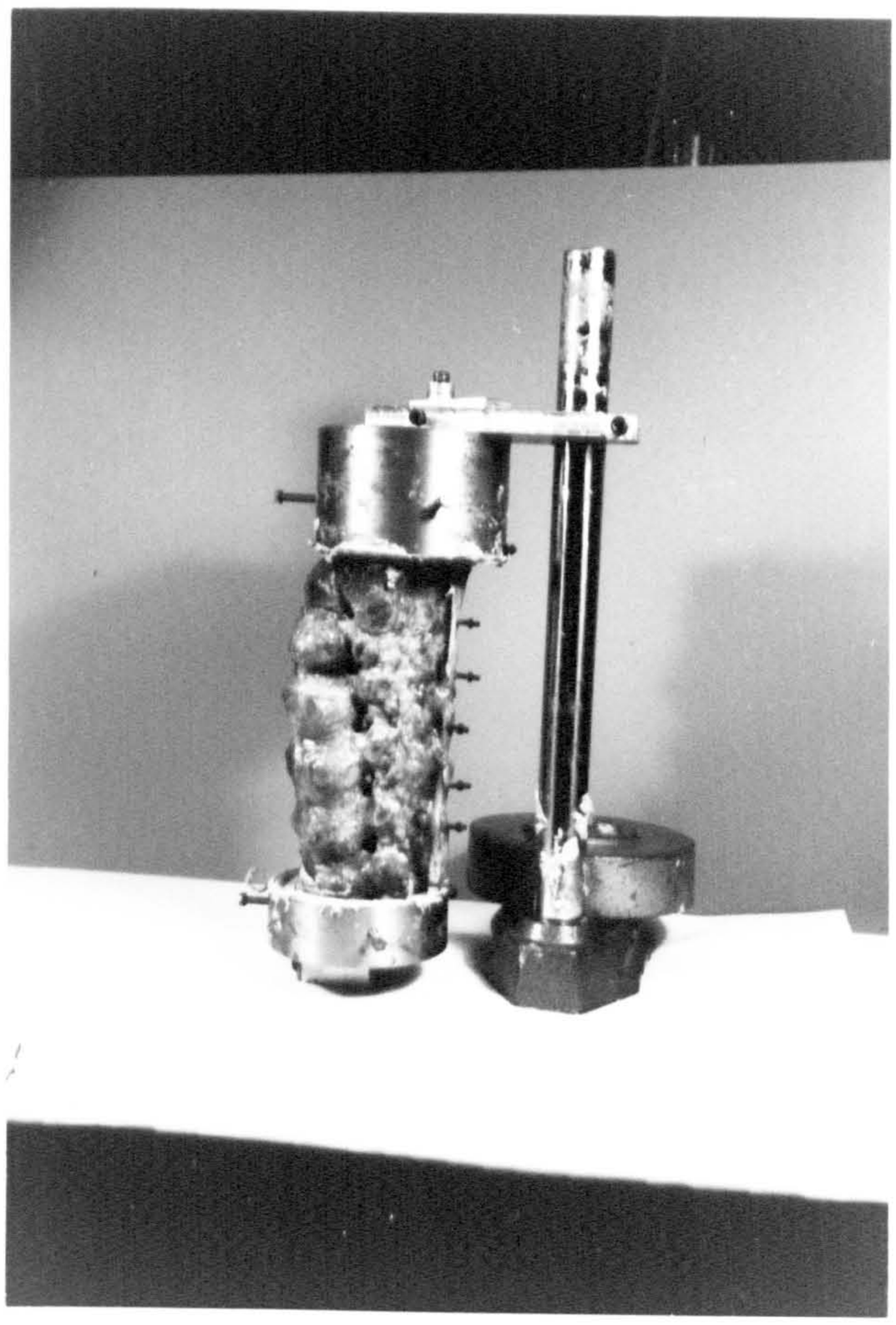

Fig 5.3 Alignment of the lumbar spine on a jig during setting of the epoxy filler.

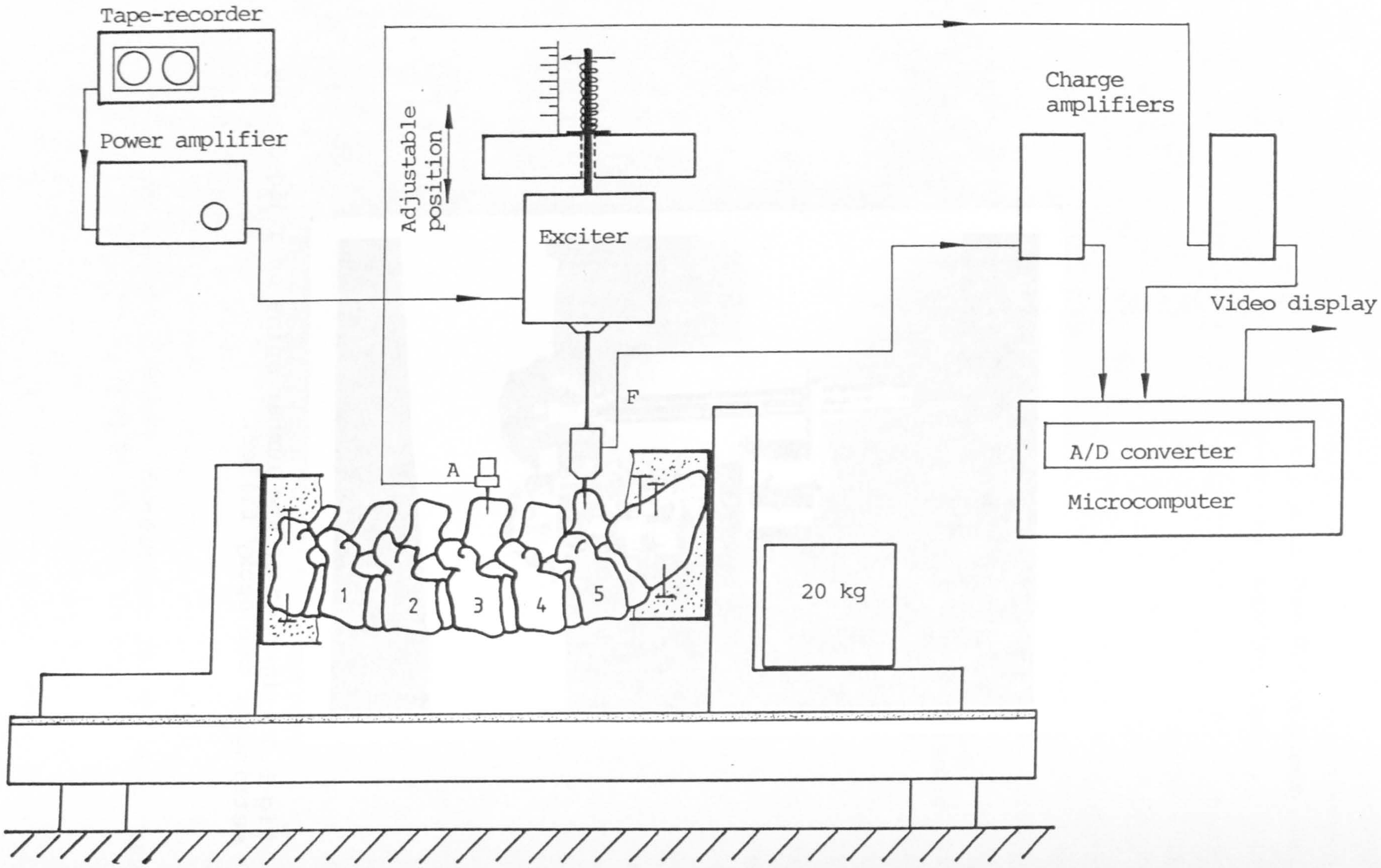

Fig 5.4 Experimental set-up of vibration tests. F and A are respectively the force and acceleration signals.

to achieve a fixed support, the ends of the specimen were embedded in epoxy-based filler set in metallic cups and further anchored using transfixing screws (fig 5.2). The specimen was aligned, with the help of an alignment jig (fig 5.3) in a vertical position while the filler was allowed to set. The L3-4 intervertebral disc was used as the reference which was placed on a horizontal plane during the alignment procedure. This corresponded to a vertical plane when the specimen was placed horizontally. These metallic cups were rigidly fixed to two angle-plates, and the amount of antero-posterior offset between the cups during the alignment procedure was maintained. The specimen was found to have a strong tendency to maintain its resting alignment fairly well, and care had been taken to avoid axial distortion of the specimen during the fixation on the angle-plates. The test specimen was then placed on a thick wooden base-board which was in turn supported on a stable bench and was effectively insulated from vibrations transmitted from the test environment by 3 cm thick rubber blocks supporting the board at the corners. The mass of the angle-plate attached at the sacral end was augmented by the addition of a 20 kg metal block. Together with the mass of the angle-plate (10 kg) and the mounting cup (1.5 kg), this was considered an appropriate approximation to 1/3 to 1/2 of an adult's body-mass to simulate pelvic inertia. Figure 5.4 depicts a lumbar spine mounted in metallic cups and fixed on the angle-plates at both ends. This set-up was considered an effective means of providing a fixed end condition for the lumbar spine. It is described as <u>fixed lumbar spine</u> in this thesis. However, the stability of the end support was also ascertained during the vibration tests. Appendix V shows the experimental set-up and accessories for mounting of the test specimen.

5.2.2 <u>Placement of Transducers</u>

Transducers were attached at the spinous process and vertebral body of the lumbar vertebra in the antero-

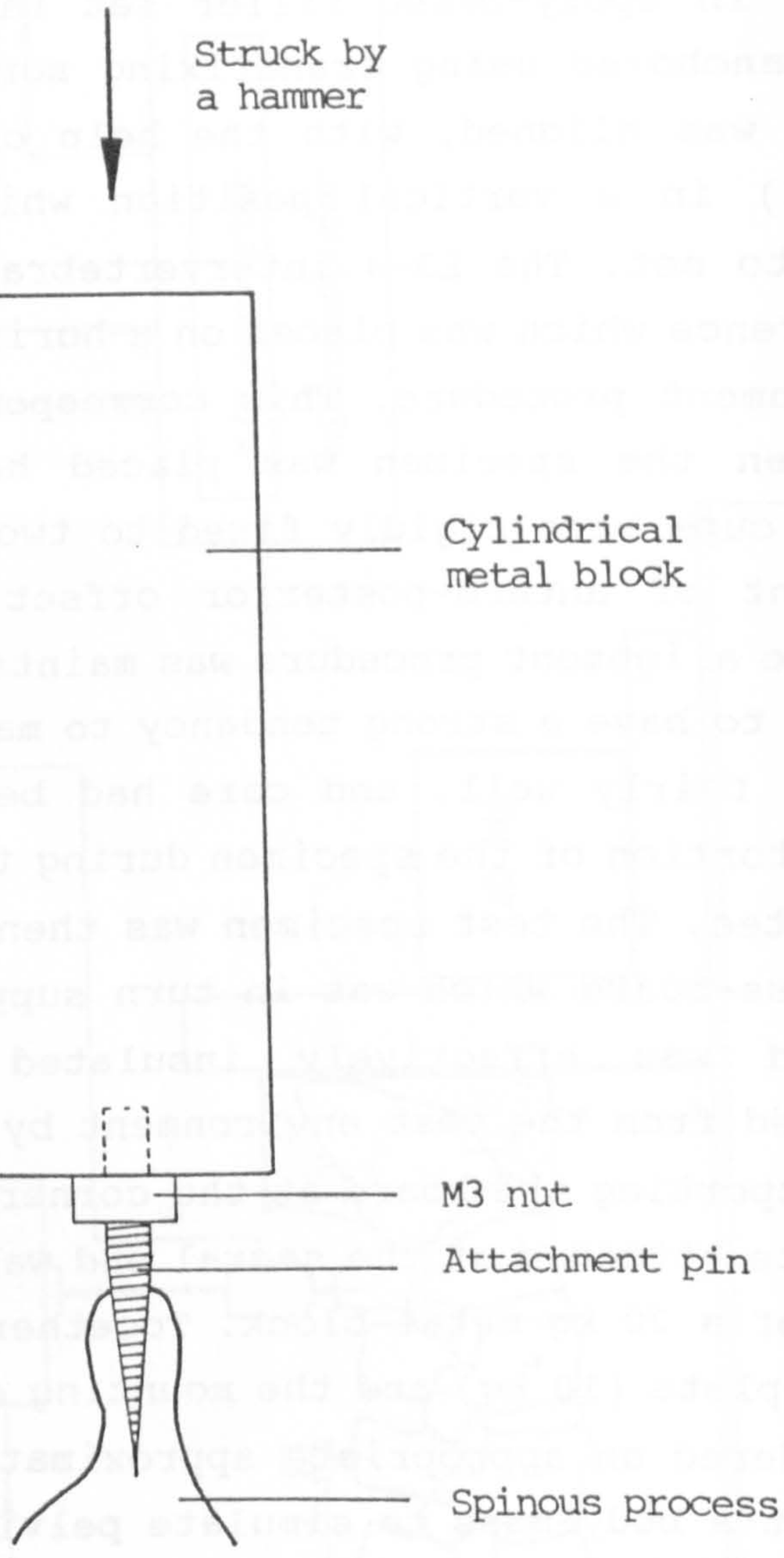

Fig 5.5 Insertion of attachment pin with the help of a cylindrical metal block for alignment.

posterior direction by the use of attachment pins modified from 2.5 cm long M3 set screws, tapered at one end (fig 4.11c). The insertion and alignment of the pin was facilitated by the use of a cylindrical block of metal (fig 5.5) which held the pin in the correct position and direction while a small hammer struck the block at its free end. The trabeculae of the bone at the spinous process and the vertebral body provided good anchorage for the pin which also because of its tapered shape, achieved a firmly plug-fitted attachment. The firmness of attachment was also checked manually by feeling the pin's stability in the antero-posterior direction.

An impedance head or force transducer was attached at the pin where the specimen was to be excited, and this pin is named as a drive-pin. A conversion screw (M3 to 10-32UNF) was used when required. The pin at which the vibration level was to be measured by an accelerometer is named as a measure-pin. The accelerometer was fixed at the threaded end of the pin and further tightened by a M3 nut to secure firm attachment. Figure 5.6 depicts the attachment of various transducers at the pins. An additional metal stud was attached on the top of the force transducer for impact testing.

5.2.3 Methods of Excitation

For impact tests, transient vibrations were initiated by a gentle impact of a hand-held dental hammer which struck the metal stud on the top of a force transducer attached at the spinous process. This gentle impact was repeated at about 1 s interval. The lumbar spine had ample time to settle before the next impact and the observed response was that induced by a single impact.

An electrodynamic exciter was used to generate excitatory force to the lumbar spine through the use of a flexible stainless steel drive-rod (diameter 0.5 mm). This drive-rod had high axial stiffness, and low bending and torsional stiffness, hence vibrations in the other axes

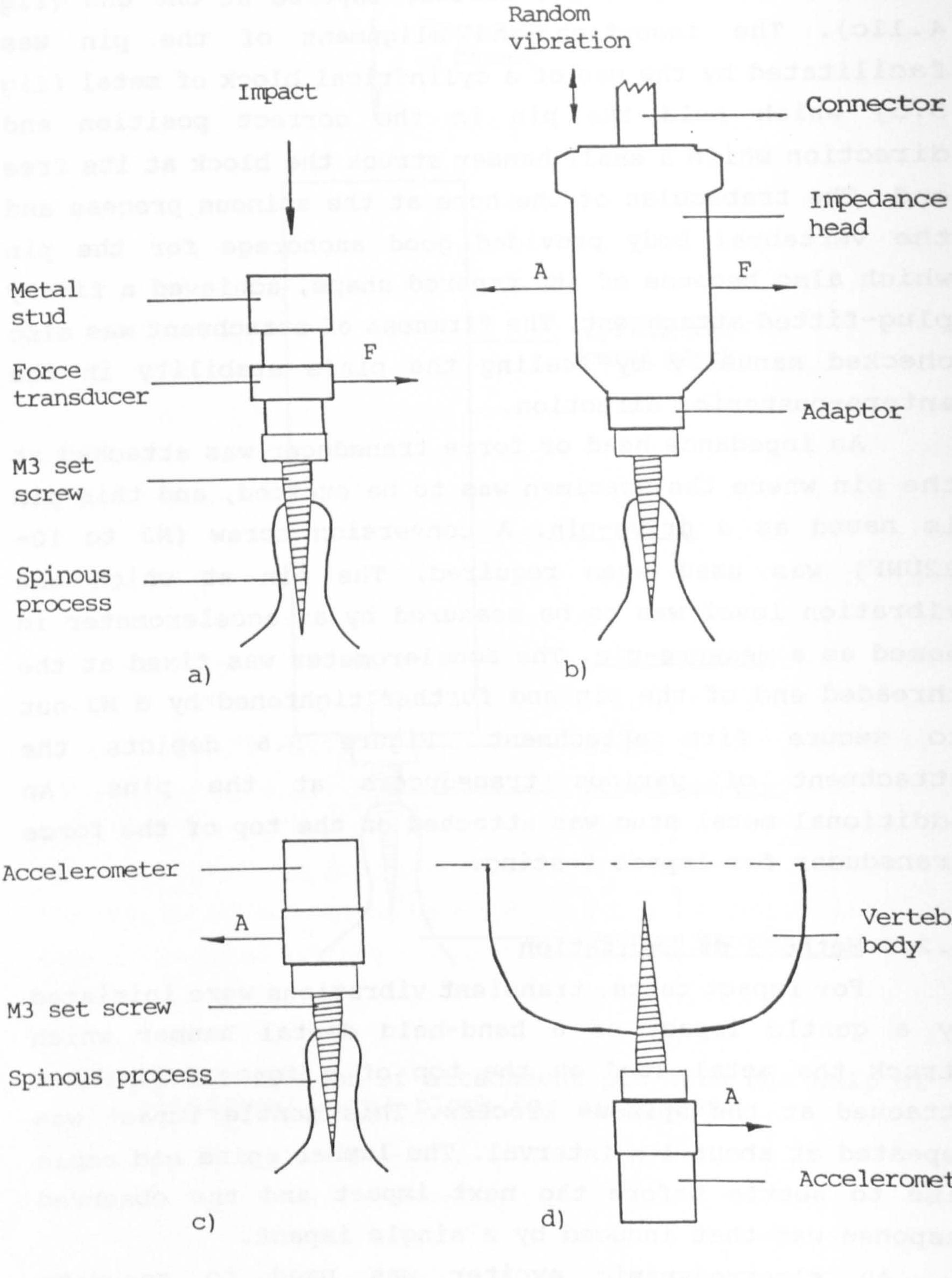

Fig 5.6 Attachment of transducers. a) Force transducer; b) impedance head; and c) accelerometer at the spinous process. d) Accelerometer at the ventral surface of vertebral body. F and A are respectively the force and acceleration signals.

were effectively decoupled (fig 5.7). Thus the imposed vibratory force was confined only to the antero-posterior direction along which the force transducer was mounted.

The exciter was supported by a spring-mounted rod of 5 mm diameter through the centre of a thick aluminium disc, and was allowed to move freely in the vertical direction. The disc was attached at the collar of the drill-holder of a bench drillstand which was bolted on the top of the test bench. Vertical adjustment of the position of the exciter was possible and it was suspended at the appropriate position set by a locking screw of the drillstand. A pointer pointing against a linear scale indicated the resting position of the exciter so as to ensure that no preload bias, compression or tension, was applied to the specimen during the vibration tests. The exciter, the drive-rod and the force transducer were aligned in the vertical direction i.e. antero-posteriorly with respect to the specimen by adjusting the position of the specimen. Figure 5.7 also shows the support mechanism of the exciter.

White noise of a flat spectrum up to 2.5 kHz was played back from a tape-recorder which was then fed to a power amplifier to drive the exciter. Random vibratory force (input) of peak amplitude lower than 5 N in the frequency range 20 Hz to 2.5 kHz was applied at the appropriate spinous process. In the discrete frequency vibration tests, 100, 200, 500, 1000 and 2000 Hz sine waves were generated from a signal generator which replaced the tape-recorder, and was then fed to the same power amplifier to supply the exciter. A push-button switch was incorporated in the circuit so as to allow a manually controlled delivery of tone bursts of the required frequency. Slowly swept sine waves from 10 to 50 Hz was generated at a sweep rate of about 5 Hz per second. Figure 5.4 also shows the schematic diagram of the experimental set-up.

Table 5.1
Annotations for figures 5.8 to 5.13.

SYMBOLS	DESCRIPTION	REMARKS
	Application of excitation to the specimen.	Pointing to the specimen; the method of excitation refers to description in the figures.
	Measurement of vibration response of the specimen.	Pointing out of the specimen.
F	Excitatory force signal measured.	
A	Vibration signal measured as acceleration at the indicated location.	
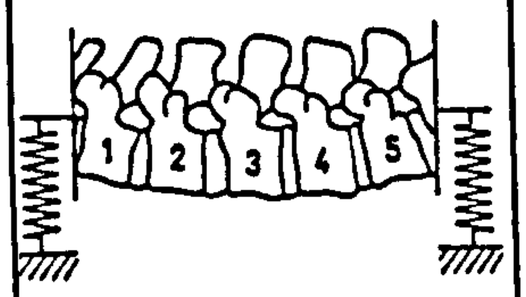	Free end support condition.	Detailed configuration refers to figure 5.1.
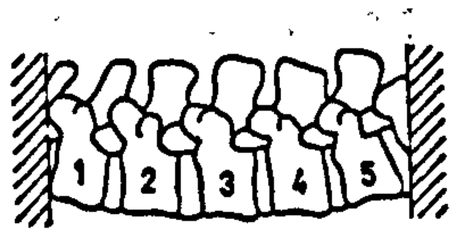	Fixed end support condition.	Detailed configuration refers to figures 5.2 & 5.4.

Notes:
1. The arrows do not necessarily indicate the positive direction of the measurands.

2. Where both F and A are drawn at the same spinous process, they refer to the measurements at the same driving point. However, in the figures, they are drawn separately for clarity.

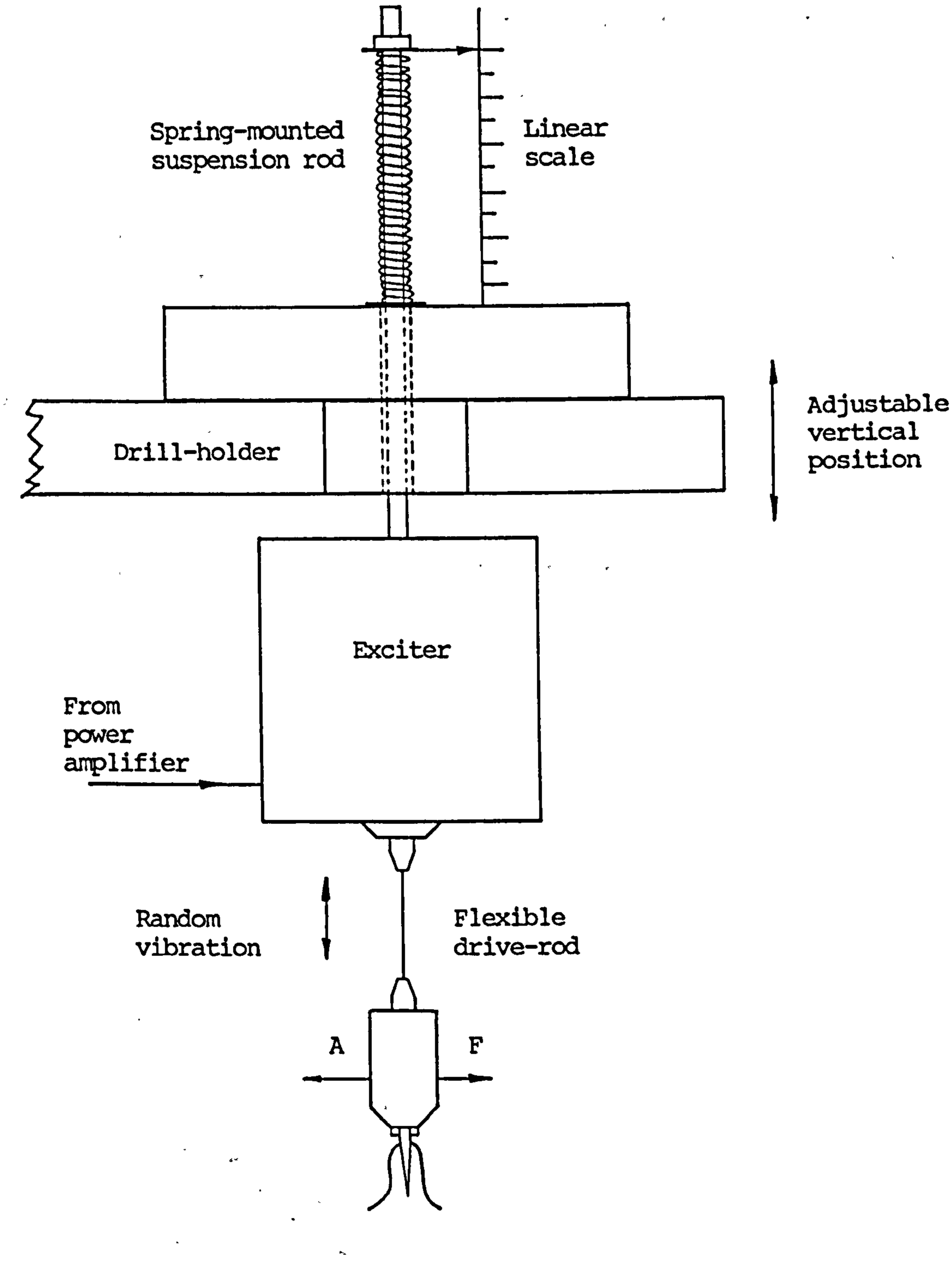

Fig 5.7 Spring-mounted suspension mechanism of the exciter and the attachment of a flexible drive-rod colinearly with the transducer. F and A are respectively the force and acceleration signals.

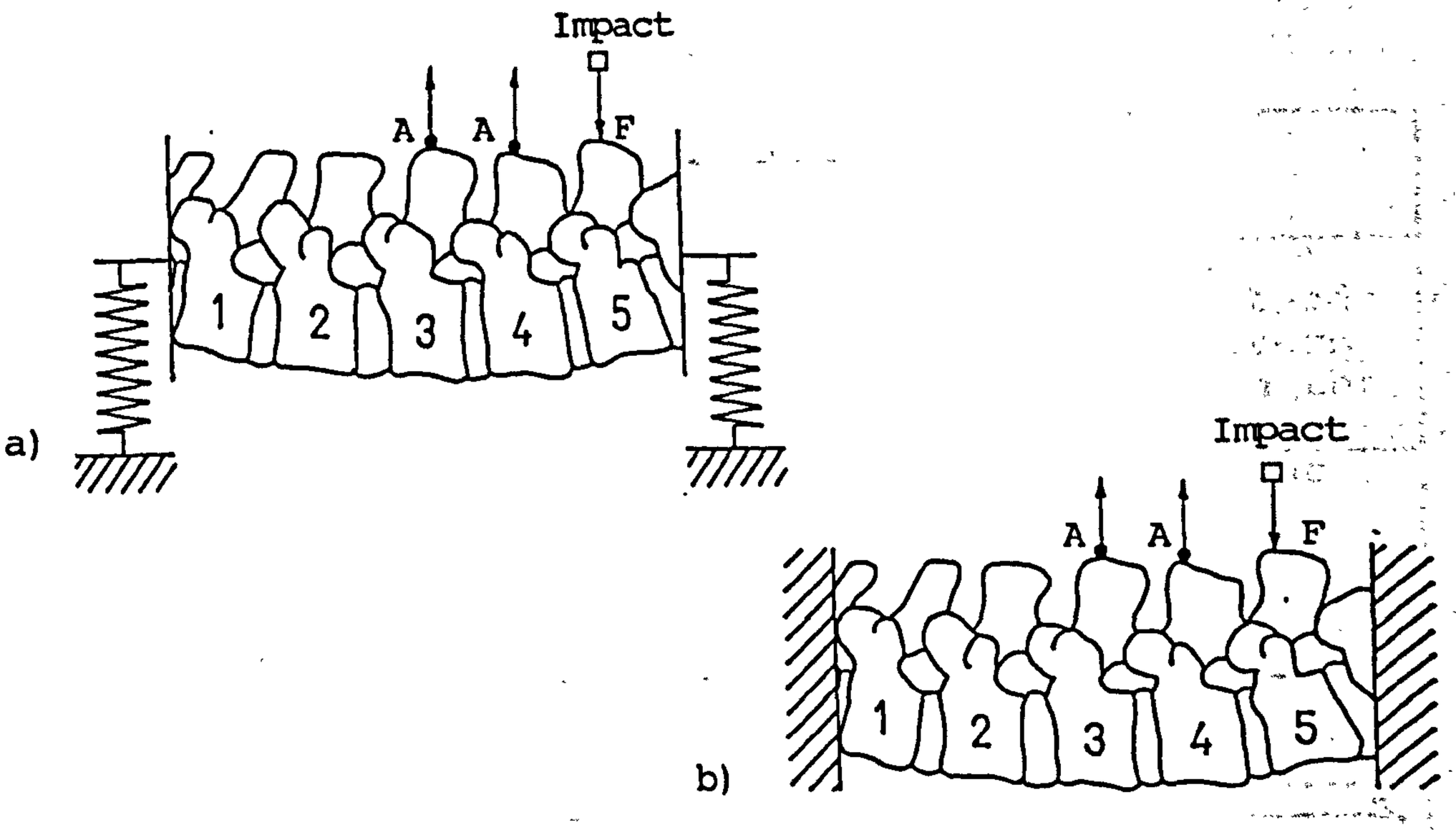

Fig 5.8 Impact testing a) on a free lumbar spine, and b) on a fixed lumbar spine.

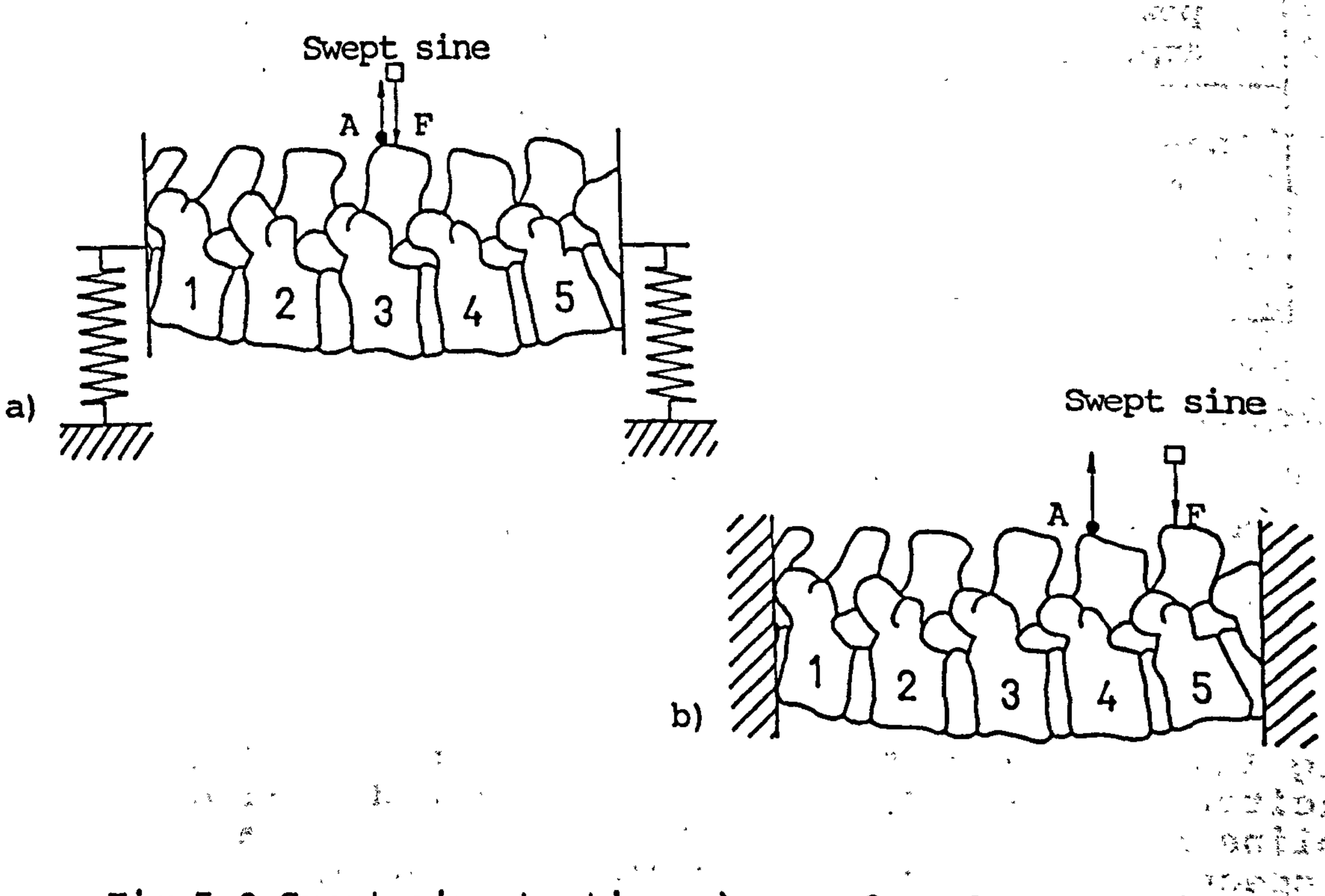

Fig 5.9 Swept sine testing a) on a free lumbar spine, and b) on a fixed lumbar spine.

5.2.4 Test Protocols

This section outlines the major experimental set-ups and protocols of vibration testing. The placement of transducers has been shown in figure 5.6. The detailed configurations of the support conditions refer to figures 5.1, 5.2 and 5.4. They are explained in table 5.1 for the purpose of illustration. The meanings of other symbols used in figures 5.8 to 5.13 are also explained in table 5.1. The following paragraphs also outline the processing of the signals to obtain the required parameters. All impact tests, swept sine tests and random vibration tests were performed at a sampling rate of 10 kHz, and with a record size of 65536 data points. The band-pass filters on the charge amplifiers were set at 2 Hz to 3 kHz. All discrete frequency vibration tests were sampled at 50 kHz.

Impact Testing. As shown in figure 5.8a, an impact force was applied at the L5 spinous process of the free lumbar spine specimen. Vibration signals were measured simultaneously as acceleration at the L3 and L4 spinous processes. The signals were analyzed in the time domain. It was aimed to examine the gross motion response of the lumbar spine to impact force in free support condition. The resonant frequency and the logarithmic decrement of the amplitudes were measured and analyzed in the time domain. The impact test was repeated when the specimen was supported in fixed condition (fig 5.8b). Acceleration signals measured at the two segments were compared and the ratio of their amplitudes and the phase difference, if any, were noted. The measurement was repeated on other pairs of spinous processes i.e. L2 & L3, and L1 & L2.

Swept Sine Testing. Slowly swept sine waves in a frequency range of 10 to 30 Hz excited the L3 spinous process of the free lumbar spine specimen. Both the excitatory force and the acceleration were measured at the L3 spinous process (fig 5.9a). The frequency response function (A(f)/F(f)) which describes the gross motion response of the specimen was obtained through the fast

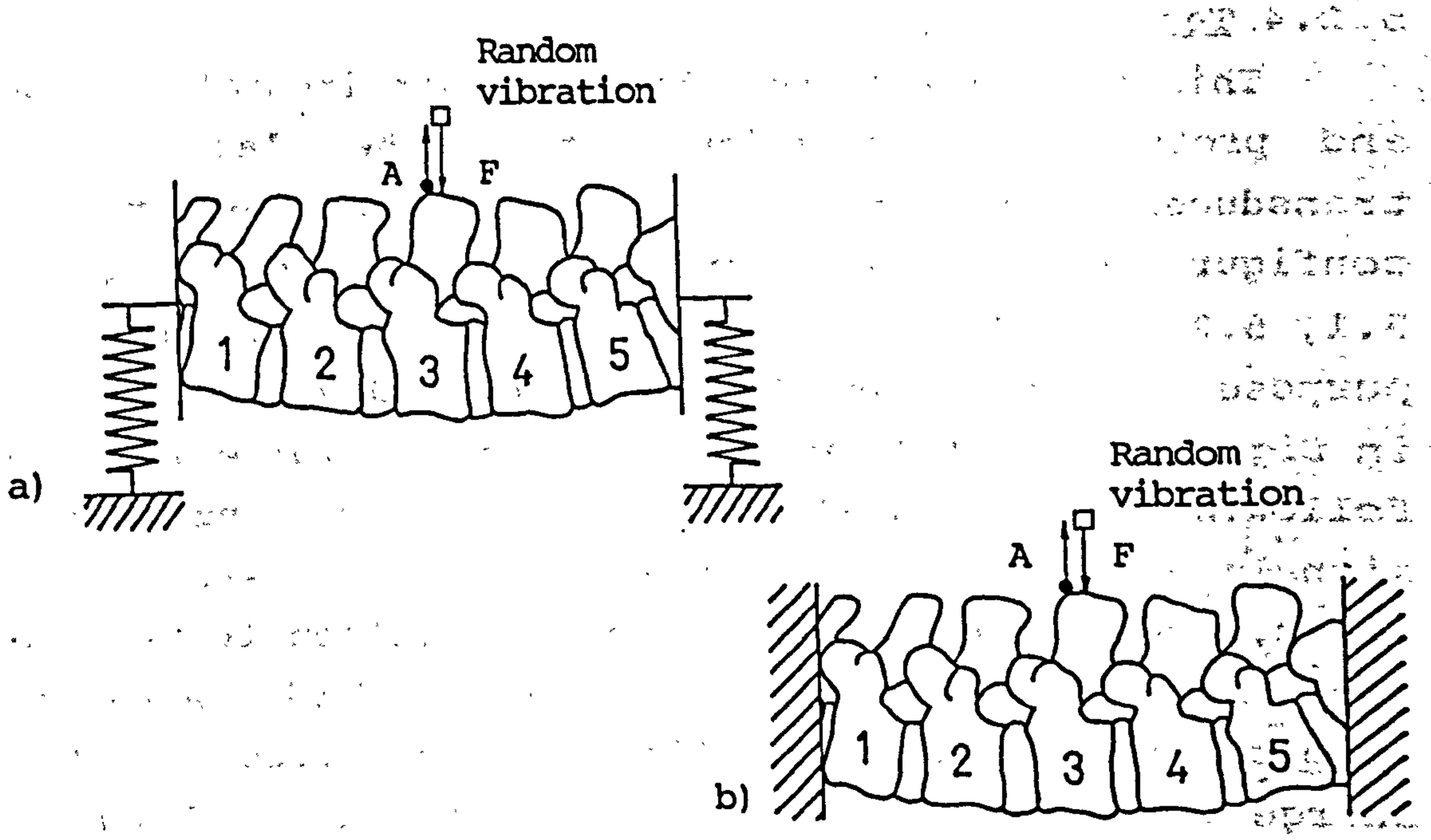

Fig 5.10 Random vibration testing for apparent mass measurement a) on a free lumbar spine, and b) on a fixed lumbar spine.

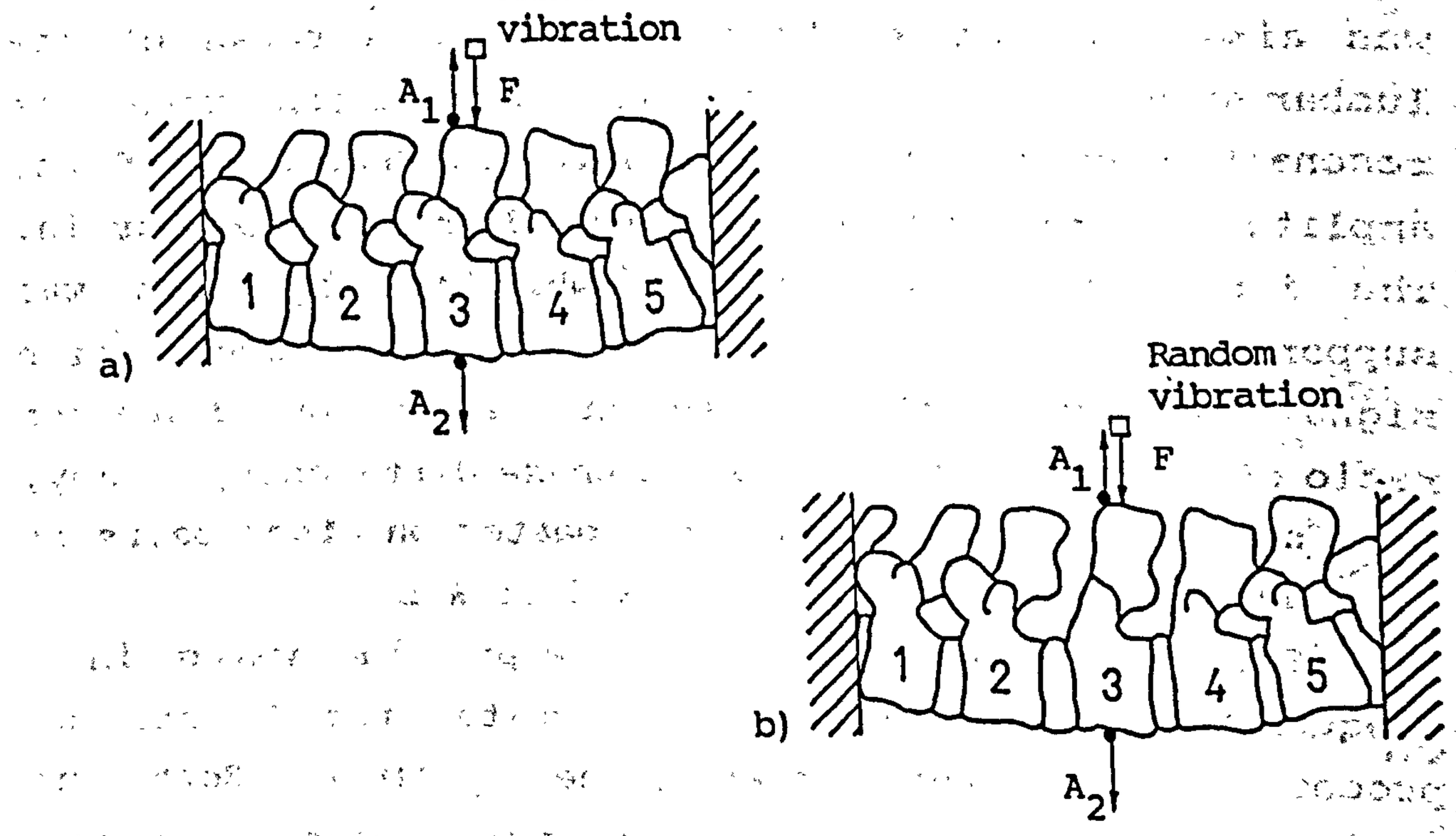

Fig 5.11 Measurement of transmissibility. a) Intact lumbar spine; b) Interspinous ligament, and L2-3 and L3-4 facet joints destroyed.

Fourier transform (section 2.4.2). The resonance characteristic of the set-up was noted. A similar swept sine test was repeated by applying the excitatory force at the L5 spinous process while the specimen was fixed. Vibration signals were measured in turn at the L1 to L4 spinous process (fig 5.9b). The frequency response function (A(f)/F(f)) was obtained by the same algorithm.

Random Vibration Testing. Random vibratory force from 20 Hz to 2.5 kHz was applied at the L3 spinous process. The peak excitatory force was controlled to below 5 N. The force and acceleration were measured simultaneously at the driving point by the use of an impedance head. The frequency response function was defined by:

$$\textit{Apparent Mass, } AM(f) = \frac{F(f)}{A(f)} \qquad (5.1)$$

where

F(f) is the vibratory force spectrum; and

A(f) is the acceleration spectrum.

The apparent mass was measured with the specimen in free and fixed conditions (fig 5.10). Tests in these experimental set-ups were also repeated with the L2-3 and L3-4 facet joints and interspinous ligaments destroyed (fig 5.11). These tests were to examine the transmissibility of vibration across the interface at the driving point. It also assessed the relative effectiveness of the excitation system in driving the specimen across the frequency range of interest. The apparent mass was also compared with the direct measurement of transmissibility which is defined as:

$$\textit{Transmissibility, } T(f) = \frac{A_2(f)}{A_1(f)} \qquad (5.2)$$

where

A_1 is the acceleration spectrum at the spinous process; and

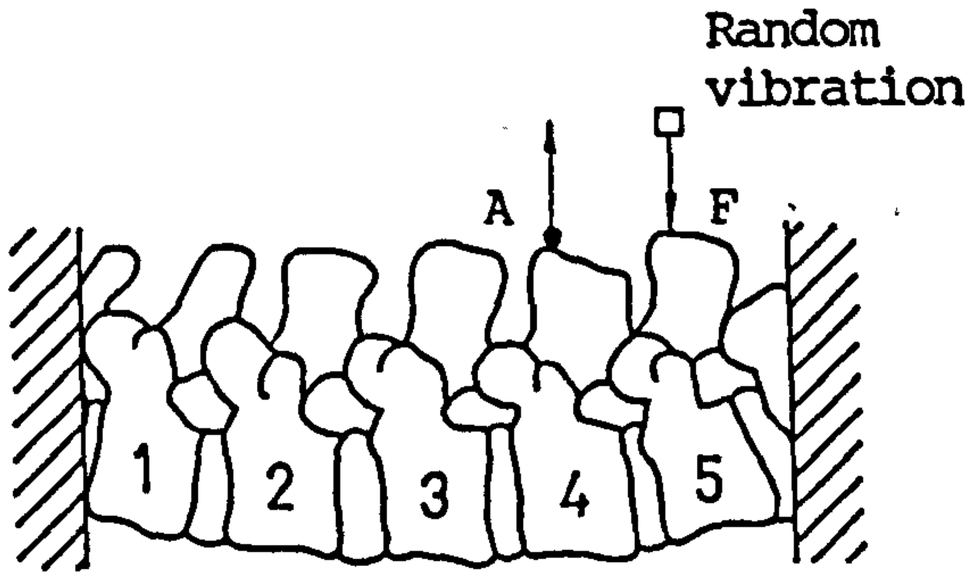

Fig 5.12 Measurement of transfer mobility.

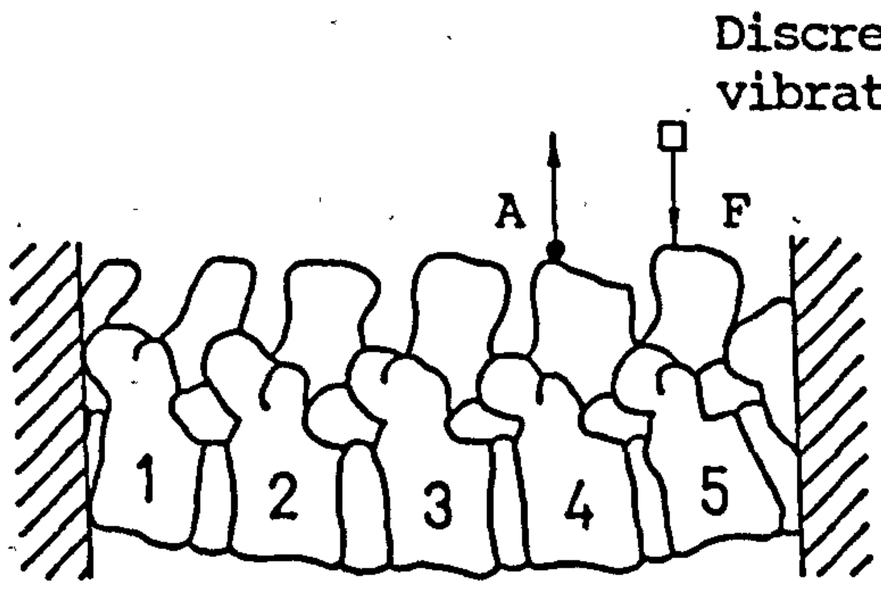

Fig 5.13 Discrete frequency vibration testing.

A_2 is the acceleration spectrum at the vertebral body.

As described in section 2.4.2, transfer mobility measures the specimen's ability in transmitting vibration. It also assesses the vibration response of the specimen to a known excitatory force input. Figure 5.12 depicts the set-up where the specimen was excited at the L5 spinous process while the acceleration signals at the other spinous processes (L1 to L4) were measured in sequence. The frequency response function defined below measures the response of the specimen to unit excitatory force as a function of frequency.

$$Transfer\ Mobility = \frac{V(f)}{F(f)} \qquad (5.3)$$

where V(f) is the velocity spectrum.

Discrete Frequency Vibration Testing. Repeated tone bursts of discrete frequencies of 100, 200, 500, 1000 and 2000 Hz were applied at the L5 spinous process as depicted in figure 5.13. The response signal was picked up as acceleration at the other spinous processes (L1 to L4) in sequence. The amplitudes of vibration signals were then converted into velocity according to the equation:

$$Velocity,\ |V(f)| = \frac{|A(f)|}{2\pi f} \qquad (5.4)$$

At each frequency, the ratio of the root-mean-square values of velocity to force was then determined in the time domain to obtain a measure of the motion response of the specimen. The magnitude of excitation was monitored and controlled to avoid non-linear response of the lumbar spine as shown in figure 3.8. As reported in section 3.9.3, the DC baseline drift was so small that it was insignificant.

Table 5.2
Vibration tests performed on the lumbar spine specimens.

SPECIMEN NUMBER	IMPACT TEST	SWEPT SINE TEST	RANDOM VIBRATION TEST	DISCRETE FREQUENCY VIBRATION TEST
1	Free	Free	Free; Fixed	
3			Free; Fixed	
4			Free; Fixed	
5			Free; Fixed	
6			Free; Fixed	
7	Fixed			Free; Fixed
8	Fixed			Free; Fixed
9			Fixed	Fixed
10			Fixed	Fixed
11			Fixed	Fixed

Notes:
Free - specimen placed on foam plastic (fig 5.1);
Fixed - specimen mounted on angle-plates at both ends (fig 5.2).

Remarks:
Specimen No. 2 was reported to have carcinoma metastasis and was not used for vibration tests.

5.3 GENERAL SYSTEM CHARACTERISTICS

Table 5.2 summarizes the vibration tests performed on the lumbar spine specimens. This section outlines the general observation on the vibration response of the specimens. Where necessary, typical examples would be included for illustration. The excitation system outlined in section 5.2.3 was effective in generating random vibratory force to the specimen in the frequency range up to 2 kHz, and even higher in some cases. However, the force spectrum was not uniform due to varying compliance of the specimen and its support condition across the frequency range. Figure 5.14 shows typical force spectra at L5 of a lumbar spine tested in free and fixed conditions. Individual variability among specimens was also noted. The excitatory force was adequate in inducing coherent response of the specimen, with coherence function very close to unity in all the tests. Slowly swept sine waves in the range of 10 to 50 Hz, were effective in producing undistorted sinusoidal responses at the L1 to L4 spinous processes within a controlled force level. In the case of impact tests, a measurable response was induced even by the gentle impact of a hand-held dental hammer at the spinous process through a drive-pin.

5.3.1 Coherence

Coherence between the input forcing signal and the response signal of a system indicates the degree of causality (section 2.4.4). Coherence functions of all the tests were very close to unity (about 0.98) except at the extremely low frequencies where the DC baseline drift, though minimal, accounted for the low coherency. The coherency also varied, depending on the spatial relation between the driving point and the measuring points. Figure 5.15 shows typical coherence functions when the response signals were picked up at various spinous processes. It was noted that the coherence function had a flat spectrum across the range of frequency when the response signal was

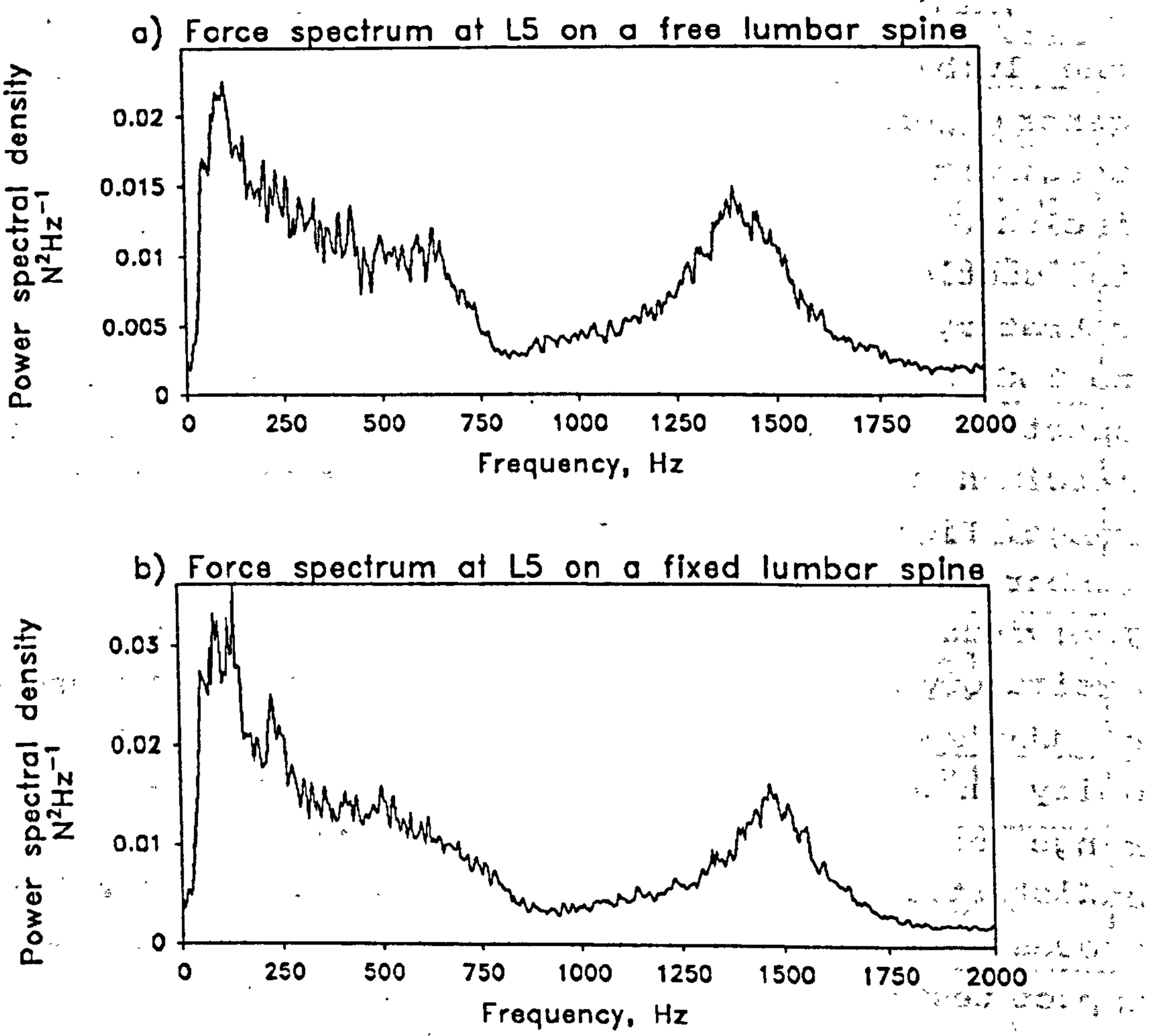

Fig 5.14 Vibratory force spectrum.

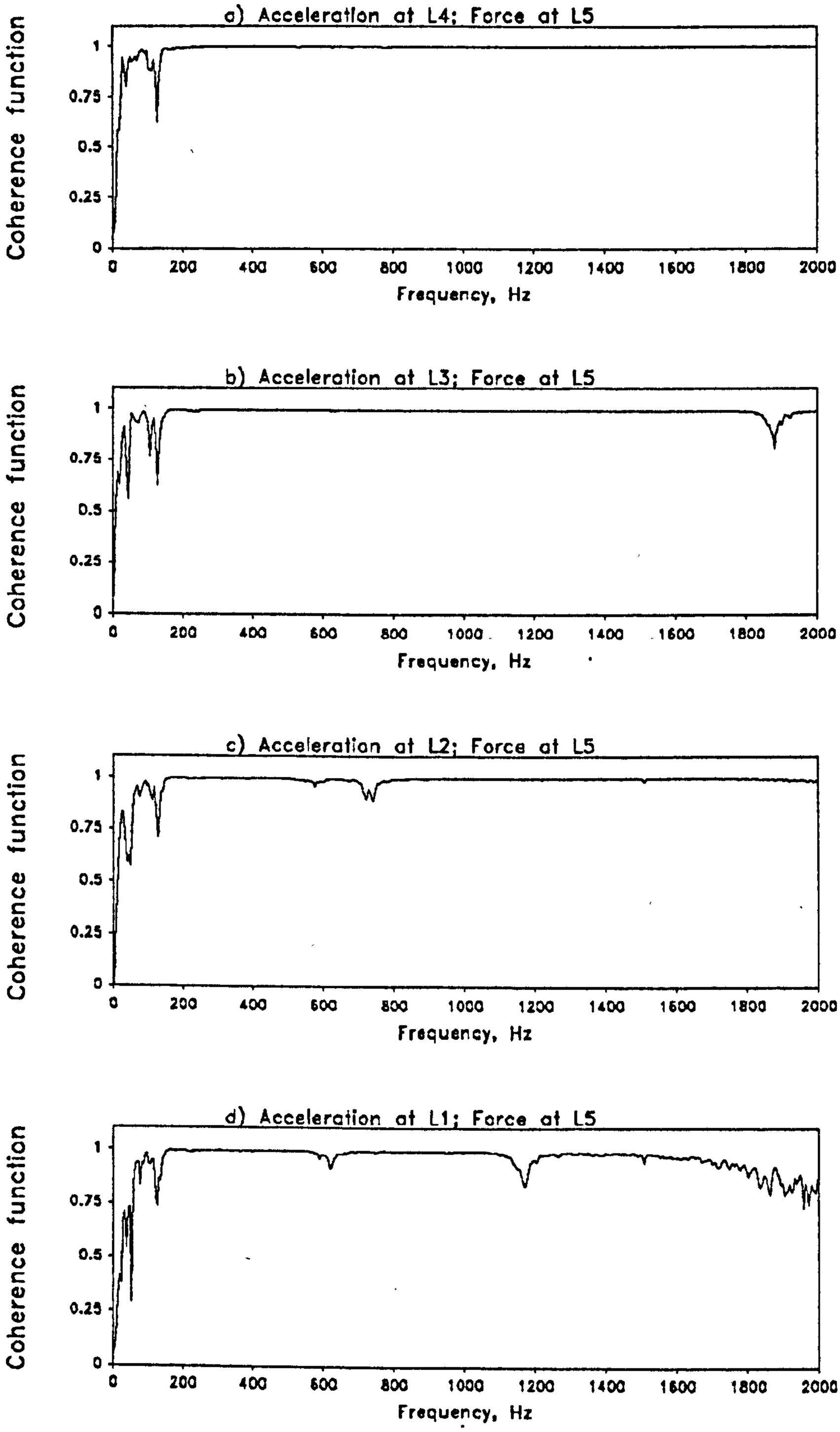

Fig 5.15 Coherence functions of vibration response measurements at different segments, showing a decrease for high frequencies at L1.

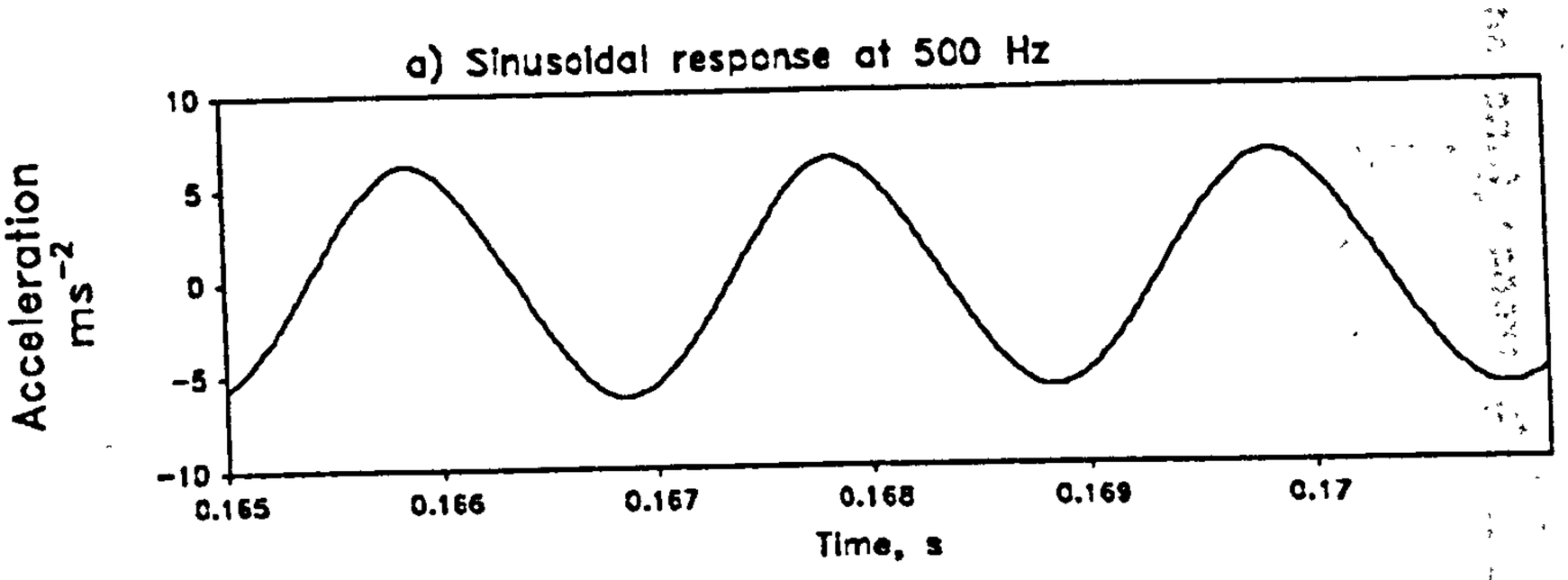

Fig 5.16 Sinusoidal response a) at 500 Hz, b) at 1kHz, and c) at 2 kHz. d) Distorted vibration at high excitatory force level of 5 N (peak).

measured at a level next to the driving point. The coherency for higher frequency ranges progressively dropped when the response signal was measured at segments farther away from the driving point. This may be explained by the attenuation of high frequencies after vibration waves had been transmitted through several intervertebral discs, and the small signal-to-noise ratio could explain the low coherency in this frequency range (section 2.4.5). High causality, as indicated by the closeness to unity of the coherence function, strongly suggests that the measured output signal was genuinely a response to the excitatory force and not one coming from artefact, noise or other incoherent source.

5.3.2 System Linearity

System linearity is a major issue which needs to be verified before an appropriate analytical process is planned. The system analysis approach outlined in section 2.4 assumes linearity of the test system (fig 3.5). Spectral averaging technique is a statistical strategy of getting the best linear fit of the system behaviour should non-linearity exist. Hence the validity of this analytical approach depends on the degree of linearity of the system. High coherency across the frequency range of interest has already indicated linearity of the system and that the previous assumption of system linearity has been met.

Sinusoidal tone bursts of discrete frequencies of 100, 200, 500, 1000 and 2000 Hz were able to induce undistorted sinusoidal vibration response, except at too high a level of excitatory force (fig 5.16). This measured 5 N (peak) at 500 Hz for a particular specimen - a level which is considered too much higher than is required for in-vitro study. In an in-vivo situation, this excitation level is considered higher than would be tolerated, and will not be required for tests on live subjects. Hence the lumbar spine specimen is considered as a linear system under vibration tests within an appropriate range of excitatory force.

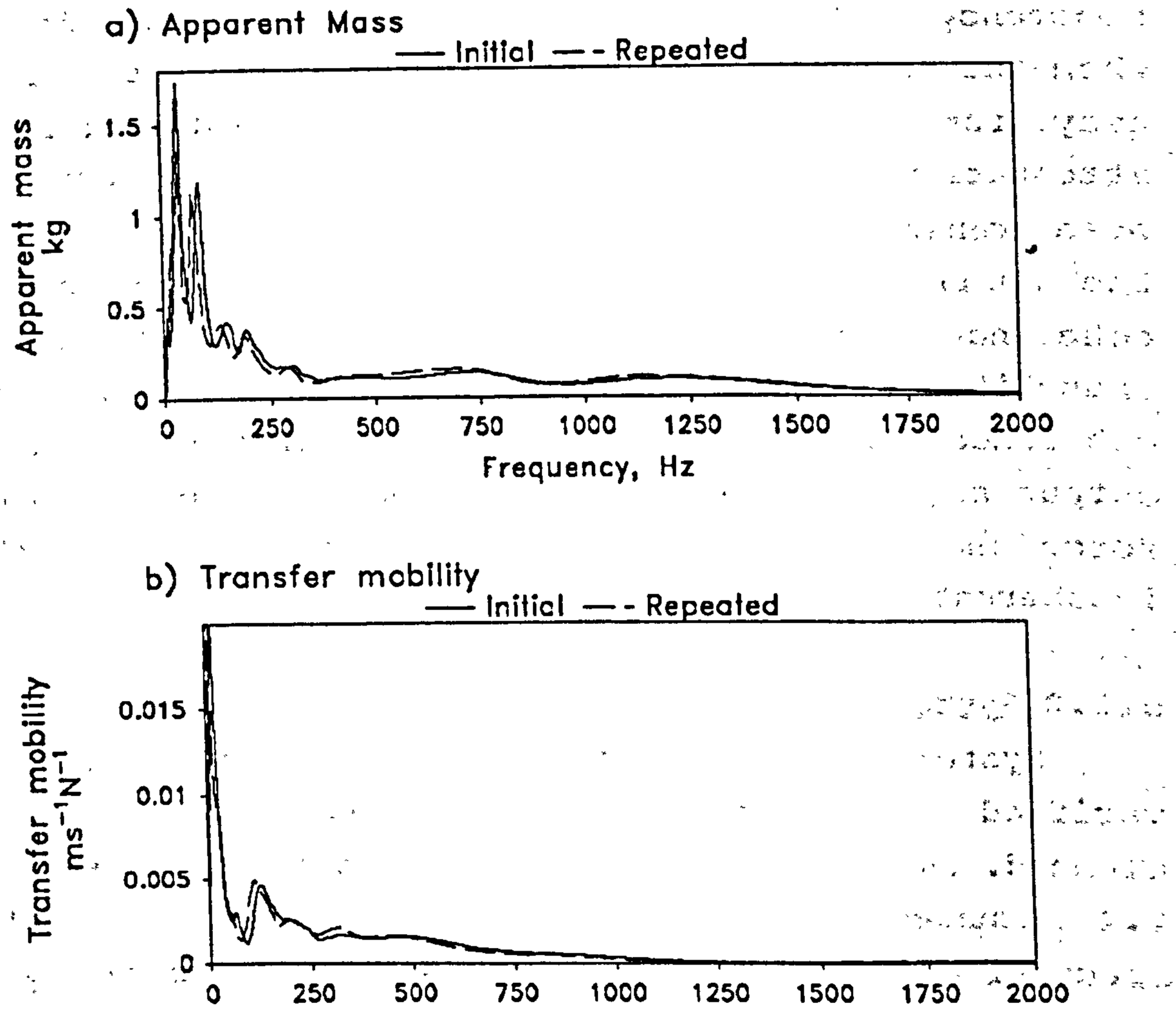

Fig 5.17 Repeatable measurements of a) apparent mass and b) transfer mobility on the 11th day.

5.3.3 Repeatability

Within the same laboratory sessions, tests were repeated three times for each set-up. It was noted that the test results were highly repeatable. Attempts have been made to repeat some of the vibration tests on a particular specimen on the 11th day after the first series of tests. In the meantime, the specimen was kept at -15 °C. As a consequence, the whole procedure of thawing and mounting the specimen, and setting up of the equipment was repeated in the second series of vibration tests. Apparent mass and transfer mobility measurements of the two test series were compared (fig 5.17). Appendix VI outlines a linear regression model to test the degree of consistency between two corresponding measurements. The degree of fit to a linear mathematical model was tested by Pearson product moment correlation and linear regression analysis. The Pearson correlation coefficients R between corresponding tests of these two series were found to be greater than 0.95, and with the level of significance $p < 0.0001$ (table 5.3). The F ratio and its level of significance indicate a highly correlated and consistent result of the corresponding tests. It therefore suggests that the vibration tests were consistent and repeatable, and that the mechanical characteristics of the specimen were stable, and not affected by the preparation procedure over that time period of the tests. Attempts were also made to repeat some of the tests on a specimen after it had undergone a series of non-destructive mechanical tensile tests in another independent study. Figure 5.18 and table 5.4 show similar findings of repeatable and consistent measurements of apparent mass and transfer mobility. It therefore suggests that pre-conditioning of the tissues (hard or soft) was not a key issue to consider for vibration tests of this nature. It also indicates that the vibration technique employed was a test of the structural characteristics. When this vibration technique is to be applied on normal subjects and patients, the level of

Table 5.3
Pearson correlation coefficients R between the initial mesurements and repeated measurements on the 11th day. R is very close to unity especially in the 500 Hz to 2 kHz range, showing consistency and repeatability in the measurements.

MEASUREMENTS	FREQUENCY RANGE	
	0 Hz - 500 Hz	500 Hz - 2 kHz
APPARENT MASS	R = 0.971	R = 0.994
TRANSFER MOBILITY	R = 0.956	R = 0.996

Notes:
For all Pearson correlation coefficients R, $p < 0.0001$.
For all F ratios, $p < 0.00005$.

Table 5.4
Pearson correlation coefficients R between the initial mesurements and repeated measurements after a non-destructive mechanical tensile test. R is very close to unity especially in the 500 Hz to 2 kHz range, showing consistency and repeatability in the measurements.

MEASUREMENTS	FREQUENCY RANGE	
	0 Hz - 500 Hz	500 Hz - 2 kHz
APPARENT MASS	R = 0.909	R = 0.990
TRANSFER MOBILITY	R = 0.835	R = 0.960

Notes:
For all Pearson correlation coefficients R, $p < 0.0001$.
For all F ratios, $p < 0.00005$.

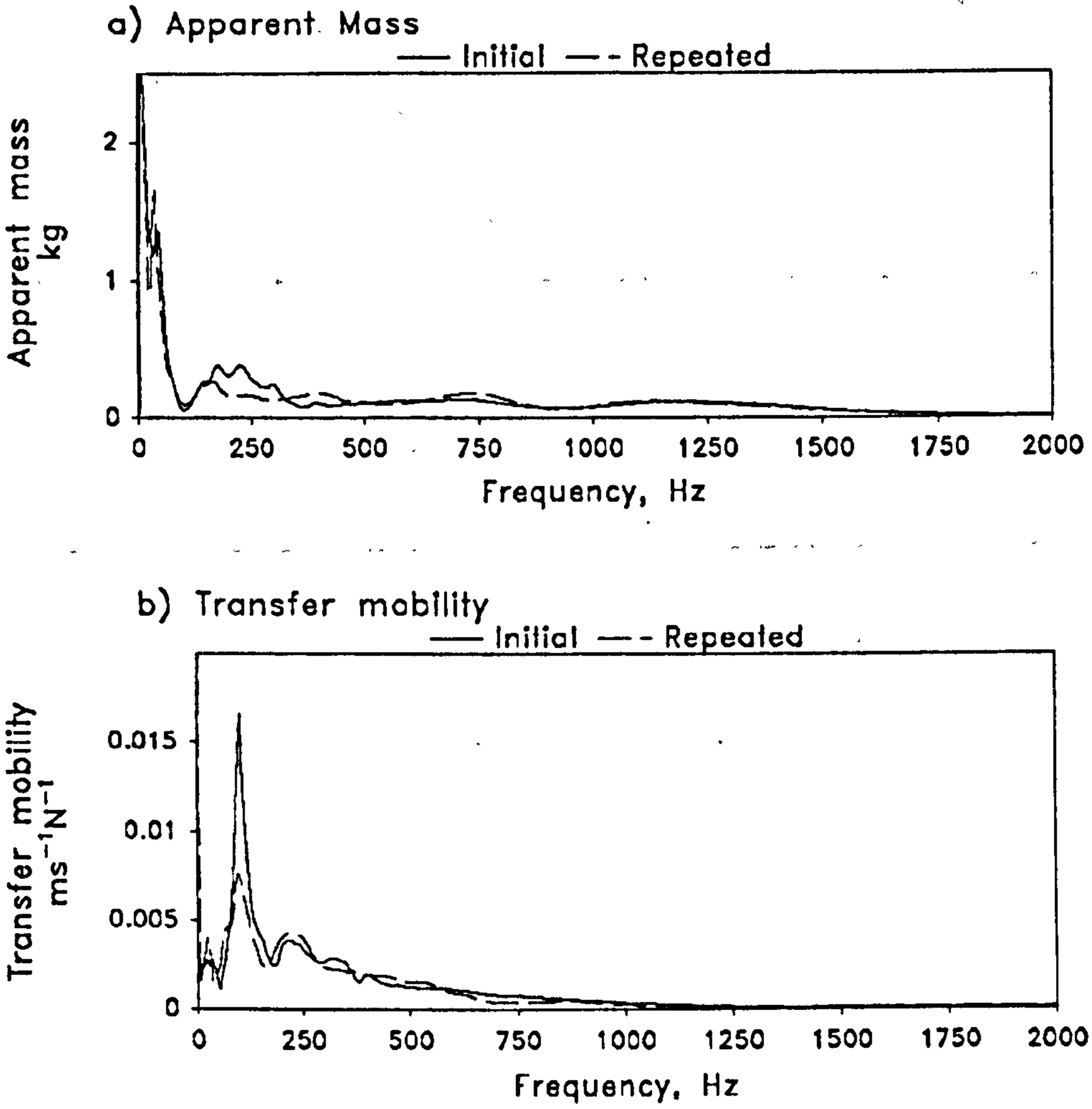

Fig 5.18 Repeatable measurements after a non-destructive mechanical tensile test on the specimen. a) Apparent mass; and b) Transfer mobility.

Table 5.5
Pearson correlation coefficients R between the apparent mass measurements taken on the same specimen in free and fixed conditions. R is very close to unity in the high frequency range (500 Hz to 2 kHz), showing consistency and repeatability in the measurements. Measurements were repeated at the L3 and L4 segments.

LOCATIONS OF APPARENT MASS MEASUREMENT	FREQUENCY RANGE	
	0 Hz - 500 Hz	500 Hz - 2 kHz
L3	R = 0.686	R = 0.995
L4	R = 0.741	R = 0.991

physical activities of the lumbar spine prior to the test would not be a key factor to be monitored.

The repeatability at different test frequency ranges was also examined, with 0 to 500 Hz arbitrarily defined as the low frequency range and that from 500 Hz to 2 kHz as the high frequency range. The figures shown in tables 5.3 and 5.4 indicate that the measurements were more repeatable in the high frequency range as defined above. Table 5.5 shows a set of apparent mass measurements taken on the same specimen in free and fixed conditions. The measurements in the low frequency and high frequency ranges were compared, using Pearson correlation coefficient to assess the repeatability. It was noted that tests at high frequency range gave relatively more repeatable results ($R > 0.99$) than those in the lower frequency range. This probably suggests that tests in the high frequency range would reveal the structural characteristics of the transmission path which is less sensitive to changes in the gross structural mechanics of the specimen and slight variation in the support condition. The tests at frequencies lower than 500 Hz would be ones for the gross structure of the specimen, and hence would be more sensitive to the mechanical integrity of the whole specimen and also of its support conditions.

5.3.4 Dynamic Range

In the course of experimentation, some tests were repeated using excitatory force of various magnitudes. Vibratory force levels of 0.1, 0.3, 0.9 and 3 N (RMS), at about 10 dB increment intervals were used. Figure 5.19 shows consistency in a series of apparent mass and transmissibility measurements for a specimen tested at different excitatory force levels. Statistical test also shows repeatability and consistency, by means of Pearson product moment correlation and by linear regression analysis ($R > 0.99$; $p < 0.0001$). It is suggested that the mechanical characteristics of the specimen were stable, and

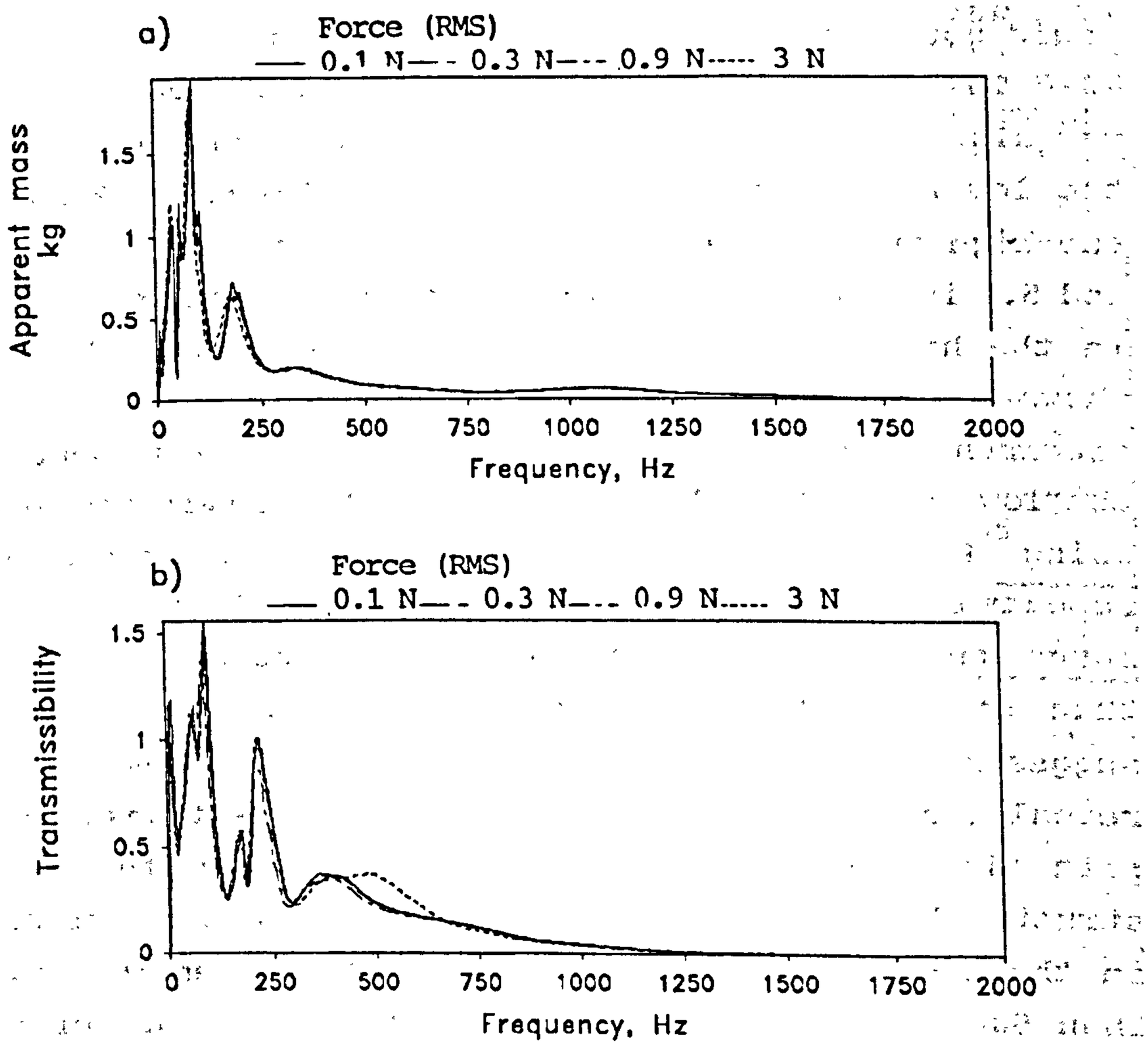

Fig 5.19 Consistent measurements of vibration response within a 30 dB range of excitatory force.

that it responded consistently to vibratory excitation over a wide dynamic range in excess of 30 dB. The working range of the vibration tests was therefore more than 30 dB and the level of excitatory force was not a critical matter of concern. From the high coherency obtained at low forcing level, it was noted that the noise level was not serious and that the vibration measurements were reliable. However, the upper limit of the excitatory force level was not extended due to the limitation of the force rating of the exciter which was 10 N (peak). Extension to an even higher magnitude of excitation has no practical benefit since this would be well above the tolerance and safety level if the vibration test is to be applied on live subjects at a later stage. Furthermore, too high a level of excitatory force would have the danger of loosening the drive-pin. The level of excitatory force is not considered as a critical matter of concern. As long as the forcing signal is strong enough to induce a measurable output response of the specimen, the problem of noise would not be a major concern. A typical random vibratory force input for this study was about 0.5 N (RMS), and the highest level used was about 1.5 N (RMS).

5.3.5 Damping

Results obtained from the pilot study on bovine specimens suggest that the vertebral column, particularly at the intervertebral disc exhibits high damping to mechanical vibration (section 4.4). It would be logical to imply that similar mechanical property could hold in the human lumbar spine. In discrete frequency vibration tests on human lumbar spines, the response signals were found to exhibit sharp cuts at the start and also at the stop in some cases, while some specimens responded with a trailing end when the excitation stopped (fig 5.20). Equation 2.5 was employed to evaluate the damping ratio according to the logarithmic decrement of the vibration amplitudes at the termination of the response signals. The results suggest that the lumbar spine had a high damping effect to the

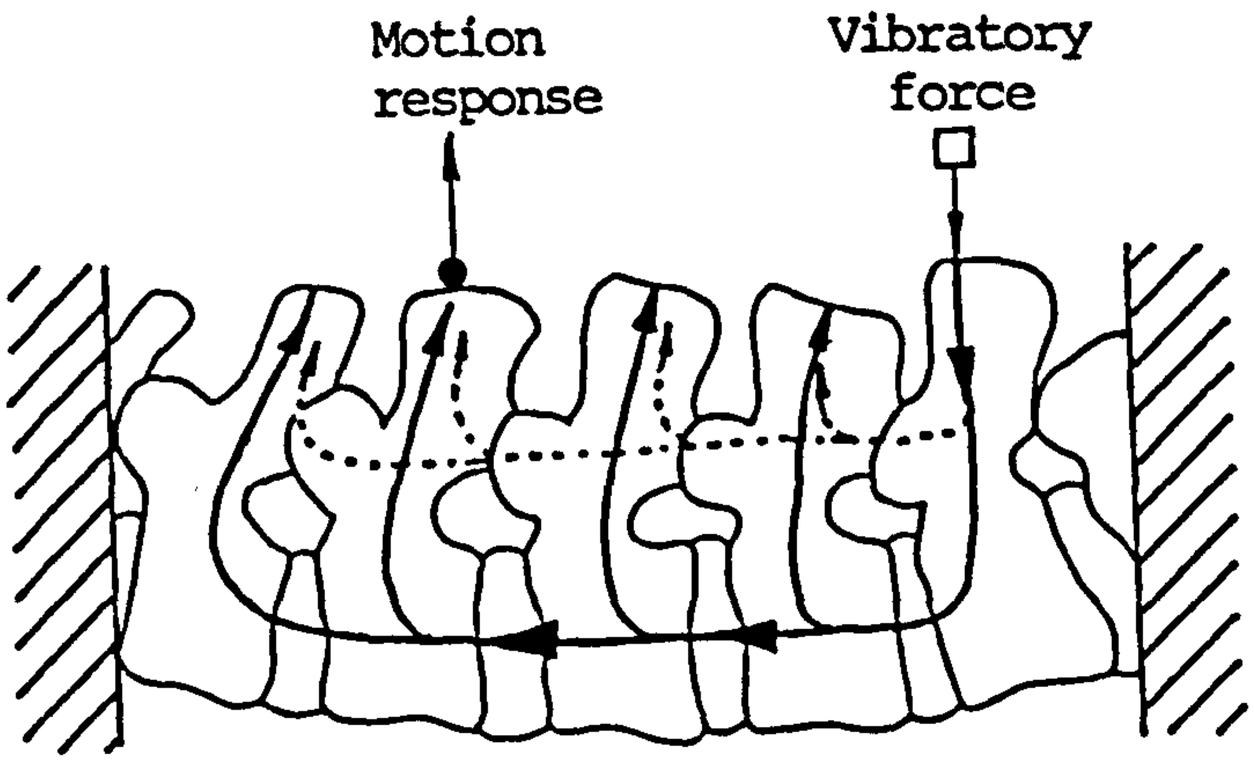

Main transmission path

Alternative transmission path

Fig 5.21 Schematic diagram showing possible transmission paths.

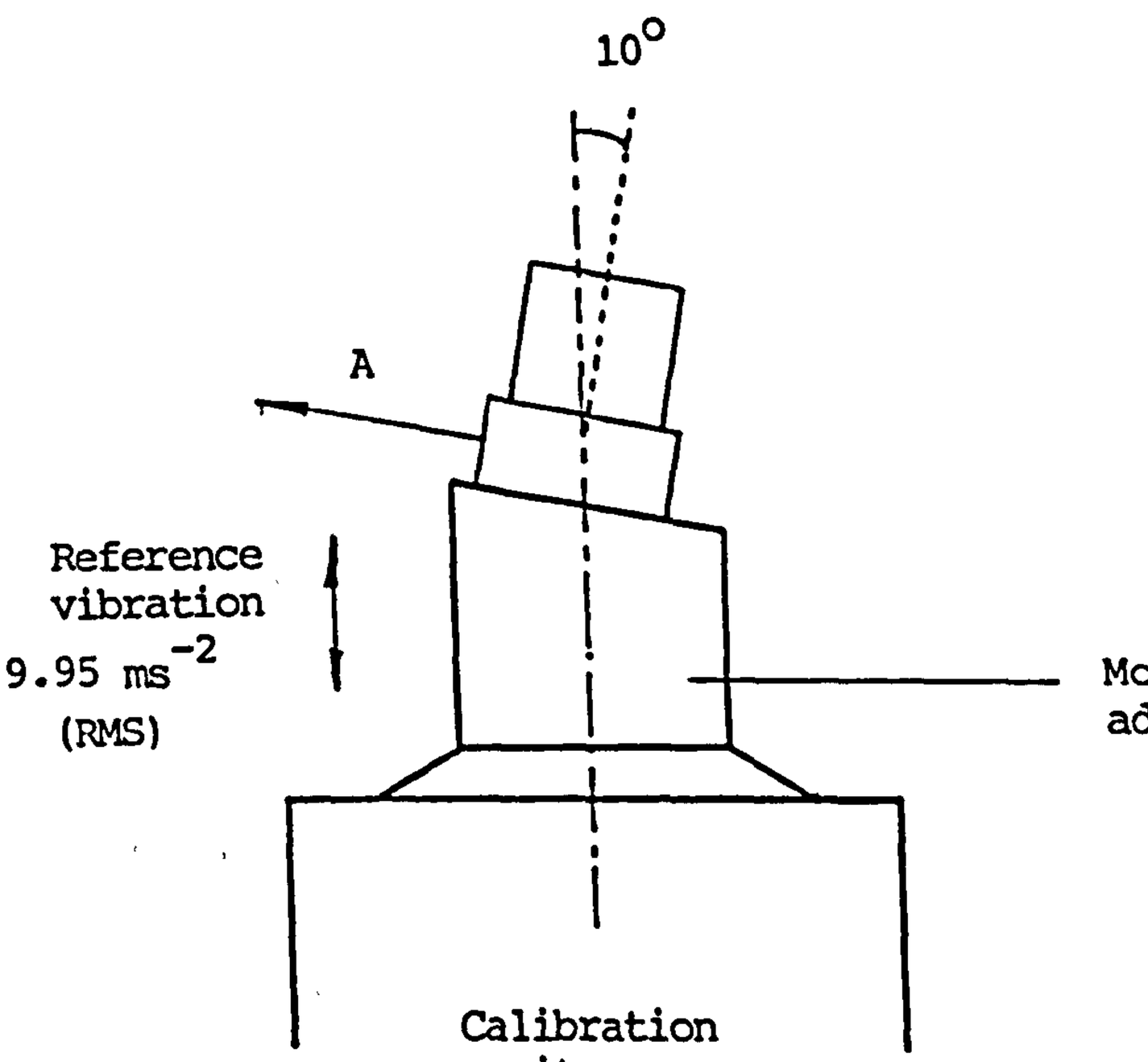

Fig 5.22 Measurement of vibration in an inclined direction of the accelerometer. A is acceleration signal.

5.3.7 Effect of Misalignment

Every endeavour has been made to align the drive-pin and measure-pins in the desired direction. They were designed to be inserted in an antero-posterior direction parallel to each other, and parallel to the plane of the L3-4 intervertebral disc. Due to technical difficulty, and the orientation of the spinous process and its trabecular structure, misalignment of a few degrees was inevitable. Tests have been carried out to assess the error in the measured signals when the transducers were mounted with a known misalignment from the desired position. Figure 5.22 shows the assessment of vibration level as measured by an accelerometer mounted on a reference calibration exciter. The accelerometer was tilted 10° with reference to the axis of vibration. It was found that a 1.5% reduction from the reference vibration level was induced with 10° misalignment of the transducer. It was close to the expected discrepancy of 1.5% for a tilt of 10°, (i.e. cos 10°). It was therefore verified that the transduction system could tolerate misalignment of a few degrees. If the angle of misalignment had been controlled to within 10°, the induced error was tolerable.

5.3.8 Error Estimation

In the spectral averaging procedure, each record length of 65536 samples was transformed with a FFT size of 2048, and the degree-of-freedom N = 32. The normalized random error from noise or incoherent signal, if any, was then reduced to a factor of 1/8 (equation 2.38). Quoting a coherence function of 0.98, the random error was about 1.8%. Results of the transform lead to a spectral analysis with frequency resolution of 4.88 Hz which was deemed acceptable for the results. As would be seen later, the motion response of the specimen to vibratory excitation did not exhibit a sharp peak at the resonant frequency. Hence a finer resolution in frequency was not demanded. For those tests for time domain analysis, such as the discrete

frequency vibration test, the signals were sampled at 50 kHz. This corresponded to a time resolution of 0.02 ms, which was adequate for the requirement of this study.

5.3.9 Effects of Support Condition

The two support conditions:- free and fixed, were designed to model two extremes of an ideal end support. The mounting cups incorporating with the angle-plates were designed to provide a fixed and stationary support to the specimen during the tests (section 5.2.1). In practice, it was difficult to create a perfectly motionless support at the ends of the specimen. The vibration level of the angle-plate at the sacral end was monitored during the random vibration test. The vibration level at the angle-plate was found to be about 0.3 ms^{-2} (RMS) while that measured on the specimen was about 40 ms^{-2} (RMS) in a typical vibration test. Thus the vibration level at the support was less than 1% of that measured on the test specimen. Hence the support device was considered effective in offering a fixed support condition to the specimen.

In the free support condition, the foam plastic offered minimal resistance to the motion of the lumbar spine. This also enabled the spine to behave as a relatively rigid body, and the test would only reveal the compliance of the supporting mechanism i.e. the foam plastic material. Hence it would not be suitable to test the behaviour of the lumbar spine at low frequency under a free condition because the structural characteristic of the specimen would not be revealed. It was noted that the motion response of the lumbar spine at low frequency was very different under these two support conditions, suggesting that the end condition had some effect on the vibration response of the specimen at very low frequency.

5.3.10 Assessment of Transmitted Vibration from the Test Environment

Attempts have been made to insulate the lumbar spine

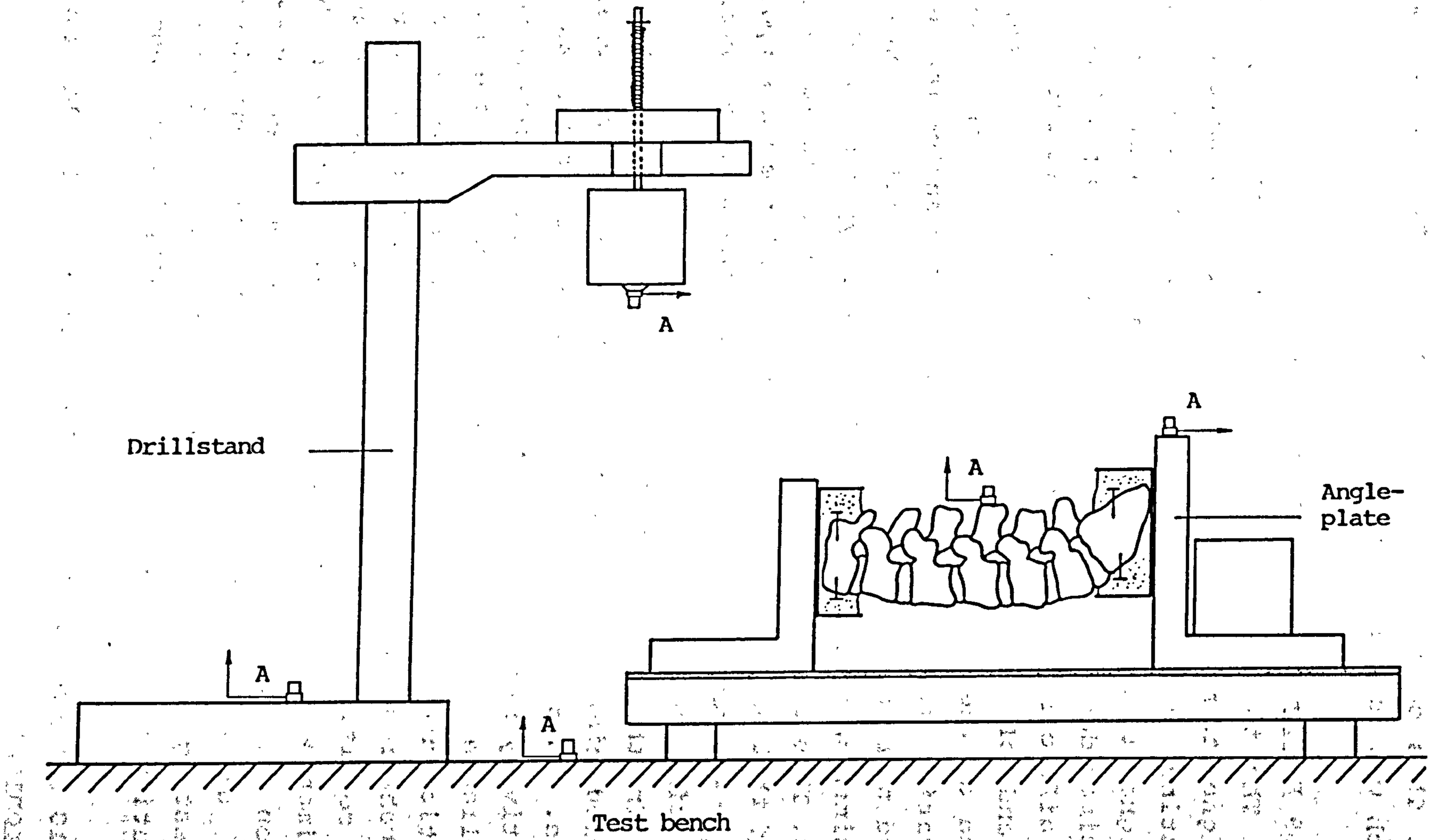

Fig 5.23 Measurement of transmitted vibrations from the test environment. A is the acceleration signal.

specimen from ambient vibration though perfect acoustical isolation from the support and its environment was not feasible. The noise from ambient vibration and other sources could be assessed by estimating the signal-to-noise ratio using equation 2.37 which refers to the coherence function estimated for each test. However, direct assessment of ambient vibration level was deemed necessary prior to proper tests. Vibration levels at the following points were monitored while the exciter was set to vibrate randomly at its full rating without attaching to the specimen (fig 5.23):-

a. the table of the exciter;
b. the base of the drillstand;
c. the bench-top;
d. the angle-plate at the sacral end; and
e. the L3 spinous process of the specimen.

Results show that the vibration levels at the points b to e were below 0.04 ms^{-2} (RMS), and that measured at the L3 spinous process was particularly below 0.01 ms^{-2} (RMS). This vibration level, when related to a typical vibration level measured in a normal vibration test, represents a signal-to-noise ratio of better than 70 dB. Vibration signals picked up at points b to e were also found to be incoherent with that measured at the freely vibrating table of the exciter. It therefore confirmed that the exciter was adequately decoupled from its support and hence the other components of the testing equipment, and that vibration from the exciter was not transmitted to the specimen through the support devices. Ambient vibration originating from the floor and neighbouring machinery, or from the bench which supported the specimen was minimal. The ambient vibration transmitted through the support device was of low level and was incoherent with the vibration signals of interest. This was dealt with as noise and was discarded by the computation algorithm of spectral averaging.

5.3.11 Other Sources of Noise and Error

When an accelerometer cable is in contact with a vibrating object the screening may be disturbed at points along its length due to bending, compression or tension. "Triboelectric" charges are formed due to local changes in capacitance (Serridge & Licht, 1986), leading to noise in the vibration signals. This "triboelectric effect" was noted and prevented by secure attachment of the cables to stable and non-vibrating objects.

Loosening of the measure-pins was easily detected by manual checking of the stability of the transducers on the pin before each test. Extraordinarily low coherency at particular frequencies which suggested pin loosening was noted only in a few cases. Hence loosening of the attachment pins was not a major problem of concern.

Excitatory force and the vibration response were measured in the antero-posterior direction (x-axis). The effect of misalignment of the transducers with respect to the defined axis has been discussed (section 5.3.7). However, the overall misalignment of the specimen with respect to the mounting cups was difficult to assess accurately, though every endeavour had been made to ensure proper alignment by the help of an alignment jig. The geometrical variations, such as the curvature of lumbar spine, specific sizes and shapes of individual segments and their other anatomical features were not assessed or taken into account. Inconsistency in the anatomical parameters and hence the geometrical variations among specimens were beyond the scope of discussion for this study.

5.4 GROSS MOTION RESPONSE IN FREE CONDITION

Under a free support condition a test specimen would exhibit a rigid-body mode of vibration which is characteristic of its mass and inertia properties (Ewins, 1991). Theoretically, there should be no flexural mode of vibration when tested at extremely low frequency in a perfectly free end support condition. However, the results

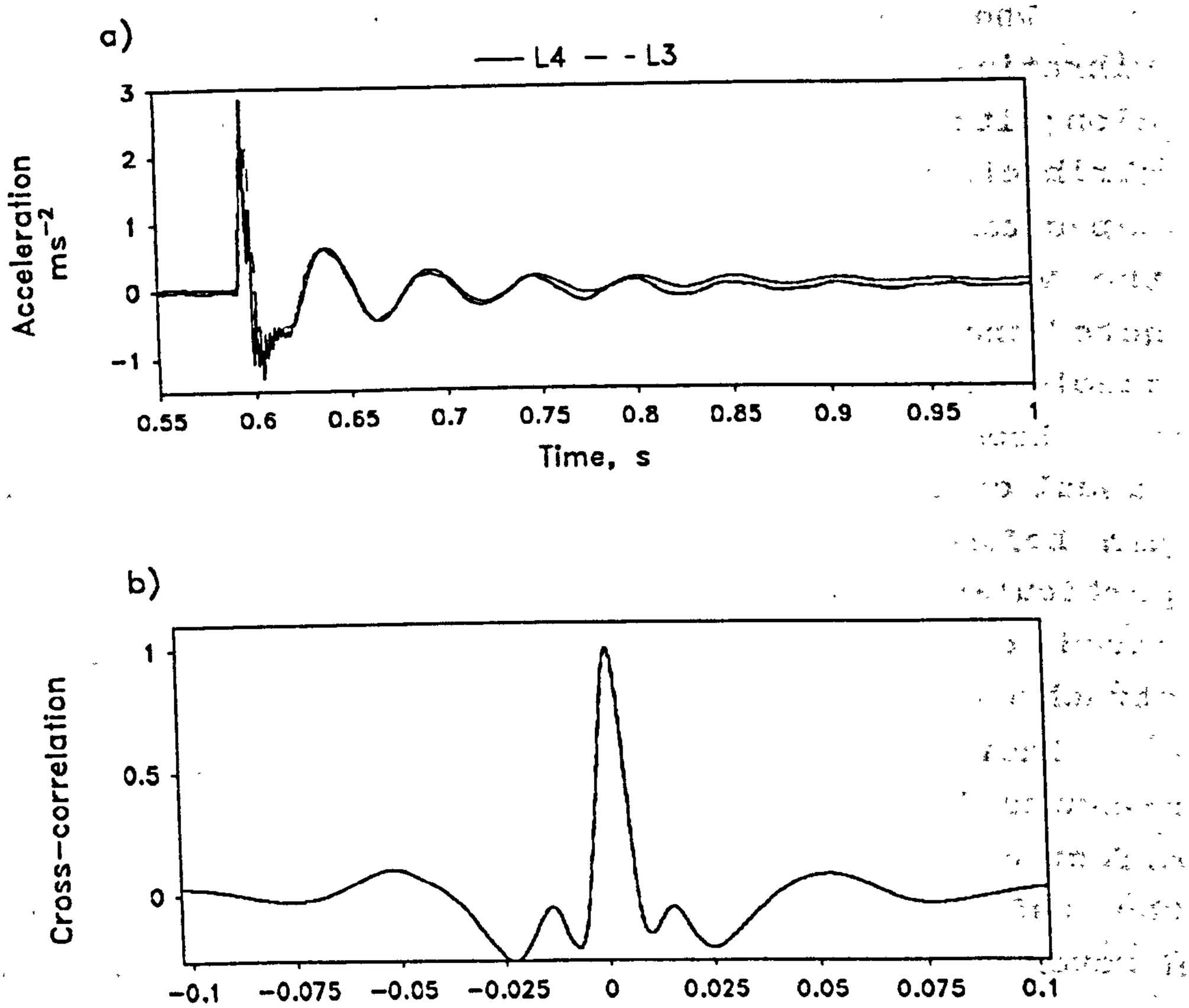

Fig 5.24 Time-signals and their cross-correlation at the L3 and L4 spinous processes.

of actual testing would show how closely to a rigid mass the specimen behaved under this test condition. The following sections outline the behaviour of the lumbar spine specimen when tested within the frequency range of below 50 Hz.

5.4.1 Impact Testing

Tests were performed with the specimen freely supported on soft foam plastic as described in section 5.2.1 (fig 5.8a). Vibration was detected by accelerometers attached at the L3 and L4 spinous processes. The excitation was induced by a gentle impact at the L5 spinous process. The initial impact signal was disregarded and only the subsequent response of the specimen was of interest for discussion. It was observed that the signals picked up at the two different segments were coherent and of equal amplitudes. The whole specimen vibrated as a rigid-body at about 19 Hz (fig 5.24). Damping was noted and a damping ratio of 0.063 was obtained by direct measurement on the logarithmic decrement of the amplitudes (section 2.2.2). Cross-correlation (section 2.3.3) of the signals picked up at the two segments revealed a time discrepancy of only 0.9 ms which corresponded to 0.0171 degree of phase difference. Thus the L3 and L4 segments were considered vibrating in coherence and both the time and phase discrepancies were considered insignificant. By the same token, it is logical to infer that the other segments i.e. L1, L2 and L5 were likely to vibrate coherently with the same amplitudes. The result therefore suggests that the specimen behaved as a rigid-body under this free test condition, and there was no flexural vibration below 50 Hz. Tests in this condition also revealed the compliance of the supporting foam plastic material, which together with the mass property of the specimen, formed a simple vibration system (fig 5.25). The results of these impact tests were also related to the tests by low frequency swept sine waves in free condition.

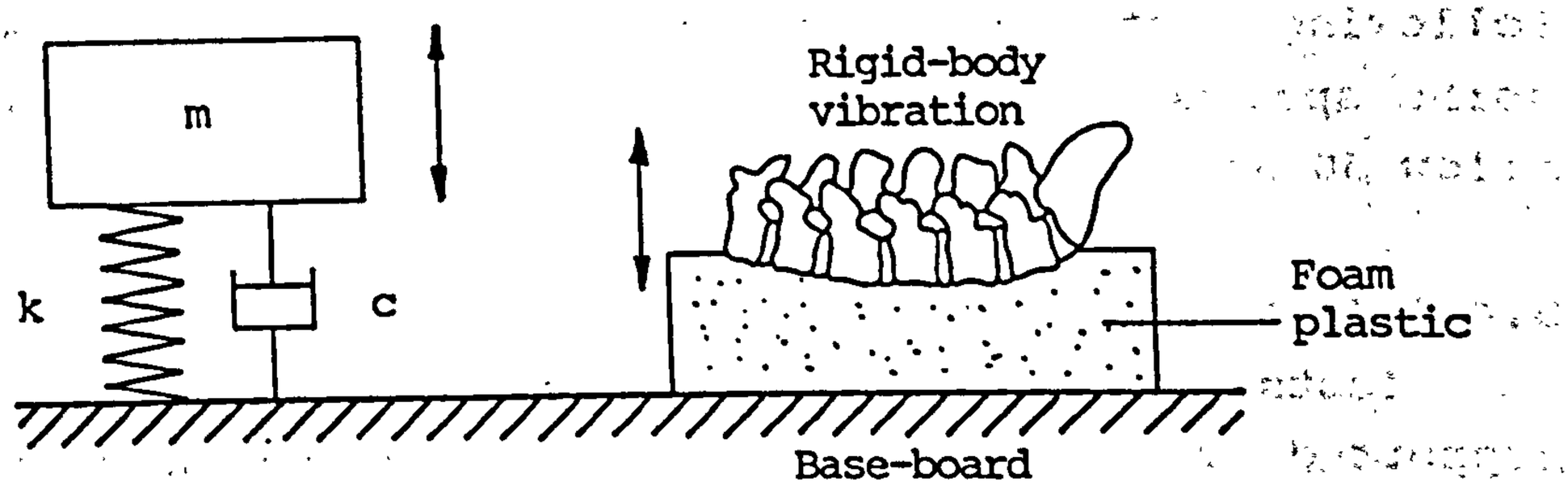

Fig 5.25 A mechanical model of the vibrating lumbar spine in free condition.

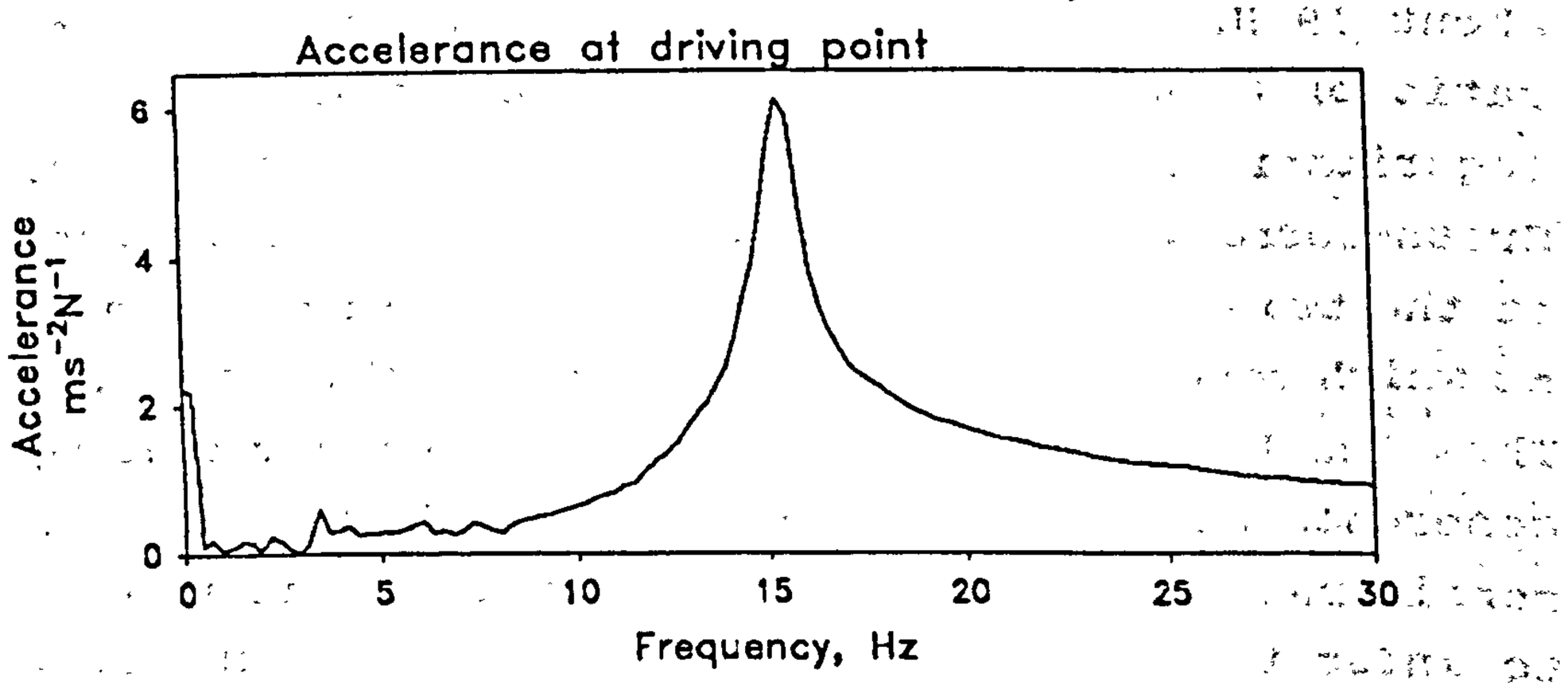

Fig 5.26 Accelerance measurement on a free lumbar spine, showing resonance at 16 Hz.

5.4.2 Swept Sine Testing

Swept sinusoidal vibration between 10 and 30 Hz was applied at the L3 spinous process of a free lumbar spine specimen (fig 5.9a). Sine waves at a sweep rate of 5 Hz per second produced a resonance at about 16 Hz. Figure 5.26 shows the peak of the accelerance (A(f)/F(f)) which indicates a significant resonant response to sinusoidal excitation at this frequency. This result suggests a mass-like behaviour of the specimen which presents only a rigid-body vibration mode, consistent with that of the impact tests reported in section 5.4.1. This swept sine testing in low frequency range was not able to reveal any structural or mechanical characteristics of the specimen apart from its behaviour as a rigid-body under the test condition. It revealed a similar behaviour of a vibration system as depicted in figure 5.25.

5.5 GROSS MOTION RESPONSE IN FIXED CONDITION

When mounted on two angle-plates as illustrated by figure 5.2 & 5.4, the specimen was effectively fixed at both ends with added mass and inertia at the T12 vertebra and at the sacrum. The specimen behaved grossly as a stiffened structure, and was less compliant to manual touch and attempted bending. Impact tests and swept sine tests were performed under this fixed condition.

5.5.1 Impact Testing

The impact was produced by a hand-held dental hammer striking gently on a small force transducer mounted at the L5 spinous process (fig 5.8b). Acceleration (A) was recorded at other segments. There was a short delay of the impulse at the segment just next to the driving point. A time-delay of about 0.3 ms was observed for each other disc level, which corresponded to a transmission speed of about 100 ms^{-1} along the lumbar spine for this particular range of vibration frequency. A damped vibration of about 100 to 150 Hz was observed. The amplitudes of vibration at the L1

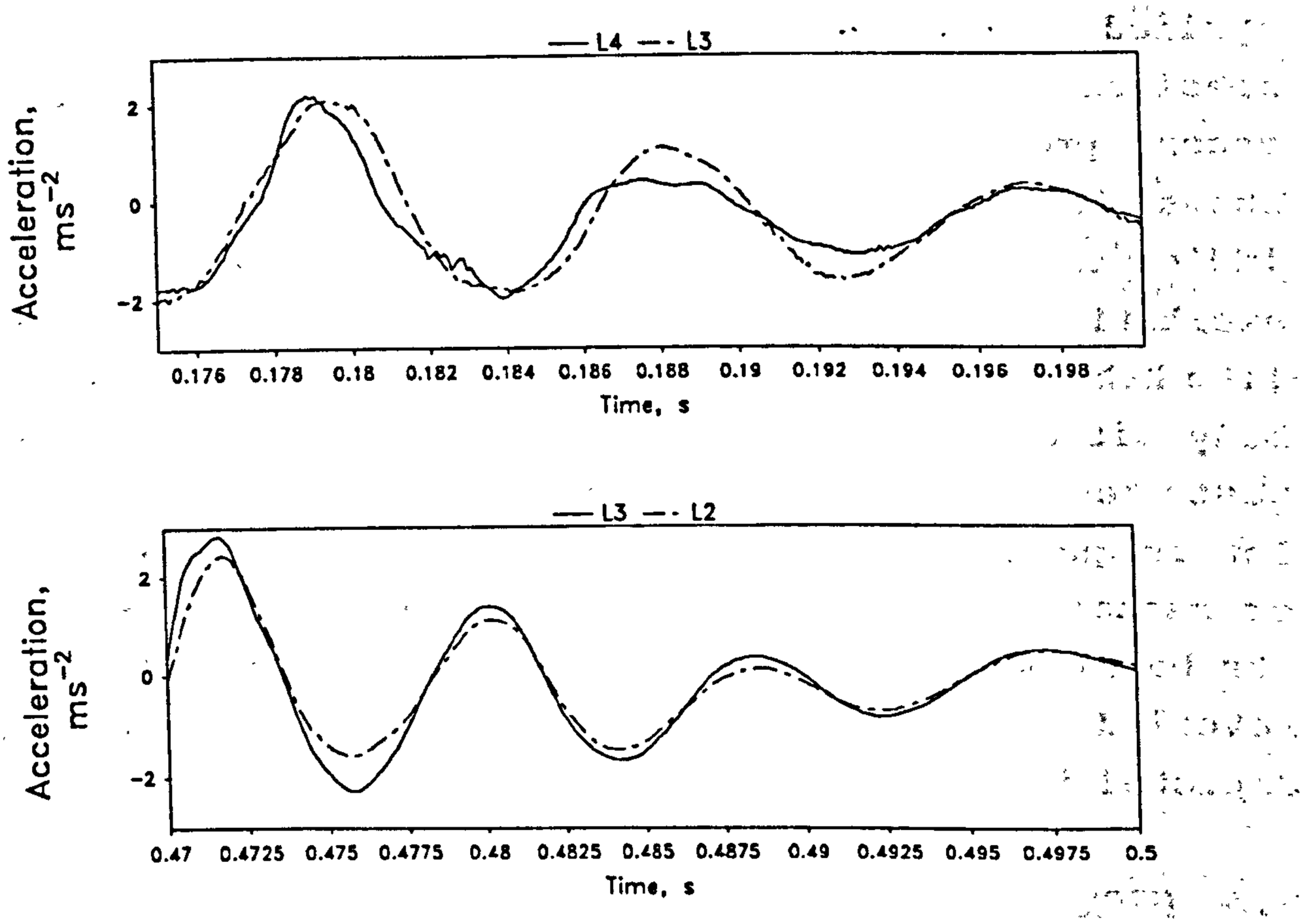

Fig 5.27 Damped vibration of different amplitudes at the L1 to L4 spinous processes.

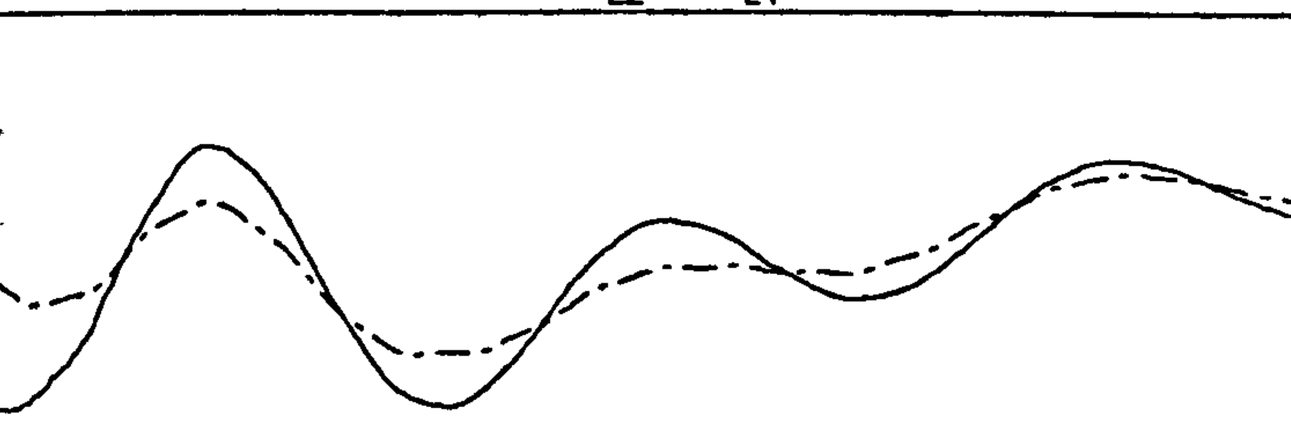

Fig 5.28 First flexural vibration mode of a fixed lumbar spine at 120 Hz.

to L4 spinous processes were compared. The L3 vertebra which was the middle segment of the specimen vibrated with the greatest amplitude. The other segments exhibited gradually decreased amplitudes when getting farther away from the L3 vertebra i.e. $A_{L1} < A_{L2} < A_{L3} > A_{L4}$. There was no significant phase difference among the measurements (fig 5.27). These results suggest that, in a fixed condition, the specimen behaved as a segmented beam, resonating with a flexural vibration at 120 Hz. Figure 5.28 depicts the first mode of flexural vibration. These results also correspond well with the findings of the random vibration tests reported in section 5.7. The variation in the response among the specimens could also be explained by inconsistent impact force generated by the hammer, in addition to individual variability. This also suggests the need of a better controlled excitation. The use of a measurable forcing excitation by random vibration technique is outlined in the appropriate sections.

5.5.2 Swept Sine Testing

This technique provided an opportunity of observing the vibration response of a fixed lumbar spine at low frequencies below 50 Hz. It was noted that low frequency vibration involved a large amplitude of movement of the drive-rod which would then correspond to a large antero-posterior displacement of the specimen. It was also observed that the specimen was effectively restricted from upward and downward movement i.e. in the antero-posterior direction. The weight of the specimen together with the stiffness of the supporting devices was offering resistance to the vibrating drive-rod. Hence the allowable excitatory force level had to be limited, otherwise non-sinusoidal or erroneous response would be induced. This might also be due to unwanted vibration set up in the fixture and some relatively weak structure in the system. With a limited excitatory force level, the fixed lumbar spine was not giving good vibration response for analysis. At this point,

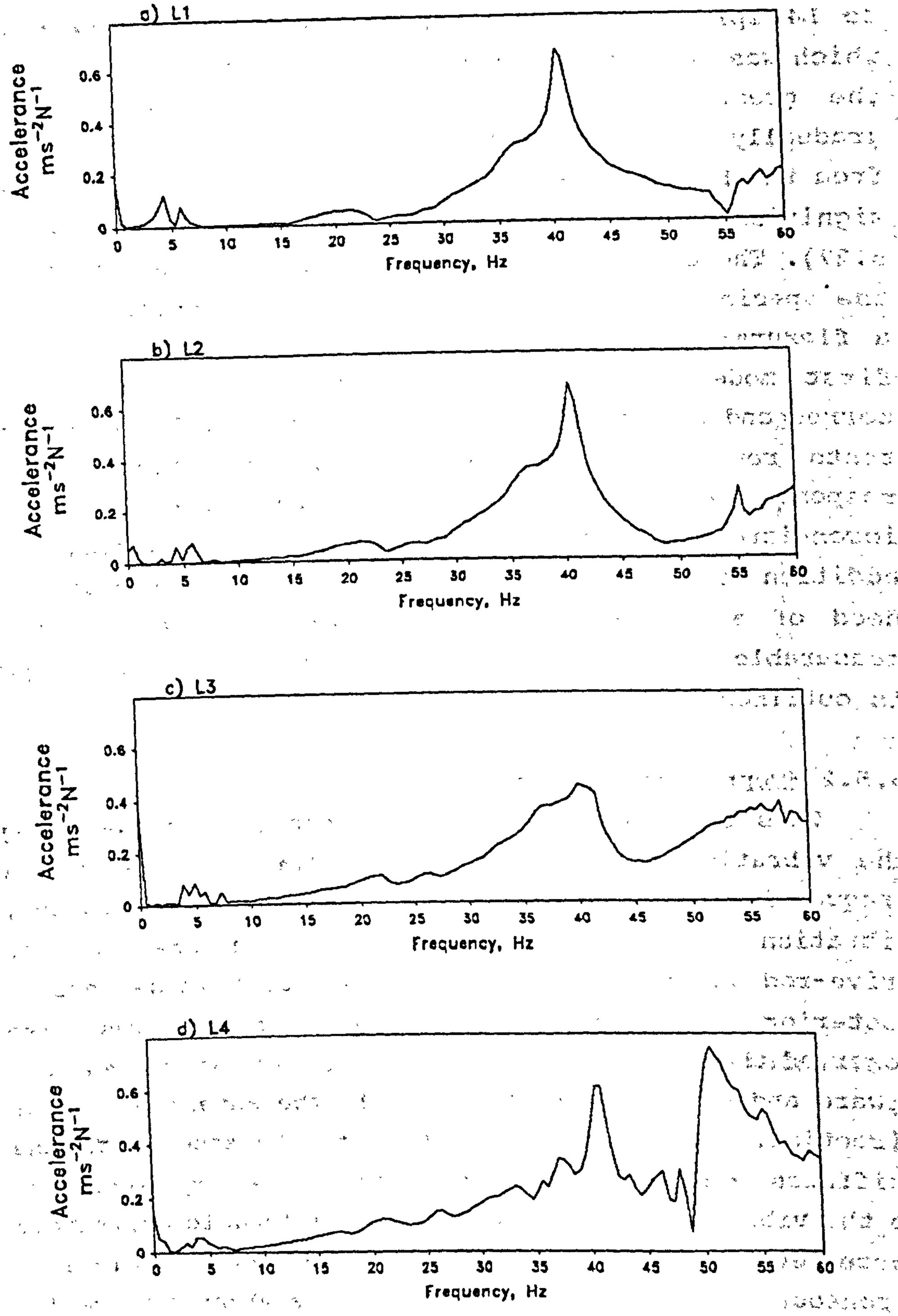

Fig 5.29 Frequency response function at different segments of the lumbar spine under swept sine testing.

it could be pointed out that the fixed specimen behaved as a "heavier" and stiffer system, showing a smaller motion response to vibration in a frequency range below 50 Hz. This observation was found to be consistent with the suggestion that the low frequency vibration response of a system is very much affected by the mechanical characteristics of its support mechanism.

Swept sinusoidal vibration between 10 and 50 Hz was applied at a sweep rate of about 5 Hz per second to the L5 spinous process of a fixed lumbar spine. The motion response (A) was measured at the other spinous processes. Driving point accelerance which is defined by the frequency response function (A(f)/F(f)) was also estimated. Similar peaks around 40 Hz were observed (fig 5.29), and there was no significant phase difference at various segments. This indicates that all the lumbar segments vibrated coherently. However the specimen did not demonstrate flexural vibration. The mechanical behaviour of the specimen under this fixed condition was different from that in a free support condition. The frequency range in this test did not cover vibration above 50 Hz so that the dynamic mechanical behaviour of the lumbar spine as observed in the impact test was not induced.

5.6 DYNAMIC RESPONSE AT THE DRIVING POINT

Dynamic response relates the measurement of motion with that of the excitatory force applied to the lumbar spine. Driving point mobility as described in section 2.4.2 is a measurement of the lumbar spine's ability to withstand or to absorb vibration. Apparent mass and mechanical impedance are inverse functions derived from the driving point mobility measurement. These are measures of the lumbar spine's ability to resist against external vibratory excitation.

5.6.1 Apparent Mass and Mechanical Impedance

These parameters have been defined in section 2.4.2,

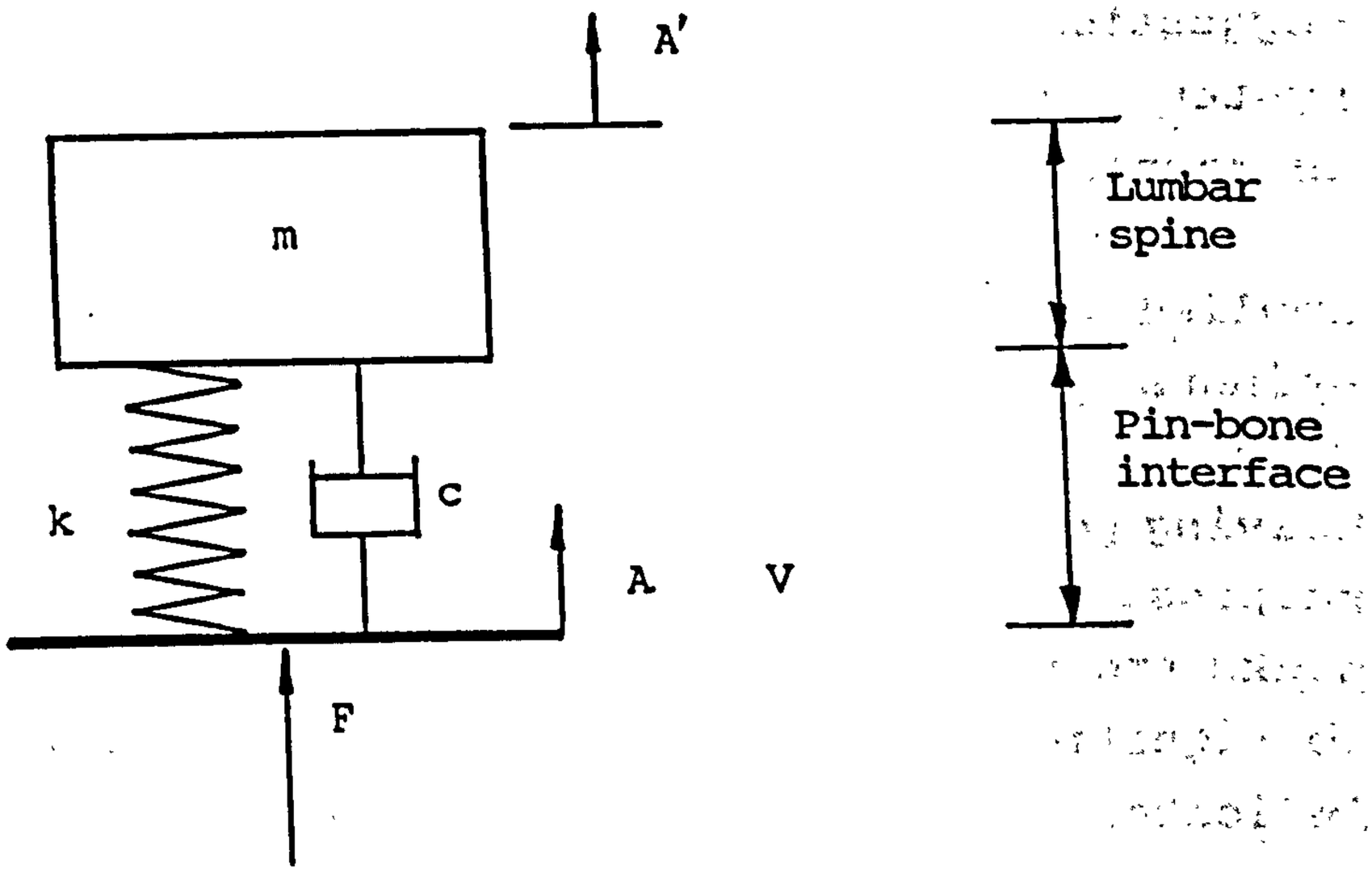

$$\textit{Transmissibility, } T(f) = \frac{A'(f)}{A(f)}$$

$$\textit{Apparent Mass, } AM(f) = \frac{F(f)}{A(f)} = \frac{mA'(f)}{A(f)} = mT(f)$$

$$\textit{Mechanical Impedance, } Z(f) = \frac{F(f)}{V(f)} = \frac{mA'(f)}{A(f)/j\omega} = j\omega mT(f)$$

where
j $= \sqrt{(-1)}$; and
ω is the angular frequency.

Fig 5.30 Transmissibility and its relations with apparent mass and mechanical impedance.

and are now shown again in figure 5.30 for convenience. As seen from the equations, apparent mass and mechanical impedance are both indicating the transmissibility of vibration across the interface and hence to the lumbar spine. From the results of the tests, it was found that these two parameters basically gave the same spectra. However, the magnitude of mechanical impedance gives more emphasis on the higher frequency, and is related mathematically to apparent mass by a frequency dependent factor of $2\pi f$. In this section, only the apparent mass is discussed. It was also observed that the apparent mass measurement at frequencies below 500 Hz was affected by the support conditions. Both in the free and fixed conditions the same spectra of apparent mass were obtained for frequencies above 500 Hz (fig 5.31). Statistical tests show that the spectra for the higher frequency range are consistent under different support conditions, with Pearson correlation coefficient $R > 0.99$ (table 5.5). This shows that the support condition has no effect on the measurements made in the frequency range higher than 500 Hz. It can be seen that the transmissibility of vibration across the interface at the driving point is then a measure of the integrity of the interface between the drive-pin and the bone. Though it is an indirect measurement of the response of the specimen to the vibratory excitation, it indicates the excitation system's effectiveness in driving the lumbar spine at various frequencies. The apparent mass measurement taken at the driving point did not reveal the structural features of the lumbar spine specimen, but it shows that the pin-bone interface at the driving point behaved as a firm contact with fairly effective transmissibility across the frequency range of interest. This mechanical characteristic was not changed even through the process of mounting. It therefore suggests that the dynamic characteristic of the interface was consistent as long as a firm anchorage of the drive-pin was maintained throughout. This also suggests that apparent mass

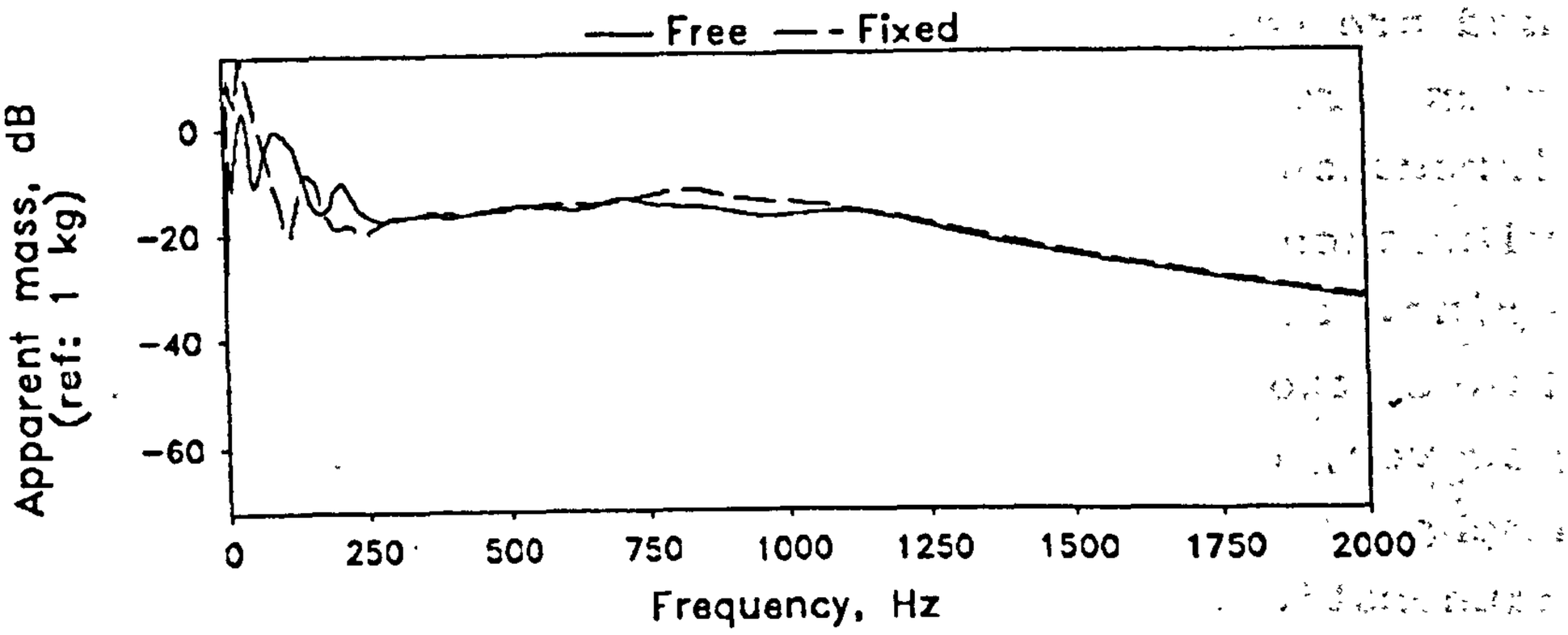

Fig 5.31 Apparent mass measurements under different end support conditions.

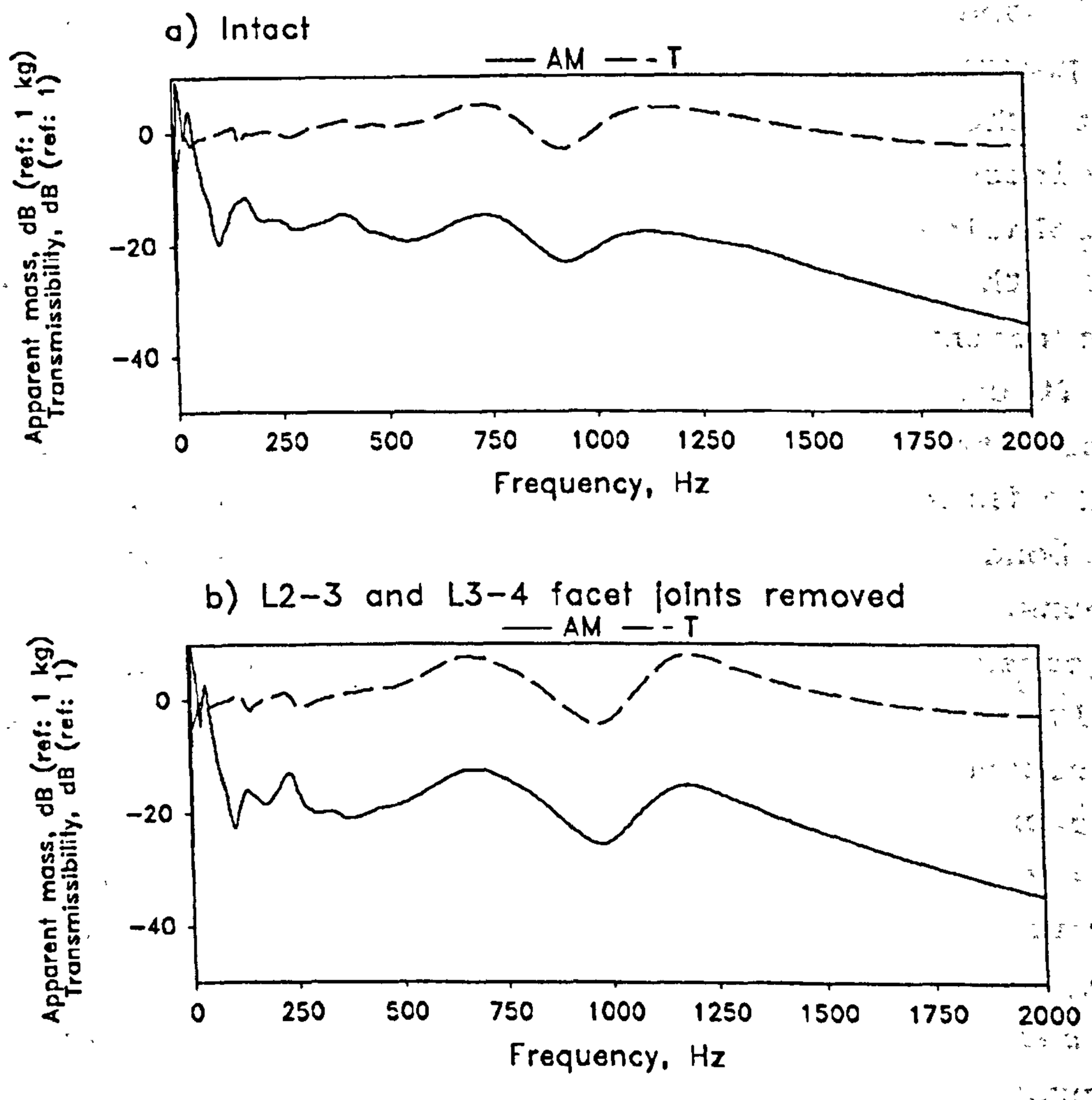

Fig 5.32 Apparent mass measurements. a) Intact specimen; b) L2-3 and L3-4 interspinous ligaments and facet joints removed. AM = apparent mass; T = transmissibility.

measurement would not reveal the lumbar spine's response to vibratory excitation. It is only an indication of the transmissibility and hence local stiffness of the pin-bone interface at the driving point.

5.6.2 Apparent Mass and Transmissibility

Following on the discussion in 5.6.1, direct measurement of transmissibility of the lumbar spine has been made to compare with apparent mass. Figure 5.11a depicts the measurement of motion response at the vertebral body of a specimen while the driving force and the motion response at the spinous process were both measured. The measurements of transmissibility and apparent mass gave the same spectra in the frequency range above 500 Hz (fig 5.32a). The difference of about 20 dB between the two curves corresponds to the mass factor m (about 0.1 kg) as indicated by the equations in figure 5.30. This estimated mass of 0.1 kg is close to the mass of a single lumbar vertebra. The spectra in frequencies lower than 500 Hz are inconsistent, suggesting again the effect of the support condition. Figure 5.32b shows the spectra obtained from the same specimen, but tested with the L3 spinous process isolated by destroying the L2-3 and L3-4 interspinous ligaments and facet joints to create a gap of at least 1 mm to ensure no contact between the posterior elements of the L2, L3 and L4 vertebrae (fig 5.11b). In this case the only links between the vertebrae concerned were the L2-3 and L3-4 intervertebral discs. It could be seen that there was no significant difference between the spectra obtained in both test conditions. Hence, it therefore strongly confirmed that the excitation at the driving point was effectively transmitted to the spinous process, and hence to the vertebral body through the laminae and the pedicles. Dispersion of vibration to other spinal vertebrae through the facet joints was not observed. Table 5.6 shows the statistics which reveal the same consistency of measurement in the frequency range between 500 and 2000 Hz.

Table 5.6
Pearson correlation coefficients R between the measurements of apparent mass and transmissibility. R is very close to unity in the high frequency range (500 Hz to 2 kHz), showing consistency and repeatability in the measurements.

PHYSICAL STATE OF SPECIMEN	FREQUENCY RANGE	
	0 Hz - 500 Hz	500 Hz - 2 kHz
Intact	R = 0.487	R = 0.967
L2-3 & L3-4 facet joints transected	R = 0.429	R = 0.972

5.7 TRANSFER MOBILITY

Transfer mobility refers to the measurement of a lumbar spine's ability to transmit vibration (section 2.4.2). It is also a measurement of motion response to unit excitatory force as a function of frequency. The measurement of transfer mobility (V(f)/F(f)) is found to be more appropriate as it gives a balanced frequency-weighting while the measurement of compliance (D(f)/F(f)) and accelerance (A(f)/F(f)) are respectively giving heavier emphasis on the lower and higher frequencies.

The transfer mobility curves also show that there was no fundamental difference whether the response was measured over a higher or lower segment than the point of excitation - L1 is referred as the highest segment and L5 the lowest in a lumbar spine. This suggests that the transmission of vibration along the lumbar spine is independent of the direction. Figure 5.33 shows the non-directional vibration response of fixed test specimens, though inter-segmental variation was noted.

Figure 5.34 shows a series of typical transfer mobility curves obtained from a fixed specimen. Vibratory force was applied at the L5 spinous process and the response was measured at the other spinous processes (fig 5.12). The transfer mobility curves can be grossly divided into two parts: a low frequency range below 500 Hz and a high frequency one between 500 Hz and 2 kHz according to the characteristics of the curves. The transfer mobility curves do not show distinct and sharp resonant peaks as would be expected of a mechanical system. There are several well defined resonant peaks of small amplitude, revealing the characteristics of a compliant and highly damped structure, presenting several degrees-of-freedom. The phase information indicates that the lumbar spine vibrated in phase at all segments at those resonant frequencies. The amplitudes of the peaks reveal that the lumbar spine vibrated in a flexural mode with the nodes at both ends i.e. the T12 vertebra and the sacrum. The antinode was at

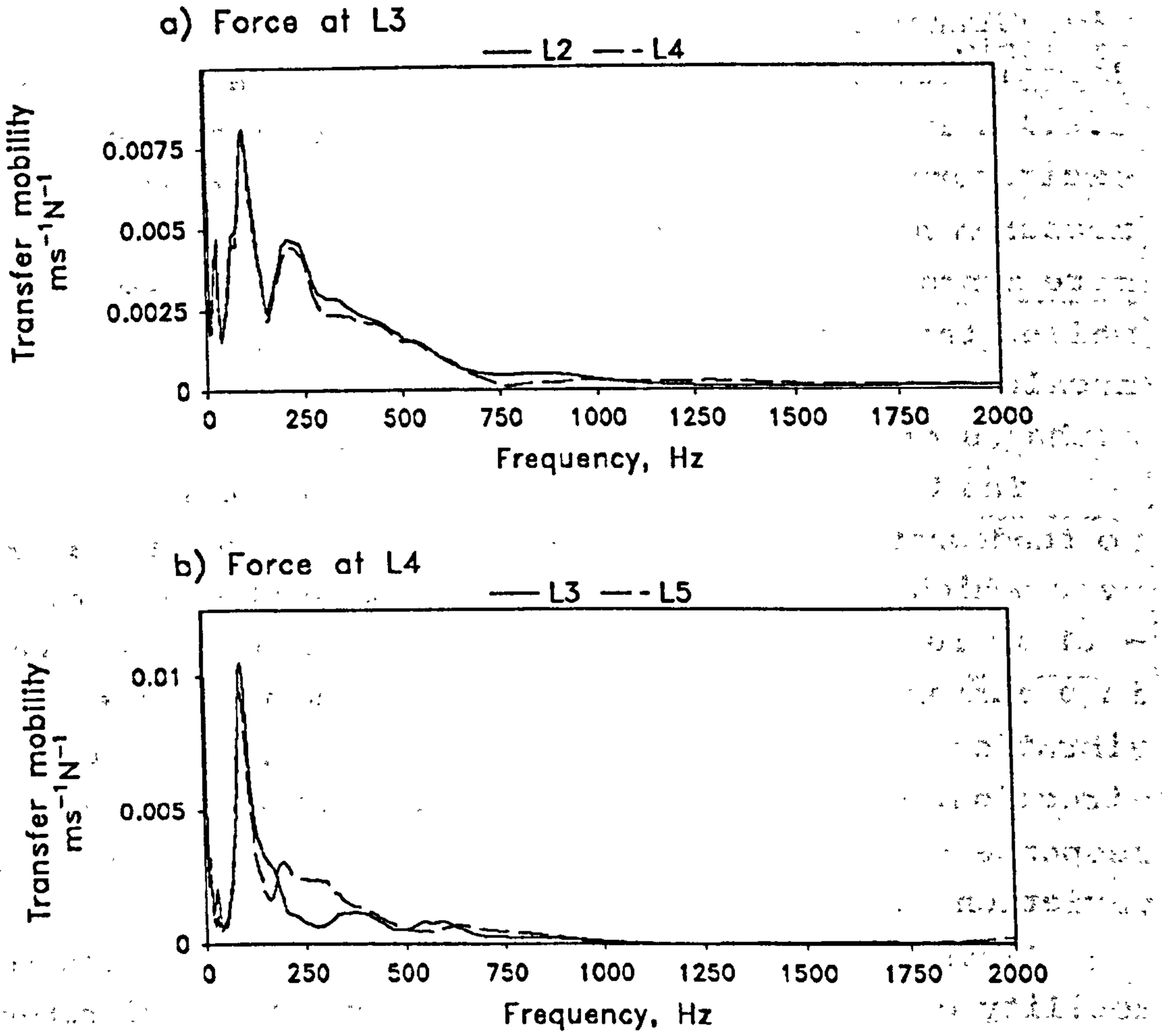

Fig 5.33 Non-directional motion response of the lumbar spine. Same transfer mobility measurements at a lower or higher segment when excited a) at L3, and b) at L4.

L3 where the biggest amplitude was detected (fig 5.34c). The modal shape presented by the vibrating lumbar spine suggests that it can be modelled as a segmented beam hinged at both ends. Mobility in the range of frequency above 1 kHz was significantly attenuated or effectively damped. The lumbar spine did not exhibit any clear mode of flexural vibration, nor was there any identifiable resonant peak in the mobility curves in this frequency range. The curves dropped close to zero beyond 1 kHz, and there was minimal motion response when the frequency approached 2 kHz.

The transfer mobility measured at various lumbar segments shows different motion response depending on the location of the measuring point. Figure 5.34 also shows the transfer mobility as measured at the other spinous processes while the excitation remained at the L5 spinous process. The curves show a gradual reduction in the transfer mobility when the measuring point was moved away from the driving point. This characteristic of the transfer mobility is particularly noticeable in the high frequency range. This result suggests an accumulative attenuation of vibration when it travelled along a series of vertebral bodies and intervertebral joints from L5 to L1. A point which is worth noting is that the high frequency vibration is dependent on the property of the transmission media i.e. the bone substance, the intervertebral disc and the facet joints. Hence the transmission (or attenuation) is dependent both on the quantity and quality of the media through which the vibration is transmitted. The high attenuation of high frequency vibration suggests strong damping effect on vibration of the lumbar spine, particularly at the intervertebral discs.

5.7.1 Summated Mobility and Total Mobility

The summation of transfer mobility is designed to provide a picture of the overall mobility of the test specimen in a specified range of frequency. It is defined by the mathematical integration of the transfer mobility

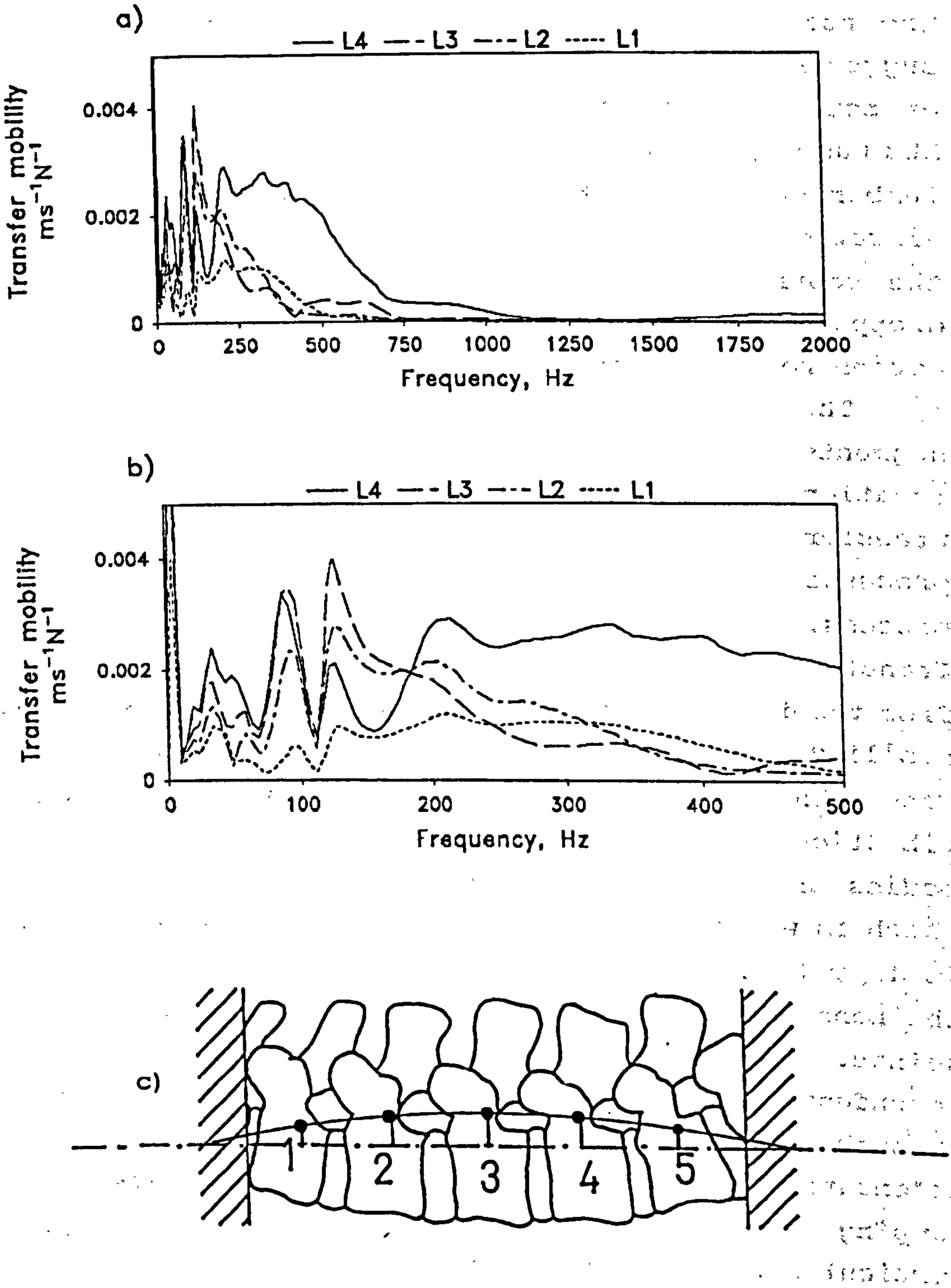

Fig 5.34 Typical transfer mobility curves. a) 0 to 2000 Hz; b) 0 to 500 Hz (expanded for clarity); c) First flexural vibration mode at 127 Hz.

curve from 0 Hz according to the following equation:

$$Summated\ Mobility,\ SM_n = \int_0^n \left|\frac{V(f)}{F(f)}\right| df \qquad (5.5)$$

where n is the designated upper frequency limit for consideration. Thus, total mobility is defined with n = 2k.

$$Total\ Mobility,\ TM = \int_0^{2k} \left|\frac{V(f)}{F(f)}\right| df \qquad (5.6)$$

It is an objective means of expressing the overall motion response of a lumbar spine specimen under forced vibration, and is a useful indicator of the specimen's overall ability in transmitting vibratory energy up to an indicated frequency. Figure 5.35 shows a series of summated mobility measurements corresponding to the transfer mobility curves shown in figure 5.34. A typical summated mobility curve comprises three major parts. At low frequency, it rises from 0 Hz with a definite slope and gradually levels off at high frequency, with a transition zone in between. Figure 5.36 illustrates the definition of total mobility by referring to the diagram of a typical summated mobility curve. This indicates the fact that mobility takes place mainly in the low frequency and the curve rises gradually due to accumulative mobility across this range of frequency. Up to a certain frequency, around 1 kHz, the mobility becomes low and the contribution of mobility in the high frequency is not significant, therefore the summation curve stops to rise, showing a trend to plateau off.

When comparing the summated mobility measured at various levels, the picture basically echoes the findings described previously. The location of mobility measurement was found to have effect on the results. The summated

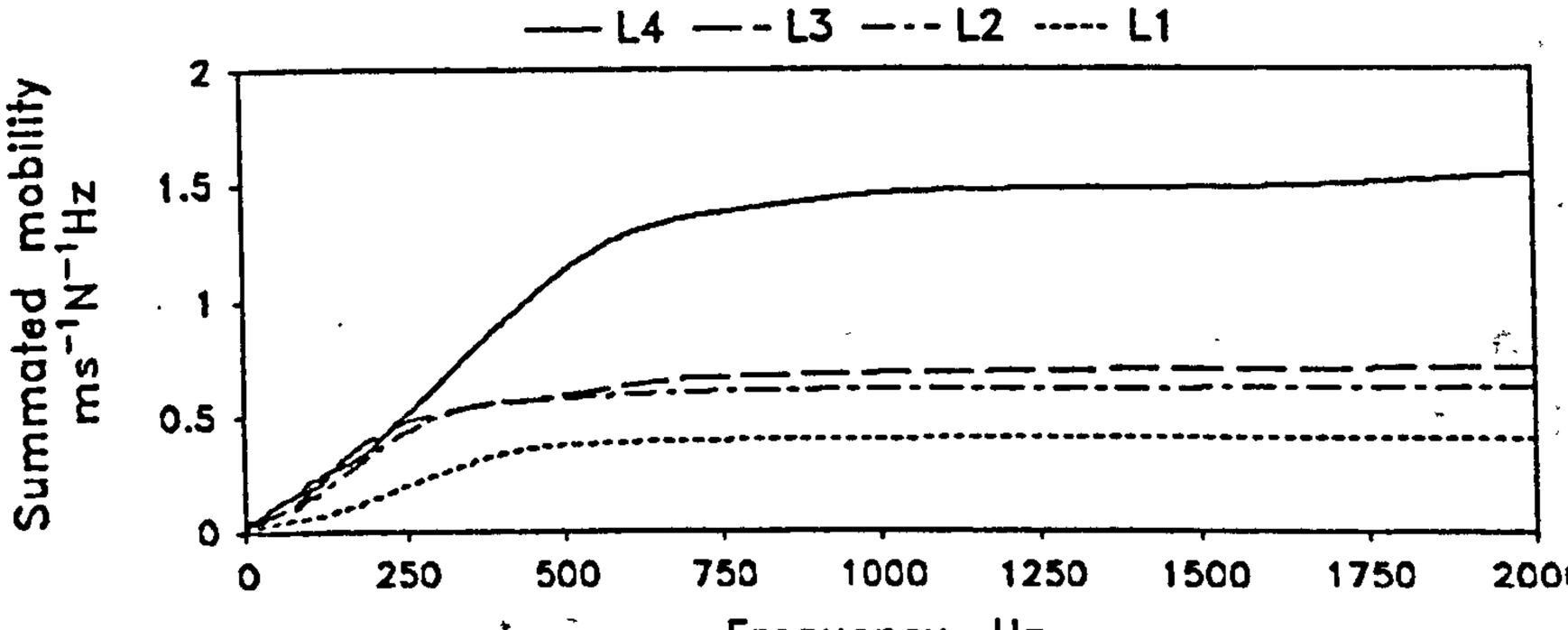

Fig 5.35 Summated mobility curves.

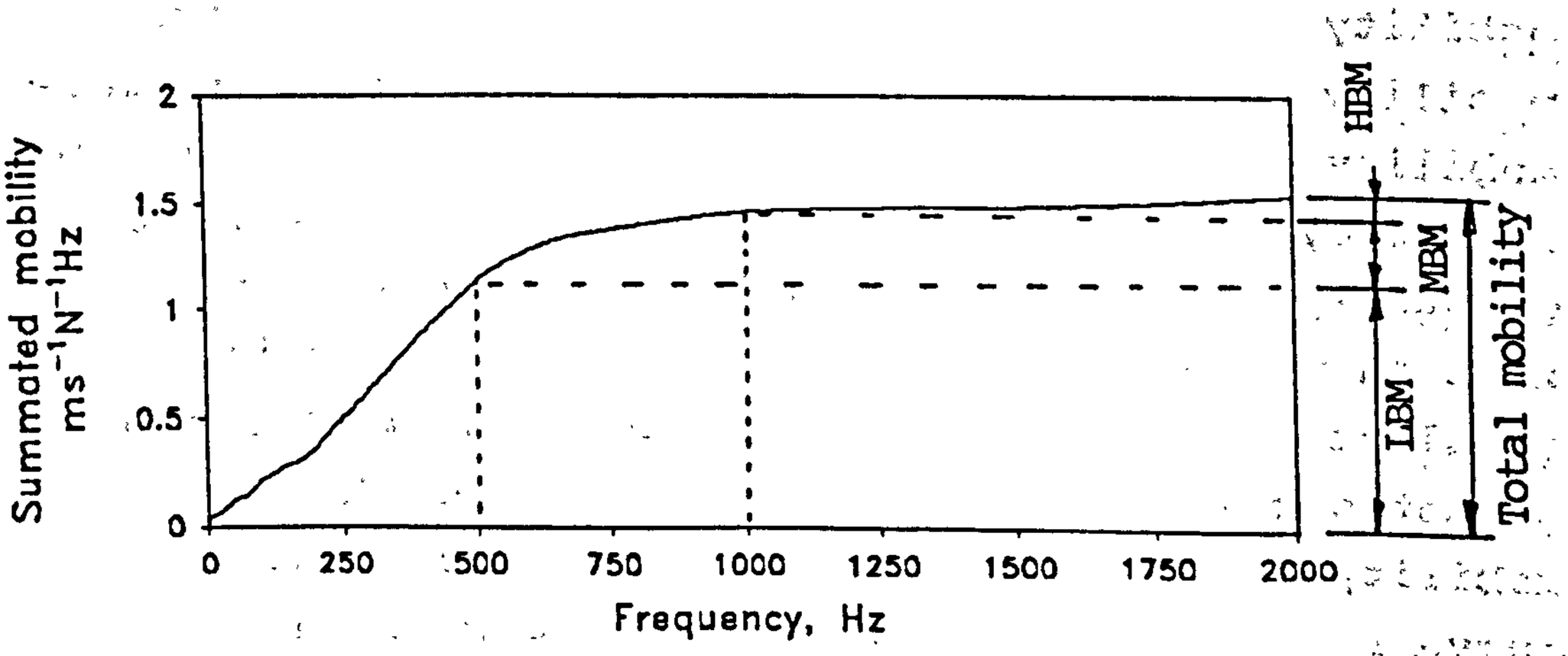

Fig 5.36 Definition of total mobility and band mobility. LBM = low band mobility; MBM = medium band mobility; and HBM = high band mobility.

mobility curves obtained at a segment farther away from the excitation source shows earlier levelling off at a lower frequency, and with a lower value. This again reflects the accumulative attenuation as a result of damping when the vibratory energy is transmitted along the lumbar spine.

An attempt was made to fit the summated mobility curve with an exponential expression indicated below:

$$Y(f) = A\ (1 - e^{-b(f-c)}) \qquad (5.7)$$

where

Y(f) is the summated mobility in $ms^{-1}N^{-1}Hz$;

A is a constant in $ms^{-1}N^{-1}Hz$;

b is a constant in Hz^{-1}; and

c is a constant in Hz.

The summated mobility curves are found to fit closely to equation 5.7 by non-linear regression, with the coefficient of determination $R^2 > 0.97$. Table 5.7 lists out the coefficients A and b determined for the Specimens No. 9, 10 and 11. The coefficient A is found to be in very close agreement with the measured values of total mobility as listed in table 5.8. Statistics by paired t-test indicates that these two sets of figures (theoretical and measured) are not different. They are also highly correlated with the Pearson correlation coefficient R = 0.9998 ($p < 0.0001$). Hence coefficient A can be taken as the theoretical total mobility of a particular segment. The constant b reflects the manner in which the curve approaches a stable level. A high value of b refers to one with a major contribution of mobility in the lower frequency, but showing low mobility in the high frequency. The curve would level off earlier i.e. at a lower frequency, and more abruptly as illustrated by SM2 in figure 5.37. A small value of b indicates a smooth transition from a slope to a plateau in the curve. This reveals a low mobility in the low frequency but the mobility remains high in the high frequency, suggesting

Table 5.7
Coefficients A and b for Specimens No. 9, 10 and 11.

COEFFICIENTS	SPECIMEN NUMBER	L4	L3	L2	L1
A ($ms^{-1}N^{-1}Hz$)	9	1.89	0.98	0.67	0.63
	10	1.56	0.71	0.64	0.42
	11	1.27	0.80	0.45	0.47
	MEAN	1.57	0.83	0.59	0.51
b (Hz^{-1})	9	0.0019	0.0025	0.0043	0.0037
	10	0.0026	0.0042	0.0049	0.0038
	11	0.0026	0.0036	0.0057	0.0038
	MEAN	0.0024	0.0034	0.0050	0.0038

Table 5.8
Total mobility measured at different segments of Specimens No. 9, 10 and 11. Measurements in $ms^{-1}N^{-1}Hz$ and in percentage with respect to L4 (as 100%). Theoretical figures are printed in italics for comparison.

	TOTAL MOBILITY (in $ms^{-1}N^{-1}Hz$) AT DIFFERENT SEGMENTS			
SPECIMEN NUMBER	L4	L3	L2	L1
9	1.93(100%) *1.89*	0.98 (51%) *0.98*	0.68 (35%) *0.67*	0.62 (32%) *0.63*
10	1.56(100%) *1.56*	0.72 (46%) *0.71*	0.64 (41%) *0.64*	0.42 (27%) *0.42*
11	1.28(100%) *1.27*	0.80 (62%) *0.80*	0.45 (35%) *0.45*	0.46 (36%) *0.47*
MEAN	1.59(100%) *1.57*	0.83 (53%) *0.83*	0.59 (37%) *0.59*	0.50 (32%) *0.51*

that the test specimen continues to contribute mobility at high frequency, as illustrated by SM1 in figure 5.37. The upper segments (L1 and L2) were found to have bigger values of b which reflects the fact that mobility was low in the high frequency range at these segments; whilst the values of b were relatively smaller at the lower segment e.g. L4.

The mean total mobility measured at different segments are listed in table 5.8, with the theoretical figures printed in italics (from table 5.7) for comparison. When the total mobility is expressed as percentage with reference to that measured at L4 which is designated as 100%, the total mobility shows a marked reduction to about 50% at L3; 40% at L2 and 30% at L1. Figure 5.38 shows the trend of attenuation when vibratory energy was transmitted from L4 to L1. Assuming an exponential attenuation, a coefficient k can be determined according to the following equation modified from Kolsky (1963):

$$M_1 = M_0 \, e^{-kn} \tag{5.8}$$

where

M_0 is the original mobility at L4 in $ms^{-1}N^{-1}Hz$;

M_1 is the mobility at other segments in $ms^{-1}N^{-1}Hz$;

k is the attenuation coefficient in neper (1 Np = 8.686 dB (Drazil, 1983)); and

n is the "distance" in terms of the number of segments.

Table 5.9 lists the attenuation coefficients determined for all segments of Specimens No. 9, 10 and 11. The attenuation was found to be highest from L4 to L3 at 5.5 dB/segment, and gradually reduced to about 3 dB/segment from L4 to L1. The result also suggests attenuation was highest at locations which was closest to the source of vibration; and gradually decreased when it was farther away. The attenuation coefficient could be a useful parameter to characterize the mechanical properties of the lumbar spine.

Table 5.9
Attenuation coefficient k of total mobility with respect to L4.

	ATTENUATION COEFFICIENT OF TOTAL MOBILITY, (dB/segment)		
SPECIMEN NUMBER	L3	L2	L1
9	5.9	4.5	3.3
10	6.7	3.9	3.8
11	4.1	4.5	3.0
MEAN ± SEM	5.5 ± 0.8	4.3 ± 0.2	3.4 ± 0.3

Remarks: SEM denotes standard error of mean.

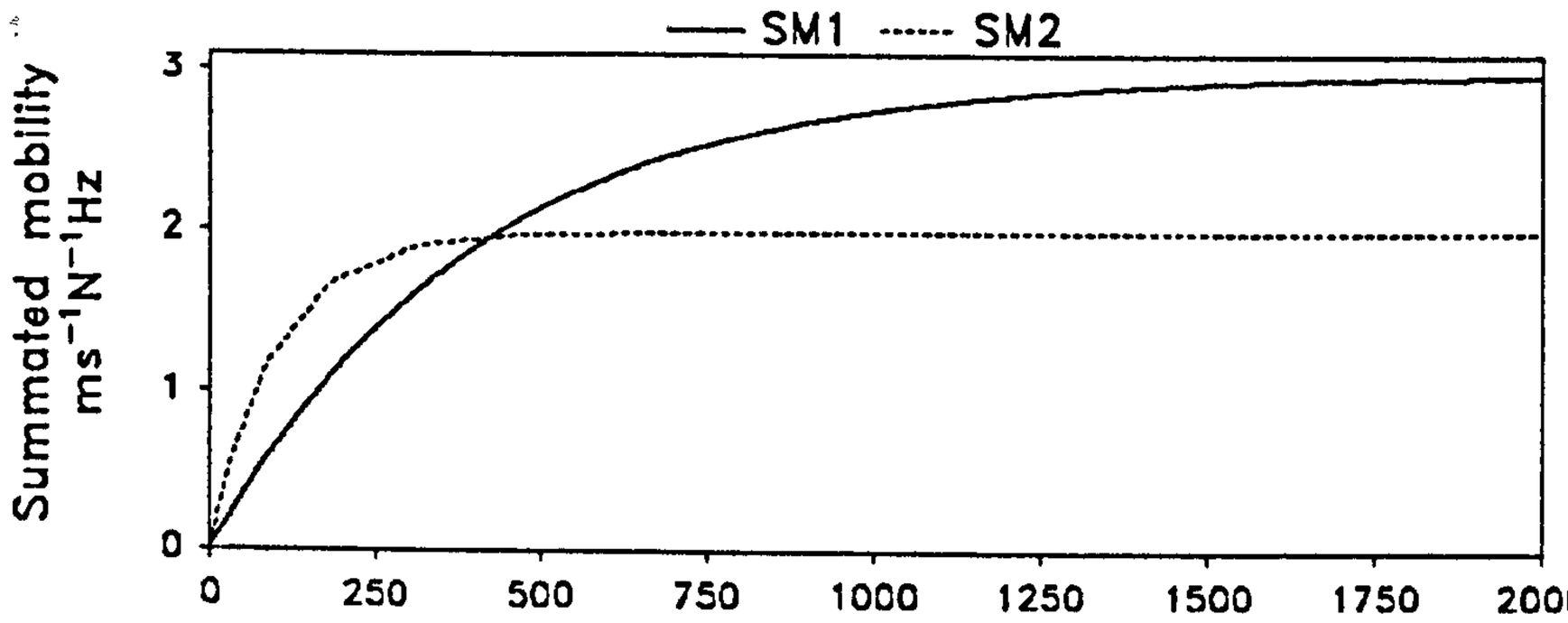

Fig 5.37 Two theoretical patterns of summated mobility curves. For SM1: A = 3, b = 0.0025; For SM2: A= 2, b = 0.01.

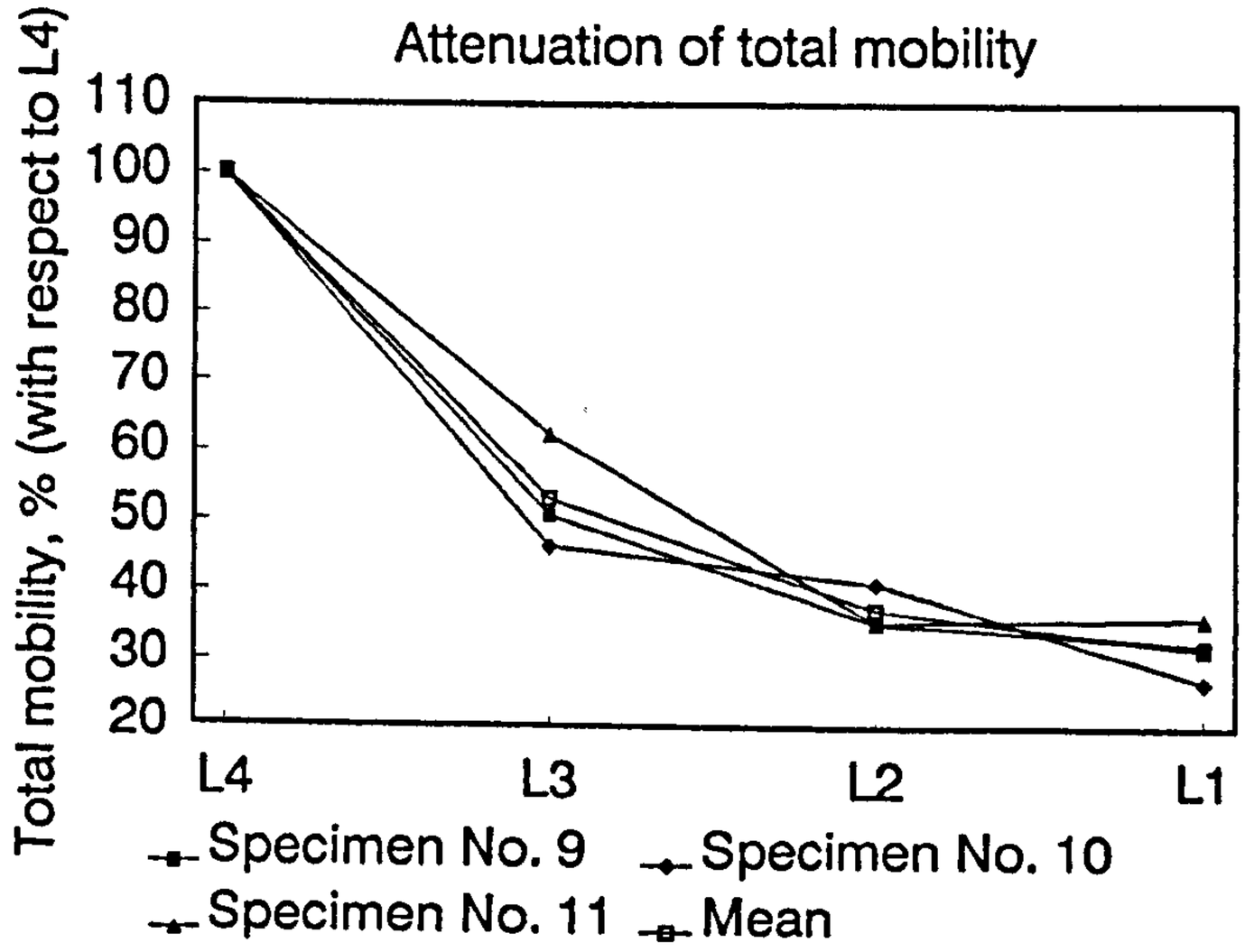

Fig 5.38 Attenuation of total mobility.

5.7.2 Band Mobility

Band mobility has been defined to allow specific measurements of the transfer mobility within different frequency bands. They are:

$$Low\ Band\ Mobility,\ LBM = \int_{0}^{500} \left|\frac{V(f)}{F(f)}\right| df \qquad (5.9)$$

$$Medium\ Band\ Mobility,\ MBM = \int_{500}^{1k} \left|\frac{V(f)}{F(f)}\right| df \qquad (5.10)$$

$$High\ Band\ Mobility,\ HBM = \int_{1k}^{2k} \left|\frac{V(f)}{F(f)}\right| df \qquad (5.11)$$

Fig 5.36 also explains the definition of these parameters on a summated mobility curve. The cut-off frequencies at 500 and 1000 Hz are arbitrarily defined, based on previous empirical findings on the characteristics of the transfer mobility curves. The low band mobility defines the dynamic response of the lumbar spine in low frequency band up to 500 Hz. Medium band mobility assesses the mobility in the transition frequency zone from 500 to 1000 Hz, within which the lumbar spine changes from a more dynamic system to a highly damped one. High band mobility defines the summated mobility in the frequency range between 1 and 2 kHz.

Figure 5.39 shows the distribution of mobility in different frequency bands for a specimen, and a similar distribution pattern was seen in other specimens. It was found that the majority of mobility took place in the low frequency band, at all segments. Mobility in the high frequency was just minimal. When the absolute measurements are tabulated and expressed as percentage with respect to L4 (as 100%), the trend of attenuation for different

Table 5.10a
Low band mobility measured at different segments for Specimens No. 9, 10 & 11. Measurements in $ms^{-1}N^{-1}Hz$ and in percentage with respect to L4 (as 100%).

	LOW BAND MOBILITY (in $ms^{-1}N^{-1}Hz$) AT DIFFERENT SEGMENTS			
SPECIMEN NUMBER	L4	L3	L2	L1
9	1.19(100%)	0.71 (60%)	0.60 (51%)	0.56 (47%)
10	1.13(100%)	0.60 (53%)	0.59 (52%)	0.38 (34%)
11	0.93(100%)	0.69 (75)	0.43 (46%)	0.42 (45%)
MEAN	1.08(100%)	0.67 (62%)	0.54 (50%)	0.45 (42%)

Table 5.10b
Medium band mobility measured at different segments for Specimens No. 9, 10 & 11. Measurements in $ms^{-1}N^{-1}Hz$ and in percentage with respect to L4 (as 100%).

	MEDIUM BAND MOBILITY (in $ms^{-1}N^{-1}Hz$) AT DIFFERENT SEGMENTS			
SPECIMEN NUMBER	L4	L3	L2	L1
9	0.36(100%)	0.19 (53%)	0.048(13%)	0.053(15%)
10	0.34(100%)	0.093(28%)	0.038(11%)	0.029(9%)
11	0.25(100%)	0.081(32%)	0.014(6%)	0.042(17%)
MEAN	0.32(100%)	0.12 (37%)	0.03 (10%)	0.041(13%)

Table 5.10c
High band mobility measured at different segments for Specimens No. 9, 10 & 11. Measurements in $ms^{-1}N^{-1}Hz$ and in percentage with respect to L4 (as 100%).

	HIGH BAND MOBILITY (in $ms^{-1}N^{-1}Hz$) AT DIFFERENT SEGMENTS			
SPECIMEN NUMBER	L4	L3	L2	L1
9	0.38(100%)	0.086(23%)	0.027(7%)	0.01 (3%)
10	0.09(100%)	0.028(32%)	0.009(11%)	0.004(5%)
11	0.10(100%)	0.027(27%)	0.011(11%)	0.004(4%)
MEAN	0.19(100%)	0.047(27%)	0.016(9%)	0.006(4%)

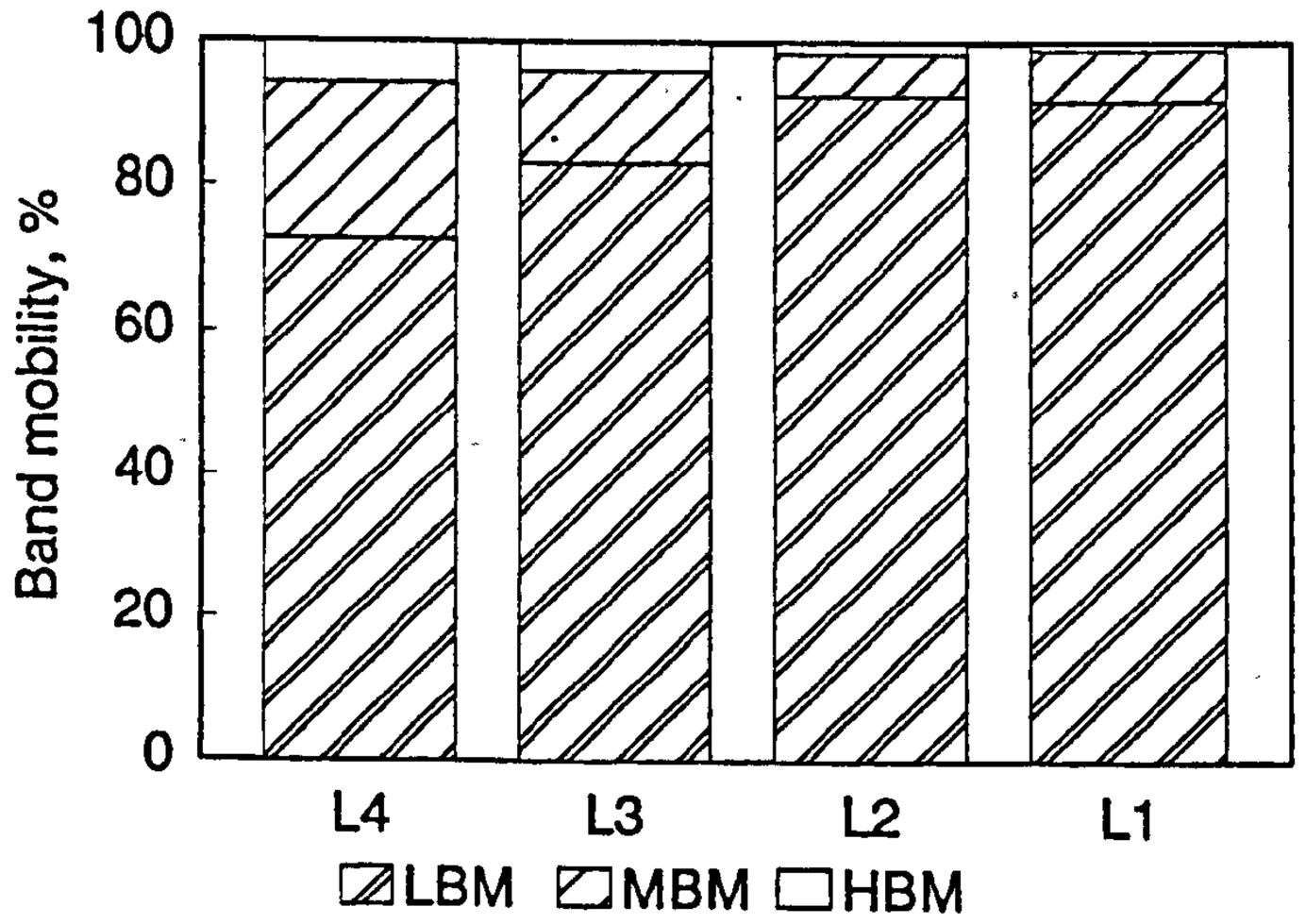

LBM = low band mobility
MBM = medium band mobility
HBM = high band mobility

Fig 5.39 Band mobility at different segments.

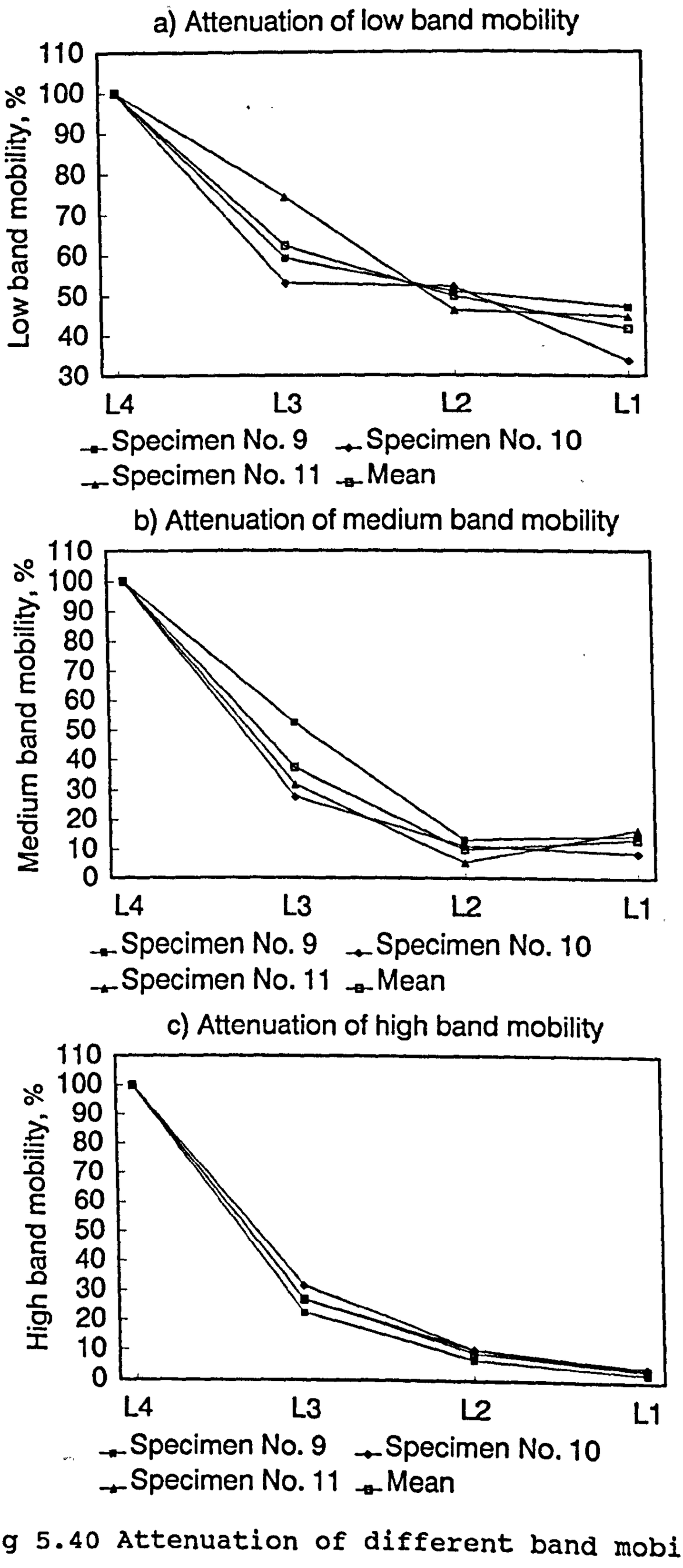

Fig 5.40 Attenuation of different band mobility.

Table 5.11a
Attenuation coefficient k of low band mobility with respect to L4.

	ATTENUATION COEFFICIENT OF LOW BAND MOBILITY, (dB/segment)		
SPECIMEN NUMBER	L3	L2	L1
9	4.5	2.9	2.2
10	5.5	2.8	3.1
11	2.6	3.4	2.3
MEAN ± SEM	4.2 ± 0.9	3.0 ± 0.2	2.6 ± 0.3

Remarks: SEM denotes standard error of mean.

Table 5.11b
Attenuation coefficient k of medium band mobility with respect to L4.

	ATTENUATION COEFFICIENT OF MEDIUM BAND MOBILITY, (dB/segment)		
SPECIMEN NUMBER	L3	L2	L1
9	5.6	8.8	5.6
10	11.1	9.5	7.1
11	9.9	12.7	5.2
MEAN ± SEM	8.9 ± 1.7	10.3 ± 1.2	5.9 ± 0.6

Remarks: SEM denotes standard error of mean.

Table 5.11c
Attenuation coefficient k of high band mobility with respect to L4.

	ATTENUATION COEFFICIENT OF HIGH BAND MOBILITY, (dB/segment)		
SPECIMEN NUMBER	L3	L2	L1
9	12.9	11.5	10.5
10	10.0	9.8	8.8
11	11.4	9.8	9.4
MEAN ± SEM	11.4 ± 0.9	10.4 ± 0.6	9.6 ± 0.5

Remarks: SEM denotes standard error of mean.

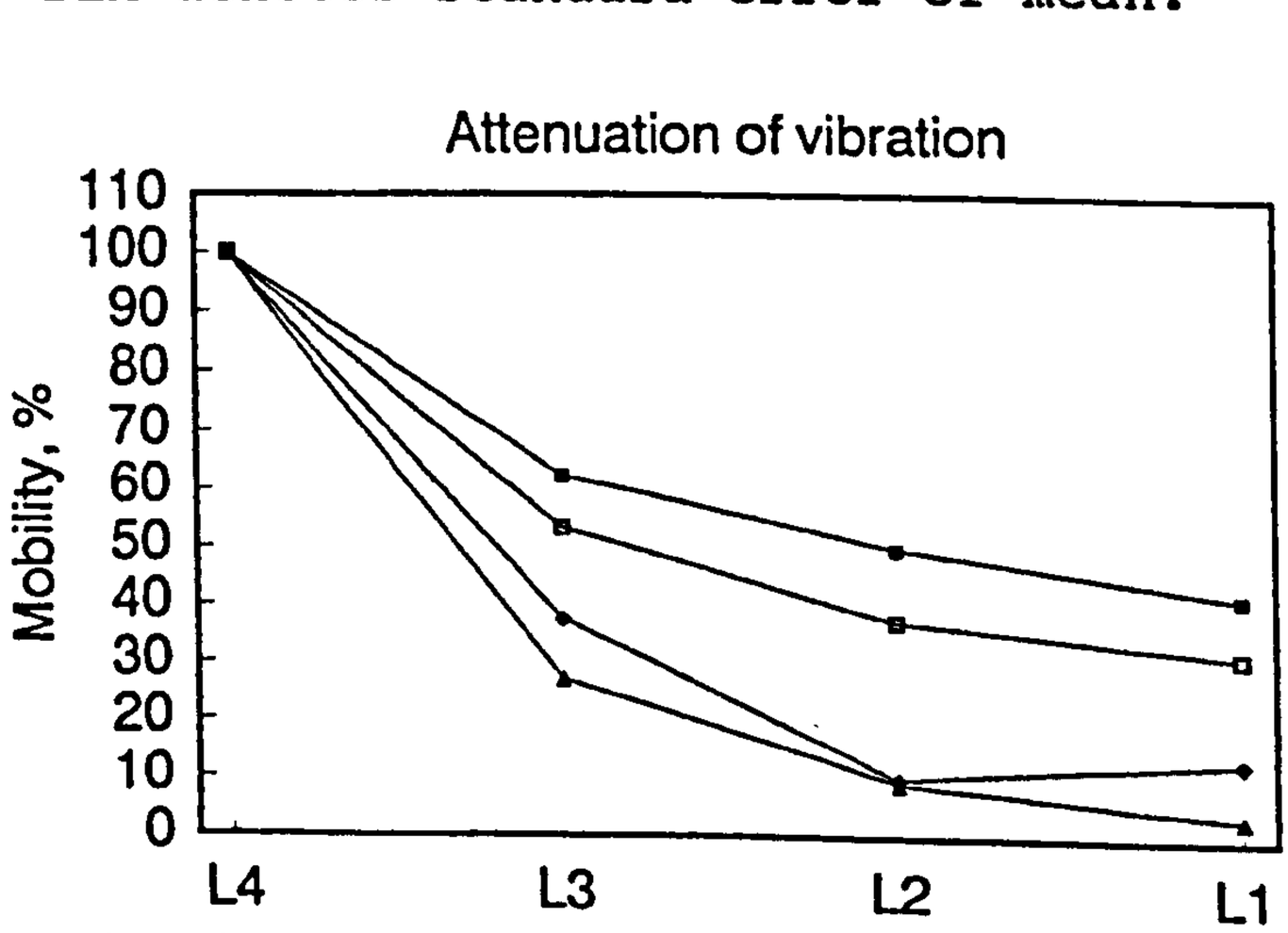

Fig 5.41 Attenuation of total mobility and band mobility.

frequency bands could be revealed (table 5.10). The mobility does not show a consistent rate of attenuation for different frequency bands, though the overall trend shows further attenuation when measurement was made at a location farther away from the excitation source. It was found that the attenuation for low frequency band was more gradual while that for medium and high frequency bands were more significant especially between L4 and L3 where a drop of mobility to about 30% was noted. Figure 5.40 shows the trend of attenuation in each frequency bands. The attenuation trend is consistent among the specimens, especially in the high frequency band. Figure 5.41 records the mean values taken for the total mobility and each band mobility. It is clearly shown that the rate of attenuation followed the order: HBM > MBM > LBM, with the total mobility positioned between LBM and MBM. Table 5.11 also shows that the high band mobility demonstrated the highest attenuation with coefficient k > 10 dB/segment; while that for low frequency band was smallest - between 2.5 and 4 dB/segment. The attenuation coefficient for medium frequency band ranged between 6 and 10 dB/segment. The findings also show that the lumbar spine exhibited various attenuation effect to different frequency bands, and the greatest attenuation was to high frequency. These results are objective measures to support findings previous interpreted from the transfer mobility curves. It is envisaged that these attenuation coefficients could be used to characterize the mechanical behaviour of the lumbar spine in different physical states.

5.8 DISCRETE FREQUENCY VIBRATION TESTING

The application of tone bursts of discrete frequency was controlled manually by a push-button (section 3.8.1), and the effective duty cycle was 1:1. Thus the lumbar spine was found to have ample time to settle before the next train of excitatory force came. The amplitude of vibratory force was controlled to avoid non-linear response, and this

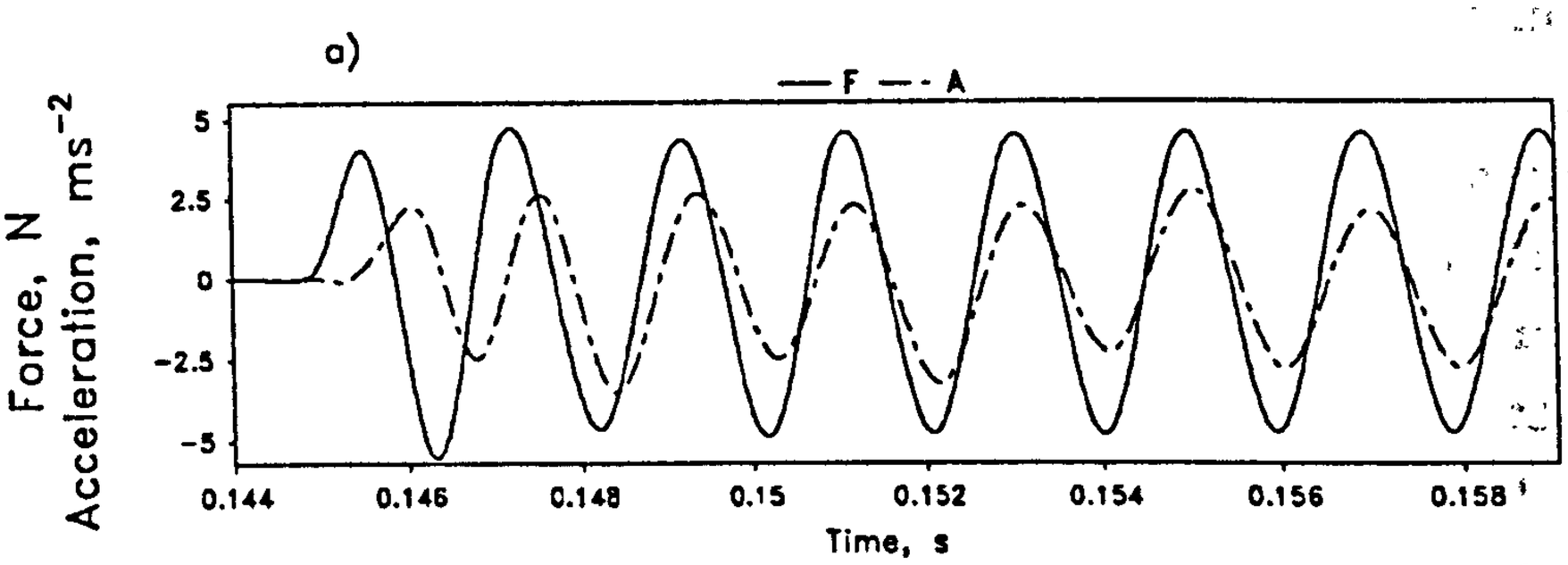

Fig 5.42 a) Sinusoidal response of the lumbar spine under discrete frequency vibration testing. a) Clear start of the response signal; and b) Phase-shift after a few cycles.

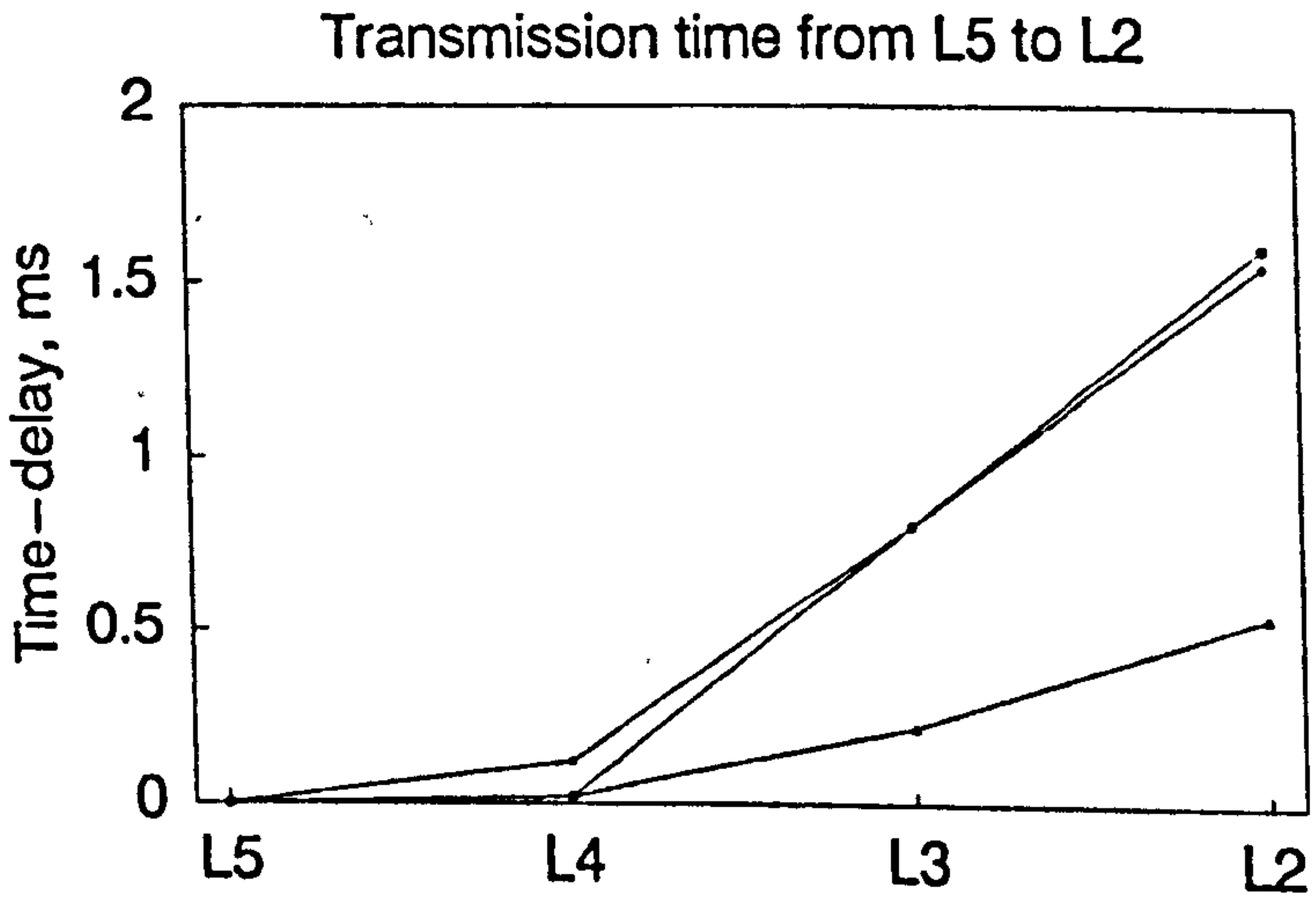

Fig 5.43 Time-delay measured at different segments of the lumbar spine specimen.

varied within the range of 5 N (peak), depending on the response of the lumbar spine under different situations. The following sections summarize and discuss the major findings in this part of the study.

5.8.1 Temporal Parameters

Short trains of sinusoidal response were obtained at the L1 to L4 spinous processes of the lumbar spine when tone bursts of sinusoidal excitation was applied at the L5 spinous process (fig 5.13). The input force magnitude was controlled to ensure sinusoidal response of the specimen. The excitation and response signals were displayed on the same time-scale for the determination of the time-delay which indicates the transmission time of the vibration from the driving point to the measuring point. In some cases, there was a sharply defined start of the signals (fig 5.42a). This allowed direct determination of the time-delay. In other cases, the start was not sharply defined, and there was a phase-shift after the first few cycles (fig 5.42b). The phase-shift posed some difficulty in direct measurement of the time-delay on the time-scale. Furthermore, this will also impose error in the determination of time-delay by cross-correlation which could only determine the overall time-delay of one signal with respect to the other (section 2.3.3). However the cross-correlation function does not manage to establish the cause i.e. whether it was due to the actual time-delay or to the phase-shift. The measurement of transmission time will be subject to uncertainty. Subsequent determination of transmission velocity based on this time-delay would be unreliable. For successful cases, the transmission time from L4 to L2 was 0.3 ms/segment for 500 Hz; 0.6 ms/segment for 1 kHz; and 0.7 ms/segment for 2 kHz. These results compare well to the transmission velocity of 100 ms^{-1} determined by impact testing (section 5.5.1). These results also suggest that the transmission velocity is also frequency dependent. Figure 5.43 shows the time-delay

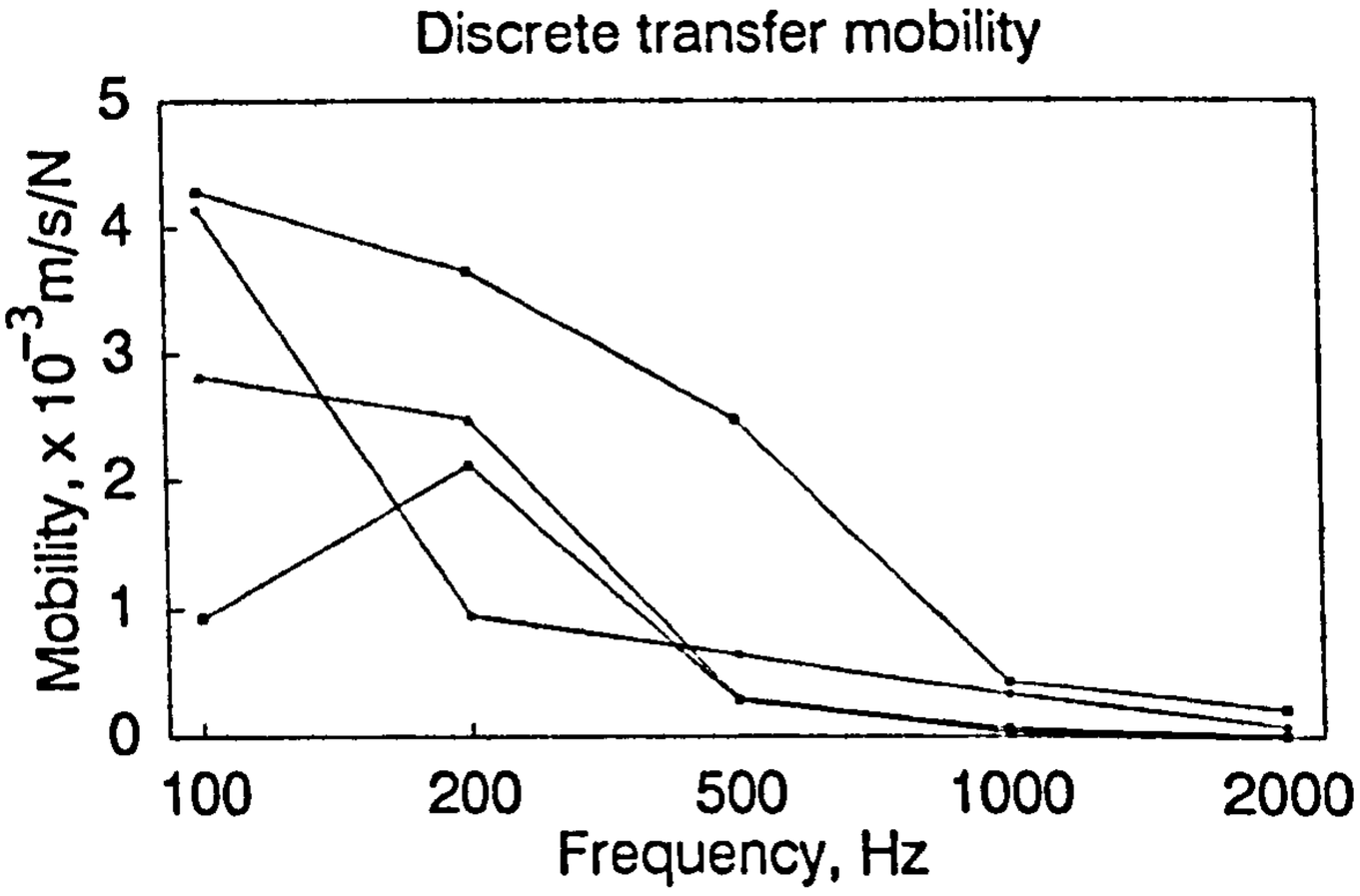

Fig 5.44 Discrete transfer mobility measured at different segments of a lumbar spine specimen.

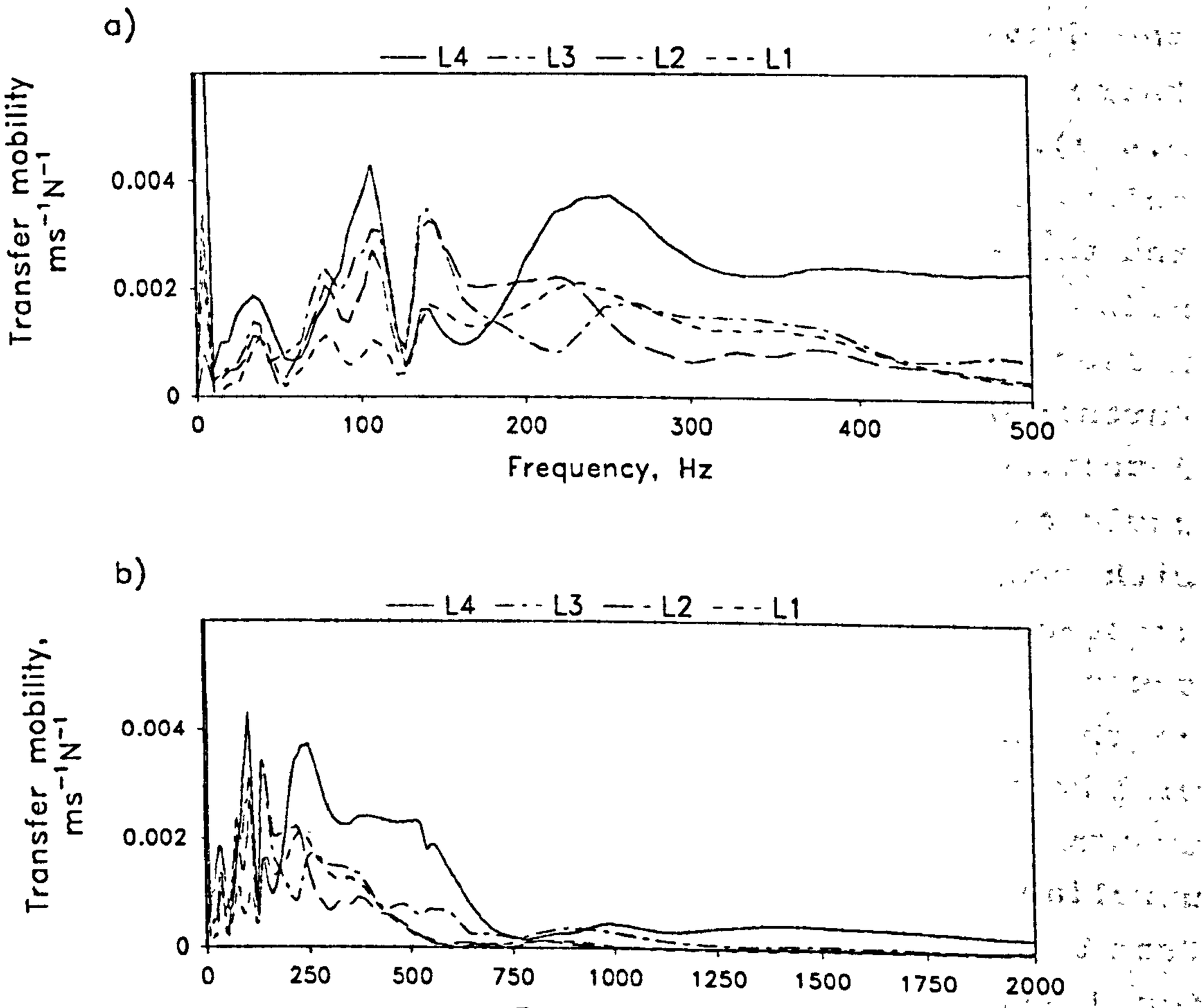

Fig 5.45 Transfer mobility measured by random vibration testing at different segments of the same lumbar spine specimen as figure 5.44.

detected at different segments when vibration travelled from L5 to L2 of a lumbar spine specimen. It was also noted that there was a "local effect" which means that the source of excitation was not confined to a single point, nor to a single vertebra. It practically extended to a bigger lumbar region including the L4 which was right next to the source of vibration. This explains why there was only a relatively short time-delay detected at the L4 segment.

5.8.2 Discrete Transfer Mobility

For each discrete frequency, the excitatory force and response signals were measured. The root-mean-square values of both signals were obtained. Discrete transfer mobility was computed for each frequency according to the following equation:

$$\textit{Discrete Transfer Mobility} = \frac{|V(f)|}{|F(f)|} = \frac{|A(f)|}{|F(f)| * 2\pi f} \qquad (5.12)$$

The pattern of discrete transfer mobility determined at different segments was found to be consistent with that obtained by random vibration testing (fig 5.44 & 5.45). The figures obtained for the same specimen by these two vibration techniques are found to be in close agreement. This can be confirmed by cross-checking the two groups of figures in table 5.12. Statistics by paired t-test did not indicate any significant difference between these two groups of figures. Linear regression procedure shows that these two sets of figures are highly correlated with correlation coefficient $R = 0.98$ and $p < 0.0001$.

Discrete frequency vibration testing was found to be technically feasible. However, the measurement of discrete transfer mobility suffers limitations in that it only allows measurement at designated frequencies while the measurement by random vibration testing covers the whole range of test frequencies. Tests by discrete vibration frequencies may be considered incomplete in this regard.

Table 5.12
Discrete transfer mobility at different segments of a lumbar spine specimen. Transfer mobility determined by random vibration testing in bracket for comparison.

Mobility in 10^{-3} $ms^{-1}N^{-1}$

LUMBAR SEGMENTS	100 Hz	200 Hz	500 Hz	1000 Hz	2000 Hz
L4	4.27 (3.44)	3.65 (2.51)	2.48 (2.33)	0.43 (0.45)	0.22 (0.25)
L3	4.13 (2.61)	0.94 (1.09)	0.64 (0.73)	0.33 (0.30)	0.083 (0.049)
L2	2.82 (1.73)	2.48 (2.15)	0.30 (0.35)	0.037 (0.033)	0.021 (0.021)
L1	0.93 (0.66)	2.12 (1.69)	0.28 (0.30)	0.067 (0.047)	0.0073 (0.0064)

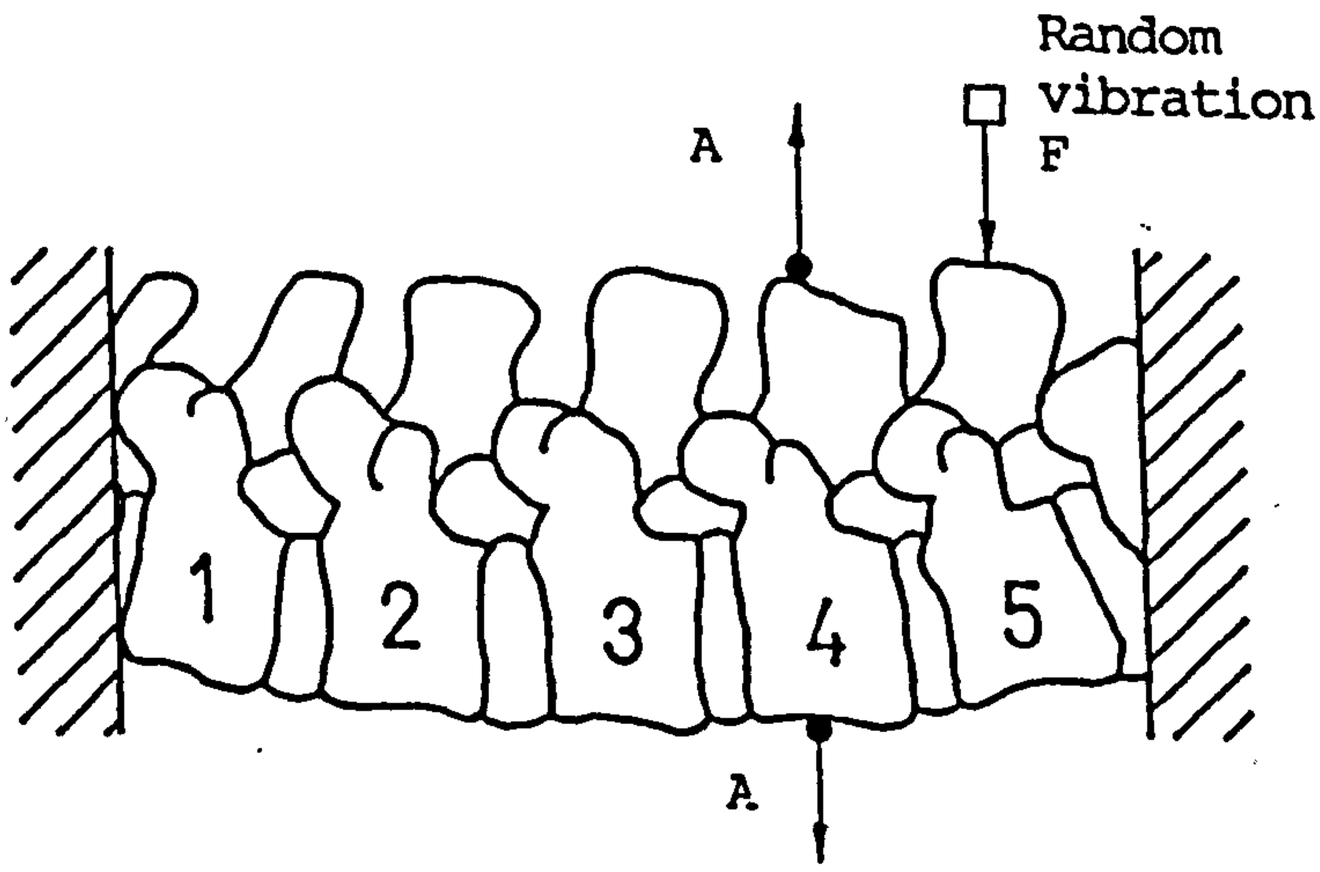

Fig 5.46 Testing protocol to compare the vibration responses at the spinous process and at the vertebral body. F and A are respectively the force and acceleration signals.

Nevertheless, this offers an opportunity to ascertain the validity and reliability of the random vibration testing by cross-referencing with the corresponding measurements by discrete frequency vibration technique.

5.9 LOCAL VIBRATION RESPONSE OF A SINGLE LUMBAR VERTEBRA

In the previous sections, the discussion was based on the assumption that the lumbar vertebra vibrated as a rigid entity such that the vibratory force measured at the spinous process effectively revealed the excitatory force applied to the whole segment. It also assumed that vibration signal measured at the spinous process was a true measure of the vibration response of the whole lumbar vertebra i.e. the transverse movement of the spinous process was the same as that of the segment. If the segment is close to a "simple" support it will show angular movements and hence the tangential displacement of the spinous process will not be the same as that of the vertebral body. However, in "small" displacements this will be a negligible effect. From the reported measurement (section 5.6.2) of the apparent mass and the subsequent comparison with the transmissibility measured directly on the vertebral body, the results suggest that this assumption is valid. However, it was deemed necessary to verify this assumption by direct comparison of the measurements of vibration at the spinous process and at the vertebral body. The local vibration response of a single vertebra in-situ (non-isolated) was examined to confirm that the vibration response measured at the spinous process was the same as that measured at the vertebral body. At the termination of the vibration tests on the whole lumbar spine, the vertebrae were isolated. The integrity of the pin-bone interfaces at the driving point, and that at the measuring point over the spinous process and on the ventral surface of the vertebral body were examined.

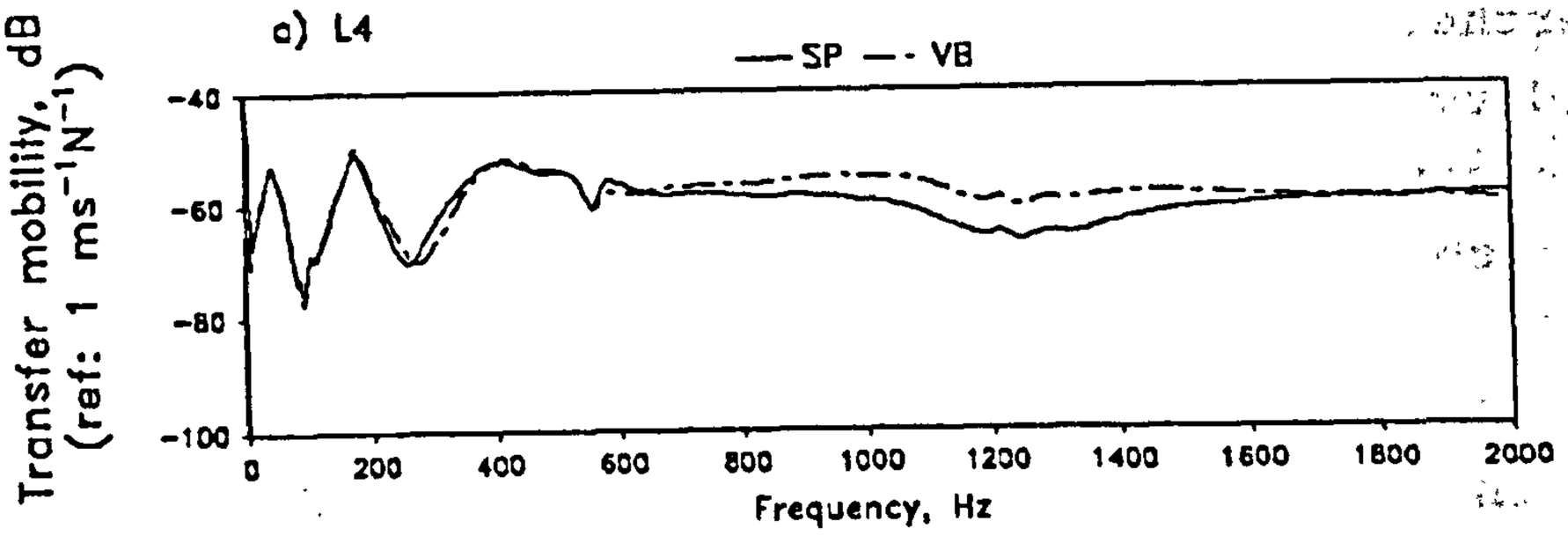

Fig 5.47 Coherent and almost identical vibration responses at the spinous process (SP) and at the vertebral body (VB).

5.9.1 Local Response of a Single Vertebra In-Situ

Figure 5.46 depicts an experimental set-up in which the vibration response of a single lumbar vertebra was measured at the spinous process and vertebral body while being excited by a random vibratory force at the L5 spinous process. The vibration response was measured as the transfer mobility at the L1 to L4 spinous processes and vertebral bodies. Figure 5.47 shows typical results of a test specimen. These curves show that both the spinous process and the vertebral body were vibrating with the same amplitude and phase across the frequency of interest. This finding further confirms that a single vertebra could be considered as a rigid entity, with the spinous process vibrating in the same manner as the vertebral body. It could also be confirmed that the signal taken at the spinous process was a genuine measure of the vibration of the whole vertebra. This is an important finding with technical implication to subsequent in-vivo study where there will be no access to the vertebral body for non-invasive measurement of vibration.

5.9.2 Integrity of the Driving Point

The integrity and hence the transmissibility of the interface at the driving point was tested in an experimental set-up shown in figure 5.48a. A spinous process was cut from the lumbar vertebra and was then fixed in a 30 mm section of steel tube by the use of epoxy filler, forming a cubic block for test. Random vibration was then applied, while the force (F) was measured at the spinous process, and the acceleration (A) at the lower surface of the cube. The same test was repeated on a dummy block which was made of a similar section of the tube, filled by epoxy filler (fig 5.48b). The transfer accelerance, defined by:

$$Transfer\ Accelerance = \frac{A(f)}{F(f)} \qquad (5.13)$$

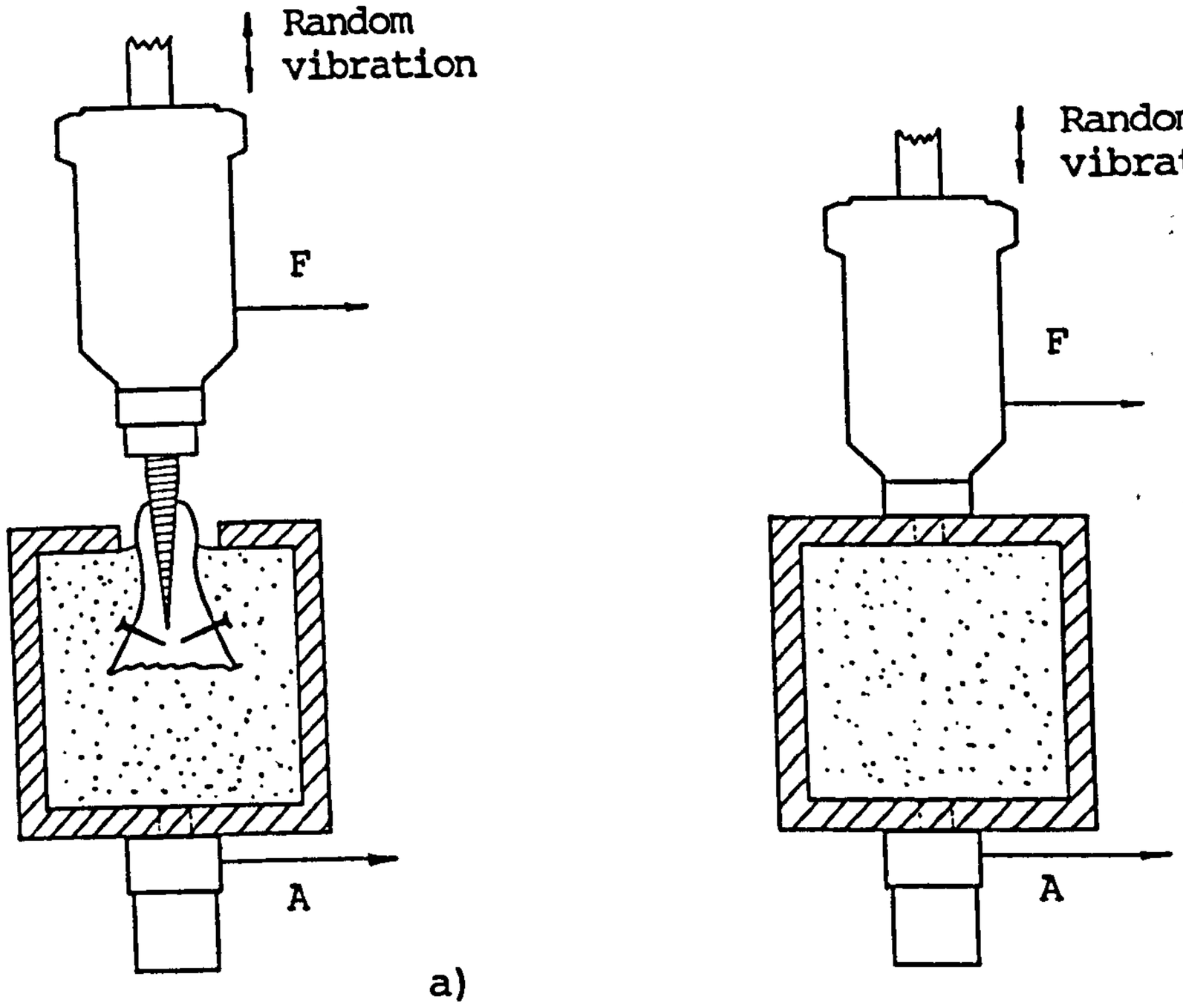

Fig 5.48 Experimental set-up to test the integrity of the spinous process as a driving point. a) A spinous process embedded in a cube of epoxy-based filler. b) A dummy cube of similar physical dimensions. F and A are respectively the force and acceleration signals.

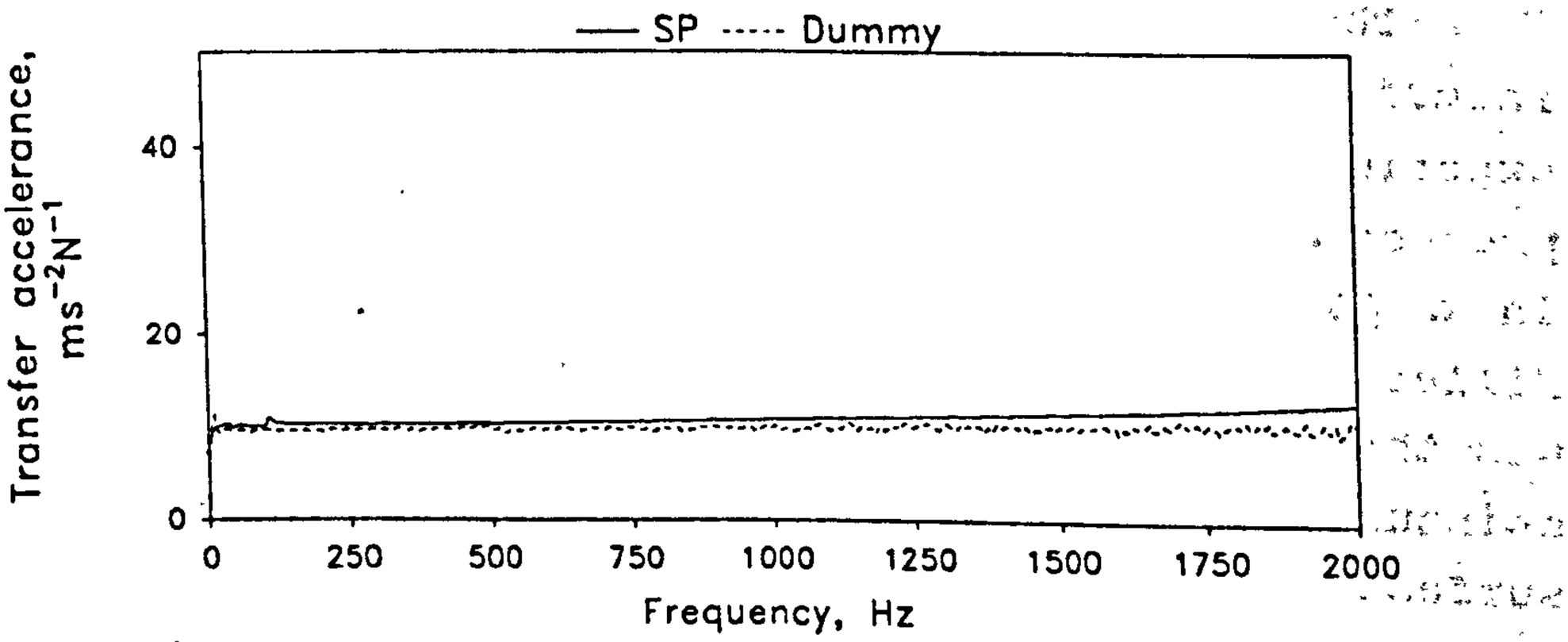

Fig 5.49 A flat spectrum of transfer accelerance measured for the cube driven at the spinous process showing the integrity of the spinous process (SP) as a driving point.

gave a flat spectrum in both cases (fig 5.49). The two spectra revealed the same mechanical response of the blocks to random vibration. The results indicate that vibratory excitation was effectively transmitted across the interface at the driving point over the spinous process, and the result was comparable to the mechanical contact by a screw for attachment. More importantly, the results also indicate that the excitatory force measured at the driving point was a genuine measurement of that applied to the lumbar vertebra. This finding also gained support from the transmissibility measurement as reported in section 5.6.2.

5.9.3 Integrity of the Measuring Point

A similar test was performed on the same cubic block with the set-up illustrated by figure 5.50a. In this vibration test, the integrity of the spinous process as a measuring point was tested. A flat spectrum was obtained for the transfer accelerance (fig 5.51), similar to that obtained for the dummy block depicted in figure 5.50b. Once again, this confirms that the acceleration measured at the spinous process was a reliable measurement of the vibration picked up from the specimen. This also confirms that the design of the measure-pin was satisfactory, and it provided a firm interface between the bone substance and the accelerometer.

A single vertebral body was isolated from the lumbar spine. Random vibratory force was applied at the dorsal surface of the vertebral body through the use of a 6.5 mm diameter screw, tapped M3 for the attachment of the impedance head. Acceleration was measured on the ventral surface (fig 5.52). A fairly flat spectrum of the transfer accelerance (A(f)/F(f)) was obtained (fig 5.53). This result indicates that the measuring point at the vertebral body was intact, and that the vibration measured on the ventral surface of the vertebral body was a reliable measurement of the vibration in the lumbar spine.

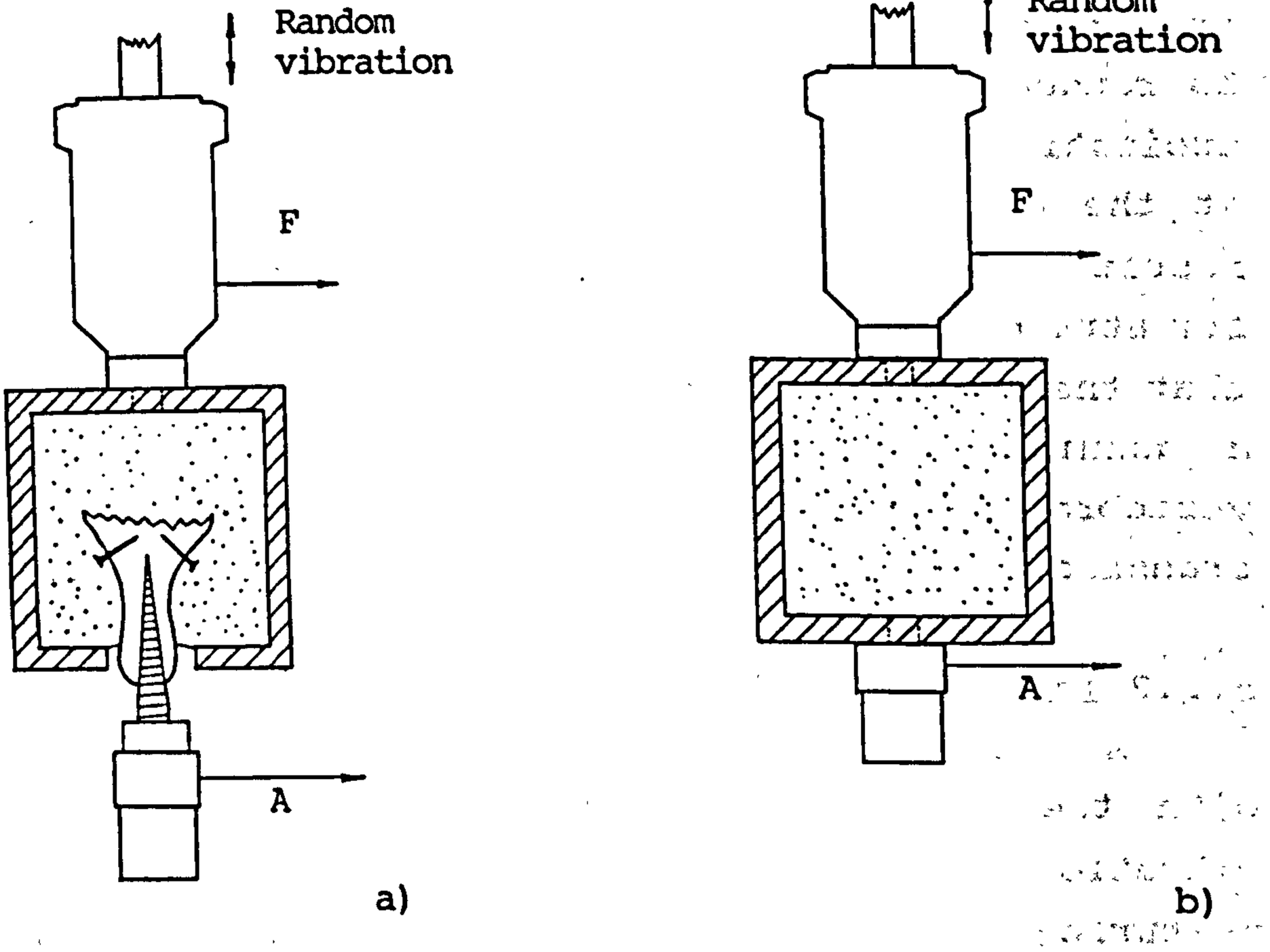

Fig 5.50 Experimental set-up to test the integrity of the spinous process as a measuring point. a) A spinous process embedded in a cube of epoxy-based filler; b) A dummy cube of similar physical dimensions. F and A are respectively the force and acceleration signals.

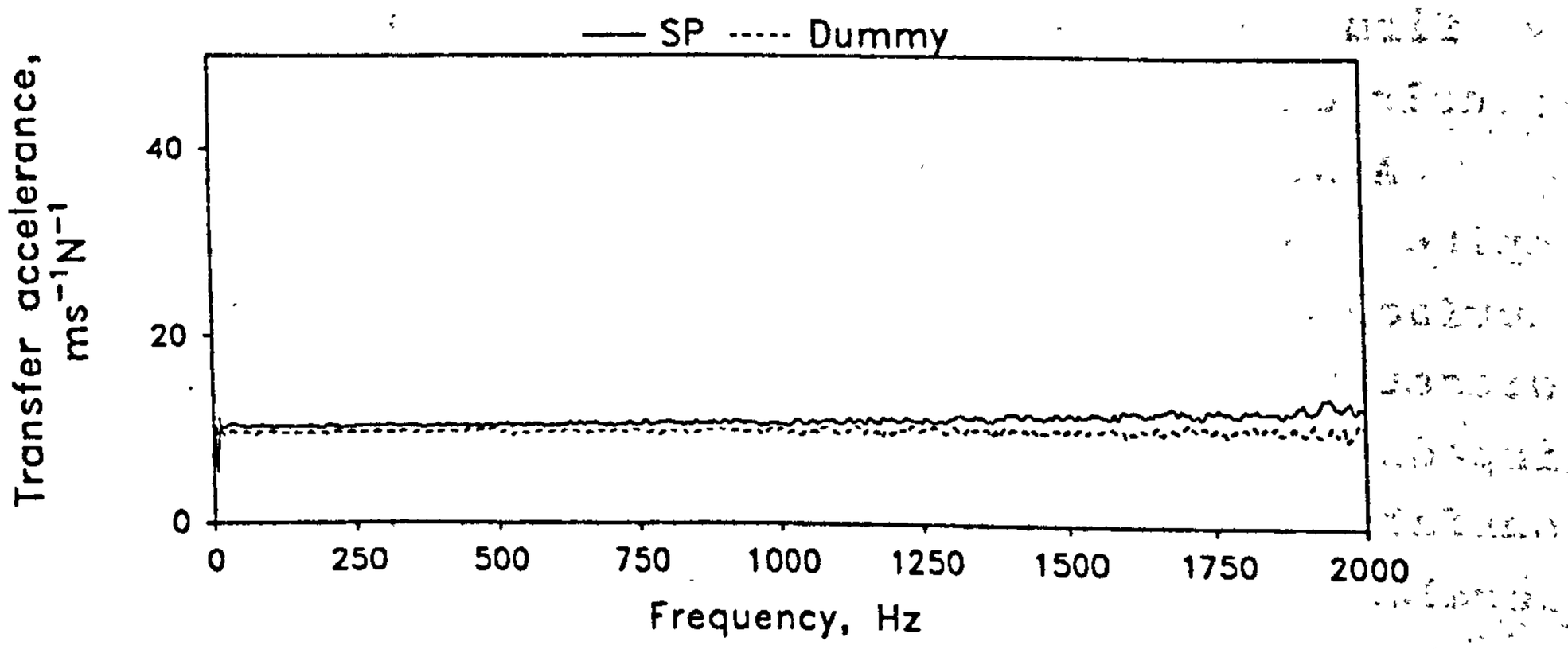

Fig 5.51 A flat spectrum of transfer accelerance measured at the spinous process (SP) showing its integrity as a measuring point.

5.10 SUMMARY

Vibration techniques have been applied to test the motion response in the antero-posterior direction of the lumbar spine specimens in both free and fixed support conditions. Random vibration testing has been found the most appropriate and complete for the examination of the lumbar spine's dynamic characteristics. Impact testing suffered from difficulty and hence inconsistency in its application of impact force whilst discrete frequency vibration testing, as anticipated, failed to reveal the mechanical behaviour of the specimens except at the designated frequencies. Swept sine testing is known to be time consuming and was not used extensively in this study. The equipment was found to be up to the requirements and the test environment was found to be suitable for testing of this nature.

The lumbar spines in a simulated anatomical condition behaved as a highly damped passive linear mechanical system, with a dynamic range greater than 30 dB. However, the results did not indicate any association between the vibration response of the specimens with their physical factors such as weight (body build), sex, age, and the grading of degeneration of the intervertebral discs. Vibration measurements were consistent, repeatable and noise-free provided the excitatory force was less than 3.5 N (RMS). The input and output signals were found to be highly coherent, and hence indicating high causality.

The test protocols were suitably designed. A free end support was found unsuitable as the test specimen exhibited only a rigid-body vibration mode. Hence the structural characteristics of the specimen would not be revealed. The measurement of excitatory force at the driving point was found adequate in the indication of vibration induced in the specimen. The measurement of transfer mobility was a useful parameter which reveals the vibration response to unit excitatory force of the lumbar spine up to 2 kHz. A fundamental mode of flexural vibration in the sagittal

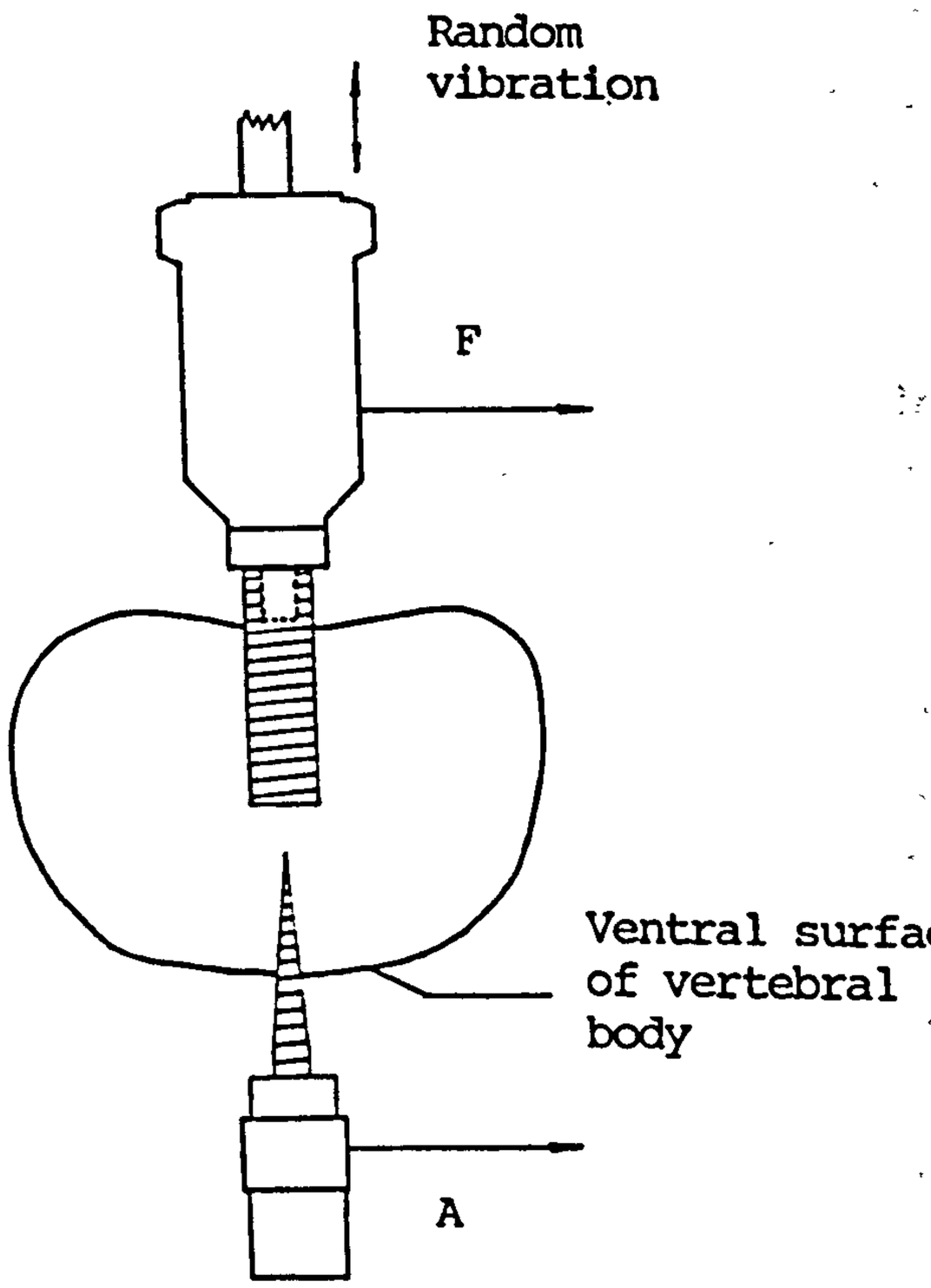

Fig 5.52 Experimental set-up to test the integrity of the measuring point on the ventral surface of a vertebral body. F and A are respectively the force and acceleration signals.

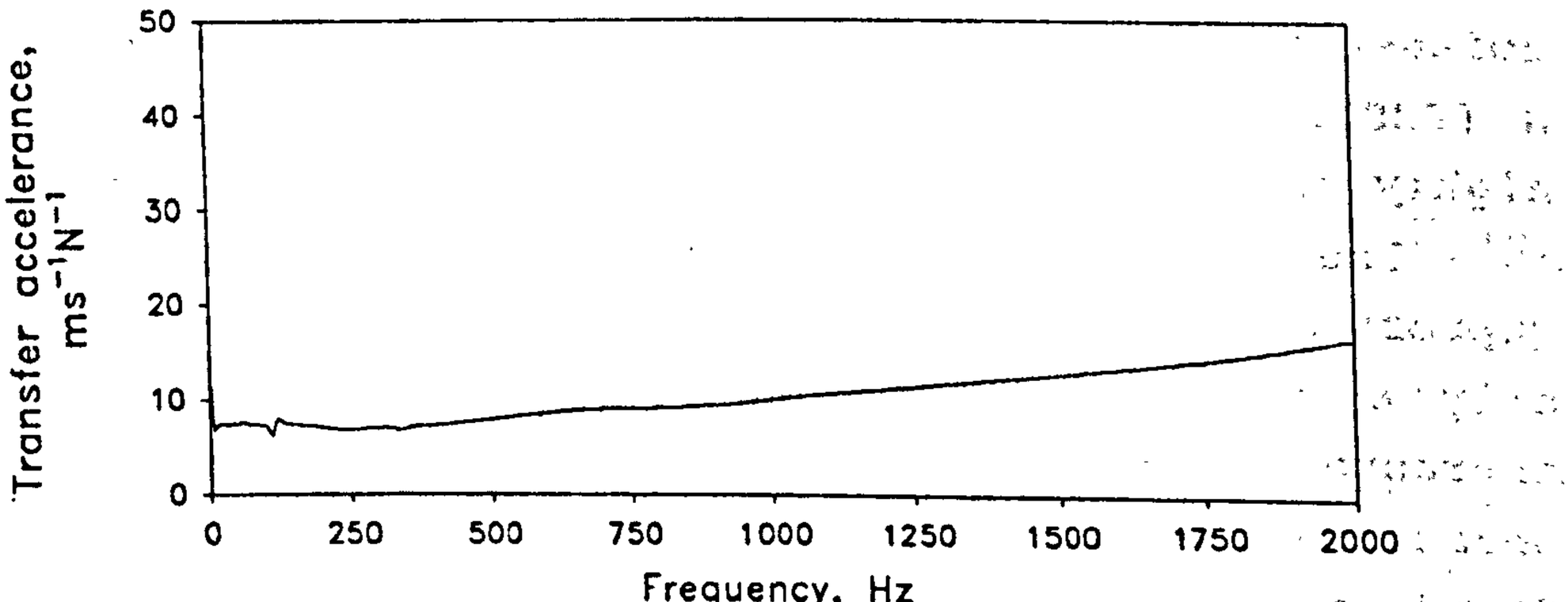

Fig 5.53 A flat spectrum of transfer accelerance measured on the vertebral body showing the integrity of the measuring point.

plane was demonstrated on the fixed lumbar spine, while the higher modes of flexural vibration were effectively damped. A fixed lumbar spine could be modelled as segmented beam hinged at both ends. Total mobility was a useful parameter to summarize the overall mobility within the same frequency range. Band mobility defines the vibration response of the lumbar spine at different frequency bands. Attenuation of vibration was observed when it was transmitted from L5 to L1. The total mobility and all band mobility demonstrated consistent trend of attenuation for all test specimens. The attenuation coefficients were greater than 10 dB/segment for high frequency band; 5 to 10 dB/segment for medium frequency band; and that for low frequency band was below 4 dB/segment. Attenuation of vibration was found to be higher in segments close to the excitation source. These are useful parameters to help understand the structural characteristics of the lumbar spine, and could be used as the basis for comparison.

Each lumbar vertebra was observed to vibrate as a single entity and there was no differential vibration detected between the vertebral body and the spinous process. The vibration testing and subsequent analysis failed to identify any differential transmission paths along the lumbar spine. This finding suggests that the lumbar spine responded to external vibration as a mechanical structure, and that the vibration was not transmitted as waves by taking any possible path through the bone substance as a transmission medium.

Discrete frequency vibration testing was found to have limited use in its time domain analysis for the determination of temporal parameters, except that a range of figures between 0.3 to 0.7 ms/segment has been determined for the transmission time. This corresponds to about 50 to 100 ms^{-1} in transmission velocity along the lumbar spine. The discrete frequency vibration testing also provided a cross-reference to the random vibration testing.

CHAPTER 6

VIBRATION RESPONSE OF SIMULATED FUSIONS OF THE LUMBAR SPINE

6.1 INTRODUCTION

This chapter reports a series of tests which were designed to investigate the changes in the vibration response of the lumbar spine with modifications of its structure. The investigation also helped to study the potential application of vibration response analysis in the detection of changes in local dynamic characteristics of the lumbar spine as a result of its structural changes. The in-vitro motion response of the lumbar spine to random vibratory force induced by simulated fusions of the zygapophyseal joints and of the vertebral bodies was studied in terms of its modal behaviour and transfer mobility. The vibration tests were carried out in the same environment as reported in chapter 5 for previous tests on unfused lumbar spines.

6.2 EXPERIMENTAL DESIGN

The same set of equipment (section 3.8) was used and the same preparation and testing procedures as described in section 5.2 were adopted. This series of vibration tests was an extension of those carried out on three lumbar spines (Specimens No. 9, 10 and 11) in their unfused form. The specimen was fixed on the angle-plates at both ends. Vibration response was measured at the L1 to L4 spinous processes while a random vibratory force was applied at L5 in the antero-posterior direction. Some simple methods were designed to create interlocking of the segments to simulate fusions of the anterior and posterior elements. A simple procedure which would not cause too much disturbance to the alignment of the lumbar spine, or any unnecessary destruction to the associated soft tissue was most preferred. Furthermore, the time constraint was a limiting factor because the specimens had already undergone an

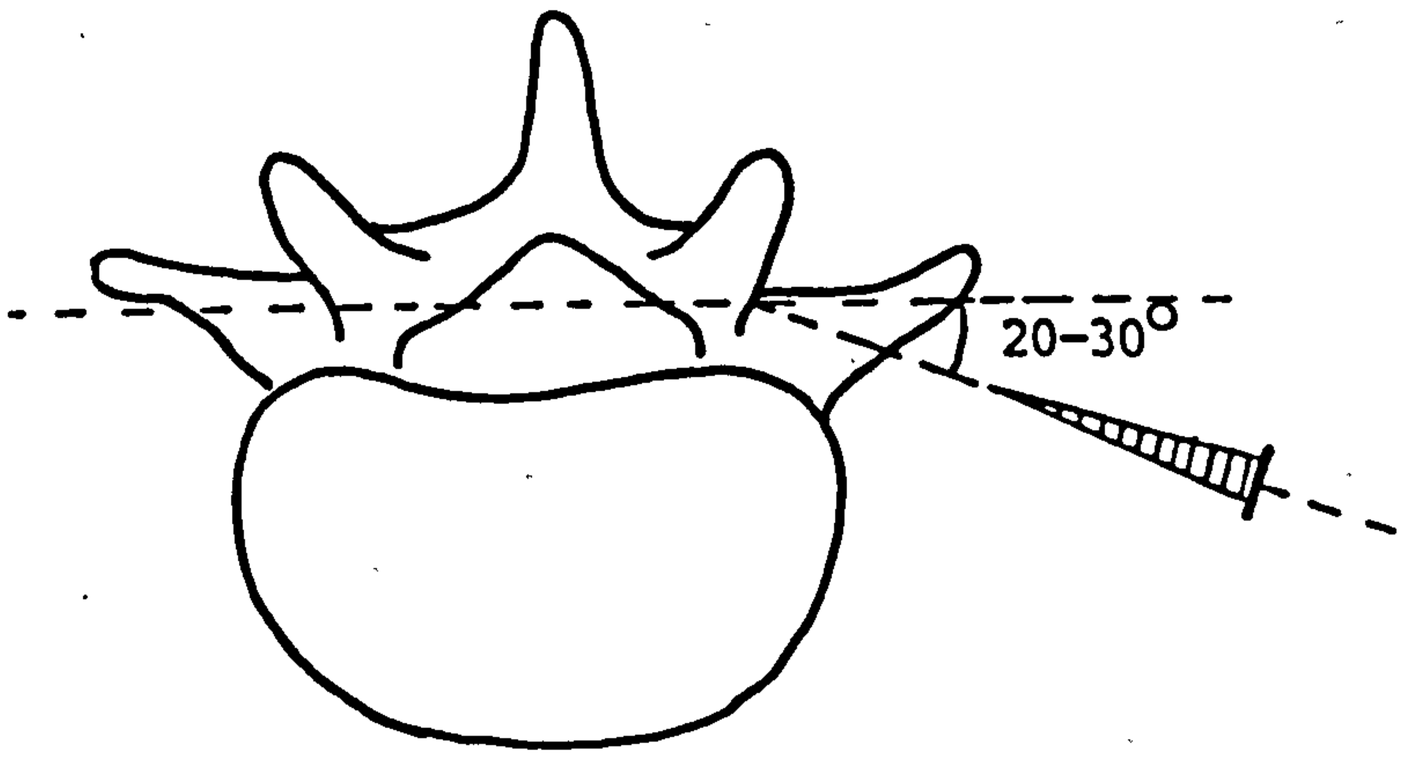

Fig 6.1 Simulated fusion of the facet joints by screws.

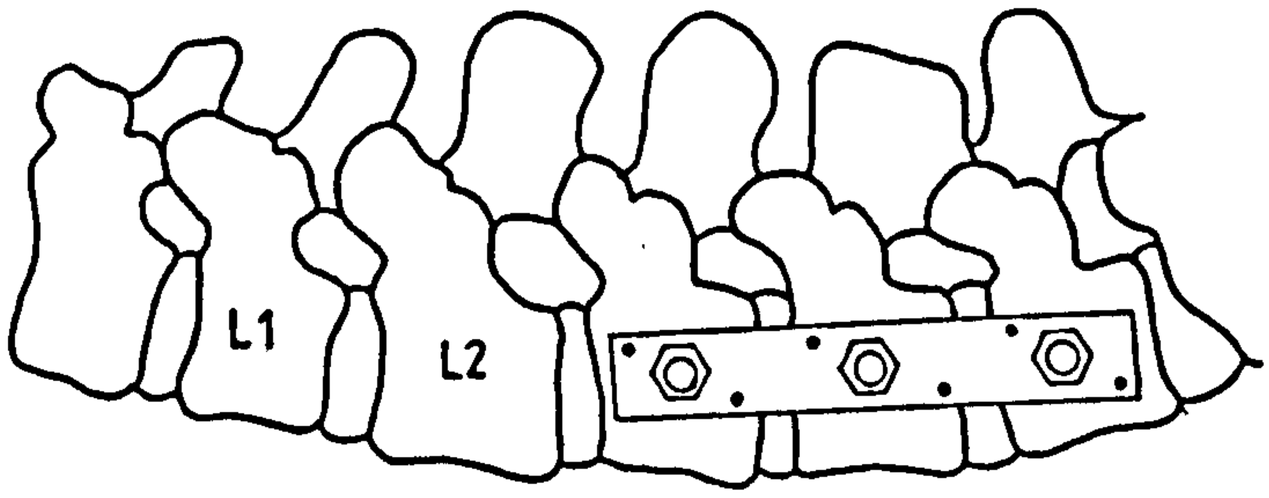

Fig 6.2 Simulated interbody fusion by bolted aluminium strips.

initial series of vibration tests, and their physical state did not permit a long period for tedious preparatory work and subsequent testing. Simulation of fusions of the vertebral bodies and the facet joints are described in the following sections.

6.2.1 Facet Joints Fusion

Fusion of the posterior element was simulated by locking the L1-2 to L4-5 facet joints on both sides, using 2 cm long self-cutting, twin-start screws of 3 mm diameter. The screws were inserted through the centre of the facet joints at an angle which varied between 20° and 30° to the coronal plane (fig 6.1). They were tightened manually to create an effective interlocking between the articular surfaces of the facet joints, and care had been taken not to over-tighten the screws to cause any crack in the bone substance. Manual manipulation of the specimen produced a feeling of overall stiffening after the insertion of screws. At the termination of all the vibration tests, the facet joints were dissected to allow direct inspection of the articular surfaces. It was confirmed that all the screws used for facet joints fusion were inserted at the centre of both articular surfaces of the joints, and that the screws were effective in creating simulated fusions of the joints. It was also confirmed that the facet joints were in a healthy state i.e. with no previous destruction or pathology which caused fusion of the joints.

6.2.2 Interbody Fusion

Interbody fusion was simulated by applying preformed aluminium strips of 20 mm width and 1.5 mm thickness across the lateral borders of the L3, L4 and L5 vertebral bodies. These strips were attached to the associated vertebral bodies using 5 mm diameter bolts passing through the centrum (fig 6.2). Two of the above-mentioned self-cutting screws were employed on both sides, penetrating the bone adjacent to the end-plates to enhance the clamping effect

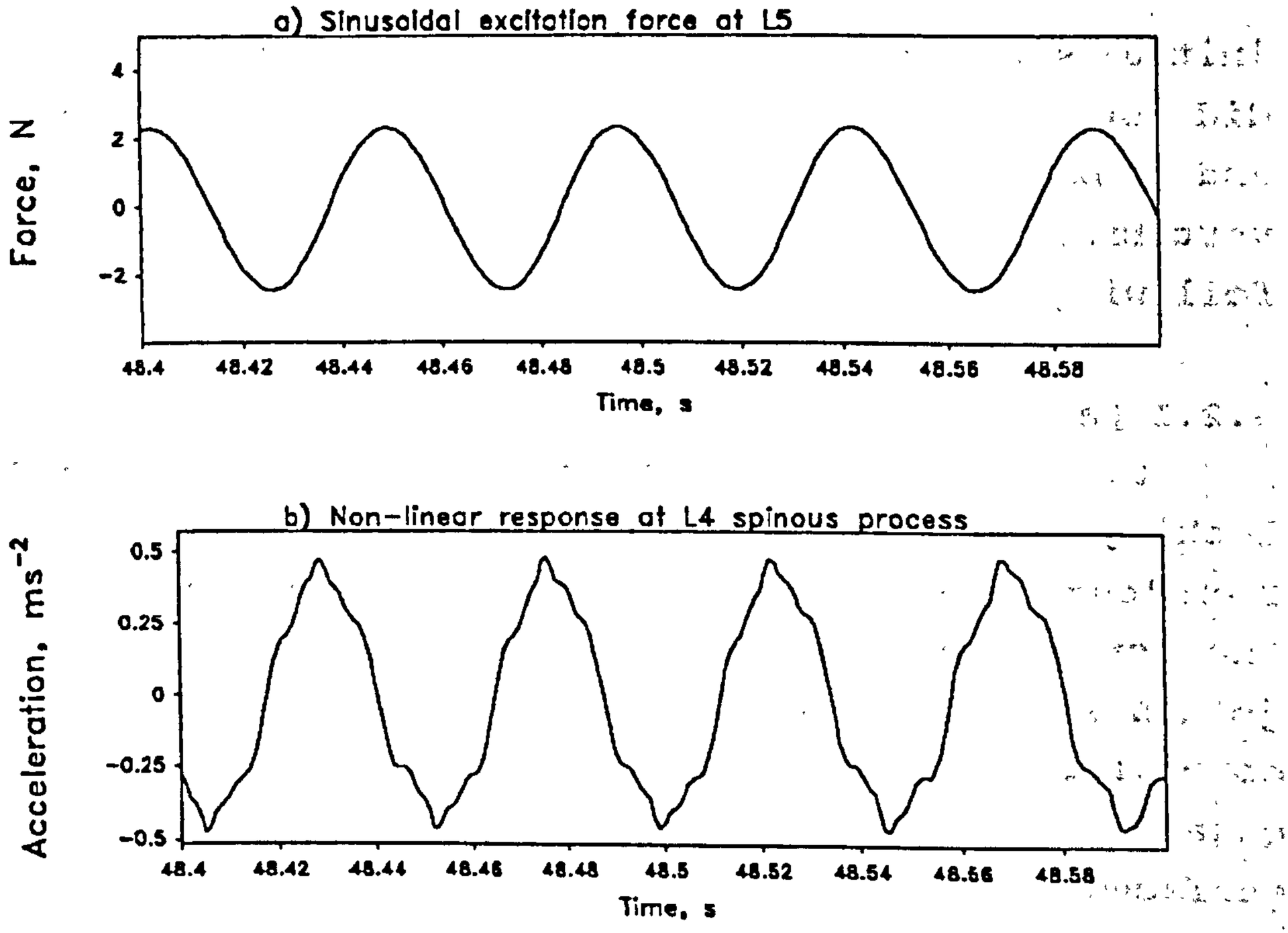

Fig 6.3 Non-linear response at L4 when a peak sinusoidal force of 2.4 N at 22 Hz was applied at L5 of the lumbar spine with simulated interbody fusion.

of the aluminium strips (appendix V). The bolted aluminium strips were found to be effective in stiffening the lumbar spine, and offering resistance to manual manipulation and attempted flexion-extension movement.

One might worry about the inadequacy of using bolted aluminium strips as a means of interbody fusion, and would suggest other methods such as that using bone cement and screws reported elsewhere (Chow, 1992). However, the vibration technique was planned to be tested of its applicability in the study of various forms of interbody fusion in addition to that caused by bridging the interbody space with bone graft. These may also include fusion due to pathological ossification of the paraspinal ligaments as in the case of ankylosing spondylitis. The technique of using aluminium strips is a close simulation of a milder or less rigid type of interbody fusion. It is envisaged that while the vibration technique is able to detect this milder form of simulated fusion, it would definitely be sensitive enough to detect more advanced fusions which involve complete bridging of the disc space through bone substance.

At the termination of all vibration tests, the specimens were dissected by cutting across the intervertebral discs for direct examination. The health state of the discs were classified according to Rolander's (1966) description. Appendix I.2 lists out the observation for each disc. Some specimens were found to have developed osteophytes, indicating degenerative changes. However, they were not severe enough to form complete bridging between the vertebral bodies, though at times, they were found to resist cutting by a sharp microtome blade. Previous interbody fusion in life was excluded.

6.3 RANDOM VIBRATION TESTING

Vibration response was measured in sequence at the L1 to L4 spinous processes while the lumbar spine was driven at L5 by a random vibratory force in the same manner as described in section 5.2.3. Transfer mobility defined as

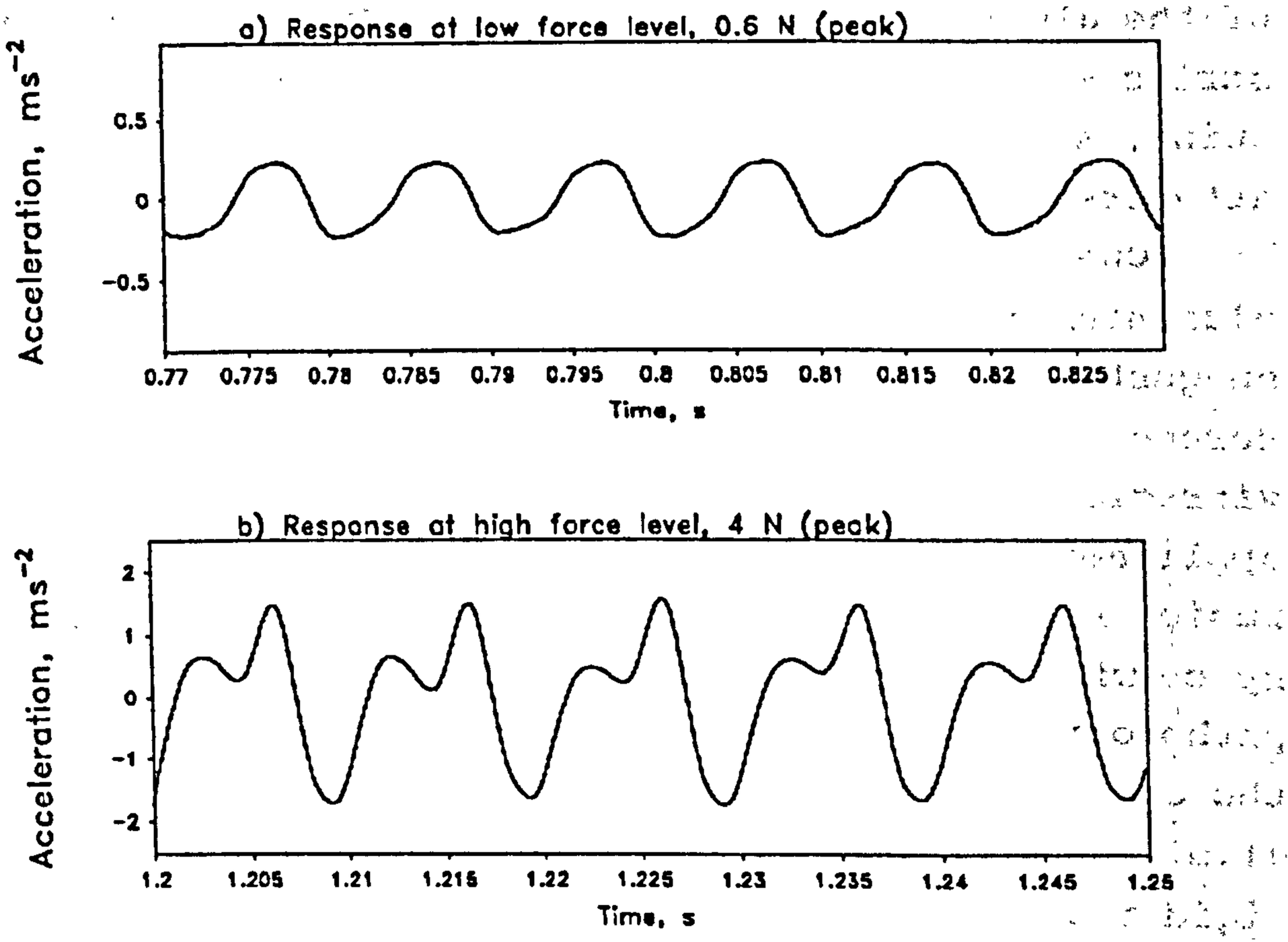

Fig 6.4 Vibration response at 100 Hz of a lumbar spine with facet joints fusion. a) Barely linear response at a low peak force of 0.6 N; b) Non-linear response when excited by a higher peak force of 4 N.

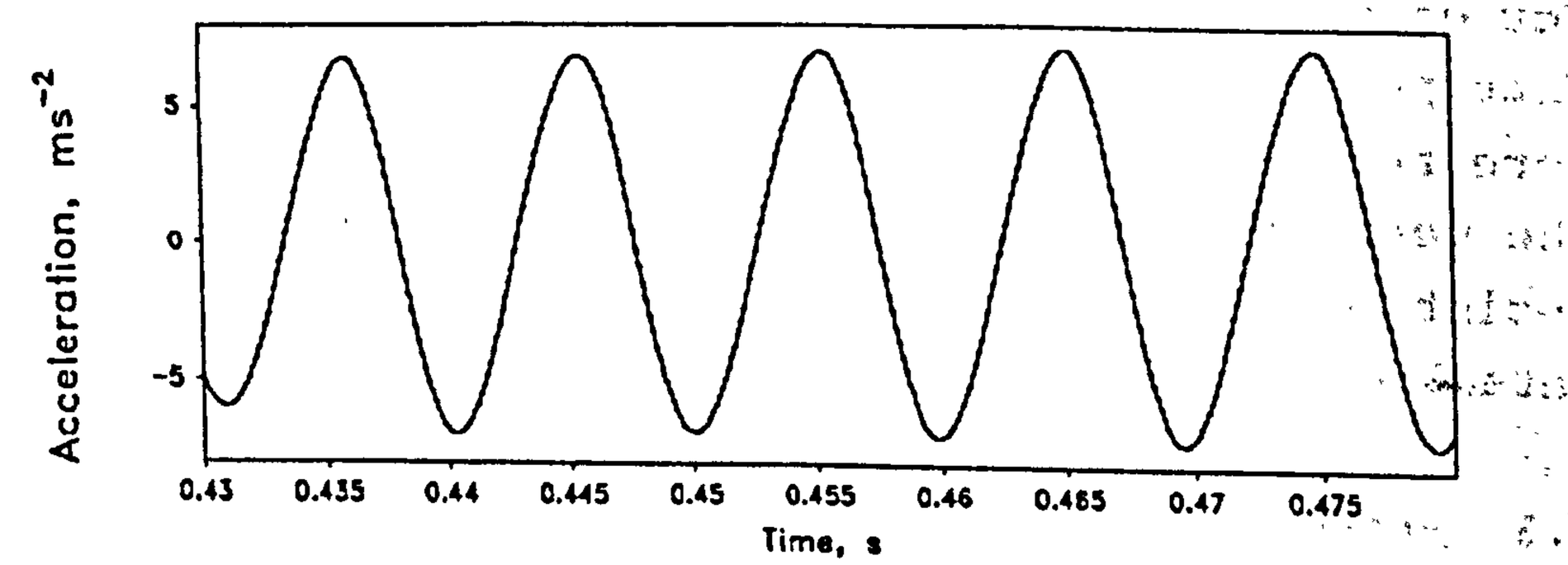

Fig 6.5 The same specimen (as fig 6.4) showed a bigger and linear response to the same force level when tested in the unfused state.

(V(f)/F(f)) was determined for each lumbar segment. The magnitude of velocity with respect to unit excitatory force was plotted for each location as a function of frequency. The mode shape of flexural vibration of the fused lumbar spine in the sagittal plane was examined. Summated mobility defined by equation 5.5 was also plotted for discussion. Curve fitting to equation 5.7 was also performed to establish the coefficients: A and b. Low band mobility (LBM), medium band mobility (MBM), and high band mobility (HBM) defined respectively by equations 5.9 to 5.11 were also determined. Typical examples of the test results are included in this chapter for discussion.

6.4 RESULTS AND DISCUSSION

6.4.1 General System Characteristics

It was found that the lumbar spine became grossly stiffened with fusion of the facet joints and interbody fusion. At low frequency, the fused lumbar spine was very easily driven to exceed its linearity limit if the amplitude of vibratory force was not carefully controlled. Figure 6.3 shows the non-linear response at L4 of a fused specimen when driven at L5 by a peak sinusoidal force of 2.4 N at 22 Hz. The fused lumbar spine was found to permit only a smaller driving force, and consequently exhibited a diminished response, if it was to maintain a linear response. Figure 6.4a shows a fused lumbar spine which responded barely linearly only to a low peak force of 0.6 N at 100 Hz. However, it responded non-linearly with harmonics to a higher peak force of 4 N (fig 6.4b). The same specimen showed a linear and stronger response to the same force level when not fused (fig 6.5). This observation indicates that at low frequency vibration, the decreased compliance of the fused lumbar spine was being challenged and there was a tendency for it to be driven to exceed its linearity limit. A fused lumbar spine exhibited a diminished response in the low frequency range due to a decrease in the overall compliance which would mean a

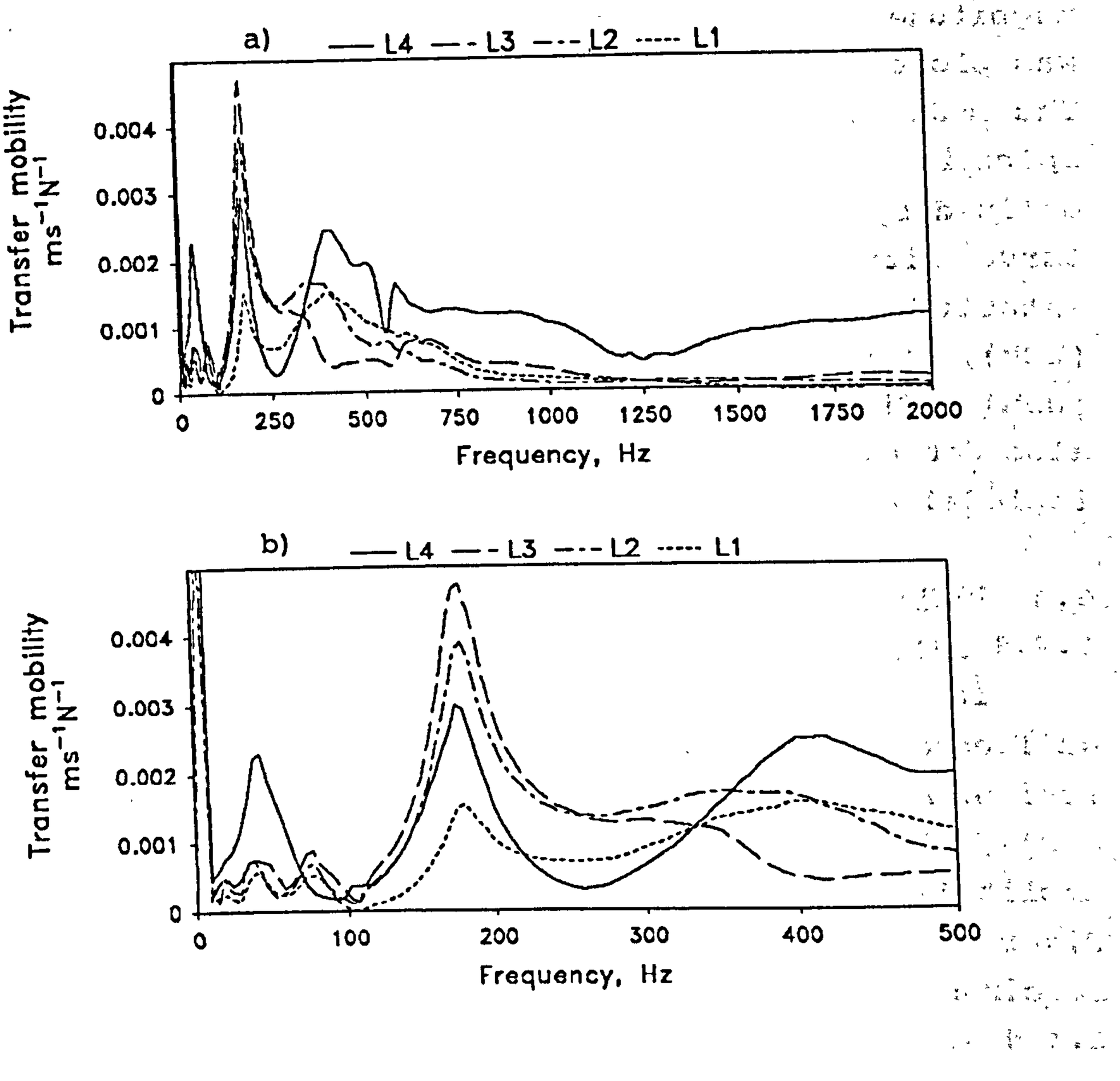

Fig 6.6 Transfer mobility measured at different segments of a specimen with facet joints fusion. a) 0 Hz to 2 kHz; b) 0 Hz to 500 Hz showing the resonant peaks; c) First flexural vibration mode at 180 Hz.

reduced displacement and hence diminished velocity in response to the same amount of vibratory force. Thus the mobility, which is defined as V(f)/F(f) decreased in the lower range of frequency.

At high frequencies, a fused lumbar spine was found to enhance transmission of vibration. A smaller driving force was required to induce a measurable response of the fused specimen. The response was coherent and linear.

The spectrum of random vibratory force applied to a fused lumbar spine did not reveal any difference except in a few case where some increase in the force spectrum in the lower frequency range was found.

6.4.2 Facet Joints Fusion

All fused specimens behaved in a stiffer manner and the transfer mobility below 100 Hz was generally suppressed showing that they behaved as a stiffer structure (fig 6.7). The transfer mobility showed clearly defined peaks below 200 Hz, and the peaks were slightly shifted to higher frequencies when compared with those of the unfused one, though there was no significant changes in their amplitudes. The specific amplitudes of the resonant peaks obtained at the L1 to L4 spinous processes revealed a first mode of flexural vibration of the fused lumbar spine, similar to that of a flexible beam hinged at both ends. In most cases, there was a marked increase in the mobility in the frequency range about 500 Hz to 1 kHz. Higher flexural vibration modes were effectively damped. Relative to an unfused lumbar spine, the mobility was significantly augmented with facet joints fusion in the frequency range extending well beyond 1.5 kHz, suggesting an enhancement of transmission of vibration with fusion of the facet joints. Figure 6.6 shows the typical transfer mobility measured at different segments of a fused lumbar spine. Figure 6.7 shows the transfer mobility of the same fused specimen in comparison to that obtained during its unfused state.

Summated mobility has been described in section 5.7.1

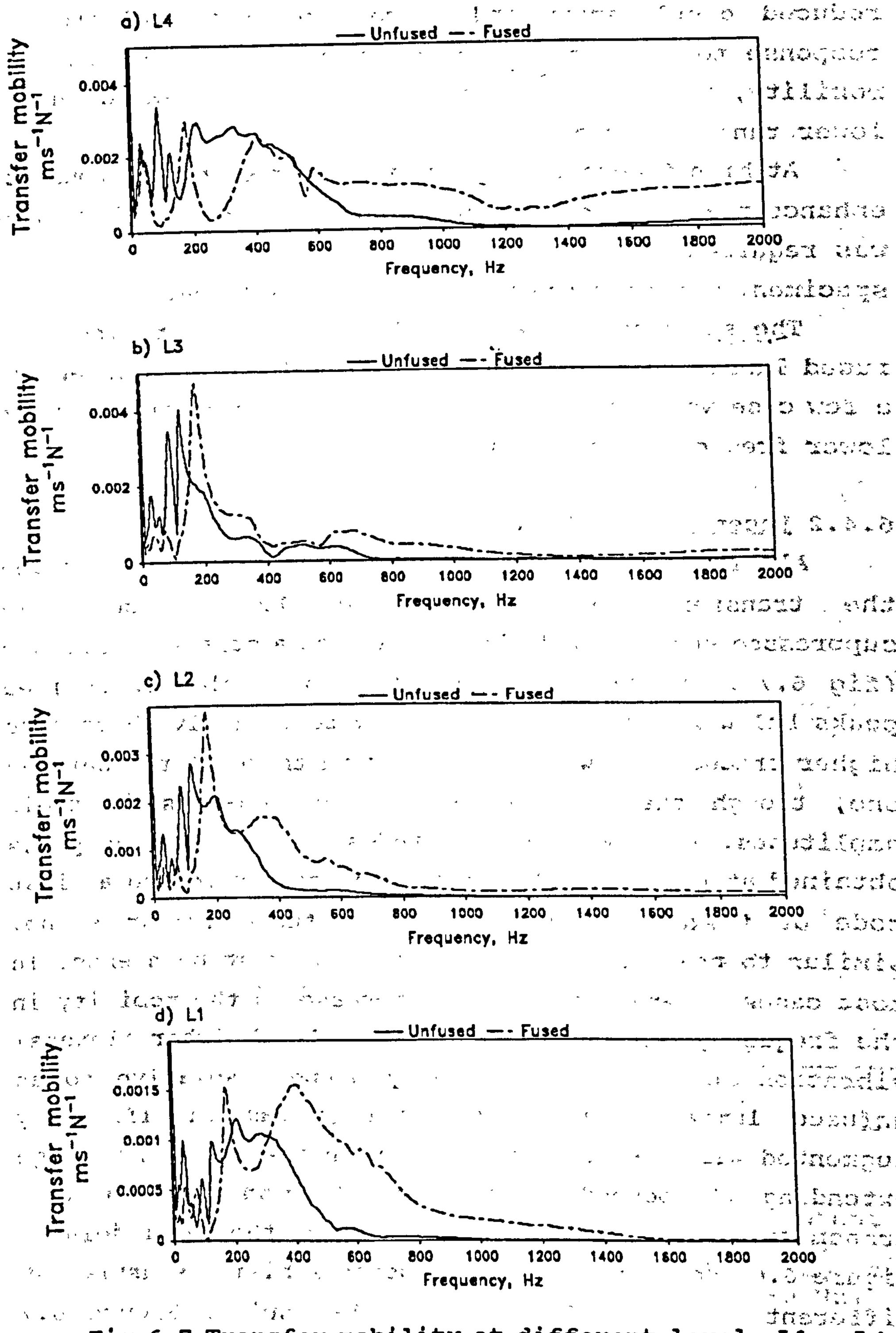

Fig 6.7 Transfer mobility at different levels L1 - L4 of a specimen when unfused, and with facet joints fusion.

as a means to show the overall trend of accumulative mobility across the frequency range of interest. It was noted that with facet joints fusion, the curves generally shift upward to a higher value. In general the slope in the lower frequency range continued to climb to above 600 Hz before any sign of levelling was seen. This might be reflected by the fact that a fused lumbar spine has higher mobility in the medium frequency range, while an unfused one is less mobile in this frequency range. This could be confirmed with the statistics on the band mobility mentioned later in this section. However, for mobility at L4 and L3, the curves continued to climb further even beyond the frequency of 2 kHz while the same specimens, when unfused, had already shown a stable plateau at about 800 Hz. This again suggests the enhancement of high frequency vibration particularly in the two segments next to the excitation source. Figures 6.8 and 6.9 show the typical summated mobility curves of a specimen in comparison to those obtained in its unfused state.

An attempt has been made to curve-fit the summated mobility curves obtained for different segments to equation 5.7 by non-linear regression. It was found that the mathematical model fits very closely to the experimental results, with the coefficient of determination $R^2 > 0.98$. There was a significant difference between the parameters determined for an unfused lumbar spine and one with facet joints fusion ($p < 0.005$). Table 6.1 lists out the coefficients determined for the fused specimens, and also includes the figures obtained in their unfused state for comparison. The coefficient A which can be taken as the theoretical total mobility was roughly doubled with fusion of the facet joints whilst coefficient b was reduced roughly to half of its value in the unfused state. The results suggest that these two coefficients from curve-fitting can be used to characterize the mechanical behaviour of the lumbar spine, or perhaps to be developed as criteria for the indication of fusions in a lumbar

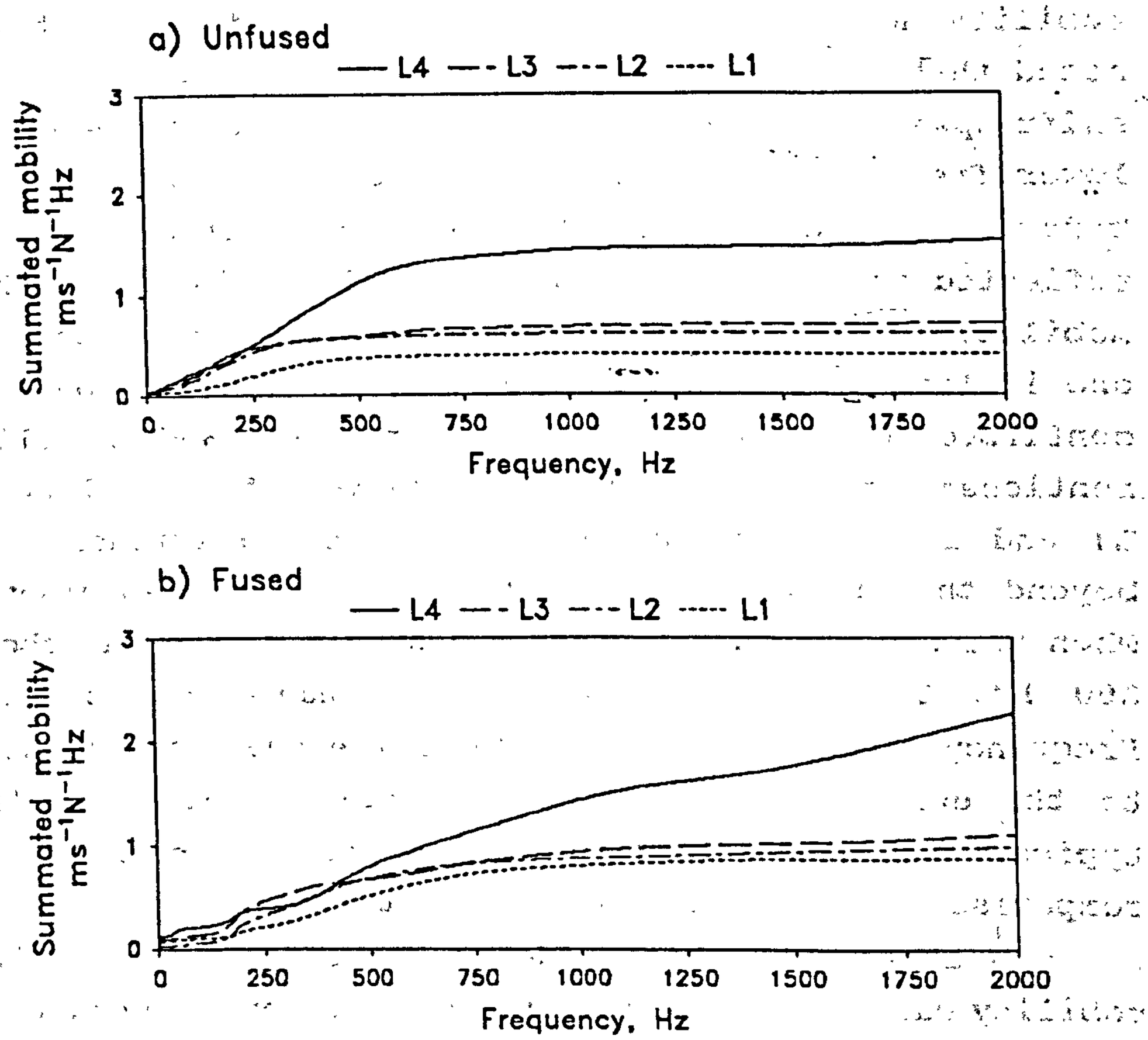

Fig 6.8 Summated mobility at different levels L1 - L4 of a specimen: a) Unfused; b) Facet joints fusion.

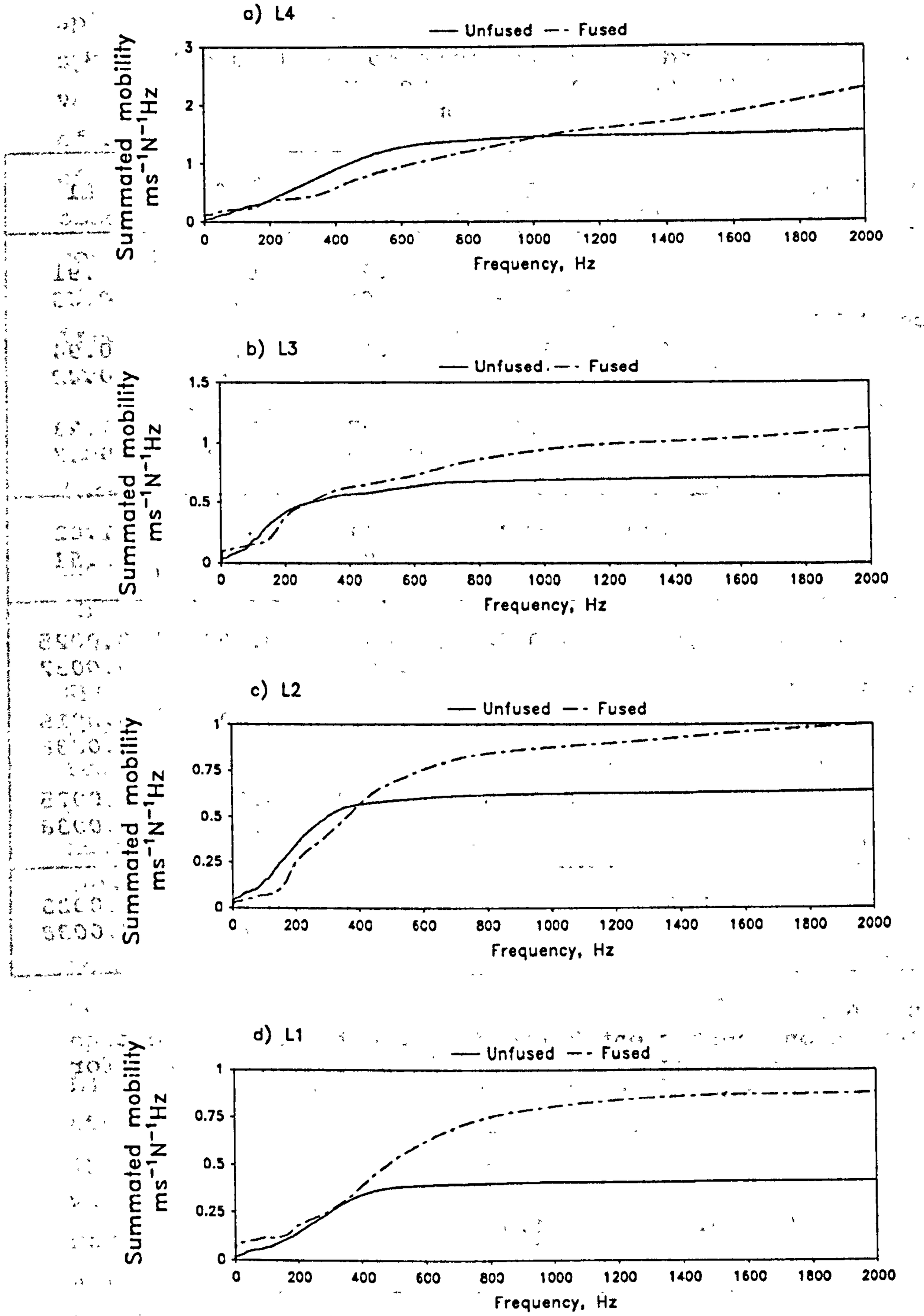

Fig 6.9 Summated mobility at different levels L1 - L4 of a specimen before and after facet joints fusion.

Table 6.1
Coefficients A and b for Specimens No. 9, 10 and 11 with facet joints fusion. Figures for unfused specimens printed in italics for comparison.

COEFFICIENTS	SPECIMEN NUMBER	L4	L3	L2	L1
A ($ms^{-1}N^{-1}Hz$)	9	4.73 *1.89*	1.23 *0.98*	0.86 *0.67*	0.91 *0.63*
	10	3.38 *1.56*	1.11 *0.71*	0.99 *0.64*	0.94 *0.42*
	11	4.22 *1.27*	1.97 *0.80*	1.09 *0.45*	1.23 *0.47*
	MEAN	4.11 *1.57*	1.44 *0.83*	0.98 *0.59*	1.02 *0.51*
b (Hz^{-1})	9	0.0004 *0.0019*	0.0017 *0.0025*	0.0029 *0.0043*	0.0025 *0.0037*
	10	0.0005 *0.0026*	0.0019 *0.0042*	0.0024 *0.0049*	0.0018 *0.0038*
	11	0.0005 *0.0026*	0.0013 *0.0036*	0.0026 *0.0057*	0.0025 *0.0038*
	MEAN	0.0005 *0.0024*	0.0016 *0.0034*	0.0026 *0.0050*	0.0023 *0.0038*

Table 6.2
Attenuation coefficient k (in dB/segment) with respect to L4 of the specimens with facet joints fusion. Figures for unfused specimens printed in italics for comparison.

SPECIMEN NUMBER	L3	L2	L1
9	5.9 *7.3*	4.5 *5.1*	3.3 *3.4*
10	6.2 *6.7*	3.6 *3.9*	2.8 *3.8*
11	3.9 *4.0*	4.3 *4.5*	2.5 *3.0*

spine. With reference to its unfused state, a lumbar spine specimen with facet joints fusion tends to show a bigger value of coefficient A in association with a smaller value of b. Following on the discussion on the physical meanings of these two coefficients in section 5.7.1, this observation can be interpreted as a overall enhancement in mobility across the frequency range of interest. Mobility of the fused lumbar spine was not just confined to lower frequencies, but extended well into the medium and perhaps the higher frequency range as seen in figure 6.7.

Total Mobility (section 5.7.1) summarizes the overall mobility of the specimen across the frequency range of interest by the mathematical summation of mobility from 0 Hz to 2 kHz. As shown in figure 6.10, the total mobility was significantly augmented in a fused lumbar spine though there were individual variations in the absolute values. The percentage of increase with respect to the same specimens in the unfused state also varied from 20% to 160%, probably due to various effect of the facet joints fusion on the transfer mobility. However, the general trend was still consistent among the specimens, and these measured figures correspond well with the coefficient A determined for the fused specimens (table 6.1).

Specific attention has been made to the attenuation of total mobility when vibration was transmitted from the L4 to L1 segments. Total mobility measured at L3, L2 and L1 are plotted in percentage with respect to that measured at L4 which is designated as 100%. Figures 6.11 shows the attenuation of vibration at various segments of the same specimen when unfused, and with facet joints fusion. There was a general enhancement of the total mobility at all segments with facet joints fusion, as indicated in figure 6.10. However, there was no relative (or proportional) changes among those measurements with fusion. There is a strong indication that facet joints fusion did not have any effect on the attenuation of vibration. Facet joints fusion was seen to enhance the overall mobility of the lumbar

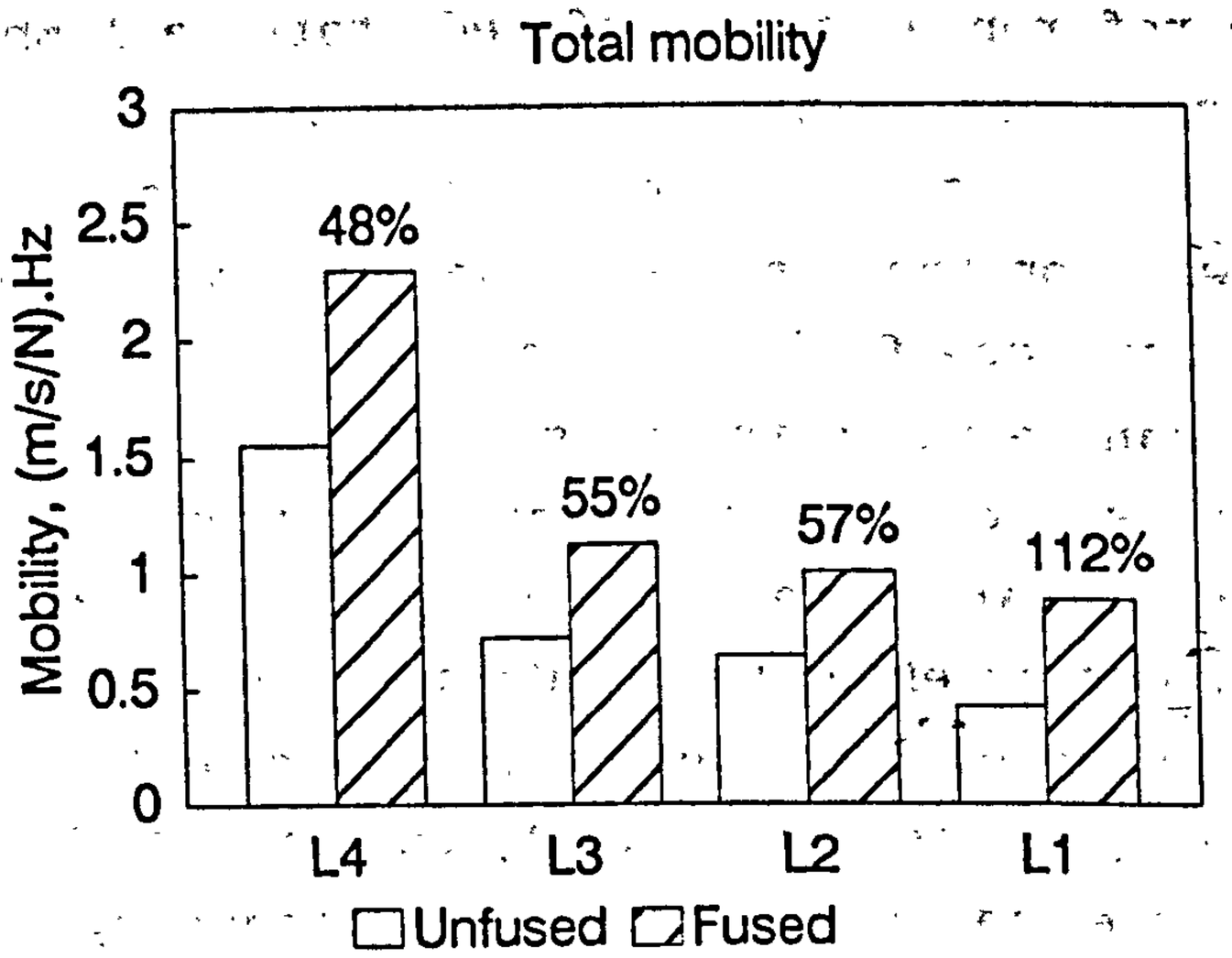

Fig 6.10 Total mobility at different levels L1 - L4 of a specimen when unfused, and with facet joints fusion. Percentage indicates increase (error = 1.8%).

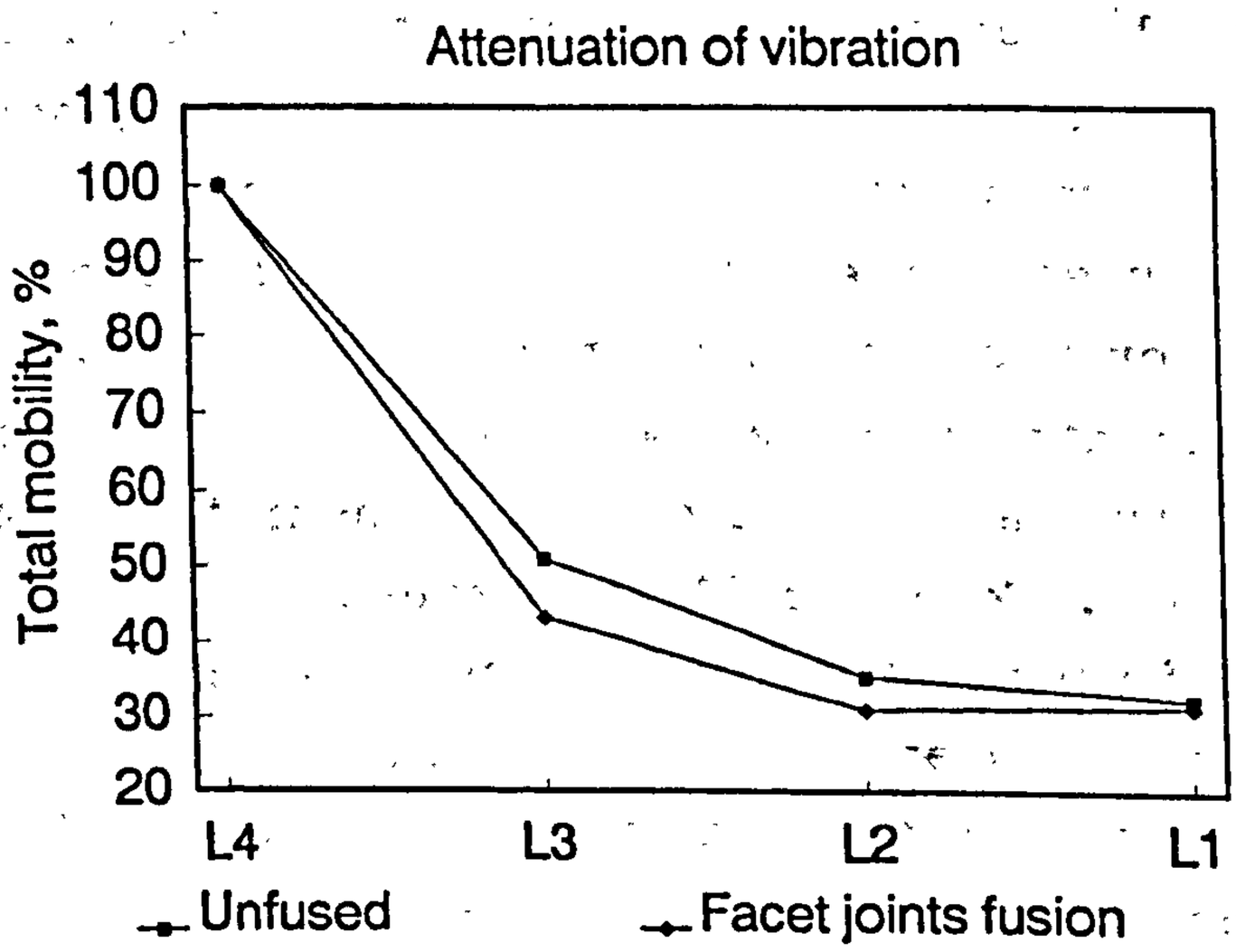

Fig 6.11 Attenuation of vibration in a specimen when unfused, and with facet joints fusion.

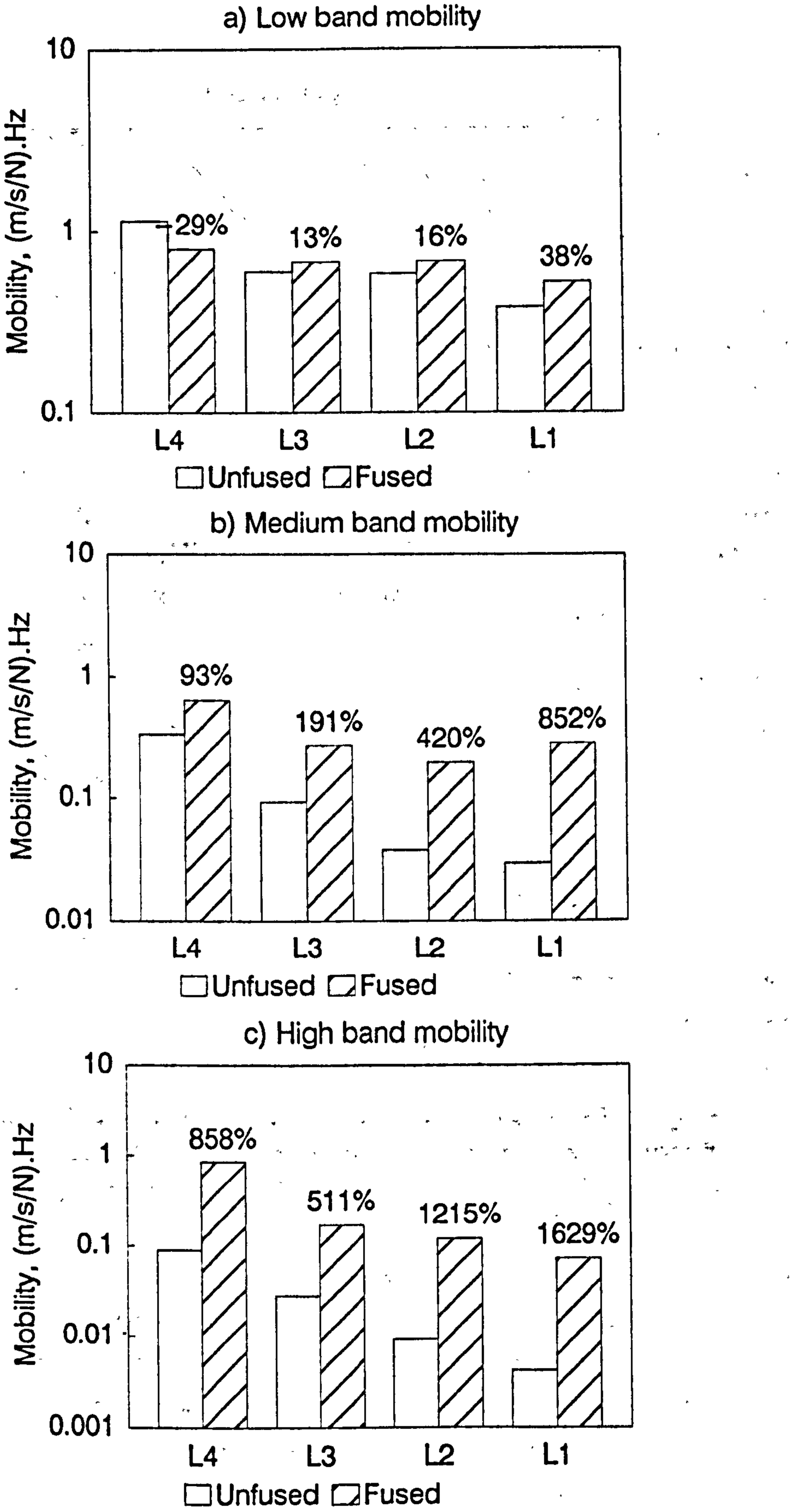

Fig 6.12 Mobility in different frequency bands measured on a specimen when unfused, and with facet joints fusion. Percentage indicates increase (error = 1.8%).

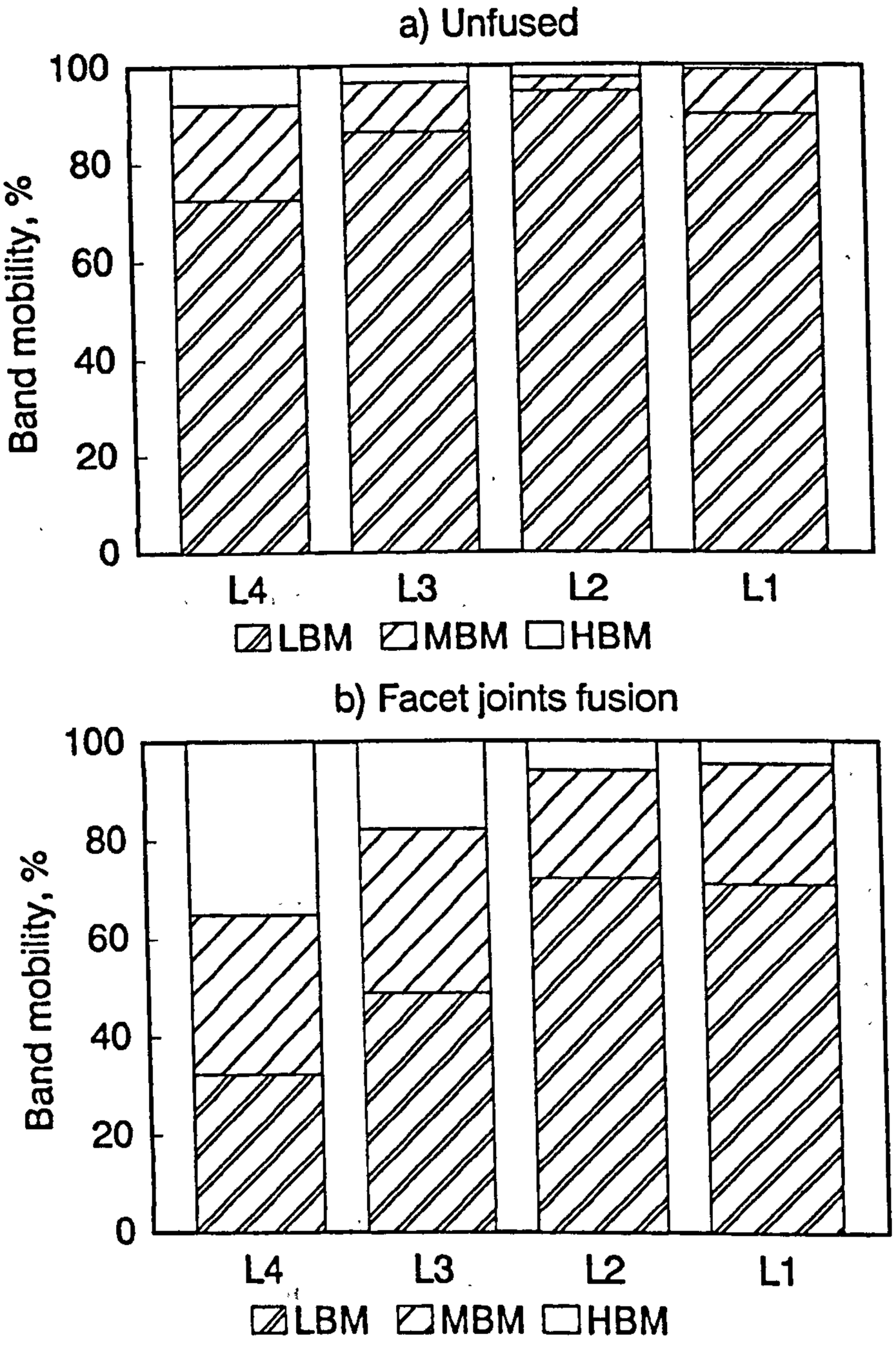

Fig 6.13 Distribution of mobility among different frequency bands of a specimen. a) Unfused; b) Facet joints fusion. (LBM = low band mobility; MBM = medium band mobility; HBM = high band mobility)

spine, but it did not change the proportionality of mobility among the segments. The attenuation coefficient k defined by equation 5.8 was determined for each segments (table 6.2). There is no significant difference between the figures obtained for the unfused lumbar spines and those with facet joints fusion.

Band mobility (section 5.7.2) shows the specific sum of mobility within various frequency ranges. Figure 6.12 shows the typical band mobility measured on a fused lumbar spine in an attempt to compare with that obtained in its unfused state. On the whole, the low band mobility (LBM, 0 to 500 Hz) showed a mild increase except in one case where the LBM demonstrated a small decrease. In the medium frequency band (MBM, 500 Hz to 1 kHz), there was significant increase ranged from 90% to 1600% in the extreme cases. The high band mobility (HBM, 1 to 2 kHz) also showed significant increase, though more remarkable at L4 which was right next to the source of excitation. These findings show that the effect of facet joints fusion on the enhancement of transfer function was most significant at the segments close to the excitation source.

It was also found that there was a redistribution of the mobility within the previously defined frequency bands. Figure 6.13 is a stack-bar chart showing the different pattern of mobility distributions for a specimen in unfused and fused states. Particular reference is made to the measurement at the L4 segment. In its unfused state, the lumbar spine demonstrated high percentage of mobility in low frequency, at more than 60%; while that for the high frequency was found to be less than 20%. With fusion of the facet joints, it was found that low band mobility decreased to less than 40% while the high band mobility increased, close to 40%. There was a similar trend in the change but in a smaller amount for the mobility at L3. However, the effect was less significant at other segments i.e. L2 and L1. It could be suggested here that the effect of facet joints fusion was highest at the two lumbar segments

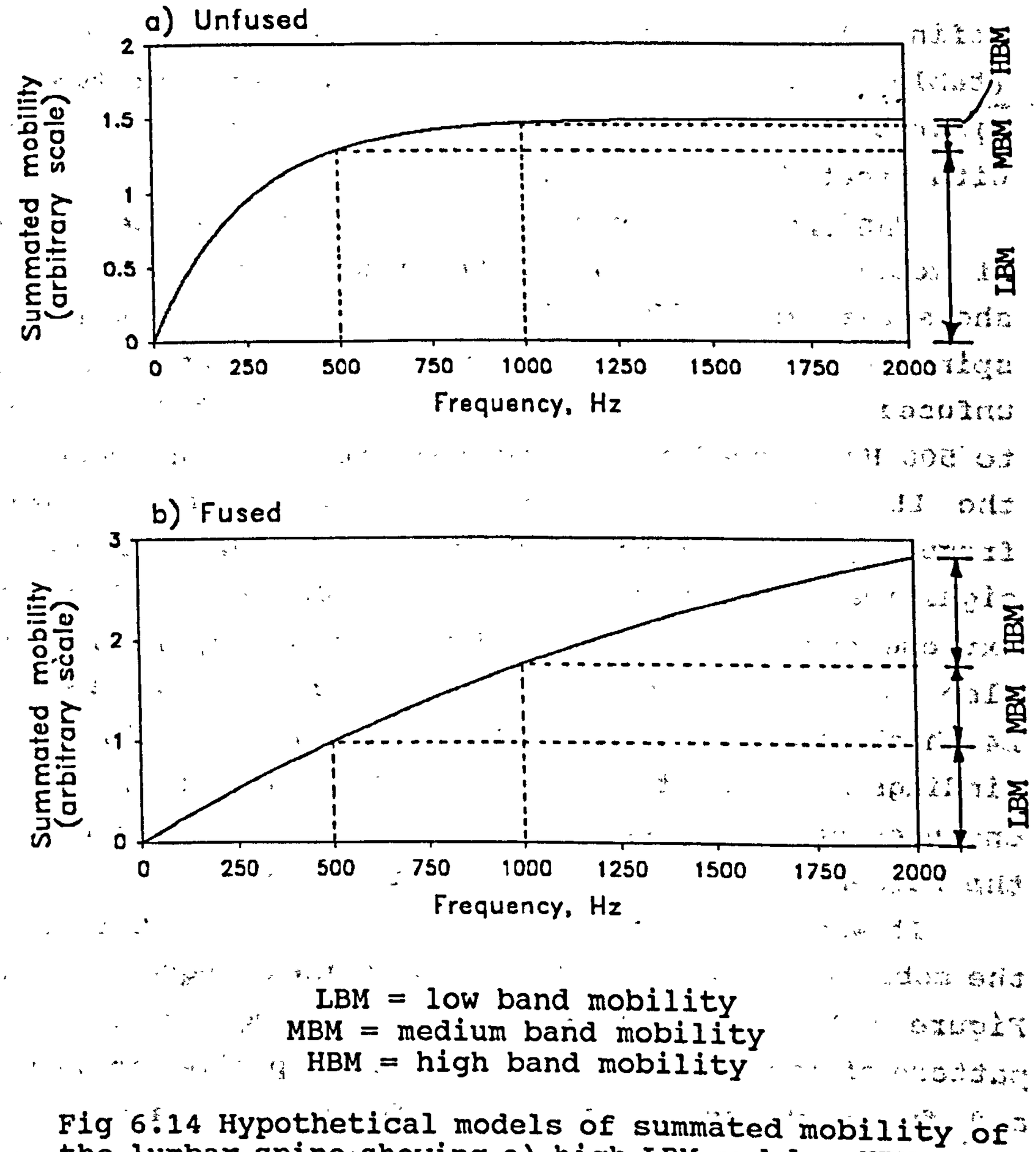

LBM = low band mobility
MBM = medium band mobility
HBM = high band mobility

Fig 6.14 Hypothetical models of summated mobility of the lumbar spine showing a) high LBM and low HBM, and b) low LBM and high HBM.

adjacent to the excitation source.

It can be hypothesized that a stiffened lumbar spine with augmented mechanical links such as fusion of intervertebral joints between the excitation source and the measuring point would offer less damping to enhance the transmission of vibration. It is envisaged that a theoretical example of a mobile lumbar spine with compliant intervening disc would exhibit a summated mobility curve similar to that depicted in figure 6.14a - with high LBM and low HBM, i.e. good mobility response in low frequency and poor response in high frequency. Figure 6.14b depicts another theoretical case where the lumbar spine is overall stiffened perhaps due to fusions between the segments. The overall characteristics of this specimen would have low LBM while HBM is high - due to decrease in gross compliance and damping which results in enhanced transmission of the high frequency. This theoretical explanation has gained support from the vibration response described previously of the lumbar spine specimens with facet joints fusion.

6.4.3 Interbody Fusion

The vibration response of the lumbar spine specimens with interbody fusion varied because it proved difficult to obtain a consistent degree of rigidity of the spine through bracing with the aluminium strips. However, simulated interbody fusion had similar effects on the mechanical behaviour as did fusion of the facet joints, except that the mobility at low frequency was not so effectively suppressed. This could be explained by the fact that the aluminium strips were placed on both sides of the vertebral bodies, lying close to the neutral plane which, for small deformations, may be assumed to pass coronally through the centroid of the vertebral bodies. Thus it can be inferred the aluminium strips were contributing little resistance to flexural vibration in the sagittal plane of the spine.

Figure 6.15 shows the typical transfer mobility measured at various lumbar segments of a specimen, and

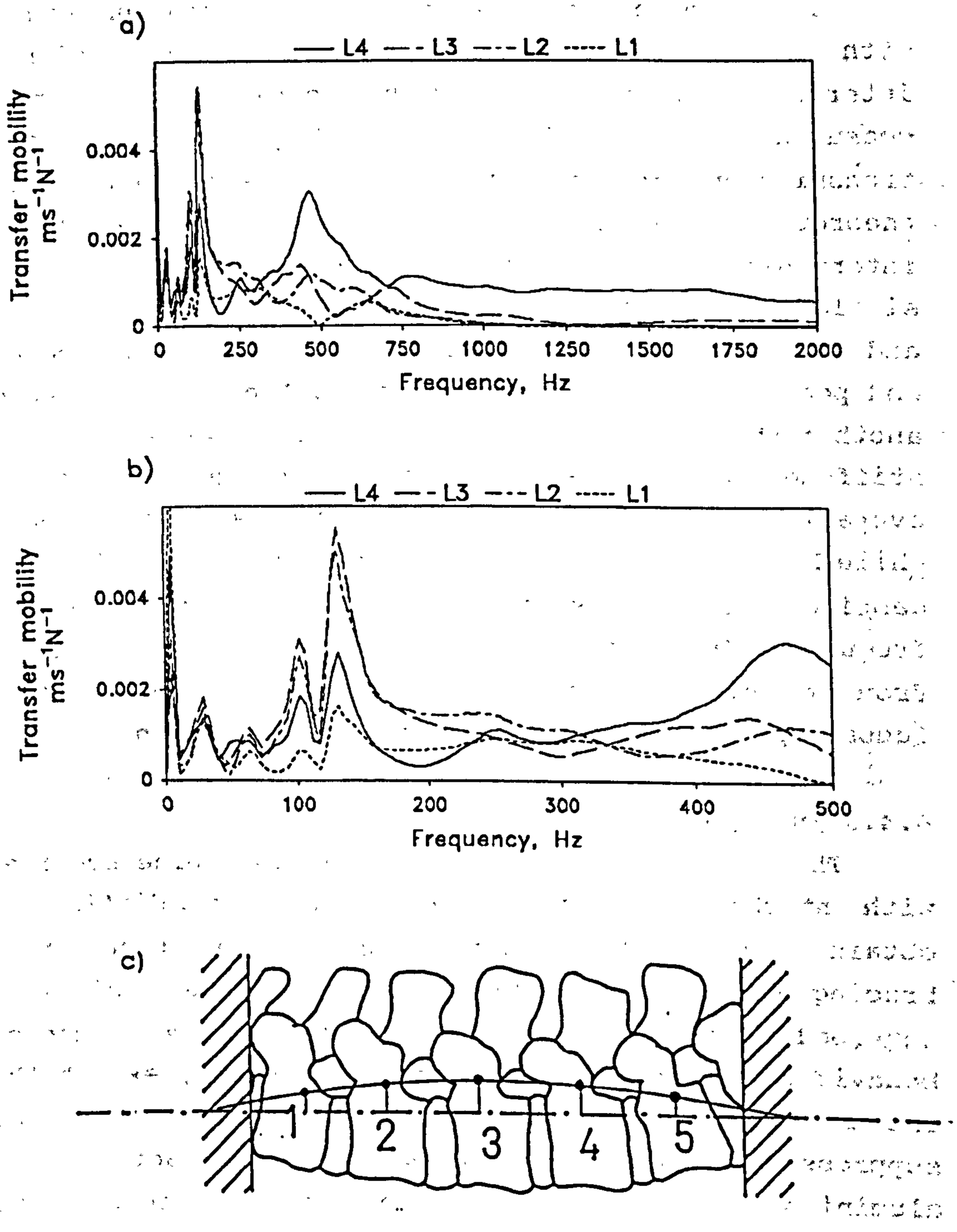

Fig 6.15 Transfer mobility measured at different segments of a specimen with interbody fusion. a) 0 Hz to 2 kHz; b) 0 Hz to 500 Hz showing the resonant peaks; c) First flexural vibration mode at 132 Hz.

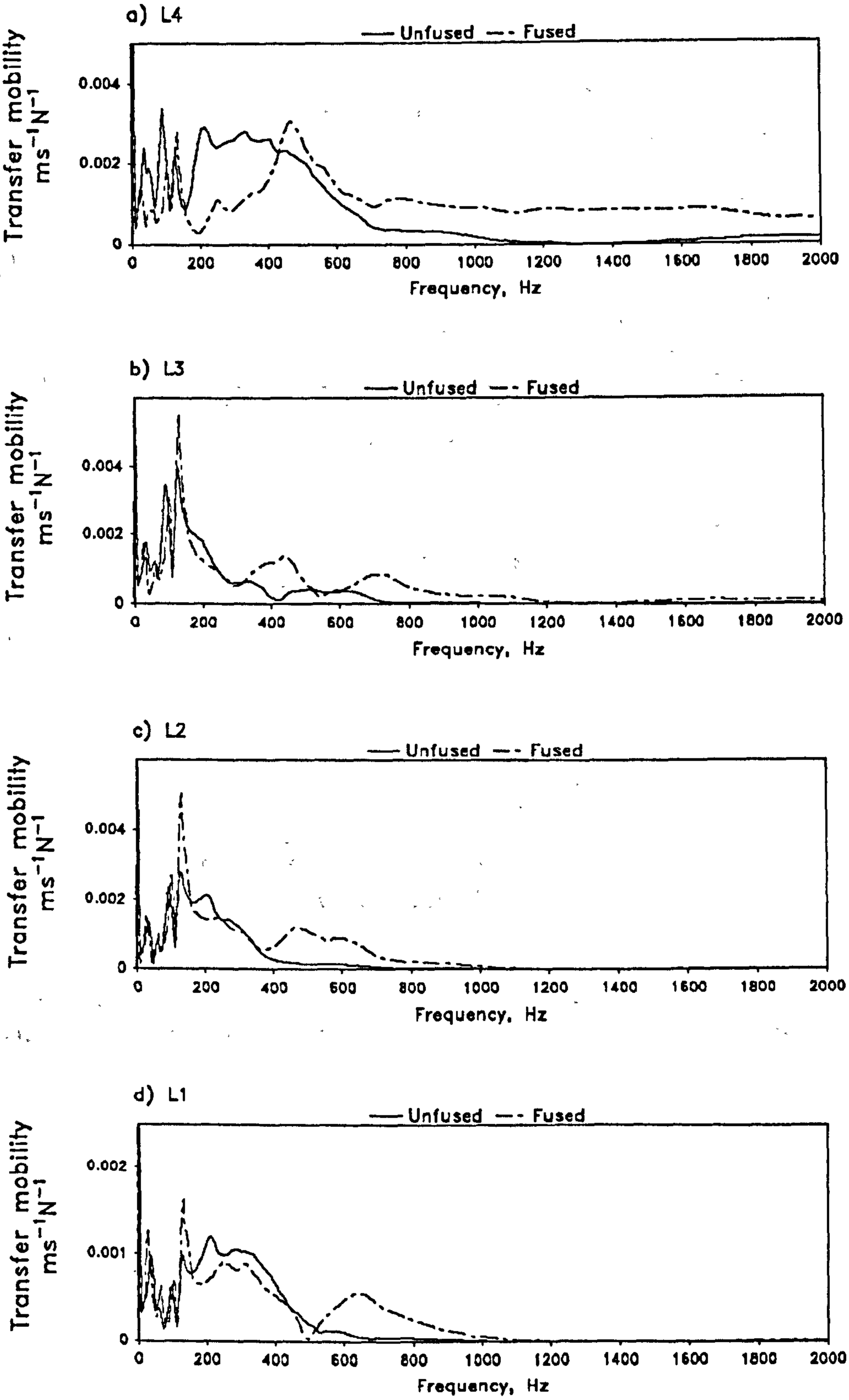

Fig 6.16 Transfer mobility at different levels L1 - L4 of a specimen when unfused, and with interbody fusion.

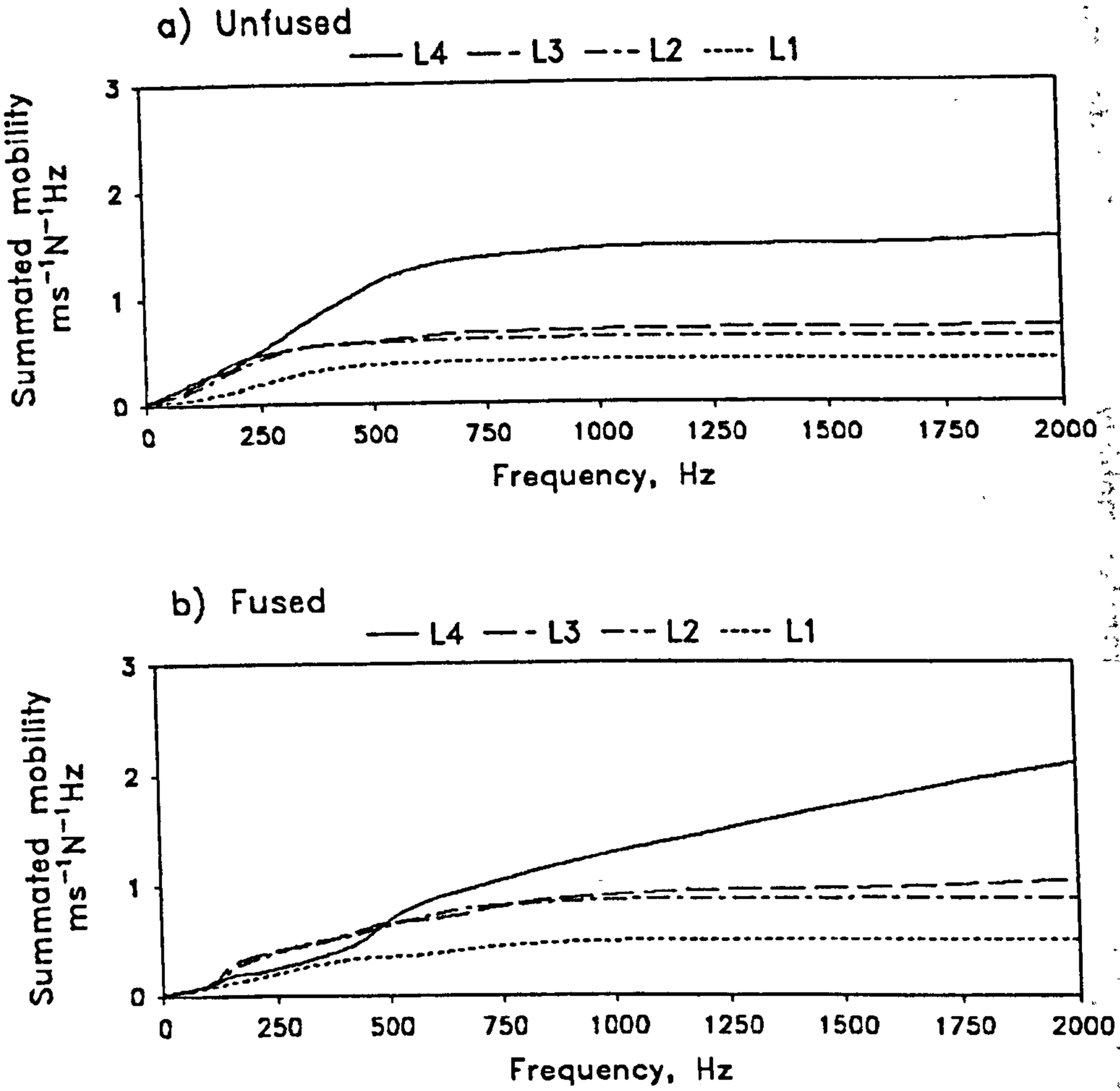

Fig 6.17 Summated mobility at different levels L1 - L4 of a specimen. a) Unfused; b) Interbody fusion.

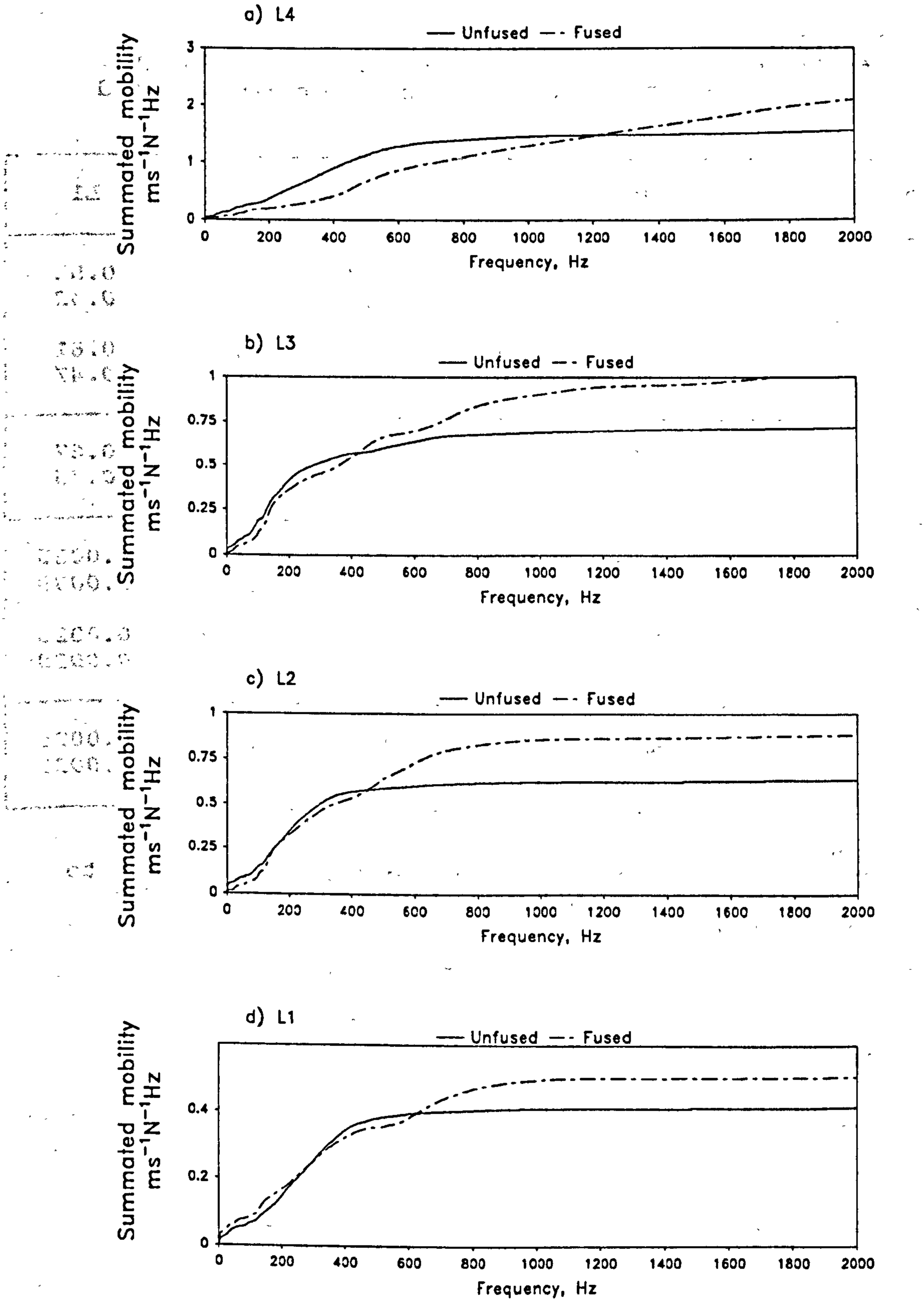

Fig 6.18 Summated mobility at different levels L1 - L4 of a specimen before and after interbody fusion.

Table 6.3
Coefficients A and b for Specimens No. 10 and 11 with interbody fusion. Figures for unfused specimens printed in italics for comparison.

COEFFICIENTS	SPECIMEN NUMBER	L4	L3	L2	L1
A ($ms^{-1}N^{-1}Hz$)	10	3.28 *1.56*	1.04 *0.71*	0.90 *0.64*	0.52 *0.42*
	11	3.35 *1.27*	3.06 *0.80*	1.00 *0.45*	0.81 *0.47*
	MEAN	3.32 *1.42*	2.05 *0.75*	0.95 *0.55*	0.67 *0.45*
b (Hz^{-1})	10	0.0005 *0.0026*	0.0021 *0.0042*	0.0028 *0.0049*	0.0025 *0.0038*
	11	0.0006 *0.0026*	0.0009 *0.0036*	0.0029 *0.0057*	0.0025 *0.0038*
	MEAN	0.0006 *0.0026*	0.0015 *0.0034*	0.0029 *0.0053*	0.0025 *0.0038*

Table 6.4
Attenuation coefficient k (in dB/segment) with respect to L4 of the specimens with interbody fusion. Figures for unfused specimens printed in italics for comparison.

SPECIMEN NUMBER	L3	L2	L1
10	6.1 *6.7*	3.6 *3.9*	2.8 *3.8*
11	3.9 *4.0*	3.6 *4.5*	3.1 *3.0*

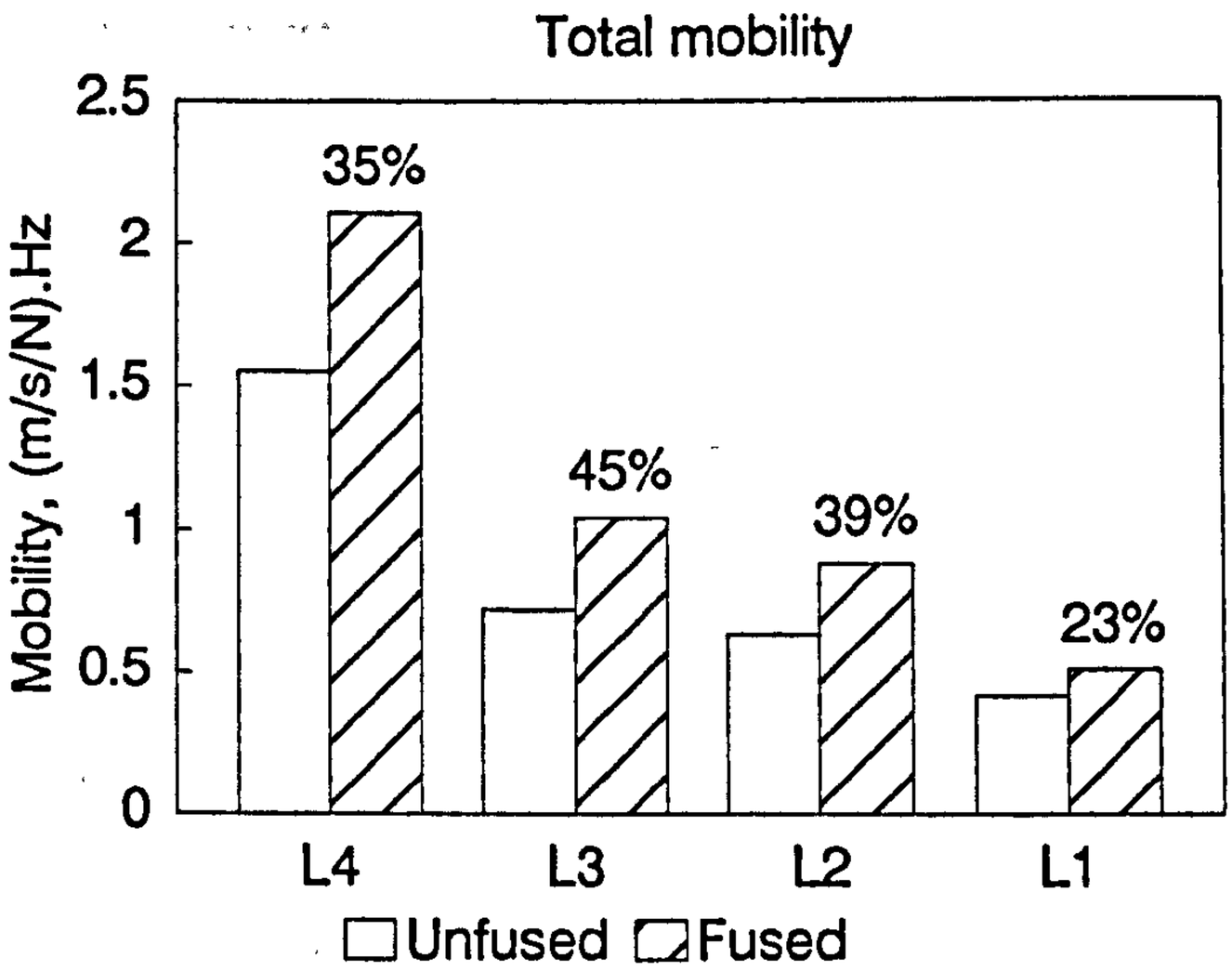

Fig 6.19 Total mobility at different levels L1 - L4 of a specimen when unfused, and with interbody fusion. Percentage indicates increase (error = 1.8%).

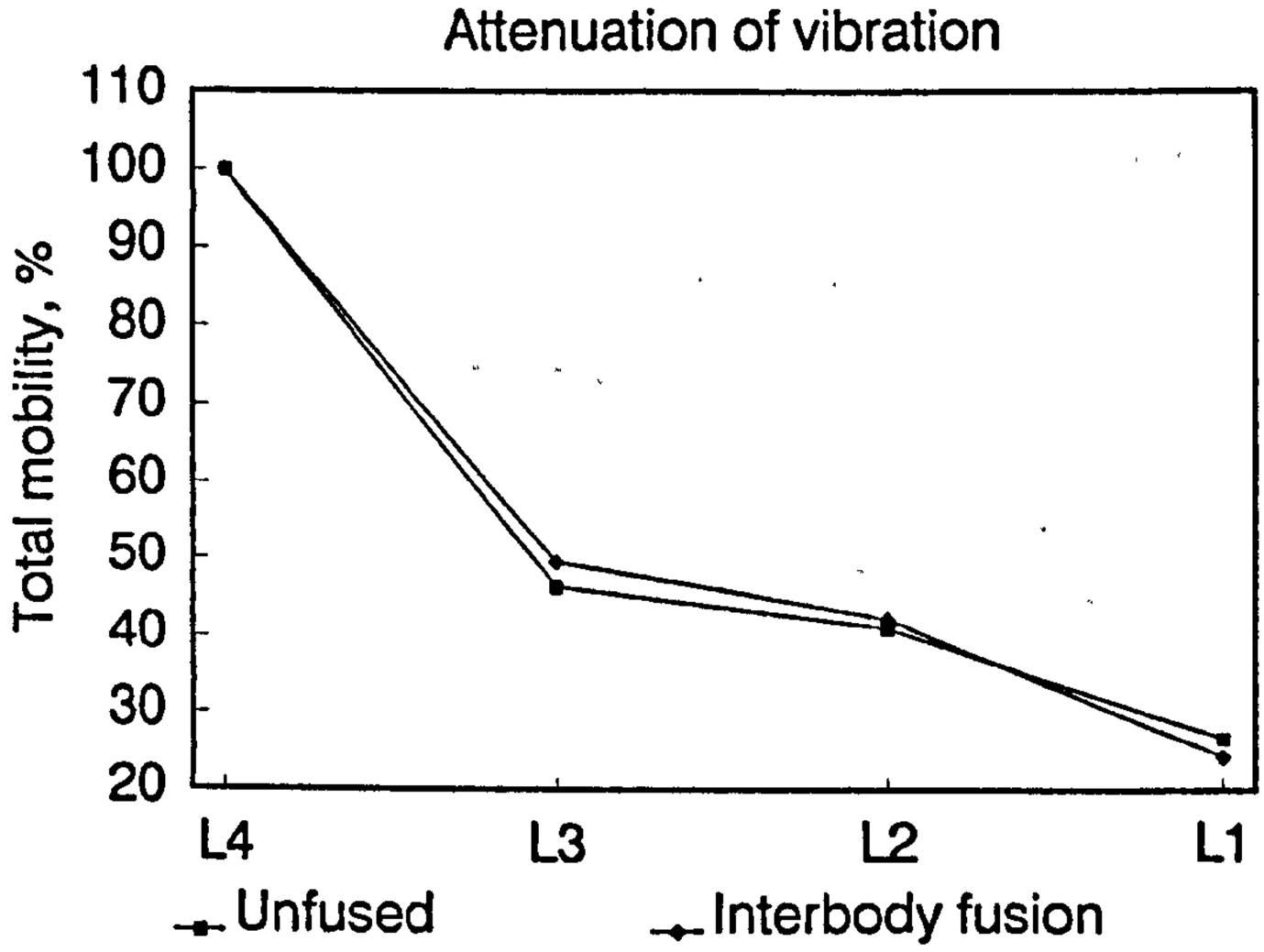

Fig 6.20 Attenuation of vibration in a specimen when unfused, and with interbody fusion.

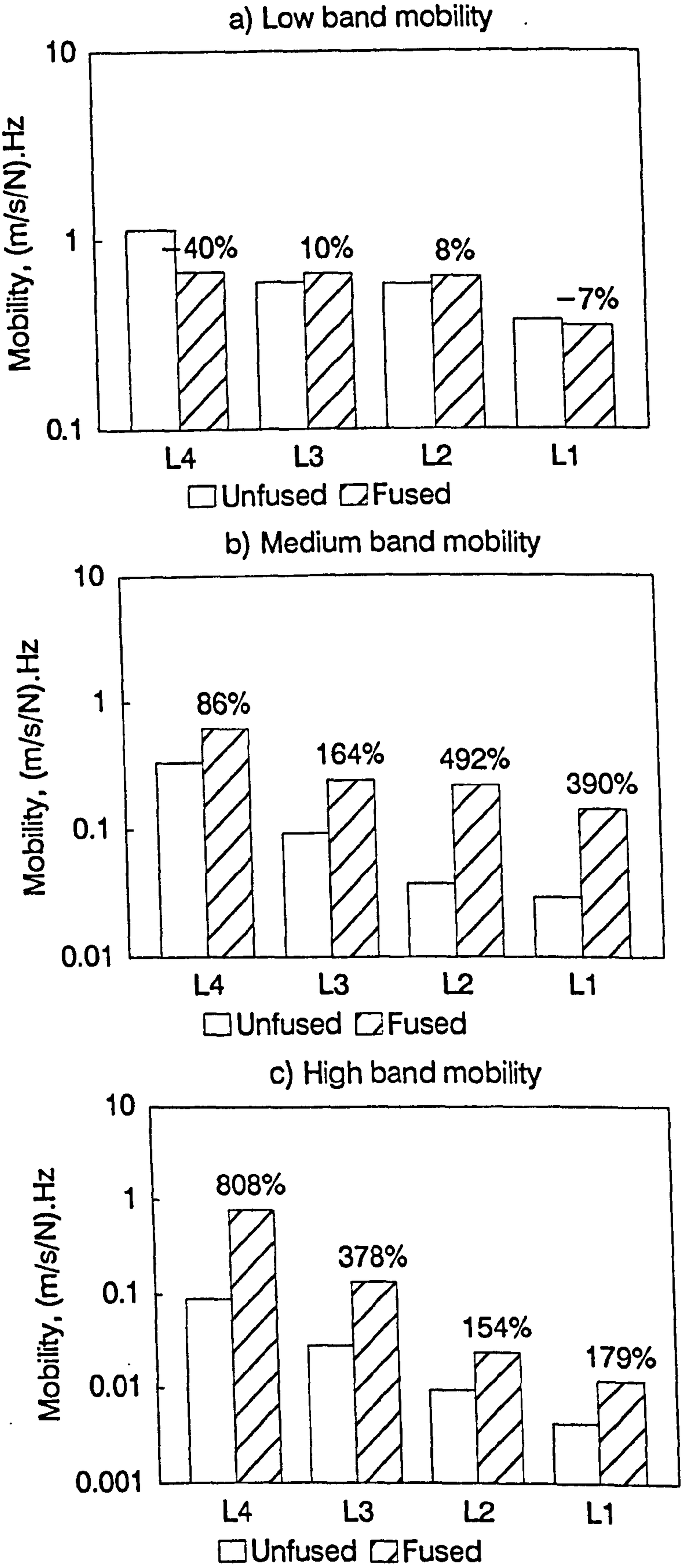

Fig 6.21 Mobility in different frequency bands measured on a specimen when unfused, and with interbody fusion. Percentage indicates increase (error = 1.8%).

figure 6.16 shows the different transfer mobility curves of the same specimen in its unfused and fused states. It could be seen that the transfer mobility curves show a similar pattern as those obtained from facet joints fusion. Both interbody fusion and facet joints fusion were noted to induce similar changes in the mechanical characteristics of the lumbar spine i.e. to increase the stiffness and decrease the damping, particularly for high frequency components. These changes induced a first flexural vibration mode at a slightly higher frequency. The higher flexural vibration modes were suppressed or effectively damped. However, the transmission of high frequency vibration in the lumbar spine was enhanced with interbody fusion.

Figures 6.17 and 6.18 show the summated mobility curves of a fused lumbar spine in comparison with its unfused state. Curve-fitting to equation 5.7 was performed for the summated mobility curves measured at different segments. The measured summated mobility curves were found to fit closely to the mathematical model, with the coefficient of determination $R^2 > 0.98$. Table 6.3 shows the coefficients A and b determined for the lumbar spines with interbody fusion, and also includes the figures obtained in their unfused state for comparison. Statistics by paired t-test shows a significant difference between these two sets of figures, with $p < 0.01$. The figures also suggest that interbody fusion induced the same effect on the summated mobility, and hence similar findings as those of facet joints fusion were obtained.

The total mobility was found to show an increase in absolute measurements at all segments, with a range of 20% to 95% increase in the extreme cases. Figure 6.19 shows a typical case. A similar trend of attenuation was observed on an unfused lumbar spine and one with interbody fusion (fig 6.20). The attenuation coefficients obtained for these lumbar spines did not show any significant difference (table 6.4). The result also suggests that interbody fusion

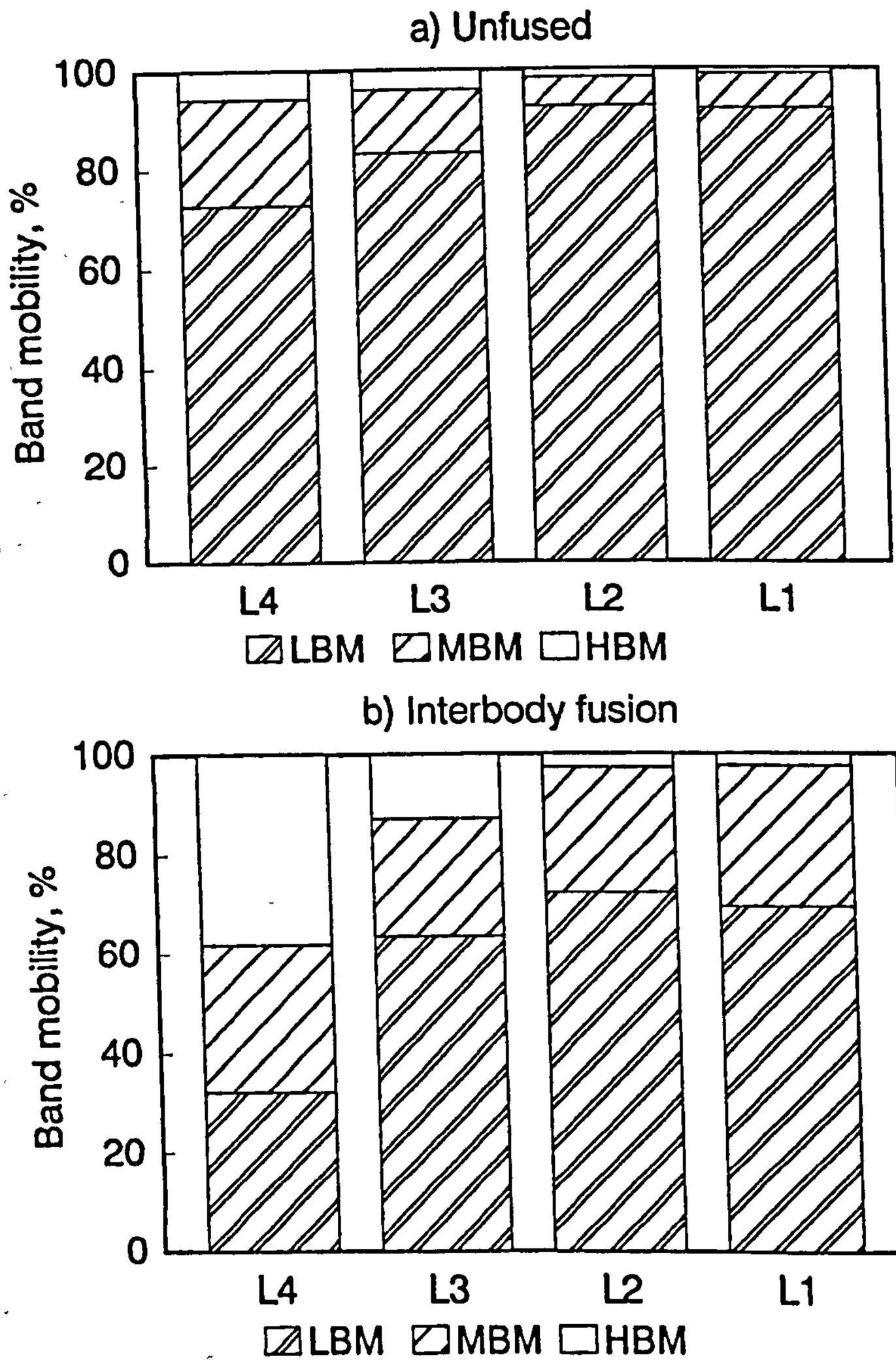

Fig 6.22 Distribution of mobility among different frequency bands of a specimen. a) Unfused; b) Interbody fusion. (LBM = low band mobility; MBM = medium band mobility; HBM = high band mobility)

induced a similar change to the mechanical characteristics of the lumbar spine as did facet joints fusion. The overall vibration response was enhanced whilst there was no induced improvement in the attenuation i.e. increase in inter-segmental transmission.

The band mobility was showing a marked decrease in the LBM for L4, but a significant increase in the MBM and HBM for L3 and L4. A point which is worth noting is that the effects of interbody fusion were more pronounced at L4 and L3, probably due to the fact that interbody fusion was only performed between the L3 to L5 segments. Hence the effect is expected to be more localized. It is anticipated that interbody fusion would produce a more extensive effect if it was performed on more segments. Figure 6.21 shows typical band mobility defined for a fused specimen to compare with the measurements obtained in its unfused state. As with facet joints fusion, there was a redistribution of mobility in the medium and high frequency bands with interbody fusion (fig 6.22).

6.5 SUMMARY

The simulation of facet joints fusion and interbody fusion is considered an analogy to sub-structuring in engineering concepts. These fusions were effective in inducing increase in stiffness and decrease in damping of the lumbar spine specimens. The overall vibration response of the fused lumbar spine did not demonstrate a significant change in the low frequency band apart from a small decrease in some cases. First mode of flexural vibration in the sagittal plane was observed in the fused lumbar spine at slightly higher frequencies, probably as a result of the increase in stiffness of the structure. However, the enhancement of mobility in the medium and high frequency bands was very distinct. These changes were most remarkable at the L4 and L3 segments which were most adjacent to the excitation source, and in some cases these increases went up to more than 10-fold. It was also noted that facet

joints fusion or interbody fusion promoted the effectiveness of vibration transmission in the whole lumbar spine. These fusions did not change the proportionality of the mobility between individual segments. Neither did these fusions induce any enhancement in the transmissibility of vibration across individual segments. However, the overall changes in the mechanical characteristics of a fused lumbar spine can be characterized by parameters associated with summated mobility curve, total mobility and band mobility measurements. The coefficient A doubled while coefficient b reduced by half of its value with simulated fusions.

The vibration technique and subsequent analysis of the response were able to detect the changes in the mechanical characteristics of the lumbar spine as a result of simulated fusions. However, the technique was not able to differentiate between the type of fusions incorporated with the specimen, neither was it able to illustrate the finer structural changes at each segment. It was only able to define the gross structural modification of the lumbar spine as a whole.

The methods of simulation of fusions, particularly the interbody fusion, were less rigid in comparison to a real fusion through grafting of bone. Surgically fused intervertebral joints would provide far more effective mechanical links between the lumbar segments. However, the vibration technique which has been found to be sensitive enough to identify the increased structural stiffness of simulated lumbar fusions could be a powerful tool for the detection of structural modifications related to changes in stiffness and damping of the lumbar spine. The technical feasibility and clinical applicability of vibration response analysis on normal subjects and patients have yet to be tested.

CHAPTER 7

VIBRATION RESPONSE OF THE LUMBAR SPINE IN-VIVO

7.1 INTRODUCTION

Previous vibration response analysis carried out on the lumbar spine specimens have identified useful parameters such as transfer mobility and band mobility. The vibration technique has been found to be sensitive enough to detect changes in the mechanical characteristics of the lumbar spine as a result of simulated fusion of the facet joints and of the vertebral bodies. The technique was extended to non-invasive vibration testing on normal subjects, and three patients with known history of surgical fusion and one with osteoporosis of the lumbar spine. The aim was to develop a non-invasive vibration technique for reliable and safe measurements and analysis of vibration response of the lumbar spine. It was hoped that useful parameters could be determined to help understand the mechanical characteristics of the lumbar spine in relation to its structural changes in a live situation. It was also the intention of this study to examine how those parameters changed under a pathological condition.

Individual variations are expected to be high. These include personal tolerance and also individual response to vibratory excitation, anatomical characteristics such as height, weight, lumbar curvature and associated anthropometrical dimensions. It would be impossible to establish a norm unless extensive measurements on a large sample were carried out. However, this study was set to investigate primarily the technical issues related to vibration response analysis on live subjects. In the light of the consistent results in the previous in-vitro study, a range of measurements could be expected and these could be useful to establish a general pattern or trend of exemplary figures for reference in an extended context.

This in-vivo study was faced with a number of technical problems at its outset. The testing was to be

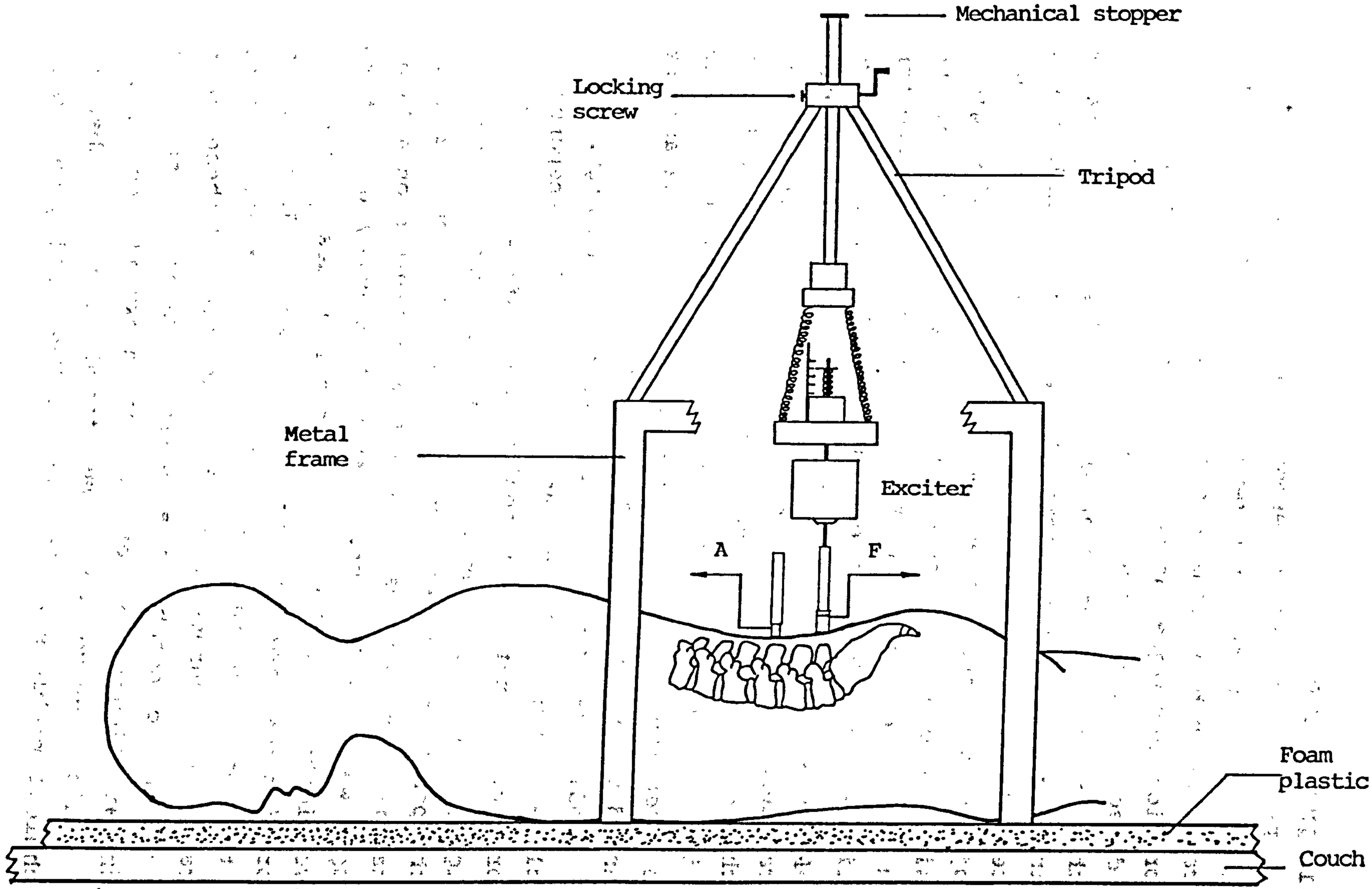

Fig 7.1 Experimental set-up of measurement of vibration response of the lumbar spine. F and A are respectively force and acceleration signals input to charge amplifiers.

confined to non-invasive techniques. This entailed an excitation system which generated non-invasively sufficient vibratory force within safe limits at a suitable point of the lumbar spine to achieve a measurable and repeatable response, but yet not be excessively strong to induce non-linearity of the system. Vibration response to the external excitatory force was to be measured at suitable locations on the lumbar spine through the use of an accelerometer attached non-invasively over the spinous process. However, the skin is known to have limited frequency response especially at the high frequency range. Some technical solution would be required to ensure reliable measurements over the skin. The problem will be more critical at the measuring point since the frequency response of the skin will be a major issue as to whether the vibration response at the bone will be genuinely measured. These are discussed further in section 7.4.

Vibration testing on normal subjects and patients basically followed that developed from the in-vitro study. The same set of testing equipment was used though the mountings of the exciter and vibration transducers were modified. The testing mainly involved the application of an excitatory force at the L5 spinous process, while vibration response was monitored and measured at L1 to L4. Vibration response analysis on the lumbar spine was carried out on normal subjects and patients. Pertinent parameters such as transfer mobility and the band mobility have been determined to establish a preliminary database for reference of these parameters for live subjects under normal and pathological conditions.

7.2 EXPERIMENTAL DESIGN

The experimental set-up and the block diagram of the equipment are shown in figures 7.1 and 7.2. The testing equipment described in section 3.8 was used. The tests were performed by an operator whose primary role was to hold the transducers at appropriate positions, and to conduct the

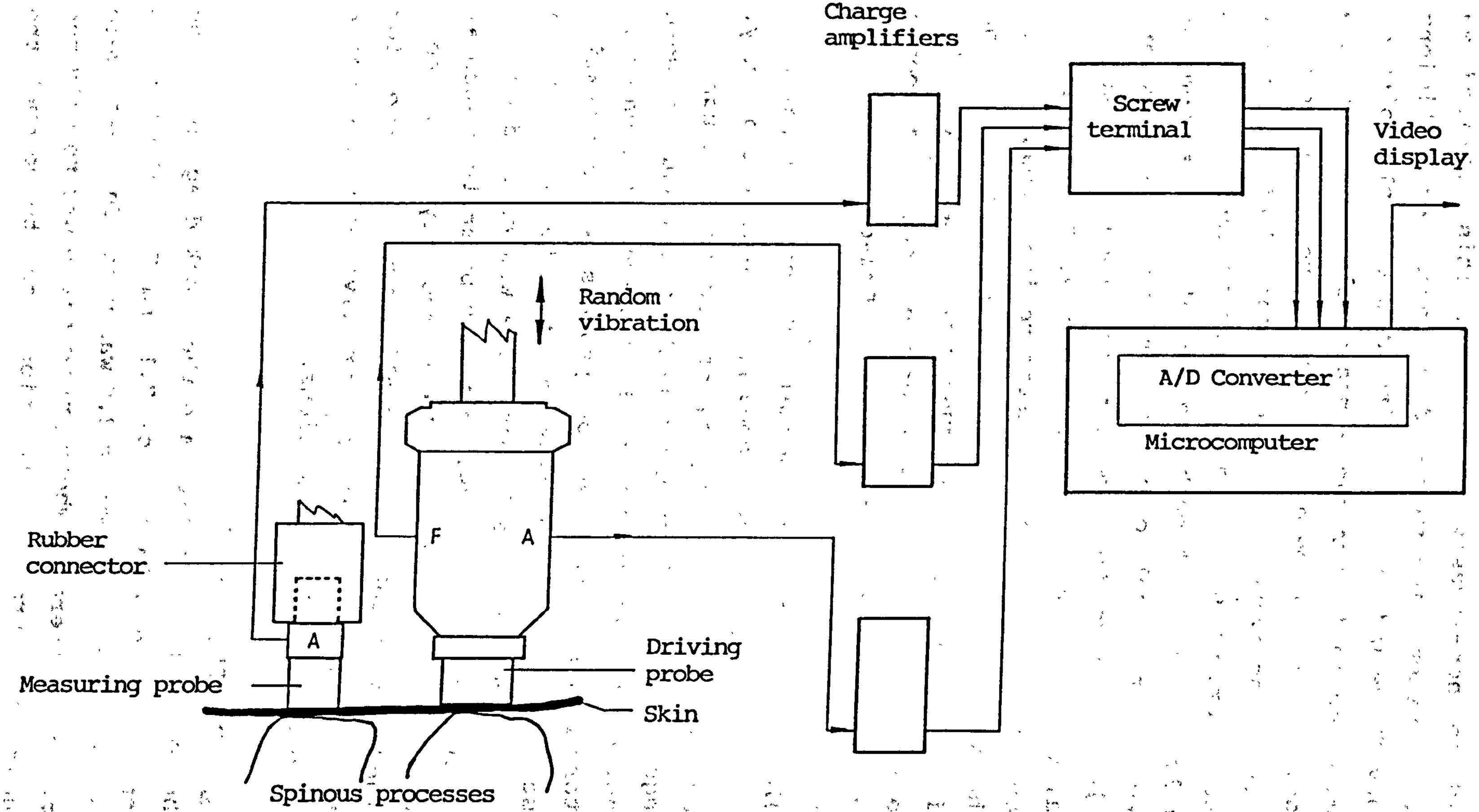

Fig 7.2 Block diagram of equipment for the vibration response analysis of the lumbar spine. F and A are respectively force and acceleration signals input to charge amplifiers.

testing procedures. An assistant was recruited to operate the equipment.

7.2.1 Selection of Subjects

Young normal subjects who did not have any known pathology or abnormality in the musculoskeletal system were recruited for the tests. The age group was between 20's and early 30's which is considered the prime period of bone maturity. The normal subjects were checked against a list of criteria stated below to exclude:

a. previous back pain;
b. known history of surgery or trauma to the back;
c. known pathology or abnormality of the musculo-skeletal system, particularly in the spine;
d. disturbance to the renal and genito-urinary functions;
e. pregnancy;
f. disturbance to gastro-intestinal functions;
g. disturbance to cardio-pulmonary functions;
h. any discomfort in the thoracic, abdominal or pelvic cavities;
i. any potential restlessness and anxiety related to excessive noise and vibration;
j. any mental disorder;
k. retinal detachment; and
l. prosthesis (internal or external, denture not to be excluded).

The patients were recruited on the recommendation of medical personnel. Criteria a, b, c and l were then suitably modified in the consideration of individual cases.

7.2.2 Preparation of Subject

The aims and arrangement of the study were explained to the subject. He was introduced to the experimental set-up and his involvement in the testing was explained to gain cooperation. Informed consent had been obtained from the subject prior to the tests (appendix III). The subject was

in appropriate clothing to ensure comfort, and to enable the lumbar spine to be exposed for the placement of vibration transducers. The subject had also been briefed on the function of the excitation system and he was also instructed to practise the use of the stop-switch implementing an over-riding stop to the vibration system.

7.2.3 Position of Subject

The subject was tested in a prone lying position on a stable, foam-padded examination couch. Suitable support by soft pillows or thick towels was used as deemed necessary to flatten the lumbar curve. Tension in the abdominal and paraspinal muscles would contribute to the rigidity and hence the stiffness of the lumbar spine. It was not quite certain how much these muscle actions would affect the results. This was a technical issue which had to be rectified before a reliable and valid testing be guaranteed. However, a restful position would ensure minimal muscle activity. The subject was reminded to maintain relaxed and natural breathing by keeping the head, the limbs and the rest of the body in a restful position. This also helped to calm down breathing and to reduce heart beat. It was not quite sure how much the breathing movement in the chest would affect the positioning and hence the results. Heart sounds and noise generated in the bowel and the abdominal cavity require attention if they contribute to noise in the measurement. This was checked in the actual testing. A restful prone lying position would also help to maintain consistent and repeatable positioning.

7.2.4 Test Protocols

Random vibratory force of less than 1 N (peak) was applied to the L5 spinous process through the use of an instrumented probe (section 7.3.3). The vibratory force and acceleration were measured at the same driving point while the vibration response was measured as acceleration at the L1 to L4 spinous processes in turn. The force and

acceleration signals were sampled at 10 kHz for 65536 data points of each record. The band-pass filter on the charge amplifier was set to the range 2 Hz to 3 kHz. Sections 7.3 and 7.4 discuss in further details the application of vibratory force at the lumbar spine and the measurement of its response by various devices.

7.2.5 Safety Measures

The power amplifier was equipped with an attenuator controllable stepwise by 10 dB intervals up to 40 dB. The output from the power amplifier was also limited by its own circuit should the output level exceed the preset rating. This ensured that the exciter was not driven by any extraneous noise which would impose excessive compressive force potentially dangerous to the test subject.

The peak force rating of the exciter is 10 N and its own weight is 11 N. Since the exciter was spring-mounted, any erroneous excitatory force above this level would only result in raising the exciter against gravity instead of pressing strongly against the subject's lumbar spine. This spring mounting mechanism ensured safety against any mechanical overload to the subject.

The operator, at any instant, could discontinue the excitation to the subject by lifting the force transducer off the spinous process should the subject complain any discomfort, or express any wish to stop the test for whatever reasons. The operator, at his discretion could terminate the test if an adverse situation arose.

A dual channel oscilloscope was available to monitor the force input to the lumbar spine. As already mentioned in section 3.8.1 an over-riding stop-switch for the subject was installed to ensure safety.

The force and acceleration transducers give a quantity of charge corresponding to the force level and vibration level. The transducers were connected to the charge amplifiers which were battery-driven. The charge amplifiers gave a peak-to-peak output voltage of 8 V, and were

connected to a screw terminal which fed to the differential inputs of an analogue-to-digital converter housed in a microcomputer. The transducers were of very high electrical resistance (20,000 MΩ), and practically drawing no current from the circuit. The transducers were placed over the spinous processes through the use of nylon probes (fig 7.4 & 7.9). These ensured safety against leakage of electrical current when they were in contact with the test subject. The power amplifier and the computer were all grounded at the same point to prevent ground-loop which would also cause contamination of the signals. The chasses of all equipment including: the signal generator, tape-recorder, power amplifier, and the computer were adequately grounded. The subjects did not form any part of the electrical circuit, and both the subject and the operator were effectively isolated from high voltage and strong current. The test set-up complied with recommendations on safety in British Standard BS 7085 (1989).

The subject was kept under supervision for at least 15 minutes after the test, before leaving the laboratory. He was able to communicate easily with the investigator and advised to seek medical care should any discomfort arise as a result of the vibration test.

7.3 EXCITATION

The random vibratory force was applied in association with a compressive force of 10 N. One may worry about the effect of compressive force on the lumbar spine which might cause non-linear response under a compressive force in the postero-anterior direction, as reported by Lee and Evans (1994). However, this vibration testing involved the application of a very small force which induced only a minute displacement. This corresponded to a very small portion of the force-displacement curve, and within this small range of force and displacement, the system could be considered linear. System linearity can also be further examined in the actual testing.

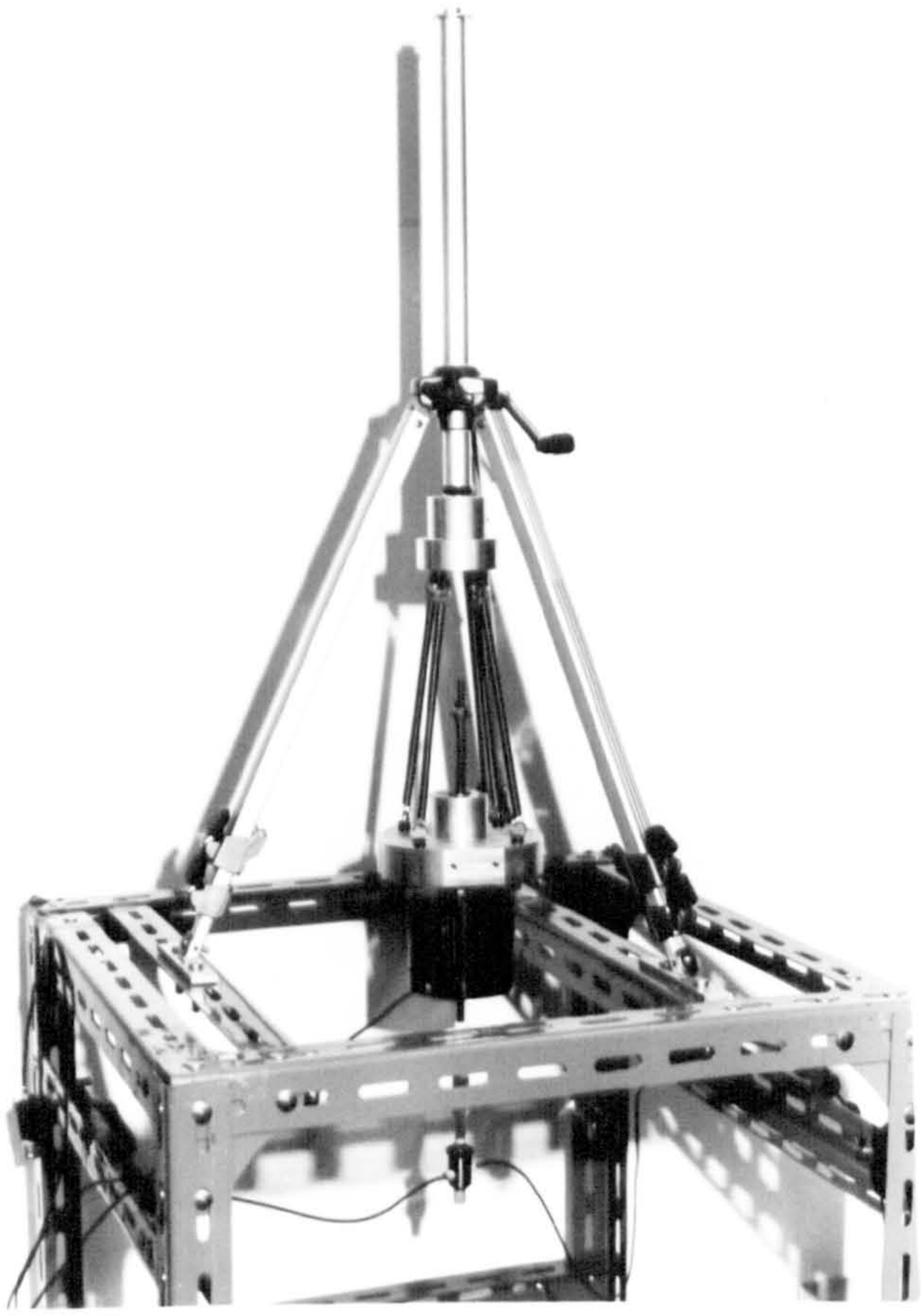

Fig 7.3 Support mechanism for the electrodynamic exciter.

7.3.1 Application of Random Vibratory Force

Random vibration of frequency range from 20 Hz to 2 kHz was played back by a tape-recorder and fed to the power amplifier. The peak vibratory force was limited to 1 N. This force level produced a vibration level corresponding to a vibration dose value VDV of less than 5 $ms^{-1.75}$ in accordance with the definition recommended by British Standard BS 6841 (1987). It was also within the total daily vibration exposure limit of 15 $ms^{-1.75}$ beyond which the attendance of medical personnel is recommended. However, this recommended safe limit assumes a whole-body exposure to continuous vibration with weighting biased to the frequency range between 0.5 Hz and 80 Hz. In this test, the subject was exposed to intermittent vibration of short duration of about 6.5 s, and with a force spectrum spreading up to 2 kHz. The excitatory force was applied only locally to the lumbar spine. Thus, the VDV involved in this testing was far less than the recommended safe limit. Furthermore, the level of exposure to vibration was much lower than those experienced in common forms of transportation and civilian working environments. This in-vivo vibration test was therefore considered safe.

7.3.2 Support Mechanism for the Exciter

A rigid frame fabricated from steel bars was used to support the exciter which was placed above the lumbar region. The exciter was held vertically by a thick spring-mounted rod through the centre of a thick aluminium disc, and it was allowed to move freely in the vertical direction. The disc was suspended by four springs attached to the lower end of the adjustable stem of a modified photographic tripod which was mounted securely over the top of the metal frame. The adjustable stem allowed vertical adjustment of position of the exciter. A locking screw fixed the stem in position and prevented it from sliding down. Safety was further enhanced by a mechanical stopper at the top of the stem to prevent it from sliding down by

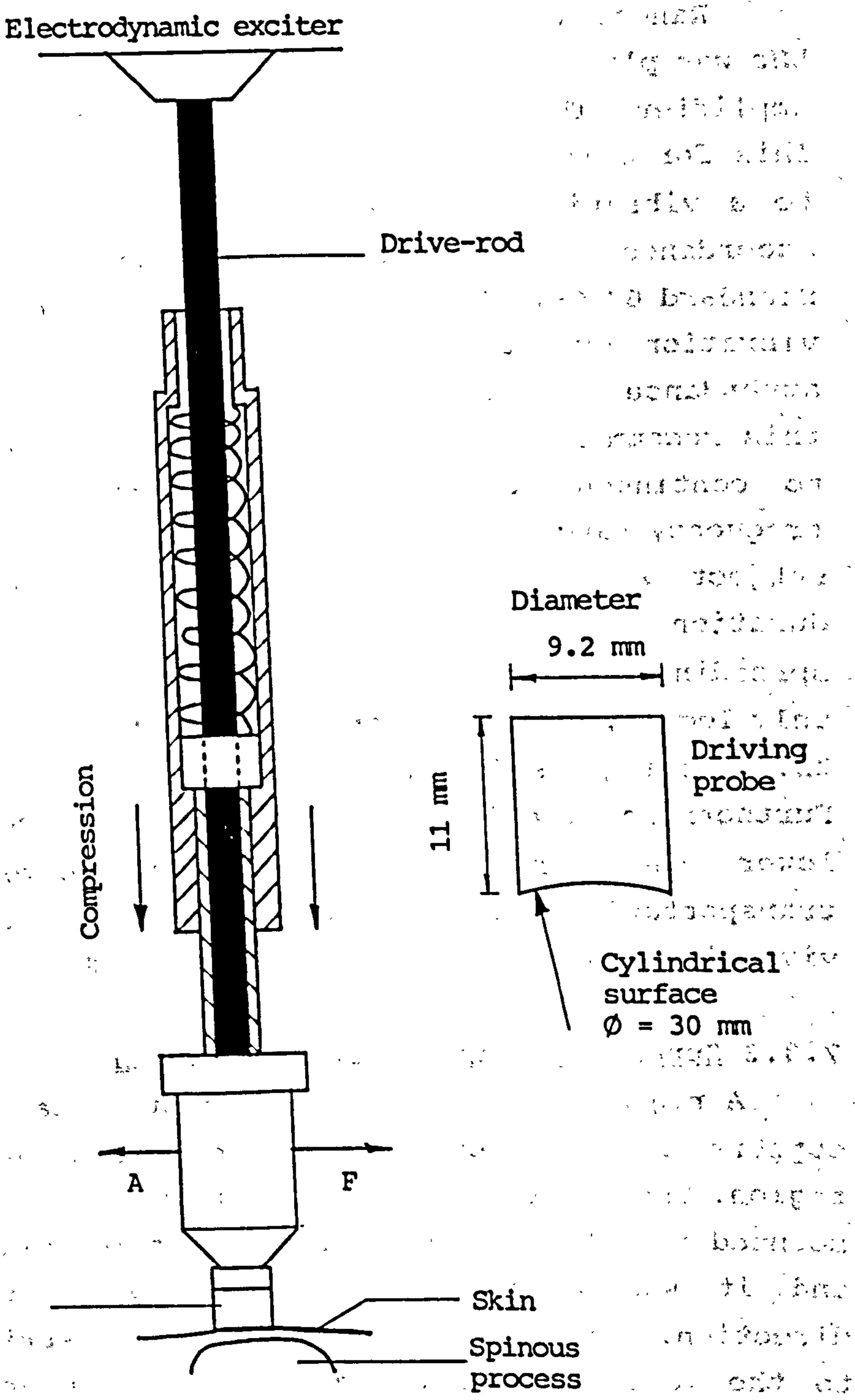

Fig 7.4 Holder of the impedance head showing the spring mechanism and the drive-rod which transmits the driving force from the exciter. F and A are respectively force and acceleration signals input to charge amplifiers.

accident. The spring mounting system also ensured that the exciter was effectively decoupled with its suspension system and prevented any vibration transmitted from the environment. Figure 7.3 shows the support mechanism for the exciter.

7.3.3 Transduction of Excitatory Force

An impedance head was attached to the lower end of a nylon drive-rod which was incorporated in a calibrated spring mechanism installed in a plastic holder (fig 7.4). The drive-rod was connected to the table of the exciter at the upper end. The holder was held manually by the operator who then pressed the transducer against the L5 spinous process to achieve a firm contact. This compressive preload to the skin was maintained to about 10 N by fully compressing the holder against the spinous process. The cylindrical surface of the driving probe which was in good contact with the skin ensured stability by preventing lateral slipping over the spinous process. The vibratory force was transmitted via the drive-rod which was flexible to decouple vibrations in other directions perpendicular to the main axis of the transducer.

It was noted that breathing would induce slight tidal movement of the lumbar spine. The test subject was advised to keep calm and relaxed during the test. Furthermore, shallow breathing only contributed movements at an extremely low frequency which was beyond the sensitivity of the transducers and these were filtered off by the band-pass filters on the charge amplifiers. The force transducer remained in good contact with the skin and maintained its position over the spinous process. The compressive preload force was maintained and undisturbed by the breathing movements.

7.4 MEASUREMENT OF VIBRATION RESPONSE

Acoustical signals emitted from bone and joints can be picked up by accelerometer or microphone though Mollan

(1981) advocated the use of the former and commented on the inadequacy of the latter. The deficiency of the microphone may relate to the problem of ambient noise and the limited frequency response of the microphone which did not fit well with Mollan's work in the lower frequency range (within 250 Hz). Mismatch in acoustical impedance would render ineffective transmission of acoustic energy across the skin. This part of the study was intended to re-investigate the technical value of acoustic transducers by implementing some modifications in the design of sensing devices using microphone and hydrophone. The attachment of the accelerometer was also investigated to achieve the best recording of vibration signals. The practical value of these transducers were compared by the signals they picked up from the medial malleolus of a tibia which was being excited by random vibratory force at its mid-span. Assuming the same vibration response at the medial malleolus, the frequency responses of these transducers were compared. The lumbar spine can be considered a less rigid system because of its irregular shapes and the complex structure with intervertebral joints. Being a solid piece of bone, the tibia is expected to show a better transmission to vibratory excitation. A vibrating tibia serves as a simpler but better controlled structure to test the applicability of various types of vibration sensors. These sensors have to perform satisfactorily on the tibia before their application at the lumbar spine be acceptable.

7.4.1 Measurement by Microphone

A miniature microphone insert (Maplin Type EM-6), diameter 6.5 mm and 5.5 mm thick, was housed in a modified neonatal stethoscope head with a vent to equalize the static pressure between the inside and outside (fig 7.5). This assembly was designed to sense the acoustic pressure set up in the small cavity inside the stethoscope head due to vibration of the medial malleolus over which it was placed. Output from the microphone was amplified with a

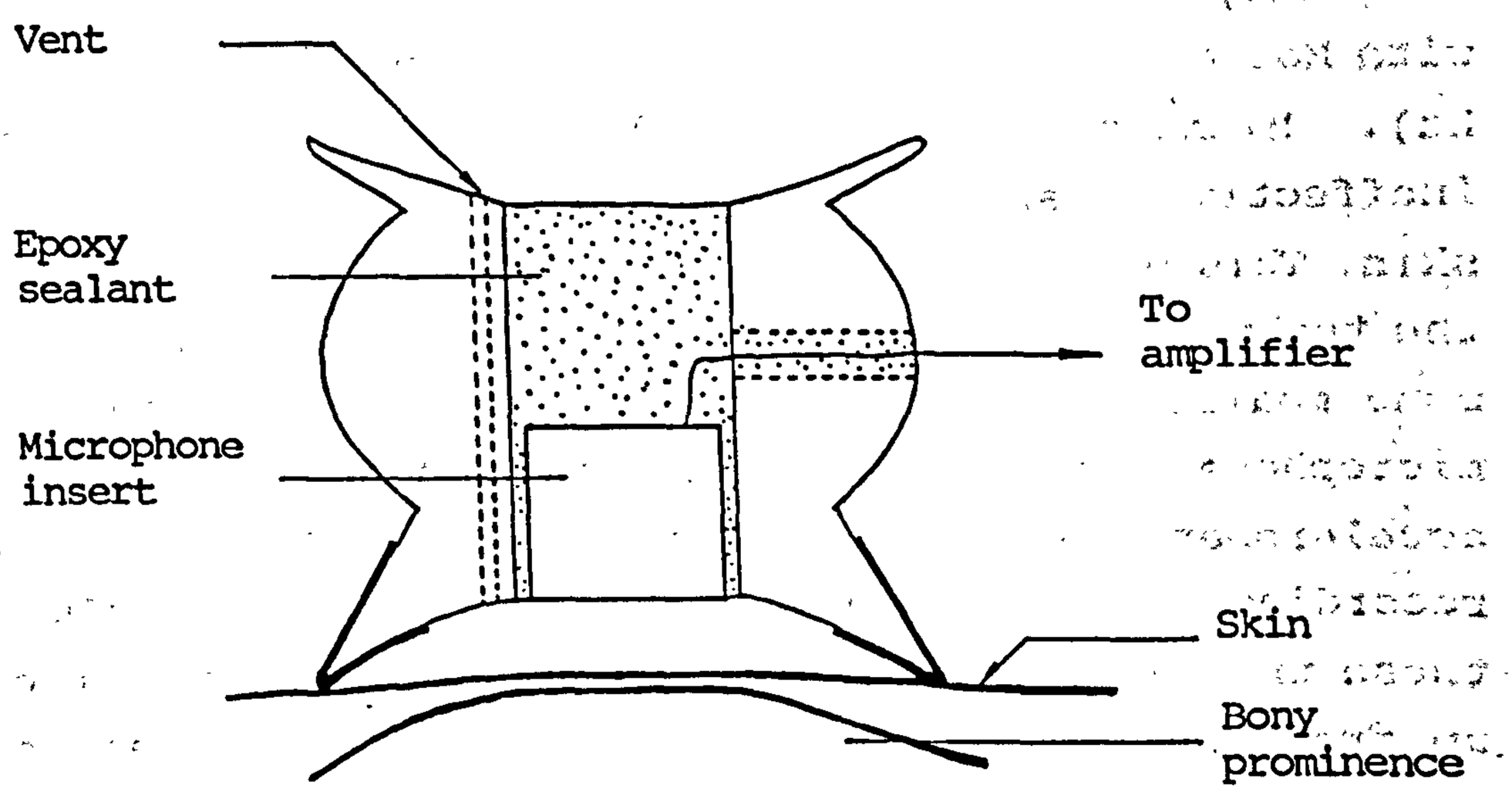

Fig 7.5 Installation of a microphone insert in a modified neonatal stethoscope head. (Dimension: 3× real-size).

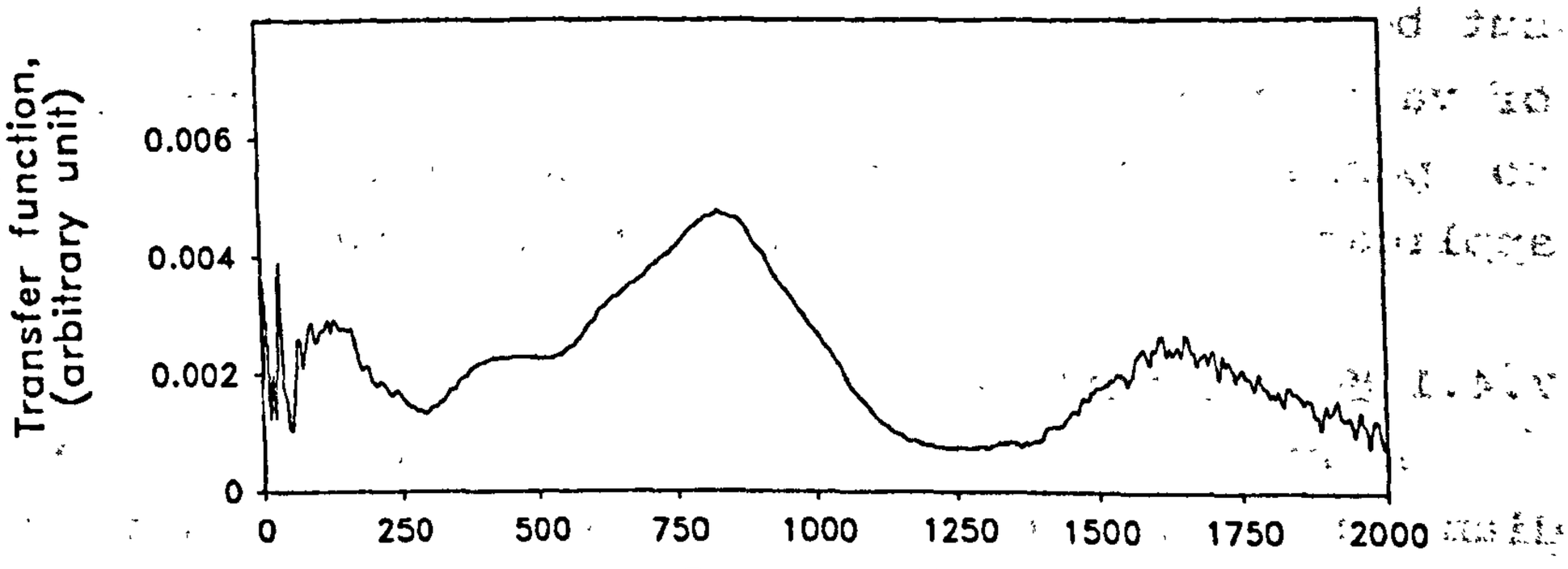

Fig 7.6 Vibration response measured by microphone over the medial malleolus of a vibrating tibia.

gain of 100 times by a custom-made ±9 V battery-driven amplifier. The microphone insert was claimed to have a frequency response from 50 Hz to 8 kHz, and it was found to be effective in picking up vibration signals from the bone. The spectrum of the signal is shown in figure 7.6. It was noted that the response signal was weak in its high frequency contents and the coherency was lower when compared to an accelerometer (fig 7.11). This suggests that this modified acoustic sensor was not a suitable device for the detection of bone vibration in the higher frequency range above 1.2 kHz. The main reason would be that this acoustic sensor did not offer any compression to the skin to enhance transmissibility. The microphone assembly was also found to be less reliable than the accelerometer in the frequency range below 250 Hz, as shown by the lower coherence function (fig 7.11). Technically this microphone-based vibration sensor has a major advantage that it is robust and is not too critical regarding its attachment over the bony prominence. It does not require great compressive force, and a firm contact is just what would be adequate for convenient attachment. The acoustic sensor was found to be insensitive to ambient noise which measured less than 1% of the signal in an ordinary laboratory environment. The amplification factor of 100 provided by the amplifier was adequate for noise-free pick-up of vibration signals from the bone. However, the acoustic sensitivity of this sensor was difficult to calibrate for quantitative measurement. Its frequency response characteristics in the actual test set-up were difficult to ascertain. Furthermore the design did not manage to achieve a better acoustic coupling and the problem of mismatch in acoustic impedance between the sensor and the bony structure has not been solved.

7.4.2 Measurement by Hydrophone

An acoustic sensor based on a piezoelectric hydrophone (Brüel & Kjær Type 8103) was initially designed to achieve

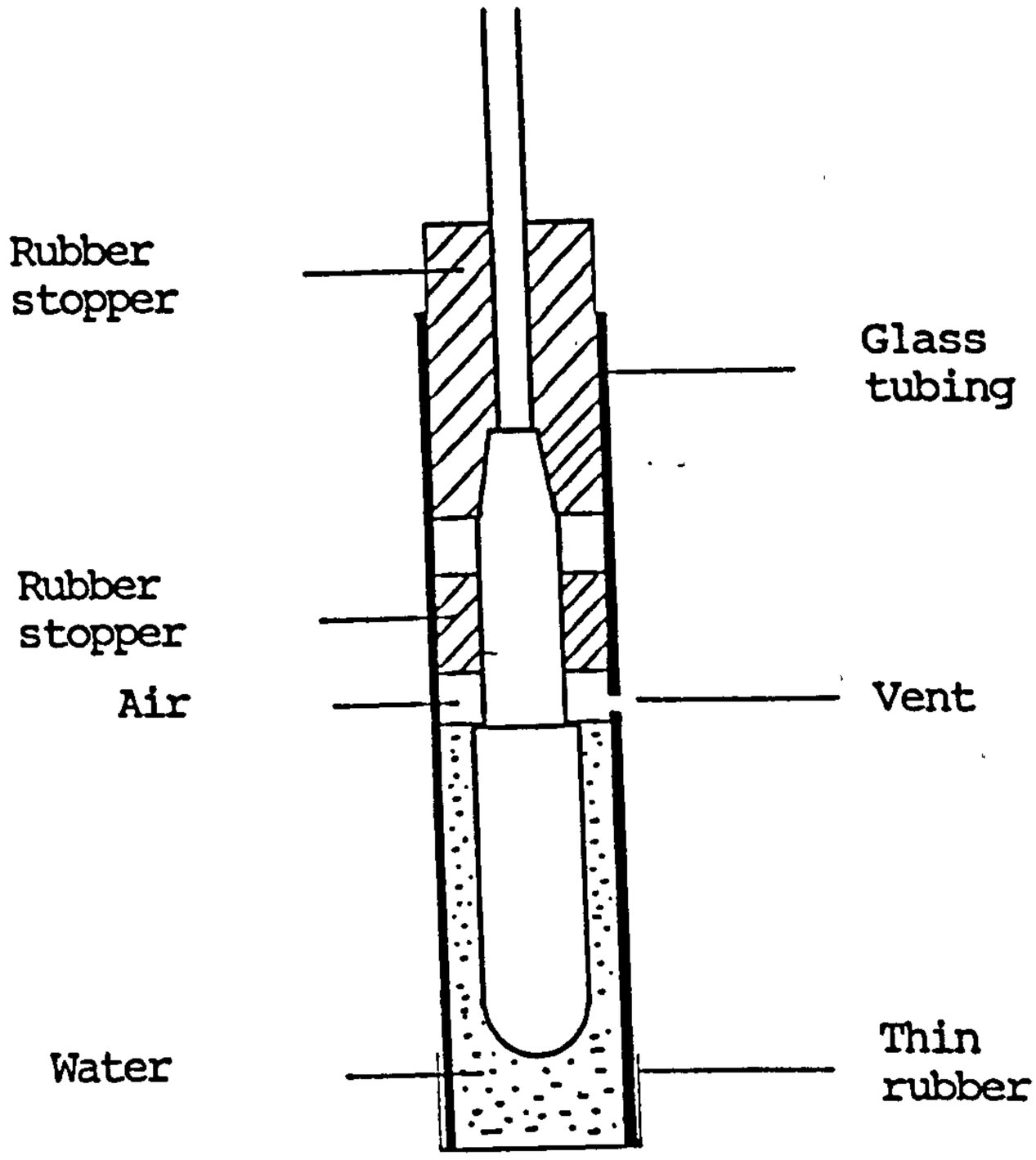

Fig 7.7 Hydrophone in a special housing. (Dimension: real-size).

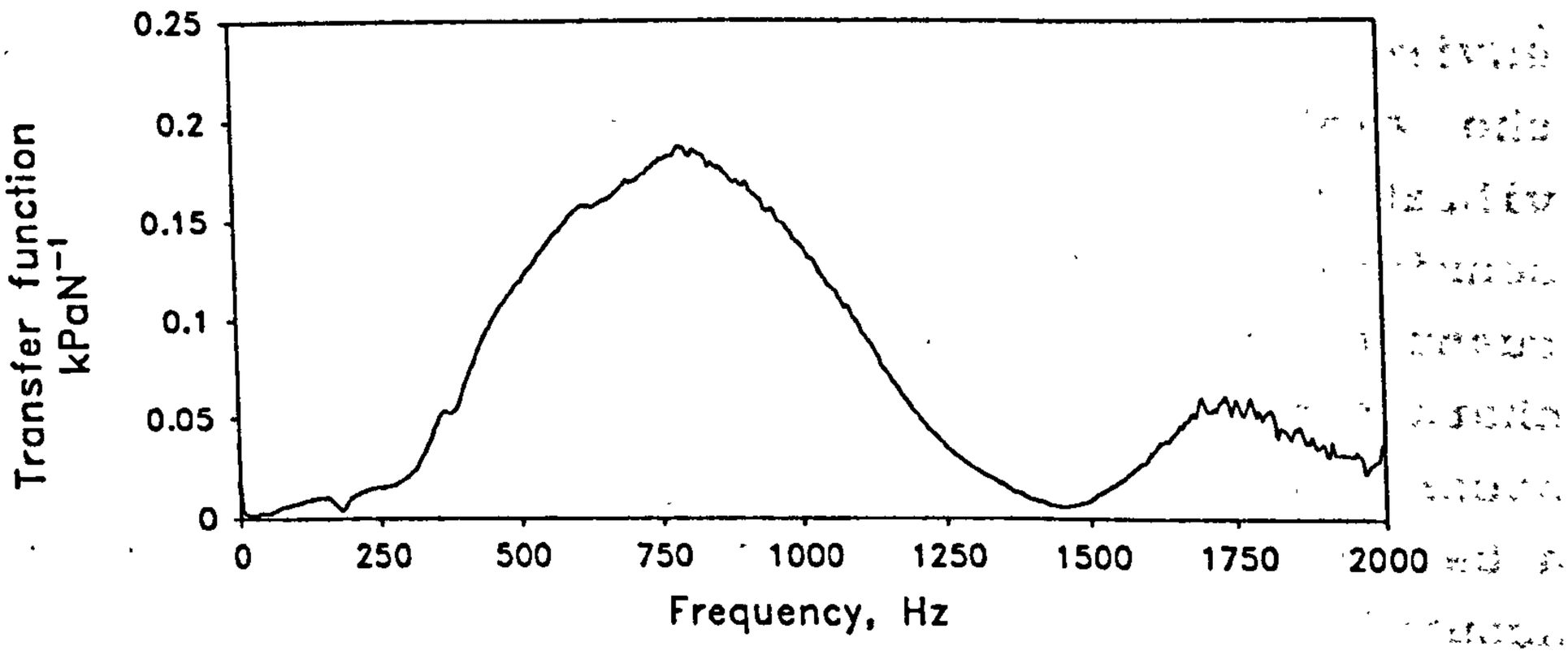

Fig 7.8 Vibration response measured by hydrophone over the medial malleolus of a vibrating tibia.

a better acoustic coupling between the sensing element and the bone. Figure 7.7 shows a hydrophone housed in a short glass tube which was filled with distilled water and sealed by a thin sheet of rubber at the distal end. The vent was designed to equalize the pressure between the inside and the outside atmosphere to eliminate static and low frequency compressive pressure on the hydrophone. The column of water served as a good acoustical transmission medium. The rubber sheet ensured good contact with the skin when the assembly was placed over the bony prominence with a gentle compression to keep the sensor in a stable position. The hydrophone picked up the change in hydrostatic pressure in the water in response to vibration transmitted at the distal end. The vibration level measured at the medial malleolus of the tibial bone was recorded while the bone was excited at its mid-span by random vibratory force within the frequency range of 20 Hz to 2 kHz.

Figure 7.8 shows the spectrum of acoustical pressure measured by the hydrophone at the medial malleolus. By referring to its lower frequency response with respect to the accelerometer (fig 7.10), the hydrophone was found less sensitive to vibration at frequencies below 250 Hz. Though the calibrated frequency response of the hydrophone extends well beyond 100 kHz, the assembly was found to have limited coherency in frequency range above 1.2 kHz (fig 7.11). The sensor was found to have limited frequency range because the design did not allow adequate compression to stiffen the skin over the bony prominence. The compliance of the skin and its underlying soft tissue limited the frequency range of acoustic transmission across the skin unless it was suitably compressed to increase the stiffness. This is consistent with the discussion in section 2.5.1 on the mechanical properties of skin. Adequate compression is the only non-invasive means of achieving a better transmissibility of vibration in the higher frequency range.

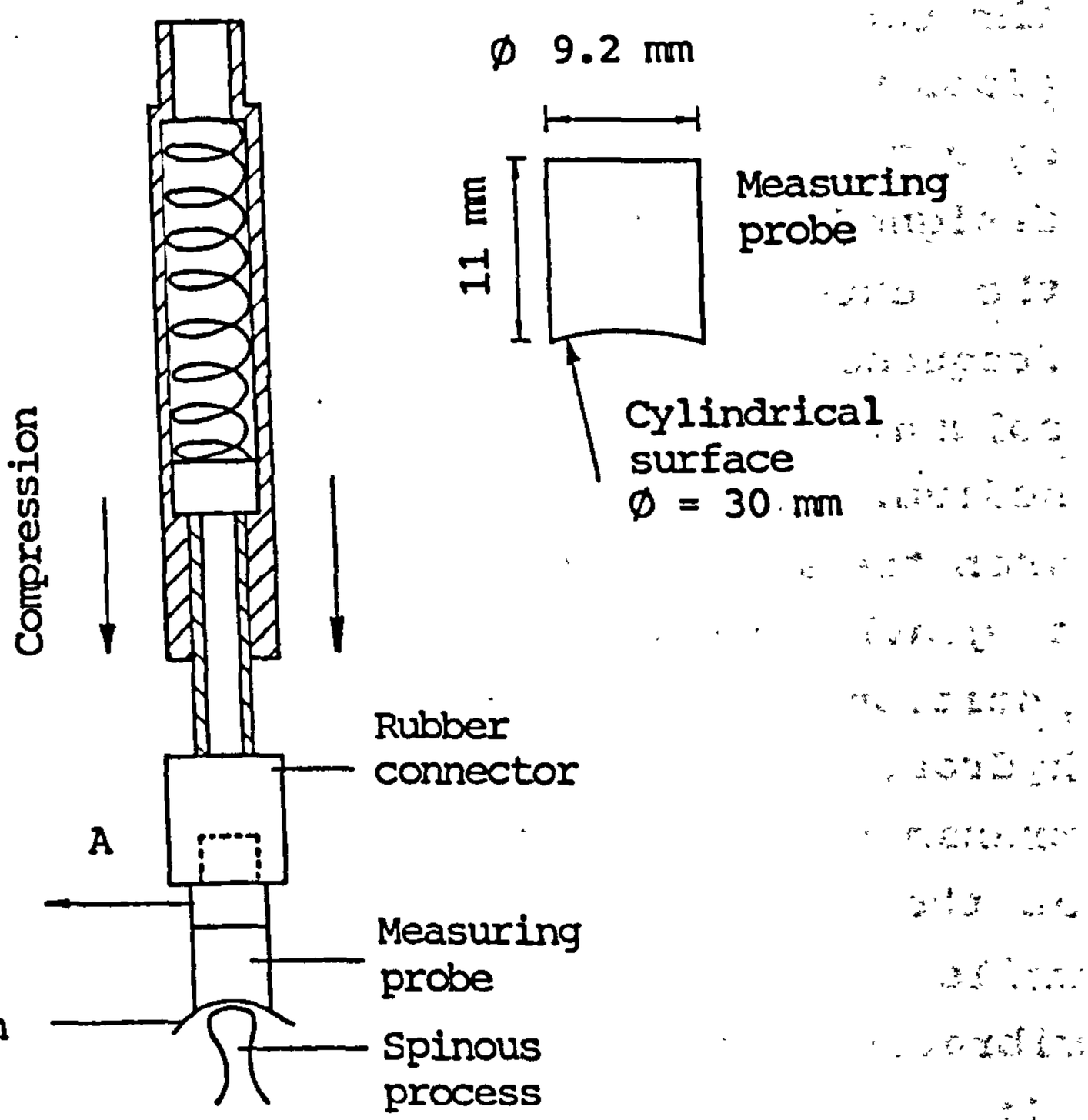

Fig 7.9 Holder of accelerometer showing the spring mechanism which applies compressive preload when compressed. A is the acceleration signal input to charge amplifier.

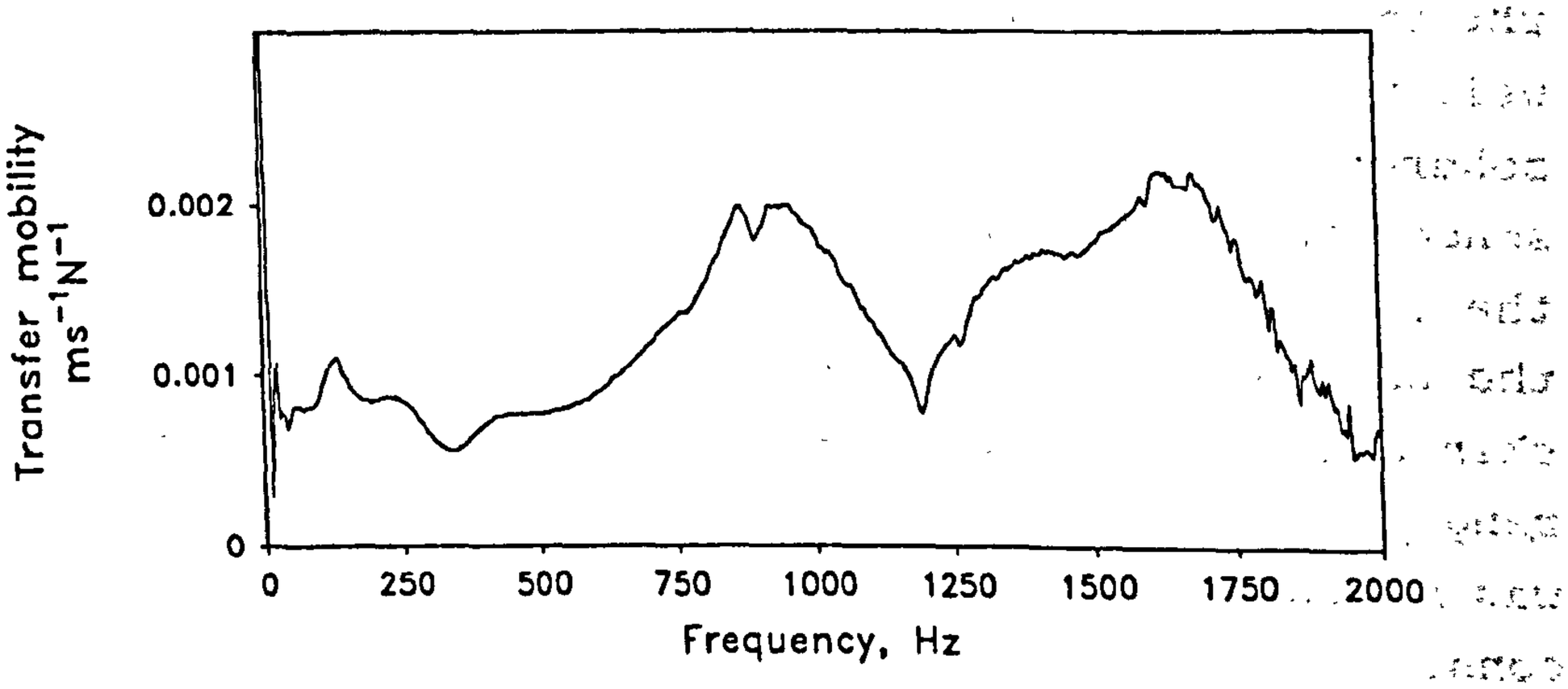

Fig 7.10 Vibration response measured by accelerometer over the medial malleolus of a vibrating tibia.

7.4.3 Measurement by Accelerometer

Referring to the previous discussion, it is clear that the skin has to be compressed to increase its stiffness, hence to enhance transmissibility. This can be achieved either by manually pressing the vibration sensor against the bony prominence, or by the use of a spring mechanism. The accelerometer was attached at one end of a plastic holder which incorporated a spring mechanism calibrated to a preload force of 10 N when fully compressed (fig 7.9). A nylon probe was machined with a cylindrical surface to maintain stability by preventing lateral slipping. The probe was attached to the base of the accelerometer, and positioned over the spinous process under compressive force to achieve a better contact with the bony prominence. Its size was also limited to avoid erroneous noise being picked up from the surrounding structures, and not to be too small to create excessive and intolerable local pressure at the point of contact with the skin.

The accelerometer has to work with a suitable compressive preload. Unfortunately an optimal compressive force level at which the frequency response of the skin is "flat" has not been established (Saha & Lakes, 1977a). Furthermore, different subjects have different tolerances to the pain caused by pressure and vibratory force. A high compressive force over a small contact area could be well above the pain threshold. It was then decided to standardize the preload force level at 10 N. Figure 7.10 shows the motion response detected by the accelerometer at the medial malleolus of a vibrating tibia. The spectrum extends well across the frequency range of interest. The accelerometer was found to be the best sensor for vibration below 250 Hz. The accelerometer also achieved coherent measurement of vibration signals within the biggest range of frequency when compared with the microphone and hydrophone (fig 7.11). The coherence function was uniform (about 0.995) up to 1.75 kHz. Hence the spring-mounted accelerometer was deemed suitable for the requirements of

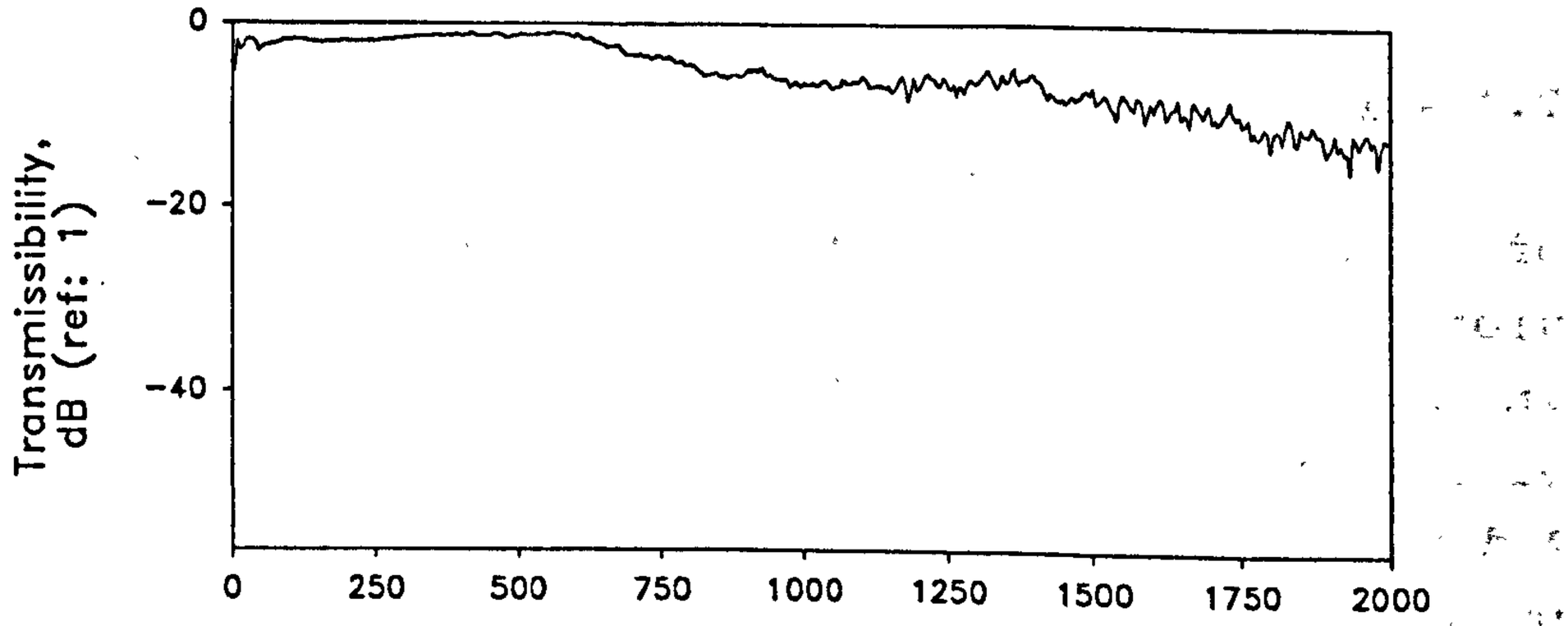

Fig 7.13 Transmissibility of skin.

in-vivo vibration response. As described in section 7.2.4, the vibratory force and acceleration were measured at the L5 spinous process of the lumbar spine. Transmissibility of vibration at the driving point was evaluated in terms of apparent mass (AM(f) = F(f)/A(f)), where A(f) and F(f) are respectively the acceleration and force expressed as a function of frequency. The transmissibility also expresses the effectiveness of the transmission of vibration from an external vibratory source to the lumbar spine. The vibration response was measured as acceleration in turn at the L1 to L4 spinous processes. Transfer mobility and summated mobility defined respectively by equations 2.34 and 5.5 were measured at each segment of the lumbar spine. Total mobility was derived from equation 5.6 by setting n = 2k. It was also attempted to fit the summated mobility curve to the exponential curve expressed by equation 5.7. The coefficients A and b were obtained by non-linear regression for curve-fitting. Band mobility defined in section 5.7.2 was also used to describe specifically the vibration response of the lumbar spine in different frequency bands. Low band mobility, medium band mobility and high band mobility were derived respectively from equations 5.9 to 5.11. Attenuation of vibration was also determined by equation 5.8 for the total mobility and the mobility in each frequency band.

7.6 VIBRATION RESPONSE OF NORMAL SUBJECTS

7.6.1 General System Characteristics

Twelve normal subjects (7 male and 5 female) have been tested with the test protocol discussed in section 7.2.4. The mean age was 22.9 years. The personal details are listed in appendix II.

All the test subjects were able to maintain a restful position in prone lying, and they managed to keep a relaxed posture throughout the vibration test. The padding underneath the abdomen effectively flattened the curve of the lumbar spine and helped to maintain comfort. There was

only gentle tidal movement of small amplitude at the lumbar spine due to relaxed and shallow breathing.

The curved surface of the probe was found to help maintain a satisfactory contact over the spinous process. The problem of dislocation of the probe due to side-slipping over movable skin was basically solved. The axial compressive preload force as was originally intended did not cause any problem of dislodging the probe from the spinous process. The compressive preload was kept at 10 N by fully compressing the spring mechanism in the holder of the accelerometer. This compressive force over a circular area of diameter 9.2 mm corresponded to a contact pressure of 150 kPa. This pressure level was higher than that of 100 kPa used by Saha and Lakes (1977a), and 55 kPa by Ziegert and Lewis (1979). None of the test subjects complained of any pain at the pressure point though some claimed discomfort after prolonged pressure. In all cases, discomfort felt at the spinous processes was relieved simply by releasing the probe. The vibration transducers were held manually. This was an effective way of placing the probes over the designated locations as the manual contact allowed sensory feedback to the operator who would then check the correct location of the probe by feeling the "firmness" over the spinous process. It was also possible to maintain the position of the probes manually throughout the test as each trial only lasted for about 6.5 s, and 3 repetitions for each location could be finished within one minute.

The excitation system was able to apply vibratory force effectively to the L5 spinous process. The vibratory force did not introduce any discomfort to the subjects, and the general feeling of the vibratory sensation was just very mild. The effective peak vibratory force was only about 0.8 N, and the RMS value less than 0.5 N. This was a very mild form of vibration when compared to what would be encountered on daily public transportation or domestic appliances. This was due to limited <u>transmissibility</u> of

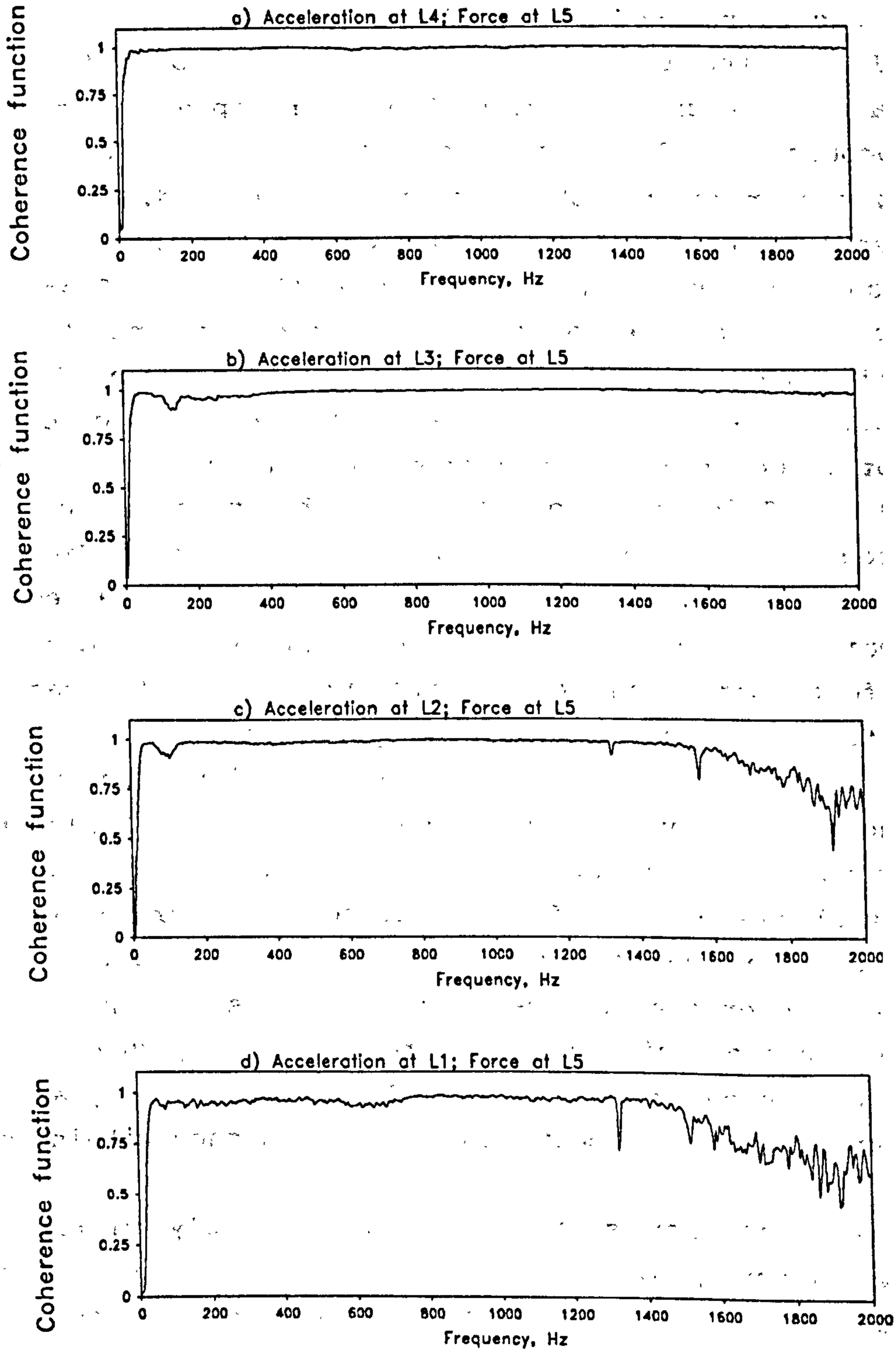

Fig 7.14 Coherence functions measured at different segments of the lumbar spine.

vibration at the driving point as a result of the compliance of skin and also of the lumbar spine, including its end supports. The general observation was that the lumbar spine was more compliant to manual compression in the postero-anterior direction when compared with a specimen of lumbar spine mounted on angle-plates at both ends.

The measurement system was sensitive in picking up vibration signals in response to external excitation at the lumbar spine. Though the vibration level at L1 was found to be very low in most cases, the accelerometer was sufficiently sensitive to pick up weak signals, and the associated amplifier enabled suitable amplification of the signals to achieve a measurable level.

The dynamic range was not specifically explored due to the limitation in the effective vibratory force that could be generated at the driving point as explained earlier. The attempt to increase the vibratory force was technically difficult and could be potentially dangerous. It was also not advisable to repeat the measurement of vibration response by increasing the vibratory force merely for the sake of exploring the dynamic range. However, it was found that the measurements of vibration response at L4 and L3 were still coherent and noise-free when the vibratory force was reduced by 12 dB. Furthermore the compliance of the skin at the measuring point accounts for some degree of attenuation to the vibration signals (section 7.4.4). Hence a reduced vibration response was recorded over the skin. This imposed further limitation in the dynamic range of the vibration response measurement when compared with an in-vitro situation.

The coherence function between the excitatory force and the vibration response was high and close to unity in all tests provided the compressive preload force for the measuring probe was adequate. Figure 7.14 shows typical examples of coherence function measured at different segments. It was found that the coherency gradually

decreased, particularly in the high frequency range when the measuring point was moved to higher levels i.e. farther away from the excitation source. The coherency also decreased when measuring on subjects with bigger body mass. In these situations, a higher compressive preload at the measuring probe would be required to solve the problem especially when the vibration response was measured at L1 and L2. Referring to discussion in section 5.3.2 on the linearity of system response, high coherency indicates that the lumbar spine also behaved as a linear system in response to vibratory excitation in-vivo. It was concluded therefore that the system analysis strategy adopted in this in-vivo study was valid. Results obtained in this series of tests could therefore be used to compare with those obtained from the in-vitro studies. Some assumptions for the in-vitro specimen could also be applied to the in-vivo situation. The lumbar spine in-vivo was also assumed as a passive linear system which only responded to external mechanical vibration. As will be described in section 7.6.4, the back extensors would change the vibratory characteristics of the lumbar spine only when they are active. However, in this in-vivo study, the lumbar spine was tested when the paraspinal muscles were relaxed. It was therefore acceptable to assume that the lumbar spine and its associated structures did not possess any active element which would generate intrinsic vibration under the test condition. As for the measurement of excitatory force, each lumbar vertebra was considered as a rigid mass which provided effective transmission of vibratory force as received at the spinous process. By the same token the vibration measured at the spinous process could be taken as the true vibration response of the whole vertebra.

In all in-vivo vibration tests carried out on the normal subjects, the mobility response of the lumbar spine did not show any clearly defined resonant peak. This is a strong indication that the lumbar spine in-vivo behaved inherently as a highly damped structure. In addition to

this mechanical characteristic of the lumbar spine, the surrounding musculature, major blood vessels and their fluid content, and other associated soft tissue structures and organs may imposed extra mass on the lumbar spine leading to diminished motion response. Vibratory energy may also be dispersed and absorbed in these soft tissue structures and organs resulting in damping. All frequency components within the range of 2 kHz were effectively damped, but to various degrees. Modal behaviour as observed on fixed lumbar specimens and reported in section 5.7 was not found in live subjects. Though a body in prone lying was in a suitable position for the vibration test, the attachment of the lumbar spine at the pelvo-sacrum complex and the thoracic cage did not provide fixed end supports. The suggestion of a segmented beam with hinged ends as for the in-vitro attachment on angle-plates (section 5.7) may not be a suitable model for the lumbar spine in-vivo. However, the mobility measured at different lumbar segments was different. This finding helped to confirm the existence of flexural vibration of the lumbar spine in the antero-posterior direction, though the mode shape could not be identified from the mobility measurement. This also helped to rule out the existence of the rigid-body vibration mode for the lumbar spine, otherwise synchronous and coherent vibrations of the same magnitude and phase should be observed on different lumbar segments. Lee (1990) reported that the centre of support for the upper end of the lumbar spine was at T8-9 level. This anatomical set-up was creating a soft support to the lumbar spine in the thoracic region. This in fact corresponded to a less rigid end support in-vivo than was modelled for the in-vitro situation, and it helped to explain the non-existence of resonance at any particular frequency.

It was not possible to fix the transducers over the spinous processes as for the in-vitro study in which the transducers were attached with pins anchored in the bone substance. Furthermore, the transducers were hand-held by

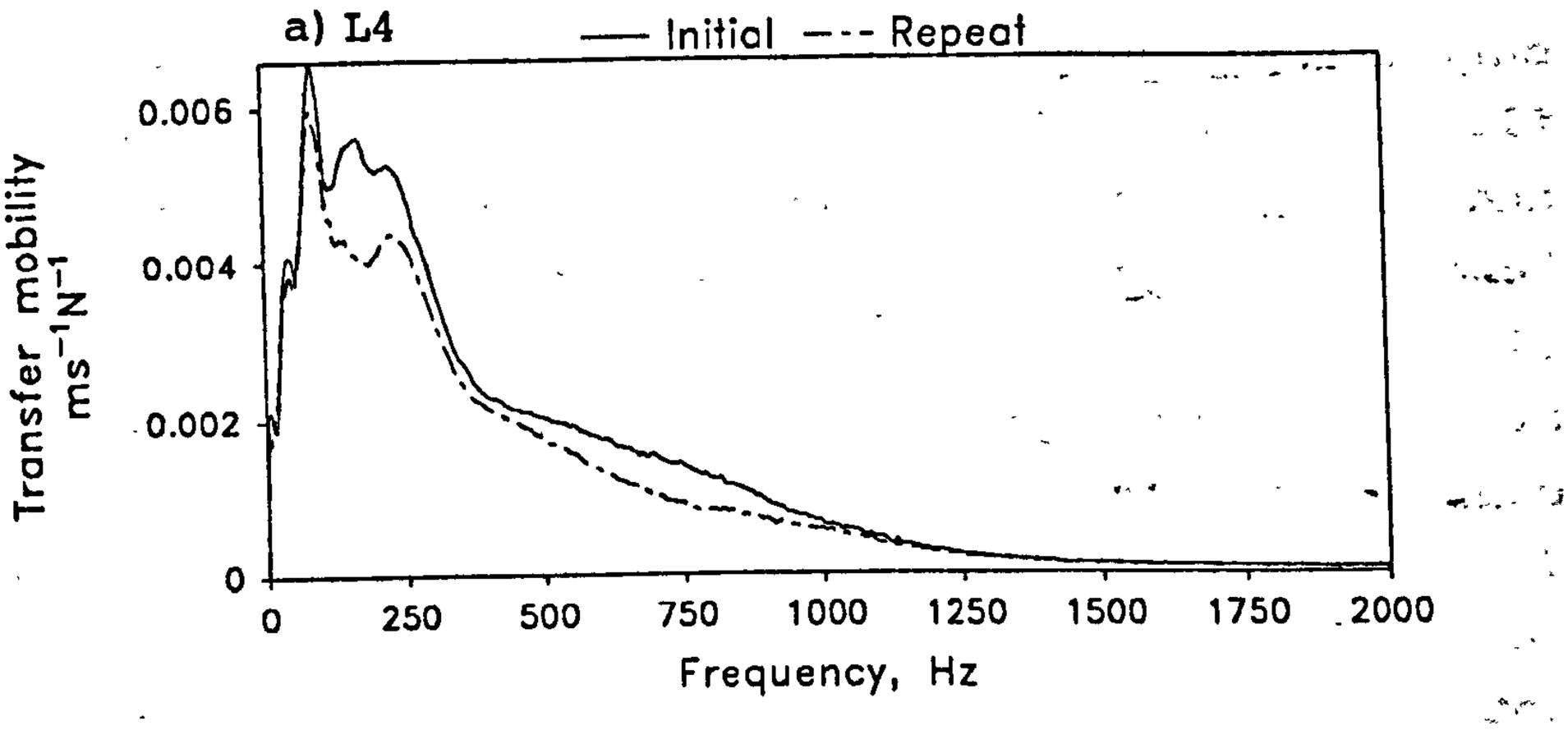

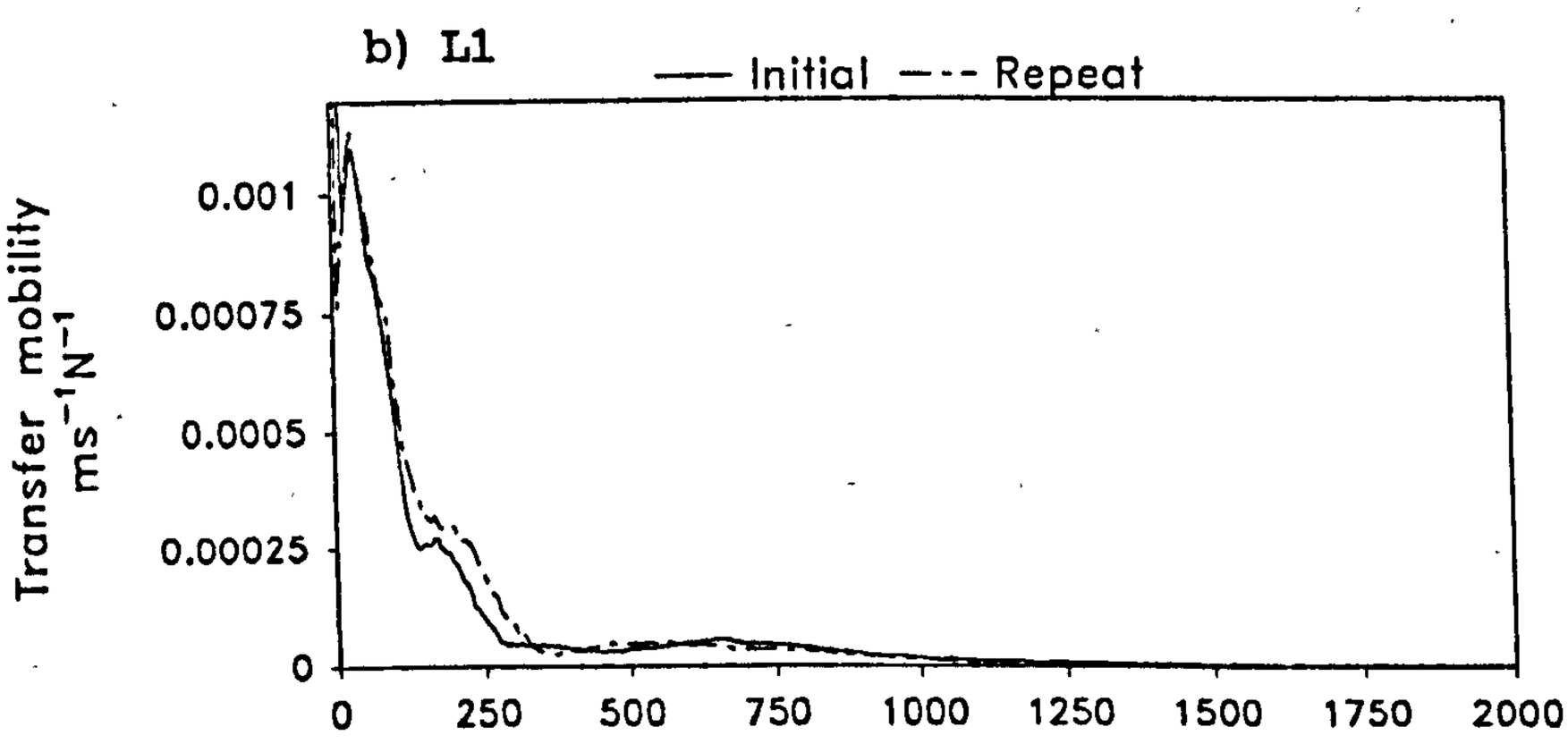

Fig 7.15 Repeatable measurements of vibration response a) at L4, and b) at L1.

the operator who from time to time had to take the transducer off to relieve the pressure over the spinous process. It was technically difficult to reproduce the same level of repeatability comparable to an in-vitro situation which was virtually undisturbed during repeated testing. However, the in-vivo vibration response of the lumbar spine was found to be reproducible when tests were repeated on some subjects with the whole process of positioning and placement of vibration probes re-run. The linear regression model described in section 5.3.3 and appendix VI was used to assess the repeatability. In all the repeated tests, the coefficient of determination R^2 ranged between 0.95 and 0.9999, and F significance < 0.0001. Figure 7.15 shows the repeatability of transfer mobility measurements at L4 and also at L1 which was the most difficult location for coherent measurements among the four lumbar segments.

The high coherency between measurements of input and output signals also confirms that the signals were noise-free. One might be concerned whether noise generated from the heart beat, from the blood flow in large blood arteries, and that from the physiological activities of other internal organs would contribute any contamination to the signals. A dummy vibration test was carried out on a test subject in the same position as in a proper test. The accelerometer was placed at the L4 spinous process and at the sacrum while the exciter was vibrating freely without attaching to the lumbar spine. The vibration levels at these two locations were found to be very minimal, and both measured less than 0.03 ms^{-2} (RMS). This was about 1% of the vibration level measured during a normal vibration test. In these vibration signals, there was no sign of any periodicity synchronous with the heart beat or breathing. This observation was consistent with the cepstrum analysis which did not reveal any periodicity in the signals. It also confirms the assumption that there is a mismatch in the acoustical impedance between soft tissues and bone. The bone would have a poor admittance to acoustical energy

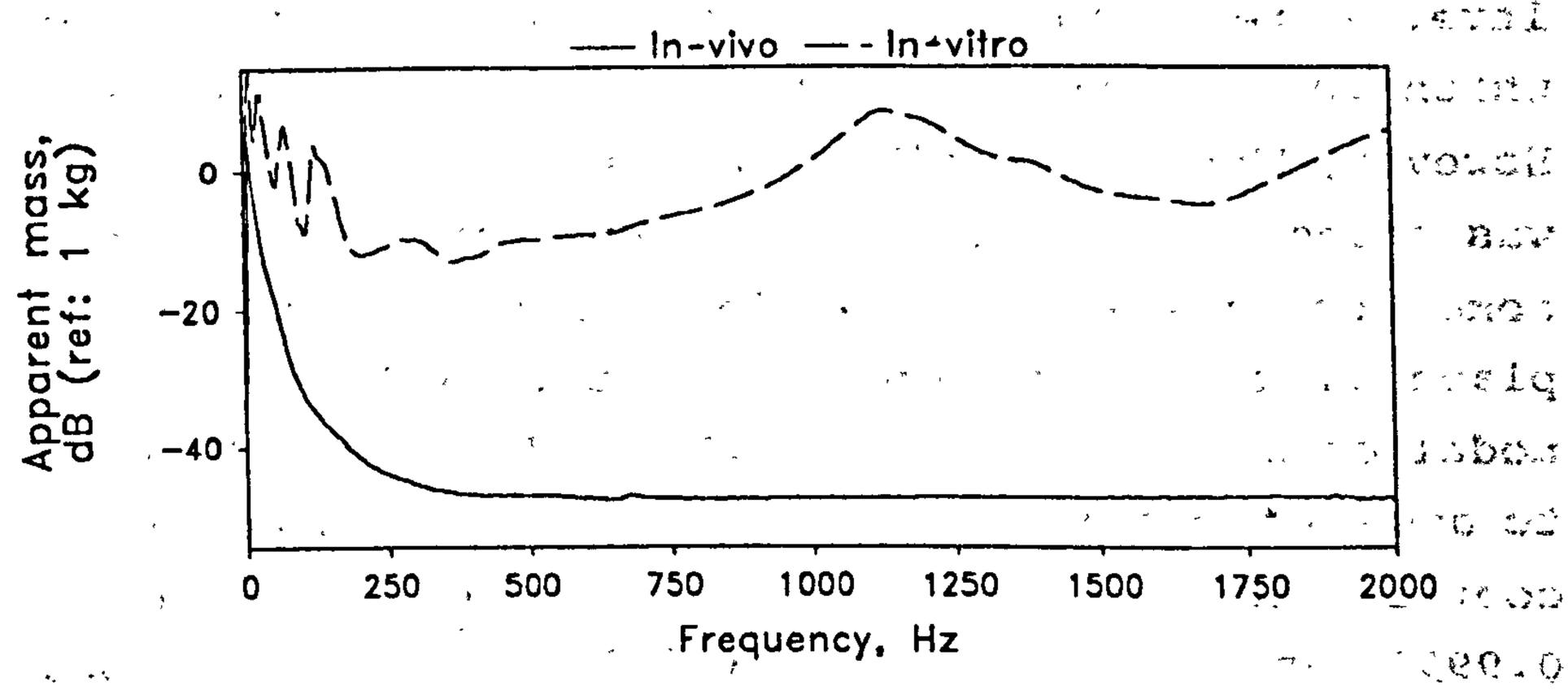

Fig 7.16 Transmissibility measurement as apparent mass at the L5 lumbar segment in-vivo and in-vitro.

generated from soft tissues or organs such as the heart. The low vibration level described previously was also found to be incoherent with that detected on the freely vibrating exciter. This observation suggests that the exciter was effectively decoupled from the lumbar spine, and the support to the body offered adequate acoustical insulation from any other source of vibration in the test environment. The vibration detected at the lumbar spine was then confirmed to be genuine response to the external excitatory force. The problem of other sources of noise such as that due to triboelectric effect (section 5.3.11) were also eliminated. In most cases the coherence function was found to be greater than 0.95. According to equation 2.38 the random error was less than 3%.

7.6.2 Apparent Mass and Transmissibility

It was important to know how effectively the vibratory force had been transmitted to the lumbar spine. Figure 7.16 shows a typical apparent mass measurement which expresses the transmissibility at the driving point of a normal lumbar spine when excited by random vibratory force. The apparent mass shows effective transmission of vibration in the frequency range below 500 Hz while that in the higher frequency range was limited. This was due to the compliance of the skin. Though it was intended to stiffen the skin by compression, it was still not possible to enhance the transmissibility any further in the higher frequency. The compliance of the lumbar spine was found to be another major factor which governed the effective transmission of vibratory force that can be applied to a lumbar spine under test. Figure 7.16 also attempts a comparison with a typical example of in-vitro measurement of transmissibility. The transmissibility was found to be much lower throughout the whole frequency range in an in-vivo situation.

7.6.3 Dispersion and Transmission in Muscles

So far the muscles have been considered primarily as

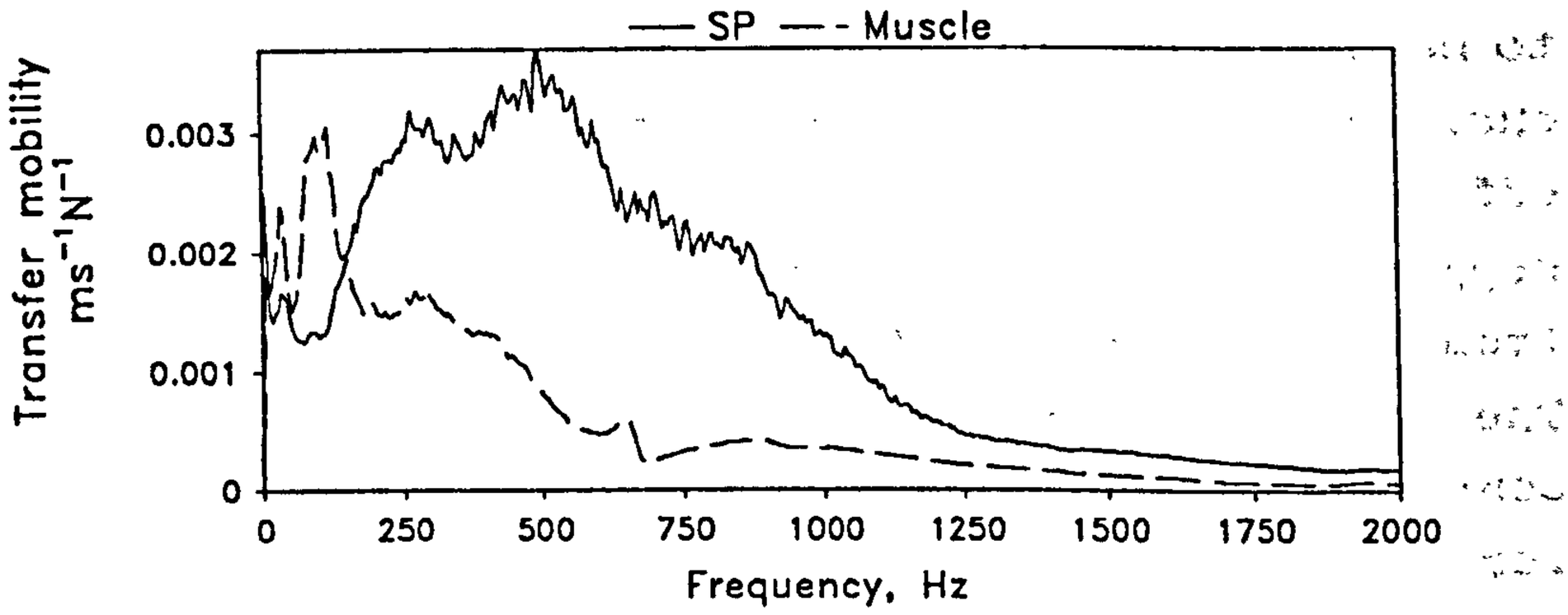

Fig 7.17 Vibration response at the L4 spinous process and over the paraspinal muscle at a point 2 cm lateral to it. (SP = spinous process).

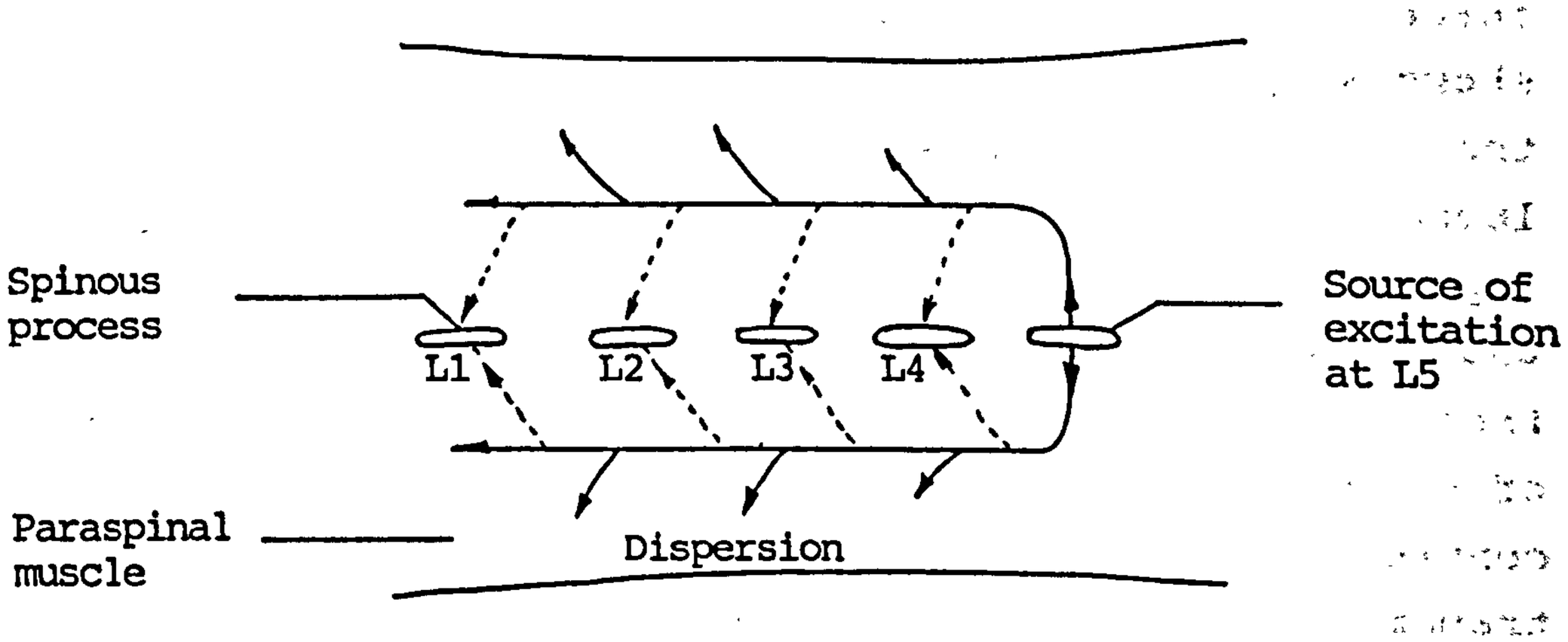

Fig 7.18 Posterior view of the lumbar spine showing the hypothetical transmission and dispersion of vibration in the paraspinal muscles. The dotted lines indicate the unlikely re-admittance of vibration to the spinous processes.

insulation material for the vibrating lumbar spine. Their transmission properties for vibration has not been specifically looked into. Due to their close association with the lumbar spine, it would be logical to presume some of the vibratory energy will be transmitted to the muscles or eventually absorbed and dissipated as heat. There was an attempt to measure the vibration level over the paraspinal muscles lateral to the spinous process. The purpose of this test was to confirm that vibratory energy was dispersed in the muscles and transmitted along to other locations, or questionably re-admitted into the bony structure. It was found that the vibration signal picked up at a point 2 cm lateral to the L4 spinous process was only about 40 to 50% of that detected at the same spinous process and was biased to frequencies lower than 500 Hz (fig 7.17). The signal was found to be coherent with the excitatory force. This confirms that part of the vibratory energy was dispersed in the surrounding muscles. Von Gierke and associates (1952) demonstrated surface waves on skin when it was in contact with a vibrating probe. Therefore it would also be logical to suggest that the vibration detected over the point lateral to the spinous process would be one result from surface waves in the skin. Furthermore, cepstrum analysis failed to identify any periodicity in the vibration signals at the spinous processes. It was therefore very unlikely that vibratory energy would take an alternative route in the muscles and then be re-admitted into the bony structure to be picked up at the spinous process as illustrated in figure 7.18.

7.6.4 The Effect of Muscle Action

The test subject was instructed to tense up the abdominal muscles, or attempt to extend the low back by lifting the limbs off the couch during a repeated vibration test. The vibration response was measured at the L3 level while the same random vibratory excitation was applied at the L5 spinous process. As revealed by the transfer

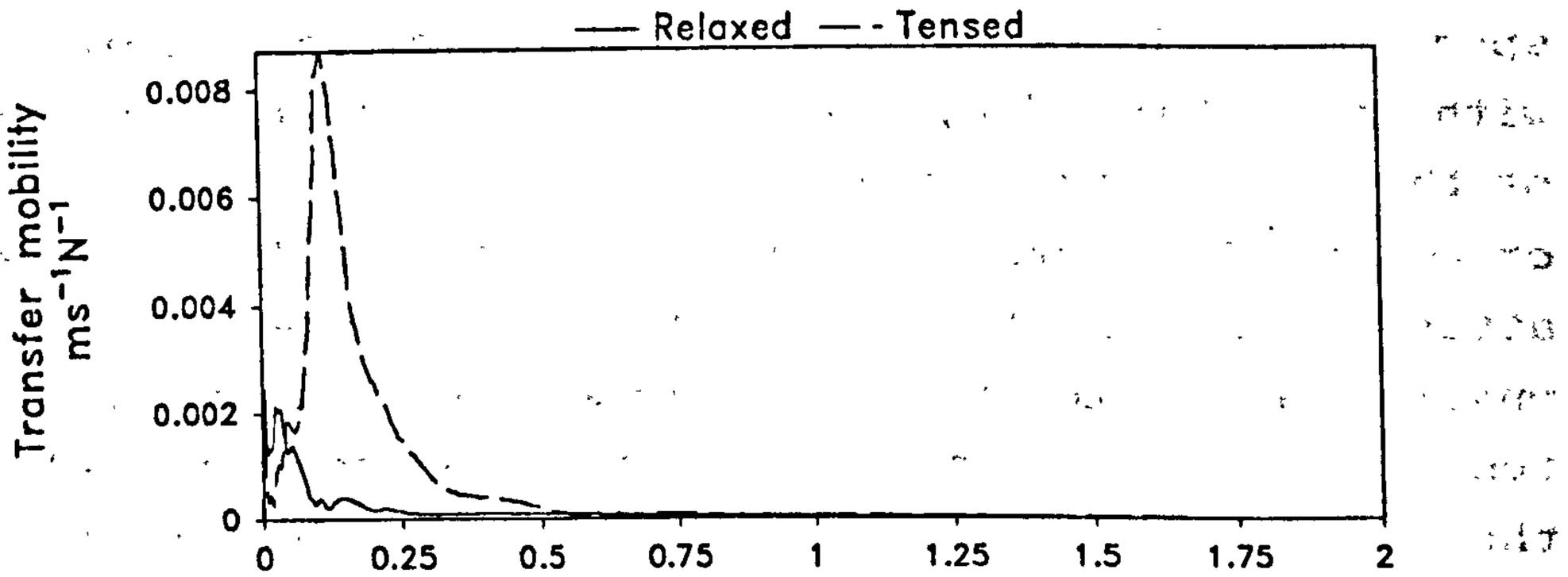

Fig 7.19 Vibration response of the lumbar spine when the subject tensed up the back extensors, showing a resonant peak at 107 Hz.

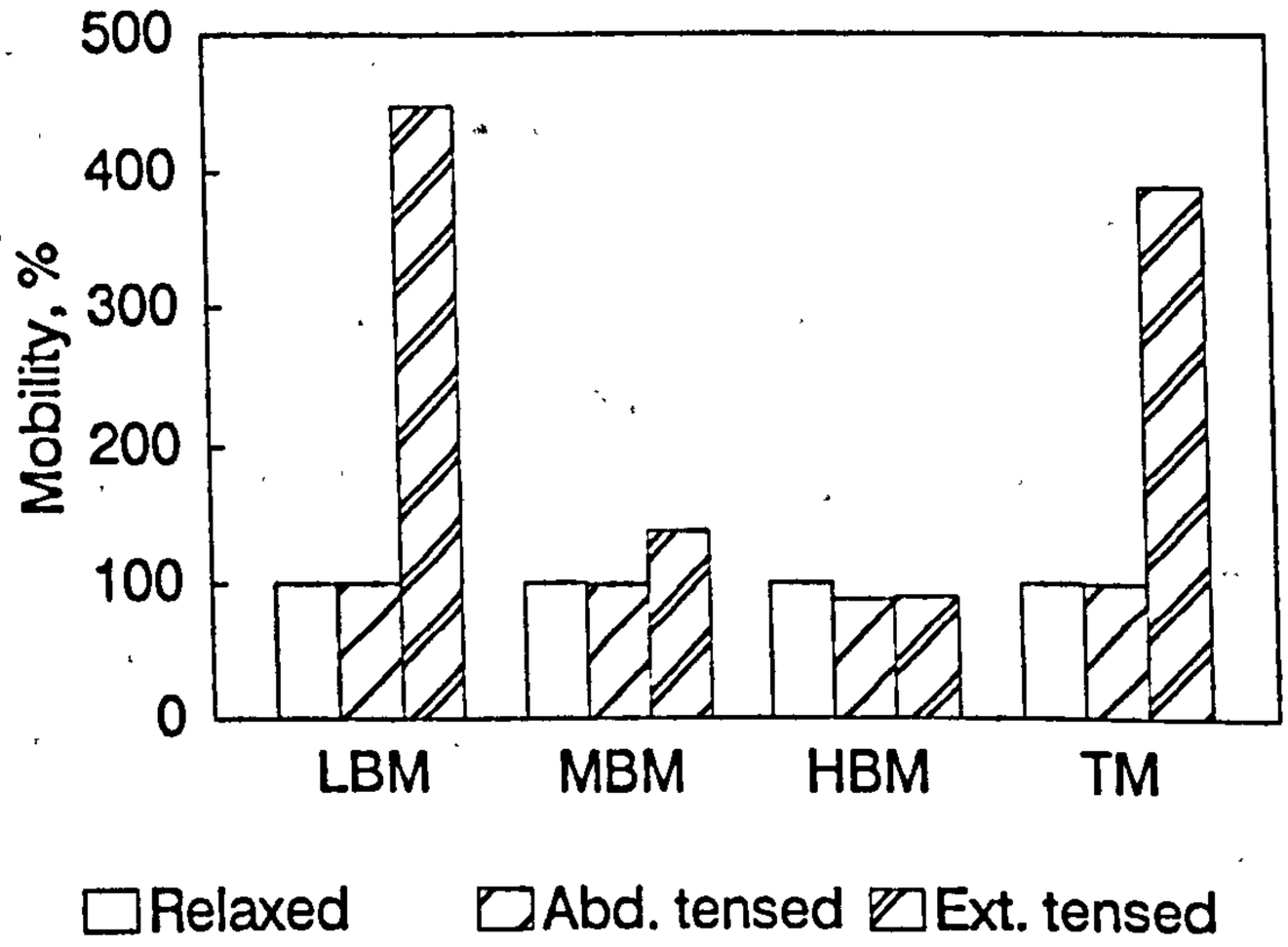

LBM = low band mobility
MBM = medium band mobility
HBM = high band mobility
TM = total mobility

Fig 7.20 Different vibratory effects of the back extensors and abdominal muscles. Mobility in a relaxed state is expressed as 100% for comparison.

mobility, the tensed lumbar spine was found to behave very differently from its relaxed state. There was a sharply defined resonant peak in the low frequency range below about 200 Hz when the subjects attempted to extend the low back (fig 7.19). Mobility in the frequencies above this range was not augmented. This vibratory characteristic is a suitable analogy to a plucked string musical instrument which gives a clear tone when the string is suitably tightened and plucked. This observation was related to what can be described as *functional stiffness* as against the *structural stiffness* which was a result of structural enhancement as in the case of simulated fusions of the lumbar spine. The behaviour of the lumbar spine under these two situations was totally different. Under the effect of the active muscles, the lumbar spine's vibratory characteristic in the lower frequency range was enhanced. It behaved more closely to a pre-stressed beam demonstrating flexural vibration with a definite resonant frequency - a feature which was not seen in a lumbar spine with its structure enhanced. The peak of the flexural vibration was observed at the L3 segment which corresponded to the middle of the lumbar spine. However, the tensed lumbar spine was a complicated structure involving some active elements whose vibratory characteristics may not be adequately explainable by the passive linear model adopted in this study. This observation of the vibratory behaviour of the lumbar spine in a tensed state helps to relieve the worry that muscle spasm would interfere with the results as might be possible in the case of measurements on patients. However, this vibratory effect of the muscle could be detected should there be any interference due to active muscle contraction or muscle spasm. Tension set up in the abdominal muscles did not show any effect on the vibratory characteristics of lumbar spine. Figure 7.20 shows the band mobility under the different effects of the action by back extensors and abdominal muscles. The hydrostatic pressure set up in the abdominal cavity may have an indirect but

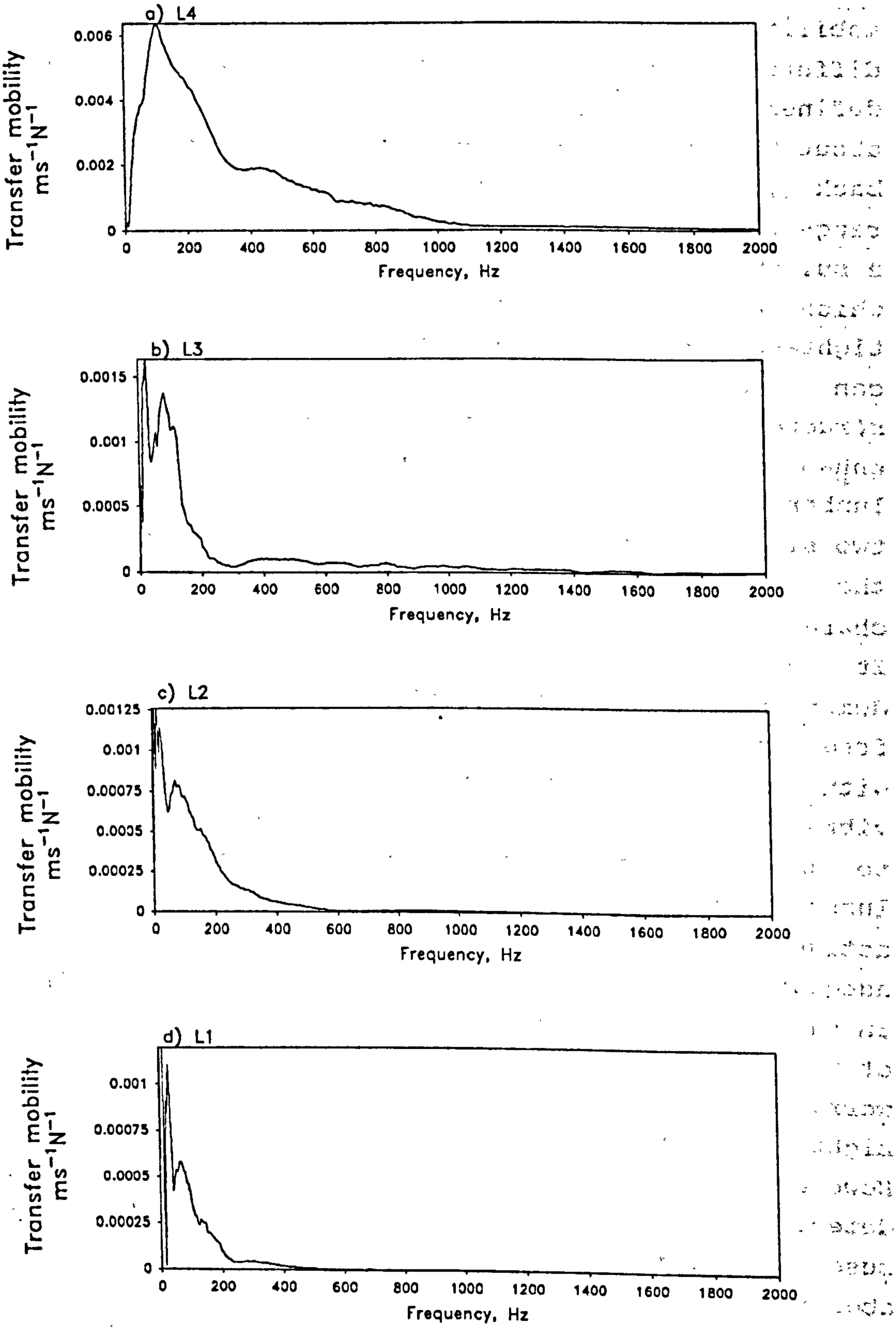

Fig 7.21 Transfer mobility measured at different lumbar segments of a normal subject.

also minor effect on the stiffness of the lumbar spine.

7.6.5 Transfer Mobility

The lumbar spine demonstrated limited mobility biased to the lower frequency range below 1 kHz or even lower if the mobility response was measured at a distant location, such as L1, from the excitation source at L5. Transfer mobility defined by equation 2.34 expresses the amount of motion response to unit vibratory force. Figure 7.21 shows typical mobility curves for a lumbar spine with the velocity obtained at different segments while it was excited by random vibration at the L5 spinous process. The mobility curves do not show any clearly defined resonant peak which reveals that the lumbar spine was highly damped and it did not resonate at any particular frequency. The lumbar spine in general behaved as a highly damped structure, not demonstrating any clear modal shape in its response to external vibratory excitation. However, the question of whether the lumbar spine behaved as a solid mass showing rigid-body vibration mode as depicted in figure 5.25 has yet to be answered. It could be revealed by the transfer mobility measured at various segments. There was a high attenuation when measurement was made at upper segments. If the lumbar spine behaved as a rigid-body, a uniform vibration response should be obtained at various segments. The response should also be of the same magnitude and phase. As reported in section 5.4, a lumbar spine with free support at both ends demonstrated a rigid-body vibration mode only at a frequency below 20 Hz. Lee and Evans (1994) reported that there were intervertebral displacements at the L3-4 and L4-5 levels when the lumbar spine was tested under a quasi-static compressive force in the postero-anterior direction at the L4 spinous process. These findings confirm that the lumbar spine does not exhibit rigid-body mechanical behaviour even under an extremely low frequency of excitation. It also implies that the free end support was not a realistic simulation of the

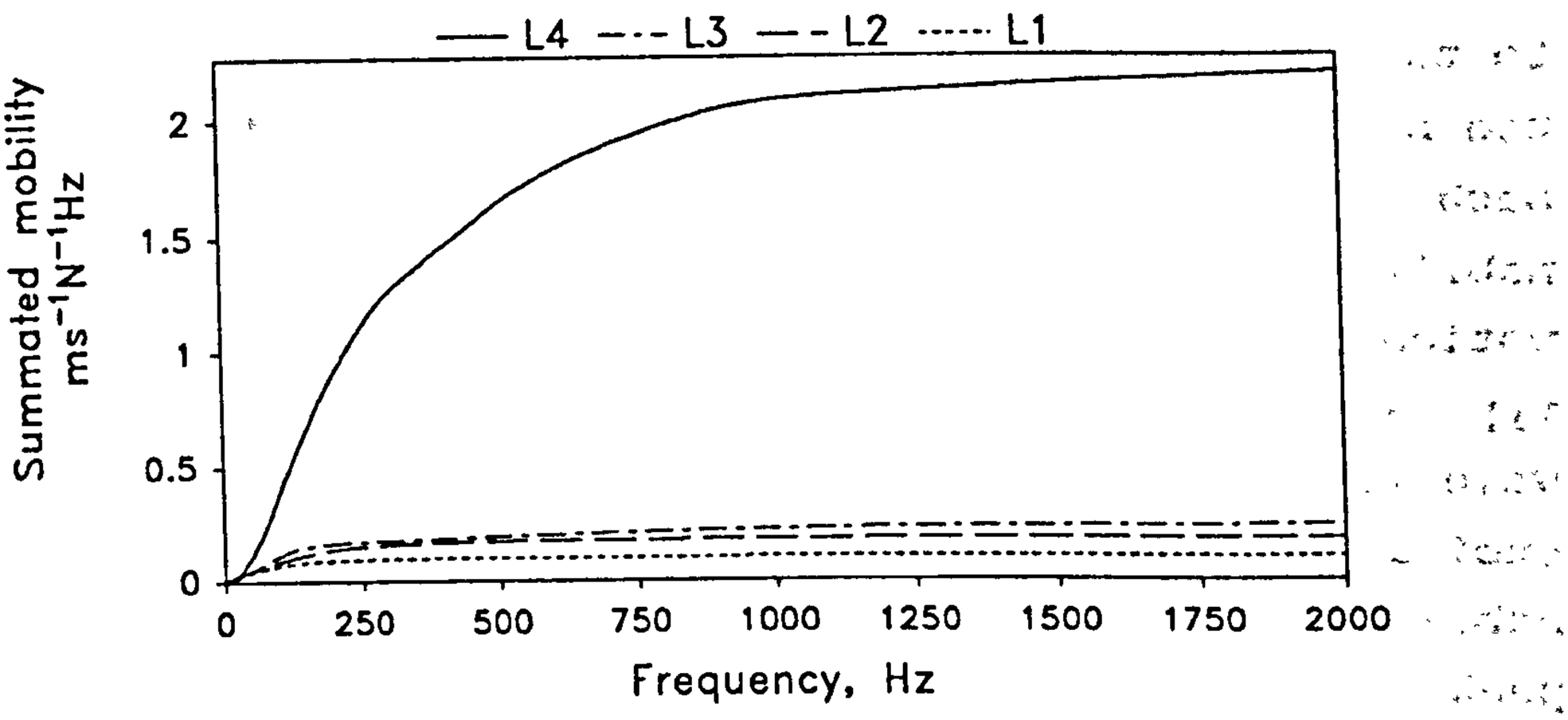

Fig 7.22a Summated mobility measured at different lumbar segments of a normal subject.

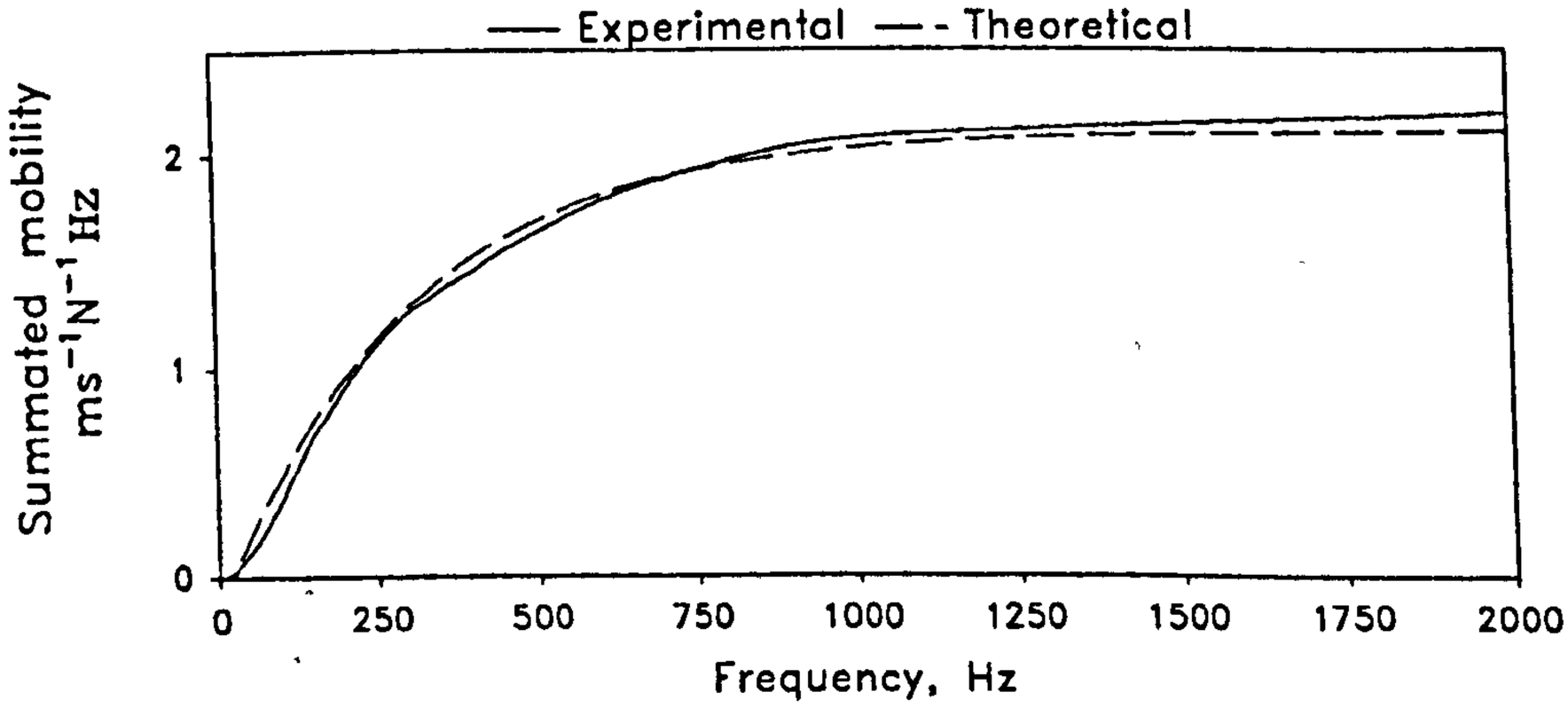

Fig 7.22b Non-linear regression of summated mobility measured at L4 of a normal subject.
Summated mobility = A $(1 - e^{-bf})$,
where A = 2.12 $ms^{-1}N^{-1}Hz$; and b = 0.00336 Hz^{-1}.

condition that a lumbar spine would experience in real life. Together with the general system characteristics discussed previously, the end condition of the lumbar spine is found to be a semi-rigid or "floating" support on a soft structure, and is definitely not a fixed end as that designed for the in-vitro study. Some degree of flexural vibration existed in a vibrating lumbar spine though it did not exhibit any clearly defined resonance. It was probably a combination of flexural vibrations at different frequencies. Flexural vibration at frequencies higher than 1 kHz was effectively damped.

It was also found that the mobility curves demonstrated a more consistent pattern in the lower frequency range. This suggests a more reliable measurement of vibration response of the lumbar spine in this frequency range. The pattern of the mobility curve was found to be less consistent in the higher frequency range, probably due to the weaker driving force and consequently a smaller vibration response. It was also due to the difficulty of maintaining a constant compressive force during different test trials. The mobility response in the higher frequency range was more susceptible to slight changes in the transmissibility of the skin.

The pattern of transfer mobility shows similarity with that obtained from in-vitro vibration tests. However it was found that the absolute mobility of an in-vivo measurement was generally higher than an in-vitro one in the lower frequency range. This may suggest the effect of more compliant end supports in the in-vivo situation which allow a greater amount of dynamic motion in response to the same level of vibratory force. This finding also corresponds well to previous discussion that the lumbar spine has compliant support at both ends. It was also noticed that the transfer mobility in the high frequency range was lower when compared with in-vitro measurements. This finding may suggest a greater damping and attenuation of high frequency vibration in the in-vivo situation. If attenuation of

Table 7.1
Coefficients A and b for normal subjects.

COEFFICIENTS	SUBJECT CODE	L4	L3	L2	L1
A ($ms^{-1}N^{-1}Hz$)	N1	3.263	1.379	0.892	1.023
	N2	4.286	0.815	0.558	0.213
	N3	3.207	0.502	0.305	0.223
	N4	4.162	1.865	0.645	0.594
	N5	2.620	0.398	0.271	0.247
	N6	4.980	0.887	1.238	0.327
	N7	3.175	0.550	0.349	0.376
	N8	3.820	0.456	0.318	0.430
	N9	1.243	0.228	0.129	0.119
	N10	2.200	0.313	0.292	0.439
	N11	2.120	0.262	0.177	0.116
	N12	1.425	0.570	0.252	0.242
	MEAN (SEM)	3.042 (0.335)	0.685 (0.142)	0.452 (0.095)	0.362 (0.072)
b (Hz^{-1})	N1	0.00192	0.00293	0.00238	0.00223
	N2	0.00175	0.00186	0.00184	0.00422
	N3	0.00246	0.00143	0.00389	0.00432
	N4	0.00233	0.00486	0.00519	0.00619
	N5	0.00230	0.00279	0.00372	0.00533
	N6	0.00164	0.00378	0.00222	0.00582
	N7	0.00136	0.00192	0.00454	0.00392
	N8	0.00249	0.00178	0.00414	0.00505
	N9	0.00441	0.00211	0.00505	0.00796
	N10	0.00312	0.00350	0.00477	0.00530
	N11	0.00336	0.00455	0.00671	0.01007
	N12	0.00289	0.00392	0.00584	0.00696
	MEAN (SEM)	0.00250 (0.0002)	0.00295 (0.0003)	0.00419 (0.0004)	0.00561 (0.0006)

Notes: SEM = standard error of mean.

vibration at the skin is taken into consideration, it would be logical to suggest that the actual in-vivo vibration response would be greater had the vibration not been attenuated by the skin. The direct transmissibility obtained for the skin reveals an attenuation factor of 0.8. This finding supports the use of a needle-mounted accelerometer for percutaneous measurement of vibration response as reported by Ziegert and Lewis (1979). A needle-mounted accelerometer was found to work more effectively and it is anticipated that this technique would help to solve the problem of attenuation of vibration by the intervening skin.

7.6.6 Summated Mobility and Total Mobility

Equation 5.5 was applied to obtain the summated mobility curve for each measurement. It was found that the summated mobility curves showed similar patterns to those obtained in the in-vitro study. A summated mobility curve could be divided into 3 parts. In the lower frequency range defined as 0 to 500 Hz, the mobility curve goes up with a definite slope. The curve then shows a transition region as the summated mobility tends to plateau off to a stable level at higher frequency range. This feature is shown in figure 7.22a as typical measurements obtained in one of the normal subjects. The summated mobility curve also fits closely to equation 5.7 (fig 7.22b). Table 7.1 lists the coefficients estimated by a non-linear regression model. The coefficient of determination R^2 is greater than 0.98 in most cases. This confirms that the experimental results fit closely to the theoretical model. However, these coefficients failed to show any relation to gender, nor did they show any links with the body build. Coefficients obtained for different normal subjects were averaged and normal curves were obtained from the statistical mean values of the coefficients (fig 7.23).

The total mobility defined by equation 5.6 was found to be different according to the location of the

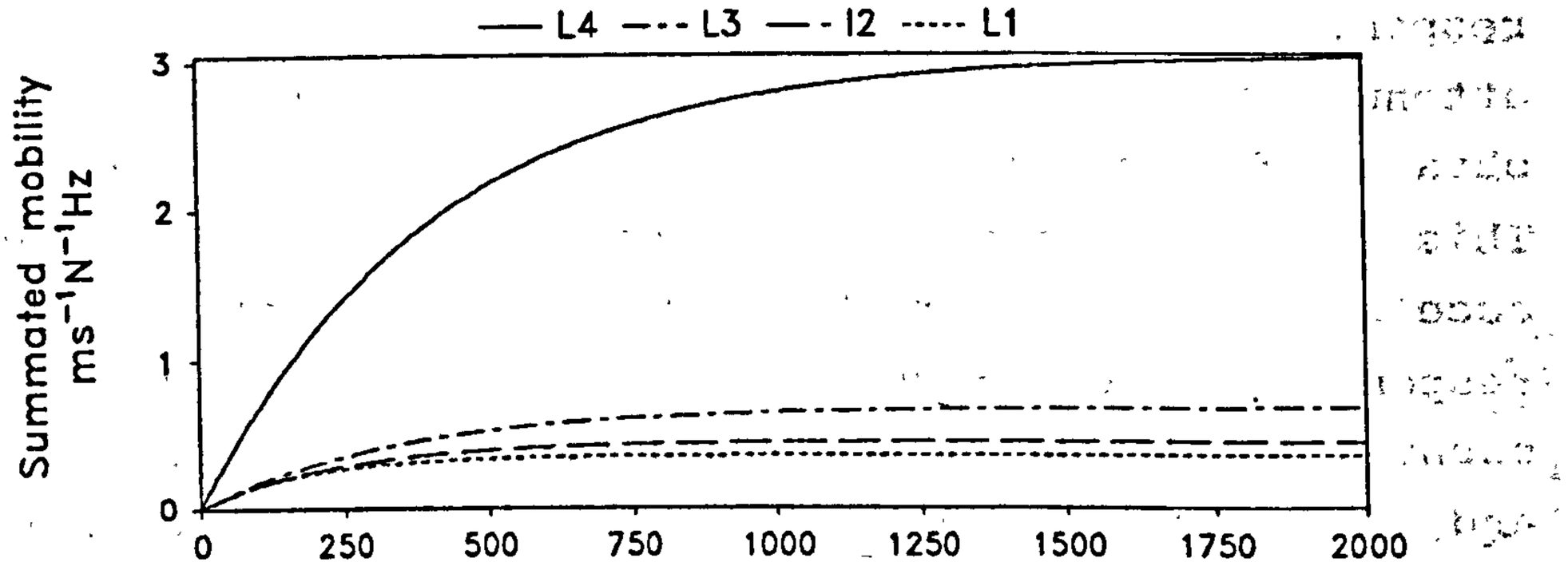

Fig 7.23 Summated mobility curves established from averaged figures of coefficients A and b of 12 normal subjects.

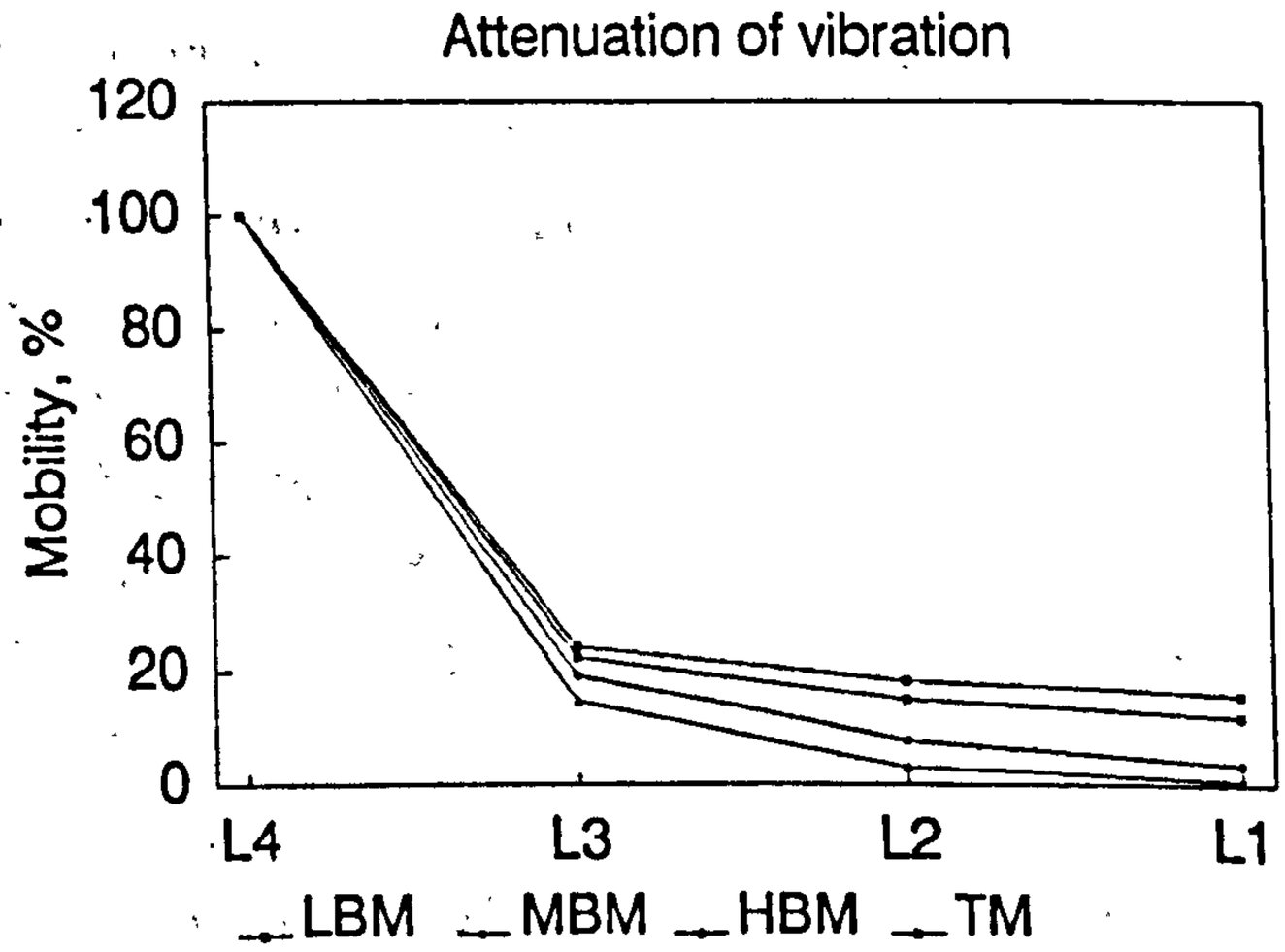

LBM = low band mobility
MBM = medium band mobility
HBM = high band mobility
TM = total mobility

Fig 7.24 Attenuation of total mobility and band mobility.

measurement of the response. Attenuation was significant when the vibration responses at L1, L2 and L3 lumbar segments were compared with that obtained at L4. There was a remarkable attenuation especially from L4 to L3 when vibration was transmitted along the lumbar spine. However, it was found that the attenuation coefficients obtained by equation 5.8 did not produce a consistent figure. It could be due to the intersubject variations as would be expected of measurements on biological systems. Figure 7.24 shows the attenuation of total mobility at different lumbar segments evaluated from the normal summated mobility curves shown in figure 7.23. Table 7.2 lists the attenuation coefficient of the total mobility determined for each segment according to the normal figures. These figures show a higher attenuation of vibration in an in-vivo situation when compared to the mean figures of the in-vitro measurements (table 5.9).

7.6.7 Band Mobility

As for the previous in-vitro study, the mobility measurement was specifically examined in different frequency bands by arbitrarily defining the low band mobility (LBM) from 0 to 500 Hz; medium band mobility (MBM) from 500 Hz to 1 kHz; and high band mobility (HBM) from 1 kHz to 2 kHz. Band mobility was obtained by applying equations 5.9 to 5.11. Figure 7.25 shows the proportion of various band mobility at different segments established from averaged normal figures. It was found that the LBM contributed the highest percentage ranged between 70% and 90%, MBM ranged between 6% and 20%, and HBM ranged between 0.5% and 8% depending on the location of measurement of mobility response. Figure 7.24 also shows the attenuation pattern observed for the mobility in different frequency bands. It was found that a nearly exponential decrease in the mobility was observed for all band mobility measurements. The greatest attenuation was seen from the L4 to L3 segments. Otherwise the general attenuation pattern

Table 7.2
Attenuation coefficient k (in dB/segment) of total mobility with respect to L4 lumbar segment. Figures (in italics) from in-vitro measurements of the lumbar spine specimens are included for comparison.

MOBILITY MEASUREMENT	EXPERIMENTAL SET-UP	L3	L2	L1
TOTAL MOBILITY	IN-VIVO *IN-VITRO*	12.9 *5.5*	8.3 *4.3*	6.1 *3.4*

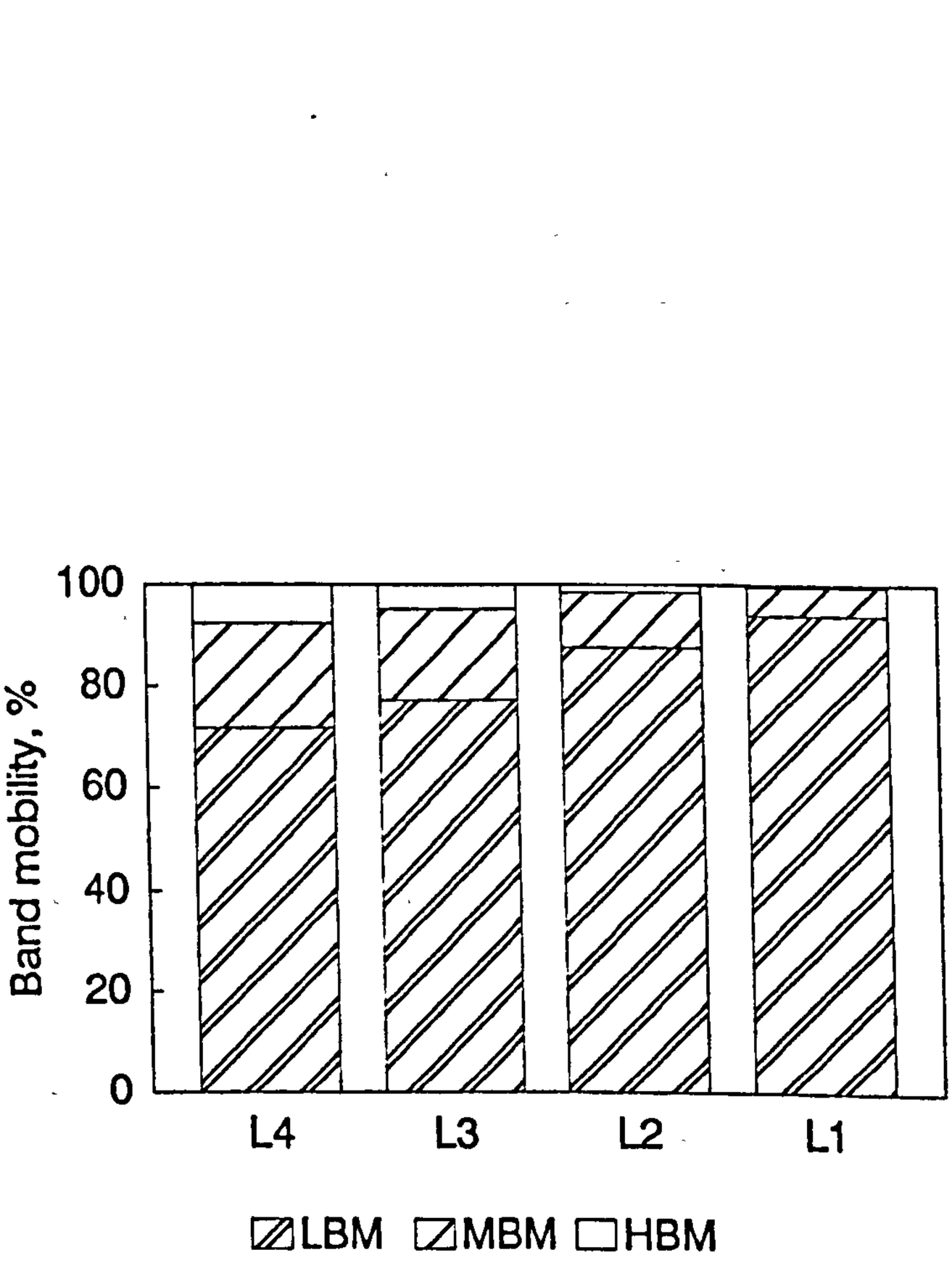

LBM = low band mobility
MBM = medium band mobility
HBM = high band mobility

Fig 7.25 Distribution of mobility in different frequency bands according to averaged figures of 12 normal subjects.

was quite similar for all frequency bands. Table 7.3 lists the attenuation coefficients of different band mobility. This finding shows an overall greater attenuation of vibration when compared to in-vitro measurements (table 5.11a to c). The finding also confirms that the vibration response obtained for the lumbar spine on live subject basically reveals the mechanical behaviour of the bony structure of the lumbar vertebrae in association with the intervertebral discs, ligaments and paraspinal musculature. These associated soft tissue structures of the lumbar spine were seen to contribute further attenuation to vibration in addition to the attenuation effect of the skin as previously discussed.

7.7 VIBRATION RESPONSE OF PATIENTS

Four female patients had been arranged for vibration tests on the lumbar spine. One of them was diagnosed with osteoporotic lumbar spine and the rest were surgically fused with instrumentation for fixation. The patients were tested in the same position as that arranged for the normal subjects. The vibration responses were measured at the L1 to L4 lumbar segments while random vibration was applied at the L5 lumbar segment. In cases where the spinous process had been cut to serve as grafting material for fusion, the most prominent bony features in the mid-line were used as the driving point or measuring point. There was no problem in defining the designated levels by palpating the bony features alone the mid-line over the lumbar region.

In this section, the motion response to vibratory excitation of individual cases are reported. Transfer mobility, summated mobility, total mobility and band mobility are the parameters used for comparison with the normal figures established from a group of 12 normal subjects, or to match with one of similar body build. The following reports on individual cases attempt to highlight vibratory features which show the differences from the normal groups, and to point out the salient features which

Table 7.3
Attenuation coefficient k (in dB/segment) of band mobility with respect to L4 lumbar segment. Figures (in italics) from in-vitro measurements of the lumbar spine specimens are included for comparison.

MOBILITY MEASUREMENT	EXPERIMENTAL SET-UP	L3	L2	L1
LOW BAND MOBILITY	IN-VIVO	12.3	7.4	5.4
	IN-VITRO	*4.2*	*3.0*	*2.6*
MEDIUM BAND MOBILITY	IN-VIVO	14.2	11.0	9.9
	IN-VITRO	*8.9*	*10.3*	*5.9*
HIGH BAND MOBILITY	IN-VIVO	16.6	15.3	15.0
	IN-VITRO	*11.4*	*10.4*	*9.6*

help to define the changes in the mechanical characteristics of the lumbar spine as a result of structural modification with spinal fixation.

The results show that the group of patients represents a wide range of the spectrum from one with osteoporotic spine to one with extensive and advanced fusion by massive bone substance and instrumentation. The following sections report the vibratory characteristics of the lumbar spines in these clinical cases. The vibration technique is not to be considered as a diagnostic tool, but rather as a means to reveal pertinent vibratory characteristics of the surgically fused lumbar spines for comparison with the normal ones. It was also the intention of this part of the study to relate the vibratory characteristics of the operated lumbar spines with clinical information.

The patients were too weak to produce active extension of the low back. Hence tests were not repeated under the action of the back extensors. However, they were able to maintain a relaxed and restful prone lying posture during the test. Muscle spasm was not particularly noticed, and the vibratory features of the lumbar spine as observed under active muscle action (section 7.6.4) was not noticeable.

7.7.1 <u>Case 1</u>

Patient Code: P1
Sex: F
Age: 58
Diagnosis: Osteoporotic lumbar spine.
Brief History: Back pain since 8 to 10 years ago. X-ray shows wedging and mild collapse fracture of the L2 and L3 vertebral bodies.

Figure 7.26 shows the transfer mobility curves measured at different lumbar segments of patient P1. The transfer mobility at L4 was greatly enhanced across the frequency range of interest. This finding suggests good

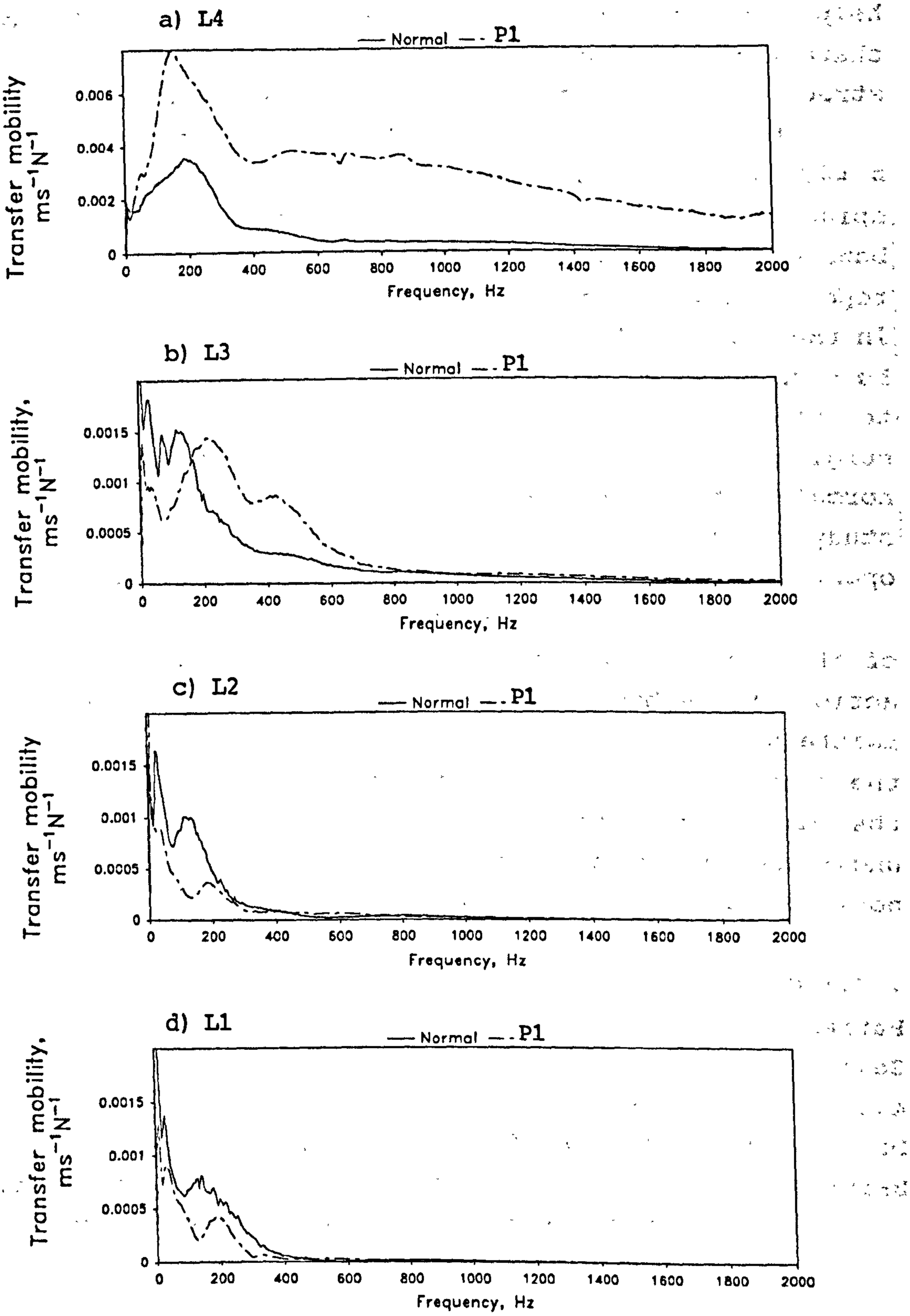

Fig 7.26 Transfer mobility measured at different lumbar segments of patient P1.

mechanical links between L5 and L4, probably as a result of substantial bony contact. For all lumbar segments, resonant frequency was not clearly defined. This suggests that the lumbar spine behaved as an overall damped system. The transfer mobility at L2 and L1 was greatly reduced when compared to the normal subject. This finding may suggest substantiated attenuation at these two levels.

Summated mobility at all lumbar segments evaluated by equation 5.5 were found to fit closely to the mathematical model described by equation 5.7. Coefficients A and b were estimated with the coefficient of determination $R^2 > 0.99$. Figure 7.27 shows the summated mobility curves for each lumbar segment, and table 7.4 lists the coefficients as compared with the averaged figures determined from the normal subjects. Coefficients A at the L4 lumbar segment was found to be much higher than the normal figure, indicating enhanced mobility; while the figures at L1 and L2 were much lower than the normal figures indicating low mobility, probably due to local attenuation. Coefficient b was about the same as the normal figures except that it was smaller at L4, which describes the trend of continuing contribution of mobility in the medium and high frequencies, according to the discussion on the physical meaning of these two coefficients in section 5.7.1.

Attenuation of vibration was found to be greater when figure 7.28 is compared to the corresponding curves (fig 7.24) for normal subjects. Table 7.5 lists the attenuation coefficients evaluated by equation 5.8. The figures show greater attenuation than normal figures by 7 to 16 dB/segment at the L2 and L3 lumbar segments in the medium and high band mobility, and the total mobility. This attenuation pattern would be more clearly shown in figure 7.29 which depicts the percentage decrease in mobility in different frequency bands when the band mobility at the L4 lumbar segment was normalized to the same level as the normal figures. There was a decrease of mobility at all lumbar segments ranged between 11% and 70% for low band

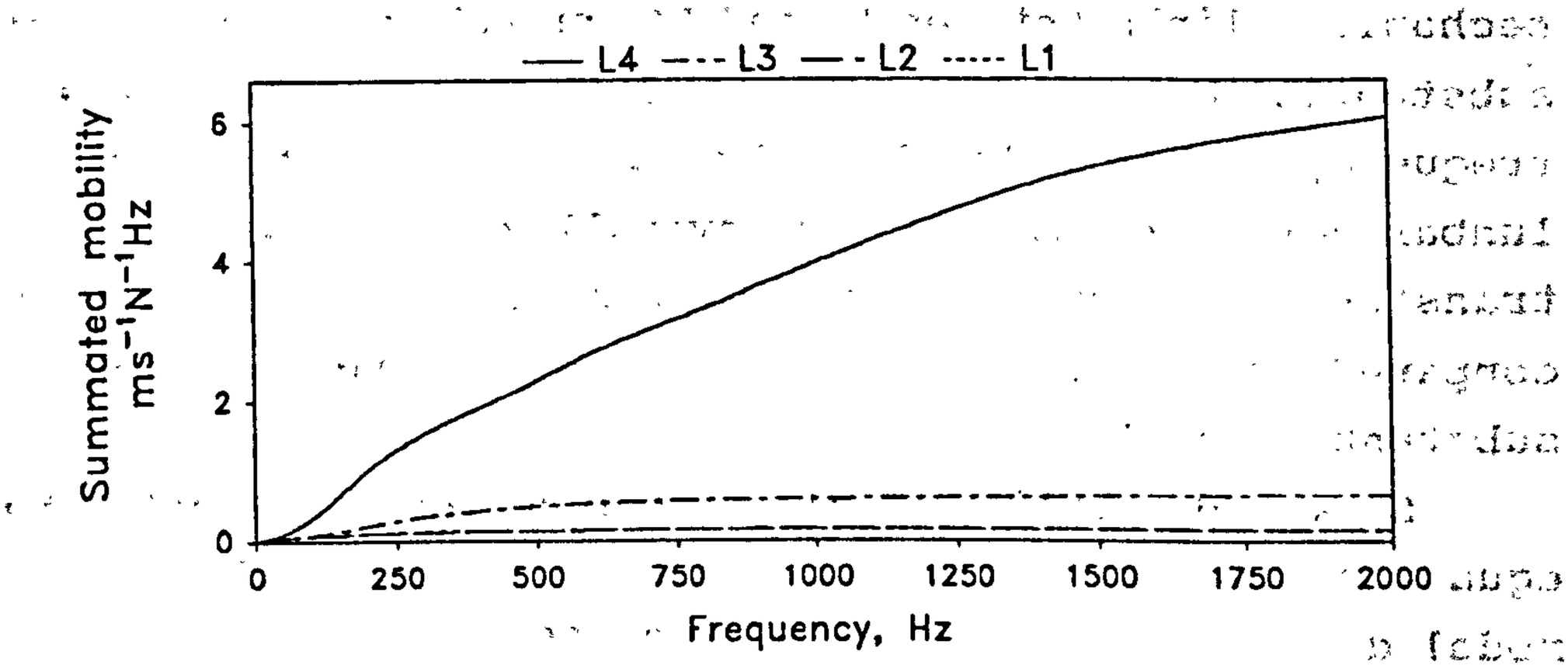

Fig 7.27 Summated mobility measured at different lumbar segments of patient P1.

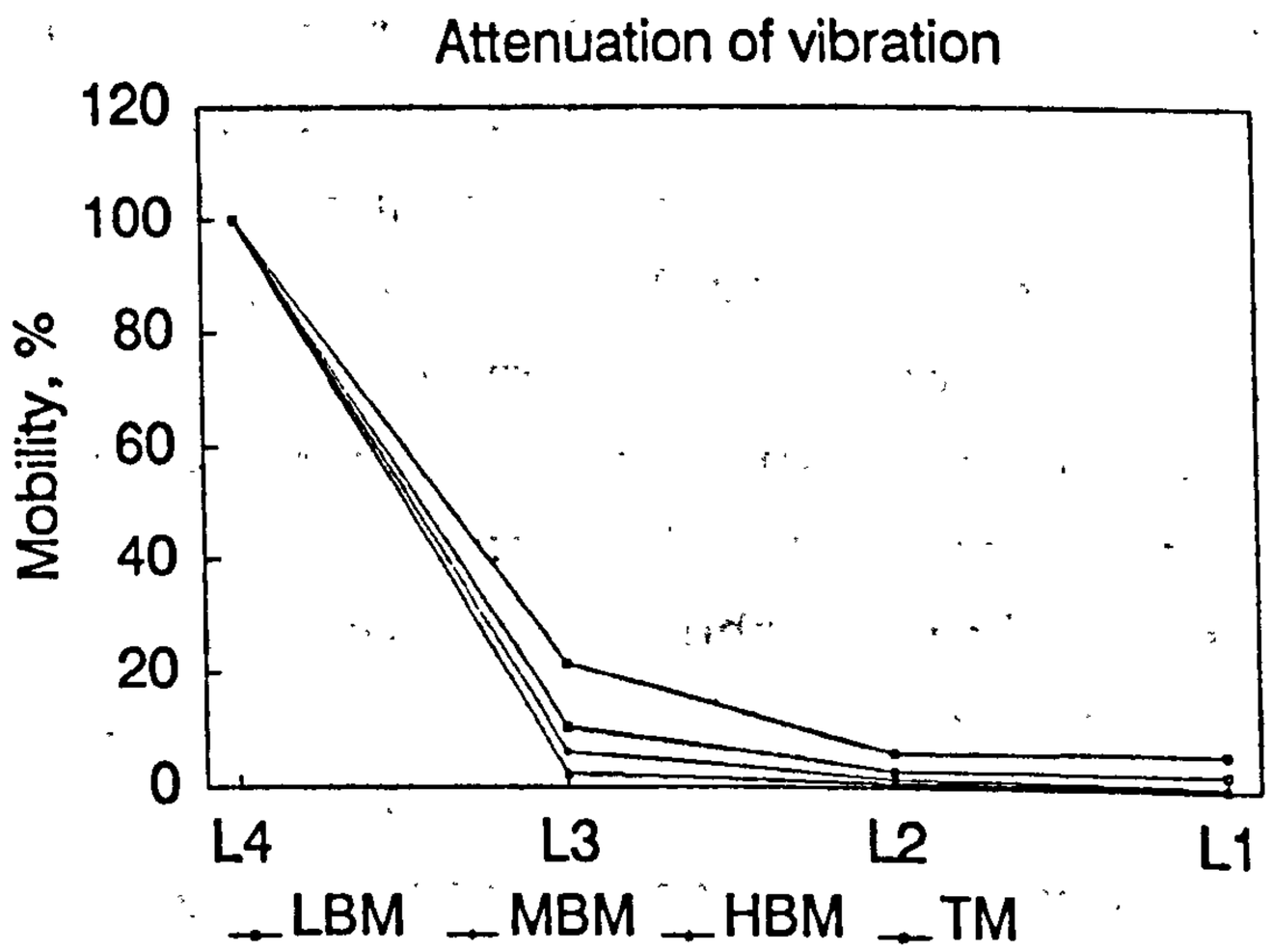

LBM = low band mobility
MBM = medium band mobility
HBM = high band mobility
TM = total mobility

Fig 7.28 Attenuation of total mobility and band mobility of patient P1.

Table 7.4
Coefficients A and b for patient P1 compared with figures (in italics) from normal subjects.

COEFFICIENTS	SUBJECT CODE	L4	L3	L2	L1
A ($ms^{-1}N^{-1}Hz$)	P1 *NORMAL*	8.586 *3.042*	0.647 *0.685*	0.167 *0.452*	0.154 *0.362*
b (Hz^{-1})	P1 *NORMAL*	0.00064 *0.00250*	0.00283 *0.00295*	0.00350 *0.00419*	0.00572 *0.00561*

Table 7.5
Attenuation coefficient k (in dB/segment) of band mobility evaluated for patient P1. Normal figures from tables 7.2 and 7.3 are included for comparison.

MOBILITY MEASUREMENT	SUBJECT CODE	L3	L2	L1
LOW BAND MOBILITY	P1 *NORMAL*	13.3 *12.3*	12.2 *7.4*	8.0 *5.4*
MEDIUM BAND MOBILITY	P1 *NORMAL*	24.0 *14.2*	18.9 *11.0*	14.7 *9.9*
HIGH BAND MOBILITY	P1 *NORMAL*	32.3 *16.6*	23.4 *15.3*	17.8 *15.0*
TOTAL MOBILITY	P1 *NORMAL*	19.4 *12.9*	15.5 *8.3*	10.6 *6.1*

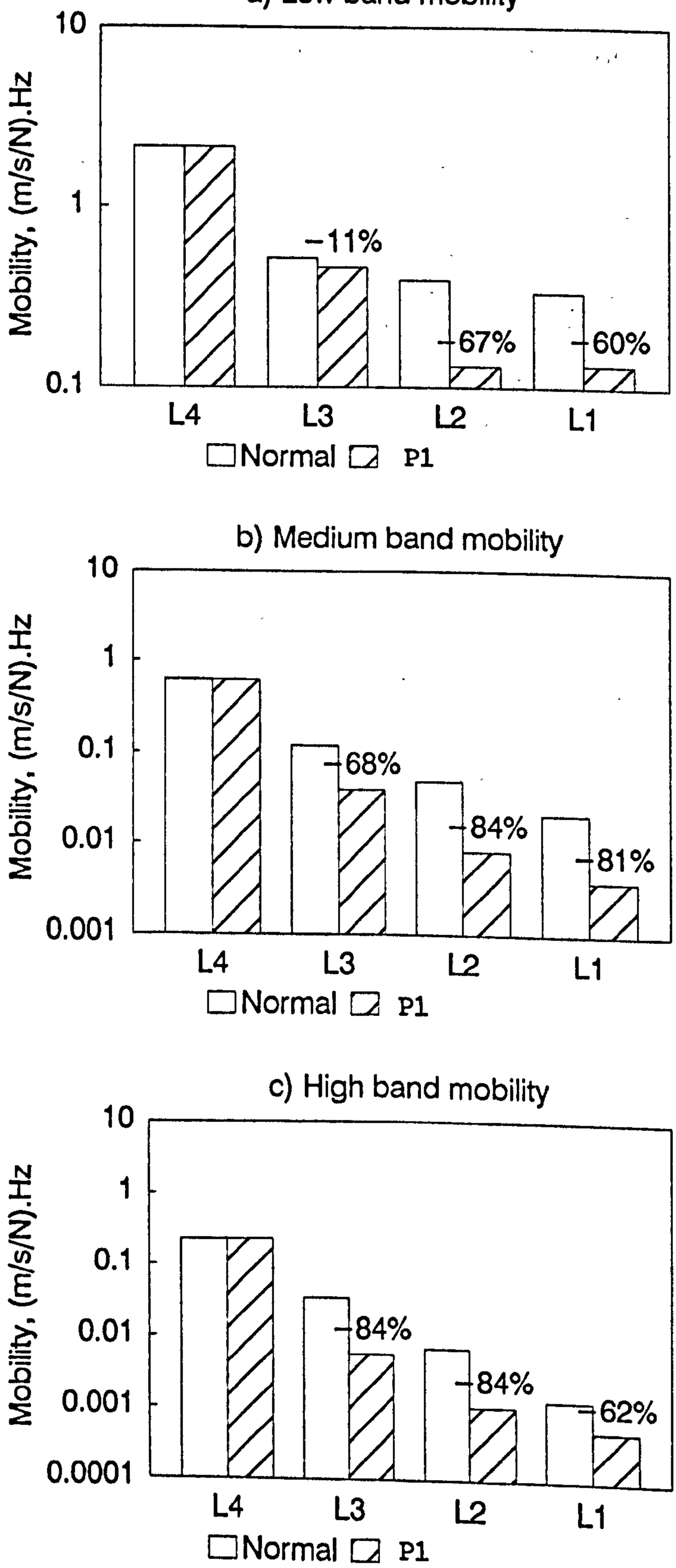

Fig 7.29 Normalized mobility in different frequency bands measured at each lumbar segment of patient P1. Percentage indicates decrease (error = 3%).

mobility; between 70% and 85% for medium band mobility; and between 60% and 84% for high band mobility. The total mobility showed a 50% to 80% decrease at all lumbar segments (fig 7.30).

The lumbar spine of P1 was presenting an example of one which shows overall attenuation to vibration. This finding is consistent with the clinical diagnosis that patient P1 sustained osteoporosis of the lumbar spine resulting in loss of bony content and collapse fracture of the vertebral bodies. However, the fact that the L4 lumbar segment gave a high motion response to random vibration might probably be due to some internal links between the L5 and L4 segments which have not been identified from the available clinical information.

7.7.2 Case 2

Patient Code: P2
Sex: F
Age: 51
Diagnosis: Spondylolisthesis L4-5 with stenosis.
Brief History: Spinal claudication for two years; Laminectomy L4 plus screw and plating of L4-5 with postero-lateral fusion done 3 months before the vibration test.

Patient P2 was a case showing good motion response of the lumbar spine to random vibration. The transfer mobility showed augmented response in frequencies higher than 300 Hz at the L3 and L4 lumbar segments in particular (fig 7.31). There was no clearly defined resonant peak, as this would be expected of a lumbar spine which behaved as a highly damped structure. Summated mobility evaluated by equation 5.5 was found to fit closely to the mathematical model with the coefficient of determination R^2 ranged between 0.96 and 0.995 (fig 7.32). The coefficients A and b determined for each lumbar segment are listed in table 7.6. The figures show more than 50% increase in the theoretical total

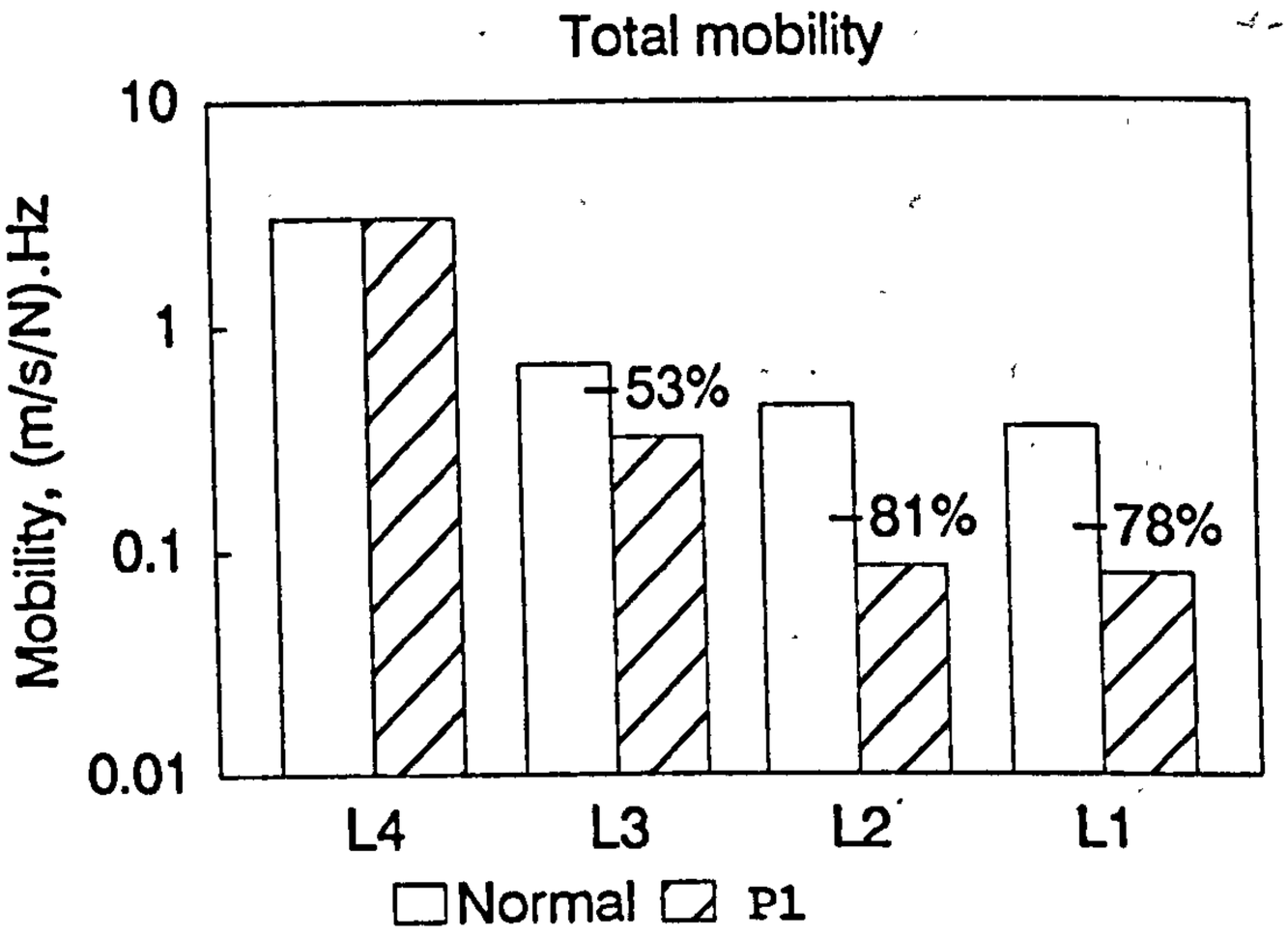

Fig 7.30 Normalized total mobility measured at each lumbar segment of patient P1. Percentage indicates decrease (error = 3%).

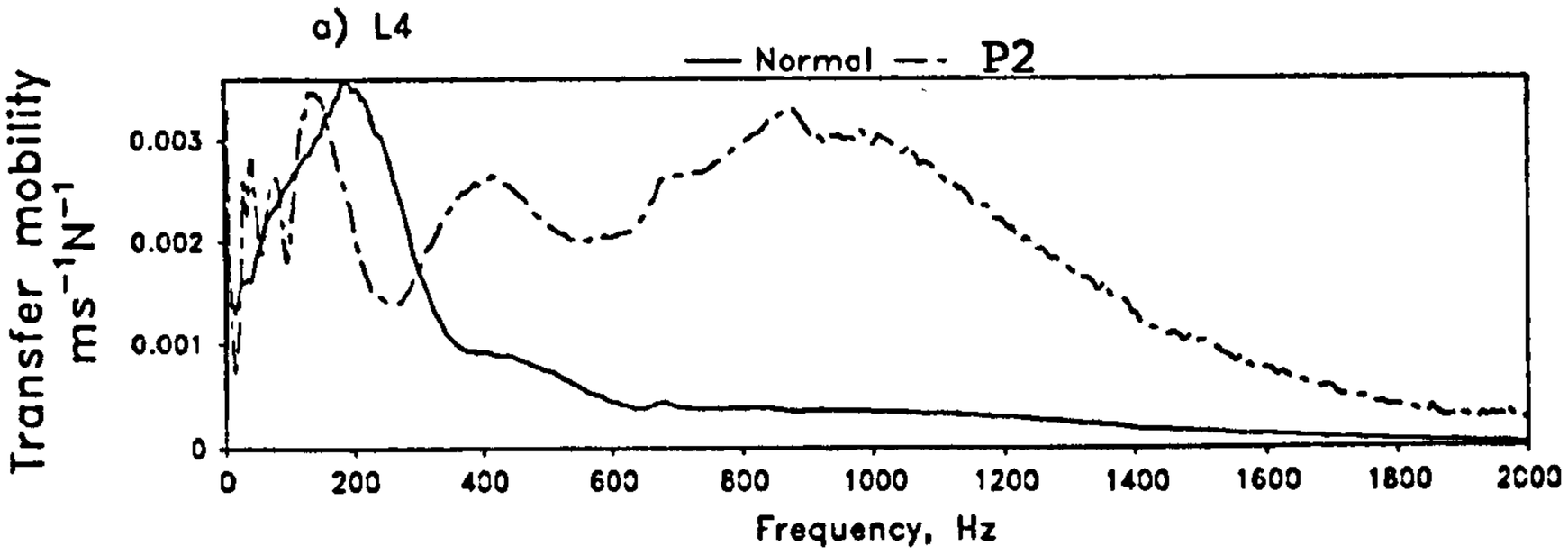

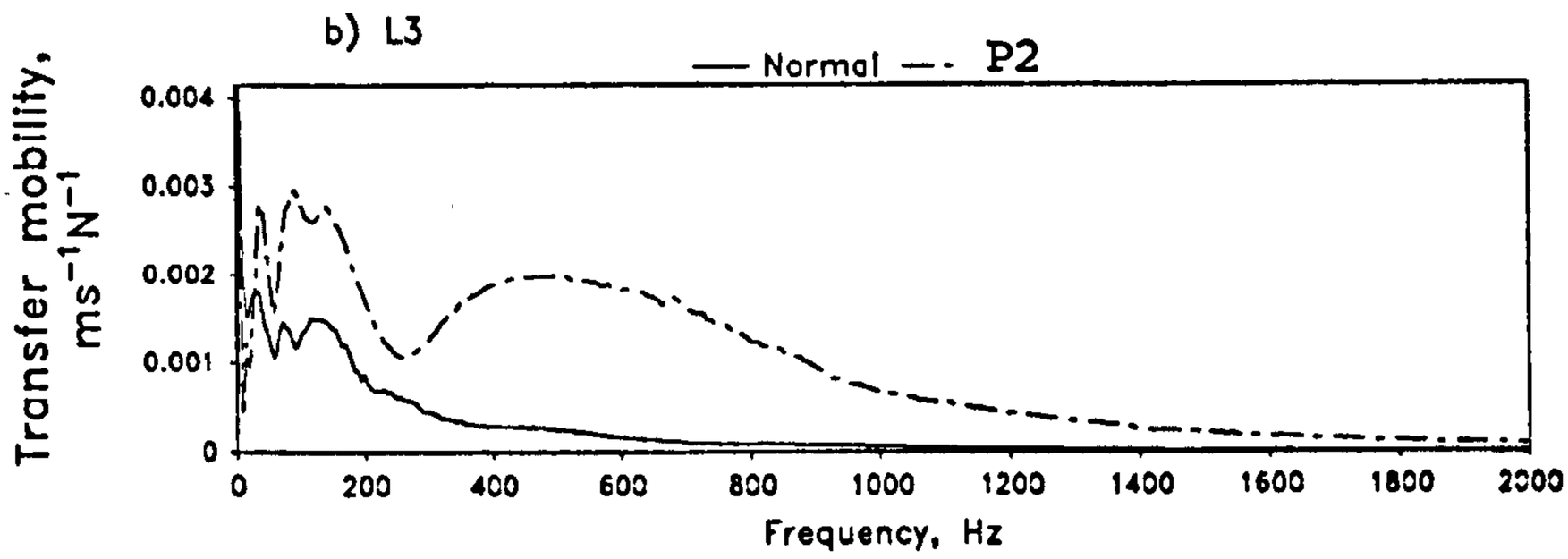

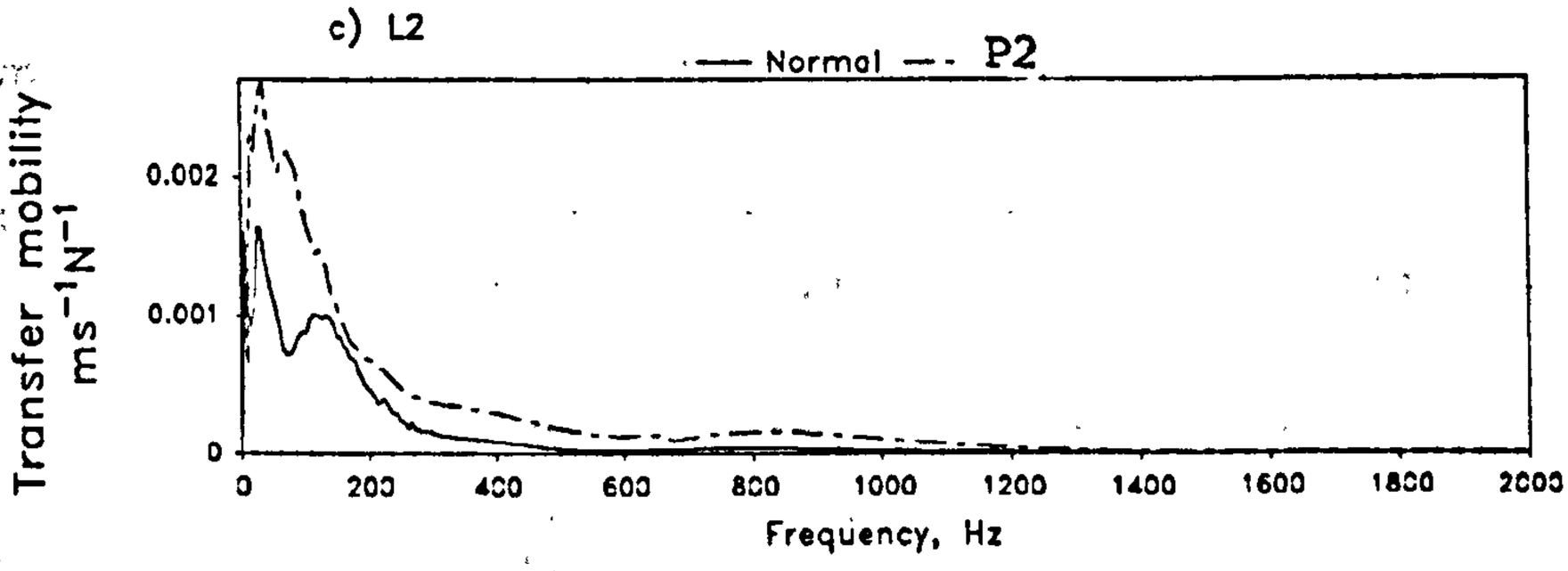

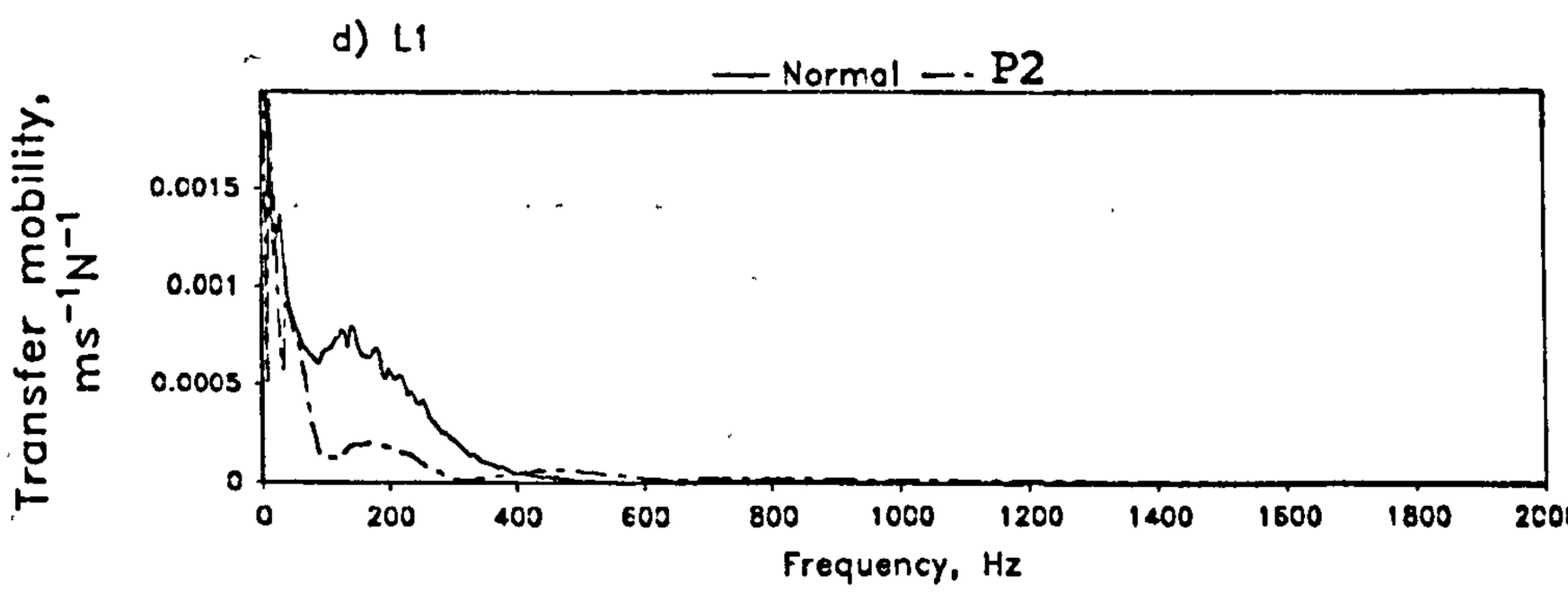

Fig 7.31 Transfer mobility measured at different lumbar segments of patient P2.

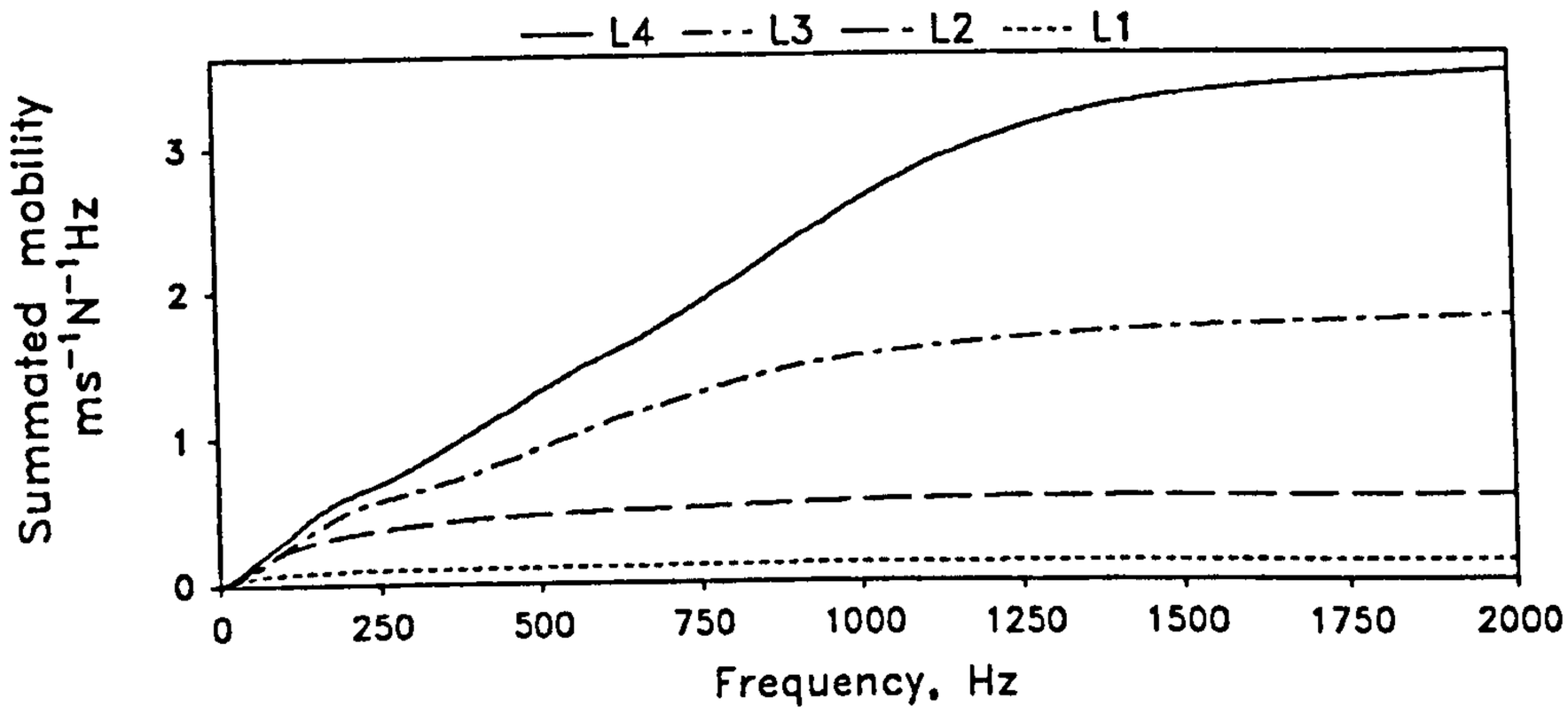

Fig 7.32 Summated mobility measured at different lumbar segments of patient P2.

Table 7.6
Coefficients A and b for patient P2 compared with figures (in italics) from normal subjects.

COEFFICIENTS	SUBJECT CODE	L4	L3	L2	L1
A ($ms^{-1}N^{-1}Hz$)	P2 *NORMAL*	4.680 *3.042*	1.955 *0.685*	0.586 *0.452*	0.140 *0.362*
b (Hz^{-1})	P2 *NORMAL*	0.00081 *0.00250*	0.00149 *0.00295*	0.00354 *0.00419*	0.00300 *0.00561*

mobility at L4, and about 200% increase at L3. The increase in mobility only in these two segments suggests a local effect of the surgical fusion which covered only the lower lumbar segments, hence the effect did not extend to upper segments. Coefficient b at L4 was only 0.00081 which reveals the trend that the accumulative mobility extended well into the higher frequency range and that the summated mobility curves climbed to a higher level before it levelled off at a stable value. A small reduction in the value of b was also observed in other lumbar segments. When the mobility in different frequency bands were analyzed, there was a clear indication that the proportion of medium and high band mobility was much higher at L4 and L3 (fig 7.33) when compared to the normal figures (fig 7.25), probably as a result of enhanced transmission. These findings could be more clearly seen in figure 7.34 which shows that the medium and high band mobility were significantly enhanced by a factor which ranged from 100% to more than 650% at the L3 and L4 lumbar segments. The enhancement of high band mobility was found to extend even further to L2 and L1. This shows that the medium and high band mobility were generally augmented in the lumbar spine surgically fused with instrumentation for fixation. The mobility in the upper segments were also affected by the effect of fusion at the lower segments i.e. L4 and L5. There was a mild decrease in the low band mobility. This could be explained by the fact that with fusion, the lumbar spine behaved as a stiffer structure with enhanced mechanical links between the lower lumbar segments and the upper ones. The excitatory force was literally exciting a bigger region of the lumbar spine. Hence a bigger portion of the structure was being excited which would mean a stronger vibratory force would be required to produce the same amount of motion. This finding of the vibratory characteristics of the lumbar spine in-vivo is consistent with the lumbar spine specimen with simulated fusions (section 6.4.2 & 6.4.3). Figure 7.35 shows the pattern of

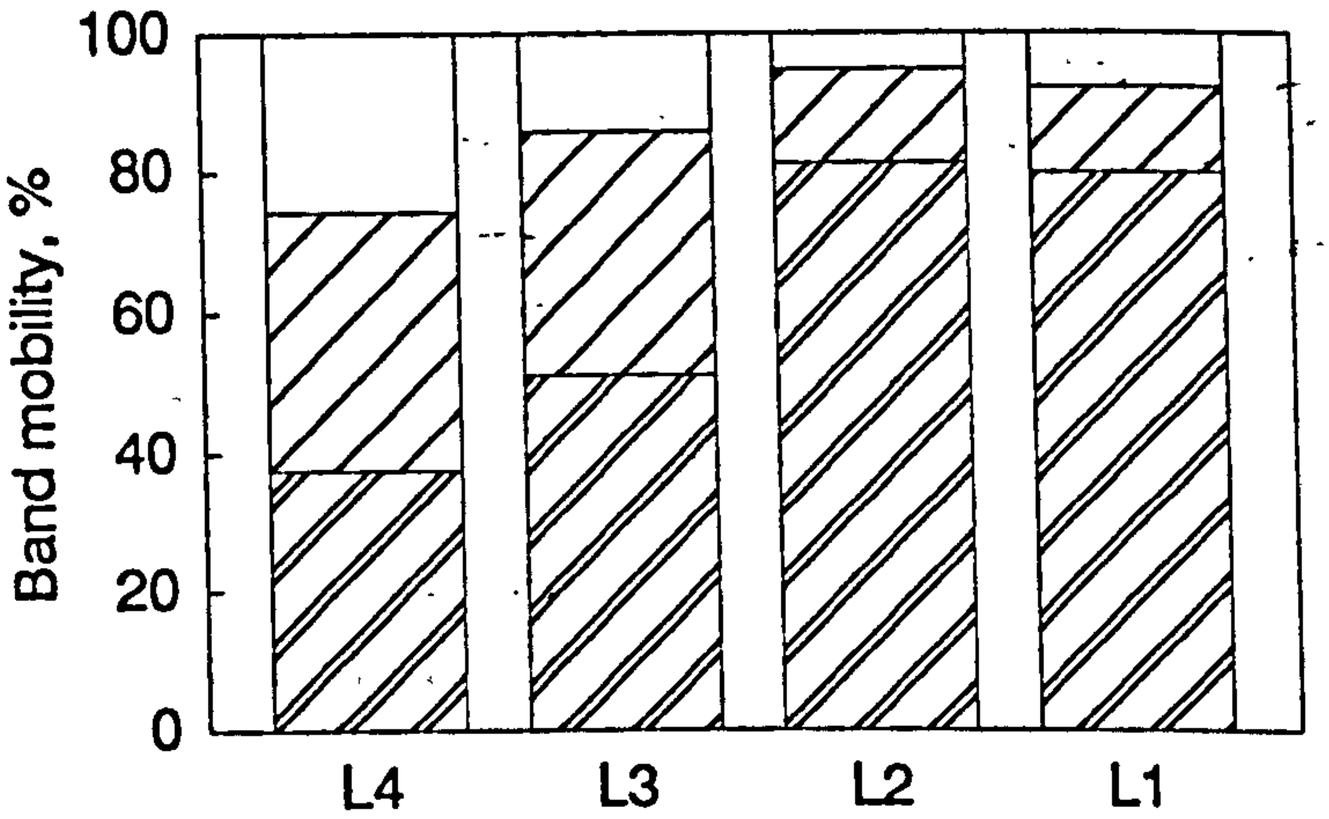

LBM = low band mobility
MBM = medium band mobility
HBM = high band mobility

Fig 7.33 Distribution of mobility in different frequency bands at each lumbar segment of patient P2.

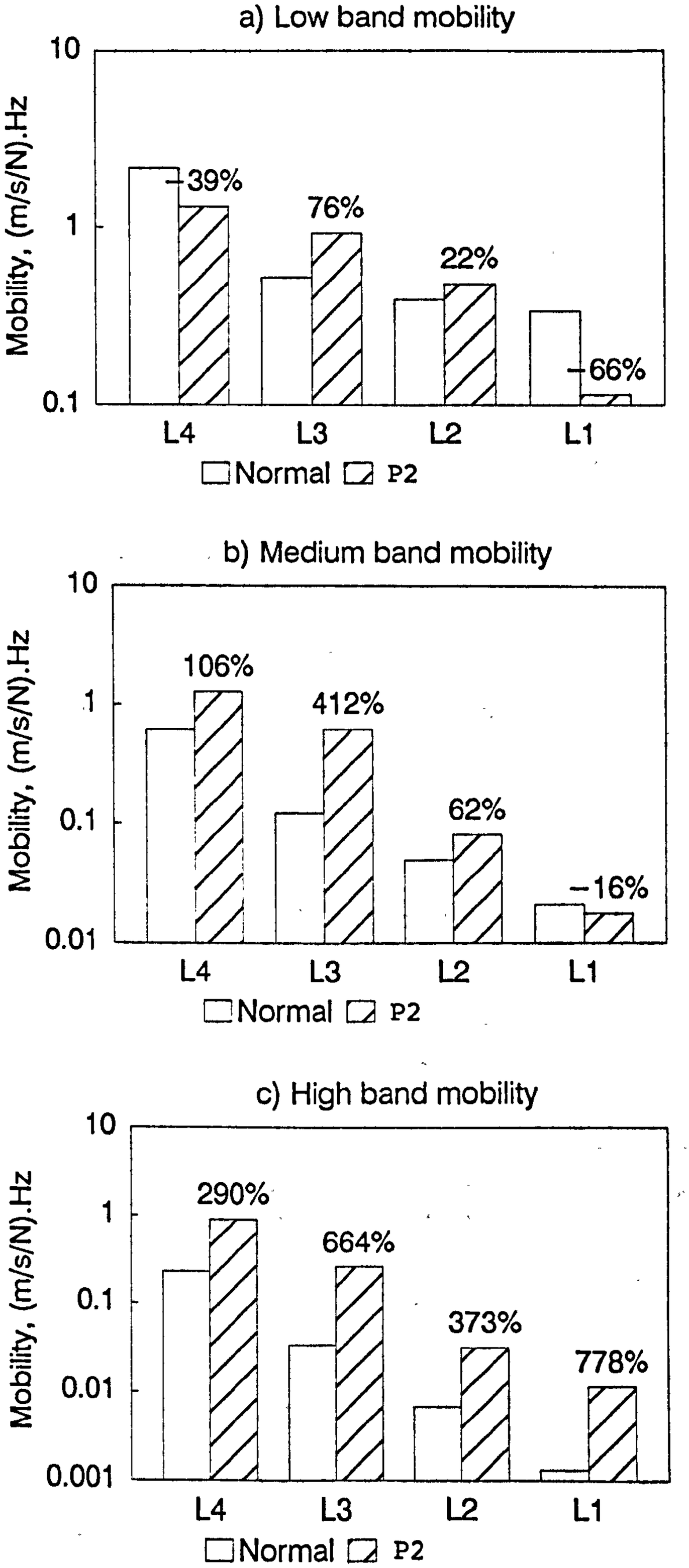

Fig 7.34 Mobility in different frequency bands measured at each lumbar segment of patient P2. Percentage indicates increase or decrease (error = 3%).

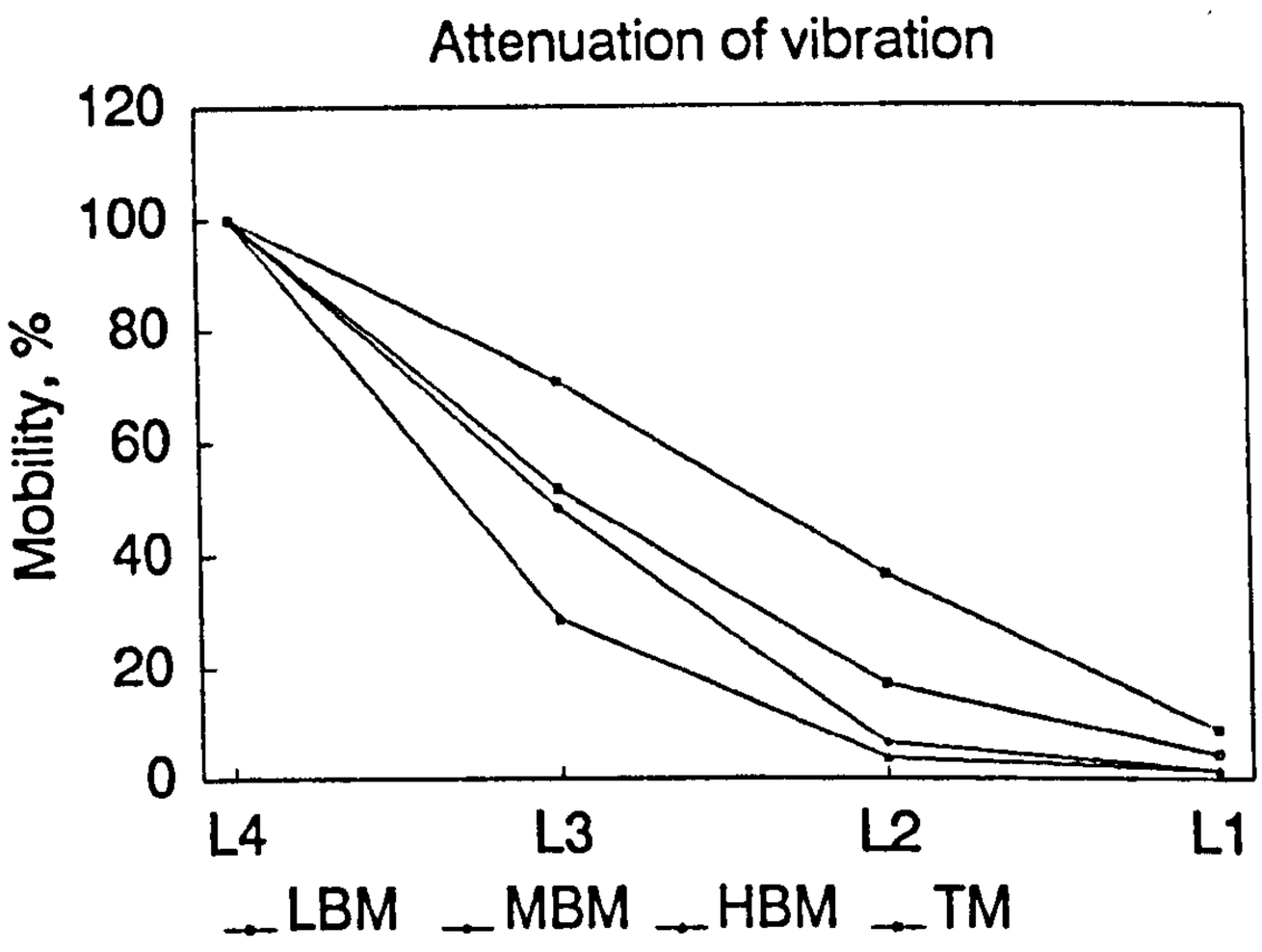

LBM = low band mobility
MBM = medium band mobility
HBM = high band mobility
TM = total mobility

Fig 7.35 Attenuation of total mobility and band mobility of patient P2.

Table 7.7
Attenuation coefficient k (in dB/segment) of band mobility evaluated for patient P2. Normal figures from tables 7.2 and 7.3 are included for comparison.

SPINAL LEVEL	SUBJECT CODE	L3	L2	L1
LOW BAND MOBILITY	P2 *NORMAL*	3.0 *12.3*	4.3 *7.4*	7.1 *5.4*
MEDIUM BAND MOBILITY	P2 *NORMAL*	6.3 *14.2*	12.1 *11.0*	12.5 *9.9*
HIGH BAND MOBILITY	P2 *NORMAL*	10.8 *16.6*	14.4 *15.3*	12.6 *15.0*
TOTAL MOBILITY	P2 *NORMAL*	5.7 *12.9*	7.6 *8.3*	9.2 *6.1*

attenuation for the band mobility. When compared with that shown in figure 7.24, patient P2 was presenting a marked decrease in attenuation to vibration particularly in the low frequency range. These were particularly noticeable from L4 to L3. Table 7.7 shows a decrease in attenuation by as much as 6 to 9 dB/segment. These findings suggest local stiffness of the lumbar spine at the L4 and L5 levels. These are consistent to the clinical information of possible structural enhancement or presence of sub-structure as a result of good bony contact in addition to the presence of instrumentation for fixation in the lower lumbar segments. The augmented medium and high frequency mobility at L3 and L4 suggests improved transmission of vibration to these two levels due to the presence of massive bone substance in the transmission path, probably as a result of united bone grafting. These findings also suggest good bony union and rigid attachment of the implant.

7.7.3 Case 3

Patient Code: P3
Sex: F
Age: 50
Diagnosis: Ankylosing spondylitis.
Brief History: Extension osteotomy at L2-3 level; Postero-lateral fusion plus CD instrumentation from the L1 to L5 levels done 7 months before the vibration test.

Patient P3 was a case which presented a very good example of a lumbar spine with advanced structural enhancement. The transfer mobility curves as shown in figure 7.36 exhibit a fairly "flat" spectrum compared with the ones from a normal subject of similar body build. Enhanced mobility was seen to extend well above 1 kHz while that in the lower frequency range was markedly diminished. These reveals that the lumbar spine behaved as a very much

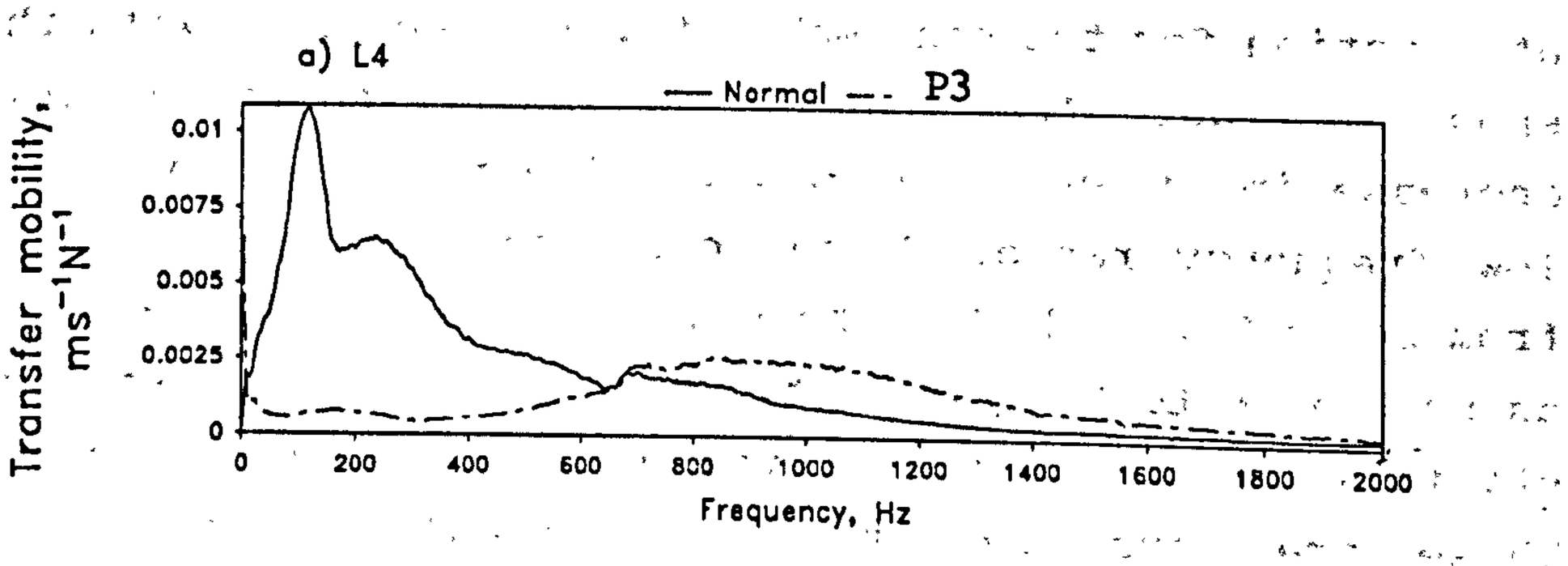

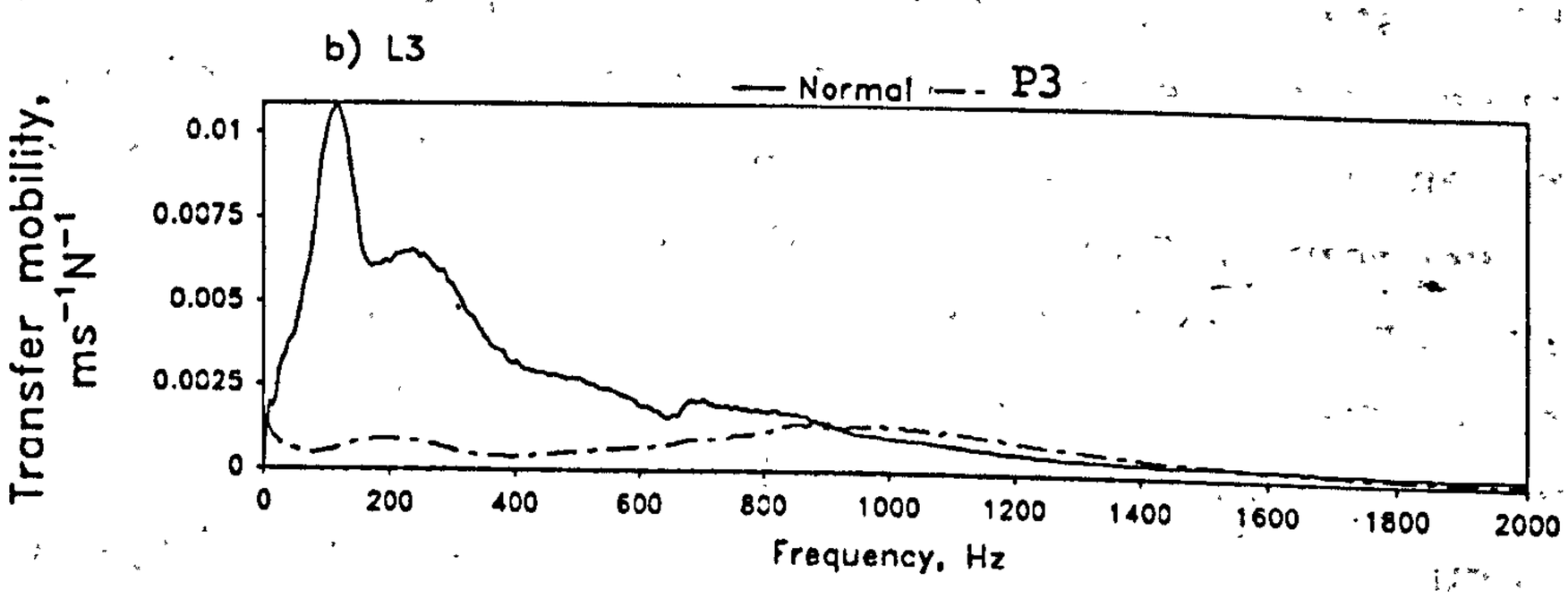

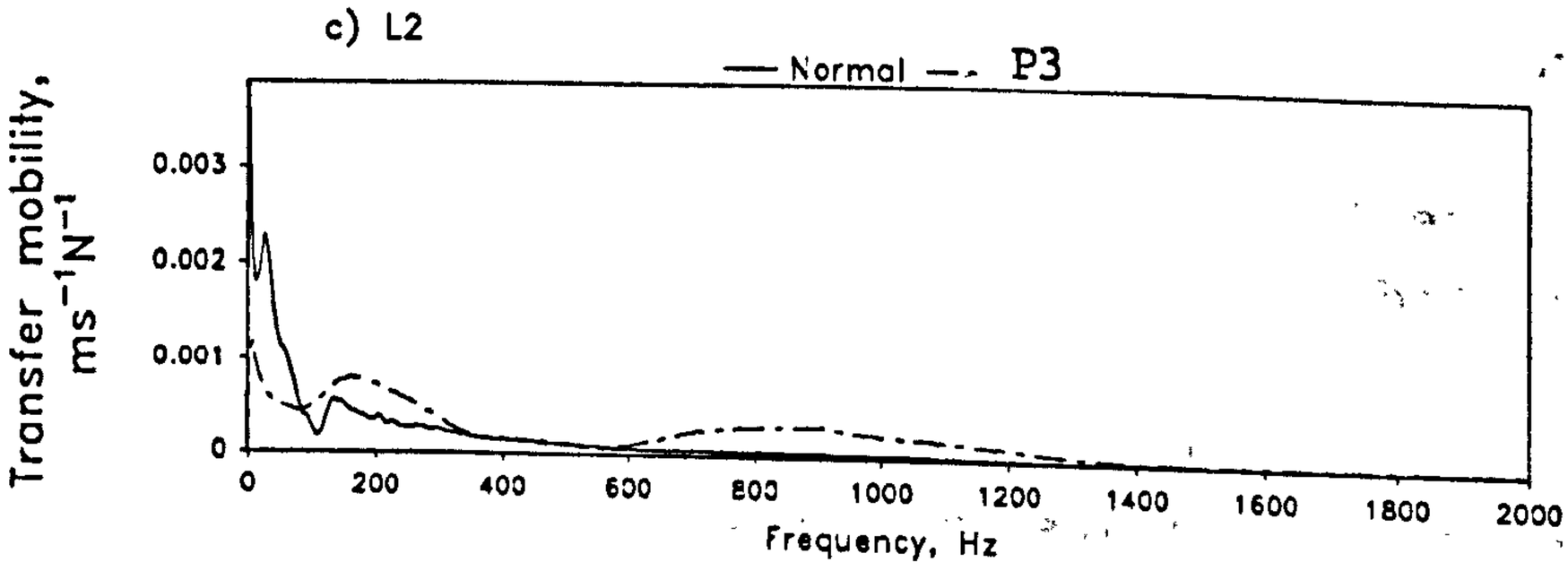

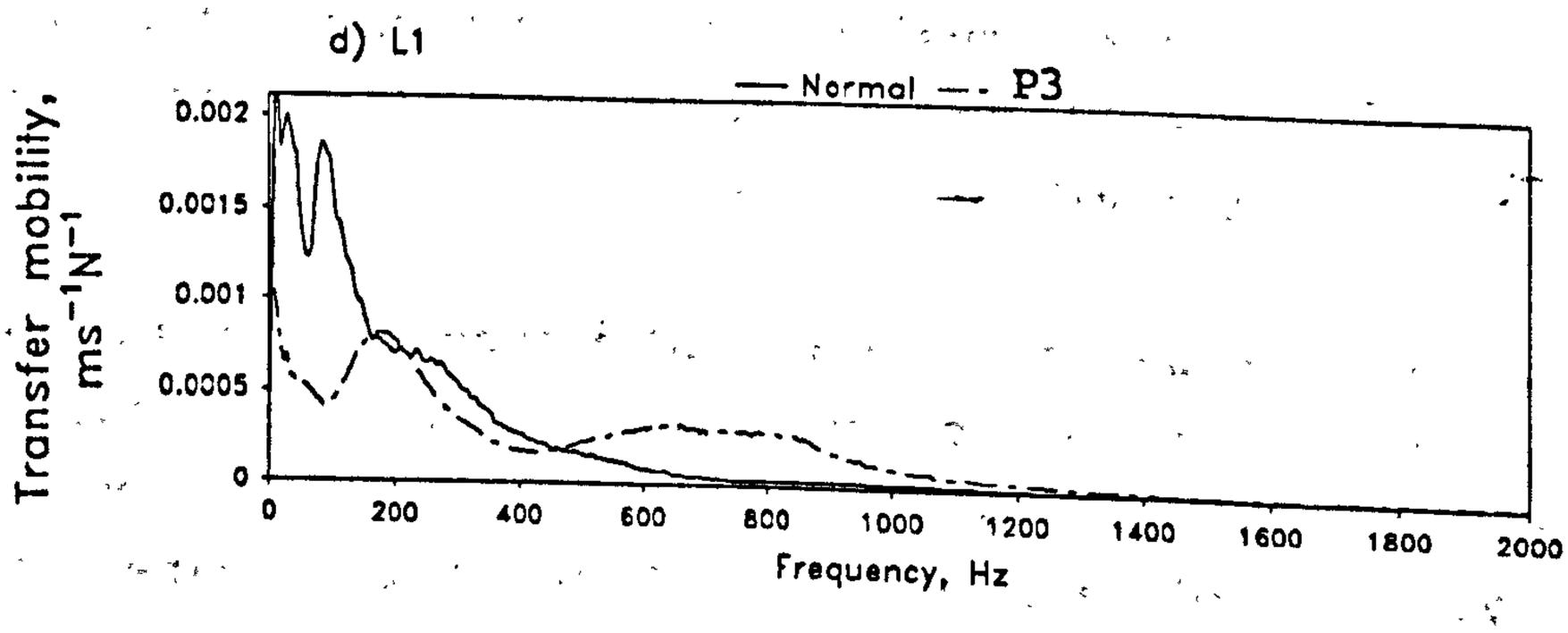

Fig 7.36 Transfer mobility measured at different lumbar segments of patient P3.

stiffened structure with solid links between segments. In the lower frequency range the lumbar spine was found to vibrate as a solid piece of structure, and therefore required a bigger amplitude of force to produce the same amount of motion. Hence the mobility in the lower frequency range was low. There were no clearly defined resonant peaks within the frequency range of interest. The summated mobility curves at L4 and L3 show a slow growth of mobility in the lower frequency range in which the curves exhibit a fairly flat region below about 500 Hz (fig 7.37). Equation 5.7 was applied to establish the coefficients A and b for the part of the curves above 500 Hz. For L2 and L1, curve-fitting by equation 5.7 was performed for the whole range of frequency. Table 7.8 lists the coefficients determined with the coefficient of determination $R^2 > 0.98$. If coefficient A is taken as the theoretical total mobility for individual segment, it could be seen that these figures were not very much different from the normal figures. This could be explained later that the increase in medium and high band mobility was roughly offset by the reduction in the low band frequency (fig 7.39), hence the total mobility would not show a significant difference in a fused lumbar spine. This implies that total mobility measurement may not be conclusive in the identification of any structural changes in the lumbar spine. Coefficient b estimated for the lumbar segments were found to be smaller than the normal figures, and statistical figures show a significant difference ($p < 0.015$). This finding was consistent with that observed on the lumbar spine with simulated fusions (section 6.4.2 & 6.4.3), and as a result of the surgical fusion coefficient b was very much reduced. Figure 7.38 shows the proportion of mobility in each frequency band at different lumbar segments. It was seen that the medium and high band mobility respectively shared a high percentage at L3 and L4 and that at L1 and L2 maintained a high percentage when compared to normal figures (fig 7.25). This is a distinctive feature of a lumbar spine stiffened by

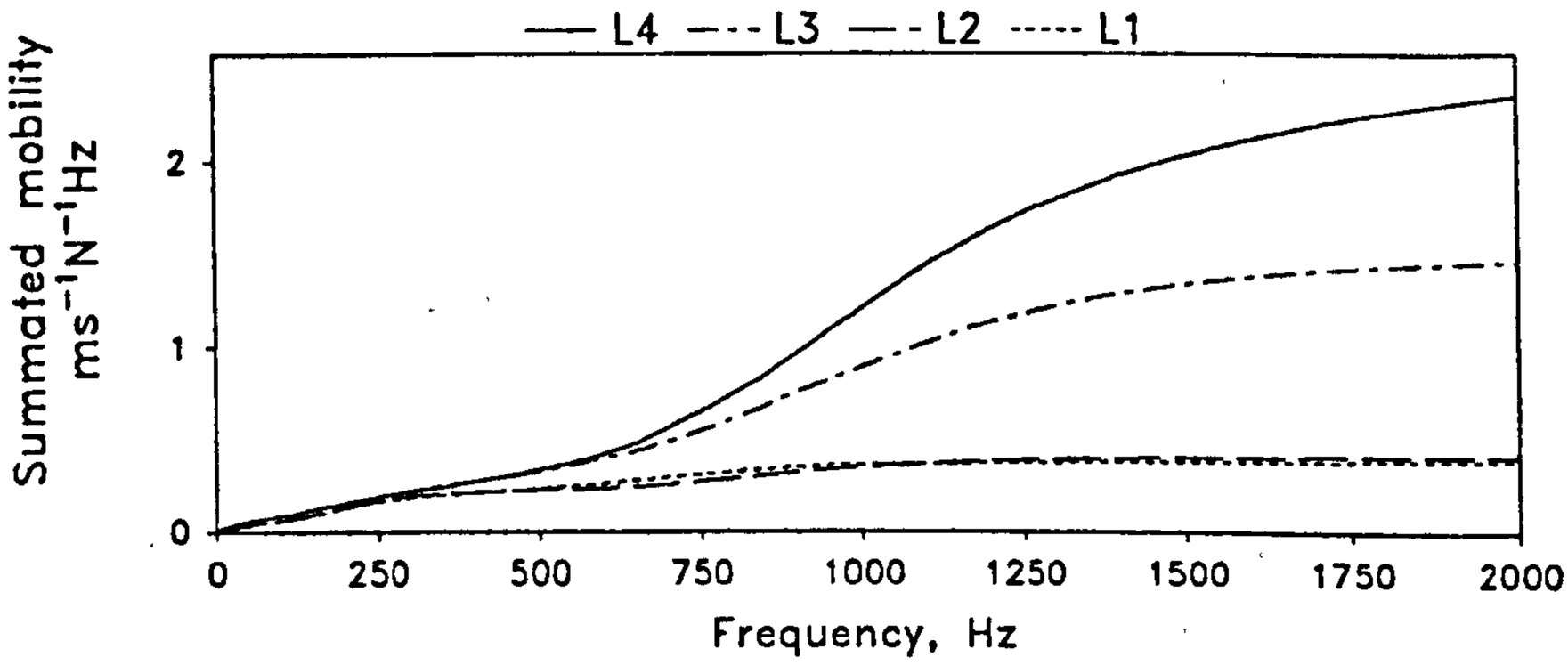

Fig 7.37 Summated mobility measured at different lumbar segments of patient P3.

Table 7.8
Coefficients A and b for patient P3 compared with figures (in italics) from normal subjects.

COEFFICIENTS	SUBJECT CODE	L4	L3	L2	L1
A ($ms^{-1}N^{-1}Hz$)	P3 *NORMAL*	3.310 *3.042*	1.769 *0.685*	0.457 *0.452*	0.406 *0.362*
b (Hz^{-1})	P3 *NORMAL*	0.00087 *0.00250*	0.00122 *0.00295*	0.00135 *0.00419*	0.00197 *0.00561*

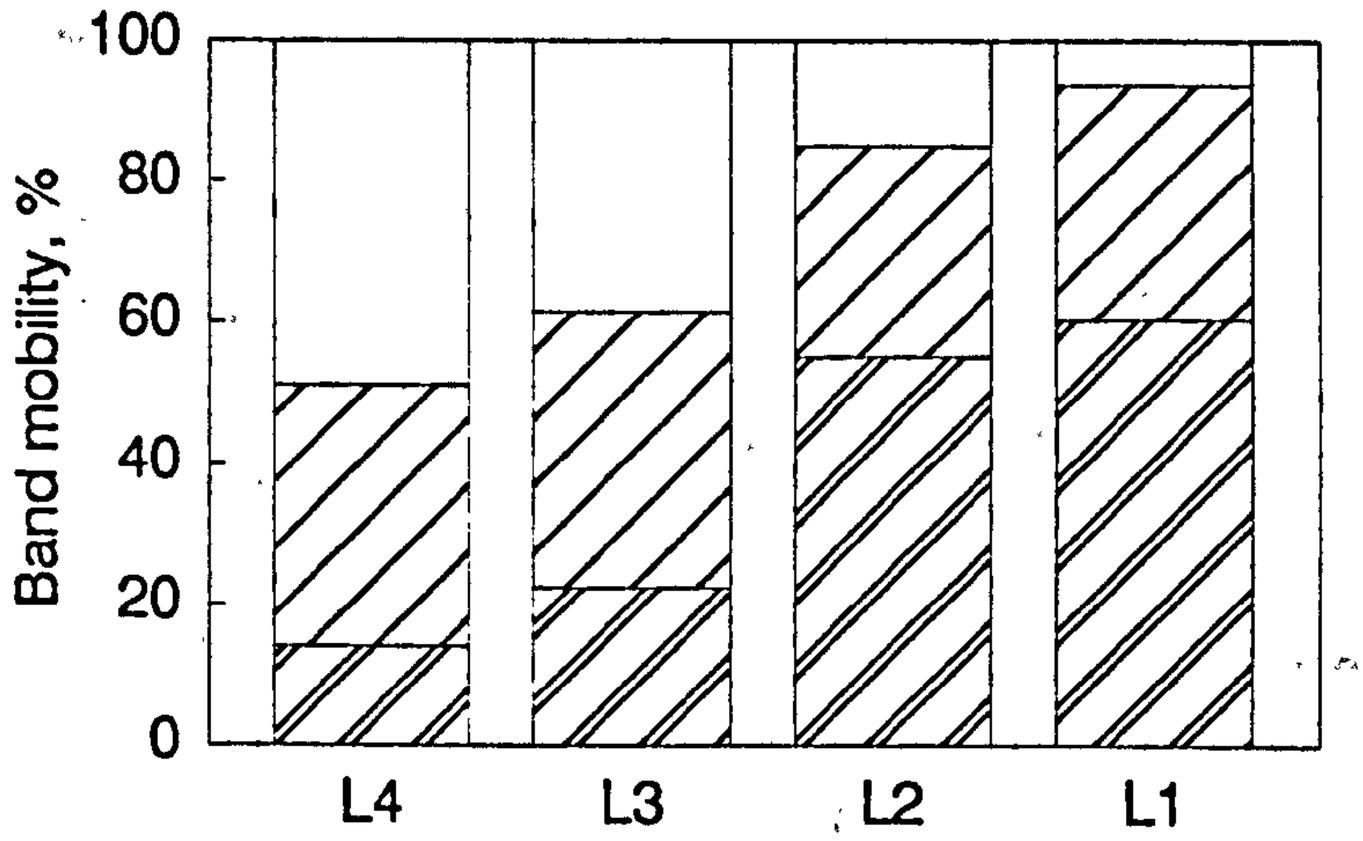

Fig 7.38 Distribution of mobility in different frequency bands at each lumbar segment of patient P3.

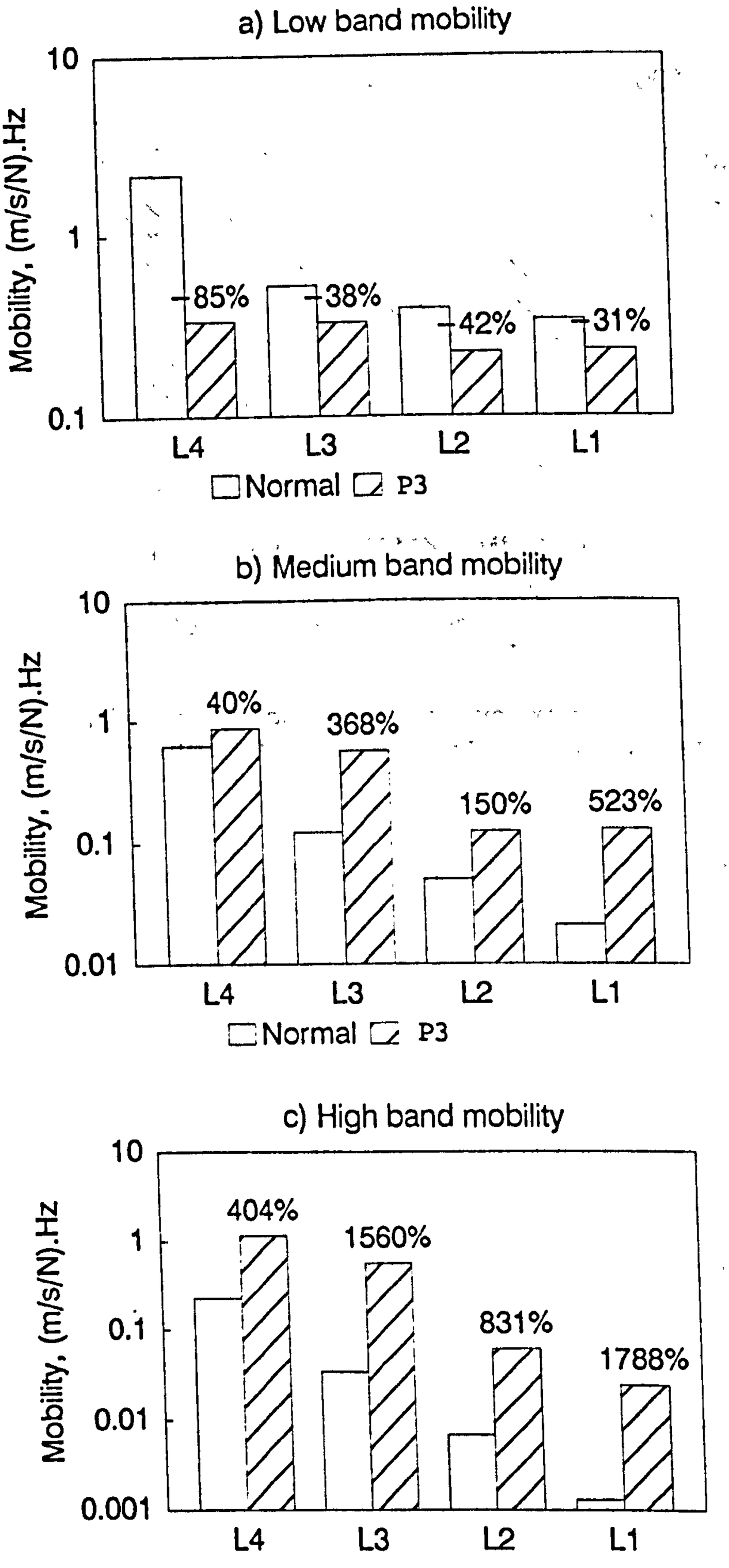

Fig 7.39 Mobility in different frequency bands measured at each lumbar segment of patient P3. Percentage indicates increase or decrease (error = 3%).

structural enhancement, probably as a result of good bony union from healed bone graft and extensive fixation by instrumentation. Figure 7.39 shows the increase of band mobility at each segment. It is seen that in the low frequency band, there was a general reduction of mobility for reasons explained previously, and the decrease ranged between 30% and 85%. There were remarkable increases in medium and high band mobility which ranged from 40% to more than 15 times the normal figures. Attenuation of vibration was seen to be much lower than normal figures, especially in the low frequency band, and also at the L3 and L2 segments (fig 7.40). The attenuation coefficient was reduced by as much as 10 to 12 dB at L3 when compared to normal figures (Table 7.9). Patient P3 was a good example of one showing greatly enhanced mobility in the medium and high frequency bands, and at the same time demonstrating reduced mobility in the low frequency band. The overall pattern of the attenuation of vibration showed a reduction at all lumbar segments. These vibratory features of the lumbar spine were found to be consistent with the clinical history.

7.7.4 Case 4

Patient Code: P4
Sex: F
Age: 39
Diagnosis: Spondylolysis L3 and L4.
Brief History: Postero-lateral fusion L3 to L5 with CD instrumentation for fixation done 8 months before the vibration test.

The transfer mobility presented by patient P4 shows all the typical features of a lumbar spine with structural enhancement. Figure 7.41 shows some reduction in the low frequency mobility while that in the medium frequency maintains a stable level and extends to above 1 kHz especially at L3 and L4. However, the picture presented

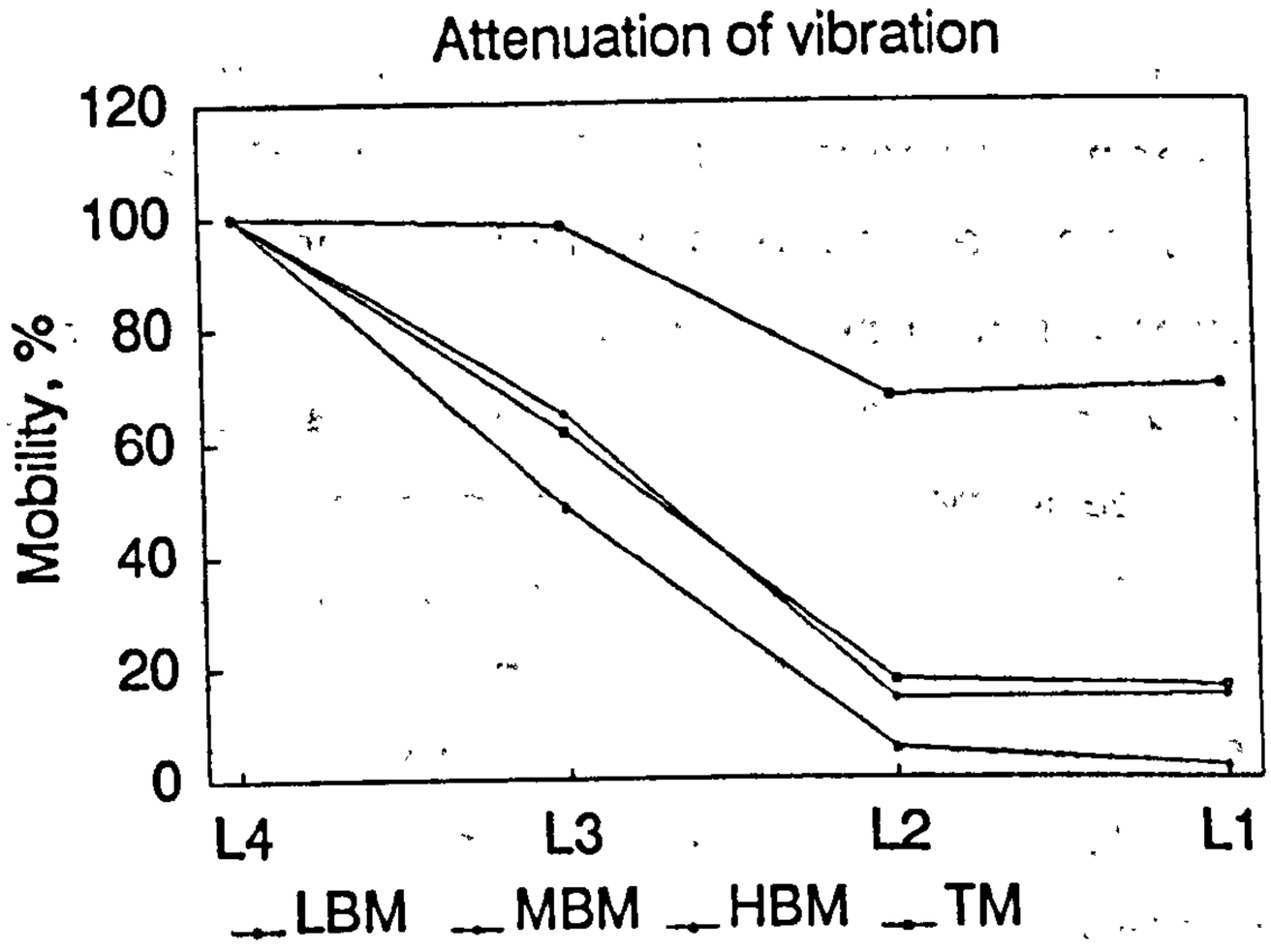

LBM = low band mobility
MBM = medium band mobility
HBM = high band mobility
TM = total mobility

Fig 7.40 Attenuation of total mobility and band mobility of patient P3.

Table 7.9
Attenuation coefficient k (in dB/segment) of band mobility evaluated for patient P3. Normal figures from tables 7.2 and 7.3 are included for comparison.

SPINAL LEVEL	SUBJECT CODE	L3	L2	L1
LOW BAND MOBILITY	P3 *NORMAL*	0.1 *12.3*	1.7 *7.4*	1.0 *5.4*
MEDIUM BAND MOBILITY	P3 *NORMAL*	3.7 *14.2*	8.5 *11.0*	5.5 *9.9*
HIGH BAND MOBILITY	P3 *NORMAL*	6.3 *16.6*	12.6 *15.3*	11.1 *15.0*
TOTAL MOBILITY	P3 *NORMAL*	4.2 *12.9*	7.6 *8.3*	5.2 *6.1*

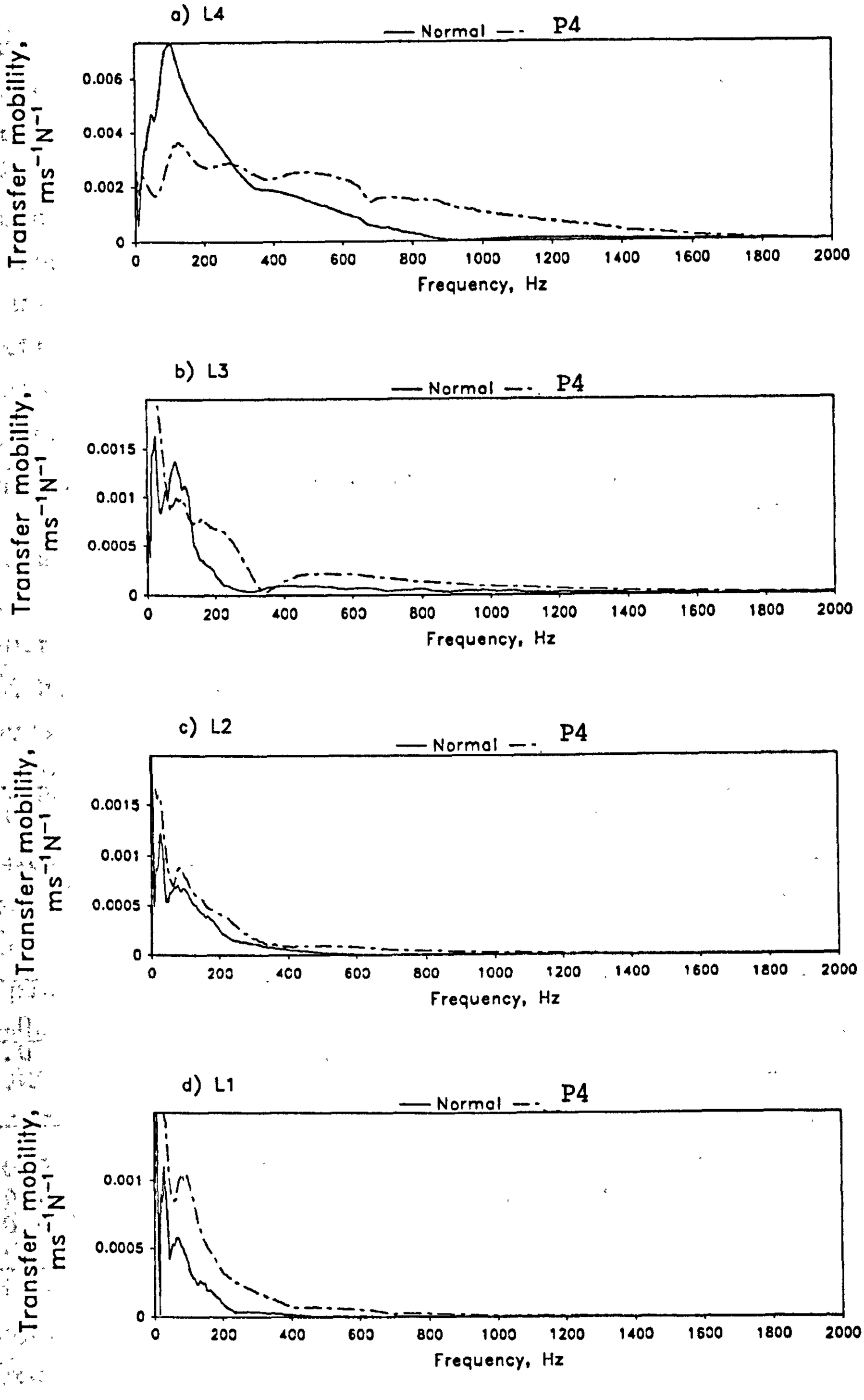

Fig 7.41 Transfer mobility measured at different lumbar segments of patient P4.

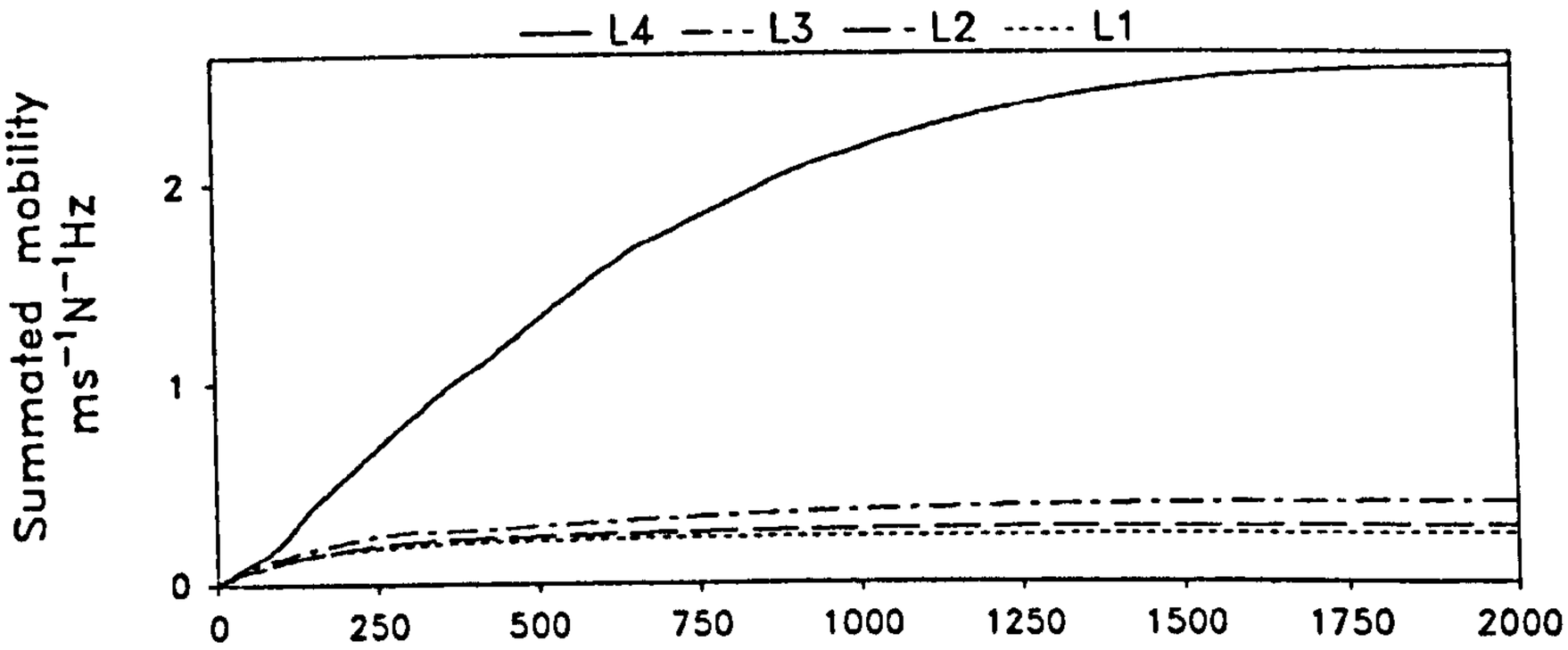

Fig 7.42 Summated mobility measured at different lumbar segments of patient P4.

Table 7.10
Coefficients A and b for patient P4 compared with figures (in italics) from normal subjects.

COEFFICIENTS	SUBJECT CODE	L4	L3	L2	L1
A ($ms^{-1}N^{-1}Hz$)	P4 *NORMAL* *N11*	2.831 *3.042* *2.120*	0.406 *0.685* *0.262*	0.281 *0.452* *0.177*	0.241 *0.362* *0.116*
b (Hz^{-1})	P4 *NORMAL* *N11*	0.00145 *0.00250* *0.00336*	0.00236 *0.00295* *0.00455*	0.00423 *0.00419* *0.00671*	0.00585 *0.00561* *0.01007*

here was only a relatively milder form when compared to patient P3 who was a case of advanced and extensive structural enhancement as a result of the surgical fusion. Summated mobility curves evaluated for this patient P4 were found to fit very closely to the exponential curve expressed by equation 5.7 (fig 7.42). The coefficient A and b were established by non-linear regression with the coefficient of determination R^2 ranged from 0.98 to 0.999. These figures are listed in table 7.10 and they are found to compare closely to normal figures. If these figures are matched with a normal subject (N11) of similar body build for the purpose of comparison, these figures show that A was slightly higher, and b was reduced by nearly half of the value of the normal subject. Patient P4 also demonstrated a higher proportion of mobility in the medium and high frequency bands (fig 7.43) when compared to this normal subject. This feature is also seen in other patients of stiffened lumbar spine with structural enhancement. Figure 7.44 shows the attenuation pattern which compares similarly to normal ones (fig 7.25). The attenuation coefficients did not show significant difference when compared with normal figures (table 7.11). This may be explained by the effect of the test subject's body structure. Among the normal subjects those with a heavier body build (e.g. N9 and N11) were found to have a higher attenuation to vibration when compared to the averaged normal figures. It could be that in patient P4 the compliance of the soft tissue structure especially that of the skin had reduced some of the effect of the structural enhancement and the vibration response was not markedly augmented as would be expected of a lumbar spine with surgical fusion. This observation in fact highlights one of the problems that vibration analysis is technically more difficult when applied on a subject of heavy body build. This problem may probably be improved by increasing the compressive preload force to a suitably higher level. During a clinical examination, patient P4 was noticed to

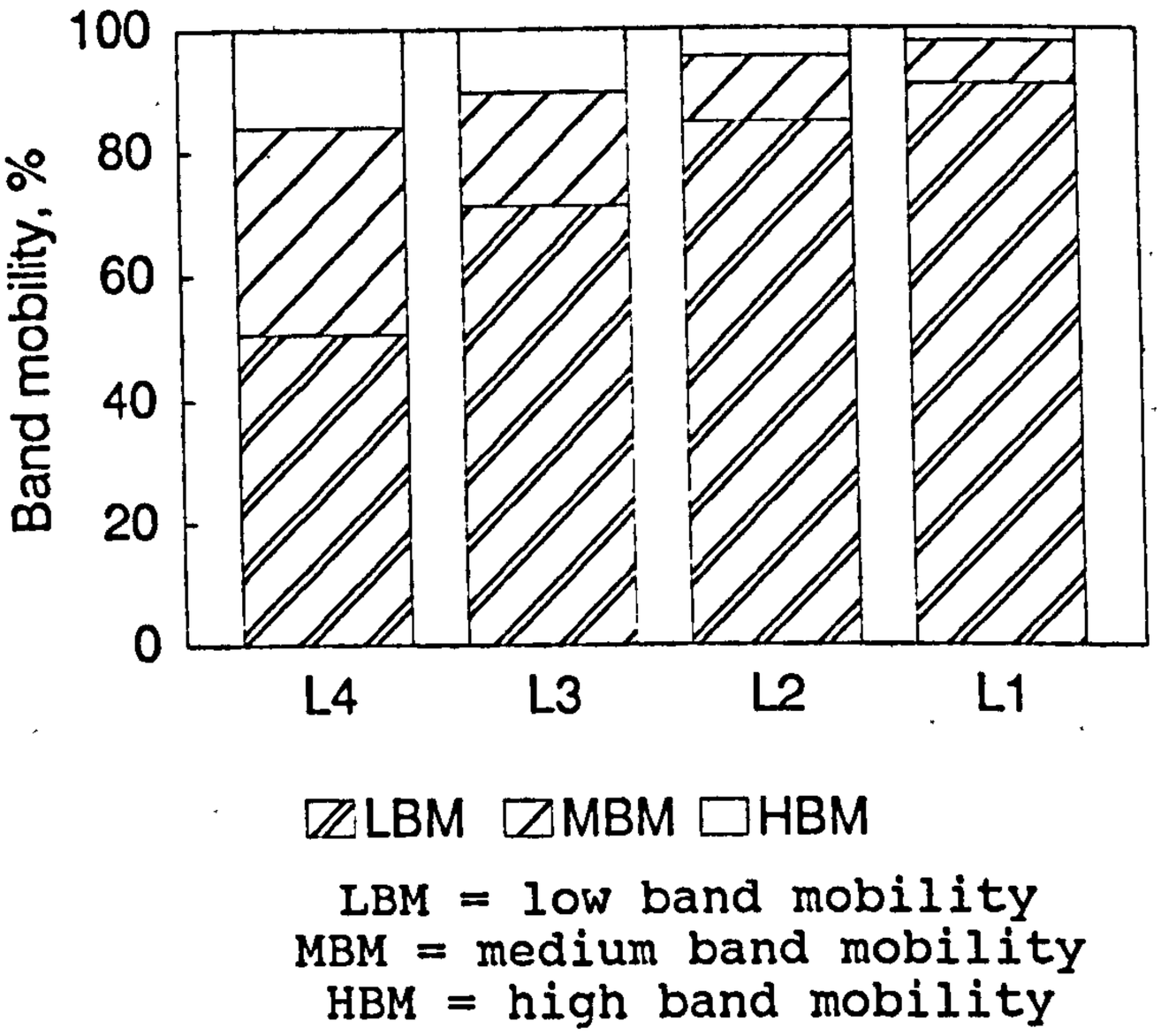

Fig 7.43 Distribution of mobility in different frequency bands at each lumbar segment of patient P4.

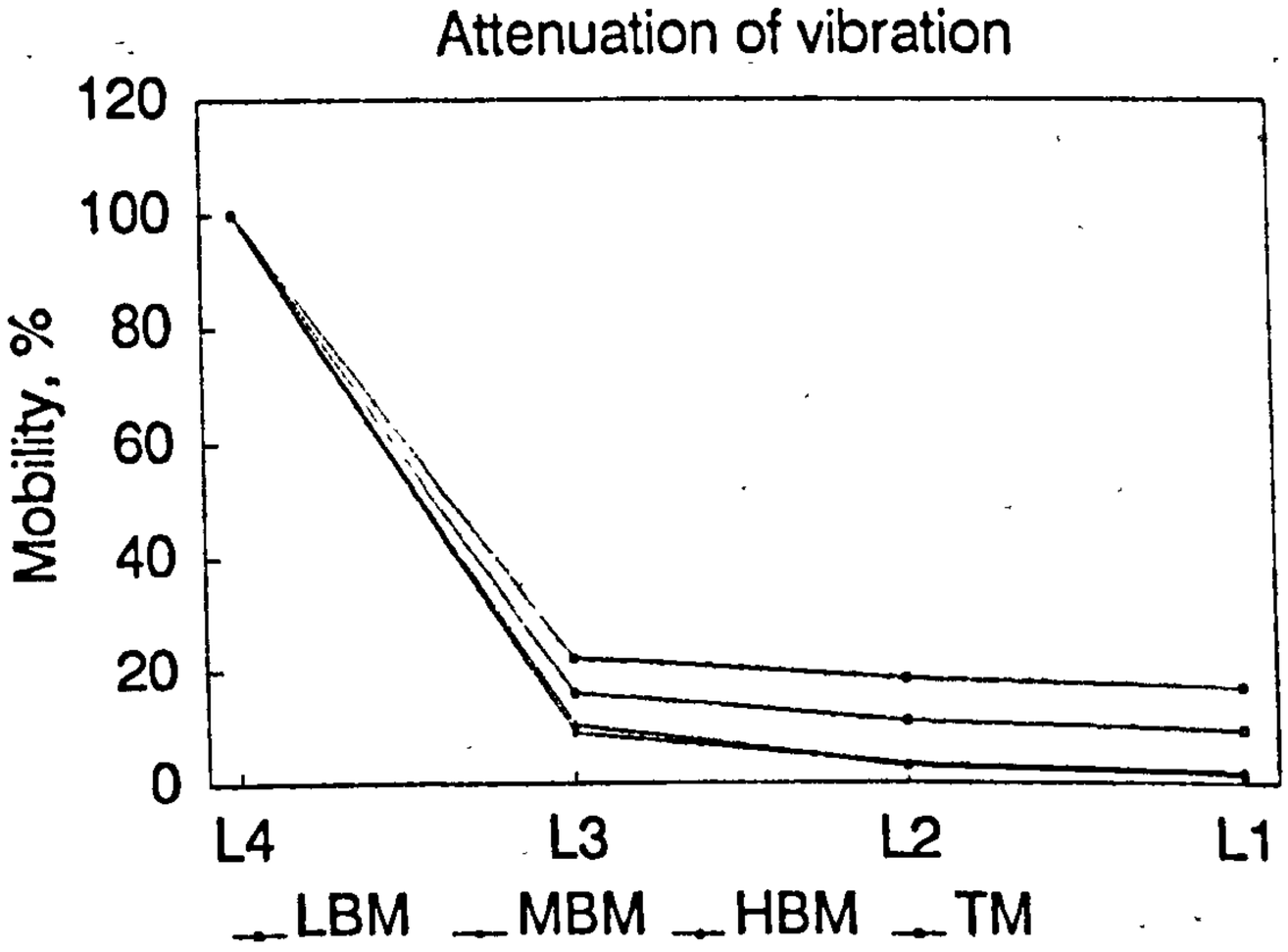

Fig 7.44 Attenuation of total mobility and band mobility of patient P4.

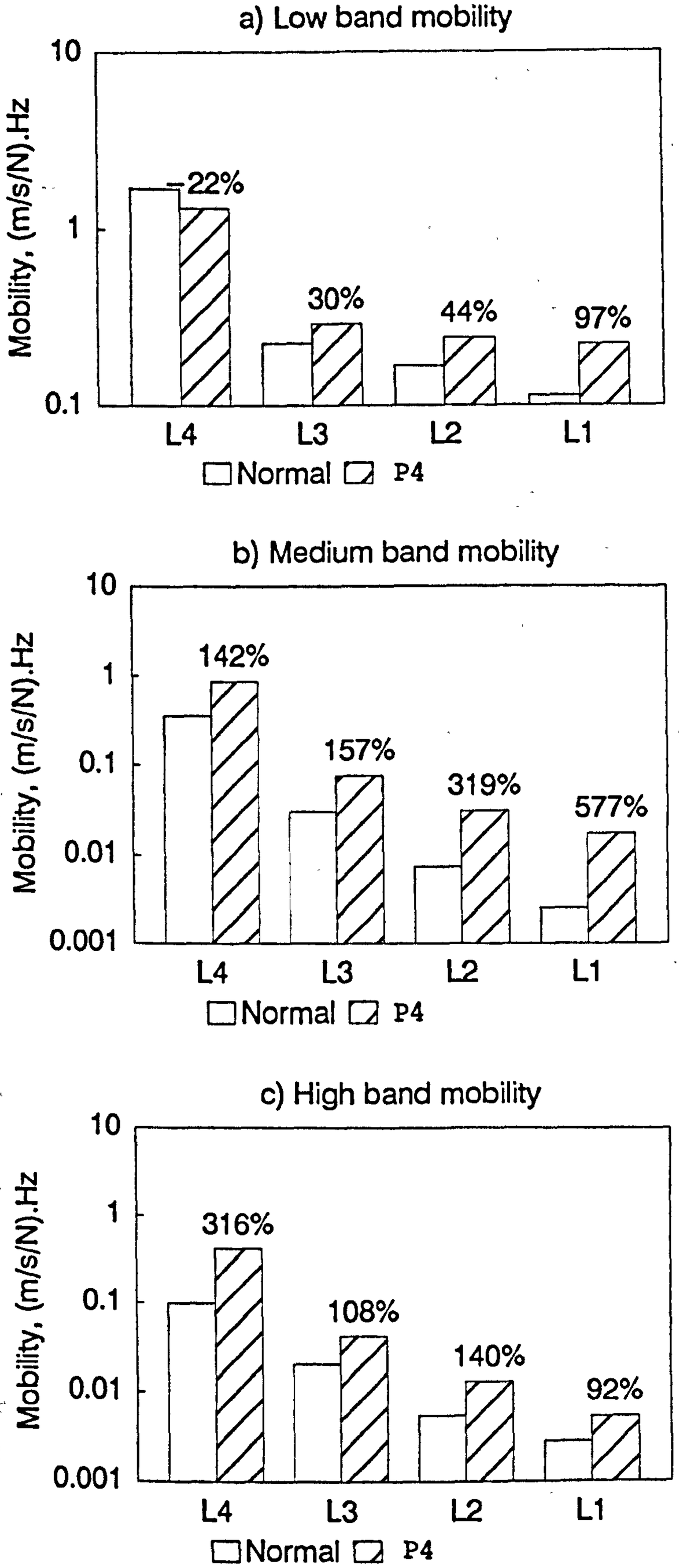

Fig 7.45 Mobility in different frequency bands measured at each lumbar segment of patient P4. percentage indicates increase or decrease (error = 3%).

Table 7.11
Attenuation coefficient k (in dB/segment) of band mobility evaluated for patient P4. Normal figures from tables 7.2 and 7.3 are included for comparison.

SPINAL LEVEL	SUBJECT CODE	L3	L2	L1
LOW BAND MOBILITY	P4	13.0	7.3	5.1
	NORMAL	*12.3*	*7.4*	*5.4*
	N11	*17.5*	*10.0*	*7.8*
MEDIUM BAND MOBILITY	P4	21.1	14.5	11.4
	NORMAL	*14.2*	*11.0*	*9.9*
	N11	*21.6*	*16.9*	*14.4*
HIGH BAND MOBILITY	P4	19.8	15.0	12.6
	NORMAL	*16.6*	*15.3*	*15.0*
	N11	*13.8*	*12.6*	*10.3*
TOTAL MOBILITY	P4	16.0	9.6	6.8
	NORMAL	*12.9*	*8.3*	*6.1*
	N11	*17.9*	*10.7*	*8.4*

have resumed a considerable amount of mobility in flexion and extension of the lumbar spine. Her low back was found to be much more mobile when compared to patient P3. This may reveal the fact that her lumbar spine was not as effectively fixed to form a rigid structure as was resulted in patient P3 who had fusion from L1 to L5. This clinical observation was consistent with the test results which showed that the vibration response of this patient's lumbar spine was not remarkedly augmented. However, the mobility measurements in different frequency bands show all the features of a lumbar spine with an overall increase when compared with a normal subject of similar body build (fig 7.45). These findings were also consistent with those observed on patient P2 (fig 7.34).

7.8 SUMMARY

System analysis has confirmed an appropriate approach to examine the in-vivo dynamic mechanical characteristics of the lumbar spine under a random vibratory test condition. The first major technical difficulty was the limited vibratory force that could be applied to the lumbar spine. The compliance of skin and the lumbar spine itself limits the effective transmission of vibratory force both in amplitude and in its frequency range. However, the magnitude of vibratory force delivered was about 0.5 to 0.8 N (RMS). This force level was very safe, and was adequate to induce a linear dynamic response of the lumbar spine. Three different acoustical sensors have been tried, and the accelerometer was found the most appropriate transducer for the detection of vibration at the lumbar spine, with respect to its working range and its broad frequency response. The compliance of skin was overcome by the application of a calibrated 10 N compressive preload force for the application of driving probe and the measuring probe though the problem of attenuation at the skin was not totally solved. However, the compressive preload was able to stiffen the skin to an extent to allow repeatable and

reliable measurements.

The measurement system established for this research was able to reveal the lumbar spine as a linear passive mechanical system with high causality between the input excitation and the output motion response. The system was not contaminated by noise generated from physiological activities internal to the human body, or that transmitted from the test environment. The paraspinal muscles did not constitute any active element to the vibratory characteristics of the lumbar spine as long as they were relaxed. The experimental set-up enabled repeatable measurements provided the test subject maintained a relaxed and restful posture.

The motion response as detected at the spinous processes revealed the vibratory characteristics of the lumbar spine. Damping was high and resonant peak was not identified both in normal subjects and in patients. Twelve normal subjects have been tested. The general pattern of the transfer mobility measurement was found to be consistent. The mobility response of the lumbar spine was found to concentrate mainly in the lower frequency range. The summated mobility was found to fit closely to an exponential expression (equation 5.7), and the coefficients A and b which characterized the motion response of each lumbar segment were established. Total mobility and the band mobility derived from the normal summated mobility curves formed the basis for comparison with the patient who was diagnosed to have an osteoporotic lumbar spine, and others of postero-lateral fusion with instrumentation for fixation. These parameters established for the patients were found to be distinctly different from normal figures. The patient with osteoporosis in the lumbar spine showed a marked decrease of 10% to 85% in mobility in different frequency bands. The attenuation was 7 to 16 dB/segment greater than the normal figures. All patients with structural enhancement as a result of surgical fusion showed features of vibration response typical of a

stiffened lumbar spine. They all showed a greater proportion of medium and high band mobility in all lumbar segments especially at those segments closer to the excitation source. The fused lumbar spine also exhibited augmented mobility by as much as 40% to 500% in the medium band mobility; and as much as 8 times the normal figures for the high band mobility. In the patient with advanced and extensive fusion, the increase was almost 18 times as much as the normal figures. The attenuation of vibration was found to be reduced in a fused lumbar spine especially for the lower frequency band. The attenuation coefficient was reduced by about 10 to 12 dB/segment in a typical case when compared with normal figures.

CHAPTER 8
DISCUSSION

8.1 INTRODUCTION

In addition to focussing on the technical issues related to the experimental work carried out for vibration response analysis of the lumbar spine, this discussion also attempts to highlight some of the main points which require further investigation or closer attention though some of these problems may not have immediate solution. It is also hoped that through this discussion, readers may be directed to new thoughts or ideas based on which a new insight into the problem would be formulated. Some of these points may help to indicate the direction for future research and broader application.

Issues related to the use of the technique in a clinical setting are also discussed and particular attention is drawn to the capabilities and limitations of this vibration response analysis technique with regards to its potential implementation.

8.2 THE EXPERIMENTAL APPROACH

The system analysis approach has been confirmed as being both feasible and appropriate as this permits a test of the lumbar spine's vibratory characteristics which is not entirely dependent of the input excitatory force. This capability is particularly important in terms of in-vivo measurement where the vibratory force is limited to low frequencies as effective excitation in the high frequencies is minimal due to attenuation at the intervening skin. Technically this approach has one major advantage in that the consistency of input excitatory force level is not critical as the vibratory characteristics are expressed as the motion response with respect to the excitatory force as a function of frequency. Surprisingly this advantage of the system analysis approach has not previously received adequate attention in the detection and monitoring of

fracture in bone by acoustic and vibration techniques. Previous acoustic technique for the identification of joint problems (Chu et al, 1976a) and the acclaimed vibration arthrometry introduced by the pioneer group from Belfast (Kernohan et al, 1990) adopt what is basically a signal analysis approach. The work on transmissibility of the pathological spine by Helliwell et al (1989) was not formally a system analysis approach as the work was based on the analysis of the output signals detected at two different locations on the spine. It is suggested here that the system analysis approach deserves more attention because of its unexplored potential for application.

Experience from this research also suggests that the measurement of driving point mobility or its derived functions, such as apparent mass, would have limited use as these do not reveal any of the vibratory characteristics of the lumbar spine. They only express the dynamic response or the transmissibility at the driving point, but lack any structural information.

The vibratory characteristics of the lumbar spine also confirm that the vibratory energy is not propagated as waves, but rather as a form of flexural vibration for which the individual vertebra of the lumbar spine could be considered as a single entity, or unit mass of definite mobility in response to the vibratory force. The lumbar spine behaves as a segmented beam in its vibratory state. Vibration concepts and associated theory have been found adequate to explain the dynamic characteristics of the lumbar spine in a vibratory situation.

8.3 THE TECHNIQUE

It has always been a technical challenge to measure the vibration of bone through overlying skin. However, to date there is no better means to ensure a reliable non-invasive measurement than the application of an appropriate accelerometer in association with a suitable level of compressive preload of the overlying tissues. The technique

outlined in this thesis has achieved acceptable reliability and repeatability as it would allow with today's technology though it still could not achieve a flat frequency response in the skin. The compressive preload force (10 N) or pressure (150 kPa) level utilized in this study has been the highest when compared to other reported studies, and it is almost the maximum level which most subjects could tolerate as determined by local pain. The designs of the driving probe and measuring probe are simple, and the dimensions are appropriate to ensure a stable placement of vibration sensor over the spinous process.

Random vibration is the most appropriate form of excitation to the lumbar spine. It allows a wide coverage of vibratory force across the frequency range of interest although a flat force spectrum could not be obtained. This technique is found to be more efficient and more complete than other techniques such as discrete frequency vibration, impact testing, or swept sine vibration. As the random vibration technique does not require a high excitatory force level this renders it more acceptable in almost all clinical test situations.

The choice of frequencies from 20 Hz to 2 kHz is appropriate and it provides a good coverage of the required test frequencies. Vibration at low frequencies corresponds to a bigger amplitude of displacement. Vibration testing in this frequency range is a test of the compliance (or, inversely, stiffness) of the gross structure of the lumbar spine, including its supports. Mobility measurement in this frequency range is a measure of the gross motion produced in the lumbar spine by the vibratory excitation. The medium and high frequency vibrations are sensitive to the modications of finer structural components. They permits the detection of any structural enhancement by demonstrating augmented motion response in these frequency bands. Such structural modifications may be the result of additional bony mass or sub-structure such as is due to the installation of metal implants. The extension to a higher

frequency range would not have any practical advantage as the greater attenuation of higher frequencies renders measurement incoherent and less reliable due to very much reduced motion response. Discrete frequency vibration testing has been found incomplete as it reveals the vibratory response of the lumbar spine only at designated frequencies though the technique has been found reliable and it provides a cross-reference with the results of random vibration testing. The use of discrete frequency vibration is not sufficiently conclusive for clinical use. The single frequency which would have discriminative power for clinical decision making has not been established though it is not certain whether the use of combined sinusoidal vibrations (multi-sine) would be of any clinical value. However, this technique may not be an appropriate choice if random vibration technique can be implemented in a clinical testing system without too much added cost or technical difficulty in operation.

The <u>end condition</u> has been found to affect the vibratory response of the lumbar spine. For both in-vitro and in-vivo studies the prone lying posture is a suitable test position. However, for in-vitro vibration testing the end support of the lumbar spine with two angle-plates seems to have been over-engineered. These two angle-plates provided too rigid a support to the lumbar spine which was consequently found to be restricted in its mobility particularly in the lower frequency range, and the system was found to be easily driven beyond its limit of linearity. Furthermore, the "resonant" characteristics demonstrated on the lumbar spine in-vitro were not clearly identified on normal subjects and patients. The in-vivo vibratory characteristics of the lumbar spine suggest a semi-rigid end support exist in life. The attachment of relaxed musculature in-vivo is not seen to have any effect on the end condition except that it may cause some damping. This is in agreement with findings on the force transmission through rabbit's tibia for which the muscle

tone did not appear to have any significant effect (Paul et al, 1978). It is also not contradictory to the observation that the muscle contraction would change the end condition of a vibrating tibia (Collier & Donarski, 1987b).

The site of excitation was suitably chosen at the L5 lumbar vertebra as it is in the lower lumbar region where surgical fusions are most commonly made. When excited at L5, the vibration responses are high at the L3 and L4 lumbar vertebrae while those detected at L1 and L2 are weaker. This may suggest that the local vibration response analysis is most suitable for the two segments next to the excitation source. For structural testing at L3-4 and L2-3 levels, the site of excitation may be better shifted to the L4 spinous process, and so forth.

The excitatory force level of about 0.8 N (RMS) has been found acceptable to all subjects. They felt only very mild stimulation when compared with domestic vibratory tools. This is definitely of very low vibration dose when compared to that delivered by motor-driven tools used in orthopaedic surgery. Hence excitation at this force level would be very safe for extensive use on normal subjects and patients with a wide spectrum of back problems, except in a situation where the patient's condition, such as pain, does not allow the application of a significant vibratory stimulus. The excitatory force so delivered is not sufficiently strong as to elicit strong muscle tone or to induce muscle spasm.

The duration of excitation of about 6.5 s for each test trial is long enough for vibration analysis, but is also sufficiently short to ensure that the test subject is not over-exposed to vibration. This short test period also opens up the possibility of developing a portable system for vibration response analysis. An extended test duration would allow a longer record of vibration signals for spectral averaging, hence a higher degree-of-freedom (N) to enhance statistical confidence. In this study N = 32, and it has been found adequate to reduce the random error to an

acceptable level. Thus a longer recording time would not necessarily introduce any further benefit.

The measurement system has been found reliable, and stable. The vibration sensors have a wide dynamic range in excess of 50 dB, and are sensitive enough to pick up weak vibration signals of high coherency with the excitatory force. A general coherence function of about 0.98 for in-vitro and 0.95 for in-vivo measurements should be considered very satisfactory. The signal-to-noise ratio of 40 dB quoted from the worst case should be taken as extremely favourable for measurements on biological systems. This corresponds to only a few percent of error. The measurement system is suitable for use in a noisy environment as seen from its high immunity from ambient noise and effective insulation from vibration transmitted from the test environment. These further support the advantage of using an accelerometer as the vibration sensor though there may still be room for improvement in terms of sensitivity to weak signals, and the technique of attachment for non-invasive measurements.

Temporal parameter, such as the time-delay between input and output signals, was very short and the transmission velocity of vibration along the lumbar spine was found difficult to determine with accuracy (section 5.8.1). There are two main reasons for this observation. Firstly, as the short distance between the two measuring points inherently demands high resolution and precision, in the order of tenths of a millisecond, in the temporal measurements, this inevitably induces inaccuracy. Secondly, the lumbar spine responds to vibration with a definite phasic relation with respect to the excitation, and measurements made at different locations on the lumbar spine would present phase discrepancies (fig 5.42). This was within about 90° at 500 Hz for that particular measurement. Hence signals detected at different lumbar segments would not by themselves show whether the discrepancy is one coming from the phasic relation or from

the actual time-delay due to definite transmission time.

Cross-correlation and cepstrum analysis are relevant analyses but with limitations in their detection of secondary signals such as echo, or vibration signals transmitted through an alternative path. Both of these mathematical analyses failed to demonstrate any utility probably for the following reasons. The secondary signals may either be too weak to be detected, or they did not actually exist. Nevertheless, the cross-correlation and cepstrum analysis only serve as a mathematical means to support the experimental observation; they should not be taken as a formal proof of the non-existence of these secondary signals.

8.4 SYSTEM CHARACTERISTICS

Linearity of the lumbar spine is confirmed within the range of the excitatory force, and within the frequency range of interest. The model, a passive linear system, is valid for the lumbar spine. The lumbar spine also presents non-resonant characteristics due to high damping. The hypothesis that the structural characteristics of the lumbar spine can be revealed by its vibratory behaviour is demonstrated.

The very limited transmissibility at frequencies above 500 Hz in an in-vivo situation imposes considerable difficulty in the measurement of vibratory response. However the measuring system was able to pick up weak but coherent vibration signals. The system was working very satisfactorily at the lower limit of its dynamic range.

It was also observed that the in-vivo and in-vitro findings were qualitatively similar, and were slightly different in quantitative terms due primarily to the additional damping effect of the associated muscles of the lumbar spine in the former situation. In both situations, the measured motion response reveals mainly the vibratory characteristics of the bony framework i.e. the lumbar spine. The associated soft tissues such as the muscles in

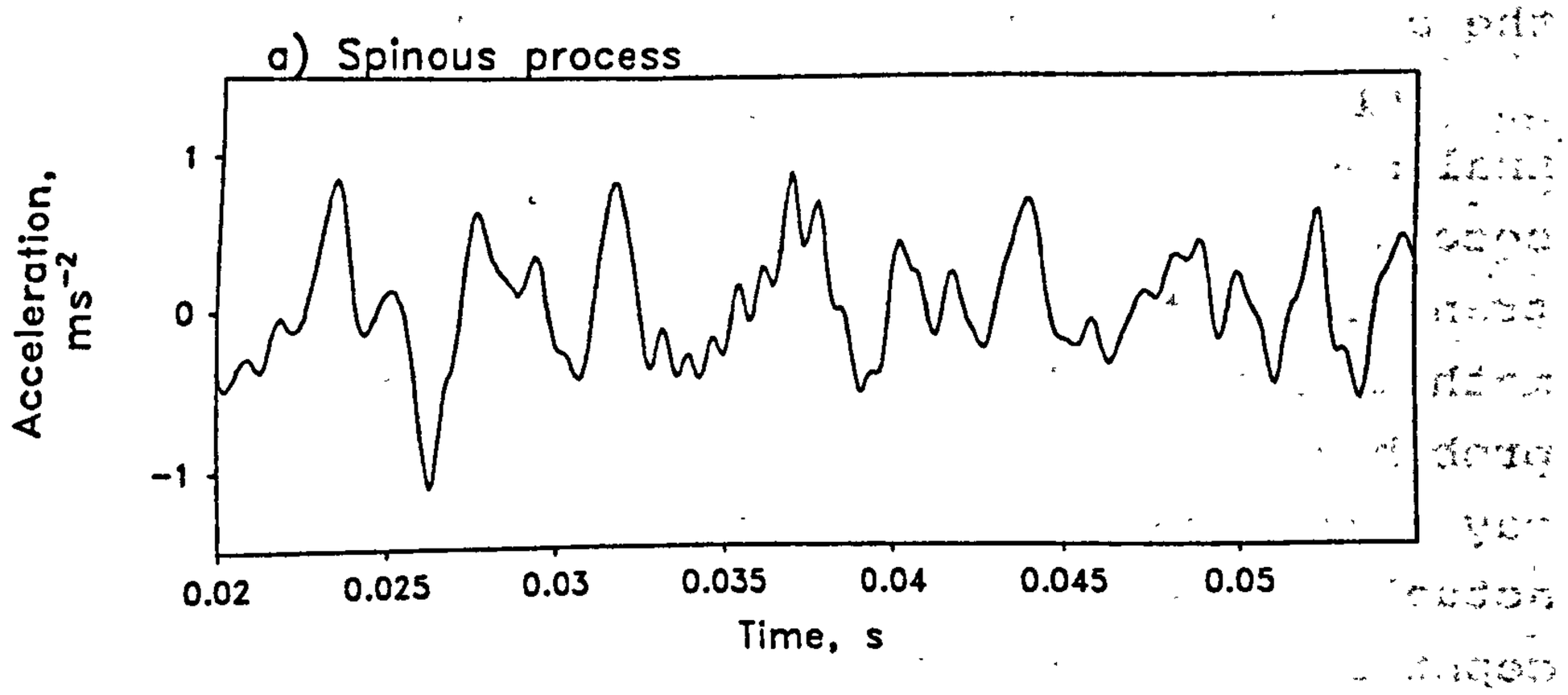

Fig 8.1 Vibration response a) at the L3 spinous process, and b) over the muscle at 2.5 cm lateral to the spinous process when the back extensors are tensed up. Excitatory force was applied at the L5 spinous process.

particular only modify the vibratory characteristics. These soft tissues enhance the damping, resulting in an ill defined resonance and unclearly identified mode shape of the lumbar spine even when surgically fused. The weaker vibration response at the higher frequencies is probably due to dispersion of energy in the overlying soft tissues and this makes the in-vivo measurement even more difficult. The skin is another major factor which modifies the vibration response by limiting the effective transmission of excitation to the bone, and attenuating the vibration signals detected over the spinous processes. This is particularly noticeable for the high frequency components.

There are no differential transmission paths detected in the lumbar spine. Individual vertebrae should each be considered as a rigid mass forming a unit entity of the segmented beam. This is an acceptable model as far as the spatial resolution of the system allows.

Relaxed muscle has been found to modulate the amplitude of motion response, but it does not have any effect on the vibratory characteristics of the lumbar spine. However, active muscle has been found to produce a different effect. As reported in section 7.6.4, the lumbar spine demonstrates a clear resonance when vibrated while under the influence of active back extensors. The tensed muscle forms a system of entirely different vibratory characteristics in association with the column of lumbar vertebrae. This was observed from the measurements made at the L3 spinous process and over the back extensor muscle at a point about 2.5 cm lateral to the L3 spinous process. The accelerometers were placed under 10 N compressive preload force over these two measuring points. The response signals were found to be almost identical but were nearly opposite in phase (fig 8.1). This finding suggests a dynamic system in which the two major components i.e. the bone and muscle were resonating. However, a clear explanation of this observation in not available, and this new system is deemed beyond the scope of the current study. It has certainly

opened up a new area in that the dynamic characteristics of the lumbar spine warrant further investigation.

8.5 SYSTEM PARAMETERS

Transfer mobility is an appropriate measure of the motion response of the lumbar spine under a controlled excitatory force. However, the non-resonant behaviour of the lumbar spine poses difficulties in the identification of resonant frequency and its related vibratory features from the transfer mobility spectrum. Furthermore, the detection of resonance may not be of any practical use because the lumbar spine does not present resonant characteristics even in the case of sound and extensive surgical fusion. As a consequence, modal parameters such as the modal frequency may not be useful, not only because they are difficult to identify, but more importantly because they do not indicate quantitatively the amount of change in the vibratory response as a result of structural modification. The mode shape is ill defined and would not be informative, and the modal damping would not allow the quantification of damping of the lumbar spine. It has not been possible to relate these modal parameters to other physical parameters of a vibrating lumbar spine. In practice, modal testing would be of very limited use on the lumbar spine.

Summated mobility and the establishment of coefficients A and b for the exponential expression (equation 5.7) has been found useful. Coefficient A is related to the theoretical total mobility projected by the summated mobility measurement. It would give some indication of the expected total mobility in absolute terms. Due to individual variability, this measurement may have some limitations in its use. Coefficient b indicates the trend at which the mobility accumulates across the frequency range of interest. It describes the mobility measurement in a quantitative term. It has demonstrated stronger discriminative power, and a statistical test shows

significant difference between normal figures and those obtained on a fused lumbar spine. However, an indicative norm of these coefficients has yet to be established. It would require an extended study to establish a series of normal figures to match with the age, gender, and other physical dimensions such as height and body mass.

Band mobility is able to characterize the motion response of the lumbar spine by giving a specific measure of its mobility in different frequency ranges. The lumbar spine has been found to exhibit varied mobility in different frequency bands. The proportionality of mobility in different bands has been established for different lumbar segments of the normal subjects (fig 7.25). This pattern of mobility distribution has been found to provide a useful basis to which mobility of surgical fused lumbar spine can be referred. It has been found that the proportionality among mobility in different frequency bands would change with surgical fusions, and some features could be identified from these changes. Different band mobility has different discriminative power. The high band mobility has been found the most sensitive to structural modifications of the lumbar spine by presenting a higher percentage of increase in a surgically fused lumbar spine. However, at this stage band mobility measurements would be of use only in a relative sense. A threshold value for this mobility for discriminative purpose has not been established. It would be most useful if measurements were made at different clinical or surgical stages so that the structural changes of the lumbar spine could be monitored. Measurement could be made in the immediate post-operative period to establish a basis so that the healing of bone graft and the integrity of the surgical implant could be monitored at a later stage.

Total mobility may not have discriminative power because a stiffened lumbar spine would present both a reduction in low frequency mobility while that in the higher frequency range is enhanced. The effect of these two

may offset each other in both in-vitro and in-vivo situations. Hence the measurement of total mobility may not produce any information on the structural changes of the lumbar spine. It could also be explained in energy terms by assuming a constant vibratory energy transmitted into a lumbar spine, and assuming also the same amount of energy loss due to damping and dissipation as heat. A reduction of mobility (energy) in a particular frequency range would be offset by a corresponding increase of mobility at another frequency. It would constitute a shift of energy to another frequency in accordance with the system's vibratory characteristics. Hence the measurement of total mobility would have limited use in indicating the changes in the vibratory characteristics of the lumbar spine.

Attenuation is a vibratory feature of the lumbar spine. It is about 5 to 17 dB/segment in a normal situation, and about 8 to 32 dB/segment in a patient with osteoporotic lumbar spine. The attenuation coefficient ranges from 0.14 to 13 dB/segment in a lumbar spine with advanced and extensive fusion. These figures are found to be very much higher than the mean attenuation coefficient 0.023 cm^{-1} (0.2 dB/cm) of the stress propagation along human long bones (Pelker & Saha, 1983). Assuming a nominal height of 3 cm for each lumbar segment, and that the nominal attenuation coefficient of a normal lumbar spine is about 10 dB/segment, it is not surprising that this figure is much higher than that in the human long bones - an estimated figure which is roughly equal to 0.6 dB for a transmission distance of 3 cm. Since the lumbar spine is a complex structure comprising intervertebral discs and the vertebral bodies which have cancellous bone as the major substance, this nominal attenuation coefficient of 10 dB/segment should be considered very reasonable when compared to a long bone with its physical continuity of cortical bone substance. In this context, it could be explained that a surgically fused lumbar spine would provide a bony continuum between segments. With the

Table 8.1
Attenuation coefficient k (in dB/segment) of total mobility with respect to a lower lumbar segment.

SPINAL LEVEL	L4 to L3	L3 to L2	L2 to L1
IN-VITRO	5.6 dB	3 dB	1.4 dB
IN-VIVO	13 dB	3.6 dB	2 dB

presence of instrumentation for fixation, this would form a more "solid" structure for the transmission of vibration. Hence the attenuation will be reduced as seen on patients with surgically fused lumbar spine.

The pattern of attenuation in-vitro has been found to possess an exponential form. However the figures listed in table 8.1 show that the attenuation of mobility was not uniform. This is more distinct for in-vivo measurements where the pattern is quite different. There is a marked attenuation (13 dB) from L4 to L3; whereas it is about 3.6 dB from L3 to L2; and 2 dB from L2 to L1. This observation is here described as a "local effect". It may be a result of the mechanical links existing between L5 and L4 in an in-vivo situation. The L4 lumbar vertebra does not behave as a purely passive element receiving vibratory excitation from L5. Instead it acts as a part of an "extend" excitation source. The L4 lumbar vertebra partly receives excitatory energy through the associated paraspinal structures such as the muscles and ligaments, and perhaps through the skin. The effect of these is only localized to the close vicinity of L5 and L4, and it does not extend to other levels due to high attenuation. As a consequence the vibratory response at L4 is higher than would result merely from transmission through the lumbar vertebrae. This "local effect" was not so obvious in an in-vitro situation as the isolated lumbar spine lacks these associated soft tissue structures. However it was not tested whether the "local effect" described above also extended to the sacral region. This requires further investigation.

Attenuation coefficients listed in table 8.1 also confirm the greater attenuation in an in-vivo situation because of the damping effect of surrounding soft tissues such as the muscles.

8.6 CAPABILITIES AND LIMITATIONS

The random vibration technique provides a structural test of the lumbar spine. This technique shows the

correlation of the vibratory characteristics of the lumbar spine with its structural modifications. The lumbar vertebra is probably the smallest unit that could be analyzed by this vibration technique. This is due to the limited spatial resolution of the testing technique. The suggestion of transmission path through material may not hold. *Functional stiffness* due to muscle contraction and *structural stiffness* as a result of additional bone mass or the installation of implant can be differentiated by the vibratory characteristics of the lumbar spine. In the former case, the lumbar spine presents a resonant characteristic at low frequencies, as already described. In the latter, a lumbar spine stiffened by structural enhancement would present non-resonant characteristics with augmented mobility both in the medium and high frequency bands.

The mobility measurement is only sensitive to gross structural changes. It is incapable of telling the nature of finer structural modifications. It may show the location in relation to the lumbar level. However, it may not indicate the cause i.e. whether it is a result of united bone graft or it is due to the presence of instrumentation. Neither does it tell the specific site of fusion.

Due to attenuation, mobility measurement is most useful for the two lumbar segments closest to the excitation source. For examining upper lumbar segments, consideration should be given to shifting the site of excitation to a higher lumbar level.

With limited information, it is still not possible as yet to establish a monitoring index of discriminative value against which a clinical decision, for example the indication of the presence (or absence) of change in structural stiffness of the lumbar spine, could be made.

The vibration system does not allow the detection of coupled movement such as rotation about the transverse axis. Information of these movements is lacking though they are expected to be minimal under such a low excitatory

force level employed in this study.

There has been no attempt to relate empirical results with gender, age, and the degree of change in structural enhancement. It was only possible to establish a general picture of the vibratory characteristics of the lumbar spine under normal or pathological conditions. It would be worthwhile to extend the study to a bigger sample so that a more reliable statistical norm would be established for future reference, and to establish a database for further clinical study.

There was only one clinical case to show the attenuation in an osteoporotic lumbar spine and the evidence should only be taken as a demonstration rather than a proof of discriminative power.

8.7 CLINICAL APPLICATIONS

With the advancement in technology and the development of new techniques of analysis, it should be possible for the vibration response analysis technique to be developed further for regular clinical applications. Possible areas of application are related to problems involving structural abnormalities of bone and joints, and those which would introduce varied acoustical transmission characteristics in the musculoskeletal system. The following are some suggested examples:

- Postoperative testing of the integrity of the spinal column for future reference. This may also apply to cervical and thoracic spine;
- Monitoring of healing bone graft by testing the vibration response at different stages after surgery;
- Testing for the integrity of bone-cement or cement-implant interfaces - possible application in the installation of implants such as total knee replacement;
- Identification of joint problems such as developmental dysplasia of the hip, ankylosing

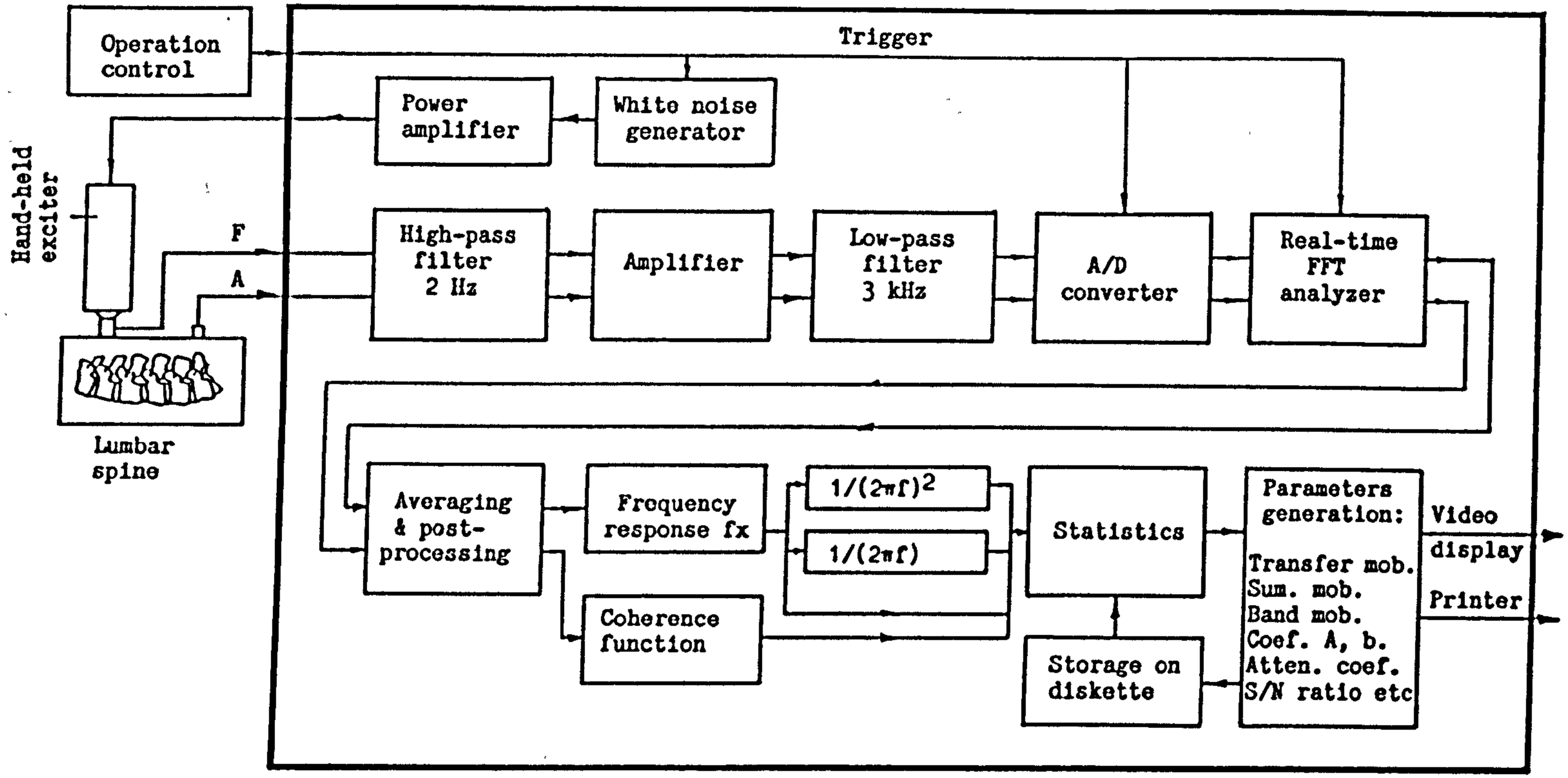

Fig 8.2 Schematic diagram of a real-time vibration response analyzer of the lumbar spine. F and A are respectively force and acceleration signals.

Parameters:

Transfer mob.	=	transfer mobility
Sum. mob.	=	summated mobility
Band mob.	=	band mobility
Coef. A, b	=	coefficients A, b
Atten. coef.	=	attenuation coefficient
S/N ratio	=	signal-to-noise ratio

spondylitis, fusion of the sacro-iliac joint, or chondromalacia patella;

- Detection of loosening of hip prosthesis;
- Monitoring of bone fracture healing; and
- Diagnosis of degenerative changes such as osteoporosis etc.

8.8 IMPLEMENTATION

Based on the evidence presented it would be highly desirable to develop a portable apparatus for non-laboratory based application of the vibration response analysis technique on the lumbar spine. This apparatus should preferably be equipped with suitable hardware and software for data acquisition, data processing, graphic display and charting of test results. A complete system should include an excitatory source which incorporates a white noise generator of controllable output, an excitation system which includes a power amplifier and a hand-held exciter with suitable vibration probes. A system with a specially designed fast processor to enable real-time analysis would be of great advantage. The ability to store test results for archiving and future retrieval would be an additional requirement for such a system. The apparatus should also be safe and user-friendly so that it could be operated by non-technical staff after suitable training. These requirements are most important if the system is to be used extensively in a clinical setting.

The schematic diagram of the major components and the suggested algorithm for data processing and analysis are outlined in figure 8.2. The major technical specifications are suggested below:

Excitation:

Random vibration 20 Hz to 2 kHz;

Force rating: 1 N (RMS), adjustable.

Transduction:

One force channel: sensitivity > 1 V/N;
Dual acceleration channel: sensitivity > 1 V/(ms^{-2});
Frequency range: 20 Hz to 2 kHz;
Input range for acceleration: 1 to 20 ms^{-2}(selectable);
Filters: high-pass at 2 Hz; low-pass at 3 kHz.

Data acquisition:

Resolution: at least 12 bits;
Sampling rate: 10 kHz;
Record size: at least 65536.

Data analysis:

Real-time dual channel FFT-based analyzer;
Frequency response function: transfer mobility;
Post-processing: summated mobility; band mobility;
Coefficient determination: A and b (equation 5.7).

8.9 SUMMARY

The technical capabilities and limitations of vibration response analysis developed for this research have been discussed. Potential areas of clinical applications in relation to the structural problems of bone and joints have been outlined. At this stage, the experimental findings have been able to establish a picture of the vibratory response of the lumbar spine under normal and pathological conditions, and the results suggest that the technique is able to relate the vibratory response of the lumbar spine with its structural modification as a result of surgical intervention. Further investigation is suggested to establish a database for clinical use. It is anticipated that this technique could be developed for clinical application or use in the objective assessment and monitoring of spinal fusions and other structural changes in the musculoskeletal system.

CHAPTER 9
CONCLUSIONS

A vibration technique based on a system analysis approach has been developed to examine the local vibratory characteristics of the lumbar spine. The problem imposed by the limited transmissibility of the skin due to its high compliance has not been fully solved, but the application of a 10 N compressive preload through the transducer is the most appropriate non-invasive means of stiffening the intervening skin to achieve an acceptable transmissibility. The test system is free from noise with signal-to-noise ratio better than 40 dB in the worst situation. The statistical confidence of vibration response measurements is high, and a typical coherence function is 0.95 which corresponds to an error of less than 3%.

The human lumbar spine behaves as a complex mechanical system similar to a segmented beam with semi-rigid supports distally at the sacrum and proximally at the thoracic cage. It presents non-resonant vibratory characteristics with multi-degree-of-freedom under a random vibratory force of less than 1 N (RMS) in the antero-posterior direction. The lumbar spine is a time-invariant and highly damped linear passive system demonstrating a high causal relationship between the vibratory excitation and its motion response. Flexural vibration could be observed though the resonant peak was not clearly identified. Modal parameters such as mode shape, modal frequency and damping factor cannot be determined from the experimental data.

Vibration response analysis on 12 normal subjects has been able to identify useful parameters which reveal the vibratory characteristics of the normal lumbar spine to external vibratory force. These parameters include the transfer mobility which defines the amount of motion response to unit vibratory force as a function of frequency.

The summated mobility curve fits well to an

exponential expression with the coefficient of determination $R^2 > 0.95$:

$$Summated\ Mobility = A\ (\ 1 - e^{(-bf)}) \tag{9.1}$$

where the coefficients A and b respectively characterize the maximum mobility and the quality of mobility response of each lumbar segment. Normal figures for these two coefficients are listed in table 7.1. The mobility defined in different frequency bands are also useful parameters as references for comparison. Attenuation coefficients with respect to the vibration at L4 range between 5 to 12 dB/segment for the low frequency band; 10 to 14 dB/segment for the medium frequency band; and 15 to 17 dB/segment for the high frequency band. However extended vibration response measurements on a bigger sample of normal subjects would be required before a norm could be established with higher statistical confidence.

Tests have been carried out on 4 patients representative of a wide range of structural modifications of the lumbar spine ranging from one with confirmed osteoporosis to one with advanced and multi-level surgical fusion plus instrumentation for fixation. The technique is sensitive in detecting structural modifications in the lumbar spine such as those resulted from surgical fusion, or a reduction in bone content as in osteoporosis. The patient with osteoporosis showed a 10% to 85% reduction in the mobility in different frequency bands, and the attenuation coefficients were 7 to 16 dB/segment greater than the normal figures. Statistical tests on the coefficient b shows significant reduction for a fused lumbar spine with reference to normal ones ($p < 0.03$). The fused lumbar spine showed 40% to 500% increase in the medium band mobility, and an increase of as much as 18 times the normal value in the high frequency band depending on the degree of stiffness. The attenuation of vibration in the lumbar spine, particularly from L4 to L3 was reduced by about 10 to 12 dB/segment with fusion.

The goal of this study has been achieved. This research has built the foundation on which further study could be based. Some fundamental questions of the vibratory characteristics of the lumbar spine and its associated soft tissue structures have been answered. Findings reported in chapter 7 have provided a strong indication that vibration response analysis is a viable technique to estimate parameters for comparison at different points in time, or to establish a clinical monitoring index for the changes in the lumbar spine's structural characteristics. However at this stage, the fact that the vibratory response of the lumbar spine shows some correlations with its physical state can only be taken as a necessary but not a sufficient criterion for the vibration technique to be used as a diagnostic tool. Results obtained so far warrant further investigation. The scope of future work would include clinical trials on a larger scale so as to establish a discriminant value against which a distinction between a normal and *abnormal* lumbar spine could be made. However, a dedicated portable vibration response analysis system with specially designed processing capability would be highly desirable for such a purpose. Suggestions have been made on the specific requirements of a purpose-built apparatus for clinical examination and monitoring of the physical state such as stiffness of the lumbar spine, with possible extension to the cervical and thoracic spine. Future work could also be extended to the transmission of vibration in other structures within the musculoskeletal system. A possible application would be in the detection of developmental dysplasia of the hip by applying vibration transmission technique and adopting a system analysis approach. Dynamic transmission or attenuation of vibration across finer structures of the joints is probably one of the areas in which the vibration analysis technique could be applied.

REFERENCES

Anderson DD, Brown TD & Radin EL (1991)
Stress wave effects in a finite element analysis of an impulsively loaded articular joint. Proc Instn Mech Engrs, 205(H):27-34.

Apley AG & Solomon L (1993)
Apley's System of Orthopaedics and Fractures, 7th edition, Butterworth-Heinemann, Oxford.

Balmer L (1991)
Signals and Systems: An Introduction, Prentice Hall, New York etc.

Barlow TG (1962)
Early diagnosis and treatment of congenital dislocation of the hip. J Bone Joint Surg 44B:292-301.

Beauchamp KG (1987)
Transforms for Engineers: A Guide to Signal Processing, Clarendon Press, Oxford, chapter 1.

Beranek LL (1972)
Acoustical definitions, in "American Institute of Physics Handbook", eds DE Gray et al, 3rd edition, McGraw-Hill Book Company, New York etc.

Bergland GD (1969)
A guided tour of the fast Fourier transform. IEEE Spectrum 6:41-52.

Beverland DE, McCoy GF, Kernohan WG & Mollan RAB (1986)
What is patellofemoral crepitus? J Bone Joint Surg 68B(3):496.

Blake RE (1988)
Basic vibration theory, in "Shock and Vibration Handbook", ed CM Harris, 3rd edition, McGraw-Hill Book Company, New York etc., chapter 2.

Blodgett WE (1902)
Auscultation of the knee joint. Boston Med Surg J 146:63-66.

Broch JT (1984)
Mechanical Vibration and Shock Measurements, 2nd edition, Brüel & Kjær, Nærum, Denmark.

Brüel & Kjær
Technical notes "Excitation signals", English BA 7343-11, Nærum, Denmark.

BS 3015 (1991)
Glossary of terms relating to mechanical vibration and shock.

BS 6841 (1987)
Measurement and evaluation of human exposure to whole-body mechanical vibration and repeated shock.

BS 7085 (1989)
Safety aspects of experiments in which people are exposed to mechanical vibration and shock.

Buturla E & Pope M (1973)
A finite element wave propagation model of pathogenic and healing bone, in "Proceedings of 1st Annual New England Bioengineering Conference", Pergamon Press, Oxford, 1973, pp.36-45.

Campbell JN & Jurist JM (1971)
Mechanical impedance of the femur: a preliminary report. J Biomech 4:319-322.

Chow DHK (1992)
The biomechanical effects of anterior lumbar interbody fusion on the juxta-fused segments, PhD thesis, University of Strathclyde, Glasgow.

Christensen AB, Ammitzbøll F, Dyrbye C, Cornelissen M, Cornelissen P & Van der Perre G (1986)
Assessment of tibial stiffness by vibration testing in situ - I. Identification of mode shapes in different supporting conditions. J Biomech 19(1):53-60.

Chu ML, Gradisar IA, Railey MR & Bowling GF (1976a)
Detection of knee joint diseases using acoustical pattern recognition technique. J Biomech 9:111-114.

Chu ML, Gradisar IA, Railey MR & Bowling GF (1976b)
An electro-acoustical technique for the detection of knee joint noise. Med Res Eng 12(1):18-20.

Chu ML, Yazdani-Ardakani S, Gradisar IA & Askew MJ (1986)
An in vitro simulation study of impulsive force transmission along the lower skeletal extremity. J Biomech 19(12):979-987.

Collier RJ & Donarski RJ (1987a)
Non-invasive method of measuring the resonant frequency of a human tibia in vivo, part 1. J Biomed Eng 9:321-328.

Collier RJ & Donarski RJ (1987b)
Non-invasive method of measuring the resonant frequency of a human tibia in vivo, part 2. J Biomed Eng 9:329-331.

Cooley JW & Tukey JW (1965)
An algorithm for the machine calculation of complex Fourier series. Math Comput 19(90):297-301.

Cornelissen P, Cornelissen M, Van der Perre G, Christensen AB, Ammitzbøll F & Dyrbye C (1986)
Assessment of tibial stiffness by vibration testing in situ - II. Influence of soft tissues, joints and fibula. J Biomech 19(7):551-561.

Cowie GH, Bogues BA, Kernohan WG & Mollan RAB (1983)
A new aid in the diagnosis of congenital dislocation of the hip. (abstract) J Bone Joint Surg 65B(5):656.

Cunningham JL, Kenwright J & Kershaw CJ (1990)
Biomechanical measurement of fracture healing. J Med Eng & Technol 14(3):92-101.

Dencker H & Moberg E (1968)
Diagnosis of soft-tissue interposition in shaft fractures of the humerus and femur by measuring the conduction of vibrations across the fracture. Acta Chir Scand 134:540-542.

Doemland HH, Jacobs RR, Spence J & Roberts FG (1986)
Assessment of fracture healing by spectral analysis. J Med Eng & Technol 10(4):180-187.

Doherty WP, Bovill EG & Wilson EL (1974)
Evaluation of the use of resonant frequencies to characterize physical properties of human long bones. J Biomech 7:559-561.

Døssing O (1988a)
Structural Testing, part 1: mechanical mobility measurements, Brüel & Kjær, Nærum, Denmark.

Døssing O (1988b)
Structural Testing, part 2: modal analysis and simulation, Brüel & Kjær, Nærum, Denmark.

Drazil JV (1983)
Quantities and Units of Measurement, Mansell Publishing Ltd., London.

Emslie-Smith D, Paterson CR, Scratcherd T & Read NW (eds) (1988)
Textbook of Physiology, 11th edition, Churchill Livingstone, Edinburgh etc., p.499.

Evans EJ (1985a)
Vibratory properties and resonances of the isolated human ulna. J Biomed Eng 7:144-148.

Evans JH (1985b)
Biomechanics of lumbar fusion. Clin Orthop & Relat Res 193:38-46.

Ewins DJ (1991)
Modal Testing: Theory and Practice, Research Studies Press,

New York etc.

Fairley TE & Griffin MJ (1989)
The apparent mass of the seated human body: vertical vibration. J Biomech 22(2):81-94.

Fischer H & Johnson EW (1960)
Analysis of sounds from normal and pathologic knee joints, in "3rd International Congress of Physical Medicine", pp.50-57.

Franke EK (1951)
Mechanical impedance of the surface of the human body. J Appl Physiol 3:582-590.

Garcia BJ (1980)
Acoustic properties of bone. Ultrason Imaging 2:184.

Griffin MJ (1990)
Handbook of Human Vibration, Academic Press, London etc, chapters 1 & 8.

Hamilton A (1989)
The measurement of physiological patello-femoral crepitus, MD thesis, Queen's University, Belfast.

Hamming RW (1983)
Digital Filters, 2nd edition, Prentice-Hall Inc., Englewood Cliff, New Jersey.

Hansson T, Keller TS, Ray JL & Magnusson M (1992)
The knee-hip-spine transmissibility in the standing subject. (abstract) Orthop Trans 16(1):248-249.

Helliwell PS, Smeathers JE & Wright V (1989)
Shock absorption by the spinal column in normals and in ankylosing spondylitis. Proc Instn Mech Engrs 203(H):187-190.

Herlufsen H (1984)
Technical Review: Dual Channel FFT Analyser, Brüel & Kjær, Nærum, Denmark, parts 1 & 2.

Hight TK, Piziali RL & Nagel DA (1980)
Natural frequency analysis of a human tibia. J Biomech 13:139-147.

Hinz B, Seidel H, Bräuer D, Menzel G, Blüthner R & Erdmann U (1988)
Examination of spinal column vibrations: a non-invasive approach. Eur J Appl Physiol 57:707-713.

Hixson EL (1988)
Mechanical impedance, in "Shock and Vibration Handbook", ed CM Harris, 3rd edition, McGraw-Hill Book Company, New York etc., chapter 10.

Hoerr NL & Osol A (eds) (1956)
Blakiston's New Gould Medical Dictionary, 2nd edition, McGraw-Hill Company, Inc., New York etc.

Huston DR, Ogden D, Wilder DG & Pope MM (1991)
Spinal mechanical properties from vibration response analysis, in "Biomecahnics Symposium", eds RL Spilker et al, AMD-Vol 120, ASME 1991, pp.365-367.

Jernberger A (1967)
A method for acoustic registration of fracture healing. Acta Orthop Scand 38:393-394.

Jurist JM (1970a)
In vivo determination of the elastic response of bone, I. method of ulnar resonant frequency determination. Phys Med Biol 15(3):417-426.

Jurist JM (1970b)
In vivo determination of the elastic response of bone, II. ulnar resonant frequency in osteoporotic, diabetic and normal subjects. Phys Med Biol 15(3):427-434.

Jurist JM & Dymond AM (1970)
Reproducibility of ulna resonant frequency measurement. Aerospace Med 41:875-878.

Jurist JM & Selle WA (1965)
Acoustical detection of osteoporosis. (abstract) The Physiologist 8:203.

Kenedi RM (ed) (1980)
A Textbook of Biomedical Engineering, Blackie, Glasgow etc., chapter 1.

Kernohan WG, Beverland DE, McCoy GF, Hamilton A, Watson P & Mollan RAB (1990)
Vibration arthrometry - a preview. Acta Orthop Scand 61(1):70-79.

Kernohan WG, Beverland DE, McCoy GF, Shaw SN, Wallace RGH, McCullagh GC & Mollan RAB (1986)
The diagnostic potential of vibration arthrography. Clin Orthop & Relat Res 210:106-112.

Kernohan WG, Cowie GH & Mollan RAB (1991)
Vibration arthrometry in congenital dislocation of the hip. Clin Orthop & Related Res 272:167-174.

Kernohan WG & Mollan RAB (1991)
Non-invasive diagnosis and prophylaxis in orthopaedics. Proc Instn Mech Engrs 205(H):173-187.

Khalil TB, Viano DC & Taber LA (1980)
Vibrational characteristics of the embalmed human femur, in "Advances in Bioengineering",ASME, New York, 1980,pp.57-59.

Kim W, Voloshin AS, Johnson SH & Simkin A (1993)
Measurement of the impulsive bone motion by skin-mounted accelerometers. Trans ASME J Biomech Engng 115:47-52.

Kolsky H (1963)
Stress Waves in Solids, Dover Publications Inc., New York.

Lee R (1990)
Biomechanics of spinal posteroanterior mobilisation, MPhil thesis, Hong Kong Polytechnic.

Lee R & Evans J (1994)
Towards a better understanding of spinal posteroanterior mobilisation. Physiotherapy 80(2):68-73.

Lim MK (1989)
Effect of swollen soft tissue on the impedance of bone for fracture healing diagnosis. J Biomed Eng 11:517-519.

Lippmann RK (1932)
The use of auscultatory percussion for the examination of fractures. J Bone Joint Surg 14:118-126.

Lowet G, Hobatho MC, Cornelissen M, Cunningham JL & Van der Perre G (1992)
Modal analysis of the human tibia in vivo: determination of the resonant frequencies and mode shapes. (abstract) J Biomech 25(6):686.

Lowet G, Van Audekercke R & Van der Perre G (1993)
The correlation between resonant frequencies and torsional stiffness of long bones. (abstract) J Biomech 26(7):780.

Lynn PA (1987)
An Introduction to the Analysis and Processing of Signals, 2nd edition, MacMillan Education, London etc., chapter 3.

MacNalty AS (ed) (1965)
Butterworths Medical Dictionary, 2nd edition, Butterworths, London etc.

Markey EL & Jurist JM (1974)
Tibial resonant frequency measurements as an index of the strength of fracture union. Wis Med J 73:S62-65.

Matthews MG, King JB, Collier RJ & Donarski RJ (1989)
The objective monitoring of stiffness of healing fractures by acoustic resonance scanning - initial clinical experience, in "Proceedings of the Institution of Mechanical Engineers, International Conference: The Changing Role of Engineering in Orthopaedics, 14-15 April 1989, London", C384/037, pp.127-132.

McCoy GF, McCrea JD, Beverland DE, Kernohan WG & Mollan RAB (1987)
Vibration arthrography as a diagnostic aid in diseases of

the knee: a preliminary report. J Bone Joint Surg 69B(2):288-293.

McGaw WH (1942)
Osseosonometry 1. the use of percussion-auscultation in fractures. Arch Surg 45:195-205.

Mollan RAB (1981)
Vibration emission in bone and joints, MD thesis, Queen's University, Belfast.

Mollan RAB, McCullagh GC & Wilson RI (1982a)
A critical appraisal of auscultation of human joints. (abstract) J Bone Joint Surg 64B:384.

Mollan RAB, McCullagh GC & Wilson RI (1982b)
A critical appraisal of auscultation of human joints. Clin Orthop & Relat Res 170:231-237.

Mubarak SJ, Leach J & Wenger DR (1987)
Management of congenital dislocation of the hip in the infant. Contemp Orthop 15(4):29-44.

Nikiforidis G, Bezerianos A, Dimarogonas A & Sutherland C (1990)
Monitoring of fracture healing by lateral and axial vibration analysis. J Biomech 23(4):323-330.

Nokes L, Fairclough JA, Mintowt-Czyz WJ, Mackie I & Williams J (1984a)
Vibration analysis of human tibia: the effect of soft tissue on the output from skin-mounted accelerometers. J Biomed Eng 6:223-226.

Nokes L, Mintowt-Czyz WJ, Mackie I, Failclough JA & Williams J (1984b)
Direct and indirect determination of tibial natural frequency - a comparison of frequency domain analysis and fast Fourier transform. J Biomed Eng 6:45-48.

Nokes LDM, Mintowt-Czyz WJ, Fairclough JA, Mackie I, Howard C & Williams J (1984c)
Natural frequency of fracture fragments in the assessment of tibial fracture healing. J Biomed Eng 6:227-229.

Nokes L, Mintowt-Czyz WJ, Fairclough JA, Mackie I & Williams J (1985)
Vibration analysis in the assessment of conservatively managed tibial fractures. J Biomed Eng 7:40-44.

Nokes LDM & Thorne GC (1988)
Vibrations in orthopaedics. CRC Crit Rev Biomed Eng 15(4):309-350.

Oestreicher HL (1951)
Field and impedance of an oscillating sphere in a

viscoelastic medium with an application to biophysics. J Acoust Soc Am 23(6):707-714.

Orne D & Mandke J (1975)
The influence of musculature on the mechanical impedance of the human ulna, an in vivo simulated study. J Biomech 8:143-149.

Paddan GS (1991)
Transmission of vibration through the human body to the head, PhD thesis, University of Southampton, Southampton.

Paddan GS & Griffin MJ (1988a)
The transmission of translational seat vibration to the head - I. Vertical seat vibration. J Biomech 21(3):191-197.

Paddan GS & Griffin MJ (1988b)
The transmission of translational seat vibration to the head - II. Horizontal seat vibration. J Biomech 21(3):199-206.

Paddan GS & Griffin MJ (1992)
The transmission of translational seat vibration to the head: the effect of measurement position at the head. Proc Instn Mech Engrs 206(H):159-168.

Panjabi MM, Andersson GBJ, Jorneus L, Hult E & Mattsson L (1986)
In vivo measurements of spinal column vibrations. J Bone Joint Surg 68A(5):695-702.

Parks TW & Burrus CS (1987)
Digital Filter Design, John Wiley & Sons Inc., New York etc., chapter 3.

Paul IL, Munro MB, Abernethy PJ, Simon SR, Radin EL & Rose RM (1978)
Musculo-skeletal shock absorption: relative contribution of bone and soft tissues at various frequencies. J Biomech 11:237-239.

Pelker RR & Saha S (1983)
Stress wave propagation in bone. J Biomech 16(7):481-489.

Peylan A (1953)
Direct auscultation of the joints. Rheumatism 9:77-81.

Pintar FA, Yoganandan N, Myers T, Elhagendiab A & Sances A Jr (1992)
Biomechanical properties of human lumbar spine ligaments. J Biomech 25(11):1351-1356.

Pope MH, Frymoyer JW & Krag MH (1992)
Diagnosing instability. Clin Orthop & Relat Res 279:60-67.

Pope MH & Hansson TH (1992)
Vibration of the spine and low back pain. Clin Orthop & Relat Res 279:49-59.

Pope MH, Kaigle AM, Magnusson M, Broman H & Hansson T (1991)
Intervertebral motion during vibration. Proc Instn Mech Engrs 205(H):39-44.

Pope MH, Svensson M, Broman H & Andersson GBJ (1986)
Mounting of the transducers in measurement of segmental motion of the spine. J Biomech 19(8):675-677.

Poss R, Pratt GW Jr & Chung JK (1984)
An evaluation of total hip replacement cementing technique using sonic resonance. Engng Med 13(4):191-196.

Radin EL & Paul IL (1970)
Does cartilage compliance reduce skeletal impact loads? The relative force-attenuating properties of articular cartilage, synovial fluid, periarticular soft tissues and bone. Arthritis Rheum 13(2):139-144.

Radin EL, Paul IL & Lowy M (1970)
A comparison of the dynamic force transmitting properties of subchondral bone and articular cartilage. J Bone Joint Surg 52A(3):444-456.

Ralis ZA (1989)
Freezing of orthopaedic specimens before mechanical testing. J Bone Joint Surg 71B:55-57.

Randall RB (1987)
Frequency Analysis, 3rd edition, Brüel and Kjær, Nærum, Denmark.

Ray J, Keller T, Magnusson M & Hannson T (1992)
In-vivo measurements of lumbar spine transmissibility in the upright human subject. Orthop Trans 16(1):244-245.

Rolander SD (1966)
Motion of the lumbar spine with special reference to the stabilizing effect of posterior fusion. Acta Ortho Scand Suppl 90:1-144.

Rosenstein AD, McCoy GF, Bulstrode CJ, McLardy-Smith PD, Cunningham JL & Turner-Smith AR (1989)
The differentiation of loose and secure femoral implants in total hip replacement using a vibrational technique: an anatômical and pilot clinical study. Proc Instn Mech Engrs 203(H):77-81.

Saha S & Lakes RS (1977a)
The effect of soft tissue on wave-propagation and vibration tests for determining the in vivo properties of bone. J Biomech 10:393-401.

Saha S & Lakes RS (1977b)
A non-invasive technique for detecting stress waves in bone using the piezoelectric effect. IEEE Trans Biomed Eng Vol BME-24(6):508-512.

Saha S, Owens G & Ray A (1992)
Resonance frequency of ulna as an indicator of its load carrying capacity. Orthop Trans 16(2):551-552.

Sandover J (1982)
Measurement of the frequency response characteristics of man exposed to vibration, PhD thesis, Loughborough University of Technology, Loughborough.

Schoenberg M, Wells JB & Podolsky RJ (1974)
Muscle compliance and the longitudinal transmission of mechanical impulses. J Gen Physiol 64:623-642.

Sekiguchi T & Hirayama T (1979)
Assessment of fracture healing by vibration. Acta Orthop Scand 50:391-398.

Selle WA & Jurist JM (1966a)
The onset of postmenopausal osteoporosis as studied by a new technique. J Am Geriat Soc 14(9):930-934.

Selle WA & Jurist JM (1966b)
Acoustical detection of senile osteoporosis. Proc Soc Exp Bio Med 121:150-152.

Serridge M & Licht TR (1986)
Piezoelectric Accelerometer and Vibration Preamplifier Handbook, Brüel & Kjær, Nærum, Denmark.

Singh VR, Yadav S & Adya VP (1989)
Role of natural frequency of bone as a guide for detection of bone fracture healing. J Biomed Eng 11:457-461.

Smeathers JE (1984)
Is the intervertebral joint a shock-absorber? (abstract) J Bone Joint Surg 66B:291.

Smeathers JE (1989a)
Transient vibrations caused by heel strike. Proc Instn Mech Engrs 203(H):181-186.

Smeathers JE (1989b)
Measurement of transmissibility for the human spine during walking and running. Clin Biomech 4:34-40.

Smeathers JE & Joanes DN (1988)
Dynamic compressive properties of human lumbar intervertebral joints: a comparison between fresh and thawed specimens. J Biomech 21(5):425-433.

Sonstegard DA & Matthews LS (1976)
Sonic diagnosis of bone fracture healing - a preliminary study. J Biomech 9:689-694.

Steele CR, Zhou LJ, Guido D, Marcus R, Heinrichs WL & Cheema C (1988)
Noninvasive determination of ulnar stiffness from mechanical response - in vivo comparison of stiffness and bone mineral content in humans. J Biomech Eng 110:87-96.

Steidel RF Jr (1989)
An Introduction to Mechanical Vibrations, 3rd edition, John Wiley & Sons, New York etc, chapters 6 & 7.

Steindler A (1937)
Auscultation of joints. J Bone Joint Surg 19(1):121-136.

Stephens RWB (ed) (1975)
International Dictionaries of Science and Technology: Sound, Crosby Lockwood Staples, London.

Stone MH, Richardson JB & Bennet GC (1987)
Another clinical test for congenital dislocation of the hip. Lancet, April 25, 1987, pp.954-955.

Summers PG (1981)
Signal testing using cepstrum analysis, MEng thesis, University of Wales Institute of Science and Technology, Cardiff.

Thomas AMC, Luo DZ & Dunn JW (1991)
Response of human femur to mechanical vibration. J Biomed Eng 13:58-60.

Thompson GA (1973)
In vivo determination of bone properties from mechanical impedance measurements (abstract), at "Aerospace Medical Association Annual Science Meeting", Las Vegas, 7-10 May, 1973.

Tortora GJ & Anagnostakos NP (1987)
Principles of Anatomy and Physiology, 5th edition, Harper and Row Publishers, New York, p.148.

Truong XT (1974)
Viscoelastic wave propagation and rheologic properties of skeletal muscle. Am J Physiol 226(2):256-264.

Van der Perre G (1984)
Dynamic analysis of human bones, in "Functional Behavior of Orthopaedic Materials", eds P Ducheyne et al, CRC Press, Boca Raton, Florida, volume 1, pp.99-159.

Van der Perre G & Cornelissen P (1983)
On the mechanical resonances of a human tibia in vitro. J Biomech 16(7):549-552.

Voloshin A & Wosk J (1982)
An in vivo study of low back pain and shock absorption in the human locomotor system. J Biomech 15(1):21-27.

Voloshin AS & Wosk J (1983)
Shock absorption of meniscectomized and painful knees: a comparative in vivo study. J Biomed Eng 5:157-161.

von Gierke HE (1959)
Transmission of vibratory energy through human body tissues, in "1957 Proc. First National Biophys Conference, New Haven, Conn.", Yale University Press, pp.647-669.

von Gierke HE (1964)
Biodynamic response of the human body. Appl Mech Rev 17:951-958.

von Gierke HE (1973)
Dynamic characteristics of the human body, in "Perspectives in Biomedical Engineering", ed RM Kenedi, Macmillan, London etc., pp.193-202.

von Gierke HE, Oestreicher HL, Franke EK, Parrack HO & von Wittern WW (1952)
Physics of vibrations in living tissues. J Appl Physiol 4:886-900.

Walters CF (1929)
The value of joint auscultation. Lancet May 4, 1929 pp.920-921.

White AA & Panjabi MM (1990)
Clinical Biomechanics of the Spine, 2nd edition, J.B. Lippincott, Philadelphia etc.

Wong ATC, Goldsmith W & Sackman JL (1976)
Flexural wave propagation in discontinuous model and in-vitro tibiae. J Biomech 9:813-825.

Wong FY, Pal S & Saha S (1983)
The assessment of in vivo bone condition in humans by impact response measurement. J Biomech 16(10):849-856.

Wosk J & Voloshin A (1981)
Wave attenuation in skeletons of young healthy persons. J Biomech 14(4):261-267.

Ziegert JC & Lewis JL (1978)
In-vivo mechanical properties of soft tissue covering bony prominences. Trans ASME J Biomech Engng 100:194-201.

Ziegert JC & Lewis JL (1979)
The effect of soft tissue on measurements of vibrational bone motion by skin-mounted accelerometers. Trans ASME J Biomech Engng 101:218-220.

APPENDIX I.

INDIVIDUAL PARTICULARS OF THE LUMBAR SPINE SPECIMENS

I.1 DEMOGRAPHIC DATA AND CAUSES OF DEATH

SPECIMEN NUMBER	AGE (yr)	SEX	HEIGHT (m)	BODY BUILD	CAUSES OF DEATH
1	56	M	1.70	Medium	Lung carcinoma
2*	---	---	---	---	Carcinoma metastasis to bone
3	66	M	1.65	Medium	Myocardial infarction
4	62	M	1.95	Medium	Respiratory failure
5	60	F	1.57	Medium	Aspiration pneumonia
6	74	M	1.88	Heavy	Bronchial pneumonia
7	49	M	1.93	Heavy	Renal failure
8	68	M	1.98	Heavy	Pneumonia
9	65	F	1.70	Heavy	C.O.A.D.
10	54	M	1.80	Medium	---
11	78	F	1.65	Small	C.V.A.

Remarks:

Age (mean ± SD) = 63.2 ± 8.9 yr
Height (mean ± SD) = 1.78 ± 0.15 m

C.O.A.D = Chronic obstructive airway disease
C.V.A. = Cerebral vascular accident

* Specimen No. 2 was used only for the practice of mounting and not for vibration tests.

I.2 DEGREE OF DISC DEGENERATION

(Grading 1 to 3 according to Rolander (1966))

SPECIMEN NUMBER	T12-L1	L1-2	L2-3	L3-4	L4-5	L5-S1
1	-	1	1	1	3	3
3	-	3+	1+	1+	2+	3+
4	-	1	1	1	1	3
5	-	1	1	1	1	1
6	-	2+	3+++	2+	2+	2+
7	-	2	2	2	2	2
8	-	1	1	2	2	3
9	1	1	3+	2+	2+	1
10	1	1+	1+	1++	2+	2+
11	1	1	3+++	1	2+	3

Remarks:

- = Grading not noted
+ = Mild osteophyte
++ = Moderate osteophyte
+++ = Advanced osteophyte

APPENDIX II.

II.1 DEMOGRAPHIC DATA OF THE NORMAL SUBJECTS

SUBJECT CODE	AGE (yr)	SEX	HEIGHT (m)	BODY MASS (kg)
N1	23	M	1.77	60.2
N2	20	M	1.67	60.0
N3	21	M	1.70	62.5
N4	20	F	1.56	46.0
N5	20	F	1.60	41.0
N6	20	F	1.59	54.0
N7	22	F	1.70	57.0
N8	21	F	1.58	47.0
N9	32	M	1.77	92.0
N10	21	M	1.74	67.0
N11	28	M	1.71	80.0
N12	27	M	1.72	65.0
MEAN	22.9	---	1.68	61.0

II.2 DEMOGRAPHIC DATA OF THE PATIENTS

PATIENT CODE	AGE (yr)	SEX	HEIGHT (m)	BODY MASS (kg)
P1	58	F	1.51	65.0
P2	51	F	1.53	60.0
P3	50	F	1.43	53.0
P4	39	F	1.57	70.0
MEAN	49.5	---	1.51	62.0

APPENDIX III.

CONSENT FORM

Consent to act as a test subject in an experiment involving exposure to mechanical vibration at the lumbar spine.
(modified from BS 7085, 1989)

Part 1. Personal details

Name: _____

Age: _____

Sex: _____

Part 2. Questions to be asked during screening

2.1 Have you ever suffered from a serious illness: (YES/NO)
If YES, please give brief particulars and approximate date(s):

2.2 Have you ever been injured seriously (i.e. badly enough to be treated by a doctor or taken to a hospital? (YES/NO)
If YES, please give brief particulars and approximate date(s):

2.3 Are you at present under medical treatment of any kind? (YES/NO).
If YES, please indicate what kind of treatment (e.g. medicine, appliances, physiotherapy, psychotherapy, dressings):

2.4 Do you suffer from any defect or disability affecting your daily life, work or travelling? (YES/NO).
If YES, please give brief particulars:

2.5 Do you suffer from, or have you in the past suffered from, any of the following conditions: back or neck problems, cardiovascular disorders, diseases of the ears or eyes; retinal detachment? (YES/NO).
If YES, please give brief particulars:

Part 3. Declaration

3.1 I hereby volunteer to be an experimental subject in a mechanical vibration test to be conducted by Mr Kevin Kwong (the principal investigator) at the Hong Kong Polytechnic University.

3.2 My replies to the questions, in part 2 above, concerning my fitness to take part are correct to the best of my knowledge and belief.

3.3 I understand that the information about myself which I have given and may give in the course of the experiment, will be treated as confidential by the investigator whose signature is:

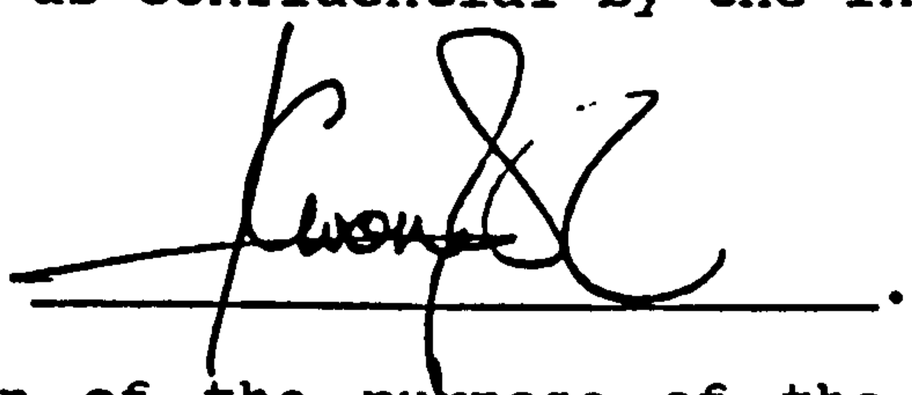

3.4 Explanation of the purpose of the experiment, the nature of the mechanical vibration to be used and the potential hazard have been given to me.

3.5 While I agreeing to attend for the purpose of the experiment at the time(s) and place(s) requested by the investigator, I fully understand that I may at any time withdraw from taking part in the experiment and that I am under no obligation to give a reason for my withdrawal or to attend again for experimentation.

3.6 While in the laboratory, I undertake to observe the regulations in force governing its use, I also agree to obey instructions given to me by the investigator regarding safety, subject only to my right to withdraw declared above.

3.7 I understand that the investigator will make every endeavour to ensure safety and to minimize any potential risks that might be imposed on me during the experiments.

3.8 I understand that I may not be compensated for any injury as a result of the experiment, unless there is a clear indication of negligence of the investigator by legal judgement.

Signature:_____ Date:_____

APPENDIX IV.

IV.1 SPECIFICATIONS OF MAJOR HARDWARE

IV.1.1 Function Generator (BK Precision Model 3040)

SPECIFICATIONS

FREQUENCY CHARACTERISTICS — **Sinewave**

All specifications apply with frequency dial setting between 1 and 13 times range, and after 30 minutes warm-up.

General

Frequency Range:	0.1 Hz to 13 MHz in 8 ranges.
Tuning Range:	Each ranges provides 100:1 frequency control.
Outputs:	Sine, square, triangle wave, ramp, TTL square wave, pulse, sync. output.
Operating Modes:	Sweep, AM, FM, gated burst, VCG (Voltage Controlled Generator).
Switched DC Offset:	Continuously variable, ± 10 V maximum open circuit (± 5 V into 50 ohm load).
Preset DC Offset:	Less than 0.1 VDC.
Variable Symmetry:	80:20:80 to 1 MHz.

Square Wave

Symmetry:	Greater than 98% from 0.1 Hz to 100 kHz.
Rise/Fall Time:	Less than 18 ns at maximum output (into 50 ohm load).
Distortion:	Less than 0.5% from 10 Hz to 50 kHz. Harmonics greater than 30 dB below fundamental 50 kHz to 13 MHz at maximum amplitude. Harmonics greater than 25 dB from maximum to 20% of maximum amplitude.
Amplitude Flatness:	Less than ±3% (0.3 dB) 10 Hz to 100 kHz. Less than ±10% (1.0 dB) 100 kHz to 10 MHz. Less than ±20% (2.0 dB) 10 MHz to 13 MHz.

Triangular Wave

Linearity:	Greater than 99% at 100 kHz.

TTL Pulse:

Amplitude:	Greater than 3 V p-p.
Rise/Fall Time:	Less than 25 ns.
Fan Out:	20 TTL Loads.

SYNC Output:

Impedance:	50 Ω ±10%.
Level:	>1 V p-p open circuit.

VCG (Voltage-Controlled Generator)

Input Control:	VCG tunable by 0 to –2 VDC ±20%. VCG tuning range is 1000:1.
Linearity:	Less than 0.5% to 1 MHz; less than 5% to 10 MHz.
Input Impedance:	3.5k ohms ±10%.

SWEEP CHARACTERISTICS

Mode:	Linear only.
Sweep Width:	Continuously variable; greater than 1000:1.
Sweep Rate:	0.01 Hz to 10 kHz; 90:10 ramp.
Ramp Output:	0 to 4 V p-p into 5k ohms.

AM MODULATION CHARACTERISTICS

Source:	Internal, external.
Modulation Ratio:	0 to 100%.
INT. Modulation:	0.01 Hz to 10 kHz.
EXT. Modulation:	DC to 1 MHz.
EXT. sensitivity:	Less than 10 V p-p for 100% modulation.
AM DC Offset:	Less than 0.1 VDC.
Carrier Amplitude Flatness:	0 to –3 dB; 100 Hz to 5 MHz.

FM MODULATION CHARACTERISTICS

Source:	Internal, external.
Deviation:	0 to ±5%
INT. Modulation:	0.01 Hz to 10 kHz.
EXT. Modulation:	DC to 50 kHz.
EXT. sensitivity:	Less than 10 V p-p for 10% modulation.

TRIGGER GATE (BURST) CHARACTERISTICS

Trigger Source:	Internal, external.
Trigger Mode:	Single, multiple.
Start/Stop Phase Range:	+90°, –80°.
Frequency Range:	0.01 Hz to 10 kHz (INT.). 0.1 Hz to 1 MHz (EXT.).
External Level:	TTL level (Hi: greater than 2.4 V, Lo: less than 0.8 V, Lo: Burst OFF, Hi: Burst ON).
Burst (Carrier) Frequency:	0.1 Hz to 1 MHz.

IV.1.2 Tape-recorder (AKAI GXC-710D)

TECHNICAL DATA

Track System .....4 track 2 channel stereo system
Tape .....Philips type cassette
Tape Speed .....1-7/8 ips.
Wow and Flutter.....Less than 0.08% WRMS
Frequency Response ....30 Hz to 14,000 Hz (±3 dB) using low noise tape
30 Hz to 16,000 Hz (±3 dB) using CrO_2 Tape,
30 Hz to 17,000 Hz (±3 dB) using Fe-Cr Tape
Distortion .....Less than 1.5% (1,000 Hz "0" VU) using low noise tape
Signal-to-Noise Ratio ....Better than 50 dB (measured via tape with peak recording level of +3 VU)
Dolby Switch ON: Improves up to 10 dB above 5 kHz
Erase Ratio .....Better than 70 dB
Bias Frequency .....60 kHz
Heads .....(2): One GX recording/playback head, One erase head
Motor .....4-pole Hysteresis Synchronous outer rotor motor
Fast Forward and Rewind Time.....80 seconds using a C-60 cassette tape
Output Jacks .....Line (2): 0.775 V ("0" VU)
Required load impedance: More than 20 k ohms
Phone (1): 50 mV/8 ohms
Input Jacks.....Microphone (2): 0.3 mV/4.7 k ohms
Line (2): 70 mV/100 k ohms
Din Jack .....0.55 V/3 mV
Semi Conductors .....Transistors 39, Diodes 48, FETs 2
Power Requirements ....U.S.A. and Canada (CSA, UL and LA) Models: 120 V, 60 Hz only
CEE Models: 220 V, 50 Hz only
Other Models: 110 to 120 V/220 to 240 V, 50/60 Hz, (Switchable)
Dimensions .....440 (W) x 142 (H) x 304 (D)mm (17.3 x 5.6 x 12")
Weight .....8.8 kg (19.4 lbs)

* For improvement purposes, specifications and design are subject to change without notice.

STANDARD ACCESSORIES

Connection Cord 1
Operator's Manual 1

IV.1.3 Electrodynamic Exciter (Brüel & Kjær Type 4810)

Specifications 4810

Frequency Range:
DC to 18 kHz

First Major Armature Resonance:
Above 18 kHz

Force Rating (Peak):
10 Newton (2.25 lbf) 65 Hz to 4 kHz
7 Newton (1.5 lbf). 65 Hz to 18 kHz

Max. Bare Table Acceleration (Peak):
550 ms^{-2} (65 Hz to 4 kHz)
383 ms^{-2} (4 kHz to 18 kHz)
(1 ms^{-2} = 0.102 g)

Max. Displacement (Peak-to-Peak):
6 mm (0.236 in)

Dynamic Flexure Stiffness:
2 Newton/mm (11.5 lbs/in)

Dynamic Weight of the Moving System.
18 grams

Magnetic Field:
Permanent magnet

Max. Input Current:
1.8 A. RMS

Coil Impedance:
3.5 Ω at 500 Hz

Connection:
Microsocket NF 10 — 32

Table Size:
14 mm (0.55 in) diameter

Fastening Thread:
NF 10 — 32

Weight:
1.1 kg (2.4 lb)

Dimensions:
Diameter: 76 mm (3 in)
Height: 75 mm (2.9 in)

Accessories Available:
Cable for connection of Mini-Shaker to Power Amplifier AO 0069

Mounting Accessories (includes isolated studs YP 0150 and non-isolated studs YQ 2960) UA 0125

Specifications for Type 4294

from Serial No.: 1466533

Brüel & Kjær

Vibration System	Electromagnetic exciter with internal built-in piezoelectric accelerometer (shear type) for servo regulation of vibration amplitude
Frequency:	159.15 Hz ± 0.02% (1000 rads^{-1})
Acceleration:	10 ms^{-2} (RMS) ± 3%
Velocity:	10 mms^{-1} (RMS) ± 3%
Displacement:	10 µm (RMS) ± 3%
Transverse amplitude:	less than 5% of main axis amplitude
Distortion:	less than 2% for 10 to 70 g load; less than 7% for 0 to 10 g
Warm-up Time:	Less than 5 seconds
Signal duration:	103 ± 1 s with automatic stop
Long Term Stability:	better than 1% per year for acceleration, velocity and displacement; better than 10 ppm per year for frequency
Transducer Mounting:	
Maximum Load:	70 g
Mounting Torque:	max. 0.5 Nm
Mounting Thread:	10 - 32 UNF
Temperature Range:	+ 10 to + 40°C (50 to 104°F) for 10 ms^{-2} reference within ± 3% – 10 to + 55°C (14 to 131°F) for 10 ms^{-2} reference within ± 5%
Humidity:	Up to 90% RH (non-condensing) at 30°C
Power Requirements:	
Built-in Battery:	One 9 V Alkaline Battery QB 0016 (IEC type 6LR61)
Battery Life:	Approximately 60 calibrations, each lasting approximately 100 s with automatic switching off at the end of each calibration
Dimensions:	
Length:	155 mm (6.1 in)
Diameter:	52 mm (2.05 in)
Weight:	500 g including battery and leather case

Certificate for Calibration Exciter Type 4294 No.: 1712693

Type 4294 Serial No.: 1712693

Calibration Conditions: **Temperature:** 23 ± 3°C
Load Mass: 40 g
Positioning: Vertical

Calibration Result: Acceleration Level*: 9,95 ms^{-2}

Uncertainty (95% confidence level): Less than 2%

93. 02. 02.
Date of calibration

O. H.
Signature

* This measurement is traceable to:
NIST - National Institute of Standards and Technology, Gaithersburg, Maryland , U.S.A.
and PTB - Physical Technische Bundesanstalt, Braunsweig, Germany

BC 0205-11

0123040

IV.1.5 Power Amplifier (Brüel & Kjær Type 2706)

Specifications 2706

POWER OUTPUT CAPABILITY:
75 VA into 3 Ω exciter or resistive load

CURRENT LIMITING:
Switchable,
Max. 5 A for Vibration Exiter Type 4809
Max. 1,8 A for Mini-Shaker Type 4810

FREQUENCY RESPONSE:
10 Hz to 20 kHz (± 0.5 dB)
2 Hz to 50 kHz (± 3 dB)

HARMONIC DISTORTION:
<0,2% (20 Hz to 10 kHz)
<0,5% (20 Hz to 20 kHz)
at full output capacity

INPUT IMPEDANCE:
15kΩ

OUTPUT IMPEDANCE:
<0,04 Ω (10 Hz to 5 kHz)
<0,08 Ω (5 kHz to 20 kHz)

PROTECTION:
Short circuit
Excessive heat sink temperature
Input overload

DC STABILITY:
<25 mV drift for ± 5% supply line variation
<25 mV drift for ambient temperature variations between 10 and 40 °C (50 and 104 °F)

HUM AND NOISE:
<5 mV RMS

MAX. VOLTAGE GAIN AT 1 KHZ:
40 dB (± 1 dB)

ATTENUATOR:
0 to 40 dB in 10 dB steps

GAIN CONTROL:
0 to −∞ dB logarithmic

ENVIRONMENTAL TEMPERATURE RANGE:
5 to 40 °C (41 to 104 °F)

HUMIDITY:
0 to 90% RH (non-condensing) at 30 °C

POWER REQUIREMENTS:
110, 115, 127, 220 and 240 V AC (± 5%, 50 to 60 Hz)
Approximately 140 VA
Complies with safety class 1 of IEC 348

DIMENSIONS:
Height: 133 mm (5,2 in)
Width: 210 mm (8,3 in)
Depth: 240 mm (9,5 in)
(KK 0042 Cabinet, 6/12 of 19 in rack module)

WEIGHT:
6 KG (13,2 LB)

ACCESSORIES INCLUDED:
1 B & K standard mains cable AN 0010
1 B & K standard coaxial plug JP 1010
Various fuses

IV.1.6 Charge Amplifier (Brüel & Kjær Type 2635)

Specifications 2635

CHARGE INPUT:
Via 10-32 NF and BNC coaxial socket
Max. Input: $\sim 10^5$ pC

SENSITIVITY CONDITIONING:
3 digit dial-in of transducer sensitivity from 0,1 to 10,99 pC/ms^{-2}

AMPLIFIER SENSITIVITY:
0,01 mV to 10 V/pC corresponding to −40 to +80 dB with transducer capacitance of 1 nF

CALIBRATED OUTPUT RATINGS:
Selectable in 10 dB steps
Acceleration: 0,1 mV to 1 V/ms^{-2}
Velocity: 10 mV to 100 V/ms^{-1}
Displacement: 0,1 mV to 10 V/mm

SIGNAL OUTPUT:
Via 10-32 NF and BNC coaxial socket
Max. Output: 8 V (8 mA) peak
Output Impedance: <1 Ω
DC Offset: < ±50 mV

FREQUENCY RANGE:
Acceleration*: Switchable 0,2 or 2 Hz to 100 kHz
Velocity: Switchable 1 or 10 Hz to 10 kHz
Displacement: Switchable 1 or 10 Hz to 1 kHz
−10 % limits quoted — see Fig. 3

LOW-PASS FILTER:
Switchable −10 % frequency limits of 100 Hz, 1 kHz, 3 kHz, 10 kHz, 30 kHz and >100 kHz with attenuation slope of 40 dB/decade

INHERENT NOISE (2 Hz to 22 kHz)
$5 \cdot 10^{-3}$ pC referred to input with maximum sensitivity and 1 nF transducer capacitance

TEST OSCILLATOR:
160 Hz (ω = 1000 rad/s) sinusoid, factory preset for test level of 1 V

OVERLOAD INDICATOR:
Overload LED lights when input or output of amplifier is overloaded by signals of too high a peak level

RISE TIME: ~ 2.5 V/μs

ENVIRONMENTAL CONDITIONS:
Temperature Range: −10 to +55°C (+14 to 131°F)
Humidity: 0 to 90% RH (non-condensing). For use in high humidities a 3 W heater may be fitted on special order

POWER REQUIREMENTS:
Int. Battery: Three 1,5 V Alkaline Cells OB 0004 (IEC LR20). Provide approximately 100 hours use
Ext. Source: +8 to +28 V (55 mA) single or ± 14 V (14 mA) dual polarity DC

DIMENSIONS:
Height: 132,6 mm (5,22 in)
Width: 69,5 mm (2,74 in)
Depth: 200 mm (7,87 in)
B & K module cassette KK 0022, 2/12 of 19 in rack

WEIGHT: 1,45 kg (3,2 lb) including batteries

ACCESSORIES INCLUDED:
3 × 1,5 V Alkaline Cells ..... OB 0004
1 × 7-pin DIN plug ..... JP 0703
2 × Overlays ..... SC 0418

ACCESSORIES AVAILABLE:
Rechargeable Ni-Cd Cells ..... 3 × OB 0008
Battery Charger ..... ZG 0113
Power Supply ..... Type 2805
7-pin Plug for Preamp. Input of B & K Measuring Amplifiers and Analyzers ..... JP 0701

*The Acceleration mode 0.2 and 2 Hz -10% limits correspond to 0,1 and 1 Hz -3 dB limits

IV.1.7 Impedance Head (Brüel & Kjær Type 8001)

Calibration Chart for Impedance Head Type 8001

Brüel & Kjær

Serial No. 1617650

Reference Sensitivity at 159,2 **Hz at** 25 **°C and including**

Cable Capacitance of 110 **pF**

Accelerometer:

Charge Sensitivity:**

3,46 pC/ms^{-2} or 34,0 pC/g*

Voltage Sensitivity:**

3,17 mV/ms^{-2}, or 31,1 mV/g*

Capacitance (including cable) 1093 **pF**

Maximum Transverse Sensitivity at 30 Hz 2,4 **%**
For Resonant Frequency mounted on steel exciter of 180 grams and for Frequency Response of Force Gauge relative to Reference Sensitivity with impedance head acceleration constant, see attached individual Frequency Response Curve.

Polarity is negative on the center of the accelerometer connector for an acceleration directed from the mounting surface into the body of the impedance head.

Date 91·02·14 Signature O.M

* 1 g = 9,807 ms^{-2} $\quad \frac{mV}{g} = \frac{mV_{RMS}}{g_{RMS}} = \frac{mV_{peak}}{g_{peak}}$

** This calibration is traceable to the National Bureau of Standards Washington D.C.

Force Gauge:

Charge Sensitivity 338 . pC/N

Voltage Sensitivity 386 mV/N

Capacitance (including cable) 876 pF

Base Strain Sensitivity of Force Gauge: 3 × 10^{-3} N/μStrain

Stiffness below Accelerometer: 25 × 10^{7} N/m

Mass below Force Gauge: 2,2 gram

Max. Screw-Down Torque: 0,5 Nm

Physical:

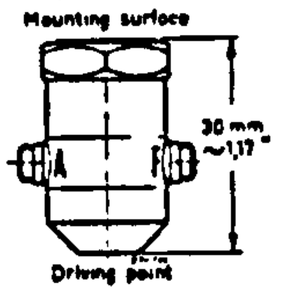

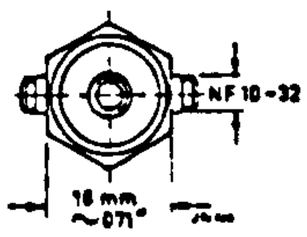

Weight: 31 gram
Material:
Titanium & Stainless Steel
Mounting Thread:
10—32 UNF-2B
Electrical Connector:
Miniature coaxial
10—32 UNF-2A thread

Environmental:

Humidity: Sealed
Max. Temperature: 260°C or 500°F
Magnetic Sensitivity (50 Hz): < 20 mV/T
Acoustic Sensitivity:
< 0,003 ms^{-2} or 0,03 g at 154 dB SPL
Resistance min. 20 000 mΩ at room temperature.

For further information see instruction book.

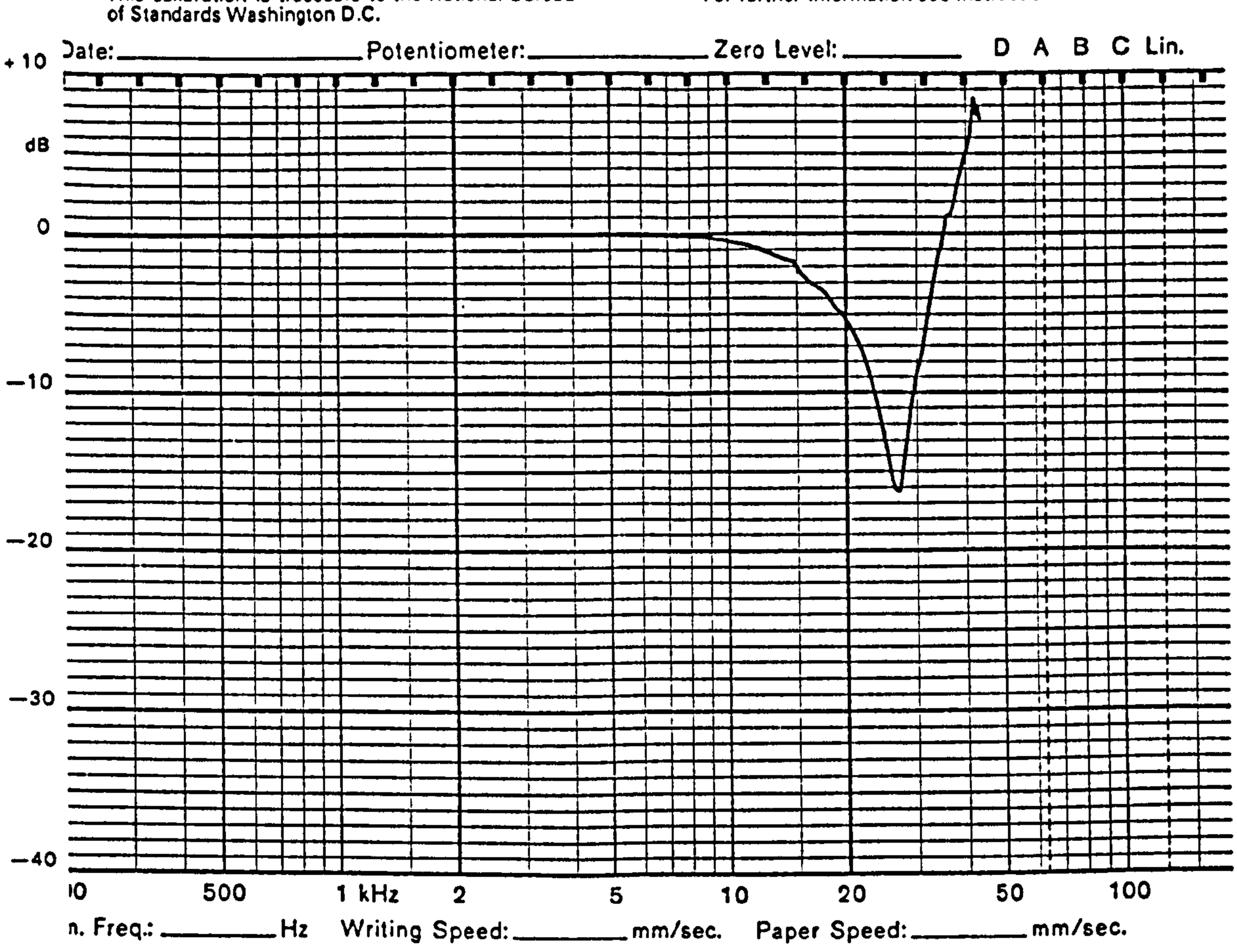

IV.1.8 Force Transducer (Brüel & Kjær Type 8203)

Brüel & Kjær

Calibration Chart for Force-Transducer Type 8203

Serial No.....1506166.....

Reference Sensitivity at 159,2 Hz (ω = 1000 s^{-1}) and room temperature: .....3,79.....pC/N

Max. Static Forces:
Tension: 250 N
Compression: 1000 N
Compression without preloading nuts: 1250 N

Linearity: typically better than ±1% of max. force or ±5% of measured force, which ever is smaller.

The frequency response curve for constant applied force shown on the attached sheet is obtained by mounting type 8203 on a vibration exciter and loading it by a mass of 2 grams (1,35 grams + accelerometer type 4374, 0,65 grams). By keeping a constant acceleration on the mass the force to the transducer is kept constant.

Polarity: Positive for compression

Leakage Resistance: > 10^5 MΩ at room temperature

Capacitance: 9 pF (without cable)

Note: The preloading nuts are assembled with a force of approx. 1000 N measured as 3600 pC output from the 8203. If disassembled and reassembled the same force should be applied. (A mounting torque of 0,6 Nm may be used).

Date 90-05-31 Signature O.M.

Typical Temperature Sensitivty Error in % rel. to the Reference Value.

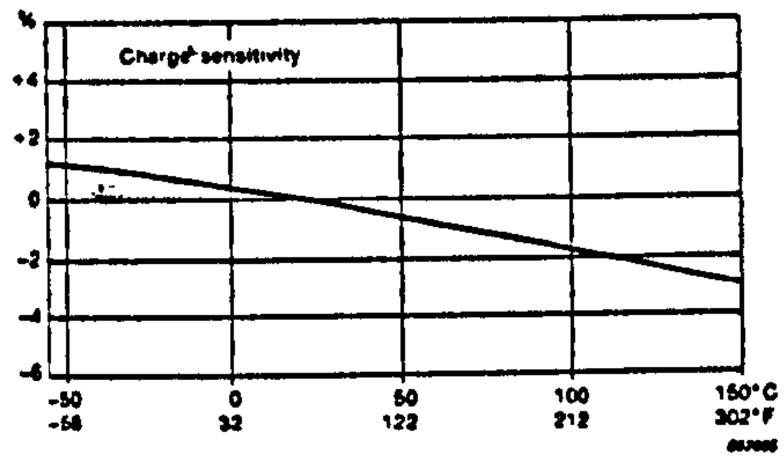

Physical:

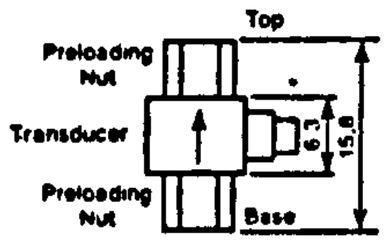

Weight: 3,2 grams
Material:
Titanium, ASTM Grade 2 and Stainless Steel, AISI 303
Mounting Thread: M3

Electrical Connector:
Coaxial M3

Environmental:
Humidity: Sealed
Temperature Range: –196° to + 150°C (–321 to +302°F)
Typical Magn. Sensitivity: 0,1 N/T
Max. Shock Acceleration: 10 000 g* ≈ 100.000 m/s^2
Max. Vibration (peak): 1000 g* ≈ 10 000 $ms/^2$
Max. Base Bending Sensitivity
0,002 N/μstrain with preloading nuts

For further information see B&K "Piezoelectric Accelerometer and Preamplifier" Handbook.

*1 g = 9,807 m/s^2 or 10 ms^{-2} = 1,02 g

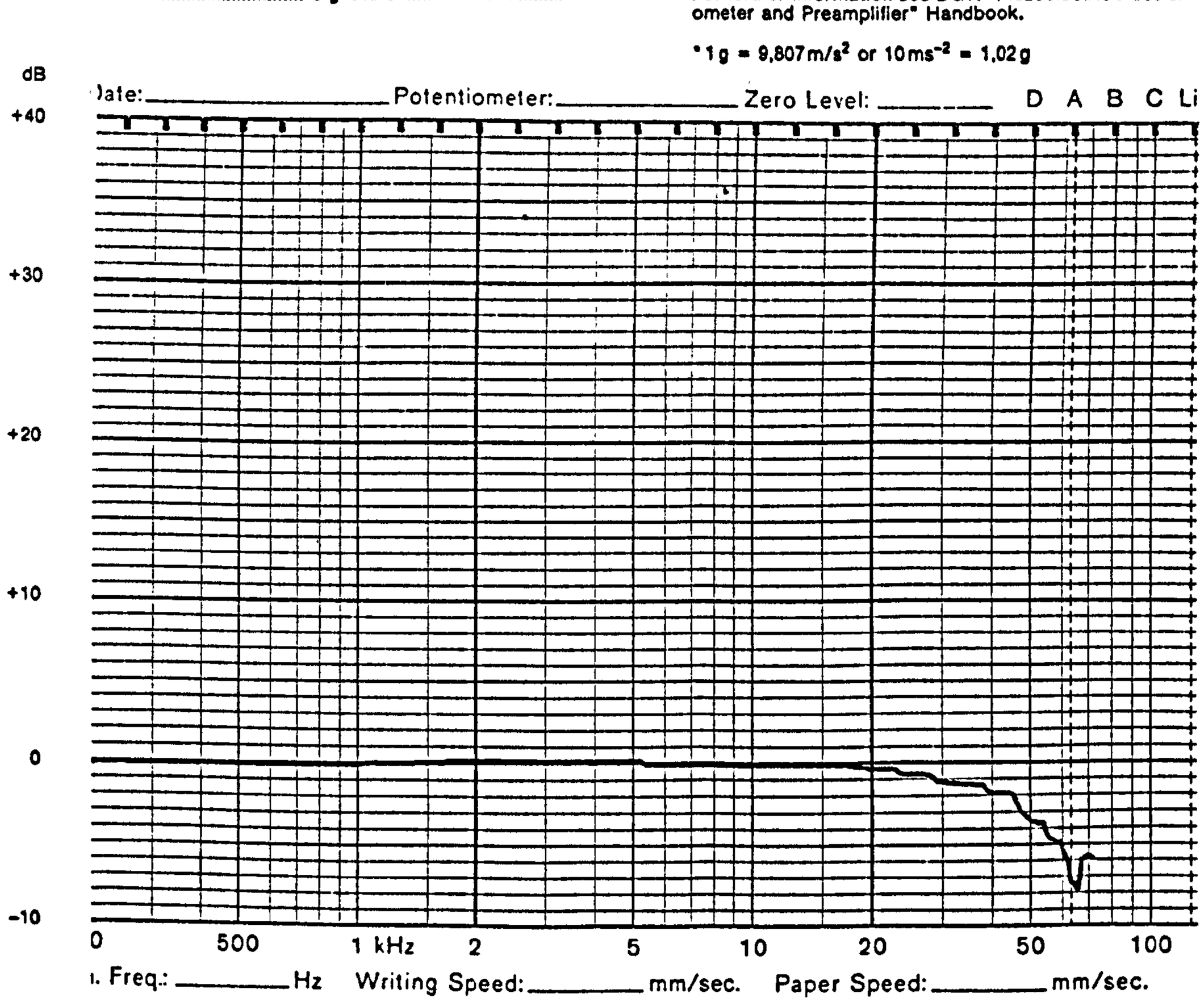

IV.1.9 Accelerometer (Brüel & Kjær Type 4393)

Calibration Chart for Accelerometer Type 4393

Brüel & Kjær

Serial No. 1581001

Reference Sensitivity at 159,2 Hz (ω = 1000 s^{-1}), 100 ms^{-2} and 24 °C

Charge Sensitivity* 0,318 pC/ms^{-2} or 3,12 pC/g

Voltage Sensitivity* (incl. AO 0283)

0,577 mV/ms^{-2} or 5,66 mV/g
(Voltage Preamp. Input Capacitance: 3,5 pF)

Capacitance (incl. AO 0283) 552 pF

Typical Capacitance of cable AO 0283 132 pF

Maximum Transverse Sensitivity (at 30 Hz, 100 ms^{-2}) 0,1 %

Typical Undamped Natural Frequency 85 kHz

Typical Mounted Resonance Frequency 55 kHz
See reverse side of chart for frequency response curve

Typical Transverse Resonance Frequency, using Exciter Table 4290, with accelerometer mounted on a titanium cube by a M3 steel screw, mounting torque 0,6 Nm and greased surfaces: 18 kHz

Polarity is positive on the center of the connector for an acceleration directed from the mounting surface into the body of the accelerometer

Resistance minimum 20 000 MΩ at room temperature

Date: 90-12-03 Signature: O.M.

1 g = 9,807 ms^{-2} or 10 ms^{-2} = 1,02 g

* This calibration is traceable to the National Bureau of Standards Washington D.C.

Environmental:
Humidity: Welded, Sealed
Temperature Range: –74 to +250°C (–100 to +482°F)
Max. Shock Acceleration: 250 000 ms^{-2} peak
Typical Magnetic Sensitivity (50 Hz – 0,03 T): 30 ms^{-2}/T
Typical Acoustic Sensitivity: 0,04 ms^{-2} at 154 dB SPL (2 – 100 Hz)
Typical Base Strain Sensitivity (at 250 $\mu\epsilon$ in base plane): 0,005 $ms^{-2}/\mu\epsilon$
Typical Temperature Transient Sensitivity (3 Hz LLF): 5 ms^{-2}/°C
Specifications obtained in accordance with ANSI S2.11-1969

Physical:

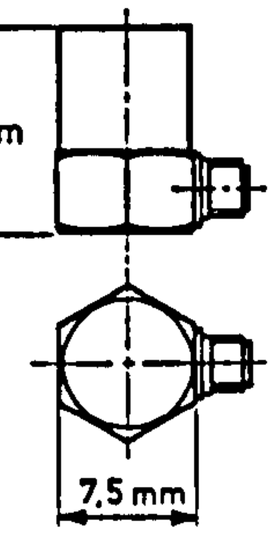

Electrical Connector:
Coaxial M3

Material: Titanium, ASTM Grade 2
Sensing Element: Piezoelectric, type PZ23
Weight: 2,2 gram excl. cable
Construction: Delta Shear
Mounting Thread: M3
Mounting Stud: M3 x 8 mm, steel
Mounting Surface Flatness: <3 μm
Mounting Torque: Normal 0,6 Nm. Max. 1,0 Nm Min. 0,3 Nm.
Seismic Mass: 0,67 gram
Center of Gravity of Seismic Mass: 7,1 mm from mounting surface on central axis
Center of Gravity of Accelerometer: 5,4 mm from mounting surface on central axis
For further information see B&K "Piezoelectric Accelerometer and Preamplifier" handbook

Typical Temperature Sensitivity Deviation:
(Piezoelectric Material PZ23)

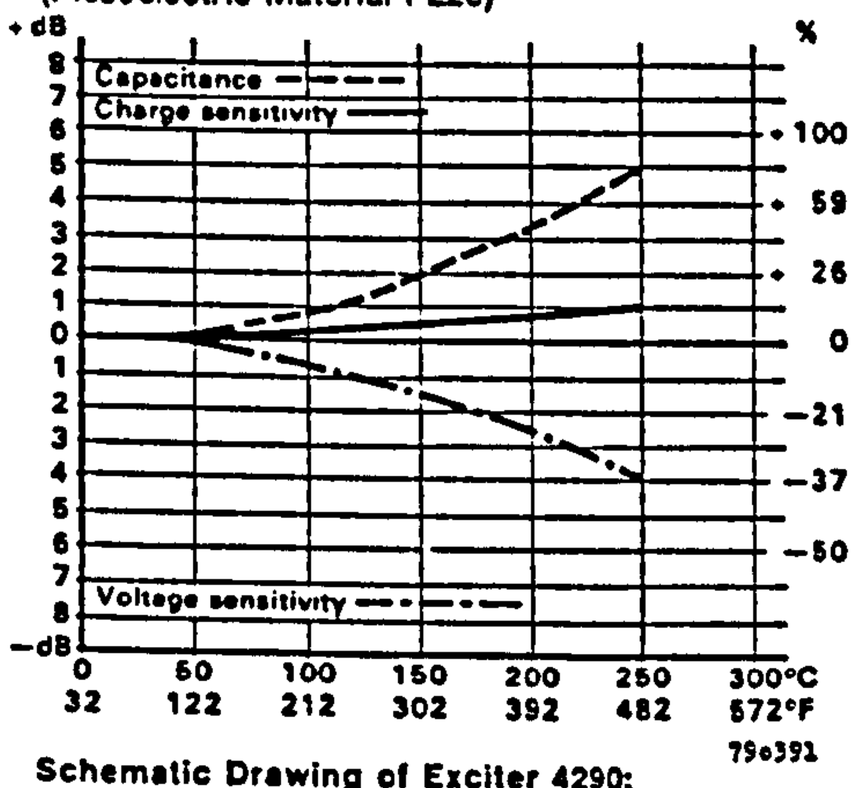

Typical Frequency Response Curve of 4393
(Corrected for response of 4290):

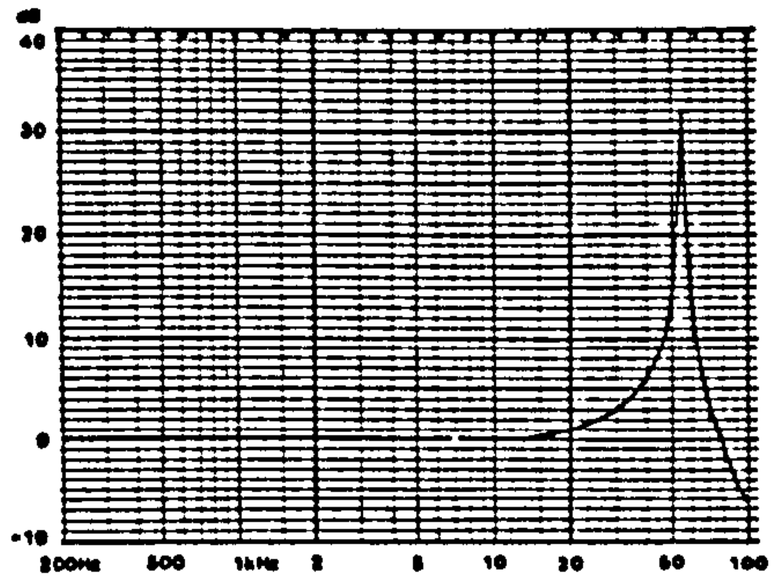

Schematic Drawing of Exciter 4290:
(Modified laboratory reference)

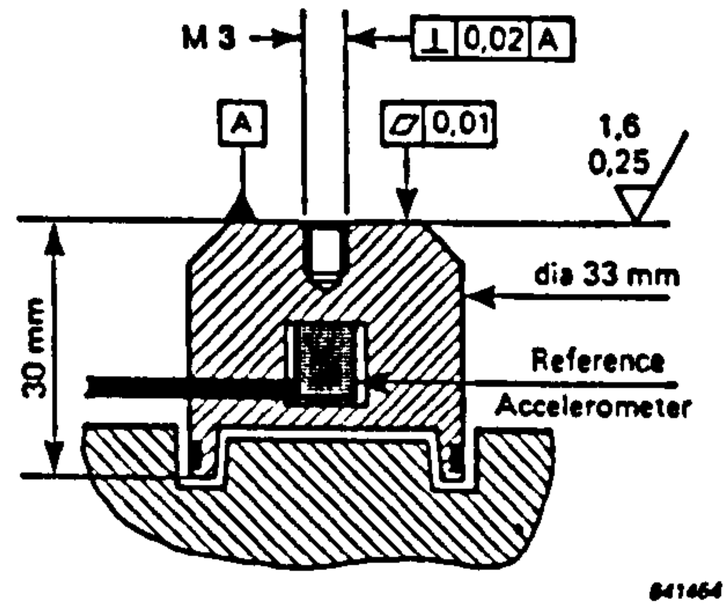

Material: Beryllium

Mass of Exciter table: 38 gram

Mounting Technique:
Examine the mounting surface for cleanliness and smoothness.
If necessary, machine surface to tolerances shown in schematic drawing of Calibration Exciter 4290.
Fasten the 4393 using a 3 mm stud. Take care not to exceed the recommended mounting torque and that the stud does not bottom in the mounting holes.
A thin film of oil or grease between the accelerometer and the mounting surface helps achieve good contact and improves mounting stiffness.
For other types of mounting, see B&K "Piezoelectric Accelerometer and Preamplifier" handbook.

Analog Inputs

	Resolution (bits)	Throughput (kHz)	Input Channels	Gain	Ranges (V)	System Error (% of FSR)	Conversion Time (µs)	CMRR (dB @ 60Hz)	S/H Aperture Uncertainty (ns)	Max. Input Volt. Protection (On/Off)
DT2821-G-16SE	12	250	16SE	1,2,4,8	0–1.25, 2.5, 5, 10	.03, G=1	2.5	—	.2	±16/± 1
DT2821-G-8DI	(.024% FSR)		8DI		± .625, 1.25, 2.5, 5, 10	.07, G=8		80		

Specifications

All specifications are typical at 25°C and rated voltage, unless otherwise specified.

DIGITAL I/O

Number of Lines
16, organized as two 8-line ports that can be set for input or output

Fanout
30 LSTTL loads

Input Load
1 LSTTL load

PACER CLOCK

Function
Pacer clock initiates A/D or D/A conversions; clock is started by software trigger or external trigger.

Usable Range
From 4µs (250kHz) to 2s (.5Hz)

Description
Pacer clock consists of a 4.00 MHz oscillator (.25µs increments), a prescaler (divides oscillator by powers of two from 20 to 215), and an 8-bit divider (divides output of prescaler by integers from 1 to 255).

OPERATING MODES

A/D

Channel/Gain Selection—16-location channel-gain list

Operation—single conversion; single scan (once through channel-gain list); continuous scan (continuous through channel-gain list)

Data Transfer—programmed I/O; single-channel DMA; dual-channel (Continuous Performance) DMA

D/A

Channel Selection—either channel singly or both channels simultaneously

Data Transfer—programmed I/O; single-channel DMA; dual-channel (Continuous Performance) DMA

GENERAL

Interface
IBM PC AT bus or EISA Bus; I/O mapped, 10-bit I/O address; 16-bit data path; one or two DMA channels

Interrupt—one line, jumper-selected level; source: A/D, D/A error; A/D done; D/A ready; A/D scan done; A/D, D/A DMA done

Power Requirements
+5V @ 2.4A typical; low-noise ±15V generated by onboard DC/DC converter

Physical/ Environmental

Dimensions—full-size PC AT board mechanicall compatible with ISA system slots only; 12.07 x 33.66 x 1.9 (4.75" x 13.25" x .5"); 12.86 x 34.29 x 1.91 (5.06" x 13.5" x .75") including bracket

Temperature—operating: 0 to 70°C; storage: –25 to 70°C

Relative Humidity—to 95%, non-condensing

IV.2 SPECIFICATIONS OF MAJOR SOFTWARE
(Only specifications relevant to this study)

IV.2.1 GLOBAL LAB Data Acquisition Module

Analogue Input Operations

- Specify gain for each channel;
- Select sampling rate;
- Select sampling duration; and
- Select software or external hardware trigger.

File Operations

- Specify memory usage;
- Specify destination A/D data file;
- Indicate amount of free space for file storage;
- Load or save A/D setup;
- Import or export non-GLOBAL LAB data file;
- Open or close a file for display;
- Edit a file for display; and
- Export a file with data reduction.

Engineering Units and Variables

- Specify units name, offset, or factor;
- Edit engineering units; and
- Calculator: add, subtract, multiply, divide, percent, square root.

Data Display

- Import, select, open, edit and export files;
- Select, label, and scale signals;
- Zoom in and zoom out;
- Automatically select next/previous file, window, or curve;
- Increase/decrease cursor speed;
- Label, select signal number, select data type, and select frequency;
- Display multiple windows, specify window layout;
- Edit window parameters, title location of axes;
- Browse quickly forward or backward through a file;
- Export a window's signal; and
- Measure exact time and amplitude at cursor.

Statistical Analysis

- Determine minimum or maximum data value;
- Determine arithmetic mean or standard deviation of sample; and
- Save results to ASCII file.

IV.2.2 STATPACK Signal Processing Module

Mathematical Operators

- +, - (change sign); and
- +, -, *, /, **, ^, =, NE (not equals), >, <, >=, <=.

Methods

- Create formulae and user-defined functions; and
- Save methods as libraries; recall methods.

Frequency Analysis Functions

- FFT, inverse FFT, autospectrum, cross-spectrum, transfer function;
- Hanning windowing etc; and
- Magnitude/phase, real/imaginary, real cepstrum, coherence, spectral analysis.

IV.2.3 GRAPHPACK Printing Module

Layout

- Zoom in or out of a select region;
- Load a graph layout from disk; and
- Save the current layout out to disk.

Add Comment

- Add text: select fonts, font size, baseline angle, subscripts or superscript text, select text alignment, text position; and
- Select scaling, range and increment for x and y axes.

Options

- Charts: select font and font size for axis scaling and legends, position legend;
- Fonts: Gothic, Roman etc.;
- Specify graph line style;
- Specify units for graph; and
- Align charts horizontally and/or vertically.

Print

- Print the current graph using the currently selected printer driver;
- Print graph to DOS files; and
- Specify printer options, output device, rotate orientation of chart.

Support Output Devices

- Most major printing devices available on the market.

APPENDIX V.

ACCESSORIES AND EXPERIMENTAL SET-UPS

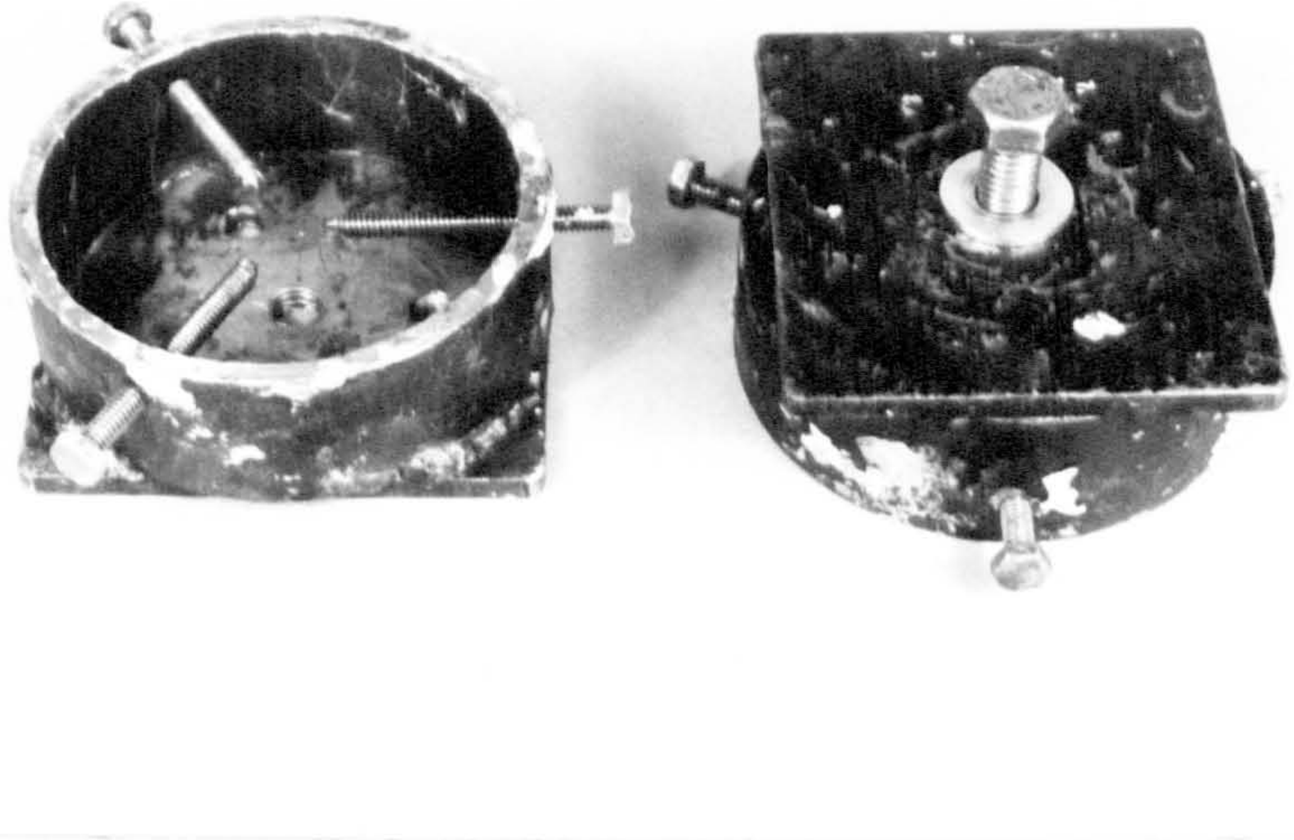

Fig V.1 Mounting cups.

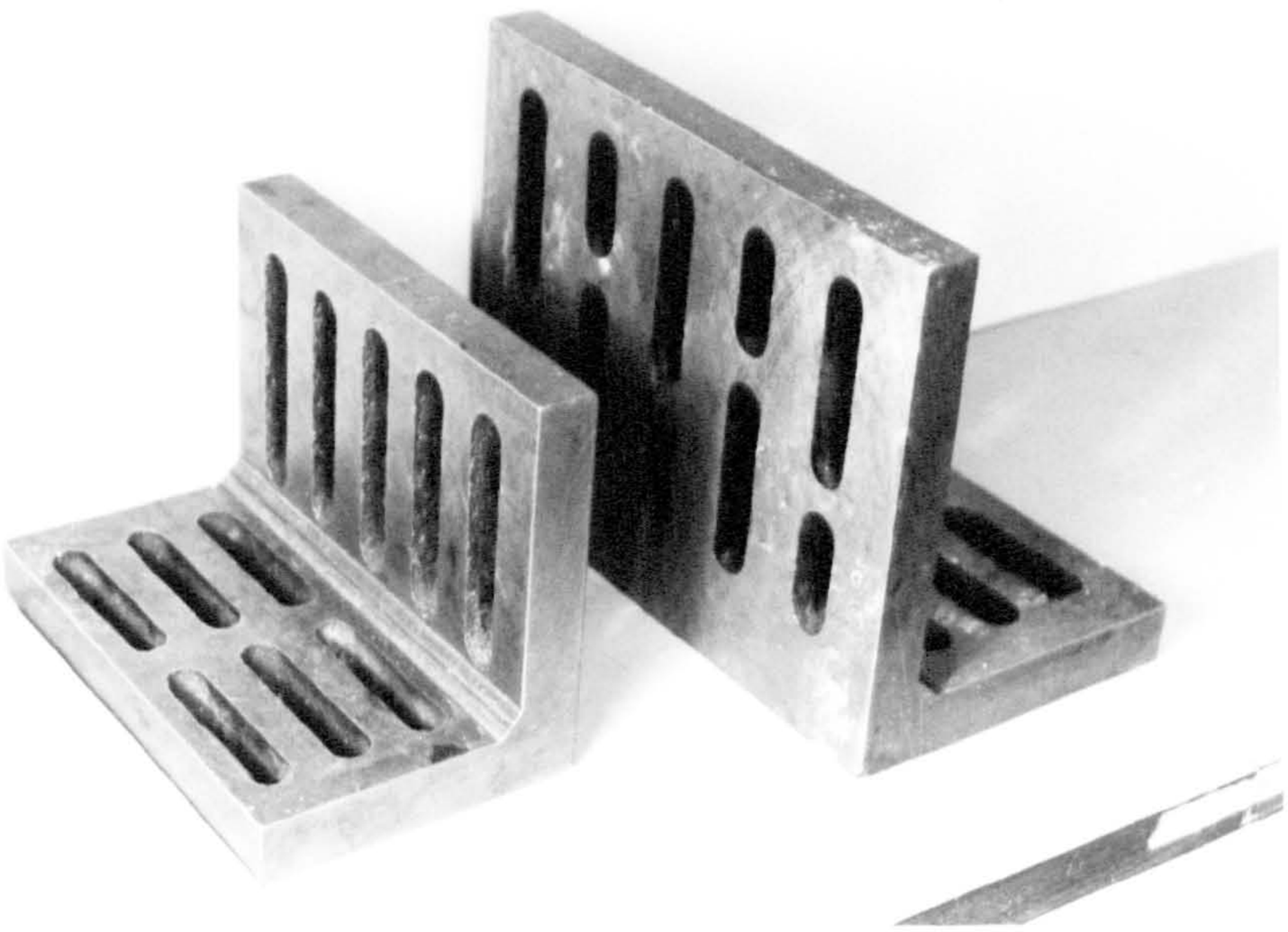

Fig V.2 Angle-plates.

a)

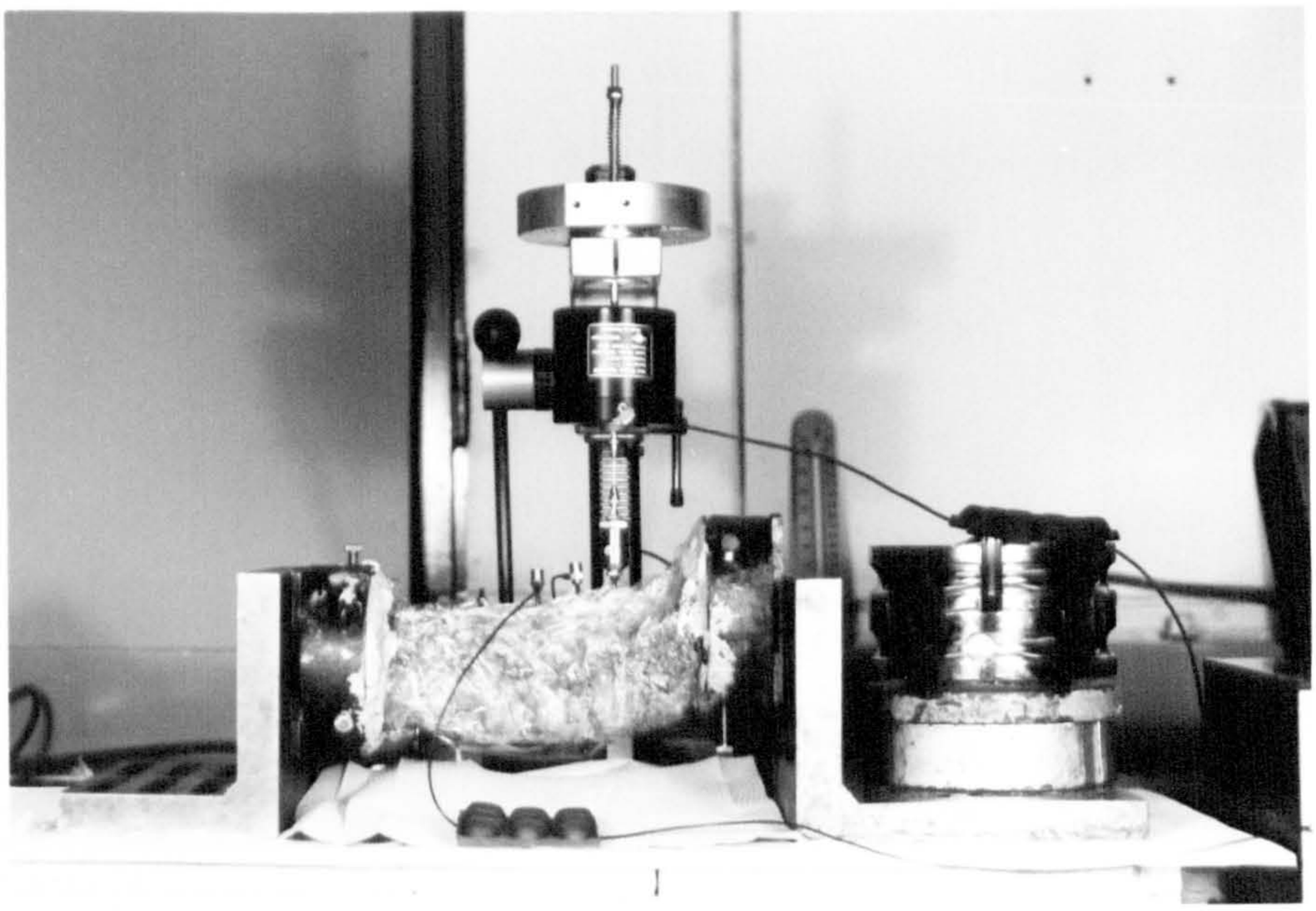

b)

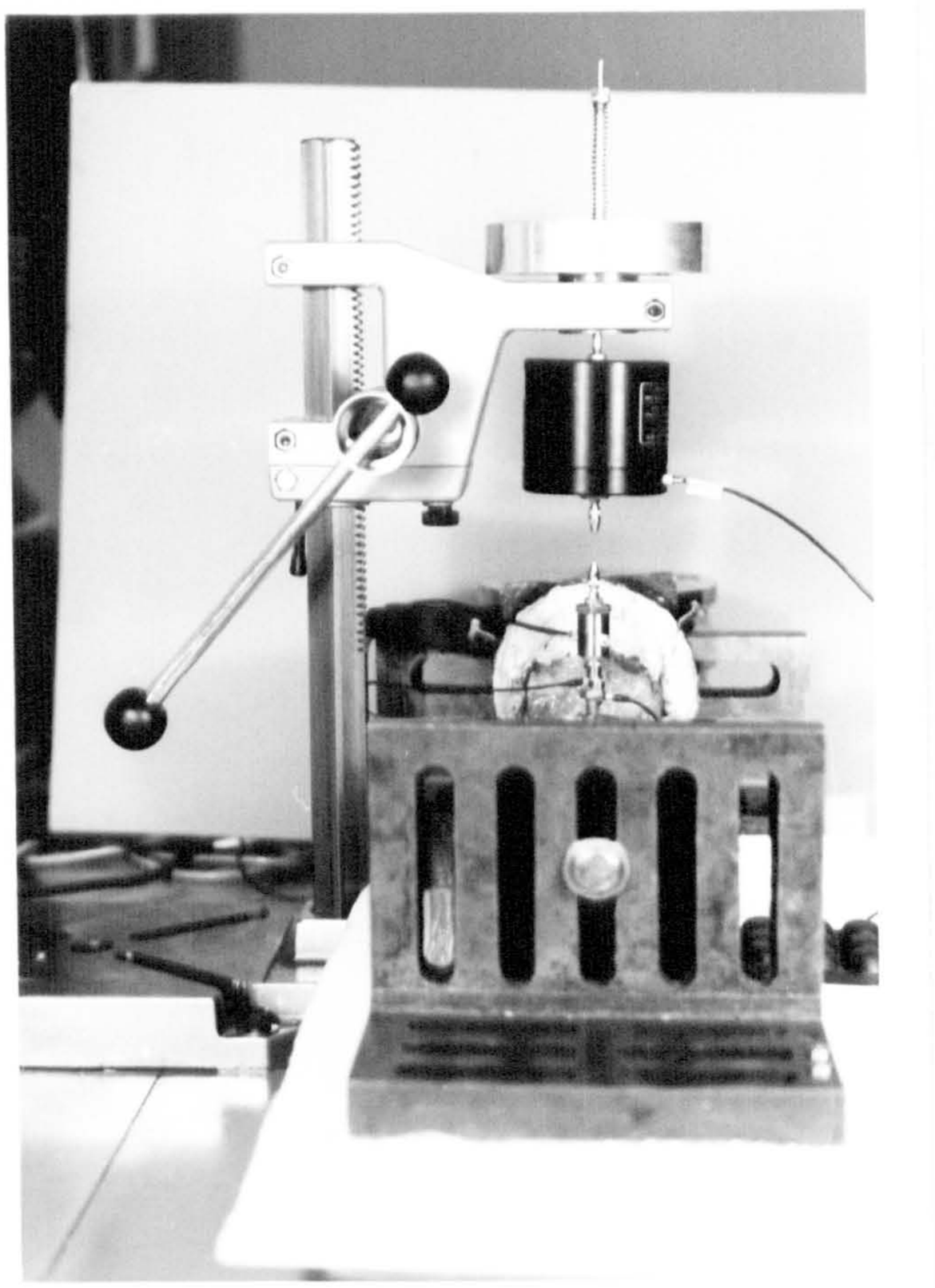

Fig V.3 Experimental set-up of in-vitro vibration tests. a) Lateral view; and b) End-on view.

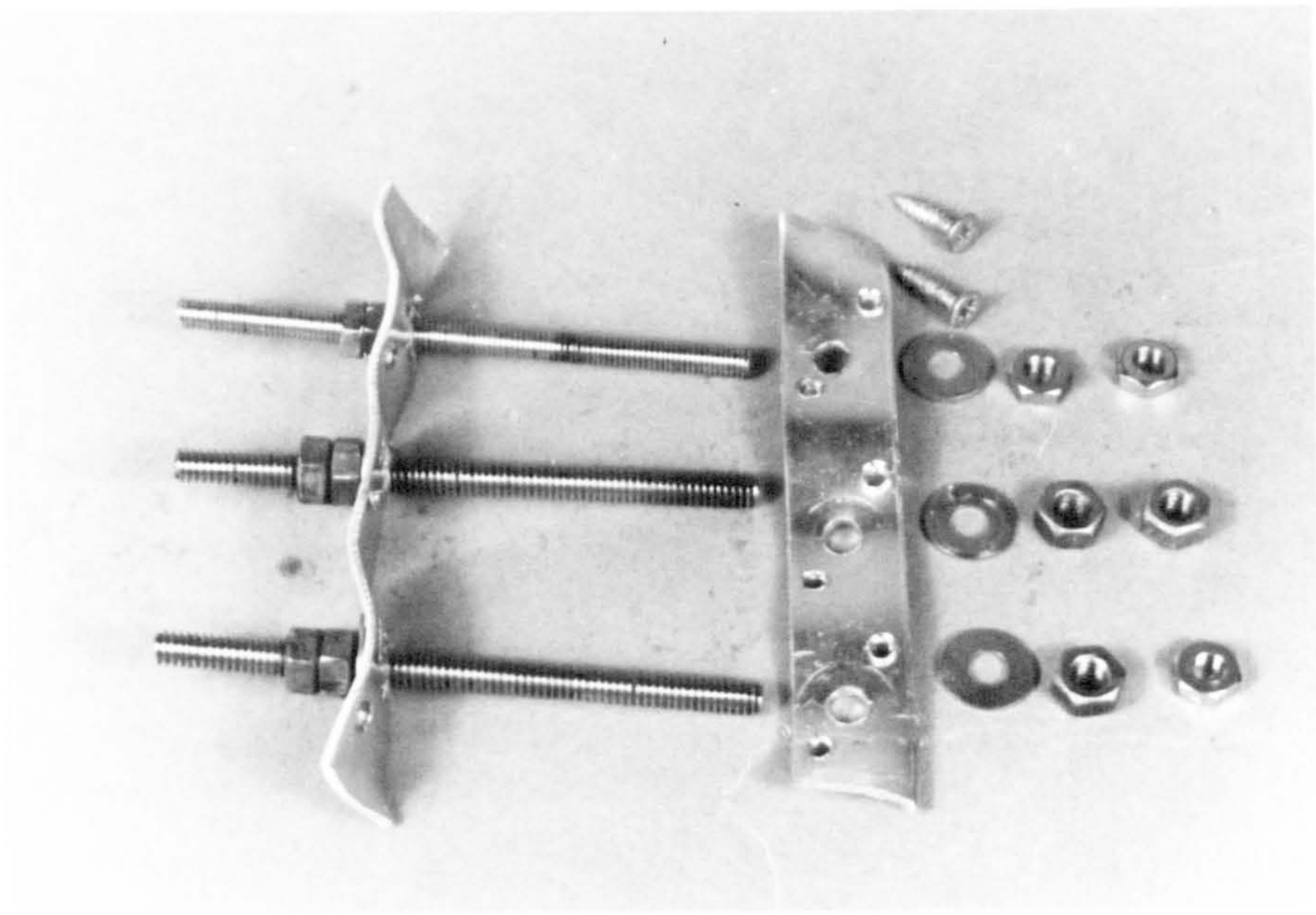

Fig V.4 Devices for simulation of fusions of the lumbar spine specimen.

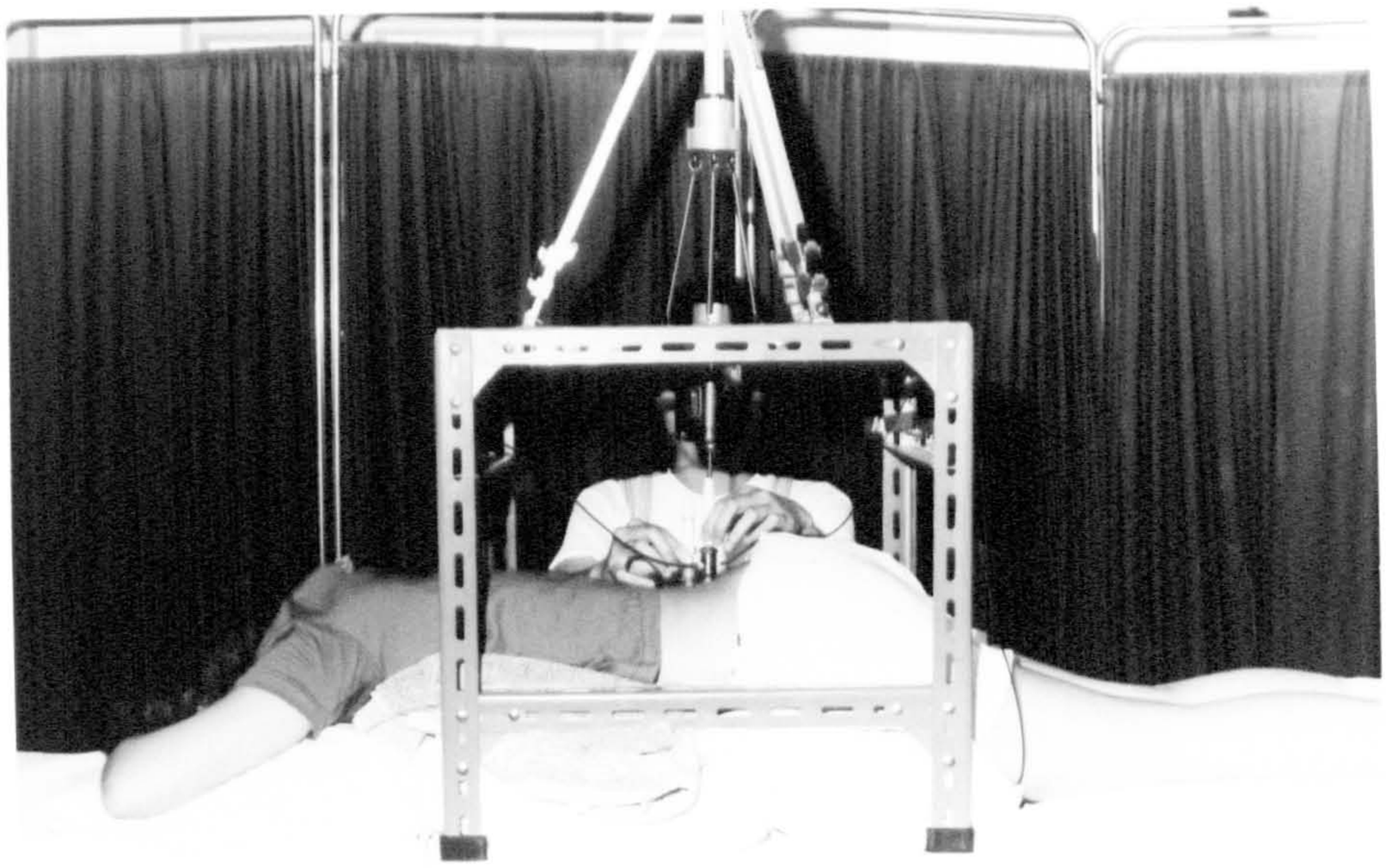

Fig V.5 Experimental set-up of in-vivo vibration tests.

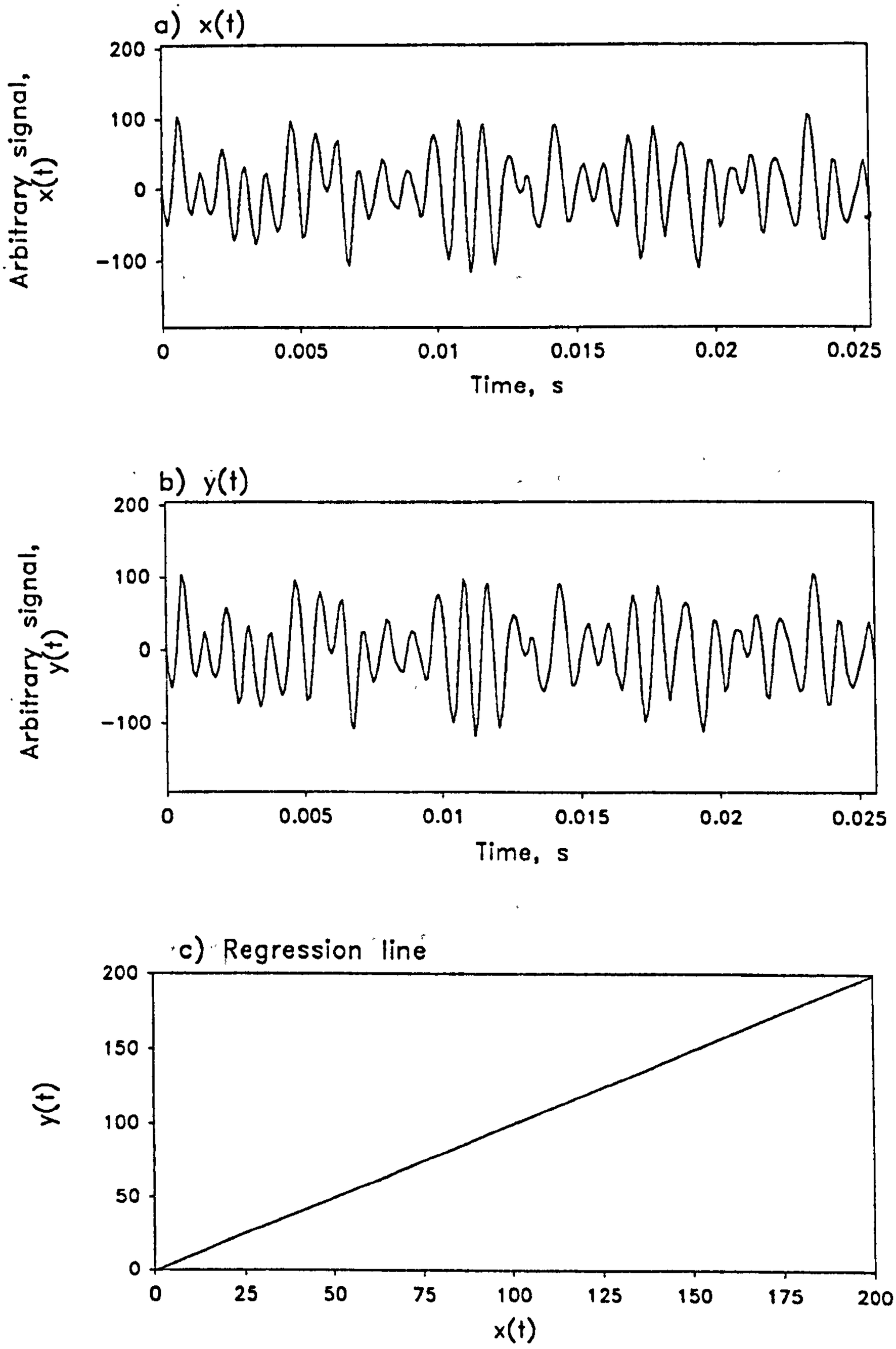

Fig VI.1 Arbitrary signals x(t) and y(t) and their linear correlation.

APPENDIX VI.

LINEAR REGRESSION MODEL:- to test correlation and repeatability

A linear regression model is designed to test how closely two time-sampled signals resemble each other. The degree of closeness is tested by the Pearson correlation coefficient R which is computed from the variances of x and y, and their covariance. The ratio of the uncorrelated component to the correlated component is given by the following equations:-

$$R_{xy}^2 = \frac{\sigma_{xy}^2}{\sigma_x^2 . \sigma_y^2} \qquad 0 \leq R_{xy}^2 \leq 1$$

$$\frac{\textit{Uncorrelated component}}{\textit{Correlated component}} = \frac{1 - R_{xy}^2}{R_{xy}^2}$$

For two highly correlated signals, R is close to unity and the small value of p indicates the level of significance.

Figure VI.1 depicts two identical time-sampled signals x(t) and y(t) which when plotted point to point on linear axes will give a straight line through the origin. This indicates a high correlation with R = 1, and p < 0.0001 which indicates very high significance.

This concept could be extended to test the repeatability of two independent measurements e.g. the frequency response function of a test system. A linear regression model can be used to assess the degree of correlation (resemblance) the two measurements have with each other, and hence the repeatability. Highly repeatable measurements would yield a coefficient of determination R^2 very close to unity, and a small value of F ratio which is defined as:

$$\textit{F ratio} = \frac{\textit{Variance between the measurements}}{\textit{Variance within the measurements}}$$

The corresponding small value of p indicates very high significance.